UNIVERSITY OF CANTERBURY
Te Whare Wānanga o Waitaha
CHRISTCHURCH NEW ZEALAND

2007

Molecular Cages of Controlled Size and Shape

A thesis submitted in partial fulfilment of the requirements for the Degree of

Doctor of Philosophy in Chemistry

in the University of Canterbury

by

Jennifer A. Zampese

Acknowledgements

About four and a half years ago I sat in the office of Prof. Peter J. Steel as he patiently explained the basics of metallosupramolecular chemistry. No other area of chemistry research had even vaguely sparked my interest until that point, and I instantly knew I wanted to be a part of this research. An honours project and PhD later, and I still feel that the anticipation of solving a crystal structure without knowing what amazing complex you may have made is one of the most exciting and rewarding experiences in science. Thanks Peter, for introducing me to this field of work and for the enormous amount of advice and encouragement you have generously provided over the past few years, as well as for all the Friday lunch drinks!

Thanks also to the people I have worked with over the past few years, in particular Matt, William, Jon, Chris R. and Chris S. for the endless help and advice on all things chemistry related. I need to deeply thank Justine, Jeni and Neroli for the fine company on this journey, I wish you guys all the best for the future! Looks like we finally made it…. Also thanks to the others who have passed through room 658 while I have been there: Thomas, Philip, Muna, Marcus, Alan, Reuben, David, Jana, Simon and Akbar. I also need to acknowledge the support and advice from others such as Prof. Ward Robinson, Dr Jan Wikaira, A. Prof. Richard Hartshorn and Prof. F. Richard Keene, along with many others in the Chemistry Department, including of course, Rob McGregor, Wayne Mackay, Sandy Ferguson and the other technical staff who make our research so much easier. Thanks too to Prof. Cameron Kepert and his group at the University of Sydney, especially to Dr Greg Halder for help with the TGA instrumentation.

Finally, a big heartfelt thank you to my parents, Lyn and Francis, and to my flatmate Clair, for the enormous amount of support and encouragement they have provided during this time.

Table of Contents

Acknowledgements **3**
Table of Contents **5**
Abstract **9**
Introduction **13**
Chemistry beyond the molecule 13
Host-guest structures 15
Metallosupramolecular chemistry 16
Nitrogen-containing heterocyclic ligands 18
Coordination polymers 21
Polygons 23
Molecular cages 24
Thesis coverage 27
Chapter Two **31**
The 1,3-disubstituted-2,4,6-triethylbenzene ligands **31**
Introduction 31
1,3-Di(bromomethyl)-2,4,6-triethylbenzene (2.2) 34
1,3-Di(pyrazol-1-ylmethyl)-2,4,6-triethylbenzene (2.4) 35
Complexes with ligand 2.4 36
1,3-Di[3-(2'-pyridyl)pyrazol-1-ylmethyl]-2,4,6-triethylbenzene (2.12) 55
Complexes with ligand 2.12 57
1,3-Di(4-pyridylsulfanylmethyl)-2,4,6-triethylbenzene (2.35) 98
Complexes with ligand 2.35 100
1,3-Di(8-quinolyloxymethyl)-2,4,6-triethylbenzene (2.44) 104
Summary 106
Chapter Three **111**
The 1,3,5-trisubstituted-2,4,6- trialkyl/trimethoxybenzene ligands **111**
Introduction 111
Synthesis of ligand precursors 114
Synthesis of the 1,3,5-tri(pyrazol-1-ylmethyl)-substituted ligands 118
Complexes with ligand 3.5 123
Complexes with ligand 3.18 130
Synthesis of the 1,3,5-tri[3-(2'pyridyl)pyrazol-1-ylmethyl] substituted ligands 131
Complexes with ligand 3.24 133
Complexes with ligand 3.25 142
Synthesis of the 1,3,5-tri(4-pyridylsulfanylmethyl) substituted ligands 143
Complexes with ligand 3.33 146
Complexes with ligand 3.34 157
Complexes with ligand 3.35 166
Synthesis of the 1,3,5-tri(8-quinolyloxymethyl) ligands 167
Complexes with ligand 3.41 171
Complexes with ligand 3.42 172
Complexes with ligand 3.43 176
Summary 177
Chapter Four **181**
The remaining C_3 symmetric ligands **181**

Introduction 181
The 4,4',4"-trisubstituted-1,3,5-triphenylbenzene ligands 182
Synthesis of ligand precursors 184
4,4',4"-Tri(pyrazol-1-ylmethyl)-1,3,5-triphenylbenzene (4.9) 185
Complexes with ligand 4.9 186
4,4',4"-Tri[3-(2'-pyridyl)pyrazol-1-ylmethyl]-1,3,5-triphenylbenzene (4.13) 190
Complexes with ligand 4.13 191
4,4',4"-Tri(4-pyridylsulfanylmethyl)-1,3,5-triphenylbenzene (4.16) . 198
Complexes with ligand 4.16 199
4,4',4"-Tri(8-quinolyloxymethyl)-1,3,5-triphenylbenzene (4.22) 199
The 4,4',4"-Trisubstituted-1,3,5-triphenyltriazine ligands 201
4,4',4"-Tri(pyrazol-1-ylmethyl)-1,3,5-triphenyltriazine (4.27) 202
4,4',4"-Tri[3-(2'-pyridyl)pyrazol-1-ylmethyl]-1,3,5-triphenyltriazine (4.31) 205
The tri(4-substituted-phenyl)methanol ligands 206
Tri(4-pyrazol-1-ylmethylphenyl)methanol (4.37) 207
Complexes with ligand 4.37 208
Tri[4-(3-[2'-pyridyl]pyrazol-1-ylmethyl)phenyl]methanol (4.38) 208
Complexes with ligand 4.38 210
Tri[4-(4-pyridylsulfanylmethyl)phenyl]methanol (4.41) 210
Tri[4-(8-quinolyloxymethyl)phenyl]methanol (4.43) 211
Complexes with ligand 4.43 212
Attempted syntheses of the tri(4-substituted-phenyl)amine ligands . 213
Summary 214
Chapter Five **219**
Complexes of 3-(2'-pyridyl)pyrazole: from decomposition and direct synthesis **219**
Introduction 219
Ligand decomposition 221
Complexes with ligand 5.1 and 5.2 224
Complexes with 8-hydroxyquinoline 245
Summary 249
Conclusions and future prospects **253**
General experimental **261**
Preparation of ligands & ligand precursors **263**
Preparation of the 1,3-disubstituted-2,4,6-triethylbenzene ligands .. 264
Preparation of the 1,3,5-trisubstituted-2,4,6-trimethylbenzene ligands 266
Preparation of the 1,3,5-trisubstituted-2,4,6-triethylbenzene ligands 268
Preparation of the 1,3,5-trisubstituted-2,4,6-trimethoxybenzene ligands 270
Preparation of the 4,4',4"-trisubstituted-1,3,5-triphenylbenzene ligands 273
Preparation of the 4,4',4"-trisubstituted-1,3,5-triphenyltriazine ligands 277
Preparation of the tri(4-substituted-phenyl)methanol ligands 279
Attempted syntheses of the tri(4-substituted-phenyl)amine ligands . 281
Preparation of complexes **284**
Preparation of complexes with the 1,3-disubstituted-2,4,6-triethylbenzene ligands 284
Preparation of complexes with the 1,3,5-trisubstituted-2,4,6-trimethylbenzene ligands 293
Preparation of complexes with the 1,3,5-trisubstituted-2,4,6-triethylbenzene ligands 298

Preparation of complexes with the 1,3,5-trisubstituted-2,4,6-trimethoxybenzene ligands 306
Preparation of complexes with the 4,4',4"-trisubstituted 1,3,5-triphenylphenyl ligands 310
Preparation of complexes with the 4,4',4"-trisubstituted triphenylhydroxymethane ligands 314
Crystallography **323**
References **341**

Abstract

This thesis details the synthesis and coordination chemistry of twenty-five nitrogen-containing heterocyclic ligands, nineteen of which were previously unreported compounds. These ligands were designed for use as synthons for the formation of molecular cages, so contain multiple coordination sites capable of bridging multiple metal atoms. The majority of molecular cages in the literature are formed by rigid bridging ligands, whereas the ligands studied in this research incorporate a higher level of flexibility, thereby lessening the degree of control over the self-assembly process and increasing the number of possible structures that can be formed upon reaction of these ligands with meal salts.

Three of the new ligands synthesised were two-armed bridging ligands, which were reacted with a wide variety of metal salts to investigate what self-assembly products were formed. The complexes characterised include a M_3L_3 cyclic trimer, a range of coordination polymers of varying dimensionality, a range of dimeric products and a series of M_4L_6 cage-like molecular squares.

However, the majority of ligands studied were three-armed, potentially tripodal compounds, which were envisaged as potential components of M_3L_2 or M_6L_4 molecular cages. The products of self-assembly of these ligands with various metals salts were shown to include a variety of discrete tri- and tetranuclear complexes, a range of coordination polymers of varying dimensionality and interpenetration, and a complex M_6L_4 assembly that appears to be a collapsed coordination cage.

Unfortunately some of the ligands synthesised were shown to decompose in the presence of various metal salts, a phenomenon already identified in the literature. Analogues of these decomposition products were synthesised deliberately to identify the potential of a known tridentate ligand as a metallosupramolecular synthon.

^{1}H NMR spectroscopy, mass spectrometry, elemental analysis, thermogravimetric analysis and X-ray crystallography were used to study the compounds synthesised. The crystal structures of five ligands and fifty-one complexes are discussed.

Chapter One

Introduction

Introduction

Chemistry beyond the molecule

Supramolecular chemistry has been portrayed by Nobel prize winner Jean-Marie Lehn as *"a sort of molecular sociology!"*,[1] as it investigates the way individual molecules recognise, associate and interact with each other when grouped together as a population.[1] More technically, he has defined this area of science as the *"chemistry of molecular assemblies and of the intermolecular bond"*, or as *"chemistry beyond the molecule"*.[1-3]

Traditionally chemistry concentrated on the step-wise construction of molecules from atomic building blocks using covalent bonds as the 'glue' to hold the components together. In contrast, supramolecular chemistry is concerned with the self-assembly of molecules into supramolecular assemblies held together by the simultaneous formation of multiple intermolecular interactions. In comparison with covalent bonds, intermolecular bonds are weak, but the additive effect of many interactions supporting a single structure can have a profound influence on the stability of that structure. The exploitation of these weaker interactions allows the often quantitative formation of a thermodynamic product, as the weak interactions are easily broken and reformed, allowing the system to cycle through a range of possible products until the most stable assembly is formed. This error-checking process is known as self-assembly.[1,3-5]

Common intermolecular interactions utilised in supramolecular chemistry are listed in Table 1.1 with approximate values for the strength of each interaction.[3] One such

Interaction	**Strength ($kJmol^{-1}$)**
Ion-dipole	50-200
Dipole-dipole	5-50
Hydrogen bonding	4-120
Cation-π	5-80
π-π stacking	0-50
Van der Waals forces	<5

Table 1.1 *– Supramolecular interactions and their relative strengths.*[3]

common interaction is the hydrogen bond, which occurs when a hydrogen bonded to an electron-withdrawing or electronegative atom is drawn towards a dipole of close proximity.[3] Also commonly encountered are π-π interactions between aromatic rings of a compound. The two types of π-π interactions are illustrated in Figure 1.1 for two benzene molecules. Face-to-face π interaction a) occurs when the rings are parallel and offset (direct overlap would be repulsive), whereas edge-to-face π interaction b) occurs when the rings are perpendicular and resembles a weak hydrogen bond.[3] Edge-to-face π interactions are often responsible for the herringbone packing formations in structures containing aromatic rings.[3]

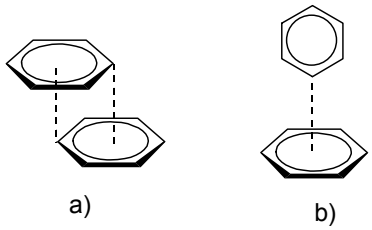

Figure 1.1 *– a) face-to-face and b) edge-to-face π-π interactions*

Although the use of weak intermolecular interactions to consciously design molecular assemblies is a recent advancement, nature has long been using these tools in biological systems. Shown in Figure 1.2[6] is an example of a well-known biological structure assembled from multiple weak intermolecular interactions.

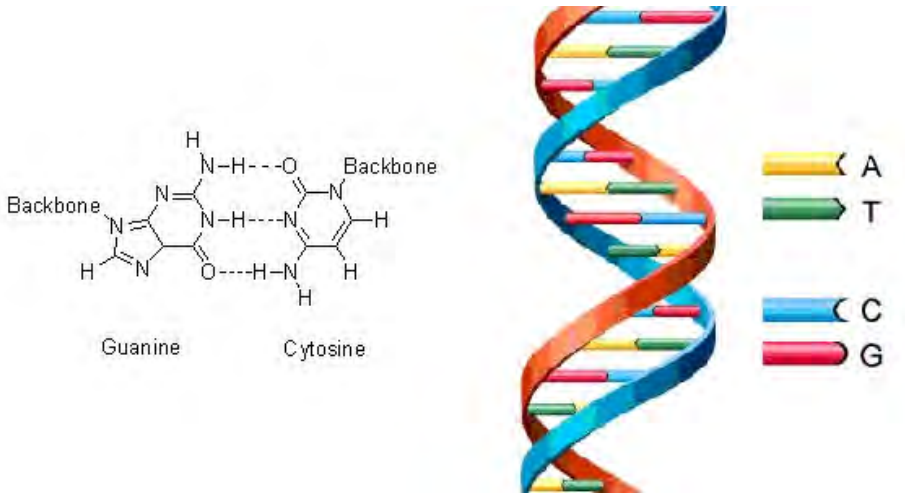

Figure 1.2 *– The classic example of supramolecular chemistry in action, DNA. Shown is an example of hydrogen bonding between two bases, and the overall double helical structure. π-π Stacking and hydrophobic interactions also strengthen this assembly.*[3,6]

Host-guest structures

A host is described as a large molecule or aggregate containing a central hole or cavity with convergent binding sites capable of binding a smaller guest molecule with divergent binding sites to create a host-guest complex or assembly.[3] Molecules commonly used as hosts include crown ethers, spherands and cryptands, while common guests include metal cations, halide anions and small organic molecules.[1,3] Host-guest assemblies are apt to form if the components are compatible due to the favorable interactions upon complexation.

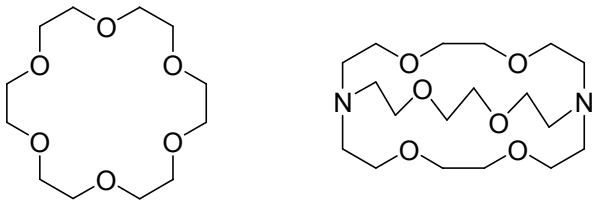

1.1 **1.2**

Figure 1.3 *– Examples of a crown-ether (**1.1**) and a cryptand (**1.2**).*

Shown in Figure 1.3 are two examples of host molecules. [18]Crown-6 (**1.1**) is a two-dimensional cyclic molecule, the right size to host a potassium cation in its central cavity.[3] This size complementarity ensures that **1.1** can extract potassium cations from mixtures, as the [$K^+ \supset$**1.1**] host-guest assembly is the most thermodynamically stable complex that can be formed. Compound **1.1** will complex with larger or smaller cations, however the interactions between host and guest will not be maximized. If the crown ether is decreased in size to [15]crown-5 the cavity becomes the ideal size to host sodium ions instead, or if the ring is enlarged to [21]crown-7 it becomes complementary to the larger cesium cation.[3] Cryptand **1.2** is a three dimensional molecule which is also the right size to host a potassium cation.[1] Unlike **1.1**, **1.2** is now a cage-like molecule, and encapsulates the potassium ion in its central cavity. It is also able to discriminate against guests which are too large or too small for its central cavity, a process which is sometimes termed spherical recognition.[1]

Host-guest structures have been developed that are much more elaborate than the two examples shown. Many can encapsulate multiple guests, through a range of different supramolecular interactions.[1] As mentioned, host molecules can be used to separate out a single component from a mixture. For another example, spherical cryptands can be

used for chiral discrimination of CHFClBr.[1] Another class of host molecules, the carcerands, completely encapsulate and imprison their guest molecule such that it can not escape even at high temperatures.[1] Carcerands can be used for the generation of highly reactive species, such as cyclobutadiene, inside the central cavity.[1,7]

Metallosupramolecular chemistry

A subset of supramolecular chemistry focuses on the construction of supramolecular assemblies using metal atoms and ligands as the primary building blocks and coordination bonds as the 'glue' that holds these formations together. The strength and lability of coordination bonds depends greatly on the metal atom and ligand used, capable of spanning the range between supramolecular interactions and covalent bonds.[1] When a compatible choice of metal atom and ligand is utilized, the coordination bonds formed during reaction are weaker than covalent bonds and labile enough to allow a one-pot spontaneous self-assembly process to take place to produce the thermodynamic product often in quantitative yield. Coordination bonds are stronger and take precedence over the supramolecular interactions listed in Table 1.1, which then become stabilising or secondary interactions in the final structure. However these secondary interactions can still have a powerful influence on the structure that forms.[8]

The addition of metal atoms into supramolecular structures has opened up a huge new area of chemistry. A fantastic range of structures have been constructed incorporating metal atoms, including frameworks, polygons, cages, catenates, knots, rotaxanes, dendrimers and helicates.[1,9,10] Not only do metal atoms act as effective and often predictable building blocks and orientation centres for the formation of these structures, but possess properties that are incorporated in the final structure such as electrochemical, photophysical, spectroscopic, magnetic and reactivity properties.[1,9,10] This has resulted in practical metallosupramolecular structures that can be developed towards a large variety of applications including functional molecular machines.[11-13]

Self-assembly takes place when pre-programmed components are capable of recognising each other and organising into a single structure dependent on the information originally encoded into the components.[2] For the metal atom component, one of the most important pieces of programmed information is the metal atom lability,

for if this is low kinetic products may be obtained from the reaction as the error-checking self-assembly process is not able to complete before competing processes in the system take over, such as precipitation or crystallisation. The other important piece of information encoded into the metal atom is its preferred geometry. This, along with lability, is controlled by the choice of metal atom for the self-assembly process. A summary of common metal atom geometries is shown in Figure 1.3.

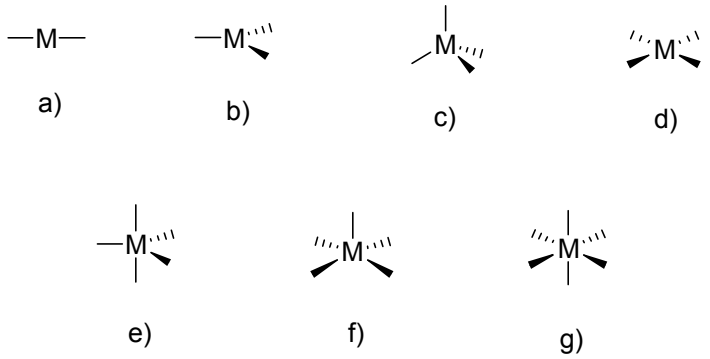

Figure 1.3 *– Examples of common metal atom geometries.*

Silver(I) is a d^{10} metal, flexible in its choice of coordination numbers and geometries, therefore often choosing to bind smaller numbers of ligands in geometries that maximise the space between the ligands. Linear and trigonal planar two- and three-coordination geometries are common for silver(I), as shown in a) and b) in Figure 1.3. For similar reasons, a four coordinate tetrahedral geometry c) is common for copper(I), allowing maximum spacing of the coordinated ligands, while d^8 metal atom palladium(II) prefers four coordinate square planar geometry d) due to its different electron configuration. Copper(II) is another reasonably flexible metal atom, capable of residing in any geometry from d) to g) in Figure 1.3, but often preferring the five coordinate geometries trigonal bipyramidal e) or square pyramidal f). It is common for copper(II) to display an intermediate five-coordinate geometry between e) and f), so definitions such as τ have been used to describe the amount of distortion around the metal centre.[14] Six-coordinate octahedral geometry g) is the most commonly preferred overall, with metals such as iron(II), nickel(II), cobalt(II), zinc(II) and cadmium(II) often displaying this coordination mode. However cobalt(II) and zinc(II) can also adopt a four coordinate tetrahedral geometry c) and nickel(II), another d^8 metal, can also obtain four coordinate square planar geometry d). Geometries other than those shown in Figure 1.3 are possible, most often displayed by large metal atoms,

especially the rare earth elements, such as lanthanum(III), which are capable of very high coordination numbers.

The choice of anion in the metal salt can have a profound effect on the metallosupramolecular structure formed (unless the ligand itself is anionic and the charges balance). Sometimes a structure will be formed with the original anion, and then the structure is precipitated or crystallised with an alternative anion, but usually the original anion from the metal salt is incorporated into the final structure. Some anions have a tendency not to coordinate to the metal atom, such as tetrafluoroborate, hexafluorophosphate, and sometimes triflate or perchlorate. This allows maximum coordination sites for other ligands on the metal atom. However it can be difficult to obtain suitable crystals for X-ray crystallography with non-coordinating anions, as the anions need to be incorporated into appropriately sized gaps in the crystal lattice and held in place by sufficient supramolecular interactions; as a consequence, non-coordinated anions are often disordered in a crystal structure. Anions with a tendency to coordinate, such as halides, nitrates, sulfates and acetates, occupy coordination sites on the metal atom. This coordination is often uncontrollable as it is hard to predict how many and which sites will be hindered from ligand coordination as some anions are also capable of chelating. These anions are also capable of bridging metal atoms, especially in the case of copper(I) iodide which is capable of forming clusters of variable nuclearity, increasing the number of potential structures which the system may produce and lessening the control the scientist has over the system. However it is possible to restrict which coordination sites on the metal atom are available for coordination by attaching a strongly chelating group to the metal atom before reaction, such as ethylenediamine (en) on a square-planar metal centre[15] or [9]aneS_3 on an octahedral metal atom.[16,17]

Nitrogen-containing heterocyclic ligands

Nitrogen-containing heterocycles are divided into two groups, azines and azoles. The π-deficient azines are six-membered aromatic rings capable of coordinating to metal atoms through the nitrogen atom, such as pyridine or quinoline. Azines bind strongly to metal atoms due to π-acceptor orbitals on the heterocycle that allow a degree of back-

bonding from the metal atom. The π-excessive azoles are five-membered aromatic rings capable of coordinating to a metal atom through a nitrogen atom, such as pyrazole, which also bind strongly to metal centres upon deprotonation due to their anionic nature.[4,18,19]

On their own, pyridines and pyrazoles are not very good ligands for use in metallosupramolecular chemistry as they can only bond to a single metal atom. However these, and other nitrogen-containing heterocycles, can be incorporated as donor groups into a larger molecule, thus creating a ligand that is capable of bridging two or more metal atoms and therefore capable of acting as a synthon for metallosupramolecular chemistry.

A ligand designed for the construction of metallosupramolecular architectures usually consists of three components: a core, which is often a single atom or an aromatic ring from which the arms of the ligand diverge; spacer groups, which extend the ligand arms away from the core; and donor groups, which terminate the ligand arms and allow the ligand to coordinate to the metal atom. Donor groups can be single atoms, electron-rich alkenes or heterocycles; in short, anything that is capable of bonding to a metal atom. In this research only nitrogen-containing heterocycles are used, so the discussion concentrates on these. If heterocycles are used, the position of the donor atom in relation to the ligand can have a profound effect on the structures formed. Furthermore, donor sites may contain multiple donor atoms designed as a binding domain to chelate to a single metal atom to form more stable complexes.

Spacer groups determine the overall size of the ligand. Spacer groups can be rigid aromatic rings or alkyne groups, or flexible amide linkers or alkyl chains. By combining a rigid ligand with a metal atom of predictable geometry in the presence of a non-coordinating anion and a non-coordinating solvent, the chemist is exerting a large amount of control over the system and decreasing the number of possible products that can be obtained from the reaction. However ligands incorporating a degree of flexibility can orient in multiple conformations, immediately increasing the number of possible products that can form. A flexible ligand may be able to choose whether it chelates to a single metal atom or bridges several. Incorporating flexibility into a ligand creates an exciting and interesting synthon that is less predictable than its rigid counterparts. The

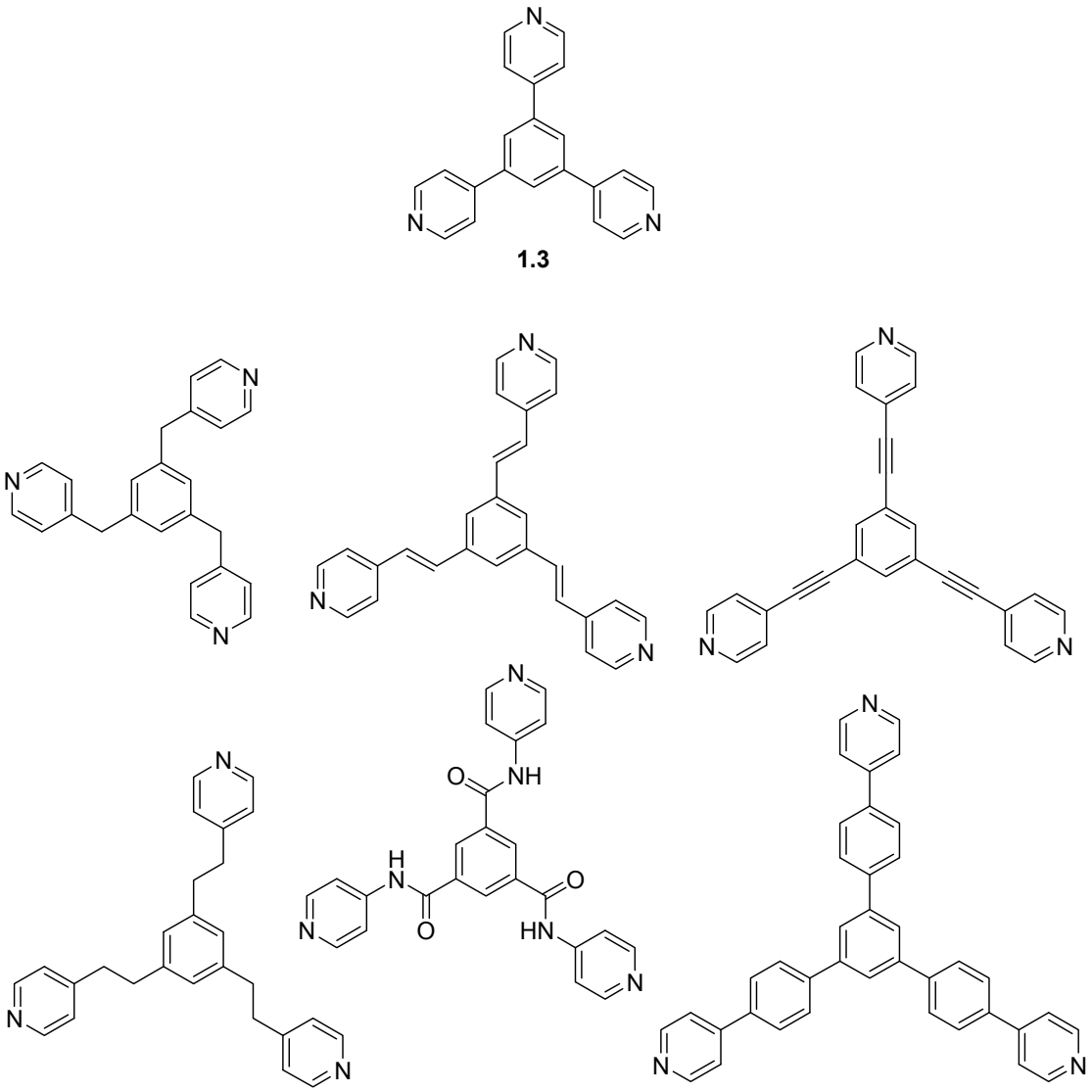

1.3

Figure 1.4 *– A series of ligands based on* ***1.3****, differing only by the spacer groups joining the pyridine donor groups to the central benzene core.*

design of ligands for metallosupramolecular chemistry is limited only by the imagination of the designing chemist.

1,3,5-Tri(4-pyridyl)benzene (**1.3**)[20,21] is shown in Figure 1.4. Ligand **1.3** is a three-armed bridging ligand based on a benzene core. The 4-pyridyl heterocyclic donor groups are linked directly to the benzene core by a 1,3,5-subsititution around the ring. The nitrogen donor atoms point directly out from the ligand core so **1.3** is capable of bridging up to three metal atoms. Also shown in Figure 1.4 are ligands which are variations on **1.3**,[20,22-26] all of which are still three-armed bridging ligands based on a benzene core, with pyridine donor groups with nitrogens in the 4-position. However these ligands contain different spacer groups which extend the pyridine rings further

away from the central core of the ligand. Some of the spacer groups are rigid,[20,23] and some are flexible.[22,24-26] Figure 1.4 shows how the size and the overall nature of the ligand can change quite dramatically with only small alterations in ligand design.

Coordination polymers

Some very basic pictorial representations of the classes of coordination polymers are shown in Figure 1.5. The purple boxes represent a linear bridging ligand with two divergent binding sites, such as 4,4'-bipyridine, capable of coordinating two metal atoms. In Figure 1.5 a), the blue sphere represents a metal atom that is binding two ligands with a linear geometry. This could represent a two-coordinative silver(I) atom, a trans-bridged palladium(II) square planar metal atom with chloride anions occupying the ancillary sites, or even an octahedral metal atom with anions or solvent molecules occupying the ancillary binding sites. The chain propagates in only one direction.

If the metal atom has a square planar geometry, like palladium(II), and is used with non-coordinating anions, or if the metal atom has an octahedral geometry and bonds two monodentate anions or solvent molecules axially, the components may self-assemble into a two-dimensional polymer as represented by Figure 1.5 b). Now each metal atom binds four different ligands. The polymer propagates in two dimensions, forming a sheet. This sheet would be defined as a (4,4) net, as it contains four four-connector nodes (the metal atoms) in each circuit.

If the metal atom prefers an octahedral geometry and is used with a non-coordinating anion, it is possible that the product will be a three-dimensional polymer, as shown in diagram c). Each metal atom now binds six ligands, and the polymer propagates in three dimensions, forming a framework.

Figure 1.5 demonstrates how the dimensionality of a structure can be altered by the choice of metal atom. In this example a rigid bridging ligand is used, so the dimensionality is limited to the metal atom. If a three or four-armed ligand is used, the ligand contributes more to the dimensionality of the structure, acting as a node itself. So variation of both the ligand, the metal ion, and other conditions of the reaction can

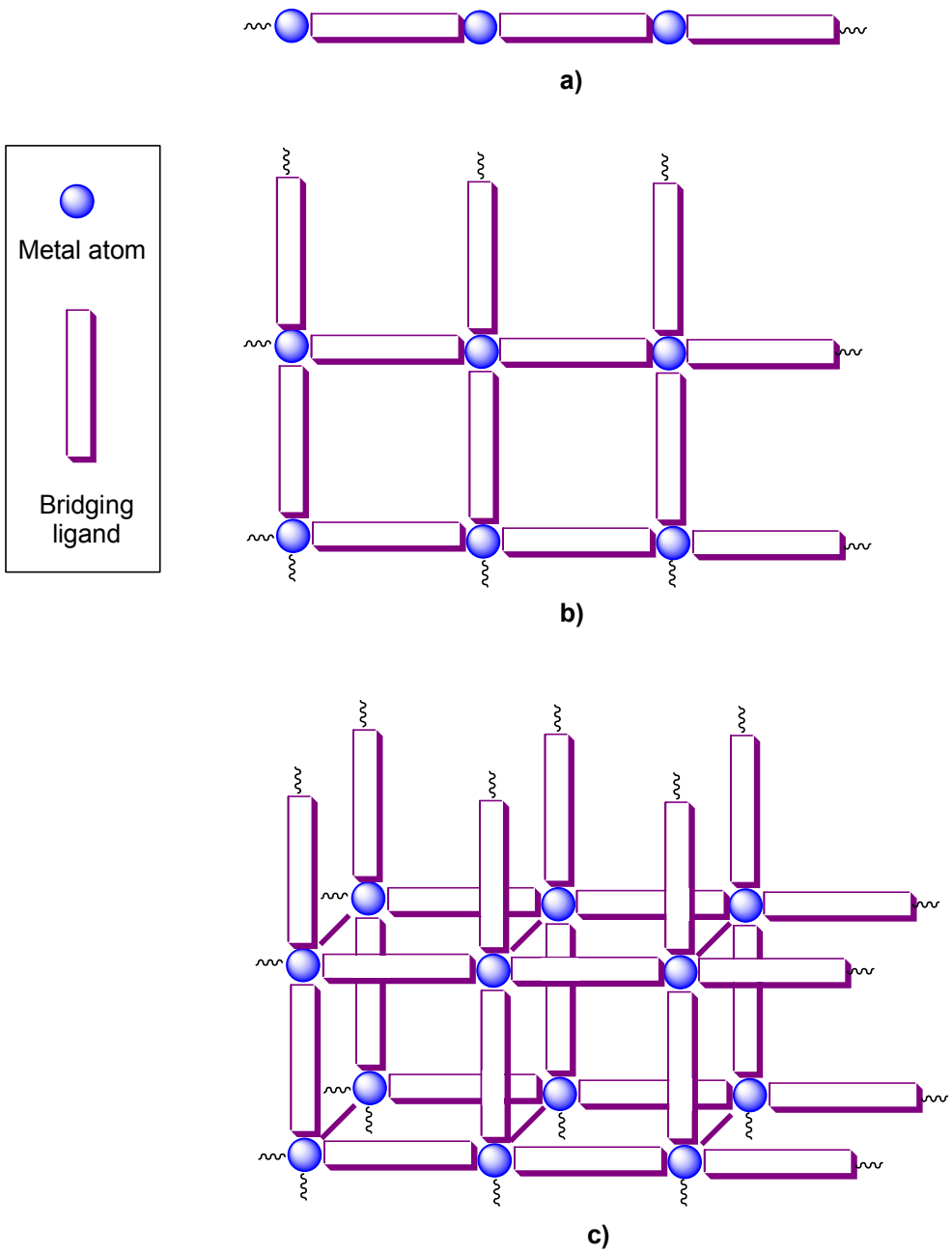

Figure 1.5 *– Schematic diagrams of* ***a)*** *one-* ***b)*** *two- and* ***c)*** *three-dimensional coordination polymers.*

produce many different polymeric products. It is not uncommon for polymers with large circuits to crystallise as multiple strands that interpenetrate through each other. An enormous range of coordination polymers of differing topology have been identified and new examples are still being discovered.[27-29]

Coordination polymers have been investigated for many possible applications. Three-dimensional frameworks are receiving a lot of attention in the field of host-guest chemistry as the channels through the framework can host ions, solvate molecules and

other small molecules.[30] These polymers can be used to separate out compounds from mixtures, acting as artificial zeolites, and for storage of gaseous molecules such as hydrogen.[30-35] Coordination polymers have also been studied for their use in such areas as catalysis, chemical sensing, magnetism, conductors, non-linear optics, and ferroelectrics.[30,32-42]

Polygons

Metallosupramolecular chemists are often more interested in the formation of discrete structures over polymeric products. The self-assembly of multiple components into a complex, single structure is a highly appealing strategy, considering the costly alternative of stepwise organic synthesis and corresponding low yields.

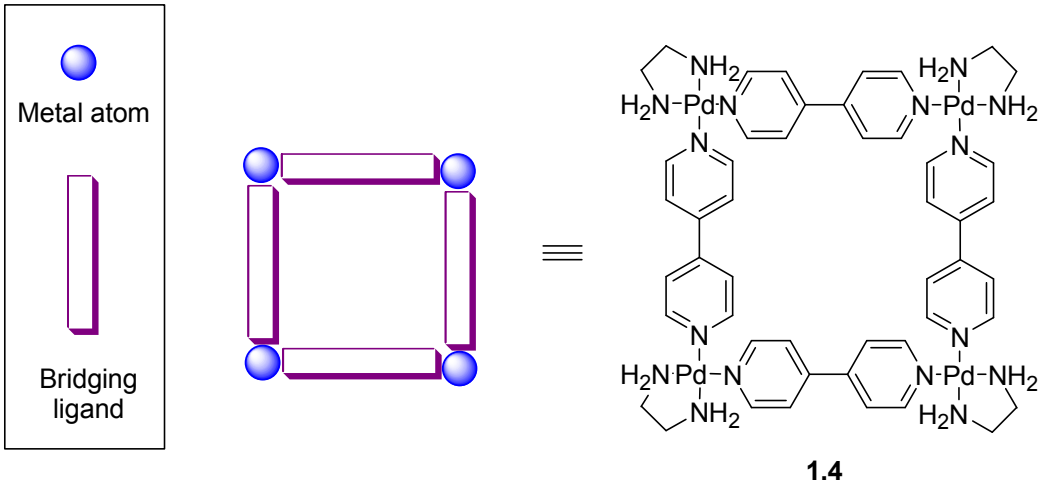

Figure 1.6 *– The self-assembly of molecular square* ***1.4****.*

Consider the formation of a molecular square. Shown in Figure 1.6 is the conceptual breakdown of a square into four 90° angular components (the metal atoms) and four linear components (the bridging ligands). This strategy has been applied towards the formation of molecular square **1.4** from eight components in quantitative yield.[43] Square **1.4** uses 4,4'-bipyridine as a linear bridging ligand to create the sides of the square, and cis-protected square planar palladium(II) as the 90° angular component to create the corners of the square. The square is held together by coordination bonds, and self-assembles due to the tendency of the components to recognise and bond to each other. The rigidity of the bridging ligand and the cis-protected metal atom limit the possible

number of products that may form. Discrete structures such as **1.4** are favoured in metallosupramolecular systems by thermodynamics (greater entropy and enthalpy) while polymers are often the kinetic product.

There are also other ways to construct a simple square. An alternative strategy is shown in Figure 1.7, where the metal atoms are used as linear bridging components to form the sides of the square, and a ligand is used as the angular component to form the corners. It is very difficult to obtain a 90° angle using organic chemistry, so most ligands only approximate this angle. This methodology was used to construct molecular square **1.5**,[44] where silver atoms linearly bridge pyrimidine ligands to form a square-like structure.

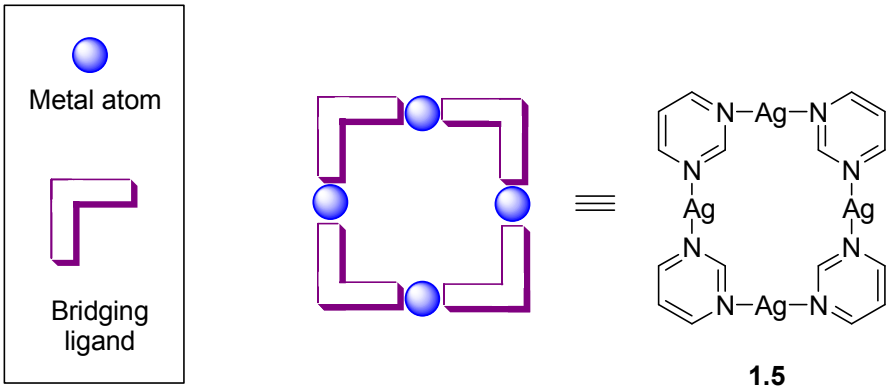

***Figure 1.7** – An alternative construction strategy to form molecular square **1.5**.*

This same methodology has been used to construct a vast range of two-dimensional polygons of varying shapes and sizes.[45-48] Polygons of large enough size contain a central cavity capable of hosting a guest molecule. Applications of metallosupramolecular polygons include molecular recognition, enantioselective sensing, photoluminescence, electrochemical sensing and catalysis.[45-48]

Molecular cages

Extension of the concept for the construction of polygons from two- to three-dimensions leads to the formation of polyhedra and molecular cages. This can be achieved by increasing the dimensionality of the metal atom by using a metal capable of bonding to more ligands, or by increasing the dimensionality of the ligand by adding extra donor groups. Examples of both these cases are shown in Figure 1.8.[17,49]

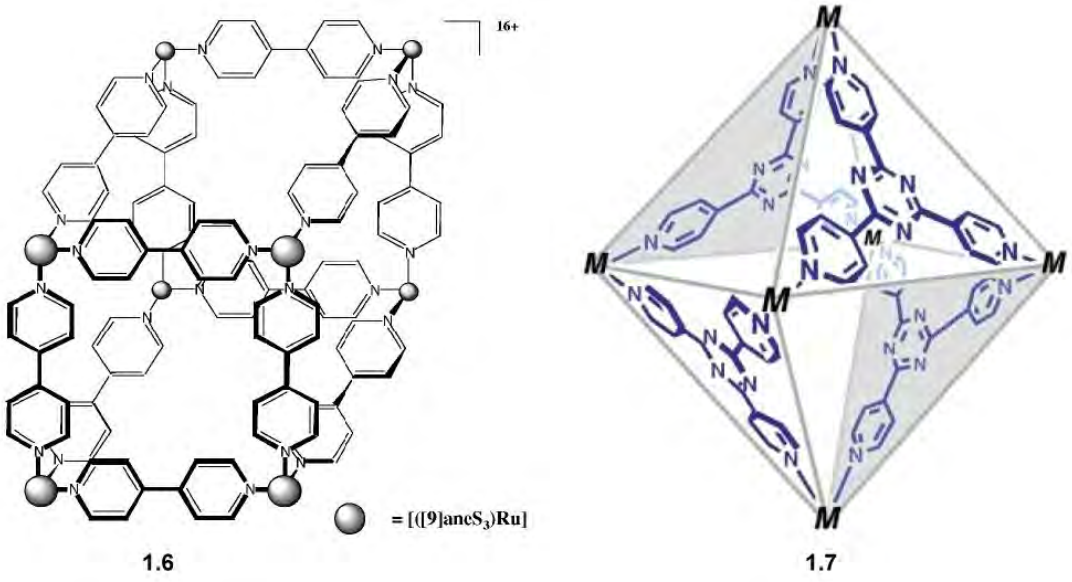

Figure 1.8 *– Two examples of three-dimensional polyhedra, an M_8L_{12} cube[17] (**1.6**) and an M_6L_4 octahedron[49] (**1.7**).*

Molecular cube **1.6**[17] in Figure 1.8 is a three-dimensional analogue of **1.4**, with the cis-protected palladium(II) metal atoms replaced by facially-protected ruthenium(II) metal atoms, the extra coordination site allowing the structure to extend into three dimensions. Molecular octahedron **1.7**[49,50] is also related to **1.4**, as the metal atom used is the same cis-protected palladium(II) salt. However the dimensionality of the structure has been increased by altering the ligand, which now consists of three 4-pyridyl groups radiating out from a central core to bridge three metal atoms, to allow the formation of this three-dimensional structure.

A cage is a polyhedron capable of encapsulating a smaller molecule, such as **1.6** and **1.7**. Many different varieties of molecular cages and cage-like discrete structures have been constructed using metallosupramolecular chemistry.[46-48,51-54] Cages of M_6L_4 stoichiometry like **1.7** are relatively common amongst these structures.[50,55-59] Three more examples of coordination cages are shown in Figure 1.9.[60-62]

Cage **1.8**[61] consists of two ligands linked together by three metal atoms, so is classified as a M_3L_2 cage. These types of small cages are relatively common.[63-68] As shown in Figure 1.9, cage **1.8** contains a central cavity large enough to host a guest molecule, in this case a CuI_3^{2-} anion. Also shown in Figure 1.9 are two views of a M_4L_6 tetrahedral

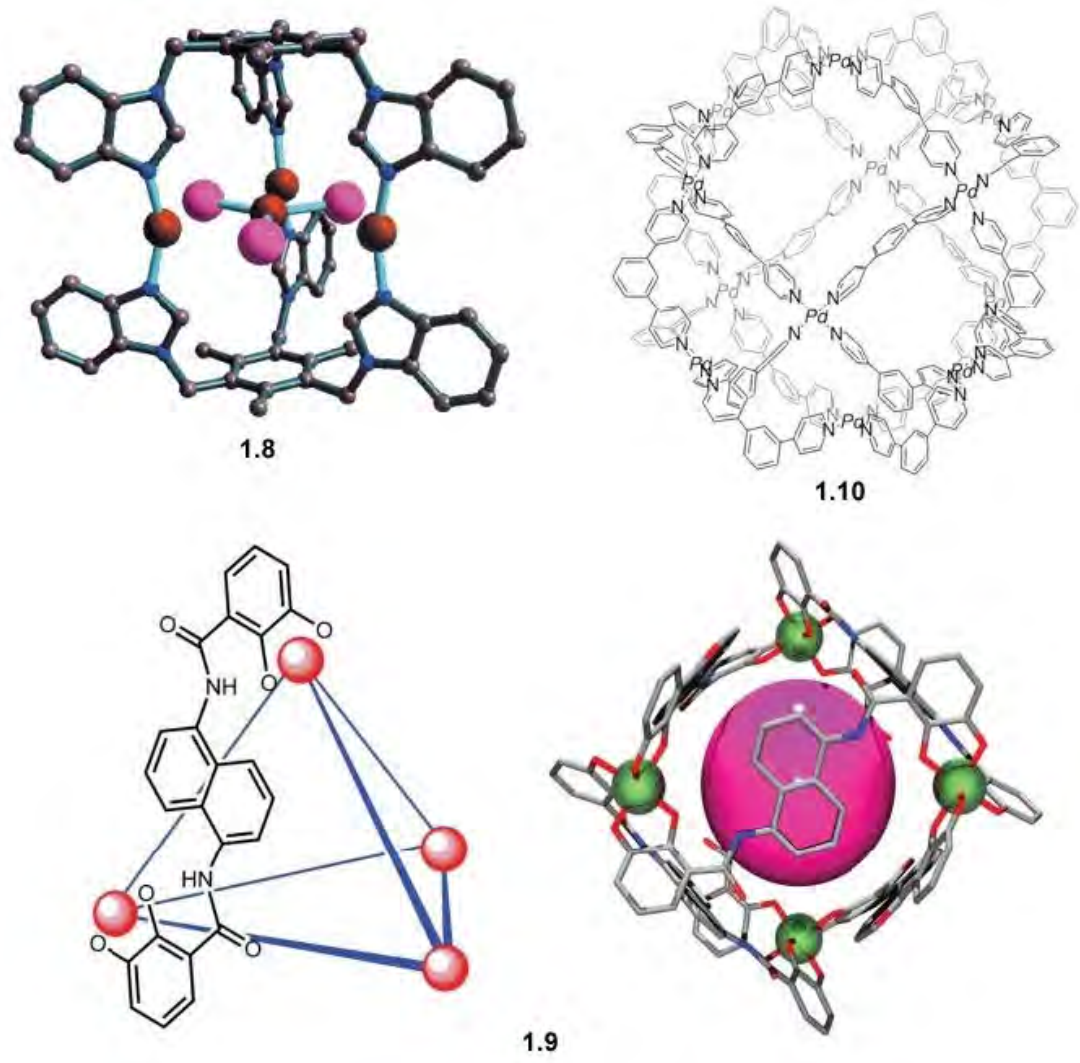

Figure 1.9 *– Examples of an M_3L_2 cage (**1.8**),[60] two views of an M_4L_6 cage (**1.9**),[61] and an $M_{12}L_{24}$ cage (**2.0**).[62]*

cage **1.9**.[61] This cage is also large enough to host a guest molecule inside its central cavity, and are relatively common.[69-75] The most common topologies of molecular cages are M_3L_2 (like **1.8**), M_4L_6 tetrahedral (like **1.9**) and M_6L_4 octahedral (like **1.7**). However many other examples exist, such as cuboctahedral $M_{12}L_{24}$ cage **1.10**.[62] Other unusual examples include M_6L_2,[8,76] M_6L_8,[77,78] M_8L_4,[79] $M_{12}L_8$,[80] $M_{15}L_6$,[81] $M_{18}L_6$[82] and $M_{12}L_{18}$[83] cages.

Strategies have been developed to encourage the formation of cage-like structures over other assemblies by ligand design.[84] Ligand rigidity or conformational restriction is recommended to reduce the likelihood of forming alternative products of lower stoichiometry which are favored by entropy.[84] Two general approaches to cage

formation exist. In both approaches the metal atoms are located at the vertices of the cage or polyhedra. Face-directed assembly links the metal atoms together by bridging ligands acting as flat panels to assemble the faces of the polyhedra, while edge-directed assembly uses the ligands as linear bridges to define the edges of the polyhedra.[51,79,84,85]

Molecular cages are interesting not just for their symmetrical and fascinating structures, but for the host-guest chemistry they provide, and the discovery that these cages can act as molecular flasks and facilitate reactions upon the encapsulated guest molecules.

> *"Unusual physical behavior is emerging from the closely-packed guests that would not occur under normal conditions. The design, synthesis and beautiful structures of these cages would be remarkable enough; but their additional applications in substantially modifying the reactivity of small compounds by confinement make them some of the most exciting compounds currently being studied."*
>
> *Michael D. Ward.*[86]

Like organic analogues such as **1.2**, the cavity size in metallosupramolecular cages is fixed, so they can be used to selectively encapsulate the preferred guest molecules from mixtures.[8,87-92] But most importantly they can be used as molecular flasks. Cages can be used to stabilise and characterise reactive intermediates,[49,88,93-96] to form single isomers of usually non-selective reactions,[49,88,93,97-100] and they can catalyse reactions that would not take place under normal conditions,[49,88,101,102] which are triggered by the closely-packed relationship between host and guest.

Thesis coverage

Molecular cages are fascinating and appealing metallosupramolecular target molecules, due to both their aesthetic structure and potential applications. Therefore, this project is based on the synthesis and study of bridging heterocyclic ligands that may potentially lead to the formation of molecular cages upon reaction with appropriate metal salts. Due to the scope of work that has already been done in this area, it was decided to incorporate a degree of flexibility into the ligands synthesised, as many molecular cages have been constructed from rigid ligands. This increases the range of products that the self-assembly process may produce.

Characterisation of the ligands was undertaken by ^{1}H NMR, mass spectrometry, elemental analysis and X-ray crystallography when suitable crystals were obtained. Characterisation of the complexes relied on X-ray crystallography. If crystals suitable for X-ray analysis could not be grown, some of the complexes were analysed by ^{1}H NMR, elemental analysis and mass spectrometry. Unfortunately, none of the complexes were found to be stable upon ionization for mass spectrometry, so only fragments of the original complex could be identified at best. Often ^{1}H NMR and elemental analysis results were ambiguous, so full characterisation of many complexes was not possible using just these techniques.

Chapter Two concentrates on the synthesis and coordination chemistry of three two-armed bridging ligands based on a 1,3,5-triethylbenzene core. The ligands vary by the heterocyclic donor groups they use to bind to the metal atom. Many complexes were prepared and crystallised from these ligands, and will be discussed in detail.

Chapters Three and Four concentrate on the synthesis and coordination chemistry of a wide range of three-armed bridging ligands based on a variety of different cores. Chapter Three focuses on ligands based on 1,3,5-trialkyl/trimethoxybenzene cores, while Chapter Four focuses on other three-armed ligands prepared during this research.

Chapter Five looks at complexes derived from decomposition processes, which occur when particular ligands from earlier chapters break apart when reacted with certain metal salts. The rational synthesis of similar complexes are also described.

During the course of the research covered in this thesis, in total twenty-five heterocyclic bridging ligands were synthesised, nineteen of which were previously unreported. Five of these ligands were characterised by X-ray crystallography. Fifty-one crystal structures of complexes derived from these ligands will be discussed.

Chapter Two

The 1,3-disubstituted-2,4,6-triethylbenzene ligands

Chapter Two

The 1,3-disubstituted-2,4,6-triethylbenzene ligands

Introduction

To construct metallosupramolecular assemblies the ligand component must be able to bridge multiple metal centres to join separate entities into a single structure. Therefore the simplest ligands contain two binding domains to link together two metal atoms. Some basic examples of ligands which are capable of bridging two metal atoms are shown in Figure 2.1.[103-106]

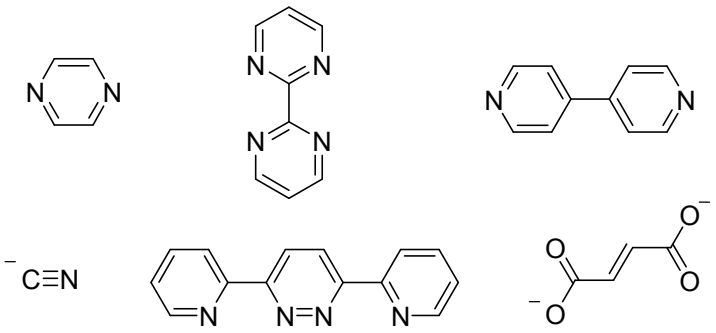

Figure 2.1 *– A few examples of ligands capable of bridging two metal atoms.*

Ligand design is often retrosynthetic, where the concept of a metallosupramolecular assembly inspires the scientist to envisage components which may be capable of spontaneously forming the desired product upon combination. Many factors need to be taken into consideration, including metal atom geometry, reactivity, and affinity for the donor atoms chosen for the ligand, the effect of anions, compatible solvent choice and ease of crystallisation, as well as other thermodynamic and kinetic factors which may influence which of the possible products could actually be observed in the system. But by far the most important factor is the restraints put on the system by the design of the ligand. A good ligand may be rigid, with the donor atoms locked into a suitable position to form the desired component. Alternatively, a good ligand may be flexible, with the ability to form many different complexes, the formation of each possibly dependent on the choice of metal salt or the adjustment of other variables in the system. The flexibility may also be inherent to the desired complex, as the ligand may be designed

to favour a particular conformation. It is even possible that the flexibility of the ligand may add properties to the final complex.

To create a particular structure, a building block is needed which has joints at the desired angles. A challenge when designing ligands is how to incorporate donor atoms at the correct positions to create a suitable building block. Often the easiest way to approach this is to increase the size of the ligand and attach multiple arms to a core. The ligand arms will often terminate in a donor atom that is capable of binding to a metal centre, or terminate with a heterocycle, which is capable of binding *via* the heteroatom. Ligand cores are often aromatic, as multiple substitutions around the ring allow for suitable spacing of the arms, however a great variety of non-aromatic ligand cores have also been exploited.

Listed in Figure 2.2 are examples of two-armed bridging ligands based on aromatic cores. These ligands are given as examples as all of these have been shown to form molecular cages or cage-like assemblies upon reaction with metal salts under appropriate conditions.[62,69,73,75,83,87,107]

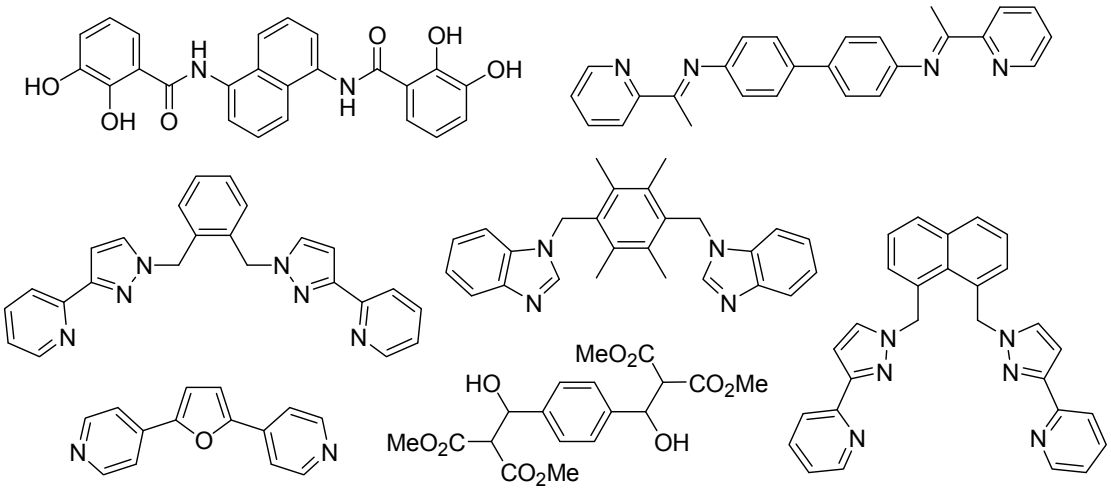

Figure 2.2 *– Two-armed ligands capable of forming cage-like structures.*

The majority of the cage complexes formed by the ligands in Figure 2.2 are of the same topology, M_4L_6 tetrahedral cages.[69,73,75,87] A schematic representation of an M_4L_6 tetrahedral cage is shown in Figure 2.3. These metallosupramolecular assemblies consist of four metal atoms at the vertices of a tetrahedron, each coordinating to three ligands, each ligand bridging two metal centres. Often an anion or solvent molecule is encapsulated inside the tetrahedron. In some cases, experiments have shown that this

guest molecule may be exchanged,[61] and even that the cage can act as a molecular flask and facilitate reactions upon the guest molecule.[88]

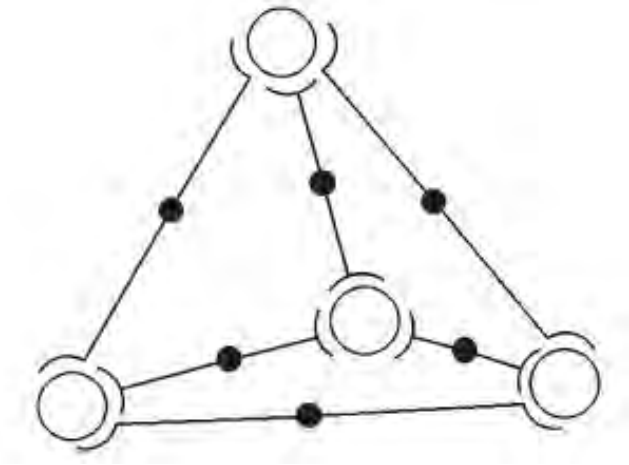

Figure 2.3 *- Schematic diagram of an M_4L_6 tetrahedral cage.*[70]

Therefore it is logical that a research project focused on the formation of molecular cages would investigate two-armed ligands that may possibly form M_4L_6 assemblies of this type.

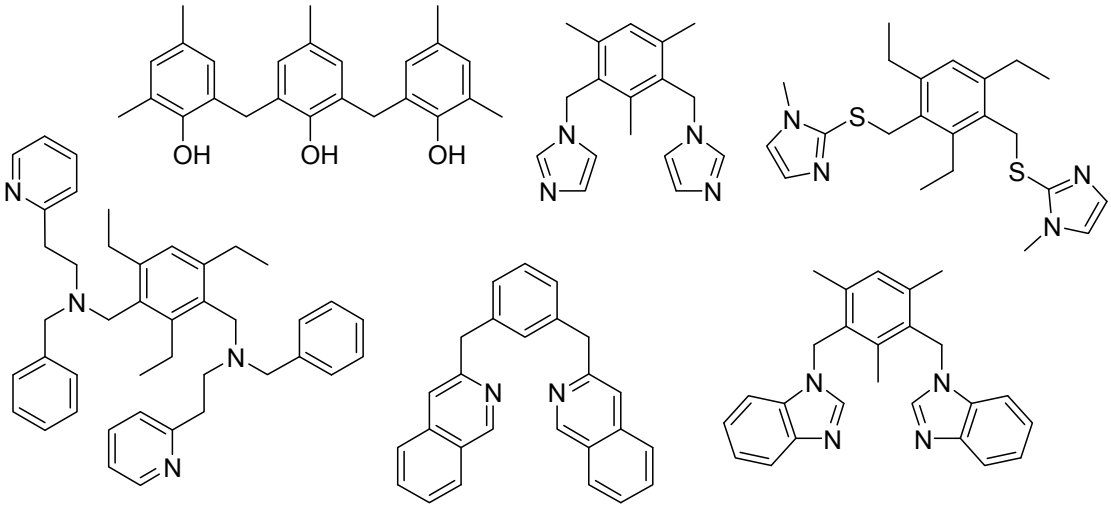

Figure 2.4 *– Two-armed ligands based on meta-substitution around a benzene ring.*

Two-armed ligands based on a 1,3-disubstitution pattern around a benzene ring are not uncommon. Figure 2.4 shows a few examples of ligands[107-110] (or potential ligands[111,112]) with this connectivity. Again, a couple of the above are known to form cage-like structures.[107,108] The 1,3-disubstitution is appealing as it creates a building

block with an angular shape. Possibly this kind of building block could have a higher preference for forming discrete (even possibly cage-like) assemblies over coordination polymers. The flexibility incorporated by attaching the binding arm to the aromatic core with a methylene group will allow the ligand to twist to different conformations, and allow adjustment of the position of the donor atoms to suit the geometry of the metal atom.

1,3-Di(bromomethyl)-2,4,6-triethylbenzene (2.2)

Other factors to be taken into account during ligand design are the ease of synthesis and the availability of starting materials. Triethylbenzene (**2.1)** is a readily available starting material, and is easily bromomethylated in the one and three positions in one step to form 1,3-di(bromomethyl)-2,4,6-triethylbenzene (**2.2)**, [109,113-115] as shown in Scheme 2.1. Precursor **2.2** is a common side product of the reaction to produce 1,3,5-tri(bromomethyl)-2,4,6-triethylbenzene (**2.3**),[109,113-116] and is easily isolated if the reaction conditions are not rigorous enough to add a third arm. Although often made unintentionally, **2.2** is not often used as a precursor to two-armed compounds[109,110,117] and has seemingly remained poorly characterised in the literature.

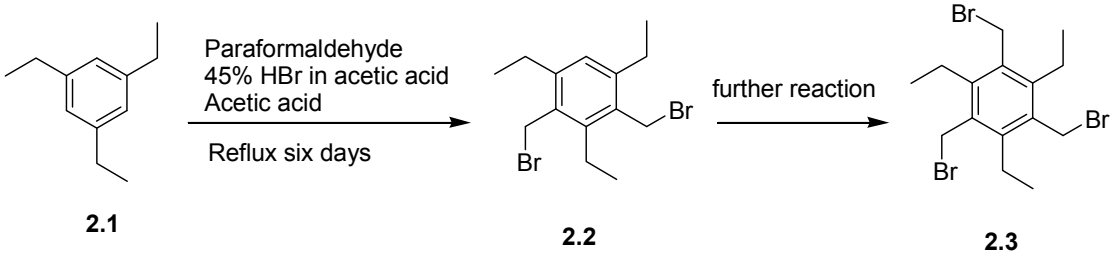

Scheme 2.1 *– The bromomethylation of 1,3,5-triethylbenzene.*

Compound **2.3** is often used as a precursor to molecules where the desired product is preorganised into an *ababab* conformation.[55,109,110,114-116,118,119] This occurs when the steric bulk around the benzene core encourages an up-down-up-down-up-down arrangement amongst the ligand arms, an alternating (a)bove-(b)elow conformation in relation to the plane of the ligand core, so all three of the substitituted arms are on one side of the benzene ring, and the three ethyl groups are on the other, as shown in Figure 2.5(A). Orienting the molecule into this conformation is useful if it is being used as a

sensor[113,115,117-120] or as a ligand where this arrangement may encourage the formation of discrete complexes such as cages.[55,109,110]

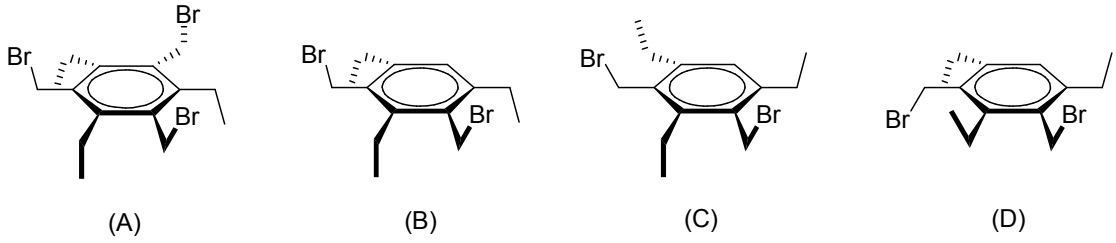

Figure 2.5 *– (A)* ***2.3*** *in a preorganised conformation, (B)* ***2.2*** *in a preorganised conformation, (C) & (D) two other possible conformations of* ***2.2****.*

However compound **2.2** does not have six arms around the benzene core, so with less steric bulk than **2.3**, it is unknown whether the ethyl groups would encourage ligands synthesised from precursor **2.2** to prefer a preorganised conformation (B) similar to **2.3**, or if the extra bulk would have negligible effect (C & D), in which case even a conformation where the binding arms are on opposite sides of the central ring might be observed (D). These conformational possibilities are shown in Figure 2.5.

1,3-Di(pyrazol-1-ylmethyl)-2,4,6-triethylbenzene (2.4)

The first ligand synthesised from precursor **2.2** is shown in Scheme 2.2. A Phase-Transfer-Catalysed (PTC) reaction substituted the bromines for pyrazoles, creating in 98% yield a two-armed ligand with two monodentate binding domains to use as a synthon in metallosupramolecular chemistry.

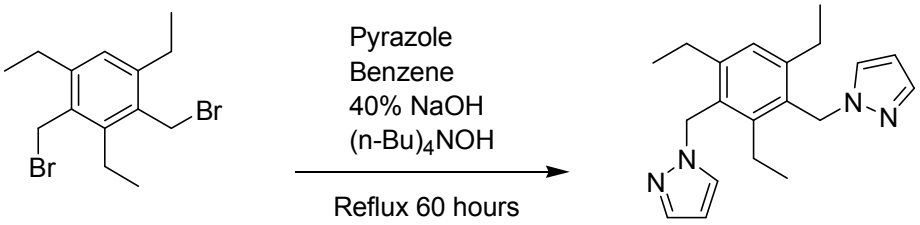

2.2 **2.4**

Scheme 2.2 *– Synthesis of ligand* ***2.4****.*

A literature search revealed that structurally similar compounds **2.5**[121] and **2.6**[122-124] have been used as ligands by other research groups. Ligand **2.5** has been shown to form

a [2+2] macrocycle in the presence of $CuBF_4$,[121] while ligand **2.6** forms one-dimensional helical polymers with $ZnCl_2$ and $CoCl_2$,[122,123] a two-dimensional sheet with $CdCl_2$,[123] and a three-dimensional network with $CuCl_2$.[124]

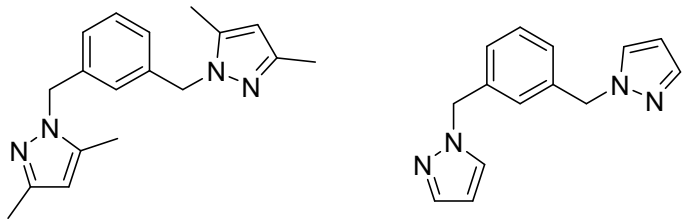

2.5 **2.6**

Figure 2.6 *– Structurally similar ligands to* ***2.4****.*

Obviously these ligands are flexible synthons that can be used to create a variety of structures. Ligand **2.4** differs due to the steric bulk and possible preorganisational effects of the ethyl groups in the 2-,4- and 6- positions around the central core. While it is possible that ligand **2.4** may form similar structures to those formed by **2.5** and **2.6**, it is likely that the difference in the central core region will lead to different structures being formed, through steric, conformational and electronic effects.

Complexes with ligand 2.4

*Crystal structure of the complex with $CoBr_2$ (**2.7**)*

The pale blue precipitate obtained from reaction of ligand **2.4** with $CoBr_2$ was crystallised by slow evaporation of an acetonitrile solution to give dark blue plates which were suitable for X-ray crystallography. The structure solved in the triclinic space group P-1 to reveal a one-dimensional coordination polymer, a section of which is shown in Figure 2.7. The asymmetric unit contains one ligand, one metal atom and two bromides, along with an acetonitrile solvate molecule. The hydrogens and solvate molecule are excluded for clarity, and the structure is grown to show the connectivity of all the atoms in the extended structure.

The cobalt atom coordinates to two bromide counterions and two pyrazole nitrogens with a tetrahedral geometry. Each cobalt binds to two bridging ligands and each ligand bridges two metal atoms. The binding arms of the ligand lie on opposite sides of the

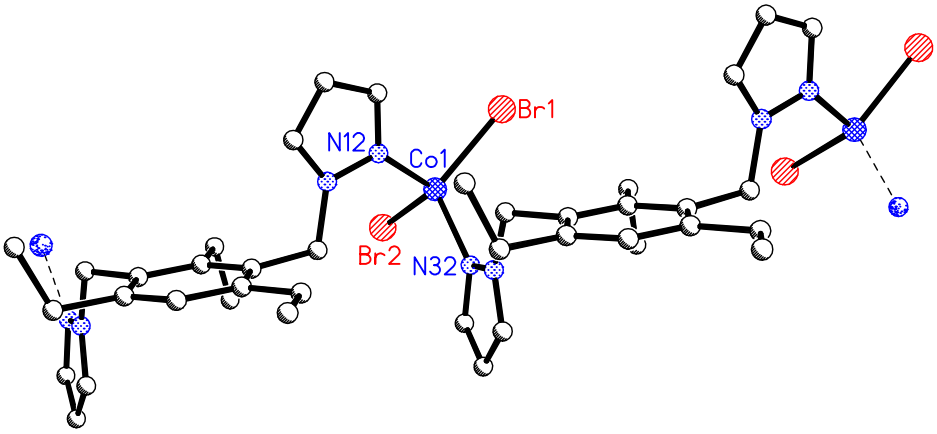

***Figure 2.7** – A section of one-dimensional polymer **2.7**. Selected bond lengths (Å) and angles (°): Co1-Br1 2.3743(4), Co1-Br2 2.3763(3), Co1-N12 2.012(2), Co1-N32 2.022(2), N12-Co1-N32 103.00(7), N12-Co1-Br1 103.95(5), N12-Co1-Br2 112.76(5), N32-Co1-Br1 118.08(5), N32-Co1-Br2 103.64(5), Br1-Co1-Br2 115.01(1).*

benzene core. The ethyl groups appear disorganised, with one pointing up, one pointing down, and one lying sideways towards the vacant position in the ring. This arrangement provides a partial *abba*- conformation around the benzene core.

The polymer propagates in one dimension, forming a straight chain. Each section is a translation from the last, with the conformation of the ligand arms accommodating the geometric constraints on the cobalt atom without the polymer deviating from its course. Complex **2.7** does not show the helicity observed in similar one-dimensional polymers formed with ligand **2.6**.

In the packing structure the benzene cores of separate chains lie facing each other, but the distance is 7.723Å, far too long for π-π stacking interactions. However the pyrazole rings of adjacent chains π-π stack which the distance between rings being 3.473Å. The closest hydrogen bonding interactions between chains are between the bromine atoms and pyrazole hydrogens of the ligand (3.070-3.097Å). The acetonitrile solvate molecule interacts with the chains of the main structure, hydrogen bonding to both Br2 (3.033Å) and the pyrazole (2.493Å).

*Crystal structure of the complex with $ZnBr_2$ (**2.8**)*

The colourless crystals produced when a solution of zinc bromide in methanol was layered over a solution of ligand **2.4** in chloroform were shown by X-ray crystallography to solve in monoclinic space group $P2_1/n$. The asymmetric unit contains two bridging ligands, two metal ions and four bromine counterions, and two and a half chloroform solvate molecules. Each ligand is bonded to two zinc atoms, but there are two independent molecules in the asymmetric unit, as shown in Figure 2.8, with the hydrogen atoms and solvate molecules omitted for clarity.

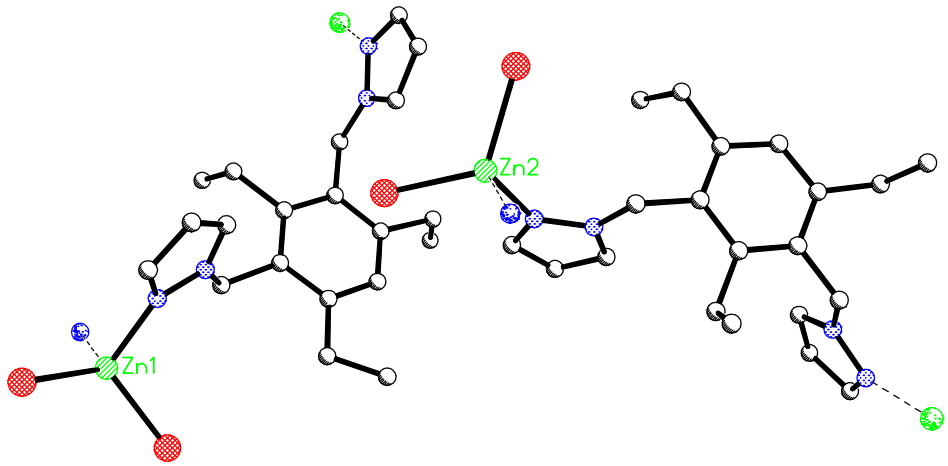

***Figure 2.8** – Asymmetric unit of **2.8**, showing the different orientations of the two independent molecules that grow into separate polymer strands.*

While the ligands are in similar conformations, they are not identical. Both ligands orient their binding arms on the same side of the benzene core. But the position of the ethyl groups vary between the two ligands. The ligand attached to Zn1 is almost in an organised conformation, with an *abab*- up-down-up-down conformation partway around the ring. However the last ethyl group lies almost sideways, filling the vacant unsubstituted position on the benzene core. The ligand attached to Zn2 lies in an *aabab* conformation, with an ethyl group beside the vacant position lying perpendicular to the plane of the benzene ring, but in the opposite direction to the expected organised conformation of *ababa*.

Chloroform solvate molecules fill the voids in the crystal lattice. Two whole solvate molecules lie in the asymmetric unit, as well as half a molecule. The carbon of the half

chloroform lies on a special position and is bonded to two chlorines also of half occupancy, and grows into a disordered chloroform when the structure is expanded.

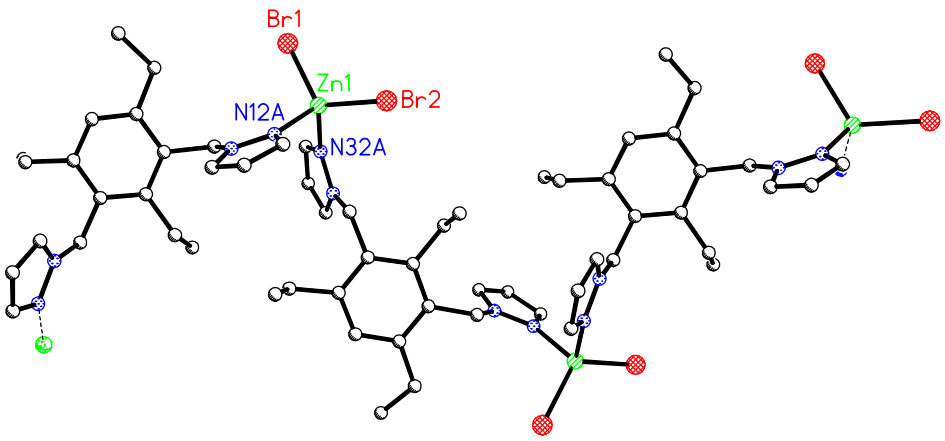

Figure 2.9 *– A section of the Zn1 polymer strand in* ***2.8****. Selected bond lengths (Å) and angles (°): Zn1-N32A 2.046(2), Zn1-N12A 2.052(3), Zn1-Br1 2.3511(5), Zn1-Br2 2.3611(5), N32A-Zn1-N12A 101.8(1), N32A-Zn1-Br1 104.96(7), N32A-Zn1-Br2 112.87(7), N12A-Zn1-Br1 111.99(7), N12A-Zn1-Br2 102.80(7), Br1-Zn1-Br2 120.93(2).*

The fragments in the asymmetric unit are sections of a one-dimensional polymer. The two independent ligand/zinc units in the asymmetric unit grow into separate independent polymer strands. A section of the polymer resulting from Zn1 is shown in Figure 2.9. The zinc atom binds two bromide counterions and two pyrazole nitrogens with a tetrahedral geometry. Each ligand bridges two metals. Both pyrazoles are on the same side of the ligand, and the ligand flips orientation between metal atoms, so each zinc is coordinated to a pyrazole above and a pyrazole below it. The overall effect is a zig-zag polymer with alternating ligand orientation.

A section of the polymer strand grown from Zn2 is shown in Figure 2.10. The two chains have an identical topology. The most obvious difference between the two strands is the different orientation of the ethyl groups, as discussed above. However there are also more subtle differences. In the two figures, Zn1 and Zn2 and the attached pyrazoles are in the same orientation, however by following the chain along the two polymers it is observed that the positioning of the other pyrazoles does vary slightly between the

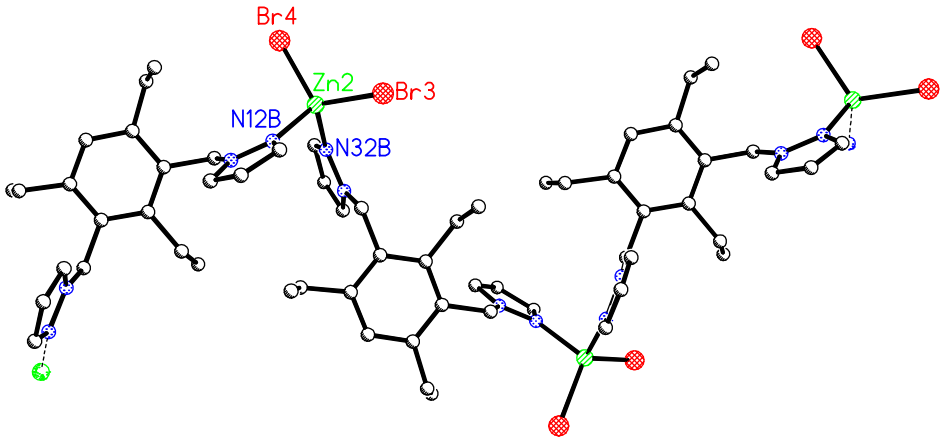

Figure 2.10 *– A section of the Zn2 polymer strand in* ***2.8****. Selected bond lengths (Å) and angles (°): Zn2-N32B 2.027(2), Zn2-N12B 2.055(2), Zn2-Br4 2.3590(4), Zn2-Br3 2.3673(4), N32B-Zn2-N12B 101.73(9), N32B-Zn2-Br4 108.87(7), N32B-Zn2-Br3 112.37(7), N12B-Zn2-Br4 112.21(7), N12B-Zn2-Br3 102.17(7), Br3-Zn2-Br4 118.15(2).*

chains. This is seen in the slight difference in bond angles between the two chains. So the different polymer chains are similar, but not identical.

In the extended structure, the chloroform solvate molecules interact extensively with the polymer strands through various hydrogen bonding interactions; however the strands do not appear to interact with each other and there does not seem to be any π-π stacking interactions between ligands of separate chains.

*Crystal structure of the complex with CuI (**2.9**)*

When ligand **2.4** in methanol was added to copper(I) iodide in acetonitrile, a white precipitate instantly forms. Overnight this precipitate crystallises as clusters of highly twinned colourless crystals. One of these crystals was selected for X-ray crystallography, and with the help of the computer programs *Cell_now*, *Saintplus*, and *Twinabs*, the crystal was shown to consist of a major twin and minor twin, and the data was processed with this taken into account to obtain a crystal structure with an impressive final R_1 value of 5.64%. The structure solved in monoclinic space group $P2_1/n$.

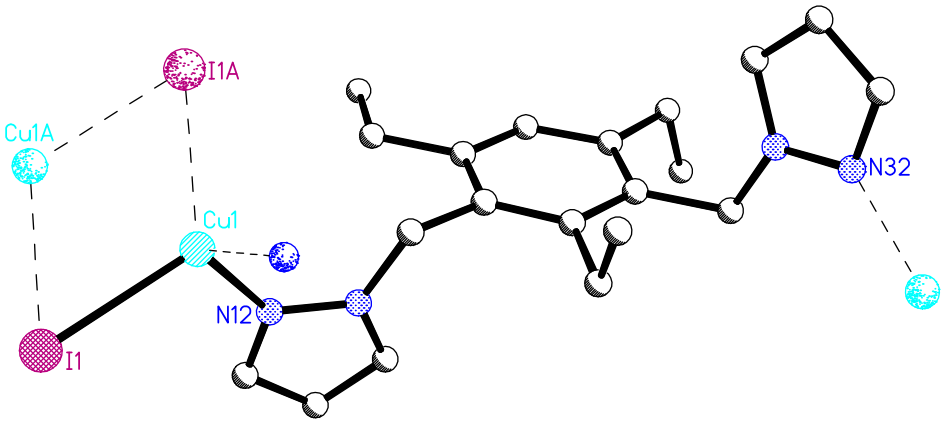

Figure 2.11 *– The asymmetric unit of* ***2.9****. Selected bond lengths (Å) and angles (°): Cu1-I1 2.620(1), Cu1-I1A 2.654(1), Cu1-N32A 2.064(6), Cu1-N12 2.069(6), Cu1-I1-Cu1A 60.40(3), I1-Cu1-I1A 119.60(3), N32A-Cu1-N12 105.9(2), N32A-Cu1-I1 110.3(2), N32A-Cu1-I1A 103.2(2), N12-Cu1-I1 105.6(2), N12-Cu1-I1A 111.5(2).*

The asymmetric unit contains one ligand, one copper and one iodine, as shown in Figure 2.11, with hydrogens removed for clarity. The pyrazole arms of the ligand lie on opposite sides of the benzene core, so the ligand is not in an organised conformation, with one ethyl group down, one up, and one lying sideways, a partial *abba*-conformation. The contents of the asymmetric unit have been expanded in Figure 2.12 to show the connectivity clearly.

The copper atom is tetrahedral, binding to two iodine atoms and two pyrazole nitrogens of separate ligands. Iodine atoms bridge two copper atoms to form a Cu_2I_2 square, a common motif for this metal salt. The copper atoms in the square are quite close together, at a distance of 2.653Å. Even though this distance is shorter than the van der Waals radius of the two atoms (2.80Å),[125] it is unlikely that this is a real bond, considering the geometric and electronic preferences of Cu(I),[126,127] however it is possible that there may be a weak interaction between the metal centres.[128,129] Each copper iodide square coordinates to four different ligands, and each ligand bridges two copper iodide squares. The resulting complex is a two-dimensional polymer. A section of the sheet is shown in Figure 2.13.

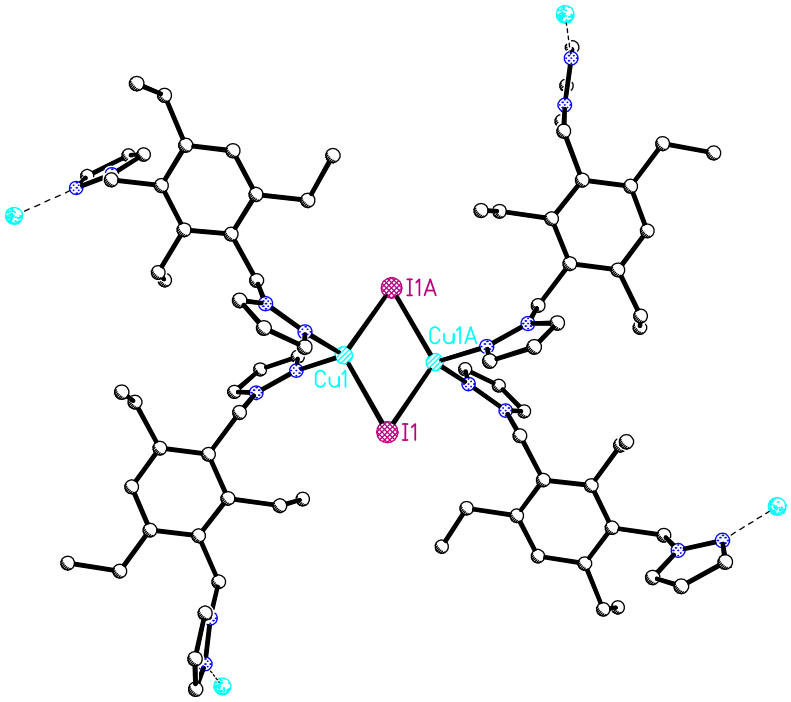

Figure 2.12 *– The bonding environment around each Cu_2I_2 square in* ***2.9****.*

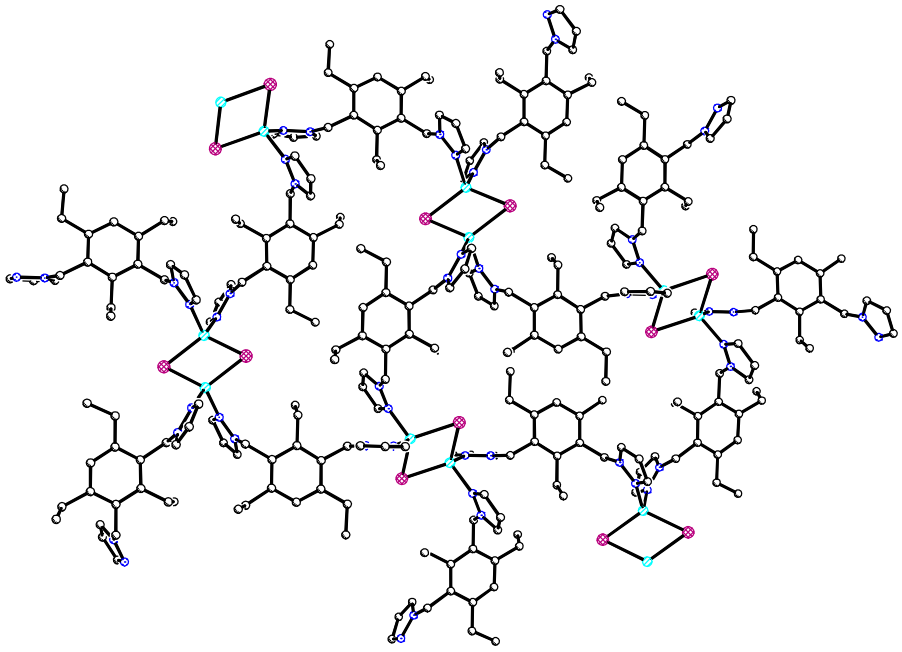

Figure 2.13 *– A section of the two-dimensional sheet* ***2.9****.*

A simplified view of the same sheet is shown in Figure 2.14. This image was created using the polymer interpretation program *Topos 4.0*, using the copper atoms as reference points to clearly show the connectivity of the sheet. If the copper iodide squares are viewed as a single moiety, each square acts as a four-connecting node. The ligands only bridge these nodes, and do not add any extra dimensionality to the structure. Therefore, there are four four-connecting nodes in each circuit, which should define the basic structure as a (4,4) net. Understandably this definition would be misleading as it suggests that each macrocycle in the net is of an equidistant size, where in reality the voids are actually rectangular in shape.

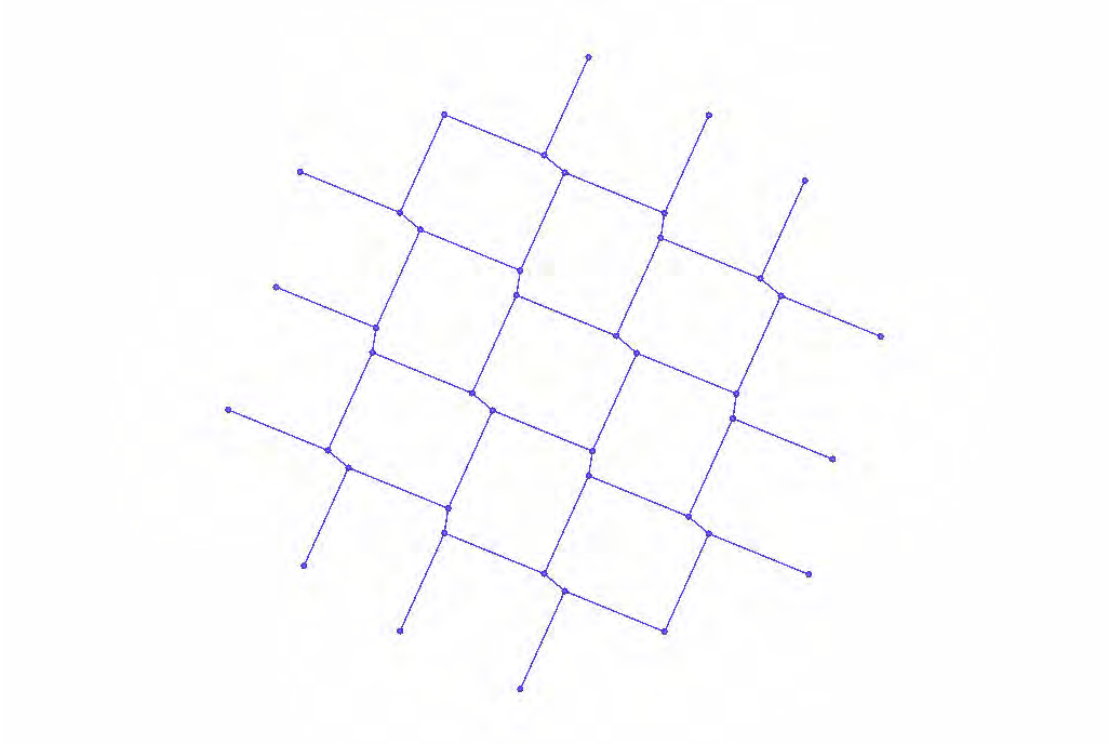

Figure 2.14 *– A simplified diagram showing the connectivity of the two-dimensional sheet* ***2.9****.*

The sheets in the structure pack vertically, with few interactions between separate sheets. While the benzene cores of each sheet are aligned, the distance is too great for π-π stacking interactions (7.162Å). There are some weak edge-face π interactions between pyrazoles of one sheet with the pyrazoles and benzene rings of the adjacent sheet (2.891Å).

*Crystal structure of the complex with CuI (**2.10**)*

An acetonitrile solution of copper iodide was layered upon a solution of ligand **2.4** in chloroform. In the last experiment discussed, a metal to ligand stoichiometry of 2:3 was used to obtain a 1:1 stoichiometry in polymer **2.9**. In this experiment, different solvents and a different metal to ligand ratio of 2:1 was used. Over a few days stacks of colourless plates grew in the reaction mixture, which proved to be suitable for X-ray crystallography. The cell was different to **2.9**, and solved in chiral orthorhombic space group $P2_12_12_1$.

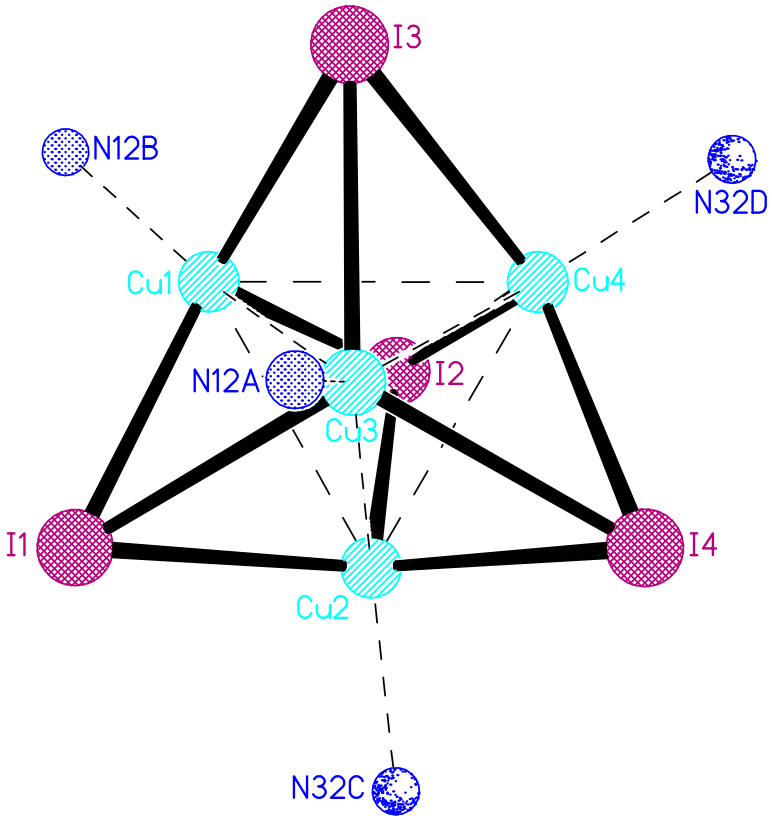

***Figure 2.15** – The Cu_4I_4 cluster in **2.10**. Selected bond lengths (Å) and angles (°): Cu1-N12B 2.03(1), Cu1-Cu3 2.649(2), Cu1-I1 2.652(2), Cu1-I3 2.661(2), Cu1-Cu2 2.721(2), Cu1-Cu4 2.721(2), Cu1-I2 2.746(2), Cu2-N32B 2.04(1), Cu2-I1 2.656(2), Cu2-I2 2.682(2), Cu2-I4 2.722(2), Cu3-N12A 2.01(1), Cu3-I4 2.658(2), Cu3-I3 2.682(2), Cu3-I1 2.737(2), Cu4-N32A 2.01(1), Cu4-I2 2.649(2), Cu4-I4 2.704(2), Cu4-I3 2.767(2), N12B-Cu1-I1 117.3(4), N12B-Cu1-I3 102.5(4), N12B-Cu1-I2 96.1(4), I1-Cu1-I2 111.02(6), I1-Cu1-I3 115.28(6), Cu1-I1-Cu2 61.68(5).*

The first feature of interest is the copper iodide motif, as shown in Figure 2.15. Four copper atoms and four iodines have bonded together to make a Cu_4I_4 cluster. The copper atoms form a tetrahedron at the centre of the cluster, and each face of the tetrahedron is capped by an iodine. Every iodine bonds to three copper atoms. The distances between copper atoms is 2.649-2.736Å, which is slightly shorter than the sum of the Cu(I)-Cu(I) van der Waals radii of 2.80Å,[125] however it seems unlikely these copper atoms are joined by actual bonds.[126,127] Therefore the copper atoms in Figure 2.15 are linked by dashed lines to show the outline of the tetrahedron they form. Each copper atom binds to three iodide atoms and one pyrazole nitrogen with a tetrahedral geometry. This copper iodide cluster arrangement is not uncommon, with 18 structures listed in the *Cambridge Crystallographic Database* (version 5.26).[130]

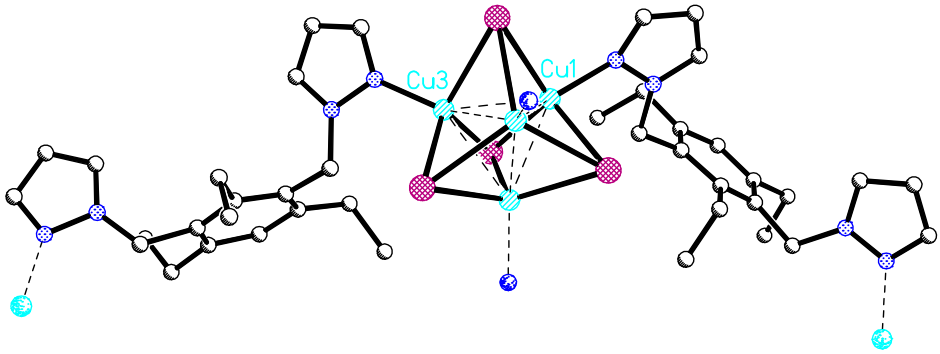

Figure 2.16 *– The asymmetric unit of* ***2.10****.*

The contents of the asymmetric unit are shown in Figure 2.16. The hydrogen atoms are excluded, along with three chloroform (one half occupancy) and one acetonitrile solvate molecules for clarity. Two ligands and one Cu_4I_4 cluster lie in the asymmetric unit. The metal cluster binds to two unique ligands and two of their symmetry equivalents in a tetrahedral geometry, acting as a single metal centre and creating a four-connector node. Each ligand then coordinates to two metal centres, bridging the clusters and creating an extended three-dimensional framework. Both ligands have similar conformations, with both pyrazole arms on the same side of the benzene cores. However the orientation of the ethyl groups differ between the ligands. The ligand bound to Cu1 lies in an organised *ababa* conformation, while the ligand bound to Cu3 lies in an *ababb* conformation.

Shown in Figure 2.18 is a simplified diagram of the extended three-dimensional framework, generated by *Topos*. Rectangular voids lie in a herringbone pattern. Each macrocycle consists of six Cu_4I_4 clusters and six bridging ligands. If the Cu_4I_4 clusters are viewed as single four-connecting nodes, the polymer can be classified as a (6,4) net, as the ligands only bridge the clusters and add no extra dimensionality to the structure. The clusters extend the network into three dimensions. These voids alternate position very slightly during alternative layers, but propagate through the entire framework, creating channels which hold solvate molecules, making this structure an excellent candidate for thermogravimetric analysis and further absorption property studies. These voids can be viewed from many different angles in the simplified structure, suggesting the network is quite porous, and any guest molecules within the framework should be able to escape easily. Shown in Figure 2.18 is an orientation where all the Cu_4I_4 clusters are aligned.

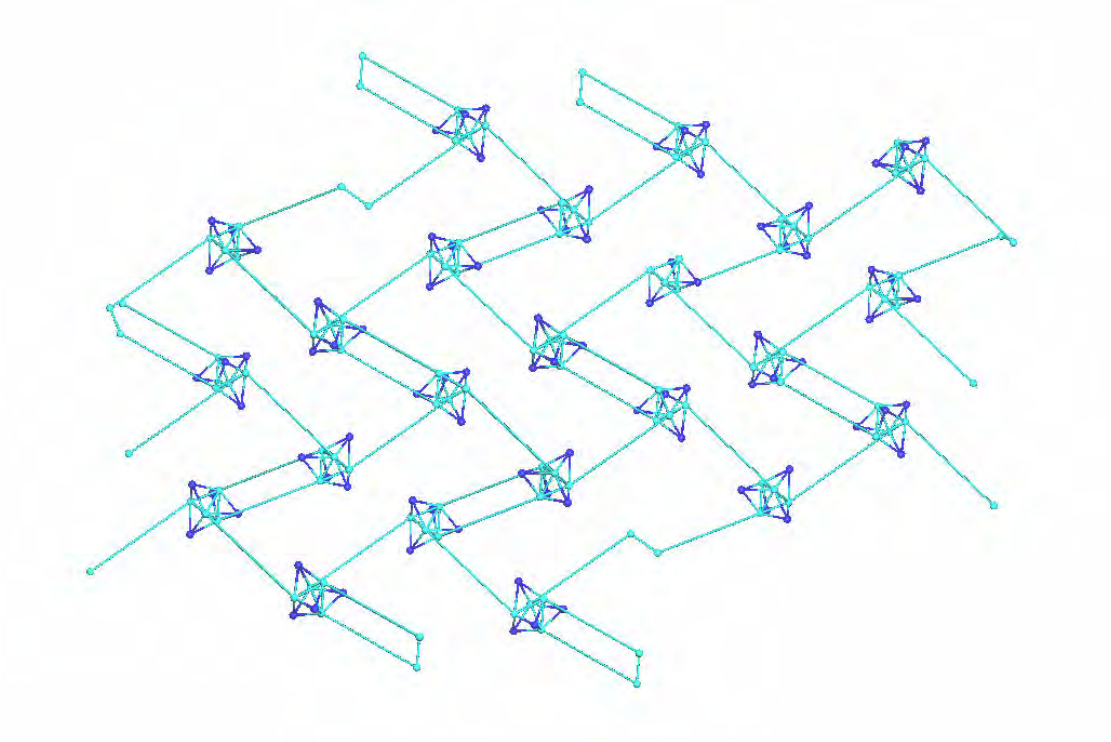

Figure 2.17 *– A simplified structure of three-dimensional polymer* ***2.10****, showing the connectivity and the voids in the net.*

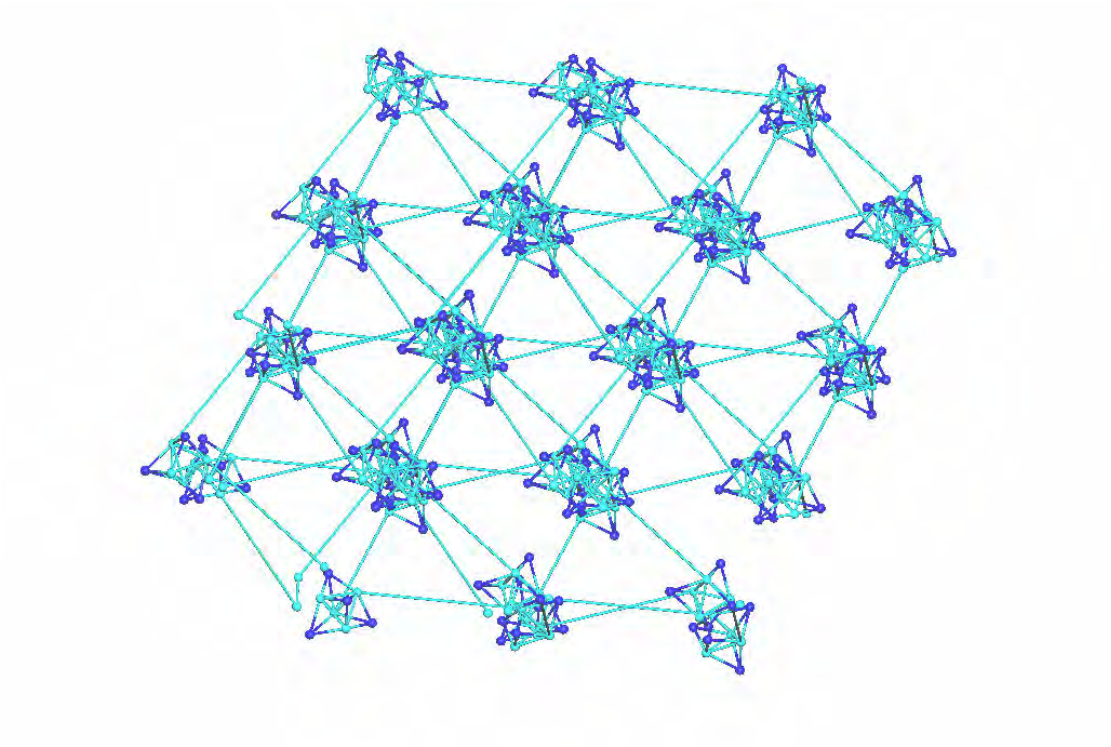

Figure 2.18 *– An alternate view of simplified three-dimensional polymer* ***2.10****, where the* Cu_4I_4 *clusters are aligned.*

There are few interactions between ligands in the packing structure. Most hydrogen bonding interactions are between solvate molecules and between solvate molecules and the main structure. No π-π stacking interactions are observed.

Crystal structure of the complex with $Pd(PhCN)_2Cl_2$ *(**2.11**)*

Slow evaporation of a solution containing ligand **2.4** and bis(benzonitrile)dichloro-palladium(II) gave orange blocks over ten days. These crystals were suitable for X-ray crystallography. The structure, as shown in Figure 2.19, solved in monoclinic space group $P2_1/n$.

The asymmetric unit reveals a discrete M_3L_3 triangular structure with guest acetone solvate molecule in the middle. Hydrogen atoms and disorder are excluded for clarity. Three palladium atoms make up the structure, each coordinating to two chloride anions and two pyrazole nitrogens of separate ligands in a trans-square planar geometry. The three ligands in the structure each bridge two metal atoms. The pyrazole arms on each ligand are both on the same side of the ring. The central core of each ligand lies below the plane of the pyrazoles inside the centre of the macrocycle. Interestingly, there is no

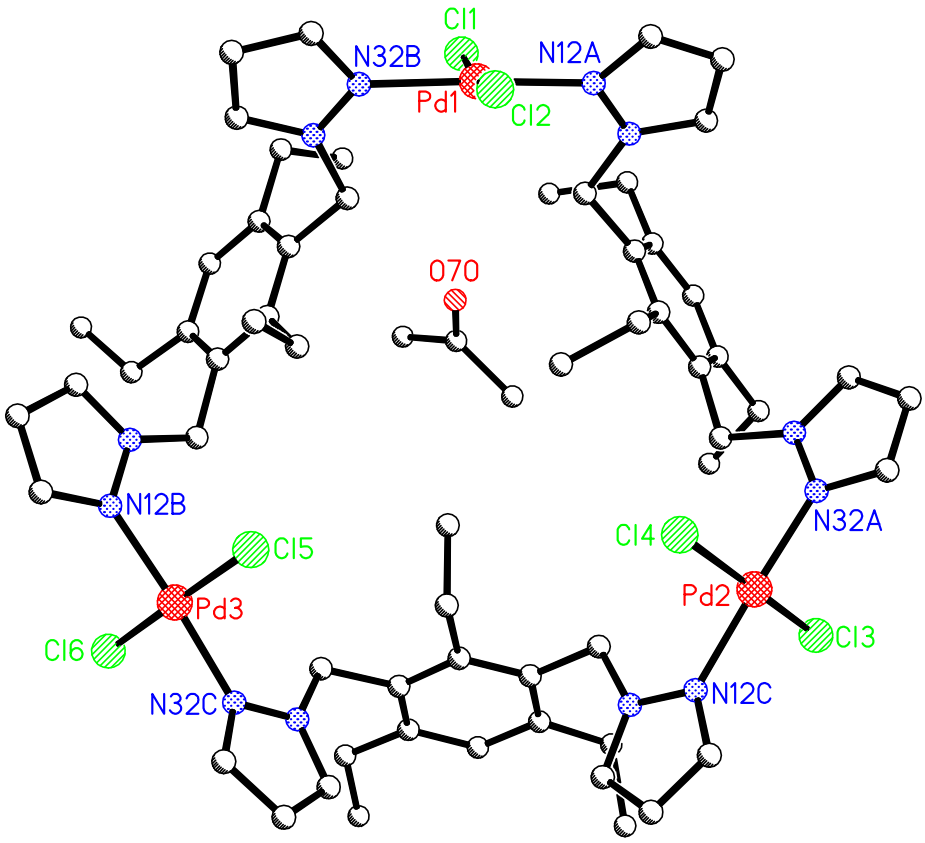

Figure 2.19 *– The M_3L_3 cyclic trimer structure* ***2.11****. Selected bond lengths (Å) and angles (°): Pd1-N12A 2.011(4), Pd1-N32B 2.018(5), Pd1-Cl2 2.286(2), Pd1-Cl1 2.316(2), Pd2-N32A 1.997(4), Pd2-N12C 1.999(4), Pd2-Cl4 2.299(2), Pd2-Cl3 2.296(2), Pd3-N12B 2.001(5), Pd3-N32C 2.005(4), Pd3-Cl5 2.275(2), Pd3-Cl6 2.297(2), N12A-Pd1-N32B 177.4(2), N12A-Pd1-Cl2 88.1(2), N12A-Pd1-Cl1 91.7(2), N32B-Pd1-Cl2 90.7(2), N32B-Pd1-Cl1 90.0(1), Cl1-Pd1-Cl2 171.01, N32A-Pd2-N12C 177.3(2), N32A-Pd2-Cl4 90.3(1), N32A-Pd2-Cl3 89.7(1), N12C-Pd2-Cl4 89.7(1), N12C-Pd2-Cl3 90.7(1), Cl3-Pd2-Cl4 174.88(6), N12B-Pd3-N32C 174.5(2), N12B-Pd3-Cl5 90.0(2), N12B-Pd3-Cl6 90.8(2), N32C-Pd3-Cl5 88.6(1), N32C-Pd3-Cl6 90.9(1), Cl5-Pd3-Cl6 177.16(7).*

more symmetry to the structure than shown, as the ethyl groups on each ligand lie in different orientations. The ligand on the top right of the diagram, bound to Pd1 and Pd2 is in an *ababa* organised conformation, with all three ethyl groups pointing into the centre of the structure. Neither of the other ligands is organised, and both have considerable disorder in the positions of the ethyl groups. The ligand on the top left of the structure, bound to Pd1 and Pd3, has ethyl groups in a down, an up, and a slightly raised sideways positions. The inner ethyl group, shown in an up position, is disordered,

with 40% of the time being located in a down position. This would make the ligand almost organised. This ethyl arm points into the void inside the structure, so it is possible that the disorder helps fill the empty space below the guest molecule. The ethyl arms of the lower ligand in the diagram, bound to Pd2 and Pd3, sit in an up, down, and sideways positions, but are also disordered. The inner ethyl group, pointing down in the figure, is 30% disordered in an up position. Again this would place that ligand in a semi-organised position, and this ethyl arm also points into the void of the structure, so again the disorder likely results from the empty space surrounding that arm. The sideways facing arm is also highly disordered, with another orientation approximating an up position, present 60% of the time. Therefore, statistically, some of the time this ligand must exist in a totally un-organised conformation, with an *aaaaa* arrangement around the central ring.

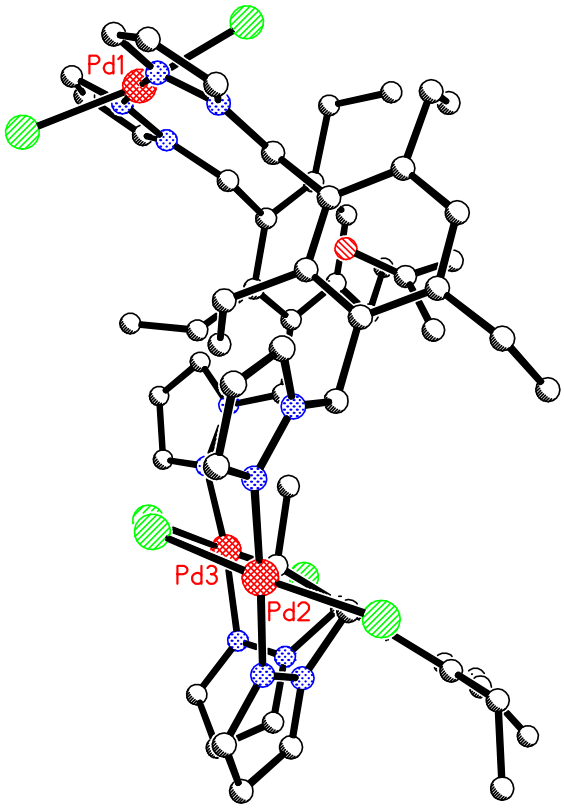

Figure 2.20 *– A side-on view of triangular structure* ***2.11****, showing how the ligands sit behind the metal centres and lean into the centre of the structure, and how the acetone guest molecule sits between the benzene cores.*

Also interesting about the ligand arrangements in this structure is their orientation with respect to each other. Each ligand faces into the centre of the structure, with the ethyl groups in the 2-position enclosing around the central cavity. This creates a tapering effect on one face of the trimer, which is shown more clearly in Figure 2.20. Also shown clearly in Figure 2.20 is how far back the central cores of the ligands sit behind the palladium atoms and the coordinated pyrazoles.

The final description point of this structure is the guest molecule in the centre. The acetone solvate molecule sits near the top of the structure, with the oxygen pointing towards the tapered face of the structure, and the two methyl groups sitting in the more open face. The acetone lies on an angle approximating 45^{o}, and along with the ethyl groups, destroys the potential mirror plane running vertically through the structure.

The host–guest interaction between the trimer and the solvate molecule is shown in Figure 2.20. The acetone sits behind the tapered end of the structure, not in the plane of the palladium atoms, but between the benzene cores of two ligands. Interestingly it is the hydrophilic end of the acetone that sits closest to the hydrophobic environment created by the ligands. Also obvious in this orientation is how high the guest molecule is sitting. There is a void in the structure below the acetone and above the bottom ligand, presumably not large enough to house a second guest molecule.

Two space-filling diagrams are shown in Figure 2.21. The first is looking at the triangle from the front, the second looking in at the acetone guest from the back. The acetone is shown in purple and red. The guest seems to fit well inside the cavity, with the methyl groups sitting where the structure is wider and the oxygen nesting in a gap of ideal size between the ligands and the chlorine. The acetone does not sit very close to the front of the structure, well hidden by the atoms in front. The space-filling diagram shows that the lowest ethyl group does partially fill the void below the guest, however this ethyl group is disordered. While the void appears large enough to possibly house another acetone the reality is that if another guest could fit it would have a tendency to do so, so the space must be slightly too small. The view from the back shows the acetone guest much more clearly. It does sit well inside the triangle, tucked in against the ligands and almost held in place by the ethyl groups. From this angle, the void below the acetone looks small, especially considering how much the lower ligand is tilted outwards.

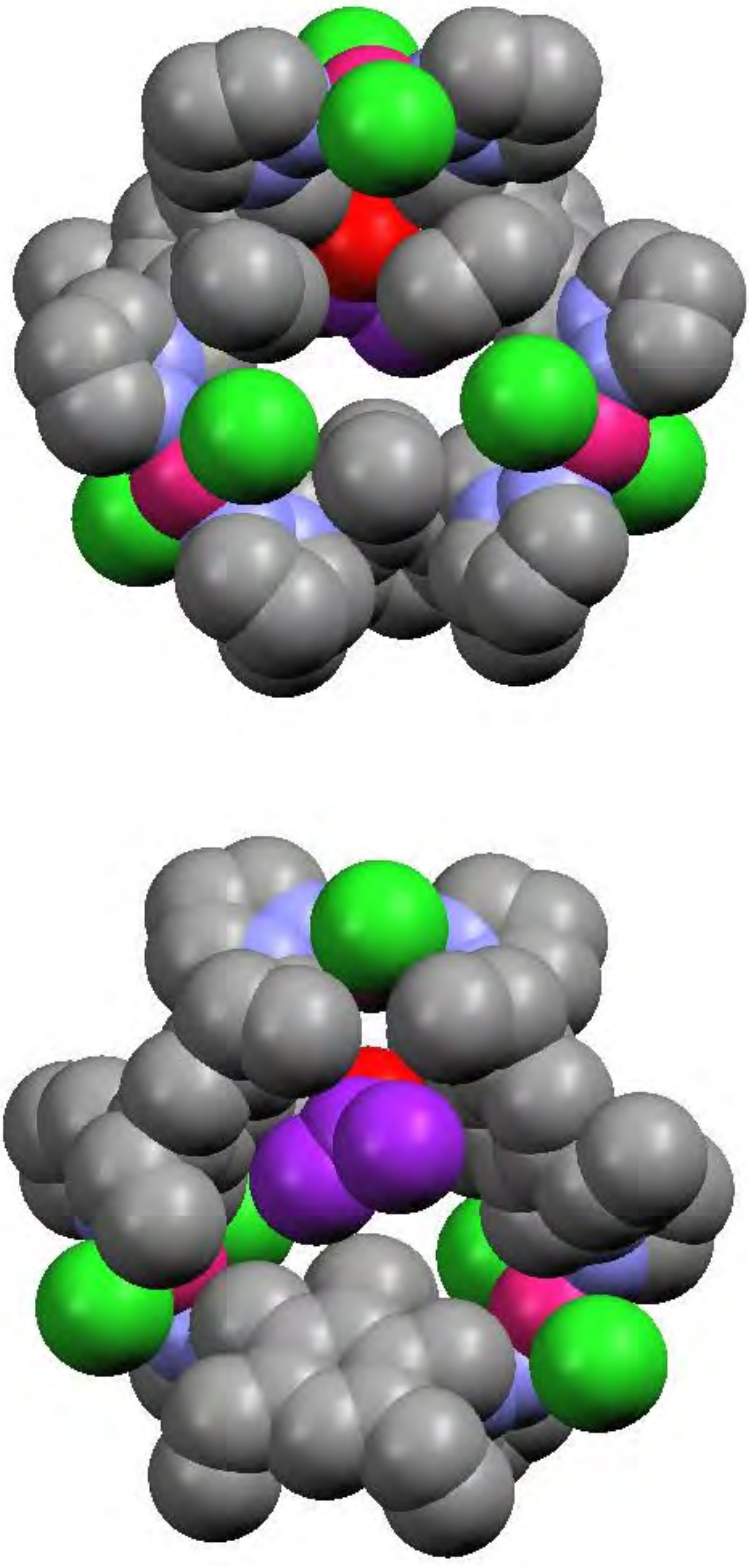

Figure 2.21 *– Space-filling diagrams of* ***2.11****. The top view is looking towards the tapered face of the trimer, the bottom view is rotated 180*^{o} *looking at the open face.*

The oxygen atom of the guest has short contacts to many atoms in the main structure, with distances ranging from 2.57-2.81Å.

In the extended structure, the triangles are offset, so no channels are created. Chlorines hydrogen bond to pyrazole hydrogens, at distances between 2.641Å and 2.749Å. The un-tapered face of the trimer nestles closely with the adjacent structure, a chlorine atom attempting to fill the void under the guest molecule.

A comparison must be made between this structure and the M_6L_4 cage first synthesised by C. Hartshorn[55] and discussed in detail in Chapter Three. This complex is really just a slice of the M_6L_4 cage, not surprising as the cage consists of $PdCl_2$ units and 1,3,5-tri(pyrazol-1-ylmethyl)-2,4,6-triethylbenzene. The only difference between the ligands is an extra pyrazole arm in the vacant position on ligand **2.4**, and this extra arm gives the Hartshorn complex more dimensionality. All the ligands in the triangle are orientated such that the addition of the extra arm would undoubtedly lead to the formation of the M_6L_4 moiety. The cage encapsulates a DMSO or a chloroform solvate molecule, guests of only slightly larger size than the acetone in this example.

This structure is unusual as it consists of a M_3L_3 macrocycle that resembles a triangle. Traditionally a triangle would be constructed from six components, three linear components that act as the sides of the shape, and three angular components which incorporate a 60^o angle which would constitute the corners. In this case the triangle is truncated. The ligand subtends a 60^o angle, but the bending of the methylene groups allows the central core of the ligand to collapse into the centre of the structure. As the core of the ligand is linear between the pyrazoles, this structure could be considered a hexagon. Metallosupramolecular hexagons can be constructed from an M_3L_3 mixture of components, as long as the length of the edges approximate each other closely enough to make a symmetrical structure. In this case, the lengths of the edges are similar, but debatably not similar enough to be considered a hexagon, therefore the description as a cyclic trimer or truncated triangle seems to fit more accurately.

However there is already terminology in place to describe this type of truncated triangular shape. The term “tricorn” is a French word originating from a style of hat popular during the late 17^{th} century,[131] where the brim of the hat is pinned up on three

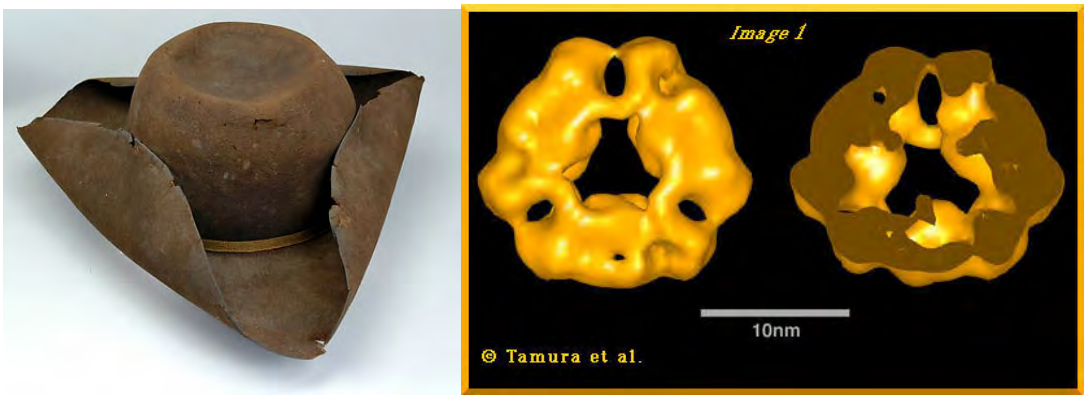

*Figure **2.22** – A tricorn hat [132] and the tricorn protease.[133]*

sides, creating a rough triangular shape, as shown in Figure 2.22. It was first adopted by chemists in the 1990's to name a high molecular weight protease shown to have an unusual shape.[133] The electron microscopy images of the tricorn protease is also shown in Figure 2.22. More recently, the term tricorn has been used to describe complexes of extremely similar topology to the truncated triangle described here.[134-136]

Shown in Figure 2.23 are examples of molecular tricorns, constructed using coordination chemistry. Example a) is built using cyclopalladation,[136] example d) using porphyrins.[137] Example c) is constructed with copper atoms and imidizole,[138] with the

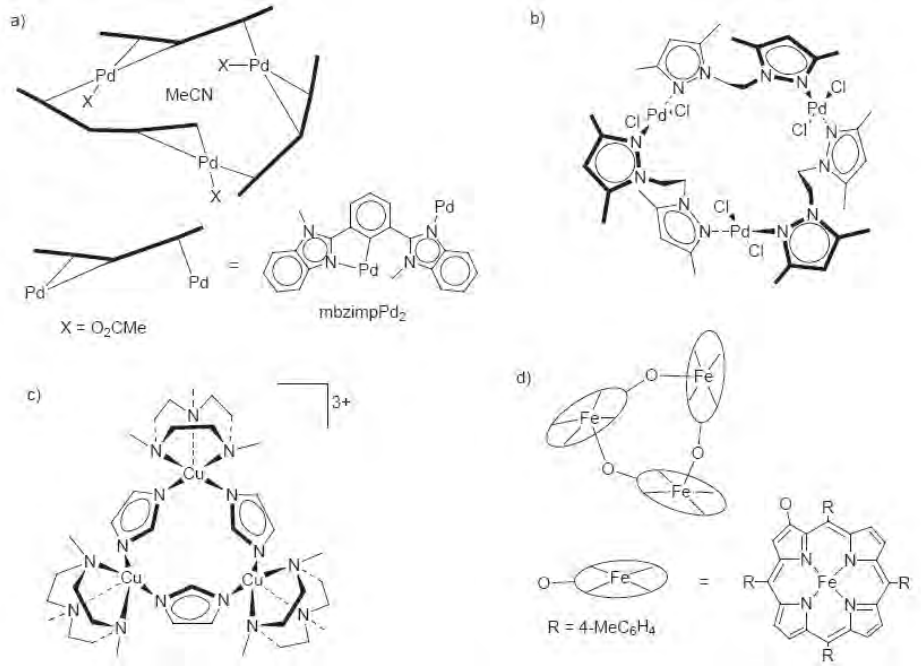

***Figure 2.23** – Other examples of molecular tricorns or cyclic trimers.[53]*

capping group on the copper atoms making the structure resemble a triangle. Example b)[134] is the closest example from the literature to the complex described here. Also made with palladium chloride, this much smaller pyrazole-based ligand is flexible enough to adopt the same conformation as ligand **2.4**. Topologically speaking, the complex described here is a much larger version of tricorn b). None of the examples above are large enough to contain a guest molecule inside the central cavity, except for example a) which is host to an acetonitrile solvate molecule.[136]

*Other complexes with ligand **2.4***

Complexation of ligand **2.4** was attempted with a wide variety of metal salts, namely CuI, $CuBF_4$, $CuCl_2$, $Cu(NO_3)_2$, $CuSO_4$, $Cu(ClO_4)_2$, $AgClO_4$, $CoCl_2$, $CoBr_2$, $Co(BF_4)_2$, $Pd(PhCN)_2Cl_2$, $Fe(ClO_4)_2$ and $ZnBr_2$. The complexes of which crystals of X-ray quality were obtained have been discussed. Many of the complexes which did not crystallise were not analysed further.

Noteworthy is the observation that, while the complex **2.8** obtained with $ZnBr_2$ has a 1:1 ratio in the crystal structure, elemental analysis results suggest the main batch of crystals actually consists of a M_2L_3 ratio. It seems that there is a mixture of products being formed, and the one-dimensional polymer may not even be the main product. With insoluble polymeric products further analysis is difficult. Another batch of this reaction in different solvents gave similar looking crystals and an almost identical melting point, but the analysis suggested a M_5L_6 ratio, different to both the crystal structure and elemental analysis of the other batch.

Complexation with CuI was attempted on four occasions, using different solvents and varying the metal to ligand ratio. Three of these products were analysed by microanalysis and two identified by X-ray crystallography. All three compounds have very similar melting points and all products contain metal to ligand ratios of 1:1. However complex **2.10** was shown by X-ray crystallography to contain a 2:1 metal to ligand ratio. Again, this suggests that the crystal analysed may not be representative of the whole sample.

The reaction of ligand **2.4** with $CoCl_2$ gives a high yield of dark blue crystals, unfortunately not suitable for X-ray crystallography. These crystals analyse in a M_5L_6

ratio. A structure containing this unusual ratio is possible, or the results could suggest a mixture of products.

Reaction of ligand **2.4** with $AgClO_4$ gives a very soluble complex which was unable to be crystallised. The complex was precipitated to give an elemental analysis result with a 1:1 ratio complex with no solvent molecules.

1,3-Di[3-(2'-pyridyl)pyrazol-1-ylmethyl]-2,4,6-triethylbenzene (2.12)

The second ligand synthesised from precursor **2.2** is shown in Scheme 2.3. A phase-transfer-catalysed reaction replaced the bromines with 3-(2'-pyridyl)pyrazole units, creating, in 98% yield, a two-armed ligand with two bidentate binding domains to use as a synthon in metallosupramolecular chemistry.

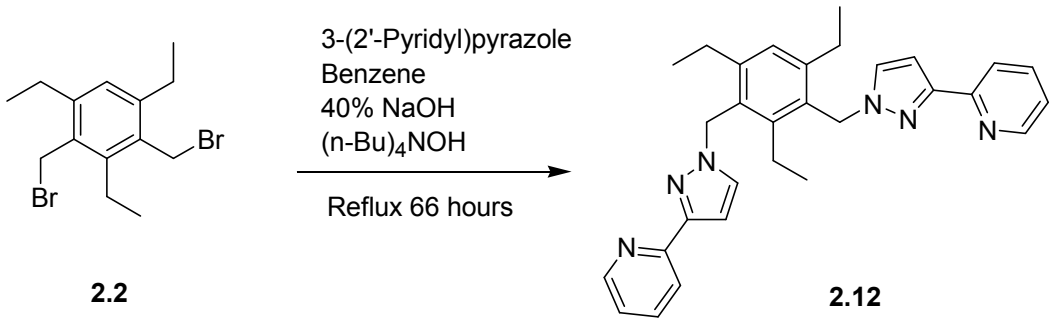

2.2 **2.12**

Scheme 2.3 *– Synthesis of ligand* ***2.12****.*

Ligand **2.12** is similar to ligand **2.4**, differing only in the addition of a pyridine to create a chelating binding domain on each arm. This should encourage ligand **2.12** to form more robust complexes than ligand **2.4**, and will also affect the complexes obtained as an extra donor will change the coordination sphere around the metal. To form a M_4L_6 tetrahedral cage, ligand **2.12** will have to be reacted with an octahedral metal atom in the presence of a non-coordinating anion.

Many ligands incorporating this 3-(2'-pyridyl)pyrazole binding domain have been synthesised. Shown in Figure 2.24 are a few examples of two-armed ligands of similar nature to ligand **2.12**. The metallosupramolecular structures constructed from these ligands are impressive, including a large number of cage and cage-like structures.

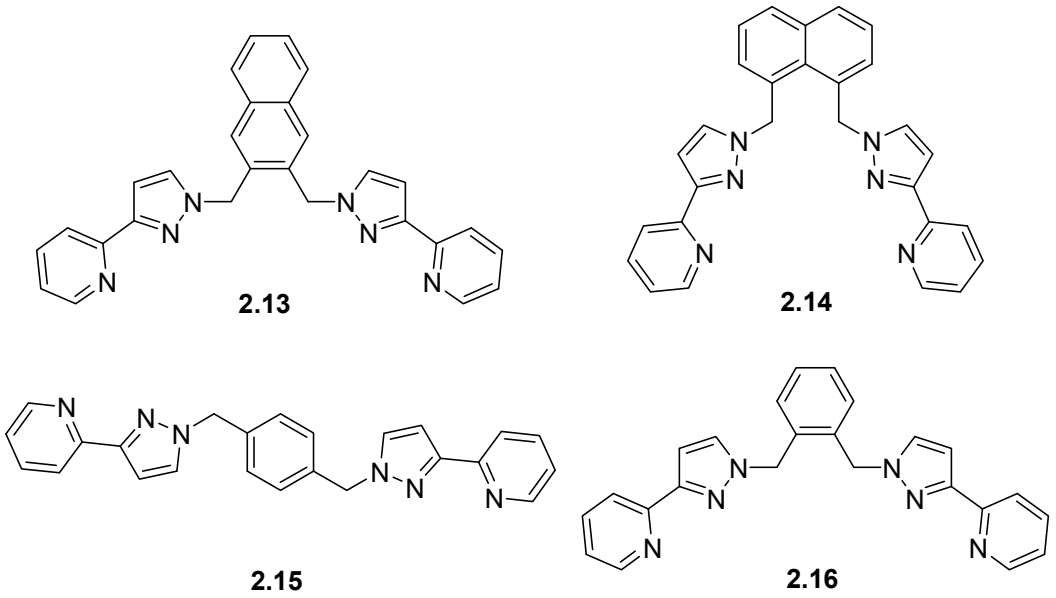

Figure 2.24 *– Two-armed ligands of similar nature to* ***2.12****.*

Ligands **2.13**[139] and **2.14**[83,139-141] are both based on naphthalene cores, with the binding arms attached closely together around the ring. Ligand **2.13** forms a M_4L_6 tetrahedral cage with $Zn(BF_4)_2$, encapsulating a BF_4^- counterion.[139] Ligand **2.14** forms discrete 1:1 complexes with CuOTf and $AgBF_4$,[140] a M_4L_4 square with $CuBF_4$ which hosts a BF_4^- counterion,[140] and large $M_{12}L_{18}$ cages when reacted with $Co(BF_4)_2$, $Cd(BF_4)_2$ or $Cu(ClO_4)_2$, encapsulating four BF_4^- or ClO_4^- counterions.[83,139,140] Ligands **2.15**[142-144] and **2.16**[69,143-146] are based on para- and ortho- substitutions of the binding arms around a benzene ring. Ligand **2.15** forms a M_2L discrete complex with $Hg(ClO_4)_2$,[144] a M_2L_2 dimer with $AgBF_4$,[144] and a large $M_{16}L_{24}$ cage when reacted with $Cd(ClO_4)_2$ which encapsulates eight counterions and six acetonitrile molecules.[142] Ligand **2.16** forms discrete 1:1 structures with $CuCl(BF_4)$,[145] $Zn(OAc)PF_6$[146] and $Hg(ClO_4)_2$,[144] a discrete M_2L_3 complex with $Ni(BF_4)_2$,[69] a M_3L_2 complex with $AgNO_3$ where the pyridine and pyrazole actually bind to different metal centres,[143] a double helical M_2L_2 complex with $CuPF_6$,[145] and a M_4L_6 tetrahedral cage with $Co(BF_4)_2$ with encapsulates a BF_4^- anion.[69]

Shown in Figure 2.25 are ligands of even closer similarity to ligand **2.12**. All three have binding arms substituted onto the 1,3 positions of the central core. The difference between the structures is in the aromatic core. In the case of ligand **2.12** the core is 1,3,5-triethylbenzene. The ligands in Figure 2.25 are less sterically crowded with ligand **2.17**[144] based on a toluene core, ligand **2.18**[141,147] a pyridine core (therefore also

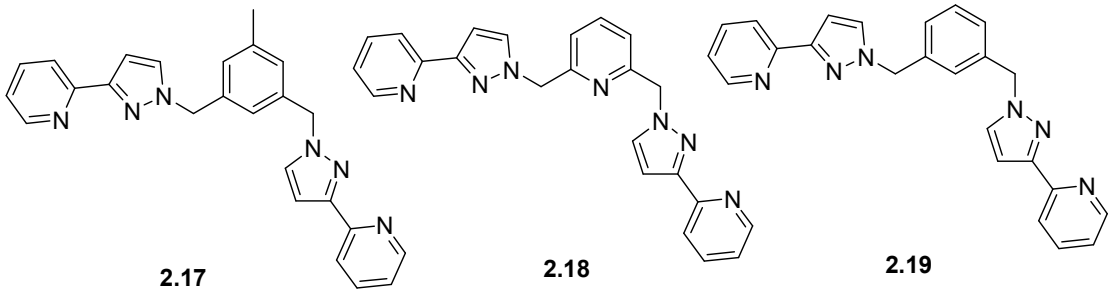

Figure 2.25 *– Meta-substituted ligands with close similarity to* ***2.12****.*

including a possible extra binding site), and ligand **2.19**[143,148] a benzene ring. Again, these ligands have produced some exciting metallosupramolecular structures, which it is possible that ligand **2.12** may replicate.

Ligand **2.17** forms a M_2L_2 dimer upon reaction with $AgClO_4$.[144] Ligand **2.18** creates a M_8L_{12} molecular cube when reacted with $Zn(ClO_4)_2$, which encapsulates a ClO_4^- anion.[147] Ligand **2.19** forms a helical one-dimensional polymer with $AgBF_4$, a discrete M_2L complex with $Hg(ClO_4)_2$, a M_6L_9 "open-book" complex with $Co(ClO_4)_2$,[148] and a M_8L_{12} molecular cube with $Zn(BF_4)_2$, encapsulating two BF_4^- anions.[148] Based on these comparisons, obviously there is potential for ligand **2.12** to become a component of a large cage-like assembly.

Complexes with ligand 2.12

*Crystal structure of the complex with CuI (**2.20**)*

A solution of copper iodide in acetonitrile was added to a solution of ligand **2.12** in acetone to give a bright yellow precipitate. Upon slow evaporation of a methanol, acetone, chloroform and acetonitrile solution of this precipitate, a few small green needle-like crystals were grown on the side of the vial. To make things more difficult, these thin delicate needles were very air sensitive, and although the crystal was mounted as quickly as possible into the cold stream of the diffractometer, some decomposition had taken place and the diffraction patterns were weak. Barely enough data was collected to solve the structure, and not enough to provide adequate information to allow all the atoms to be treated as anisotropic. Multiple crystals were tried, and recrystallisations attempted, however this isotropic structure with an R_1 value of 8.36% remains the best data collection for this structure.

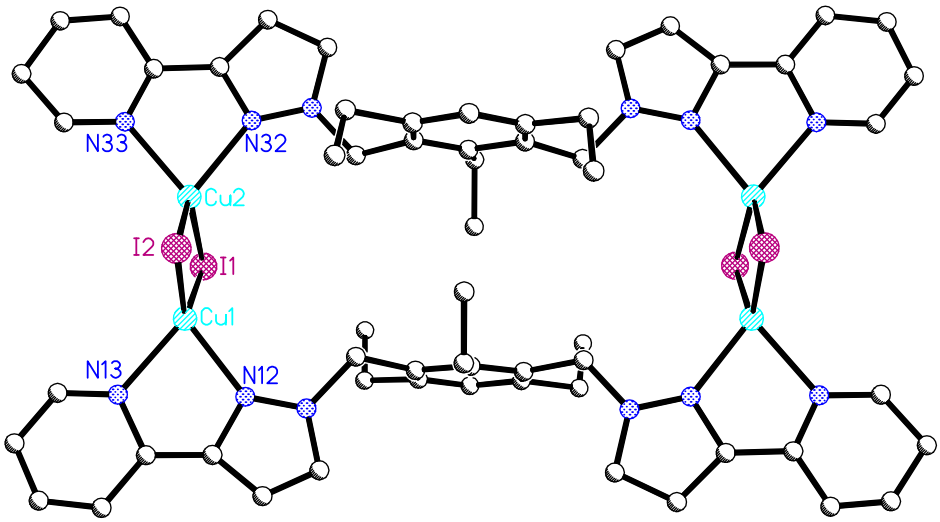

Figure 2.26 *– The M_4L_2 macrocycle* ***2.20****. Selected bond lengths (Å) and angles (°): Cu1-N12 2.12(2), Cu1-N13 2.13(2), Cu1-I1 2.584(4), Cu1-I2 2.601(4), Cu1-Cu2 2.604(4), Cu2-N32 2.12(2), Cu2-N33 2.15(1), Cu2-I1 2.601(4), Cu2-I2 2.604(4), N12-Cu1-N13 78.7(8), N12-Cu1-I1 114.4(6), N12-Cu1-I2 108.7(6), N13-Cu1-I1 116.6(6), N13-Cu1-I2 111.4(6), I1-Cu1-I2 119.8(1).*

The rectangular metallomacrocycle solves in triclinic space group P-1, and is shown in Figure 2.26 with the hydrogen atoms and solvate molecules excluded for clarity. The asymmetric unit contains one ligand, one Cu_2I_2 square, one acetone and two chloroform solvate molecules. The discrete structure, as shown in Figure 2.26, contains four copper atoms, four iodide counterions, and two ligands, lying about a crystallographic centre of inversion. Each copper atom bonds to two iodines, and chelates in the binding domain of a single ligand arm, coordinated to both the pyrazole nitrogen and the pyridine nitrogen to give an overall tetrahedral geometry. The copper-copper distance is only 2.604Å, which in comparison to the sum of the van der Walls radii of two Cu(I) atoms of 2.80Å[125] is reasonably short; however considering the geometry of each atom the copper centres can not be bonded together.[126,127] Iodine atoms bridge two copper atoms to form a square. Each ligand bridges two copper atoms in a linear fashion, thereby creating a rectangular shape, as the ligands make up the length and the Cu_2I_2 squares make up the sides. If the Cu_2I_2 squares are considered a single unit, this complex may be classified as a [2+2] macrocycle. The rectangle created has a length of 12.041Å (Cu2-Cu1A) and a height of 4.615Å (C2-C2A). Unfortunately the ethyl groups reduce

the volume of the void in the centre of the structure, so the rectangle does not play host to a guest molecule.

The ligands sit in an *ababa* organised conformation, with the coordinated arms on one side of benzene ring, and all three ethyl groups on the other. An alternative view of the structure is shown in Figure 2.27. Emphasised in this view is the orientation of the ligand arms, which form a horizontal plane. This orientation would be less surprising from a para-substituted derivate than this meta-substituted example. It is the flexibility of the methylene group linking the coordinating arm to the central core that allows the ligand to be this generous in its orientation. Both ligands are vertically in line, constrained as such by the copper atoms.

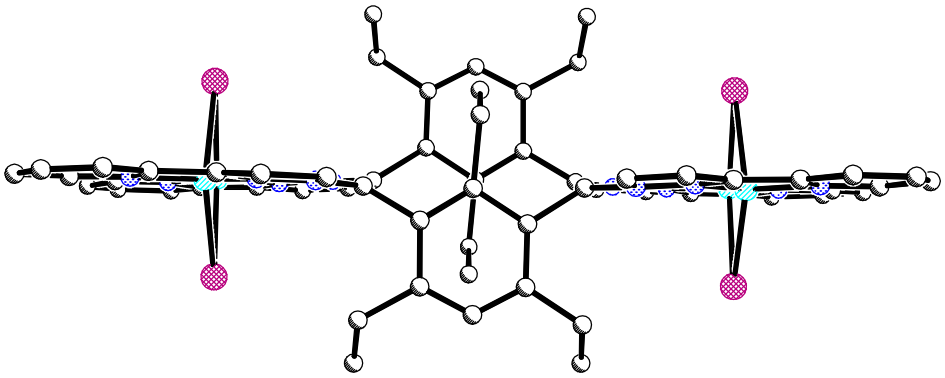

Figure 2.27 *– An alternate view of macrocycle* ***2.20****, looking down on the ligand arms from a birds eye view.*

As the binding substituents are displaced in a meta-arrangement around the ring, the benzene cores sit out of plane with the ligand arms. As the ligands are related by a centre of inversion, each sits on opposite sides of the plane. This allows the internal ethyl group of each ligand to sit above the benzene core of the opposing ligand. These interactions are quite long due to the distance between the ligands (C-H distances of 2.94-3.03Å), and therefore weak; however this effect is still stablising to the structure.

In the packing structure the dimers are aligned in channels, each channel offset from the ones beside it. There are few hydrogen bonding interactions between dimers, however the channels are formed by each dimer π-π stacking to those beside it *via* the coordinating arms of the ligand (3.483Å).

*Crystal structure of the complex with $CuSO_4$ (**2.21**)*

Crystals of complex **2.21** were grown by a procedure adapted from that used by Sun et al.,[64] and, as this procedure was used throughout this research, this technique will be described further as demonstrated in Figure 2.28. The metal salt, copper sulfate in this case, is dissolved in 4mL of water. Very carefully, 12mL of methanol solvent is layered on top of the aqueous copper sulfate solution. As methanol and water are very miscible, this layering process is not very successful, but if done carefully, a gradient can be created where the lower solution is more aqueous than the higher solution. The ligand is dissolved in a small amount of chloroform, which is added dropwise to the solution with care. Chloroform is a dense solvent and would normally sink to the bottom of such a solution. However if the layering process has been done correctly, as the chloroform sinks it is repelled by the increasing aqueous gradient (as chloroform and water are not miscible) and slowly rises to the surface of the solution. Therefore a thin organic layer containing the ligand develops at the surface of the solution. Depending on the solubility of the ligand, the ligand may diffuse across the chloroform/methanol boundary to react with the metal salt. Otherwise over a few days the chloroform and methanol layers will slowly mix, gradually releasing the ligand into the solution. Copper sulfate is soluble in methanol and therefore capable of diffusing above the most aqueous section of the solution.

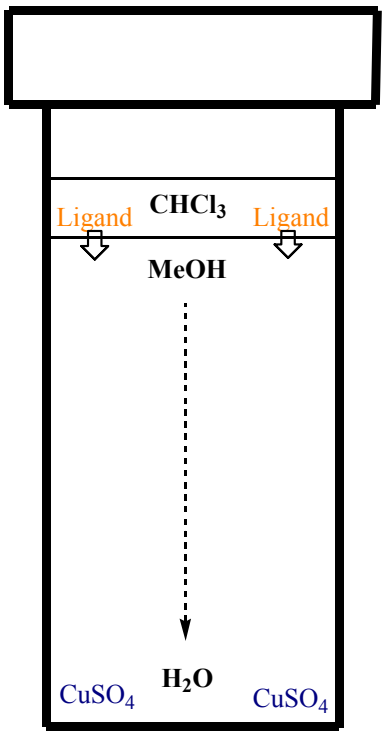

***Figure 2.28** – The solvent layering procedure used to crystallise **2.20**.*

The crystallisation process depends on the solubility of the complex. If crystals do not appear in solution within the first few days, slow evaporation often achieves this task. Chloroform is the most volatile of the solvents, so evaporates first, followed by methanol. As more methanol evaporates the remaining solution becomes more and more aqueous in nature, and along with the increasing relative concentration, often promotes crystallisation.

The copper sulfate complex of ligand **2.12** was synthesised in this manner, with blue blocks forming in solution after a few weeks of slow evaporation. These blocks were suitable for X-ray crystallography, although the crystals were very air sensitive and lost solvent within seconds of being removed from solution, even when immersed in oil. Although mounted as quickly as possible, the crystal had started decomposing and turned opaque by the time it was relocated under the cold nitrogen stream of the diffractometer, therefore the poor quality data only refines to an R_1 value of 16.5%.

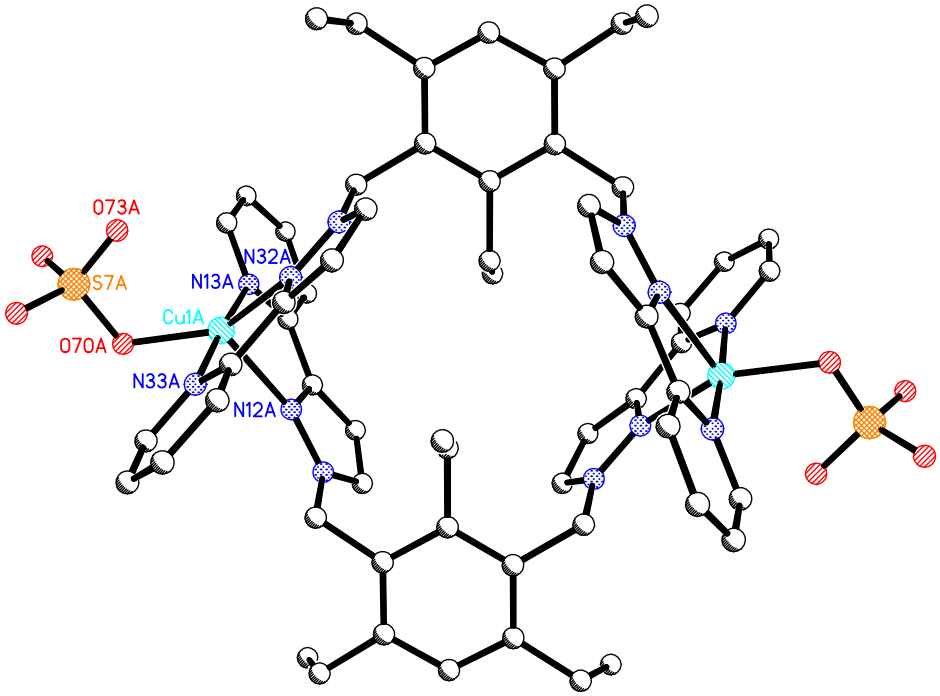

Figure 2.29 *– The M_2L_2 macrocycle* ***2.21****. Shown is the dimer grown from Cu1A. Selected bond lengths (Å) and angles (°) for the Cu1A dimer: Cu1A-N33A 1.982(7), Cu1A-N13A 2.000(7), Cu1A-O70A 2.005(6), Cu1A-N32A 2.090(7), Cu1A-N12A 2.23(7), N33A-Cu1A-N13A 176.9(3), N33A-Cu1A-O70A 90.6(3), N33A-Cu1A-N32A 80.4(3), N33A-Cu1A-N12A 98.3(3), N13A-Cu1A-O70A 90.9 (3), N13A-Cu1A-N32A 99.8(3), N13A-Cu1A-N12A 78.7(3), O70A-Cu1A-N32A 147.8(3), O70A-Cu1A-N12A 109.3(3), N32A-Cu1A-N12A 102.3(3).*

The crystal solves in triclinic space group P-1. In the asymmetric unit are two half molecules, consisting of one ligand, one metal and one counterion each, and a mess of disordered solvate molecules. There are two methanols, a partial occupancy chloroform, and at least twelve waters in the asymmetric unit. Obviously this crystal structure

contains large voids which must be filled with solvent, which explains the instability of the crystals.

Shown in Figure 2.29 is the grown structure of one of the half molecules in the asymmetric unit. Hydrogens and solvate molecules are excluded for clarity. There are two copper atoms in the structure, each bonding to one counterion and two ligands. The copper coordinates to both the pyrazole and pyridine nitrogens in each binding domain, making four bonds to the ligand, and one bond to an oxygen of the sulfate counterion. However there is pseudo-octahedral distortion of the 5-coordinate square pyramidal copper centre, as it makes a weak bond to another sulfate oxygen (2.705Å to O73A). The sulfates on each side of the dimer are related by a centre of inversion, with one pointing up and the other down. Two ligands bridge the two metal atoms creating a M_2L_2 dimer, very similar to that reported in the literature with ligand **2.17** and $AgClO_4$.[144] Each ligand has both binding arms on the same side of the benzene core, and both arms coordinate to the copper atom on the same face. As they are also related by a centre of inversion, the top ligand faces forward with both arms above the copper atoms, while the other ligand faces down with both arms below the copper atoms. The ethyl groups are not organised, lying in an *aabaa* conformation. Thus all the substituents on the central core are facing the same direction, except the ethyl group in the centre of the macrocycle.

The other half molecule in the asymmetric unit also grows into a M_2L_2 dimer. Comparison of the two structures show that although they are similar, the dimers are not identical. An overlay of the two structures is shown in Figure 2.30. The darker structure shown is grown from Cu1B. The overlay is poor as the structures are slightly different. Most obvious of the differences are the orientations of the sulfate groups, which are much more twisted towards the copper centres in the Cu1A dimer. Analysis of the copper centres in each of the dimers shows the extent of the distortion of each copper atom is different. Cu1A shows more distortion than Cu1B, with the distances to the closest non-bonding sulfate oxygens being 2.705Å and 2.817Å respectively. Understandably, this also alters the geometry of the other bonds surrounding the copper atoms, and causes the small alterations to each structure seen in Figure 2.30.

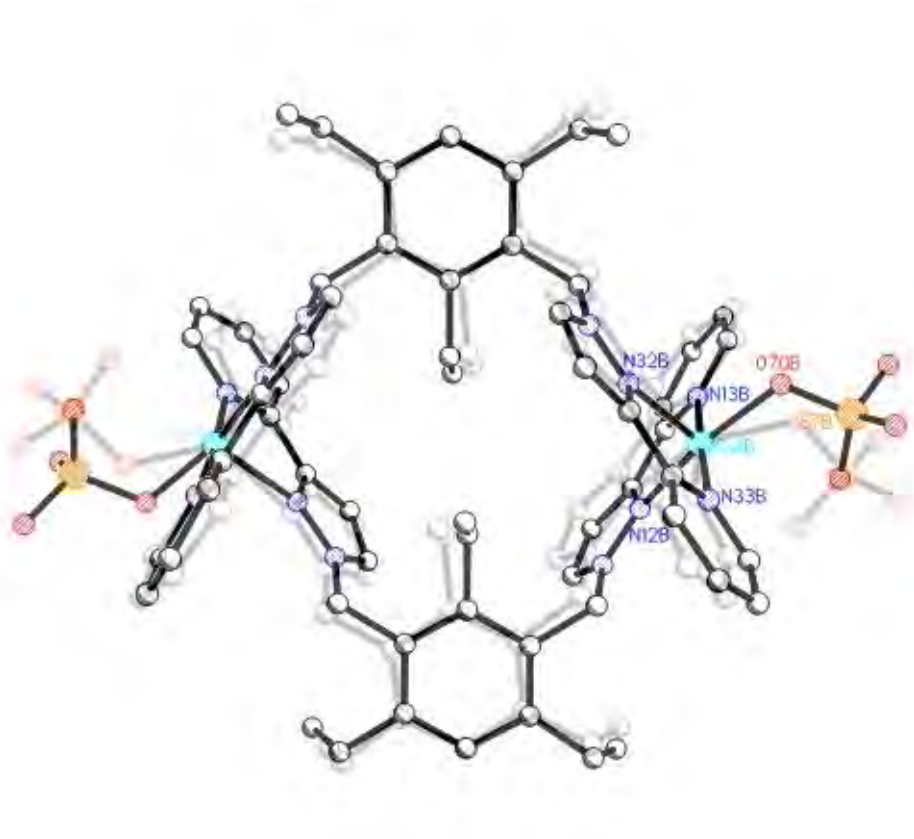

Figure 2.30 *– An overlay of both the dimers in* ***2.21****, showing the differences between the two structures. The darker structure of the two is the Cu1B dimer. Selected bond lengths (Å) and angles (°) for the Cu1B dimer: Cu1B-O70B 1.978(6), Cu1B-N33B 1.978(7), Cu1B-N13B 2.016(7), Cu1B-N12B 2.058(7), Cu1B-N32B 2.230(7), O70B-Cu1B-N33B 90.5(3), O70B-Cu1B-N13B 90.7(3), O70B-Cu1B-N12B 163.6(3), O70B-Cu1B-N32B 90.4(3), N33B-Cu1B-N13B 175.3(3), N33B-Cu1B-N12B 97.6(3), N33B-Cu1B-N32B 78.3(3), N13B-Cu1B-N12B 80.2(3), N13B-Cu1B-N32B 106.2(3), N12B-Cu1B-N32B 105.3(3).*

An interesting feature of these structures is the position of the ethyl groups. Shown in Figure 2.31 is a space filling diagram of the Cu1B dimer. No hydrogens are shown for clarity. The ligands are coloured differently so they are easy to distinguish. The one ethyl group on the lighter coloured ligand that points above the ring, sits directly in the "V-shape" made by the binding arms of the darker ligand. This same interaction occurs on the underside of the molecule in the same fashion, where the ethyl group of the darker ligand is nestled between the binding arms of the lighter ligand. The distance between the hydrogens on the ethyl group to the aromatic carbons is 2.718Å. This interaction must stabilise the complex, and could be a defining factor of why this is the structure these components choose to form.

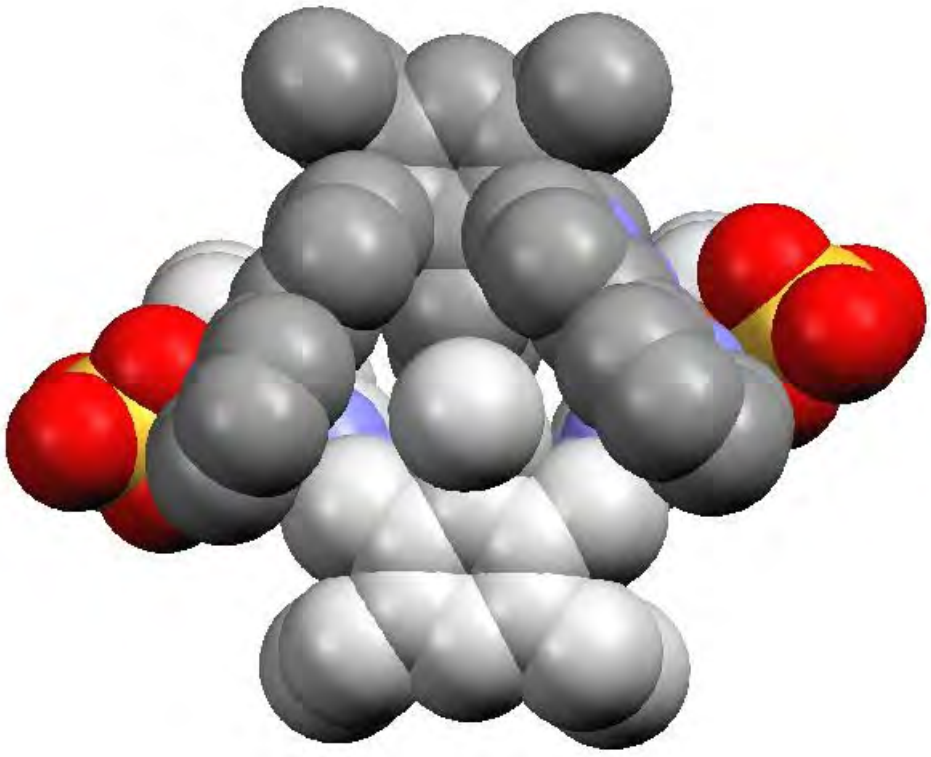

Figure 2.31 *– A space filling diagram of the Cu1B dimer of* ***2.21****, with the ligands shown in different shading to distinguish.*

In the packing structure, the large solvent voids are obvious. There is an extensive hydrogen bonding network between the solvate molecules and the main structures. The dimers are packed close together, with π-π stacking interactions between the binding arms of adjacent molecules (3.414Å). Supporting this π-stacking are two hydrogen bonds between the sulfate oxygens and the hydrogens of the binding arms (2.396Å and 2.302Å).

Crystal structure of the complex with $FeSO_4$ ***(2.22)***

After a few days of slow evaporation, several yellow crystals grew on the sides of the vial from a methanol solution containing ligand **2.12** and iron(II) sulfate. Although suitable for X-ray crystallography, these crystals were air sensitive and decomposed after removal from the solvent, only stable for less than a few minutes in oil. The chosen crystal was quickly mounted and relocated into the cold nitrogen stream before too much solvent loss had taken place, giving a reasonable R_1 value of 7.26%. The structure solved in triclinic space group P-1.

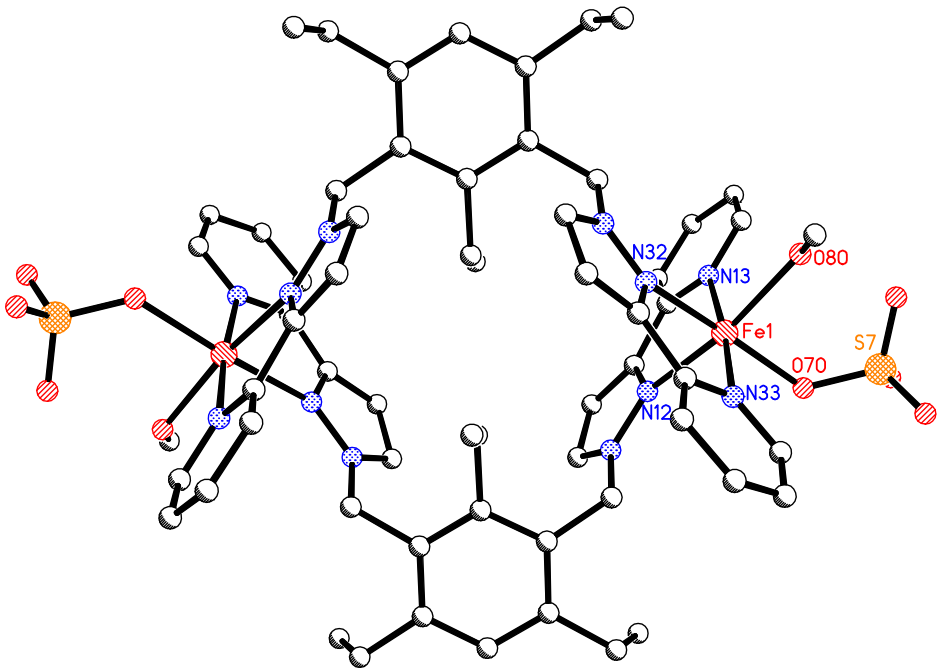

Figure 2.32 *– The M_2L_2 dimeric structure of* ***2.22****. Selected bond lengths (Å) and angles (°): Fe1-O70 2.051(4), Fe1-O80 2.165(4), Fe1-N13 2.178(5), Fe1-N33 2.178(5), Fe1-N12 2.188(4), Fe1-N32 2.196(4), O70-Fe1-O80 91.1(2), O70-Fe1-N13 91.7(2), O70-Fe1-N33 91.8(2), O70-Fe1-N12 91.6(2), O70-Fe1-N32 167.3(2), O80-Fe1-N13 90.7(2), O80-Fe1-N33 92.2(2), O80-Fe1-N12 166.6(2), O80-Fe1-N32 85.8(2), N13-Fe1-N33 175.4(2), N13-Fe1-N12 76.1(2), N13-Fe1-N32 100.6(2), N33-Fe1-N12 100.9(2), N33-Fe1-N32 76.0(2), N12-Fe1-N32 94.3(2).*

The asymmetric unit contains one ligand, one metal atom and one sulfate counterion, along with one coordinated methanol and five methanol solvate molecules. The structure grows into a M_2L_2 macrocycle, as shown in Figure 2.32. Hydrogen atoms, the disorder of the sulfate anion, and solvate molecules are excluded for clarity. There are two metal atoms and two **2.12** ligands in the structure. The iron atom coordinates to two bridging ligands *via* the pyrazole and pyridine nitrogens, one oxygen of the sulfate counterion, and the oxygen of a methanol ancillary ligand with an octahedral geometry. Each ligand bridges two metal atoms, holding each in a binding domain of its arms. The ligands are related by a centre of inversion. The substituents lie in a *aabaa* conformation, with the ethyl group at the 2-position in the centre of the macrocycle sitting opposite to the others, to fit in between the "V-shape" made by the coordinating

arms of the other ligand. The sulfate anion is disordered, 25% of the time sitting in a slightly different position.

This structure is very similar to **2.21**, with the most obvious difference being the geometry of the metal atom. Iron prefers a six-coordinate octahedral geometry instead of the five-coordinate square pyramidal geometry that copper chose in **2.21**, and therefore chooses to bind a methanol to complete its coordinative sphere. Like **2.21**, the ligands sit in the same conformation, with the ethyl group nestled between the "V"-shape made by the arms of its adjoining ligand. Both crystals were air sensitive, and both contain large voids in the structure which are filled with solvate molecules. However the dimers pack differently in each of these structures.

There is extensive hydrogen bonding between the sulfate anions and solvate methanol molecules. This time there is no π-π stacking between the binding arms of adjacent dimers, however there is π-π stacking between the benzene cores of adjacent dimers (3.458Å), whereby these dimers are packed back to back instead of side by side.

Iron(II) has the option of two spin states, high spin (HS) or low spin (LS). The electron configuration it chooses depends on the coordinated ligands and the effect they have on the relative energies of the molecular orbitals.[149,150] The adoption of either a HS or a LS state can also be influenced by temperature. These crystals are a pale yellow colour, indicative of a HS electron state at room temperature. The X-ray data was collected at -180^{o}C. The long bond lengths in the crystal structure of 2.177-2.188Å correspond to a HS state, as does the observation that these crystals do not change colour when immersed in liquid nitrogen.

*Crystal structure of the complex with $CoCl_2$ (**2.23**)*

Slow evaporation of an acetone solution containing ligand **2.12** and cobalt chloride gave large pink crystals. Almost surprisingly, these crystals were air stable, and a single crystal fragment from these stacks of plates was analysed by X-ray crystallography to reveal structure **2.23** in monoclinic space group C2/c.

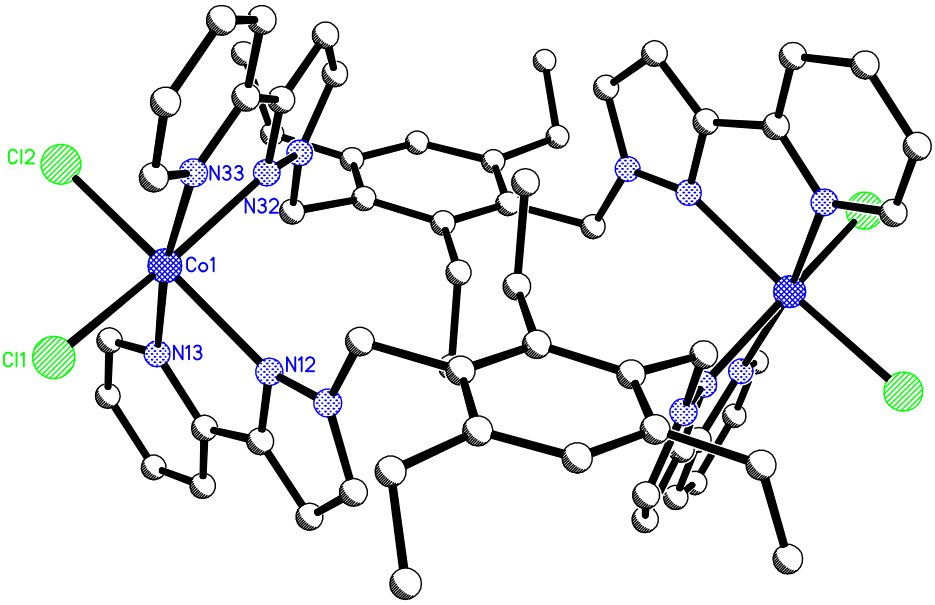

Figure 2.33 *– The M_2L_2 dimeric structure of* ***2.23****. Selected bond lengths (Å) and angles (°): Co1-N33 2.157(1), Co1-N13 2.169(1), Co1-N32 2.210(2), Co1-N12 2.218(1), Co1-Cl2 2.2790(5), Co1-Cl1 2.4080(5), N33-Co1-N13 172.43(5), N33-Co1-N32 75.34(5), N33-Co1-N12 98.69(5), N33-Co1-Cl2 92.42(4), N33-Co1-Cl1 92.09(4), N13-Co1-N32 100.11(5), N13-Co1-Cl2 93.15(4), N13-Co1-Cl1 92.19(4), N32-Co1-N12 92.23(5), N32-Co1-Cl2 84.52(4), N32-Co1-Cl1 167.30(4), N12-Co1-Cl2 167.26(4), N12-Co1-Cl1 87.84(4), Cl2-Co1-Cl1 98.03(2).*

As this structure is so similar to the last few discussed, the structure in Figure 2.33 is shown in a different orientation for variety. Hydrogen atoms and solvate molecules have been omitted for clarity. The asymmetric unit contains one ligand, one cobalt with two chloride counterions, and one and a half acetone solvate molecules. The half acetone lies on a two-fold axis, so three acetones are associated with every dimer. The cobalt atoms are octahedral, bonding to two chlorides and four ligand nitrogens. Each metal atom joins two ligands and each of the two ligands bridges two metal atoms, creating the dimeric structure seen in Figure 2.33. Like **2.21** and **2.22**, the ligand sits in an *aabaa* conformation, with the inner ethyl group sitting inside the "V" made by the coordinating arms of the adjacent ligand. This structure contains less solvate molecules than **2.21** and **2.22**, which may contribute to the higher stability of the crystals.

In the crystal packing, the chlorine atoms have short contacts with other dimeric structures (2.742Å-2.875Å). The oxygen atom on one of the acetones also interacts with

a pyridine hydrogen at a distance of 2.462Å. Dimers are π-π stacked with each other through the binding arms, at a distance of 3.562Å.

*Crystal structure of the complex with $CuCl_2$ (**2.24**)*

Green block-like crystals were obtained after a methanol solution containing ligand **2.12** and copper chloride(II) was left to slowly evaporate over two weeks. These crystals were suitable for X-ray crystallography, even though they started decomposing after removal from solvent, cracking even when submerged in oil. It was a struggle to get a crystal onto the fibre before crystallinity was lost, but eventually a crystal was mounted quickly enough to provide a reasonable diffraction pattern.

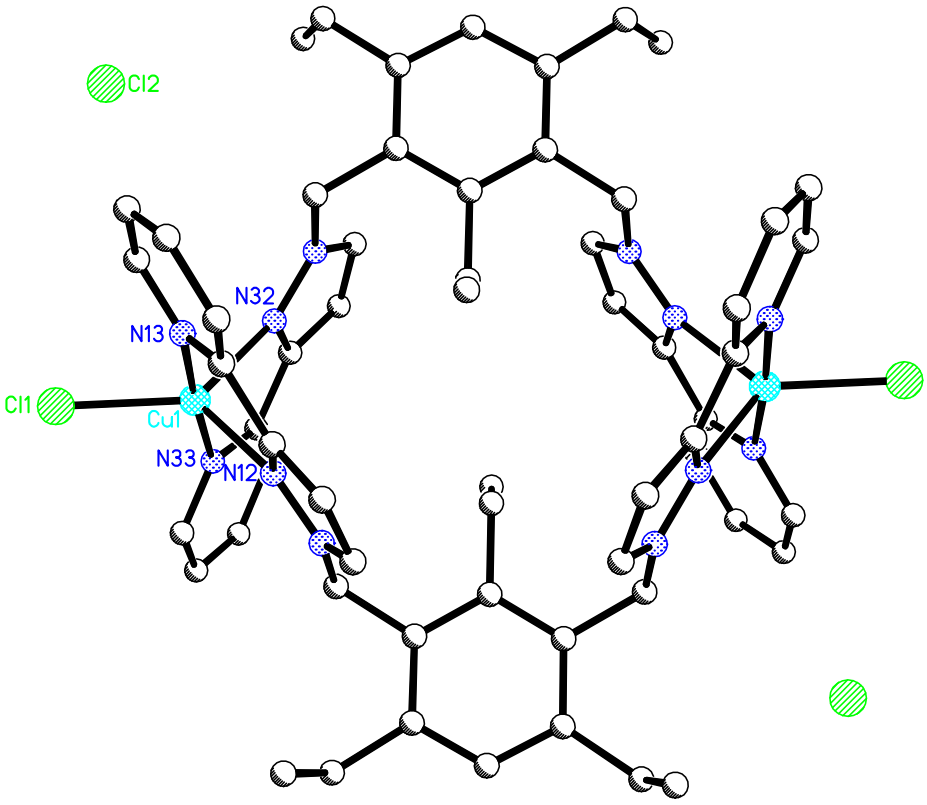

***Figure 2.34** – M_2L_2 dimer **2.24**. Selected bond lengths (Å) and angles (°): Cu1-N33 1.978(4), Cu1-N13 1.985(4), Cu1-N12 2.149(3), Cu1-N32 2.167(3), Cu1-Cl1 2.269(1), N33-Cu1-N13 176.8(1), N33-Cu1-N12 98.4(1), N33-Cu1-N32 79.1(1), N33-Cu1-Cl1 91.6(1), N13-Cu1-N12 79.3(1), N13-Cu1-N32 99.3(1), N13-Cu1-N32 91.6(1), N12-Cu1-N32 106.8(1), N12-Cu1-Cl1 128.1(1), N32-Cu1-Cl1 125.1(1).*

The structure solved in monoclinic space group $P2_1/c$. The asymmetric unit contains one ligand, one copper atom, two chlorides and three methanol solvate molecules. The full dimeric structure is shown in Figure 2.34, with hydrogen atoms and solvate molecules omitted for clarity. Like the majority of the structures already discussed for this ligand, two ligands and two metal atoms form a dimer. The ligand sits in the same *aabaa* conformation seen in the other examples. In this case, the copper atoms bind to four ligand nitrogens, and one chloride anion with a five-coordinate trigonal bipyramidal geometry. Copper(II) can adopt either five-coordinate or six-coordinate geometries, so it is interesting in this case that the copper ion has chosen to only bind one anion, letting the other anion float alone in the crystal lattice. In the previous example, **2.23**, cobalt forms a similar structure but achieves it in an octahedral geometry coordinating both chloride counterions. Given the option, copper(II) has chosen to relax the geometrical constraints imposed by a six-coordinate sphere, suggesting that two chloride ions may be a tight fit against the steric bulk of the ligand arms. An alternative factor is that the ligand may favour an orientation with its limbs at different angles than that provided by an octahedral metal geometry; however the flexibility at the methylene group should allow adjustments in the binding angle without too great an energetic penalty. It seems more likely that a crowded metal sphere is the reason for the five-coordinate geometry in this example. Interestingly, the metal in the $CuSO_4$ structure **2.21** also chooses to bind to five donor atoms, however in a square pyramidal geometry instead of the trigonal bipyramidal geometry seen here. It appears this dimeric topology is reasonably flexible with not only the choice of metal atom but the geometry around the metal centre.

In the crystal packing there are extensive hydrogen bonding interactions between both the chloride anions, the solvate methanol molecules and some of the atoms on the main structure. The dimers are aligned in channels, with strong π-π stacking interactions between the benzene cores (3.357Å) and weaker stacking between the binding arms of alternate ligands (3.590Å).

*Crystal structure of the complex with $Cu(NO_3)_2$ (**2.25**)*

Ligand **2.12** and copper nitrate were mixed in methanol and provided green rectangular block-like crystals after a few days. Like similar crystals described previously, these crystals were very air sensitive, losing solvent and crystallinity within seconds of

removal from the solvent. Immersing the crystals in oil slowed this decomposition process down to a few minutes. Despite these difficulties, a data set of reasonable quality was obtained. Initial analysis showed this crystal to have a similar cell to **2.24** and also solved in monoclinic space group $P2_1/n$.

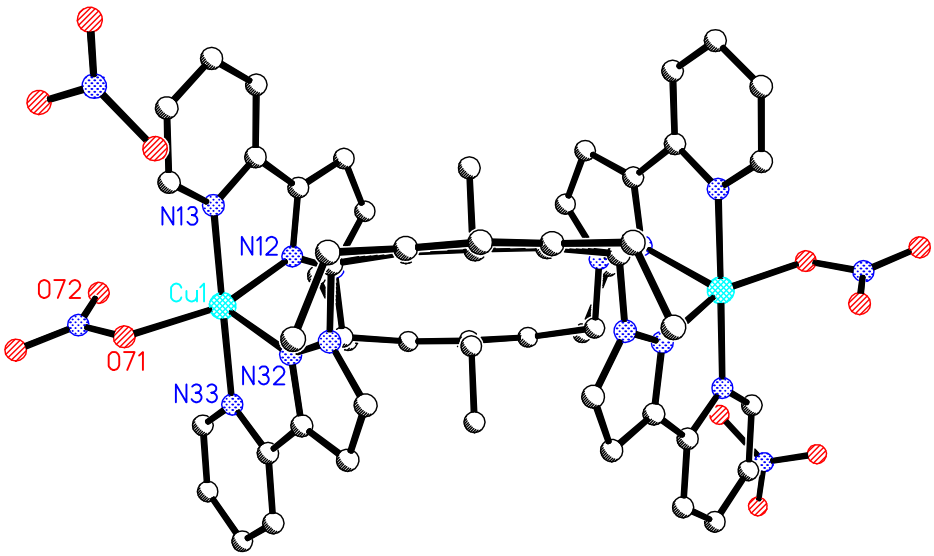

Figure 2.35 *– A view of M_2L_2 macrocycle* ***2.25*** *looking perpendicular to the central benzene rings on the ligands. Selected bond lengths (Å) and angles (°): Cu1-N13 1.983(3), Cu1-N33 1.989(2), Cu1-O71 2.012(6), Cu1-N12 2.073(3), Cu1-N32 2.199(3), N13-Cu1-N33 178.9(1), N13-Cu1-O71 93.6(2), N13-Cu1-N12 80.6(1), N13-Cu1-N32 99.7(1), N33-Cu1-O71 86.3(2), N33-Cu1-N12 99.9(1), N33-Cu1-N32 79.2(1), O71-Cu1-N12 157.1(2), O71-Cu1-N32 97.2(2), N12-Cu1-N32 105.6(1).*

As similar dimeric structures have been shown multiple times, the view of structure **2.25** in Figure 2.35 is shown in a different orientation to emphasise the conformation of the ethyl groups and the geometry of the copper atoms. Excluded from the diagram are hydrogen atoms, the disorder associated with all four nitrates, and seven methanol solvate molecules disordered over fourteen positions. The asymmetric unit contains half of these molecules.

Again two ligands in *aabaa* conformations link together two metal atoms to create a M_2L_2 dimer. Each copper atom coordinates four ligand nitrogens, sitting in the chelating binding domains of two ligand arms of separate ligands. In the fifth coordination site a nitrate oxygen is bonded. A weak interaction also exists from the

copper atom to another nitrate oxygen (2.636Å to O72). The geometry of this copper atom is different to the copper atom in **2.24**, but similar to the geometry of the copper in **2.21**. The second nitrate counterion floats uncoordinated in the crystal lattice, so again the copper atom has chosen a five-coordinate geometry over binding both of its counterions. Both the nitrate anions are disordered. The coordinated nitrate lies in a slightly different orientation 17% of the time, while the uncoordinated nitrate is disordered over two sites each occupied 50% of the time. The surrounding methanol solvate molecules adjust their positions accordingly, also disordered over two positions.

These dimers also pack in channels. There are short contacts between ligand hydrogens and oxygens of the nitrates and solvate methanols. There are π-π stacking interactions between the benzene cores (3.639Å) and between coordinating arms (3.519Å) of alternating dimers.

*Crystal structure of the complex with $ZnBr_2$ (**2.26**)*

Zinc bromide and ligand **2.12** were mixed in methanol. Slow evaporation of this solution over a few weeks yielded colourless blocks. Although perfect for X-ray crystallography, these crystals were very air sensitive, decomposing to powder even when stored in oil. The selected crystal was mounted quickly but had still turned opaque by the time it was placed in the cold nitrogen stream. A data set was collected, which provided a structure but refined poorly, giving a final R_1 value of 9.60%.

The dimeric structure solved in monoclinic space group $P2_1/c$, and is shown in Figure 2.36, with hydrogen atoms and solvate molecules excluded for clarity. The asymmetric unit contains one ligand, one metal ion, two bromide counterions, one coordinated methanol and one and a half solvate methanol molecules and one water solvate molecule. Again two ligands in *aabaa* conformations bridge together two metal ions to form a [2+2] macrocycle. The zinc atom is in a six-coordinate octahedral geometry, coordinating to four ligand nitrogens, and rather surprisingly, binds one bromide anion and one methanol oxygen, while the second bromide anion floats alone in the crystal lattice. It appears that while zinc prefers an octahedral geometry, there is not enough space in its coordination sphere for both bromide ions, so one coordination site is replaced by the smaller methanol ancillary ligand.

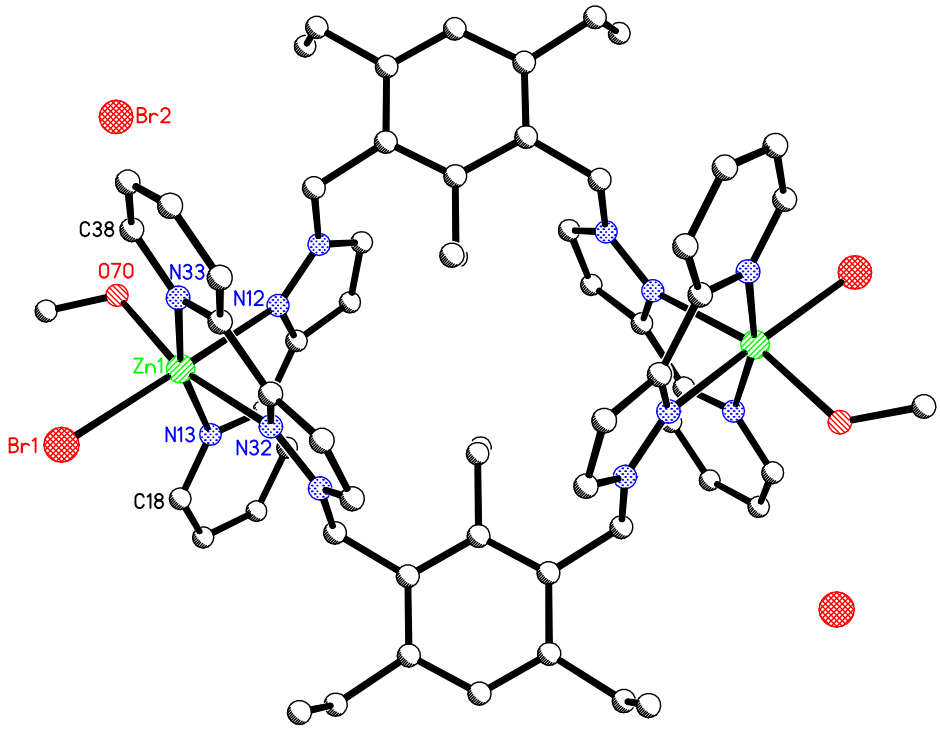

Figure 2.36 *– The M_2L_2 dimeric structure of* ***2.26****. Selected bond lengths (Å) and angles (°): Zn1-N33 2.111(8), Zn1-N13 2.119(8), Zn1-O70 2.175(7), Zn1-N32 2.286(8), Zn1-N12 2.293(8), Zn1-Br1 2.523(2), N33-Zn1-N13 166.3(3), N33-Zn1-O70 97.3(3), N33-Zn1-N32 76.0(3), N33-Zn1-N12 94.0(3), N33-Zn1-Br1 91.9(2), N13-Zn1-O70 91.2(3), N13-Zn1-N32 93.4(3), N13-Zn1-N12 76.6(3), N13-Zn1-Br1 98.3(2), O70-Zn1-N32 166.7(3), O70-Zn1-N12 81.5(3), O70-Zn1-Br1 93.9(2), N32-Zn1-N12 87.4(3), N32-Zn1-Br1 97.8(2), N12-Zn1-Br1 173.0(2).*

So why is the environment around the zinc atom too crowded in this case when zinc often forms octahedral complexes with two cis-bound bromine atoms? A space-filling diagram is shown in Figure 2.37, with nitrogens shown in blue, the zinc atom in pink, methanol oxygen in red, and the bromides in dark green. As the nitrogen donors on the ligand are part of heterocyclic rings, the atoms surrounding the nitrogen also stretch across the environment surrounding the zinc, causing more steric bulk. The main problem is the pyridine ring, where C38 and H38A partially occupy the adjacent binding site. These two atoms are in very close proximity to the large bromide in one of these positions (2.883Å to H38A), however the atoms fit more nicely together when the smaller oxygen atom is attached, as shown in Figure 2.37. This steric hindrance caused by C38/C18 and H38A/H18A is also possibly responsible for copper to choose to

repeatedly adopt five-coordinate geometries in these complexes, also letting an anion roam free.

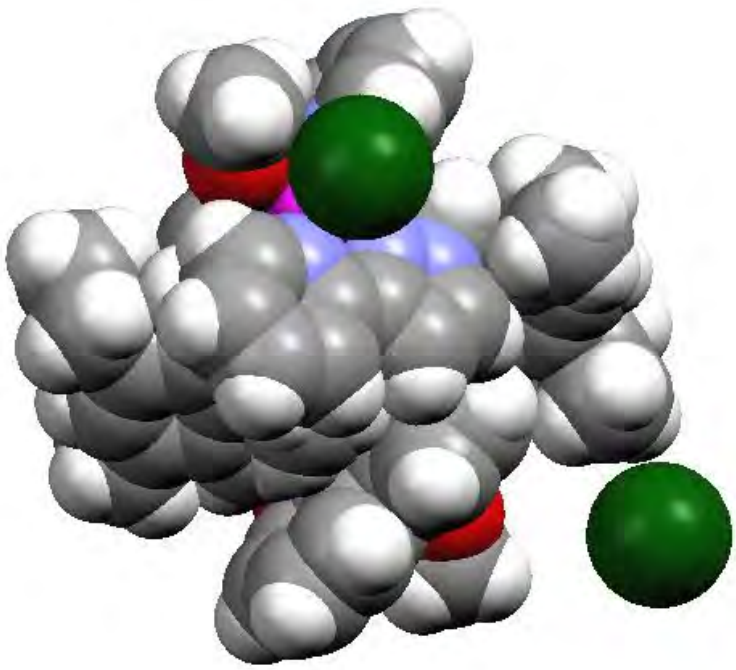

Figure 2.38 *– A space-filling diagram of* ***2.27****, showing the crowding around the zinc atom by the pyridine rings on the ligand.*

The dimers pack similarly to **2.24** and **2.25**, which crystallise in the same space group. The molecules are aligned in channels, with hydrogen bonding interactions between the solvate molecules, both bromide counterions and the main structure. There are also π-π stacking interactions between adjacent molecules, both through the benzene cores (3.395Å) and the coordinating arms of the ligand (3.493Å).

*Crystal structure of the complex with $AgClO_4$ (**2.27**)*

Acetone solutions of ligand **2.12** and $AgClO_4$ were combined, and evaporated to give an oil, which was crystallised by slow evaporation of an acetone and methanol solution over a few months. These colourless plate-like crystals were air stable and suitable for X-ray crystallography, solving in monoclinic space group C2/c.

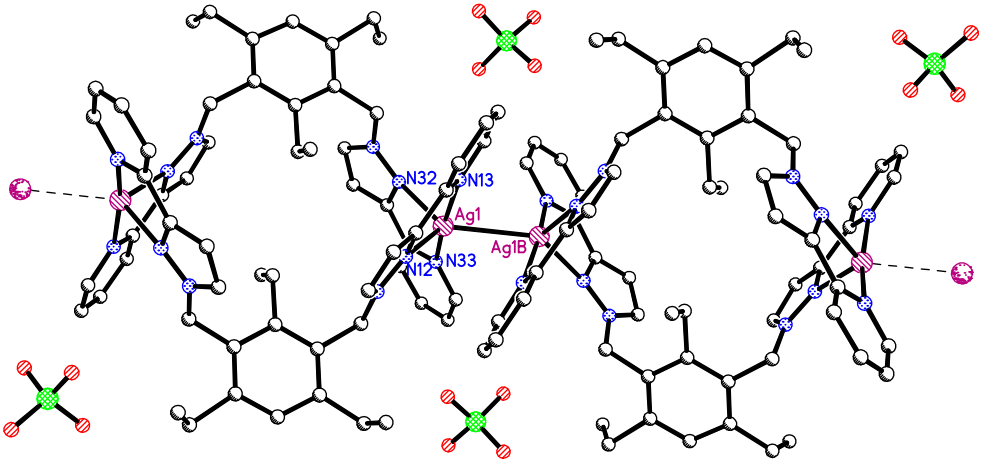

Figure 2.38 *– A section of one-dimensional polymer* ***2.27****. Selected bond lengths (Å) and angles (°): Ag1-N13 2.303(5), Ag1-N33 2.216(5), Ag1-N12 2.338(5), Ag1-N32 2.393(5), Ag1-Ag1B 3.088(4), N13-Ag1-N33 163.3(2), N13-Ag1-N12 72.0(2), N13-Ag1-N32 102.4(2), N13-Ag1-Ag1B 76.3(1), N33-Ag1-N12 124.4(2), N33-Ag1-N32 73.1(2), N33-Ag1-Ag1B 92.8(1), N12-Ag1-N32 120.3(2), N12-Ag1-Ag1B 112.2(1), N32-Ag1-Ag1B 124.2(2).*

A section of the one-dimensional polymer is shown in Figure 2.39. The diagram is idealised – the perchlorates shown have only half occupancy, and the other half occupied perchlorates are badly disordered and so are excluded for clarity. Also omitted from the diagram are the hydrogen atoms, the disordered methanol solvate molecules, and the disorder surrounding the silver atom. The asymmetric unit contains one ligand, one silver, two half occupancy perchlorate anions, one of which is well resolved and sitting on a special position, and the other badly disordered, two partial occupancy methanol solvate molecules, disordered about special positions, and likely a partial occupancy acetone solvate molecule, alternating occupancy with the disordered perchlorate. So formidable is the disorder and partial occupancy of the molecules not shown in Figure 2.38 that the crystallography program *Squeeze*[151] has been used to remove additional electron density and make this structure more manageable. This program deletes all evidence of troublesome electron density attributed to disorder and therefore can be used to ignore the presence of poorly defined anions and solvate molecules. This barely affected the R_1 value.

The structure consists of two silver atoms, bridged by two ligands in *aabaa* conformations to create the dimer unit well identified in this section. However, the

silver atom then makes another bond, to the silver atom of the adjacent dimer. This creates propagation in one dimension and therefore these dimer units are linked together in a polymer chain. Each silver atom coordinates to four ligand nitrogens, chelating into two binding domains, and to one silver atom, in a five-coordinate trigonal bipyramidal geometry. A d^{10} metal, silver(I) is adaptive towards many coordination numbers and geometries.

There is a discrepancy between the actual silver-silver bond distance in this structure. The problem arises as the silver atom is slightly disordered, so the location of the mid-point of the highest occupancy silver atom is difficult to locate. The two versions of this structure treat this disorder slightly different, which is where the discrepancy originates from. In the original 'unsqueezed' structure, the silver-silver distance is 3.088Å, a long distance for this kind of metal-metal bond. However in the 'squeezed' version, the silver-silver distance is 2.876Å. The classification of what distance constitutes a silver-silver bond is heavily debated.[143,152-157] The sum of the van der Waals radii of two Ag(I) atoms is 3.44Å,[125,155] considerably longer than the distances considered here. The interatomic distance between two atoms in metallic silver is 2.889Å.[143,152,154-156] The majority of non-bridged silver-silver distances lie in the vicinity of 2.8-3.3Å,[154] but the longer of these are not usually considered bonding interactions. It has been suggested that a silver-silver length of 2.916Å corresponds to a bond order of a third.[154] Examples of silver-silver distances where bonding is though to occur range from 2.740 to 3.085Å,[152] in which case both the distances obtained for **2.27** would seem to suggest at least a partial bonding interaction is present between the two silver atoms. The silver-silver distance between the highest occupancy atoms in the 'squeezed' version of 2.88(2)Å is less precise than the distance in original 'unsqueezed' version 3.088(4)Å, therefore the longer distance of 3.088Å seems more likely to be correct. Also, since there is doubt in this case, it is more logical to take the value from the data which has not been tampered with by *Squeeze*.[151] This distance of 3.088Å is longer than the bonding distance in metallic silver, but the interaction between the atoms appears to be a bond as the silver atom has a distinct geometry, with the adjacent silver atom making a definite contribution to the coordination sphere of the metal atom. Noteworthy is that this silver-silver interaction is unsupported, as no species is bridging these metal centres and forcing them to bond. The only interaction supporting this bond is π-π stacking between one pair of coordinating ligand arms between the dimers (3.472Å).

This supporting interaction between silver centres has been noted before in the $AgNO_3$ complex of **2.16**, although weaker.[143] The geometry of the silver atom does not allow the other corresponding ligand arms to interact in this way.

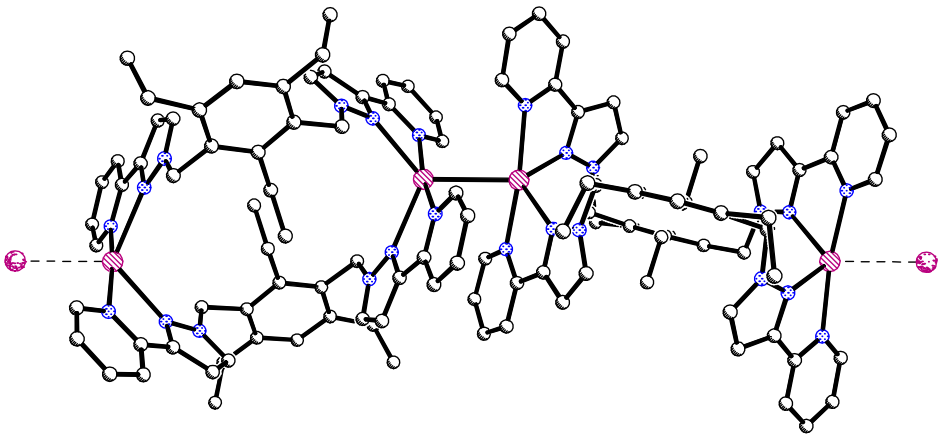

*Figure **2.39** – The undulation of polymer **2.27**.*

Figure 2.39 shows a different view of the polymer. This time all species excluding the polymer backbone are omitted, as well as hydrogen atoms, to give an unobstructed view of the main structure. Each dimer is offset from the previous, which causes the direction

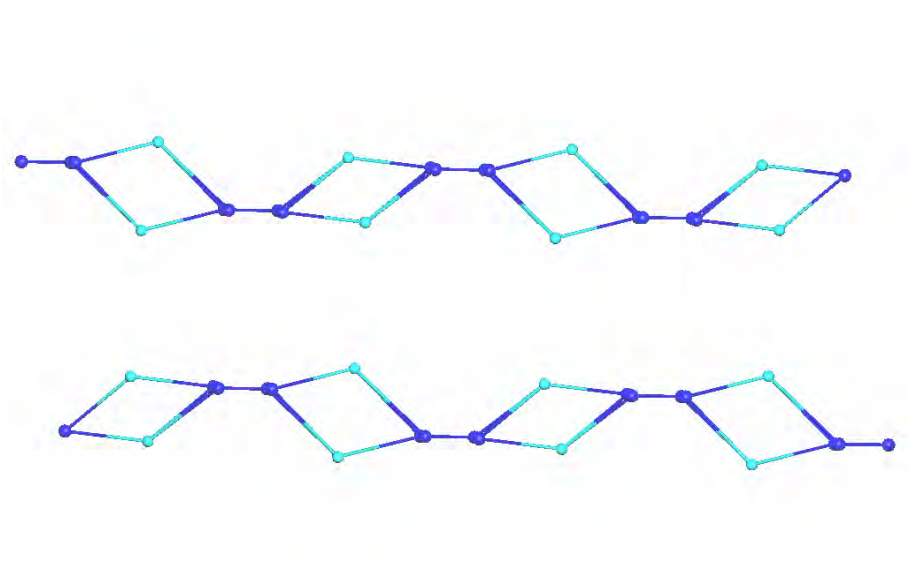

***Figure 2.40** – A simplified diagram of the polymer chains of **2.27** and their undulations in respect to each other.*

of the chain to rock. This rotation of each dimer from the last is necessary to align the aromatic rings for π-π stacking interactions. This curve-like undulation translates down the chain, in repeating units of two dimers. Overall, the chain propagates in a snake-like fashion in one dimension. A simplified view of this undulation is shown in Figure 2.40 for two strands of the structure.

The undulations of one chain is mirrored in the adjacent chains, as seen in Figure 2.40 so large pockets exist in the packing structure, filled with disordered counterions and solvate molecules. These pockets are only visible from one orientation, and form channels through the crystal. In the other dimensions the chains are packed tightly together; however there do not seem to be any strong interactions between the chains.

*Crystal structure of the complex with $Ni(ClO_4)_2$ (**2.28**)*

Nickel perchlorate was dissolved in acetone and added to an acetone solution of ligand **2.12**. Within 24 hours large block-like crystals had formed, which were suitable for X-ray crystallography.

The structure solved in orthorhombic space group Pmmn, and is a M_4L_6 square, as shown in Figure 2.41, with hydrogens, most anions, and solvate molecules removed for clarity. The majority of the species surrounding the main structure are disordered. Mirror planes run vertically and horizontally through the structure, so only a quarter of the structure is present in the asymmetric unit. Four nickel atoms and six ligands make up the main structure. Eight perchlorate anions are also present, however some are disordered and/or partial occupancy over multiple positions which is complicated as the relatively small unit cell constrains the perchlorates to special positions. The same problem is also found with the solvent molecules. Some waters and possibly some acetone is present, but again disorder makes location difficult, and these factors restrain the R_1 value to 10.65%. Disorder problems and high R_1 values are not uncommon amongst large structures of this size.

The square is based on the dimeric unit seen repeatedly in this chapter. Two nickel atoms are bridged by two ligands, each in an *aabaa* conformation. The metal coordinates to four ligand nitrogens, chelating in the binding domain of two separate ligands. This leaves two cis-coordination sites on the metal atom vacant. This allows

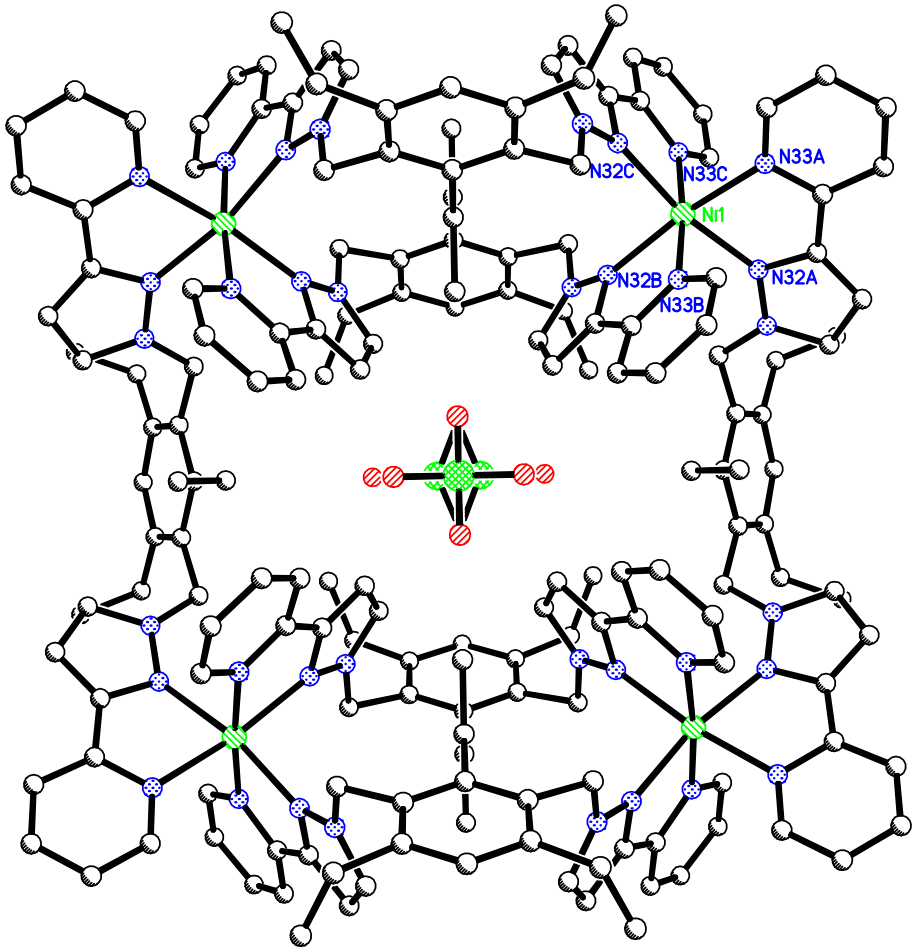

Figure 2.41 *– The M_4L_6 square* ***2.28****. Selected bond lengths (Å) and angles (°): Ni1-N33C 2.068(8), Ni1-N33A 2.089(8), Ni1-N33B 2.096(8), Ni1-N32B 2.107(7), Ni1-N32C 2.120(7), Ni1-N32A 2.125(8), N33C-Ni1-N33A 89.9(3), N33C-Ni1-N33B 174.8(3), N33C-Ni1-N32B 97.8(3), N33C-Ni1-N32C 79.1(3), N33C-Ni1-N32A 95.8(3), N33A-Ni1-N33B 93.9(3), N33A-Ni1-N32B 171.7(3), N33A-Ni1-N32C 92.3(3), N33A-Ni1-N32A 78.7(3), N33B-Ni1-N32B 78.7(3), N33B-Ni1-N32C 97.2(3), N33B-Ni1-N32A 88.5(3), N32B-Ni1-N32C 92.4(3), N32B-Ni1-N32A 97.2(3), N32C-Ni1-N32A 169.7(3).*

another ligand to coordinate to the nickel atom, linking two dimer units together. Another ligand binds on the other side of the dimer, joining together the two dimers and completing the square. The dimers at the top and bottom of the structure are mirror images of each other. The front top ligand reaches over the top of two metal ions, while the front bottom ligand reaches under the bottom metal ions. As each metal ion binds three bidentate groups, each metal ion is a stereogenic centre. Due to the mirror planes,

the square is heterochiral, and possesses two delta and two lambda centres at opposite corners of the square. The linking ligands on the sides of the square are also mirror images of each other. Interestingly, all the ethyl groups are on the same side of these ligands as the binding arms, creating the *aaaaa* conformation that steric bulk was expected to repress. As binding arms of the ligand are substituted in the meta-positions, the ligand has to bridge the metal ions together in an angular fashion. Both ligands are bent in the same direction, which causes the vertical sides of the square to withdraw from the plane of the nickel atoms, as shown in the side-on view in Figure 2.42. Again, hydrogens and selected anions and solvate molecules have been omitted for clarity.

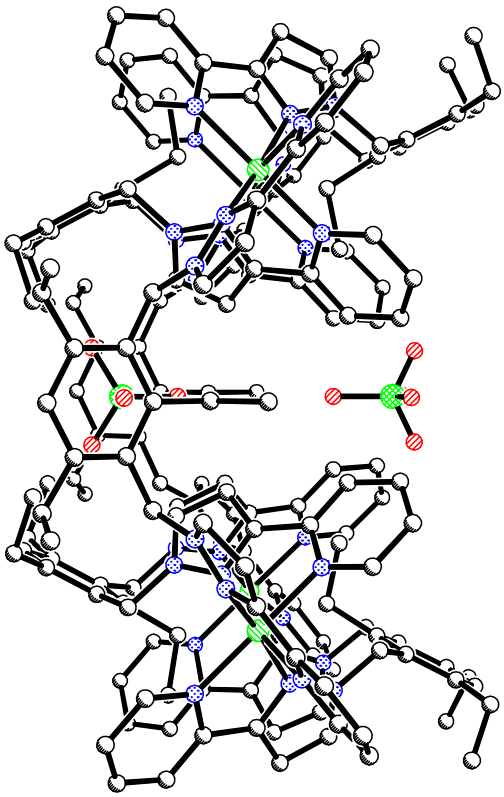

Figure 2.42 *– A side-on view of M_4L_6 square* ***2.28****, showing the bending of the bridging ligands and the positioning of the two perchlorate anions within the centre of the square.*

Two perchlorate anions are shown in both Figure 2.41 and Figure 2.42. These two are shown as they sit in the central cavity created by the square. Both these perchlorates are disordered. The perchlorate to the right in Figure 2.42 shows rotational disorder through

an axis that runs though the chlorine atom and the internal oxygen. This suggests the internal oxygen is interacting while the orientation of the rest of the molecule is less important. The perchlorate to the left in Figure 2.42 shows positional disorder, where two half occupancy anions sit side by side, sharing the positions of three oxygen atoms. This disorder likely occurs as the cavity is slightly too large for the size of the anion, allowing the position of the perchlorate to shuffle horizontally without affecting the rest of the structure.

Both perchlorates are guest molecules inside the cationic host square. As seen in Figure 2.41, one perchlorate does sit in the centre of the void created by the square, but Figure 2.42 shows it sits in the hollow where the linking ligands have withdrawn back from the plane. This anion is still strongly interacting with the structure, filling the pocket created by the bend in the vertical ligands. Figure 2.43 shows space-filling diagrams of the square and its anion guests. Hydrogen atoms and unnecessary counterions are omitted for clarity. Three different views are shown. View a) shows the interaction of this anion with the main structure. Four pyridine rings angle into the centre of the square from each corner, creating a diamond-shaped void in the centre of the square. The perchlorate fills this void with rotational disorder, with oxygens pointing into the corners of the diamond-shaped void at different times. View b) shows the same orientation but the anion of concern removed, so the empty void can be seen. The red oxygen atoms of the other anion can be seen. The void narrows, so is nicely filled by one oxygen arm of the perchlorate.

While the first perchlorate discussed is interacting with the square in a host-guest fashion, the second perchlorate appears to be encapsulated by the structure. This perchlorate sits further back than the first perchlorate, and as seen in Figure 2.42, sits directly between the benzene cores of the linking ligands. Thus it is boxed in on two sides by the linking ligands, and also boxed in top and bottom by the benzene cores of the dimer ligands, and seemingly held in place by the orientation of the ethyl groups.

The space-filling diagrams in Figure 2.43 show how the perchlorate sits in the enclosed cavity in the centre of the square, and the degree of encapsulation surrounding it. View b) shows the front face of the square, with the other perchlorate removed. The perchlorate sits behind the pyrazole rings of the ligand binding arms that run through

a)

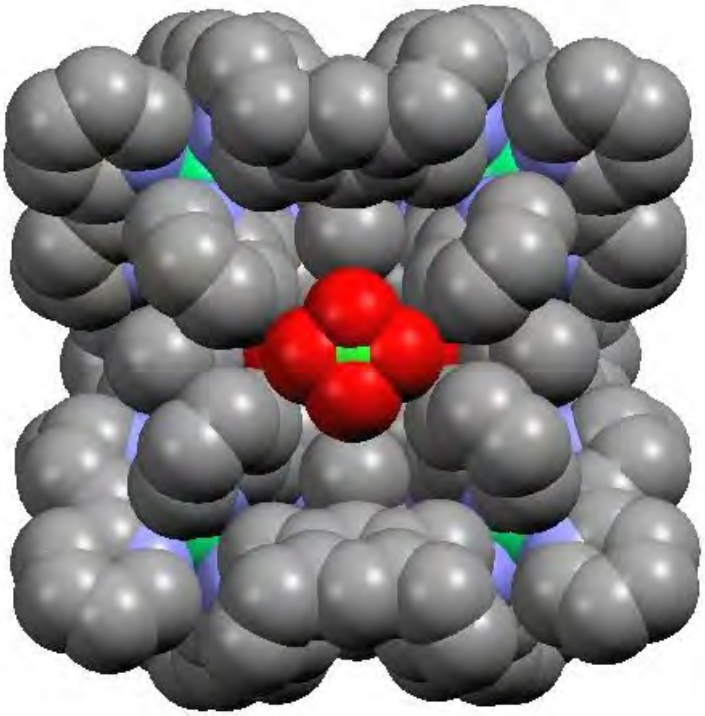

b)

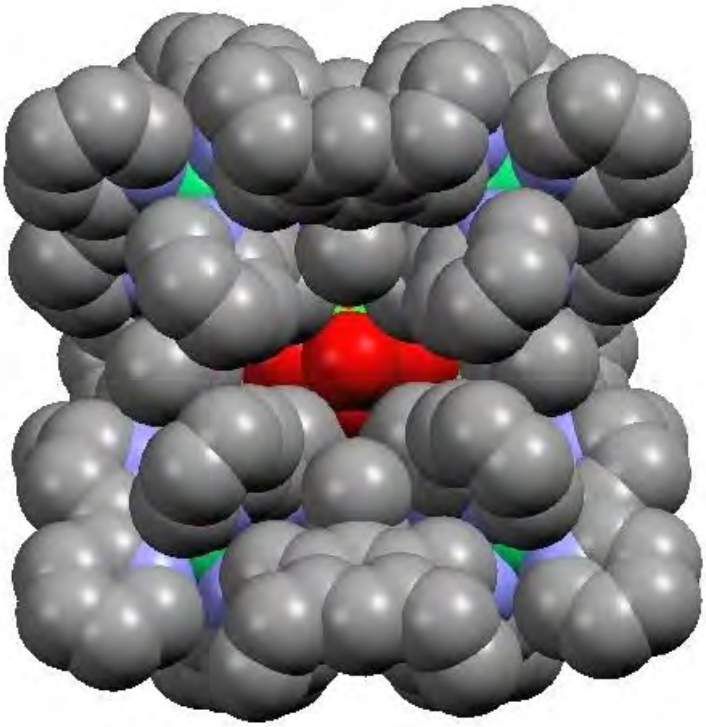

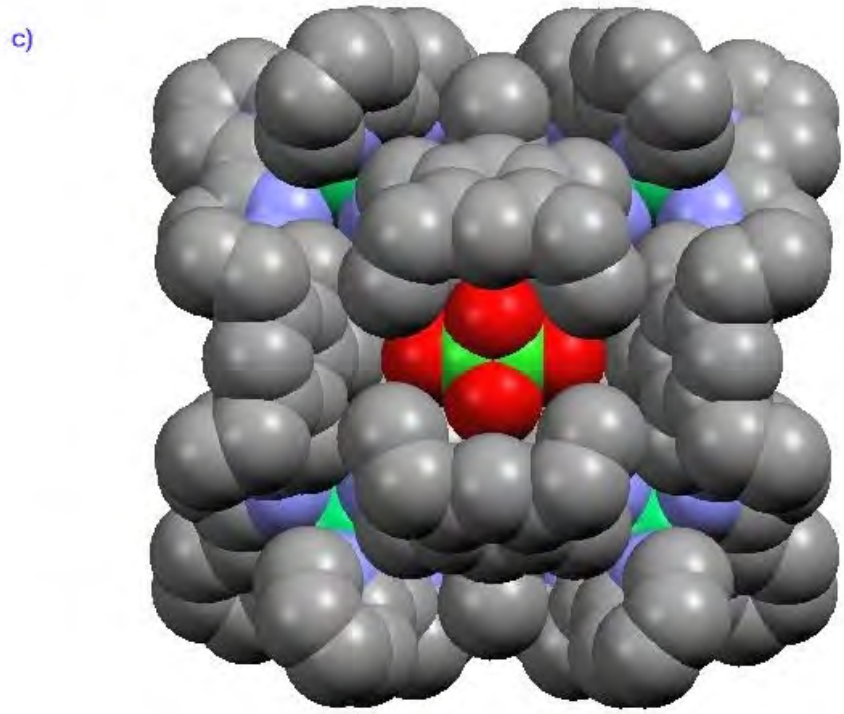

Figure 2.43 *– Space-filling diagrams of M_4L_6 square* ***2.28*** *and its guest anions.* ***a)*** *Looking at interacting anion 1,* ***b)*** *same view, with anion 1 removed so encapsulated anion 2 can be seen* ***c)*** *rotation 180° looking at the degree of encapsulation of anion 2 from the back face of the square.*

the central corners of the square. Also blocking this entrance are two ethyl groups from the top and bottom dimer units. From this view, the window for the perchlorate to escape its cavity is small, and the structure would have to expand for the perchlorate to be removed. View c) shows the orientation from the back face of the square, rotated 180° from view b). The benzene cores from ligands of the top and bottom dimers stretch over the perchlorate, seemingly holding it in place by the orientation of the ethyl groups. From this view the window is rather large; however the perchlorate could not escape from the cavity without difficulty and adjustment of the square, especially considering hydrogen atoms would further narrow the gap. Therefore, the central perchlorate appears to be encapsulated by the square, and the square is acting like a cage. Examples are known where the guest templates the formation of the host structure. As the cavity fits the perchlorate so well, it is possible that the structure was templated by the anion, possibly by organising two dimer units into the correct orientation to allow the linker ligands to form the square. Alternatively, it is possible

that the square formed first, and the perchlorate was drawn into the central cavity as the square breathed to fill the void.

This M_4L_6 square is an isomer of the target compound, a M_4L_6 tetrahedral cage. In both cases the metal atoms are surrounded by three ligand donors of separate ligands, but the connectivity within each of the structures is different. The M_4L_6 cage has the metal atoms oriented at the vertices of a tetrahedron, creating a three-dimensional structure which often encapsulates the corresponding anions. In contrast, the metal atoms in this M_4L_6 structure are located at the corners of a square, a two-dimensional structure that still manages to encapsulate an anion due to the dimensionality added by the ligand. Literature searches have failed to locate structures of a similar nature to the M_4L_6 square, although this topology is identified in smaller structures of this type discussed in Chapter Five.

In the crystal packing, the squares are aligned in channels that run right through the lattice. There are π-stacking interactions between aligned squares, through the benzene cores of ligands in the dimers (3.429Å). Because each dimer consists of one ligand lying up and one lying down, the adjacent ligand cores are perfectly placed for this interaction. The channels of squares are not aligned, and there are no interactions between channels, with disordered anions and solvate molecules filling the spaces.

*Crystal structure of the complex with $Cu(ClO_4)_2$ (**2.29**)*

Acetone solutions of ligand **2.12** and copper(II) perchlorate were combined, and crystallisation occurred almost immediately, with green elongated blocks appearing in solution within ten minutes. The reaction was repeated in the fridge, however the crystals obtained were of poorer quality than the original batch. The original crystals were suitable for X-ray crystallography, providing a very similar cell to **2.28** and solving in Pmmn, but gave a poor R_1 value of only 20.95%.

As expected from the cell constants, **2.29** is isomorphous with **2.28**. A picture of the structure is shown in Figure 2.44, with all hydrogens, counterions and solvate molecules removed for clarity. The poor quality data is obvious from the distortion of the central cores of the linking ligands. Despite this, the structure is proven unambiguously. Again the structure is a M_4L_6 square, containing four copper atoms in octahedral geometries, and six ligands. Unlike earlier examples with copper(II) and ligand **2.12** where the

dimeric complexes were terminated by one counterion bonding to the metal atom to create a five coordinate geometry, in this case two dimeric units are linked by two bridging ligands, to create a square. Perchlorate can weakly coordinate to a metal atom, so it is notable that the discrete dimer with terminal perchlorates is not the product of this reaction. This strengthens the hypothesis that the perchlorate anion may be templating the formation of the square.

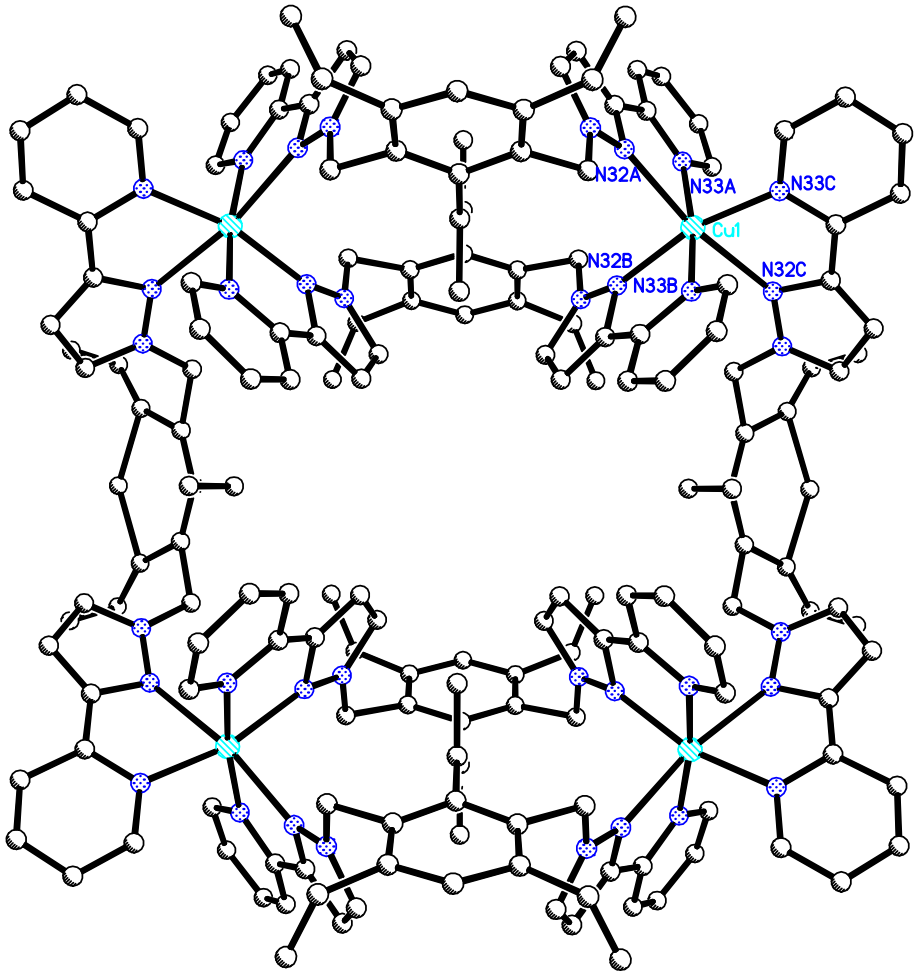

Figure 2.44 *– M_4L_6 square* ***2.29****. Selected bond lengths (Å) and angles (°): Cu1-N33C 2.02(2), Cu1-N33A 2.04(2), Cu1-N33B 2.07(2), Cu1-N32B 2.11(2), Cu1-N32A 2.35(2), Cu1-N32C 2.44(2), N33C-Cu1-N33A 93.0(7), N33C-Cu1-N33B 90.7(7), N33C-Cu1-N32B 166.4(8), N33C-Cu1-N32A 98.8(7), N33C-Cu1-N32C 73.9(8).*

Copper is a more labile metal than nickel, so this probably explains the much more rapid crystallisation process of this square compared with the previous nickel example. Not shown in Figure 2.44 are the two perchlorate anions in the centre of the square. Although more poorly defined, the two anions are in the same positions as in **2.28**.

So is the presence of perchlorate anions templating the formation of the square over the dimer? Octahedral metal ions have been shown to form both dimeric and square complexes with ligand **2.12**, but square complexes only result when perchlorate is used. However perchlorate does not always template the formation of the square, as seen in **2.27**, but silver is not predisposed to an octahedral geometry. A test for this hypothesis is to combine ligand **2.12** with an octahedral metal ion, a coordinating anion, and a perchlorate anion, and observe if a square is formed.

*Crystal structure of the complex with $Co(NO_3)_2$ and $AgClO_4$ (**2.30**)*

Combination of acetone solutions of cobalt nitrate and ligand **2.12** in a 2:3 ratio resulted in a pink precipitate, which dissolved upon addition of silver perchlorate. A few days of slow evaporation yielded orange block-like crystals suitable for X-ray crystallography. A cell check revealed these crystals to have remarkably different cell constants to **2.28** and **2.29**, and the structure solved in triclinic space group P-1.

Rather surprisingly, X-ray analysis showed the product to be another dimer, as shown in Figure 2.45. Hydrogens and the disorder in one of the anions (20% of the time a nitrate resides in the perchlorate position) are excluded. The asymmetric unit contains half the structure. Two cobalt atoms are bridged by two ligands, creating a dimeric structure. The cobalt binds four ligand nitrogens and two waters with an octahedral geometry. Two non-coordinating anions are present for every metal ion, one nitrate and one perchlorate (although 20% of the time the anions are two nitrates). Neither the presence of perchlorate nor two ‘vacant’ cis-coordination sites on the cobalt atom have triggered the formation of the square.

This dimer also differs from the other dimers by the conformations of the ethyl groups surrounding the ligand core. Usually these are oriented in a two up one down fashion, causing an *aabaa* conformation of substituents around the ring. In this case, the internal ethyl group sits in the usual location, opposite to the coordinating arms so it sits in the

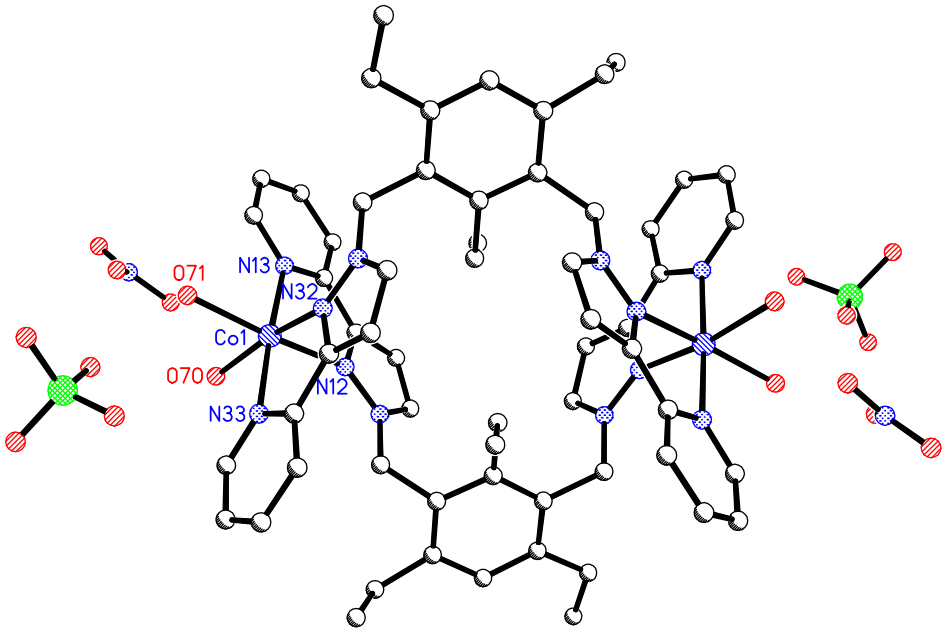

Figure 2.45 *– M_2L_2 macrocycle* ***2.30****. Selected bond lengths (Å) and angles (°): Co1-O71 2.081(2), Co1-O70 2.119(1), Co1-N33 2.121(2), Co1-N13 2.122(2), Co1-N32 2.125(2), Co1-N12 2.141(2), O71-Co1-O70 85.11(6), O71-Co1-N33 92.51(6), O71-Co1-N13 91.07(7), O71-Co1-N32 94.39(6), O71-Co1-N12 166.95(6), O70-Co1-N33 91.22(6), O70-Co1-N13 88.19(6), O70-Co1-N32 168.74(6), O70-Co1-N12 87.35(6), N33-Co1-N13 176.31(7), N33-Co1-N32 77.55(7), N33-Co1-N12 98.29(7), N13-Co1-N32 103.07(6), N13-Co1-N12 78.05(7), N32-Co1-N12 95.07(6).*

"V"-shape made by the binding arms of the adjacent ligand. However, the other ethyl groups have assumed a completely different orientation to all the other complexes of this nature. One ethyl group lies sideways, towards the vacant site on the ring. The other lies in the same orientation as the internal ethyl group, the opposite orientation to where it usually lies. It is unknown why the conformation is different in this lone example.

In the crystal packing, the dimers are aligned in channels. There are extensive hydrogen bonding interactions between anion oxygens and the hydrogens on the main structure. There are close interactions between coordinating arms of adjacent dimers (3.249Å), but no π-π stacking interactions.

In a related experiment, silver perchlorate was added to a solution of ligand **2.12** and zinc bromide. The resulting precipitate was filtered off. Small colourless blocks grew in the filtrate over a few days, and were shown by X-ray crystallography to have the same

cell constants as M_4L_6 squares **2.28** and **2.29**. Unfortunately, the insolubility of silver bromide is a driving force for the anion exchange process, and the bromide is then removed from solution by precipitation, so the formation of the square has not been triggered by the choice of perchlorate over bromide anions. The crystals grown in this experiment were too small to obtain a structure, so this reaction was repeated using commercial zinc perchlorate to confirm the existence of this square.

*Crystal structure of the complex with $Zn(ClO_4)_2$ (**2.31**)*

Ligand **2.12** and zinc perchlorate were each dissolved in acetone and combined to give a colourless solution from which the product started crystallising within an hour (when this reaction was repeated in gently refluxing acetone the solution crystallised almost instantly, suggesting the square is very insoluble and crystallises out as soon as it forms). The colourless blocks were suitable for X-ray crystallography, revealing cell constants very similar to **2.28** and **2.29**, and also solving in orthorhombic space group Pmmn. Several crystals were examined, the final crystal having the best R_1 value of 9.39% (7.11% when disordered anions and solvate molecules are removed by the program *Squeeze*[151]). All these squares are weak diffractors despite growing large crystals, and this is reflected in the poor refinements, along with all the disorder surrounding the squares.

Figure 2.46 shows the structure complete with all eight anions, excluding hydrogens and the disorder surrounding the perchlorates at the top and bottom of the diagram. As expected, the structure is isomorphous with **2.28** and **2.29**. There are four zinc atoms, six ligands and eight anions. The ligands at the top and the bottom of the structure are in *aabaa* conformations and bridge two metal ions, then these two dimers are linked together by ligands in *aaaaa* conformations. The zinc atoms each bind to three different ligands, and each centre is chiral, but overall the square is a meso compound. Like the other structures two perchlorates sit in the centre of the square, one interacting in a host guest manner, displaying rotational disorder, while the other is encapsulated, displaying disorder between two positions. Four of the other anions sit close to the metal centres, the final two above and below the square.

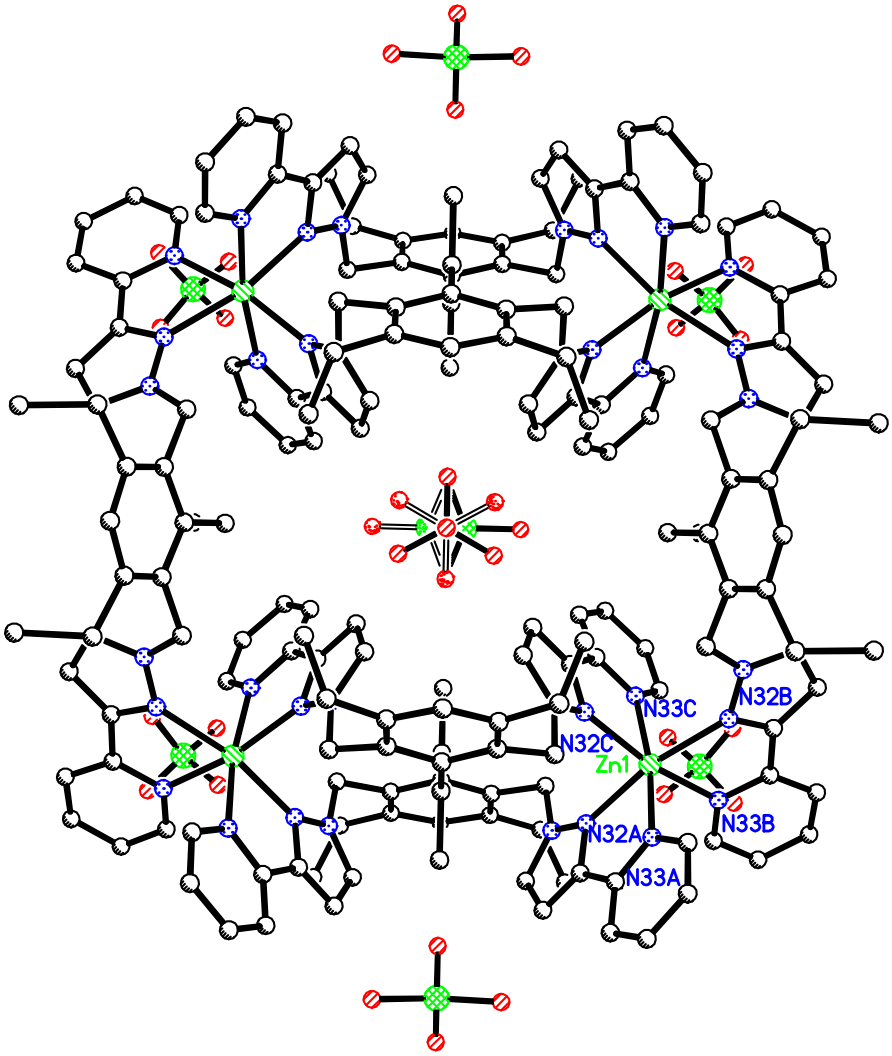

Figure 2.46 *– M_4L_6 square* ***2.31*** *and anions. Selected bond lengths (Å) and angles (°): Zn1-N33A 2.127(4), Zn1-N33C, 2.132(4), Zn1-N33B 2.142(4), Zn1-N32C 2.187(4), Zn1-N32A 2.209(4), Zn1-N32B 2.221(4), N33A-Zn1-N33C 171.9(2), N33A-Zn1-N33B 92.3(2), N33A-Zn1-N32C 97.4(2), N33A-Zn1-N32A 97.0(2), N33A-Zn1-N32B 97.6(2), N33B-Zn1-N32B 76.4(2), N32C-Zn1-N32B 97.7(2).*

*Crystal structure of the complex with $Zn(BF_4)_2$ (**2.32**)*

Zinc tetrafluoroborate and ligand **2.12** were combined in acetone to give a colourless solution, which yielded large colourless blocks by the next morning. These crystals were suitable for X-ray crystallography, and were revealed to have the same cell constants and to solve in the same space group (Pmmn) as **2.28**, **2.29** and **2.31**.

Unfortunately a good refinement of these crystals could not be obtained, with the best crystal only producing a final R_1 value of 21.87%. Despite this, the structure shows unambiguously that the M_4L_6 square can also form with a tetrafluoroborate counterion.

The structure is a M_4L_6 square, as shown in Figure 2.47. A different orientation is shown for variety and to show the central anions. Excluded from the diagram are

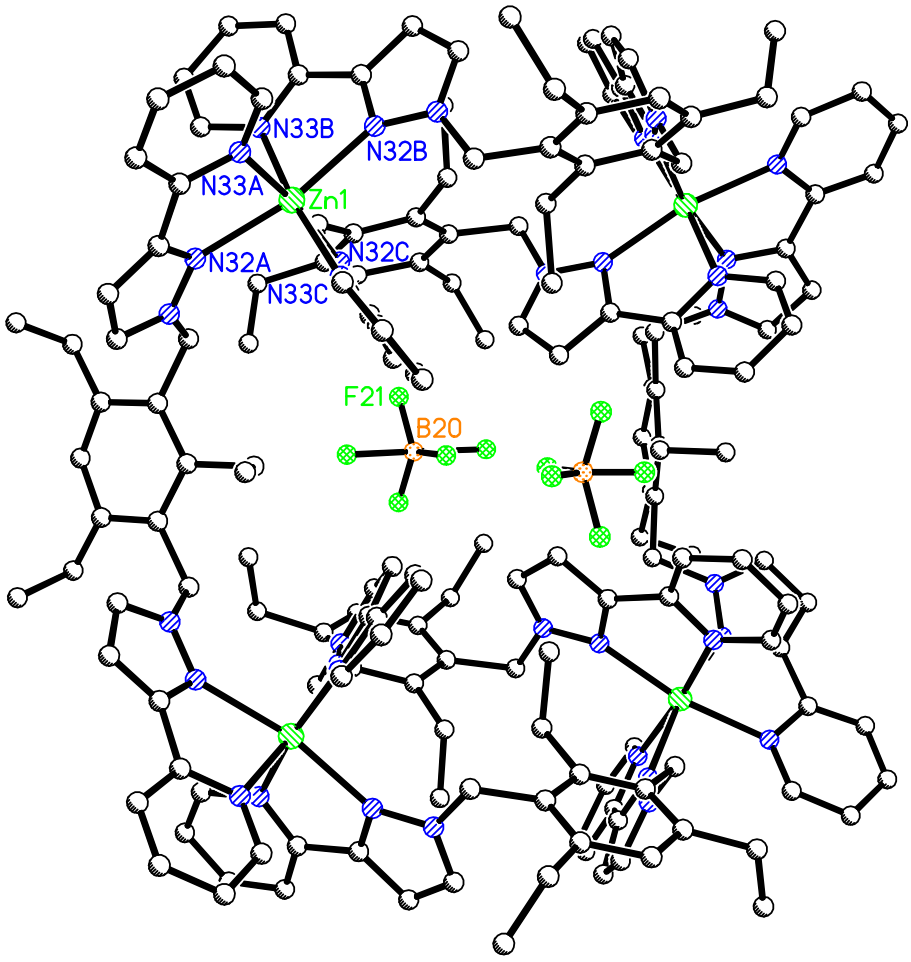

Figure 2.47 *– M_4L_6 square* ***2.32****, showing the central tetrafluoroborate anions. Selected bond lengths (Å) and angles (°): Zn1-N33B 2.08(1), Zn1-N33C 2.13(1), Zn1-N32C 2.157(9), Zn1-N32B 2.19(1), Zn1-N33A 2.14(1), Zn1-N32A 2.23(1), N33B-Zn1-N33C 171.4(4), N33B-Zn1-N32B 76.6(4), N33B-Zn1-N32A 97.9(4), N33C-Zn1-N32C 78.1(4), N33C-Zn1-N32B 97.5(4), N33C-Zn1-N32A 92.9(4), N33C-Zn1-N32A 88.9(4), N32C-Zn1-N32B 93.2(4), N32C-Zn1-N33A 169.5(4).*

hydrogen atoms, the majority of the anions, and solvate molecules. Again, one quarter of the square is present in the asymmetric unit, and the majority of the anions and solvate molecules are disordered about special positions. The square consists of four zinc atoms and six ligands, like two dimer units joined together. The ligands at the top and bottom of the structure are in *aabaa* conformations, and the linking ligands are in *aaaaa* conformations.

Like the perchlorate square, the tetrafluoroborate square contains two counterions in the central cavity of the square. One of the anions sits in the cavity at the face of the structure, with one fluoride arm pointing into the centre of the square and the rest of the anion rotationally disordered just like the perchlorate examples. The other anion sits further back in the centre of the cavity, encapsulated by the components of the structure. Tetrafluoroborate is smaller in size than perchlorate, so it is of no surprise that the central tetrafluoroborate is even more disordered than the perchlorate in the other squares. The fluoride arms are disordered over five sites, and the axial arms appear to stretch to implausible lengths. In reality the anion may be located in two positions side by side to each other. The central boron atom probably does not lie where it is plotted in the diagram, but alternates in positions to the left and right. The central three fluorides are probably always located where they are drawn, but the boron and the axial fluorine alternate between the left and right positions. The boron atom is simulated at the centre of the disorder due to special position complications.

*Crystal structures of the complexes with $Fe(ClO_4)_2$ (**2.33** and **2.34**)*

Iron(II) perchlorate and ligand **2.12** were combined in acetone and yellow block-like crystals started appearing after 24 hours. These were suitable for X-ray crystallography and provided the same cell constants as the other M_4L_6 complexes. The structure also solved in orthorhombic space group Pmmn. Like the other structures, this large crystal was a poor diffractor, and the final R_1 value sits at 9.25% for the 'squeezed' version where residual electron density from disordered counterions and solvate molecules is removed. Without *Squeeze*,[151] the R_1 value is 13.10%.

The M_4L_6 square is shown in Figure 2.48 in a different orientation to help show the disorder in the central anions. The other perchlorates, solvate molecules and hydrogens are excluded for clarity. This structure is isomorphous with the other metal perchlorate

squares discussed. Four octahedral iron atoms are bound together by six ligands, in a square-like arrangement. As the same ligands link every metal atom, the length of each side are very similar, except that the linking ligands are stretched slightly further than in the dimer ligands. Thus the Fe1-Fe1B length across the dimer is 9.594Å, whereas the Fe1-Fe1A length across the linking ligand is 10.745Å. The diagonal distance from Fe1-Fe1C is 14.404Å.

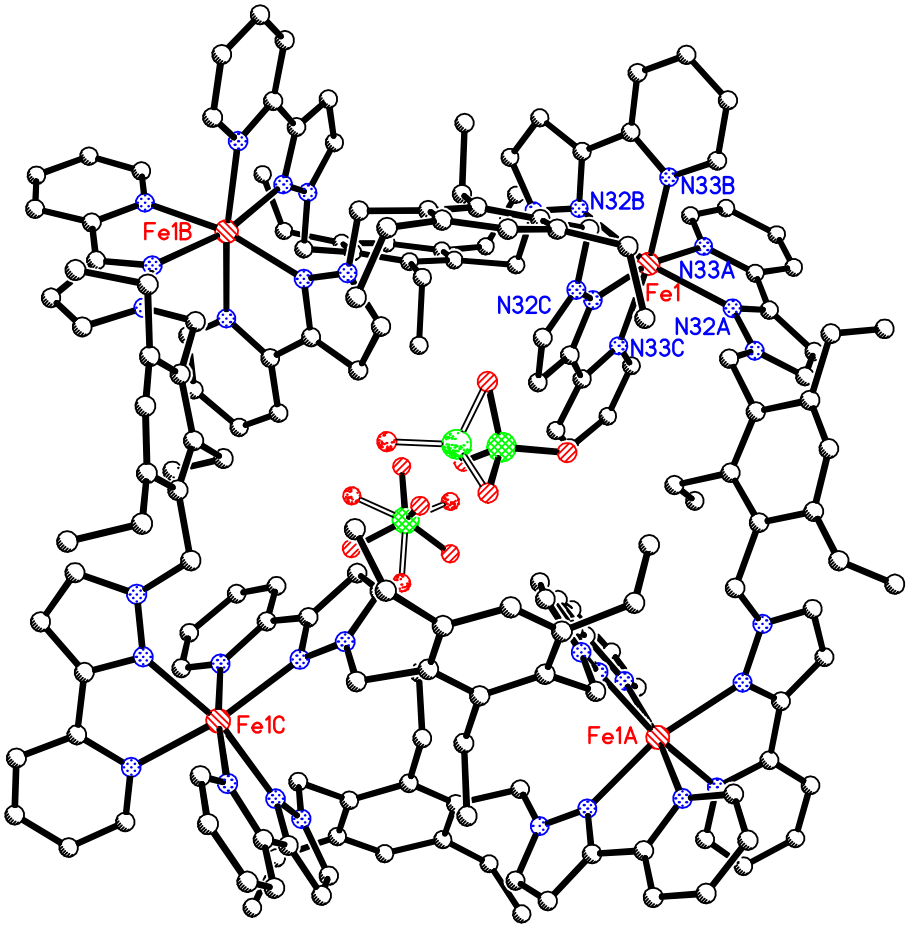

Figure 2.48 *– M_4L_6 square* ***2.33****, showing the disorder of the central anions. Selected bond lengths (Å) and angles (°): Fe1-N33C 2.143(8), Fe1-N33A 2.145(8), Fe1-N33B 2.140(9), Fe1-N32C 2.143(7), Fe1-N32B 2.171(7), Fe1-N32A 2.176(8), N33C-Fe1-N33A 93.0(3), N33C-Fe1-N33B 173.3(3), N33C-Fe1-N32C 76.9(3), N33C-Fe1-N32B 98.1(3), N33C-Fe1-N32A 88.3(3), N33A-Fe1-N33B 91.7(3), N33A-Fe1-N32C 168.9(3), N33A-Fe1-N32B 92.4(3), N33A-Fe1-N32A 76.2(3), N33B-Fe1-N32C 98.7(3), N33B-Fe1-N32B 76.9(3), N33B-Fe1-N32A 97.5(3), N32C-Fe1-N32B 93.5(3), N32C-Fe1-N32A 98.6(3), N32B-Fe1-N32A 167.3(3).*

Like the other structures, two perchlorates lie in the centre of the square. One perchlorate, shown in the background of Figure 2.48, interacts in a host-guest manner, with one oxygen pointing into the central cavity, with the other oxygens rotationally disordered. The other perchlorate, shown in the foreground, is disordered over two sites, just like the tetrafluoroborate in the last example.

Iron(II) can rest in a high spin (HS) or a low spin (LS) state. These crystals are pale yellow, indicative of a HS state. The X-ray data were collected at -180^{o}C, a temperature difference sometimes great enough to flip the iron centres into a LS state. However the bond lengths in the structure (2.137Å -2.180Å) are characteristic of a HS state. A final test was undertaken, to see if the colour of the crystals darkened upon submersion in liquid nitrogen. A colour change to dark purple is characteristic for a spin-crossover complex. The crystals did not change colour that dramatically; however, the crystals did darken from pale yellow to dark orange. As some Fe(II) complexes surrounded by bidentate nitrogen donors are known to exhibit spin-crossover properties, a sample of the Fe_4L_6 square was sent to Prof. Keith Murray and his research group at Monash University for further analysis.

The results are shown in Figure 2.49. The plot shows that **2.33** is HS over the temperature range 2-300K and very weakly coupled, typical of an octahedral d^6 $^5T_{2g}$ ground state.[158] A spin crossover complex would show a sudden drop in μ_{eff} when the critical temperature is reached, and a spin state switch is initiated. Unfortunately, the square itself does not show spin crossover properties. However the graph shows that the crystals are doped with a small amount of a substance which does show spin crossover.[158] It is not known what this contaminating substance is. Spin crossover properties are very sensitive to the anion present and the amount of water in the crystal lattice, so it is possible that subtle changes to the complex like anion exchange may initiate crossover.[158-160]

The absence of spin crossover capabilities is interesting. Fe[3-(2'-pyridyl)pyrazole]$_3$(ClO_4)$_2$ displays crossover, as do the BF_4^-, PF_6^- and $CF_3SO_3^-$ salts.[159,160] Therefore, in the case of the Fe_4L_6 square, the attachment of the 3-(2'-pyridyl)pyrazole units to a benzene core must have weakened the ligand field around each iron centre.[158]

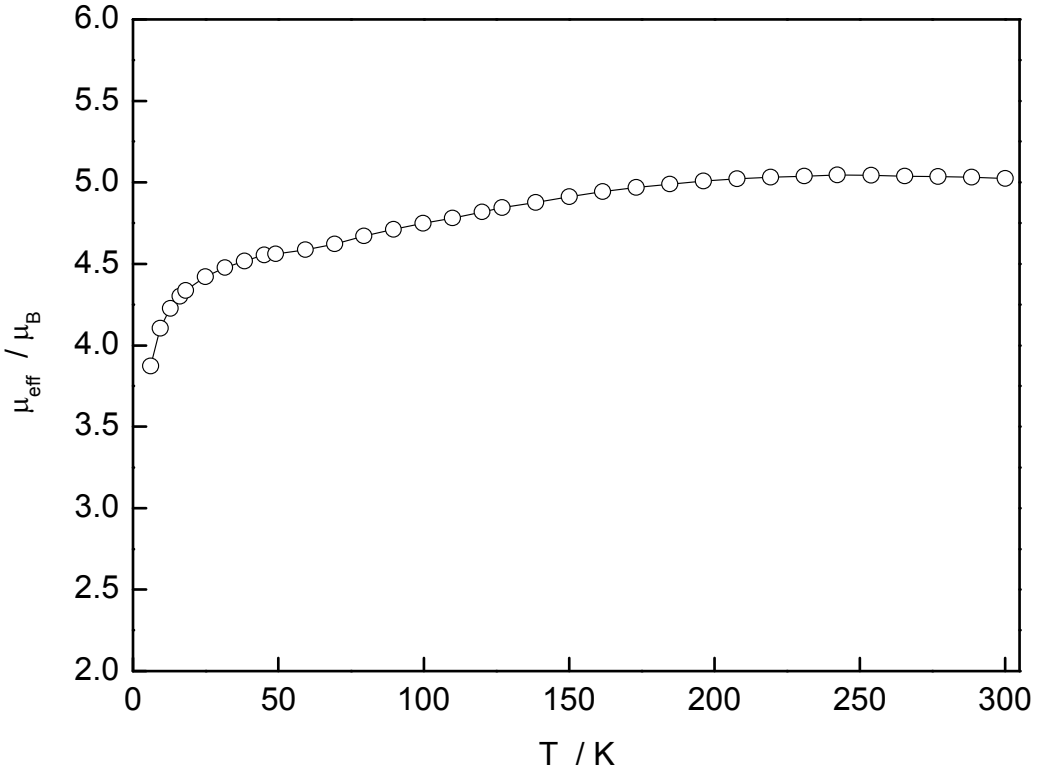

Figure 2.49 *– The lack of spin-crossover properties of M_4L_6 square* ***2.33****.*

The biggest surprise was unveiled when a second batch of the Fe_4L_6 square was synthesised, by repeating the initial procedure at greater concentration. Once again a metal to ligand ratio of 2:3 was used. Crystals did not appear within the 1-2 day mark as expected, and when crystals did appear, after a week, the yellow octahedra did not resemble the rectangular blocks originally obtained. The vial was placed in the fridge overnight, after the first few octahedra appeared in solution, but this did not seem to induce more cystallisation. Within the next few days many more octahedral crystals formed, followed a few days later by large messy blocks that appeared to be stacks of plates. These blocks were not suitable for X-ray analysis, and were very air sensitive. However elemental analysis suggests they may have the same chemical composition as the octahedral form, which was suitable for X-ray crystallography. The cell constants for these new crystals were very different from the square, and solved in orthorhombic space group Cmca.

The structure is shown in Figure 2.50, excluding the hydrogens, the disorder surrounding the coordinated acetones, the disordered perchlorate counterions, and the solvate acetone molecules for clarity. The asymmetric unit contains half a ligand, half an iron atom, a disordered coordinated acetone, two half disordered perchlorates, and half a solvate acetone. The coordinated acetones are each disordered over two sites with half occupancy. One acetone always sits towards the middle and one always points away. One perchlorate is rotationally disordered, the other is slightly positionally disordered, which probably corresponds to the location of the coordinated acetone. The solvate acetone is well behaved.

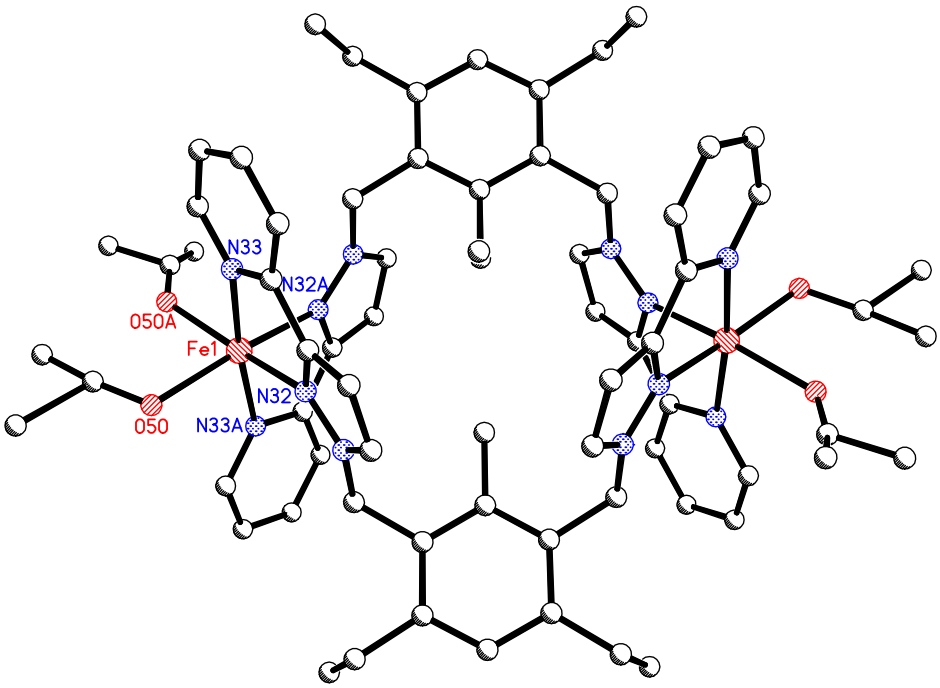

Figure 2.50 *– The M_2L_2 dimer* ***2.34****, crystallised from the same procedure which initially produced M_4L_6 square* ***2.33****. Selected bond lengths (Å) and angles (°): Fe1-O50 2.110(4), Fe1-N32 2.137(3), Fe1-N33 2.152(3), O50-Fe1-N32 90.8(2), O50-Fe1-N33 92.5(1), N32-Fe1-N33 76.7(1), O50-Fe1-N32A 166.9(1), O50-Fe1-N33A 91.5(1), N33A-Fe1-N33 174.6(2), N32A-Fe1-N33 99.6(1), N32-Fe1-N33A 99.6(1), O50A-Fe1-O50 84.0(3).*

The complex is a M_2L_2 dimer, not the M_4L_6 square previously synthesised by this same procedure. The dimer resembles the majority of the other dimers formed upon complexation of ligand **2.12** with metal atoms and coordinating anions. Two iron atoms

are bridged by two ligands. Unlike all the other dimers, the ligand lies in an organised *ababa* conformation, with all the ethyl groups lying on the same side of the benzene core. The internal ethyl group still lies in the "V"-shape formed by the coordinating arms of the adjacent ligand. The iron is six-coordinate, binding to four ligand nitrogens, and surprisingly, two acetone oxygens. Acetone is a very weak ligand, and it is very surprising that the metal atom has chosen to coordinate two acetones over the chelating binding domain of another ligand to form the Fe_4L_6 square.

In the crystal diagram the dimers are aligned in channels running through the lattice. The perchlorate oxygens and the solvate acetone oxygen make close contacts with hydrogens on the binding arms of the ligand. There are π-π stacking interactions between pyridine rings of separate dimers (3.435Å).

It is logical and straightforward to suggest that octahedral metal ions with coordinating anions form dimeric structures with ligand **2.12,** as the tendency for the anions to coordinate is a stronger driving force than the coordination of an extra binding domain to the metal to form the square. Likewise, if a non-coordinating anion is present, then the octahedral metal will prefer to use the vacant cis-coordination sites to bond to another chelating ligand to form the square. To take this a step further, based on the good fit of the perchlorate anion inside the cavity of the square, it is possible that the presence of this anion helps template the formation of the square.

This crystal structure, along with that of **2.30**, complicates this story. In both examples, weak monodentate ligands occupy the vacant cis-binding sites on the metal atom, which should be very easily substituted with a chelating binding domain of the ligand. However, for some reason the extra ligand chooses not to bind. In both examples perchlorate anions are present, which have not templated the formation of the cage as predicted. And the formation of the dimer from the same procedure that initially produced the square suggests more kinetic and thermodynamic factors must influence which product crystallises out, and there must be a fine balance between which product is favoured.

When the procedure to form the Fe_4L_6 square was repeated, the same starting materials were used. The same metal to ligand ratio was used each time, a 2:3 ratio to favour formation of the square. It is possible, since $Fe(ClO_4)_2$ is hygroscopic, that one sample

might have been slightly wet, so maybe slightly less metal salt was used in one of the preparations, in which case the relative excess of the ligand may encourage formation of the square. When the square was formed, the metal solution was added to the ligand solution, but when the dimer was formed, the ligand solution was added to the metal solution. As no product forms for at least a day and the same solvent was used so the solution was fully mixed, this should be irrelevant. Much less solvent was used when the dimer was formed. This higher concentration should lower the solubility and favour the formation of the least soluble product, and should also favour the formation of the larger macrocycle over the smaller dimer. However the crystals took longer to form than when the solution was much more dilute. Finally, as these reactions were undertaken on different days, the room temperature may have been different enough to favour the formation of one product over the other. The solution which yielded the dimer was placed in the fridge overnight, but only after the first crystals of the dimer had already appeared. Lower temperatures should favour the kinetic product by reducing the solubility of the intermediates on the way to the thermodynamic product. In summary, there do not seem to be any outstanding differences between the syntheses that explain the formation of the dimer over the square.

To try to isolate the defining factor which triggers the formation of dimer or square, the procedure that formed the dimer was repeated exactly. This concentrated solution was then split into three portions. Portion a) was left at room temperature untouched, and was expected to yield the dimer. Portion b) was left in the fridge, to determine if the lower temperatures would encourage formation of the square, or if the dimer would still form. Portion c) was diluted three-fold and left at room temperature, and expected to yield the square. Surprisingly, all the vials yielded the square, portion a) within two hours, and portions b) and c) overnight. As portion a) was an exact repeat of the conditions which yielded the dimer, it seems the formation of the dimer by this route may not be reproducible.

It seems reasonable that the square is the kinetic product, which crystallises out first due to lower solubility than the dimer, which is the thermodynamic product due to its higher entropy. Typically squares are thermodynamic products, the synthesis of which is often only achieved at high temperatures.[45] It seems obvious in this case that the formation of the dimer unit is the favoured product of the reaction, where there is a delicate balance

between it and the square. While the square gains enthalpy by the substitution of the weakly binding ancillary ligands with a ligand chelating binding domain, it does so at the cost of entropy, as more components make up the square.[45] Therefore the dimer and the square may be in equilibrium in solution, with very little thermodynamic energy difference between them.[45]

*Other complexes with ligand **2.12***

Complexation of ligand **2.12** was attempted with a wide variety of metal salts, namely CuI, $CuBF_4$, $CuSO_4$, $Cu(NO_3)_2$, $CuCl_2$, $Cu(ClO_4)_2$, $AgClO_4$, $CoCl_2$, $CoBr_2$, $Co(BF_4)_2$, $Co(PF_6)_2$, $Co(NO_3)(ClO_4)$, $FeSO_4$, $Fe(ClO_4)_2$, $Ni(ClO_4)_2$, $ZnBr_2$, $Zn(ClO_4)_2$, $Zn(BF_4)_2$, $Cd(ClO_4)_2$ and $La(NO_3)_3$. Luckily the majority of these products crystallised, leaving no ambiguity about their structure. These structures have already been discussed in this chapter. Most of the complexes which did not crystallise were not analysed further.

Of the fifteen crystal structures obtained of complexes of this ligand, ten are M_2L_2 dimers of a particular type. The majority of these crystals were air sensitive, so it is not surprising that the solvate molecules seen in the crystal structures are not seen in the elemental analysis results. Instead, water has often been absorbed into the compounds.

The $FeSO_4$ dimer **2.22** only crystallised as a few crystals on the side of the vial. The bulk precipitate obtained is a different compound. Elemental analysis results suggest a M_2L compound, which is probably discrete.

The M_4L_6 squares are much more air stable than the dimers, but also slowly lose solvent over a time period of days to months. According to elemental analysis they too absorb water from the atmosphere, anywhere from four to fourteen water molecules per square. This suggests thermogravimetric analysis on these compounds could be interesting, as the crystals may contain pores in the lattice for guest exchange.

Reaction of ligand **2.12** with $CoBr_2$ and NH_4PF_6 produced a precipitate which analysed as $CoL(PF_6)_2$, so is likely a dimeric species again, and not a square containing the PF_6^- counterion as hoped. Similarly, reaction of ligand **2.12** with $CdCl_2$ and $AgClO_4$ precipitated AgCl, but the product obtained analysed as $CdLCl_2$, which again appears to be a dimeric species and not a square, even though all the chloride ions should have been precipitated.

The product of reaction of ligand **2.12** with $La(NO_3)_3$ was shown by elemental analysis to have a stoichiometry of M_3L_2. This is unlike any product identified by crystallography, but not surprising considering the different coordination nature of the lanthanides.

1,3-Di(4-pyridylsulfanylmethyl)-2,4,6-triethylbenzene (2.35)

The third ligand synthesised from precursor **2.2** is shown in Scheme 2.4. A base-catalysed reaction substitutes mercaptopyridine groups onto the benzene core in 52% yield after purification. Obtained is a two-armed ligand with two mono-dentate binding sites to use as a synthon in metallosupramolecular chemistry.

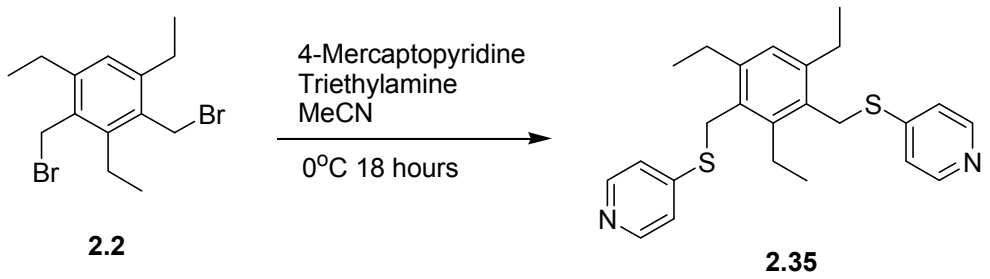

2.2 **2.35**

Scheme 2.4 *– The synthesis of ligand* ***2.35****.*

Unlike the other ligands discussed so far, ligand **2.35** is based primarily on a pyridine heterocycle as the donor group. Ligand **2.35** varies from ligands **2.4** and **2.12** in the orientation of the donor atoms, with the nitrogens pointing directly out from the ligand core, as opposed to the sideways orientated binding sites of the other ligands which bring the metal atom closer to the central core of the ligand. These small changes in orientation should make ligand **2.35** a much different building block than the ligands already discussed. Ideally, the angle imposed between the binding nitrogens by the meta-substitution of the central core will encourage the formation of closed cage-like structures over coordination polymers.

Shown in Figure 2.52 are ligands displaying structural similarities to ligand **2.35** which have been used as synthons for metallosupramolecular chemistry. Ligands **2.36** to **2.38**[161-164] have 4-pyridine units attached to meta-positions on the benzene (or pyridine) core *via* two linker atoms, like ligand **2.35**. However the amide groups constrain the

conformations these ligands can adopt more than the methylsulfanyl linkers used in ligand **2.35**. The electronic and steric environments within the ligands are also much different, but it is still possible that they may form similar structures. Ligand **2.36** forms M_2L_2 macrocycles with Ag(I) salts with various anions,[161] ligand **2.37** M_2L_2 macrocycles with $Pd(CF_3SO_3)_2$,[163] and ligand **2.38** either M_2L_2 macrocycles, or one-dimensional zigzag polymeric chains, depending on the ancillary ligands also attached to the $Pd(CF_3SO_3)_2$ complex.[163,164]

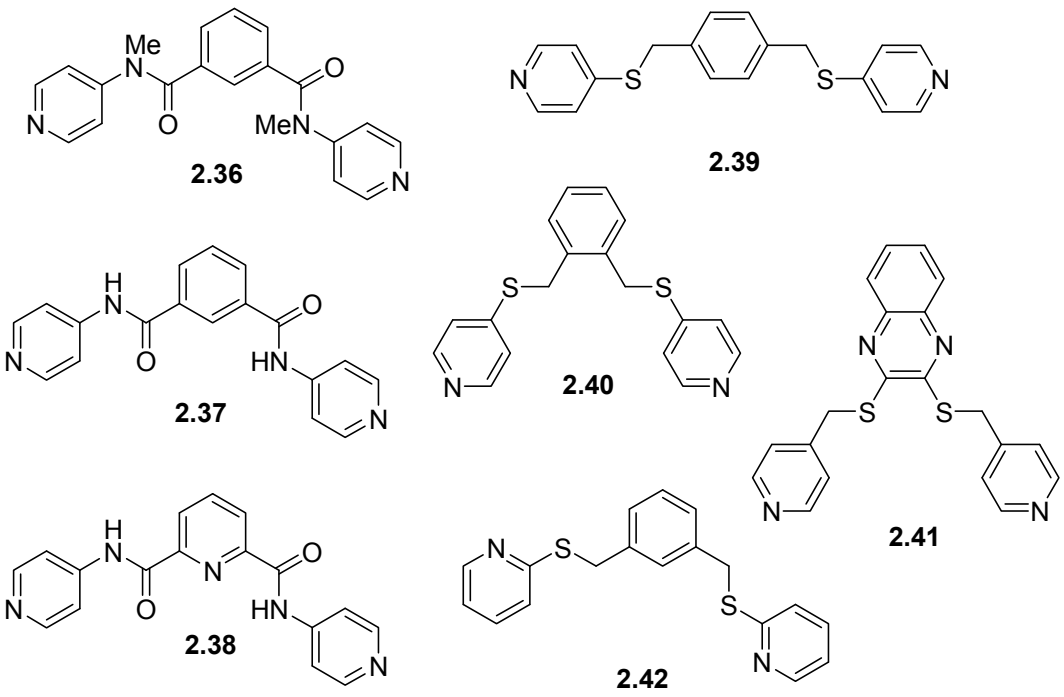

Figure 2.52 *– Similar ligands to* ***2.35****.*

Ligand **2.39**[165] differs from ligand **2.35** by having its 4-pyridylsulfanylmethyl groups para-substituted on a benzene core, and is reported to form one-dimensional and two-dimensional polymers with many cobalt, nickel, and copper salts.[165] Ligands **2.40**[166-168] and **2.41**[167] contain ortho-substituted 4-pyridylsulfanylmethyl groups. Ligand **2.40** forms M_2L_2 macrocycles with $AgClO_4$,[166,167] and a one-dimensional chain with $CuBr_2$, where four ligands bind to every metal centre creating a necklace-like polymer of ML_2 squares,[168] while ligand **2.41** forms a one-dimensional zigzag chain with $AgClO_4$.[167] Ligand **2.42**[169] differs from ligand **2.35** by the absence of ethyl groups surrounding the benzene core, and by the movement of the pyridine substituent to the 2-positon. When ligand **2.42** is reacted with $AgNO_3$, the sulphur atom also binds to the silver atoms to create a double stranded one-dimensional polymer chain.[169]

*Crystal structure of ligand **2.35***

Crystals of ligand **2.35** can be grown by slow evaporation of a chloroform and methanol solution. The colourless needles obtained are air sensitive, and decompose rapidly upon exposure to the atmosphere. Eventually a crystal was mounted on the X-ray diffractometer before crystallinity was lost, and a data set collected. The crystal solves in orthorhombic space group Pnma, with half a ligand and a methanol solvate molecule in the asymmetric unit. The ligand structure is shown in Figure 2.53, with the hydrogen atoms and solvate methanols excluded for clarity.

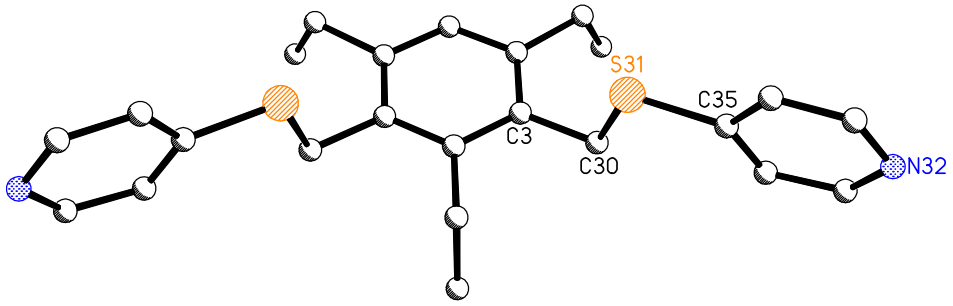

***Figure 2.53** – Crystal structure of ligand **2.35**. Selected bond lengths (Å) and angles (°): S(31)-C(35) 1.754(4), S(31)-C(30) 1.821(4), C(30)-C(3) 1.512(5), C(3)-C(30)-S(31) 107.2(2), C(35)-S(31)-C(30) 105.2(2).*

The ligand lies in an organised *ababa* conformation, with the sulphur atoms and pyridine groups lying above the plane of the benzene ring, and the ethyl groups lying below the plane. A mirror plane runs vertically through the middle of the structure. In the packing diagram the nitrogen atoms hydrogen bond to the hydrogens on the methanol oxygens (1.960Å). The sulphurs do not interact. The ligands pack side by side, each rotated 180° from each other, with no π-π stacking interactions between molecules.

Complexes with ligand 2.35

*Crystal structure of the complex with $Cu(NO_3)_2$ **(2.43)***

The blue precipitate obtained by reaction of copper nitrate in methanol with ligand **2.35** in chloroform, crystallised overnight into clusters of dark blue crystalline material.

DMSO was added to dissolve the product, and after a few months of slow evaporation small purple needles grew. These very small thin crystals were poor diffractors, but a structure was obtained using X-ray crystallography. Due to the poor diffraction and large amount of disorder, the program *Squeeze*[151] was used to remove additional electron density from the voids in the structure, which lowered the final R1 value from 10.76% to 6.73%.

The structure solved in hexagonal space group P6/m. A view of the extended structure is shown in Figure 2.54, to show the connectivity of the atoms as well as the nature of the overall one-dimensional polymer. Excluded from the diagram are hydrogen atoms, disordered counterions and solvate molecules. The asymmetric unit contains half a ligand, half a copper atom, half a nitrate disordered over three sites, half a DMSO solvate molecule, and possibly a water molecule or two.

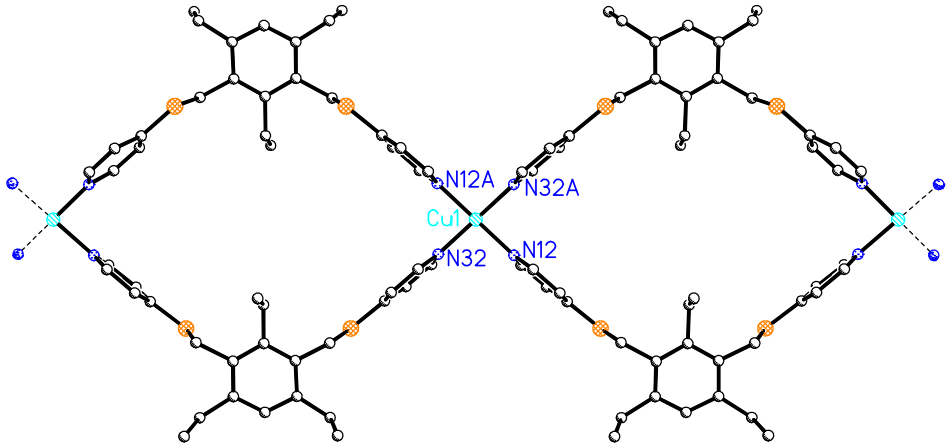

Figure 2.54 *– One-dimensional polymer* ***2.43****, consisting of M_2L square units. Selected bond lengths (Å) and angles (°): Cu(1)-N(32) 2.000(7), Cu(1)-N(12) 2.040(7), N(32)-Cu(1)-N(32A) 180.0(0), N(32)-Cu(1)-N(12) 88.1(3), N(32)-Cu(1)-N(32A) 91.9(3), N(12)-Cu(1)-N(12A) 180.0(0).*

The copper atoms are four-coordinate square planar, binding to four pyridine nitrogens of separate ligands. Each ligand bridges two metal atoms, and there are two ligands for every metal in the structure. Each ligand is in an organised *ababa* conformation, and is related to its adjacent co-bridging ligand by a centre of inversion. The copper atoms act as spiro centres to link together two square units, and the polymer propagates as square

ML_2 units linked at the corners. In this nature, the polymer resembles a necklace-like chain, and is the same kind of structure as formed by ortho-substituted ligand **2.40**.[168]

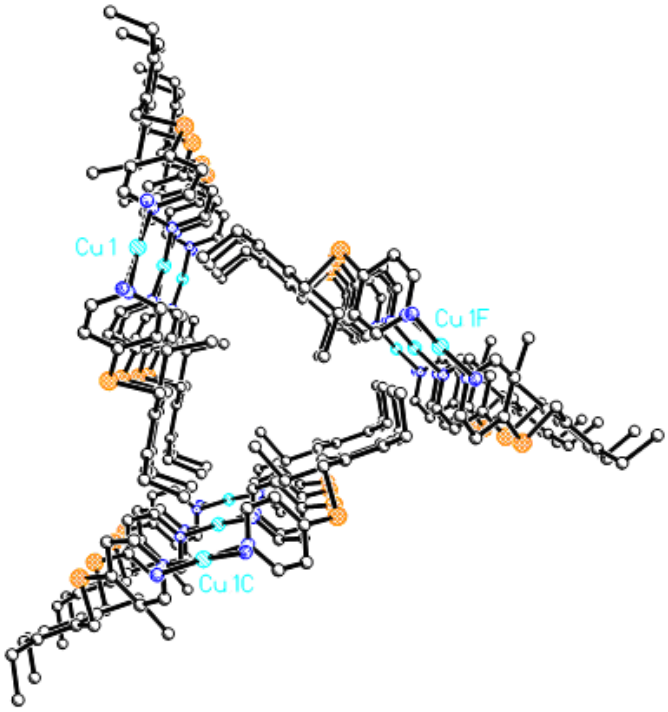

Figure 2.55 *– The triangular packing of* ***2.43*** *allows the ethyl groups of the ligands to point towards the cavity created between the copper atoms of each chain, as demonstrated by three strands in this diagram.*

The copper-copper distance is 16.096Å, and the distance between co-bridging ligands is 6.530Å (from ethyl group to ethyl group). No anions or solvate molecules sit inside the cavity in any kind of host-guest manner. The disordered nitrates sit above the plane of the polymer, reasonably close to the copper centres but not interacting. Instead the voids in each chain are filled with the benzene cores of ligands in other chains, in an interdigitated manner. In the packing diagram the three-fold nature consistent with the space group is obvious, with each chain rotated 120° from the last to form a triangular shape, as demonstrated by three separate chains in Figure 2.55. The ethyl groups from each ligand point towards the copper atoms in another chain, but the chains are aligned such that the ethyl groups point into the middle of the void, without actually entering the void. Another set of ethyl groups from another ligand chain reach towards the void

from the opposite side in the same manner. The nitrate counterions are aligned down the centre of the triangular channels.

There are weak interactions between the DMSO oxygens at the axial coordination sites on the copper atom. The distance is 2.646Å, too long to be a formal bond. The nitrate oxygens hydrogen bond with the ligand in the main structure. There are no π-stacking interactions between ligands in the extended structure.

*Other complexes with ligand **2.35***

Complexation of ligand **2.35** was attempted with a wide variety of metal salts, namely CuI, $Cu(NO_3)_2$, $CuCl_2$, $CuSO_4$, $AgClO_4$, $CoBr_2$, $CoCl_2$, $Ni(NO_3)_2$, $Pd(PhCN)_2Cl_2$, and $FeSO_4$. Almost all of these complexes precipitated immediately, and were so insoluble they would not even dissolve in DMSO, which means recrystallisation was not possible. Unfortunately only one of these complexes was fully characterised by X-ray crystallography.

Some of the other precipitates were sent for elemental analysis. Complexes with 1:1 ratios were obtained from reaction of ligand **2.35** and $Pd(PhCN)_2Cl_2$, $CoCl_2$, and $CuCl_2$. These could be discrete complexes, or more likely polymers. Noteworthy is the observation that all these metal salts are the chlorides, and it is possible that all three compounds could have similar structures.

The precipitate obtained from reaction with $FeSO_4$ analyses as a M_2L compound. As the ligand can only bind a maximum of two metal atoms, this is either a discrete complex, or the M_2L units are linked into a polymer by bridging anions or solvate ligands.

The product of ligand **2.35** and $CuSO_4$ analyses as an M_2L_3 complex. This could be a discrete M_2L_3 structure, possibly a triple helicate, or a M_4L_6 tetrahedral cage, or M_4L_6 square, or a complicated coordination polymer. Similarly, the product from CuI and ligand **2.35** has a M_4L_3 stoichiometry, and since CuI usually dimerises into squares, the product probably also contains an effective "M_2L_3"-type ratio.

1,3-Di(8-quinolyloxymethyl)-2,4,6-triethylbenzene (2.44)

The target compound, 1,3-di(8-quinolyloxymethyl)-2,4,6-triethylbenzene (**2.44**), shown in Figure 2.56, is a potentially exciting synthon for the construction of metallosupramolecular assemblies, due to the unique binding angles that the ligand can undertake. Would the bulky quinoline group encourage preorganisation of the ethyl groups? For the quinoline nitrogen to bind, the heterocycle has to rotate out of the plane of the ligand. It is possible that a metal atom binding to the nitrogen may lie over the core of the ligand, possibly even interacting with the aromatic core. Alternatively the methylene spacer may allow the arm to lie back far enough that the nitrogen donor atom is pointing directly upwards. It is also possible that a metal atom may coordinate to or interact with the oxygen attaching the quinoline group to the central ligand.

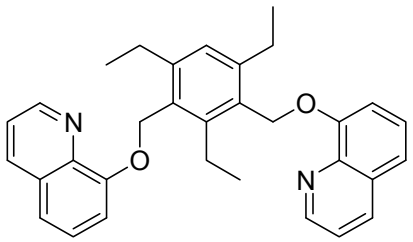

2.44

Figure 2.56 *– Ligand* ***2.44****.*

Molecules similar to **2.44** with two or more 8-hydroxyquinoline groups substituted around an aromatic core are often used for sensor applications. Also, some 8-hydroxyquinoline derivatives have been proven to create interesting structures upon metal complexation.[170]

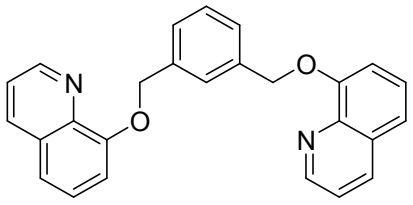

2.45

Figure 2.57 *– A similar ligand to* ***2.44****.*

Ligand **2.45**[171-173] is closely related to ligand **2.44**, shown in Figure 2.57, only lacking the ethyl substituents around the benzene core. Upon reaction with $Cu(NO_3)_2$, ligand **2.45** forms discrete M_2L complexes, the structure of which varies with the solvents

used.[172] Most excitingly, reaction with $AgCF_3SO_3$ creates a M_3L_3 circular helicate.[173] The procedure to synthesise **2.45** has been applied to the synthesis of **2.44**.

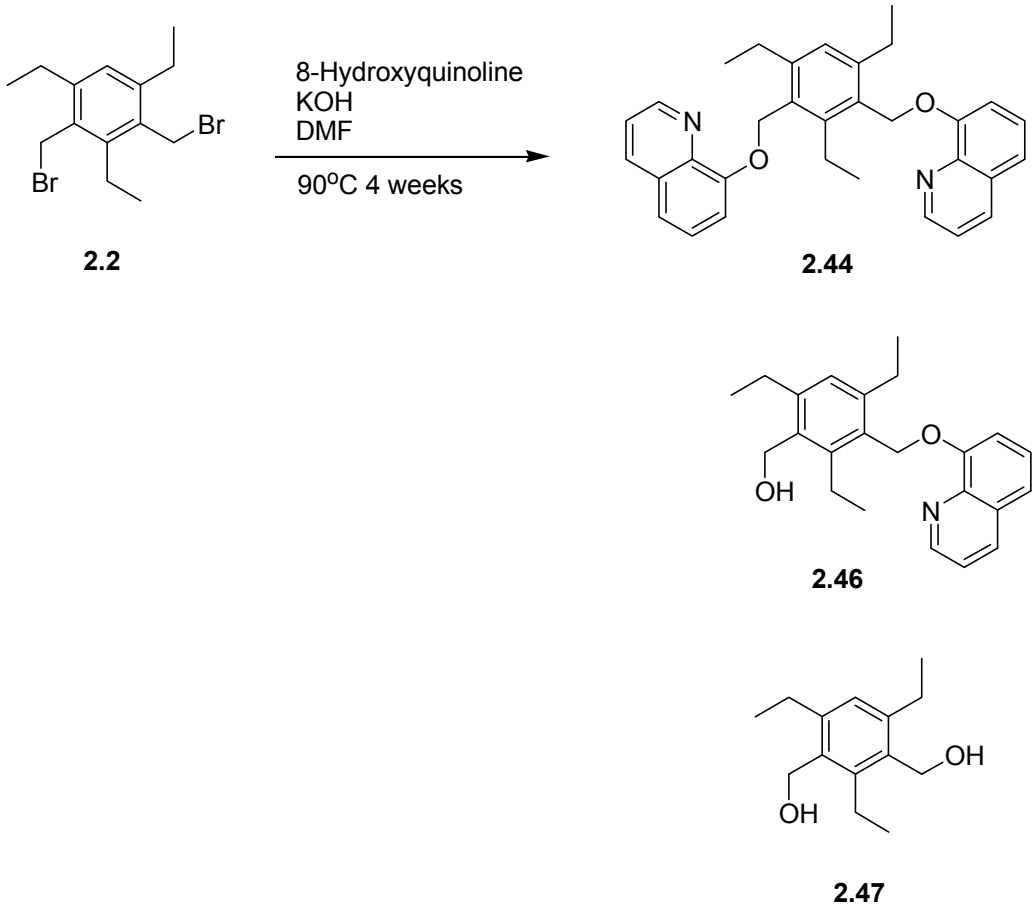

2.2 **2.44** **2.46** **2.47**

Scheme 2.5 *– The synthetic route to a mixture of **2.44** and side-products.*

A base-catalysed substitution reaction with potassium hydroxide in DMF proceeded slowly over time, presumably due to the steric hindrance caused by the ethyl groups and the conformational adjustments needed to accommodate the large quinoline substituents. The reaction was left running for a period of four weeks, until no further changes in the ^{1}H NMR were observed. Unfortunately, although a small amount of ligand **2.44** was synthesised, the main product of reaction was the di-alcohol substituted side product **2.47**, as shown in Scheme 2.5. The ^{1}H NMR shows a roughly 2:1 ratio of alcohol substituents to hydroxyquinoline substituents on the methyl carbon, so a large amount of side-product **2.46** was also obtained. These isomers were separated by column chromotagraphy, but not as cleanly as desired. A pure sample of ligand **2.44** was not isolated and other routes to this ligand were not attempted.

Summary

The 1,3-disubstituted-2,4,6-triethylbenzene ligands have proved to be successful synthons for metallosupramolecular chemistry, not only creating a wide variety of polymeric and discrete structures, but, most importantly, creating complexes that are able to be crystallised and therefore fully characterised.

Ligand **2.4** provided a diverse range of coordination polymers with a variety of metal salts, with one-, two- and three-dimensional products identified. The flexibility of ligand **2.4** has led to this range of products, and is exciting as a synthon as the products cannot be predicted. Most interesting is the M_3L_3 tricorn structure **2.11** that ligand **2.4** forms with $PdCl_2$.

Ligand **2.12** has proved to be a successful component in the formation of discrete metallosupramolecular structures. First a rectangular dimer was formed with CuI (**2.20**), then a M_2L_2 dimeric motif was established with a variety of metal salts, which extends into a large M_4L_6 molecular square when two of these dimeric units are linked together. The processes which lead to the crystallisation of either the square or the dimer warrant further investigation, as does a possible study of the degree of encapsulation of the anion in the central cavity of the square.

Unfortunately due to low solubility, the complexes with ligand **2.35** did not crystallise as readily as the complexes with ligands **2.4** and **2.12**, leading to the full characterisation of only one complex of **2.35**, a one-dimensional necklace-like polymer (**2.43**).

The degree of preorganisation the ethyl groups would induce within these ligands was unknown before synthesis, due to the vacant substitution site on the ring. It seems that the possibility of coordination is a stronger driving force on the conformation of the ligand than minimising steric bulk around the ring. Many different conformations were observed in complexes, from the organised *ababa* conformation to the completely un-organised conformation *aaaaa*. There does not seem to be much preference for the ligand to conform to an organised conformation in the solid state complexes characterised. However the X-ray structure of the only free ligand crystallised does show the ligand preorganised. It is possible that in the absence of other factors, the

ligands do prefer a preorganised conformation but the energy barrier upon rearrangement into a new conformation is low enough that it is easily compensated for by the energy gains associated with other interactions.

Unfortunately, no molecular cages of M_4L_6 topology or otherwise were characterised from these ligands. However the M_4L_6 squares are fascinating structures which deserve further attention and seem to display cage-like properties by encapsulating an anion. The other complexes obtained, such as the M_3L_3 tricorn **2.11**, the numerous dimeric complexes and the variety of coordination polymers, while serendipitous and not cage-like, are each exciting and worthy of attention in their own right.

Chapter Three

The 1,3,5-trisubstituted-2,4,6-trialkyl/trimethoxy-benzene ligands

Chapter Three

The 1,3,5-trisubstituted-2,4,6-trialkyl/trimethoxybenzene ligands

Introduction

Tripodal ligands offer a route to metallosupramolecular assemblies of more complex topology than those offered by simpler ligands. While two-armed-ligands are capable of bridging two metal centres, three-armed ligands can bridge three metal centres, incorporating another level of dimensionality into the structure. While complexes containing two-armed ligands are dependent on the metal atom to create nodes to increase the depth and complexity of the structure, three-armed ligands act as more elaborate puzzle pieces, capable of interlocking up to three metal atoms and acting as a node themselves, giving rise to different assemblies. Primarily of interest are tripodal ligands capable of forming either M_3L_2 or M_6L_4 cage structures, such as the ligands shown in Figure 3.1.

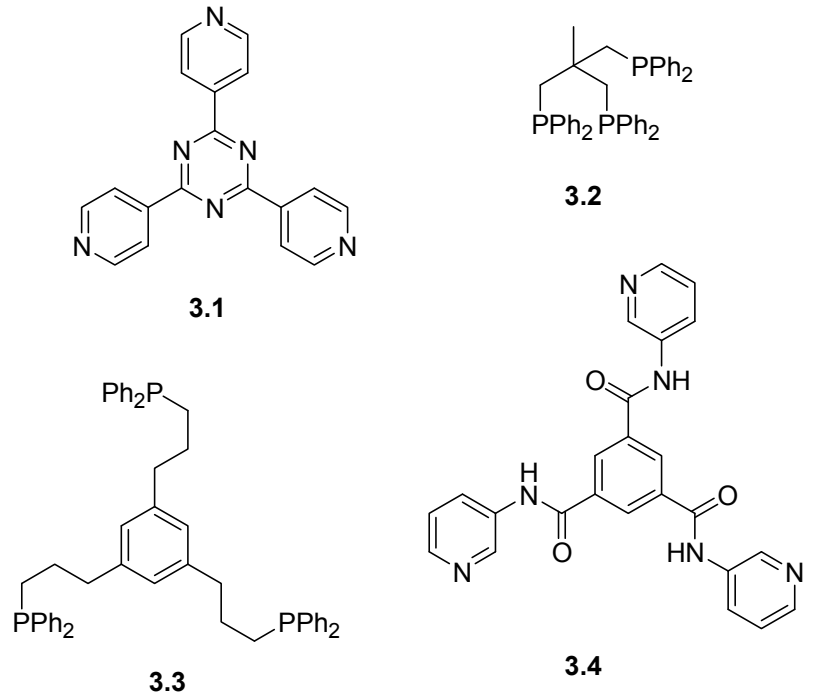

Figure 3.1 *– Examples of three-armed ligands capable of forming molecular cages.*

Like the two-armed ligands, often the easiest approach to creating a tripodal ligand is to attach three binding arms to a central core. The core may be a single atom, like carbon in **3.2**,[56] or nitrogen or boron, for example, or the core might be aromatic, as in **3.1**,[50,174-178] **3.3**[67] and **3.4**.[179,180] Benzene cores are very popular as 1,3,5-trisubstitution evenly spaces the three arms 120° from each other. The donor atom capable of coordinating to a metal atom may be an atom, like phosphorus in **3.2** and **3.3**, or part of a heterocycle like pyridine in **3.1** and **3.4**, and is either attached directly to the central core so the ligand is quite rigid, as in **3.1**, or attached *via* a methylene linker (**3.2**) or an alkyl chain (**3.3**) that incorporates flexibility into the ligand.

Ligand **3.1** is a component of the most referenced molecular cage reported.[50,89-96,98-102,174,181-199] The M_6L_4 structure consists of four ligands and six palladium atoms, forming an octahedron with a hollow cavity that not only hosts guest molecules, but functions as a molecular flask, facilitating reactions inside the cavity of the cage.[90,93-96,99-101,187-199] Although very different to **3.1**, ligand **3.2** also forms a M_6L_4 molecular cage of the same topology, but the cage is smaller and does not encapsulate any guest molecules.[56] Both **3.3** and **3.4** form cages of the M_3L_2 type.[67,179] This type of cage often hosts guest molecules but is usually a quite open structure that does not fully encapsulate the guest. Schematics of both types of cage are shown in Figure 3.2.

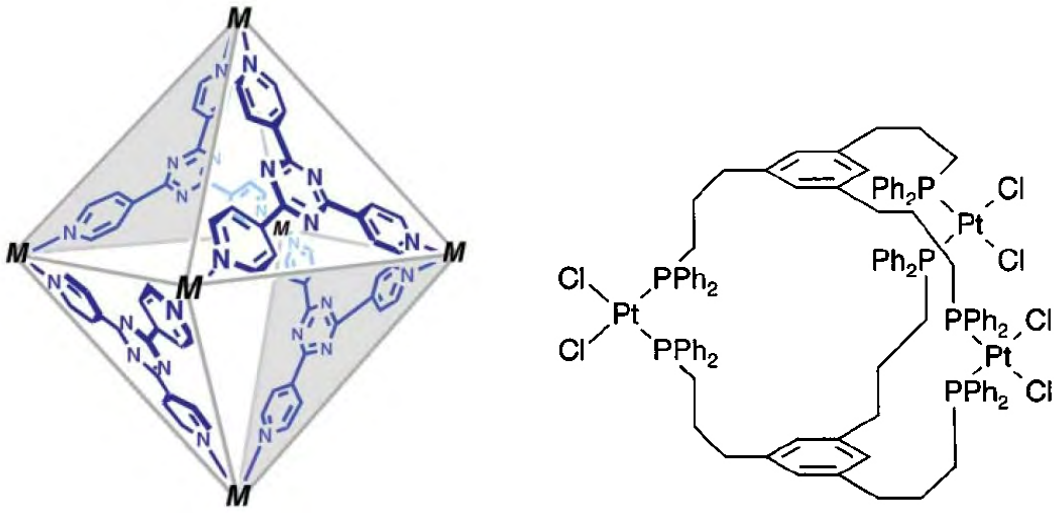

***Figure 3.2** – Schematic diagrams of an M_6L_4 octahedral cage formed by **3.1** (left)[49] and a M_3L_2 cage formed by **3.3** (right).[67]*

Of popular design are tripodal ligands based on heterocyclic donor arms attached *via* a methylene group in a 1,3,5-substitution pattern around a benzene ring. Shown in Figure

3.3 are examples of such ligands, all of which have been shown to form molecular cages upon reaction with appropriate metal salts.[55,63-65,68,78,200] Therefore this type of substitution appears to be a good template for the design of ligands potentially capable of forming molecular cages.

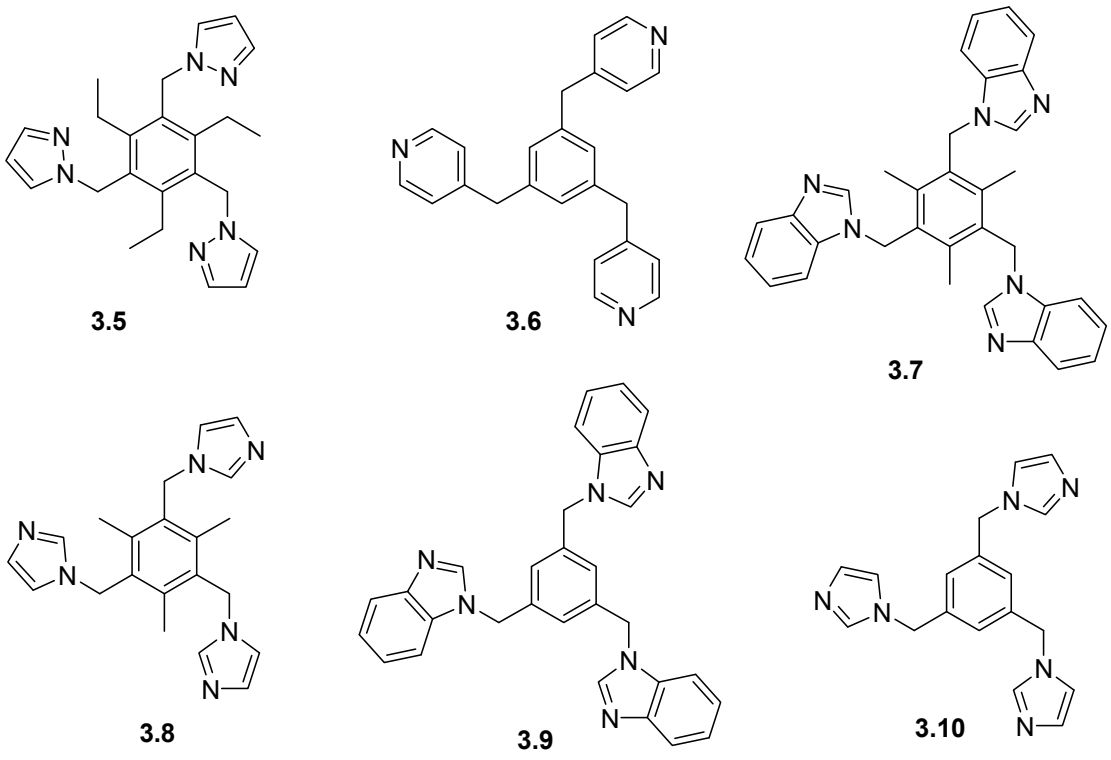

Figure 3.3 *– Examples of tripodal heterocyclic ligands based on 1,3,5-substitution around a benzene core that have been shown to form coordination cages.*

Ligand **3.5**[55] is perhaps the most famous of the ligands shown, forming one of the first examples of a M_6L_4 cage when reacted with palladium chloride,[55] and will be discussed in much more detail in the next few pages as it was the starting point for the research undertaken in this project. All of the other ligands shown in Figure 3.3 form M_3L_2 cages.[63-65,68,200] Some of these cages encapsulate guest molecules.[64,68,200] These ligands have relatively less substitution around the benzene cores than **3.5**, and the donor atom in **3.5** is adjacent to the atom which links the heterocycle to the ligand core, whereas in the other ligands the donor atom is further around the ring. The flexibility of the methylene linker allows the heterocycle to bend away from the plane of the ligand core to bind to the metal atom to form these small discrete M_3L_2 capsules. Obviously planar rigid ligands would not be able to form M_3L_2 cages of this type. Ligand **3.8** also reacts

with palladium chloride to form a large M_6L_8 cage which encapsulates eight chloride anions.[78]

This chapter concerns ligands similar to those in Figure 3.3, heterocyclic tripodal ligands with substitution in the 2,4,6-positions around the benzene core, and the effect these ancillary substituents have on the structures formed. Three different ligand cores are utilised, the first being mesitylene, so the ancillary substituents are methyl groups. The other cores are 1,3,5-triethylbenzene and 1,3,5-trimethoxybenzene, so the substituents are ethyl or methoxy groups. Once the ligand binding arms are attached the ligands have six groups attached to the benzene core, which may induce preorganisation around the ring if the substituents are bulky enough.

Synthesis of ligand precursors

Mesitylene (**3.11**) is a commercially available starting product which is readily bromomethylated in the vacant 2,4,6-positions around to the ring to produce 1,3,5-tri(bromomethyl)-2,4,6-trimethylbenzene (**3.12**)[201] in 87% yield, as shown in Scheme 3.1. No further purification is necessary. This is a well known and utilised reaction, and many ligands and other molecules in the literature are synthesised from **3.12**.[107,202-211]

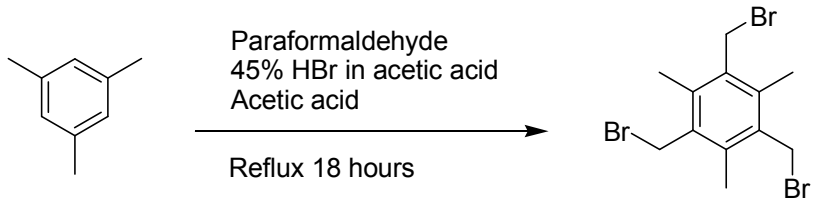

3.11 **3.12**

Scheme 3.1 *– Synthetic route to precursor* ***3.12****.*

The crystal structure of **3.12** shows the molecule in a disorganised conformation, with two brominated arms on one side of the ligand core, and one brominated arm on the opposite side.[212] This is not surprising, as the methyl groups are unlikely to induce preorganisation to the system. Statistically, 25% of the time all three substituted arms should sit on the same side of the benzene core if no other factors are influencing the conformation. To examine this, a search of the *Cambridge Crystallographic Database*

(v. 5.26)[130] was undertaken, concentrating on hexasubstituted molecules based on mesitylene cores with substituents in the 1,3,5-positions connected to the central core with flexible linking groups. Of the 123 hits, 56% of molecules crystallise with all three of the heavily substituted arms on the same side of the benzene core. This percentage is much greater than statistically predicted, suggesting that other factors encourage this conformation.

The reaction to produce the triethyl analogue of **3.12** does not occur as smoothly. As discussed in the previous chapter and shown in Scheme 3.2, reaction of 1,3,5-triethylbenzene **(2.1)** under similar conditions but longer reaction times was shown to give 1,3-di(bromomethyl)-2,4,6-triethylbenzene (**2.2)**. Hartshorn reported a 46% yield of 1,3,5-tribromomethyl-2,4,6-triethylbenzene (**2.3)** under the same conditions and reaction time,[116] but seems to have been fortunate as other researchers have also struggled to add the final arm *via* this technique,[109,113-115] most probably due to the steric hindrance of the ethyl groups. It has been repeatedly reported that further reaction of **2.2** under the same conditions will provide **2.3**,[109,113,115] but after multiple attempts it was concluded that this was not an efficient route to **2.3,** even when the reaction duration was highly extended.

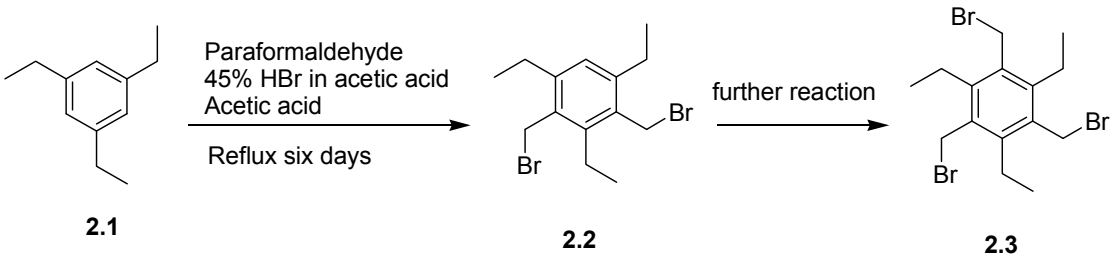

Scheme 3.2 *– One synthetic route to precursor* ***2.3*** *which proved unsuccessful on this occasion, not producing* ***2.3*** *in the yield or purity desired.*

An alternate literature procedure to synthesise **2.3** was attempted[114] which proved highly successful. Zinc powder was added to the reaction flask and **2.3** was produced in 74% yield after six days of reaction. The successful procedure is shown in Scheme 3.3.

Precursor **2.3** has been used extensively to synthesise ligands[55,109,110,114,213] or sensor molecules[113,115,118,119,214,215] where the product is desired to adopt a preorganised *ababab* conformation around the ring, with each substituent around the ring alternating (a)bove

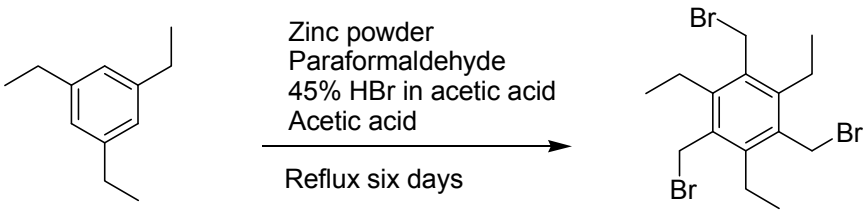

2.1 **2.3**

Scheme 3.3 *– The preferred synthesis of* ***2.3****.*

or (b)elow the plane of the benzene core.[55,109,110,114-116,119,120,209,213,216] It has been shown in these compounds that the steric bulk provided by the ethyl groups is often enough to discourage adjacent arms to sit on the same side of the ring, and the X-ray crystal structure of **2.3** shows a preorganised conformation.[213] This conformation is useful as it brings all three binding arms onto the same side of the molecule, so the arms can congregate around a molecule as a sensor,[113,115,118,119,215] or bind to metal atoms in such a way that may promote the formation of discrete coordination structures[110,213] such as cages.[55] A schematic of **2.3** in an *ababab* preorganised conformation is shown in Figure 3.4.

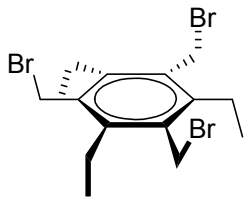

Figure 3.4 *– Ligand precursor* ***2.3*** *in a preorganised* ababab *conformation.*

Six flexible substituents around a benzene ring can orientate in 64 ways, of which only two possibilities describe an *ababab* system. So statistically, if no other factors are influencing the arrangement of substituents, there is only a 3.1% probability that a fully preorganised conformation will take place by chance. A search of the *Cambridge Crystallographic Database* (v. 5.26)[130] was undertaken to examine how often the addition of ethyl groups in the 2,4,6-positions around the ring in a hexasubstituted compound induces an *ababab* arrangement. Out of the 102 molecules identified, 64% crystallise in an organised conformation. This includes the conformation of ligands in coordination complexes and molecules in other environments where the organisation may be influenced by other factors. Therefore the list of compounds was reviewed to concentrate on compounds where the conformation appeared to be unrestrained by factors external to the arrangement of the core of the molecule in question. This is a

hard factor to judge, as almost every molecule has interactions in the solid state that may encourage the formation of one conformation over another, and the influence of these factors is difficult to determine. Of the 30 molecules selected, 50% possess an organised conformation. However, of the fifteen molecules which do not lie in an *ababab* conformation, 53% still lie with all three major substituents on the same side of the benzene core, and the disorganisation is only amongst the ethyl groups. So although the technique of using ethyl groups to increase steric bulk and initialise preorganisation may not be 100% effective, it does increase the chances that all three arms will be on the same side of the aromatic core.

The final precursor synthesised for this section was produced from 1,3,5-trimethoxybenzene (**3.13**). Methoxy groups resemble ethyl groups in size, but orientate slightly differently due to the geometry of the oxygen atom. It is unknown if a compound with methoxy groups would be more or less prone to preorganisation than the corresponding compound substituted with ethyl groups. 1,3,5-Tribromomethyl-2,4,6-trimethoxybenzene (**3.14**) has not received as much attention in the literature as its methyl and ethyl counterparts, with only five hits in *Scifinder Scholar*, with none of the products used as ligands for coordination chemistry.[209,217-220]

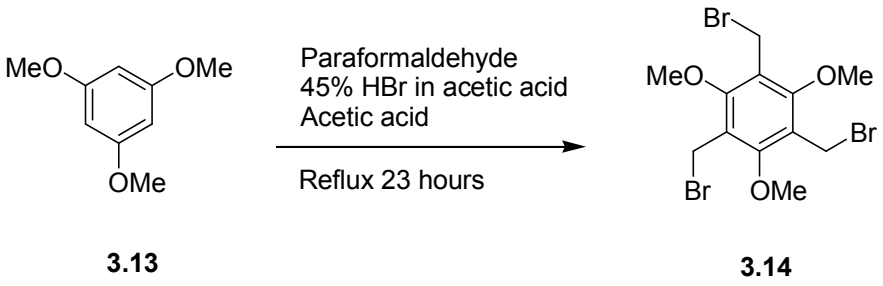

3.13 **3.14**

Scheme 3.4 *– Synthetic route to precursor* ***3.14****.*

According to literature reports, the same experimental conditions used to produce **3.12** and **2.2** can be used to synthesise **3.14** in the much shorter reaction time of three hours and at the lower temperature of 60-70^{o}C.[220] This seems logical as methoxy groups are electron-donating and would activate the benzene core to electrophilic attack and allow the reaction to proceed more readily, even considering the greater steric bulk compared with methyl groups in **3.12**. However it was found that the product after four hours of reaction at 70^{o}C was 1-bromomethyl-2,4,6-trimethoxybenzene. Longer reaction time at higher temperature was found to produce **3.14** in 61% yield, as shown in Scheme 3.4.

A search of the *Cambridge Crystallographic Database* (v. 5.26)[130] showed that if there are sufficient vacant sites around the benzene core, the methoxy groups prefer to lie sideways in the plane of the aromatic ring. However, hexasubstitution around the ring causes the substituents to sit perpendicular to the ligand core. Of eight crystal structures in the database of hexasubstituted molecules with methoxy groups in the 2,4,6-positions around the central core, only three displayed an *ababab* conformation around the ring, suggesting that methoxy groups may be less effective at inducing this type of preorganised conformation than ethyl groups.

Synthesis of the 1,3,5-tri(pyrazol-1-ylmethyl)-substituted ligands

Known literature compounds 1,3,5-tri(pyrazol-1-ylmethyl)benzene (**3.15**),[116,205,221,222] 1,3,5-tri(pyrazol-1-ylmethyl)-2,4,6-trimethylbenzene (**3.16**)[116,205,222-224] and 1,3,5-tri(pyrazol-1-ylmethyl)-2,4,6-triethylbenzene (**3.5**)[55,116,118] have all been used as ligands in coordination chemistry and have been shown to form complexes of different topology from each other.[55,116,221,223] The only differences between the ligands, as shown in Figure 3.5, are the substituents in the 2,4,6-positions around the central core. Obviously small adjustments in ligand structure can have large effect on the products obtained upon reaction with metal salts.

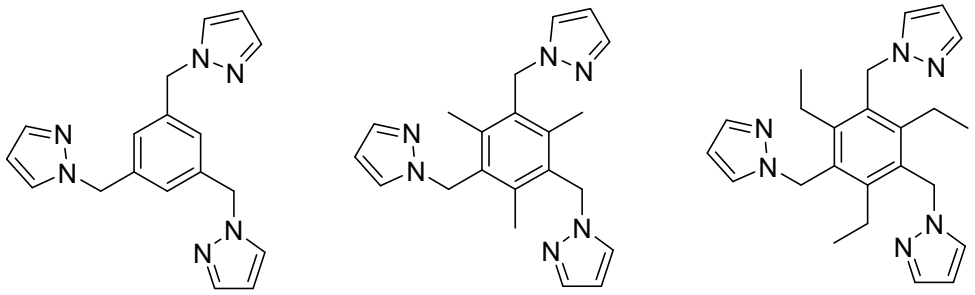

Figure 3.5 *– Known ligands based on 1,3,5-tri(pyrazol-1-ylmethyl)benzene, with different substituents in the 2,4,6-positions around the central core.*

Ligand **3.15** is known to form a discrete ML_2 complex with $Cu(ClO_4)_2$, where only one nitrogen of the ligand bonds to the metal atom,[221] and one- and two-dimensional polymers upon reaction with $CuCl_2$ and $CoCl_2$.[221] Ligand **3.16** has been shown to form a one-dimensional polymer with $AgNO_3$,[116] and a coelenterand structure with

$Ru(DMSO)_4Cl_2$, where the metal atom is encapsulated by the ligand, bonding to all three pyrazole nitrogens as well as the benzene core.[116] Ligand **3.16** has also been used as a sensor for $NH_4^+$and K^+,[224] as well as for the formation of ball-shaped ionic assemblies in water.[205]

Ligand **3.5** has been shown to form a one-dimensional polymer with $AgNO_3$,[116] and significantly, a M_6L_4 cage with $PdCl_2$.[55] Therefore **3.5** was the starting point for the research in this project, as it was of interest to attempt the crystallization of complexes of **3.5** with other metal salts to determine if other cage structures could be formed. Two different literature methods have been used to produce **3.5**.[116,118] The route chosen is the phase-transfer-catalysed alkylation of pyrazoles common for these types of compounds, as shown in Scheme 3.5. Ligand **3.5** was obtained in 78% yield.

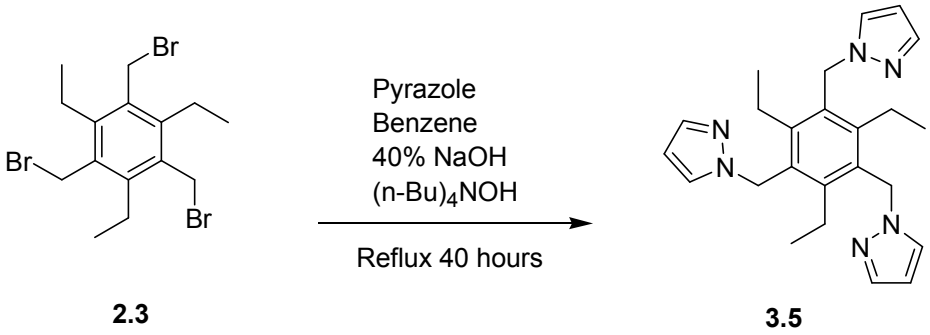

2.3 **3.5**

Scheme 3.5 *– Synthetic route to ligand **3.5**.*

The predominant difference between **3.5** and similar ligands **3.15** and **3.16** is the presence of bulkier substituents in the 2,4,6-positions around the ring, encouraging preorganisation of all three flexible arms to point towards the same face of the ligand. Preorganisation of the binding arms arranges the ligand into a conformation ideal for bonding to metal atoms in such a way that should encourage the formation of closed polyhedral structures. However it should still be possible for ligands **3.15** and **3.16** to form the same kind of cage structure as **3.5**, as it is still possible for all three arms to sit on the same side of the ligand for coordination, even though they may be less predisposed to this conformation. The product of reaction of **3.16** with $PdCl_2$ was not crystallised but was determined to have a M_3L_2 stoichiometry,[116] so is possibly an analogue of the cage produced by **3.5**. Instead of repeating the work already done on **3.16**, a chiral analogue of **3.16** was prepared by fusing bornane groups to the pyrazoles.

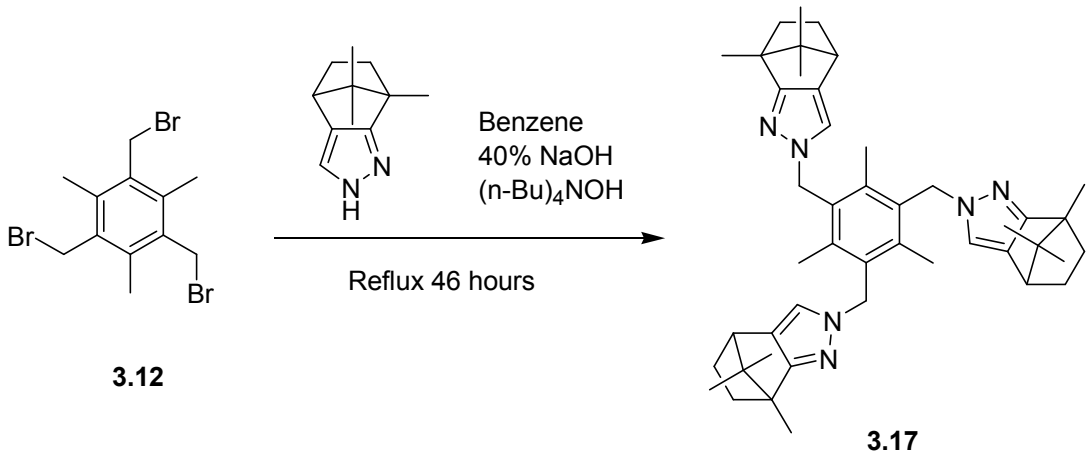

Scheme 3.6 *– The synthetic route to chiral ligand* ***3.17****.*

1,3,5-Tri[((4S,7R)-7,8,8-trimethyl-4,5,6,7-tetrahydro-4,7-methano-2H-indazol-2-yl)methyl]-2,4,6-trimethylbenzene (**3.17**) was synthesised to incorporate chirality into any cage structures constructed from this component. A chiral cage may have the potential to separate out single enantiomers of guest molecules from racemic mixtures. The phase-transfer-catalysed alkylation of the pyrazole went to completion within 46 hours of reaction to give a crude yield of 79%. However the characteristic minor products of attachment at the more hindered nitrogen are seen,[225] a 3:1 ratio of attachment at each reaction site, giving **3.17** as the major product along with a complex mixture of minor isomeric products. It has been shown that radial chromatography can separate out isomers like these,[225] but this was not attempted. The isomer mixture containing **3.17** was reacted with K_2PdCl_4 in case the dominant isomer would form the desired complex and separate out by crystallisation. However, as no crystals were obtained, the coordination chemistry of this ligand was not investigated further.

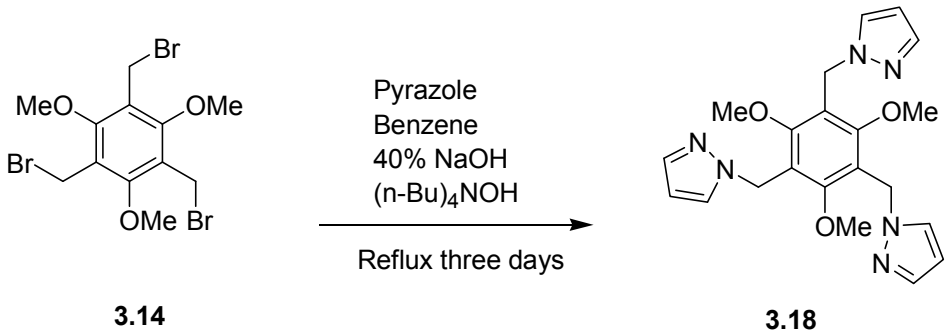

Scheme 3.7 *– The more successful of the two synthetic routes to ligand* ***3.18****.*

The synthesis of 1,3,5-tri(pyrazol-1-ylmethyl)-2,4,6-trimethoxybenzene (**3.18**) was not quite as straightforward as counterparts **2.4**, **3.5** and **3.17**. The phase-transfer-catalysed alkylation of pyrazole did produce **3.18** as an orange oil in 73% yield, but the reaction did not proceed as cleanly as the analogous reactions and so another route was investigated. However this synthesis, using potassium carbonate in DMF,[116] produced **3.18** in even lower yield and purity than the original reaction. Therefore, the product from the phase-transfer-catalysed synthesis, as shown in Scheme 3.7, was used in subsequent reactions.

*Crystal structure of **3.19***

Slow evaporation of an acetone solution produced a few colourless crystals of the product of the reaction of ligand **3.5** with an excess of silver hexafluorophosphate. These crystals proved to be suitable for X-ray crystallography, and the structure solved in monoclinic space group $P2_1/c$.

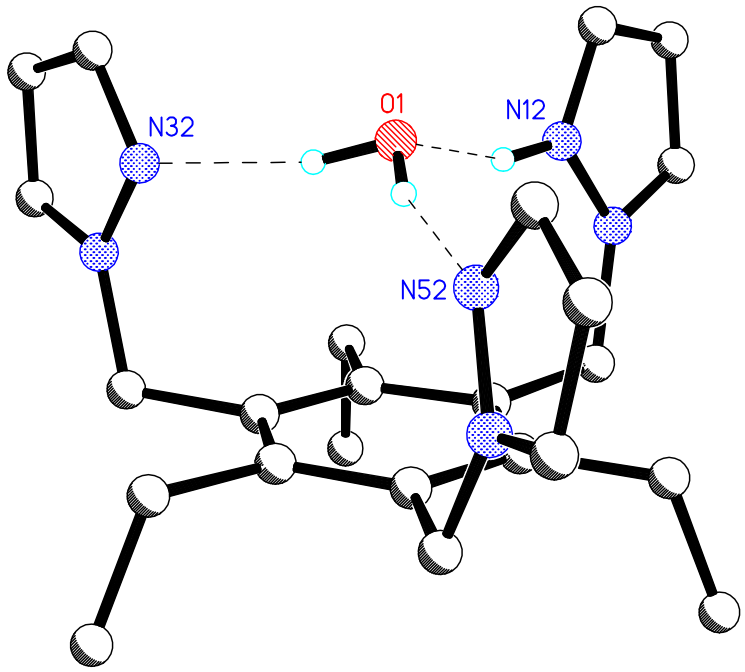

***Figure 3.6** – A view of the X-ray structure of **3.19**, showing the protonated ligand encapsulating a water molecule. Selected bond lengths (Å) and angles (°): O1-H32 0.89(3), O1-H52 0.85(3), O1-H12 1.63(3), N12-H12 0.96(3), N32-H32 1.96(3), N52-H52 1.93(3), H32-O1-H52 102(6), H32-O1-H12 110(6), H52-O1-H12 118(6).*

Surprisingly, no silver is present in structure **3.19**, as shown in Figure 3.6, with the majority of the hydrogen atoms, the hexafluorophosphate anion and a solvate water molecule excluded for clarity. The asymmetric unit contains protonated ligand **3.5** with a water molecule nestled between the arms, a disordered hexafluorophosphate counterion and a solvate water molecule with partial occupancy. The ligand is strongly hydrogen bonded with the water molecule, such that it resembles a H_3O^+ with a neutral ligand. The data quality allowed the hydrogen atoms to be located in the difference map. The pyrazole nitrogens N32 and N52 point directly to the hydrogens on O1 with N-H distances of 1.960Å and 1.928Å, respectively. N12 is protonated, with a hydrogen bonding distance of 1.636Å to O1. A bird's eye view of the structure is shown in Figure 3.7. The oxygen lies above the centre of the ligand core. The N12 and N52 pyrazoles point directly towards the centre of the ligand, as expected, but the N32 pyrazole lies differently, twisted so that it points away from the central oxygen. N32 still hydrogen bonds to the water molecule, even though the nitrogen lone pair is not pointing directly at the hydrogen.

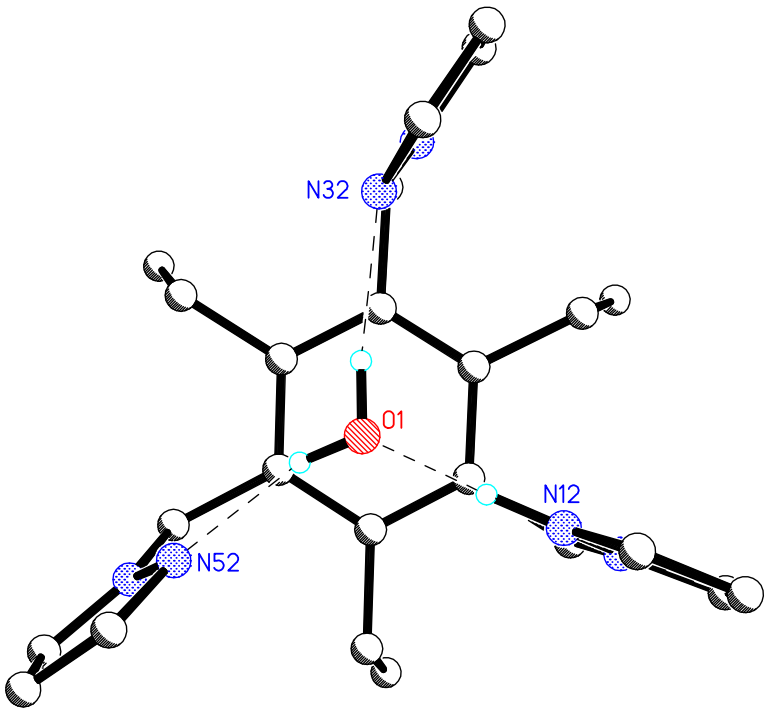

Figure 3.7 *– An alternate view of* ***3.19****, looking at the position of the water molecule and the relative distortion of the N32 pyrazole.*

Ligand **3.5** is organised in the expected *ababab* conformation, but as the pyrazoles are hydrogen bonded to the water molecule, it cannot be confirmed that this is the preferred conformation of the naked ligand. The H_2O/ligand **3.5**H^+ entity has an overall positive charge which is counterbalanced by the hexafluorophosphate anion in the asymmetric unit. The anion is rotationally disordered around one axis. A partial occupancy water molecule is also present in the asymmetric unit, in such a way to interact with the central water molecule and hexafluorophosphate anion by hydrogen bonding.

Structure **3.19** packs with the ligands lying back to back and offset. There are no π-π stacking interactions between the benzene cores as the distance between rings is 6.122Å. However two pyrazoles on each ligand π-π stack with two pyrazoles on the adjacent ligand, at a distance of 3.416Å. This explains why the N32 pyrazole ring lies in an odd orientation, to be coplanar with the N52 pyrazole to maximize π stacking while still hydrogen bonding to the central water molecule. The fluorines on the counterion are hydrogen bonded to surrounding pyrazoles with H-F distances around 2.262Å.

This crystal structure is very similar to that of the product of the 3,5-dimethylpyrazole analogue of **3.5** reacted with perchloric acid.[118] The counterion in that structure is perchlorate, and the ligand is protonated and the pyrazoles hydrogen bonded to a water molecule as in structure **3.19**. In this case, the ligand based on **3.5** was prepared as a receptor to selectively bind NH_4^+. The conclusion of the authors was that receptors of this nature are not selective to NH_4^+ and are capable of detecting H_2O.[118] Ligands similar to **3.5** have been thoroughly investigated for their possible use as sensors for $NH_4^+$and other molecules.[115,118-120,214,215,224] It is not known why ligand **3.5** preferred to bind H_2O over Ag(I) in this example.

Complexes with ligand 3.5

*Crystal structure of the complex with $AgClO_4$ (**3.20**)*

The product of reaction of ligand **3.5** with excess silver perchlorate gave colourless crystals suitable for X-ray crystallography upon slow evaporation of an acetonitrile solution. The larger crystals decomposed rapidly and were shown to be $Ag(MeCN)_4ClO_4$ by X-ray crystallography; however the smaller crystals were revealed

to be a complex of greater interest. This structure solved in monoclinic space group $P2_1/c$.

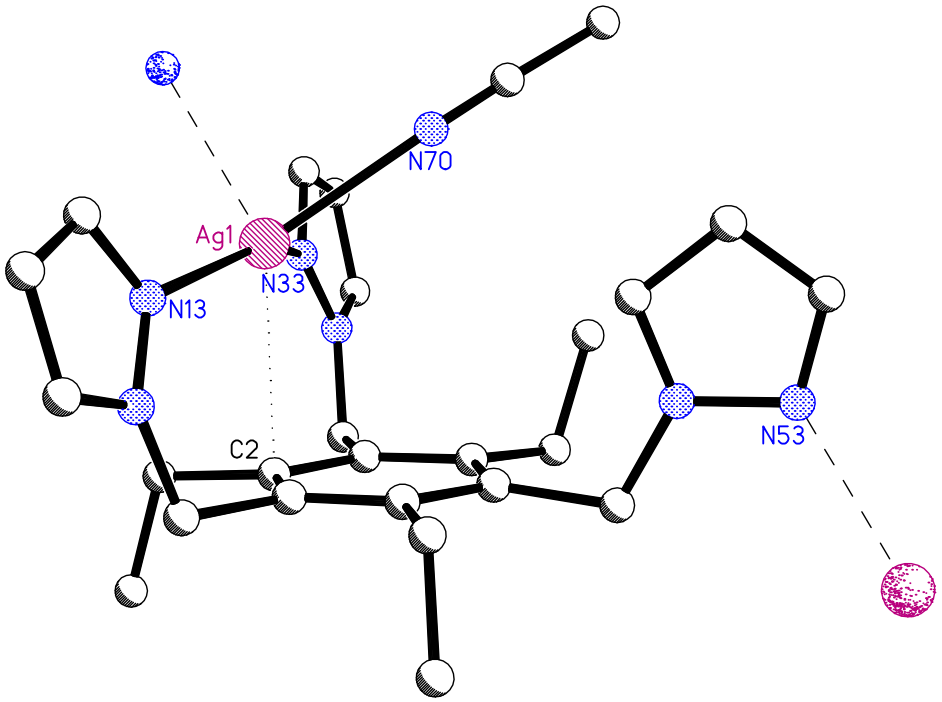

Figure 3.8 *– The asymmetric unit of* ***3.20****. Selected bond lengths (Å) and angles (°): Ag1-N13 2.296(6), Ag1-N33 2.317(6), Ag1-N70 2.408(7), Ag1-N53A 2.435(6), Ag1-C2 2.804(6), N13-Ag1-N33 149.5(2), N13-Ag1-N70 120.0(2), N13-Ag1-N53A 92.5(2), N33-Ag1-N70 90.3(2), N33-Ag1-N53A 91.9(2), N70-Ag1-N53A 86.5(2), C2-Ag1-N13 81.2(2), C2-Ag1-N33 79.7(2), C2-Ag1-N70 122.8(2), C2-Ag1-N53A 148.2(2).*

The asymmetric unit of **3.20** is shown in Figure 3.10, with hydrogen atoms, the perchlorate anion and solvate acetonitrile molecule excluded for clarity. There is one ligand **3.5** and one silver atom and counterion in the repeating unit. The silver coordinates to three pyrazole nitrogens of two separate ligands, as well as an acetonitrile nitrogen and has a weak η^1 interaction with the C2 carbon in the benzene core of the ligand, indicated by a dotted line in the diagram. The silver atom binds these five atoms in a distorted trigonal bipyramidal geometry, the distortion likely due to the weaker interaction with the benzene ring. Ligand **3.5** chelates to the silver atom with two pyrazoles through N13 and N33, while the third pyrazole has rotated to bind the silver atom in the next unit through N53. Although the ligand has three arms capable of

binding to three separate metal atoms, in this instance it has chosen to bridge only two metal centres. Even though the pyrazoles are bound to different metals, the pyrazole arms are all organised on the same side of the ring. Two of the ethyl groups point down, while the other ethyl group is disordered between up and down, so the ligand lies in an *ababab* conformation approximately 35% of the time.

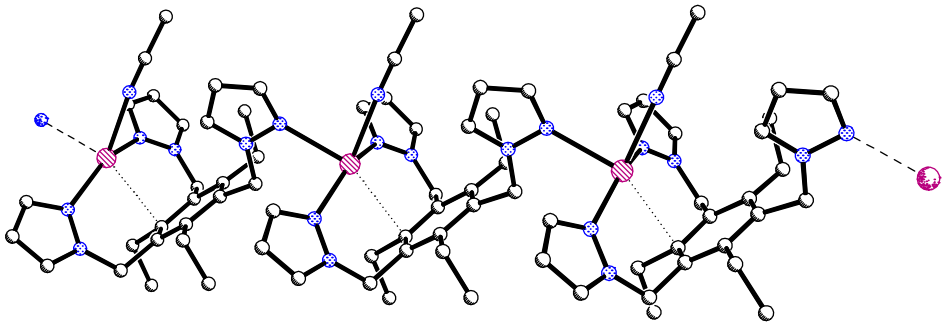

Figure 3.9 *– A representative section of one-dimensional polymer* ***3.20****.*

The complex propagates in one dimension as shown in Figure 3.09, with perchlorate counterions, solvate molecules and hydrogen atoms excluded for clarity. The units link together in a linear fashion, propagating along the a-axis. In the crystal packing there are no π-π stacking interactions between chains. The oxygens on the perchlorate anions weakly interact with hydrogen atoms on the ligands.

Silver-arene interactions are not uncommon.[116,226-229] The η^1 interaction seen here is much less common,[116,226] probably resulting from the way the position of the silver atom is restrained by the pyrazole groups, holding it directly over the C2 atom, instead of allowing it either to lie in the centre of the ring and interact with all the atoms in an η^6 fashion, or to bind unsymmetrically to two atoms in the benzene ring, as usually seen in η^2 interactions.[116,226] Interestingly, this type of η^1 interaction and overall general polymer structure are seen in two very similar structures of silver complexes prepared with **3.5** and **3.16**. The silver nitrate complex of **3.16** is almost identical to **3.20**, with the counterion coordinated to the silver atom in place of the acetonitrile, and the η^1 C2 interaction being slightly shorter (2.771Å).[116] The silver nitrate complex of **3.5** is slightly different, with two independent silver atoms and only pseudo-polymeric in

nature, but a silver atom bonds to two pyrazole nitrogens, two nitrate oxygens, and interacts in an η^1 fashion with C2 at a distance of 2.785Å.[116]

*Crystal structures of the complexes with $PdCl_2$ (**3.21** and **3.22**)*

In 1996, Hartshorn reported the formation of one of the first M_6L_4 cages upon reaction of **3.5** with palladium chloride.[55,116] To determine the reproducibility of this assembly process, potassium tetrachloropalladate was added to a D_6-DMSO solution of ligand **3.5** and the resulting solution monitored by ^{1}H NMR for a few days without any sign of complex formation. Vapour diffusion of chloroform into this solution eventually led to orange block-like crystals over a period of ten months. These crystals were suitable for X-ray crystallography, and were shown to display the same cell constants as the original Hartshorn cage. Not surprisingly, the structure also solved in triclinic space group P-1, and was shown to be the same M_6L_4 structure as Hartshorn reported, as shown in Figure 3.10, with hydrogen atoms and poorly defined solvate molecules excluded for clarity.

The cage consists of six palladium atoms and four ligands. Each palladium coordinates to two chloride anions and two pyrazole nitrogens of separate ligands in a distorted square planar geometry. Each ligand bridges three metal atoms, linking the metal atoms together into a spherical structure. Like the schematic in Figure 3.2 of an octahedral cage,[49] the ligands occupy half of the faces of the octahedron. The six palladium centres sit on the vertices of the octahedron. Unlike the famous M_6L_4 cage formed by ligand **3.1**,[50] the flexibility of ligand **3.5** allows the ligand core to collapse into the centre of the structure, creating a smaller but more enclosed hydrophobic cavity. One of the ligands sits in an *ababab* organised conformation with all three ethyl groups pointing into the central cavity, but the ethyl groups on the other three ligands are not as ordered, having *abaaab* conformations. In contrast to the original structure which encapsulates a DMSO molecule, **3.21** has chosen to encapsulate a chloroform molecule. It appears that this guest is occasionally a DMSO molecule, but the refinement of this data was not good enough to accurately determine the relative ratio of occupation. However it has now been determined that a chloroform molecule must be a slightly better fit inside the cavity of this cage than DMSO for it to be preferentially encapsulated.

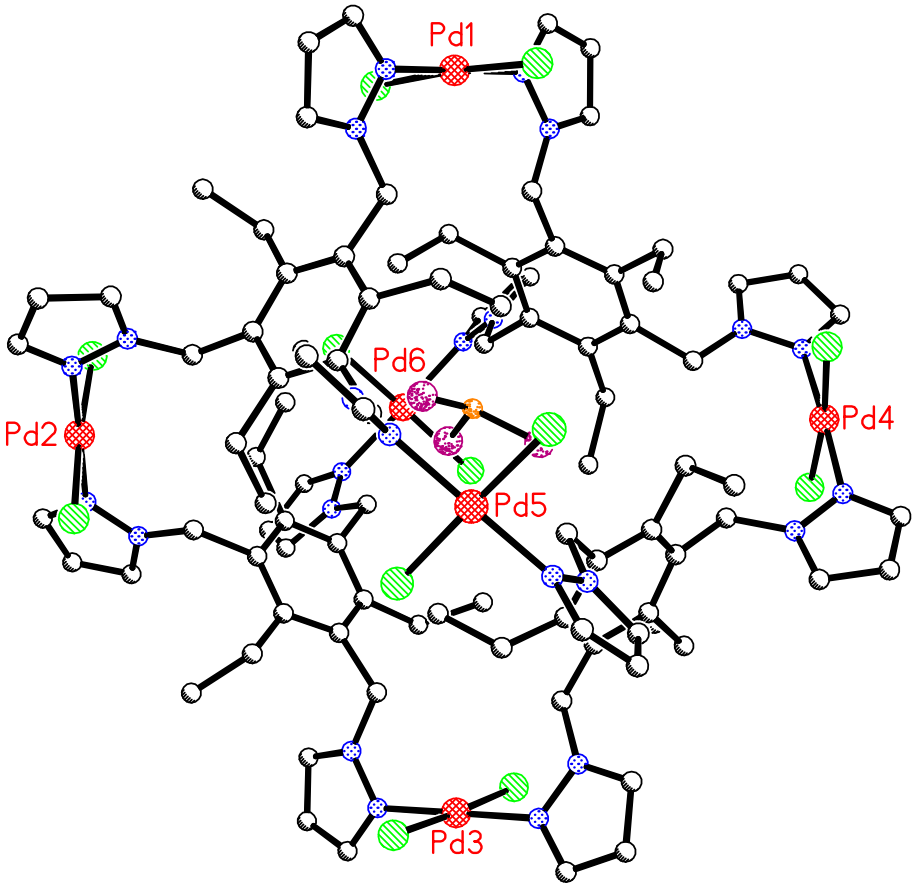

Figure 3.10 *– The M_6L_4 cage* ***3.21*** *first synthesised by Hartshorn.*[55] *The encapsulated chloroform molecule is shown in pink.*

This cage was crystallised twice more, both from less direct syntheses. The less labile palladium(IV) salt potassium hexachloropalladate was added to a solution of **3.5** in D_6-DMSO. Not surprisingly, ^{1}H NMR did not show any signs of complex formation over the course of a few days, but after a month of vapour diffusion of dichloromethane into this solution orange blocks crystallised. So over time, Pd(IV) was reduced to Pd(II) to form **3.22**.

Another component used regularly to construct metallosupramolecular cages is dinitrato(ethylenediamine)palladium, so the complex of this metal salt and **3.5** was prepared. The M_6L_4 cage **3.21** has palladium dichloride providing a linear connection between the trans-coordinated ligand donor atoms. Dinitrato(ethylenediamine)-

palladium is capable of binding ligands in a cis-coordination and acting as a 90° angular component in metallosupramolecular assemblies, so the possibility of using this to form a different cage structure relying on the flexibility of **3.5** is intriguing. Elemental analysis suggested the product might possibly have the desired M_6L_4 stoichiometry, and even more exciting was the signal in the ^{1}H NMR spectrum characteristic of an encapsulated DMSO molecule, but the complex could not be crystallised. In an attempt to aid crystallization, zinc chloride in dilute hydrochloric acid was added to the solution to form an alternative anion ($ZnCl_4^{2-}$). The result was that the chelating ethylenediamine ligand on each palladium was substituted by two chlorine ions, and orange block-like crystals of **3.22** were obtained. The M_6L_4 cage must be very stable to form under both these very different reaction conditions.

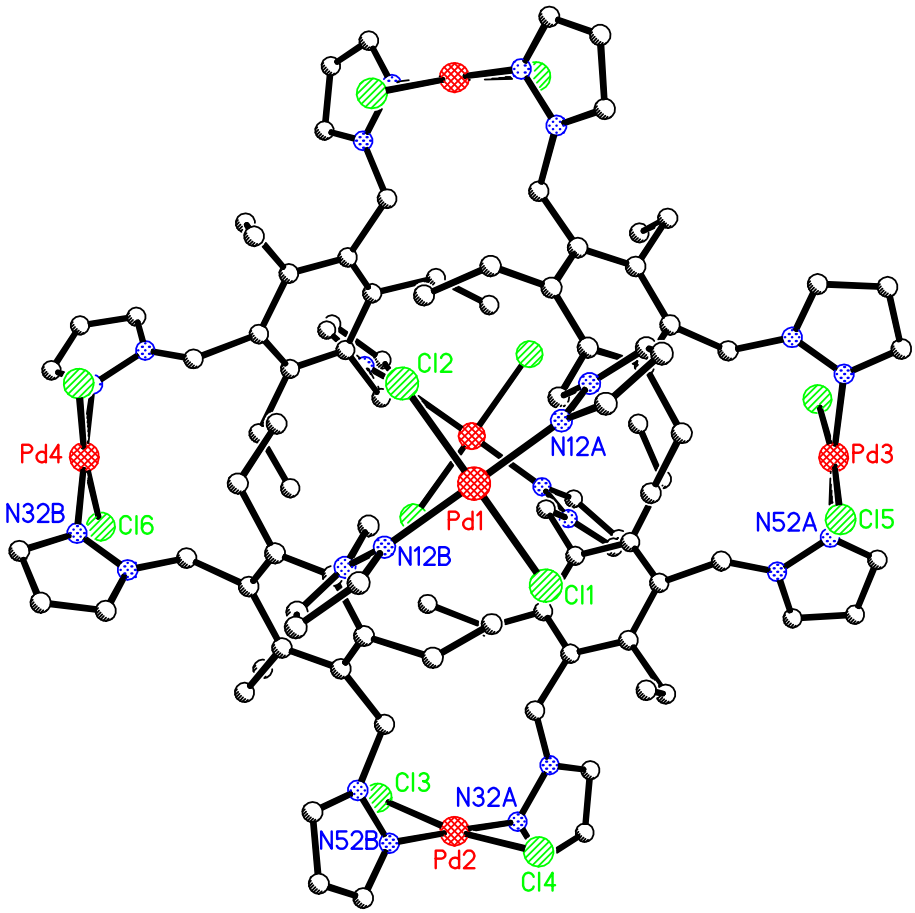

***Figure 3.11**. – The M_6L_4 cage **3.22**, of higher symmetry than **3.21**. Selected bond lengths (Å) and angles (°): Pd1-N12A 1.99(2), Pd1-N12B 2.00(2), Pd1-Cl1 2.287(7), Pd1-Cl2 2.300(6), Pd2-N32A 2.00(2), Pd2-N52B 2.00(2), Pd2-*

Cl3 2.319(6), Pd2-Cl4 2.302(7), Pd3-N52A 2.02(2), Pd3-Cl5 2.287(5), Pd4-N32B 1.99(2), Pd4-Cl6 2.326(5), N12A-Pd1-N12B 173.9(7), N12A-Pd1-Cl1 90.3(5), N12A-Pd1-Cl2 90.5(5), N12B-Pd1-Cl1 89.4(6), N32A-Pd2-N52B 178.2(7), N32B-Pd2-Cl3 88.4(5), Cl3-Pd2-Cl4 172.6(2), N52A-Pd3-Cl5 91.08(5), N32B-Pd4-Cl6 89.1(6).

The cage resulting from both these syntheses crystallises in a different space group to **3.21**, solving in orthorhombic group Pbcn. The structure is shown in Figure 3.11, excluding hydrogen atoms and poorly resolved solvate molecules. Only half of the cage is in the asymmetric unit, two ligands and two whole and two half palladium chloride units. The refinement on both the crystals is poor, probably due to twinning. The cage is surrounded by a large number of solvate molecules, but the resolution is not good enough to distinguish these, nor to unambiguously identify the solvate molecule present in the central cavity of the cage.

The main difference between **3.22** and **3.21** is the organization of the ethyl groups. In **3.22** all the ligands lie in an *ababab* conformation, with all the ethyl groups pointing into the central cavity. In both **3.21** and the original structure collected by Hartshorn,[55] one ligand is fully organised while the other three are not. The reasons for this lack of organisation in one of the two polymorphs are unknown. It seems logical that the more symmetrical structure **3.22** should be preferred. Hartshorn showed *via* ^{1}H NMR that the ethyl groups on the ligands are equivalent in solution,[55] so the symmetry disruption must only occur in the solid state.

The distances between opposite palladium atoms in **3.22** are 13.130Å, 15.423Å and 15.534Å, and surprisingly the cage is slightly compressed in one dimension, as was observed in **3.21**. Likewise all the pyrazole rings trans-coordinated to palladium atoms are significantly offset from the plane, except for the pyrazole rings bonded to Pd1 which are inline with each other. One trans-coordinated pyrazole pair in **3.21** also roughly approximates this. Again these small lapses of symmetry are surprising in a structure that has the option of being perfectly symmetrical.

The cages in both **3.21** and **3.22** pack similarly, in close packed columns, the spaces between molecules filled with disordered solvent molecules.

*Other complexes with **3.5***

As the coordination chemistry of **3.5** has been studied previously, complexation attempts in this research concentrated on silver and palladium reactants. One complex that has not yet been discussed was formed by the reaction with dinitrato(ethylenediamine)palladium, and subsequent conversion to the hexafluorophosphate salt. The resulting product analyses with Pd_5L_6 stoichiometry. This ratio is certainly possible but unusual. The ^{1}H NMR spectrum in acetonitrile shows an unsymmetrical complex is present in solution. It is a pity that multiple crystallization attempts were unsuccessful at providing crystals for full characterization.

Complexes with ligand 3.18

Complexation of ligand **3.18** was attempted with a variety of metal salts, namely CuI, $CuCl_2$, $Cu(NO_3)_2$, $CoCl_2$, $CoBr_2$, $FeSO_4$, $Pd(PhCN)_2Cl_2$ and K_2PdCl_4. Despite repeated attempts, none of these complexes produced X-ray quality crystals, and most were not analysed further.

The product of reaction of **3.18** with CuI was shown by elemental analysis to have a M_4L stoichiometry. As copper iodide is renowned for dimerising into Cu_2I_2 units or greater in complexation,[230,231] this could be an effective "M_2L"-type stoichiometry, which could have a number of possible structures, most likely a coordination polymer. Reaction with $CuCl_2$ formed a yellow powder that was shown to consist of a M_2L stoichiometry.

Of more interest was to explore whether **3.18** could complex to palladium and form a M_6L_4 cage analogous to **3.21** and **3.22**. Initially **3.18** was reacted with $Pd(PhCN)_2Cl_2$ in acetone to instantly form a yellow precipitate, which unfortunately analyses as M_2L stoichiometry. This was dissolved in DMSO in the hope it might react further, but vapour diffusion of various solvents into this solution failed to produce crystals. Reaction with K_2PdCl_4 was also attempted, both in acetone under hydrothermal conditions and in DMSO at room temperature, but the former only produced an oily solid upon slow cooling and vapour diffusion of acetone into the later has not yet produced any crystalline material.

Synthesis of the 1,3,5-tri[3-(2'pyridyl)pyrazol-1-ylmethyl] substituted ligands

The coordination chemistry of the known compound 1,3,5-tri[3-(2'pyridyl)pyrazol-1-ylmethyl]-2,4,6-trimethylbenzene (**3.23**) has been well studied.[141,142,144,232] Structurally related to ligand **3.16**, **3.23** includes an extra pyridine group to create a hexadentate ligand with three bidentate binding domains, as shown in Figure 3.12. The crystal structure of the free ligand shows that two arms lie on one side of the benzene ring and one on the other. This ligand has been shown to coordinate to three copper atoms, one in each binding domain, to form a discrete complex with copper perchlorate.[232] Reaction with silver tetrafluoroborate creates a complex one-dimensional chain, with weak silver-silver interactions linking the chains together into a two-dimensional sheet.[144] Ligand **3.23** was also used as a component of large heteroleptic cuboctahedral cages with ligand **2.15** and $Cu(BF_4)_2$ or $Co(BF_4)_2$, of the formula M_{12}(**2.15**)$_{12}$(**3.23**)$_4$.[142]

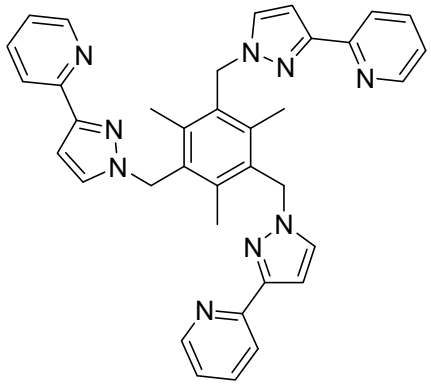

3.23

Figure 3.12 *– Literature compound **3.23**.*

As the coordination chemistry of **3.23** has been well-studied by separate groups, this ligand was not synthesised for this research. However, its ethyl and methoxy analogues have not previously been reported.

1,3,5-Tri[3-(2'pyridyl)pyrazol-1-ylmethyl]-2,4,6-triethylbenzene (**3.24**) was synthesised in one step from precursor **2.3** by a phase-transfer-catalysed alkylation of pyrazole to give the product in 96% yield. It is hoped that **3.24** will prefer a preorganised conformation and act as a metallosupramolecular synthon to form M_3L_2 or M_6L_4 molecular cages upon reaction with appropriate metal salts.

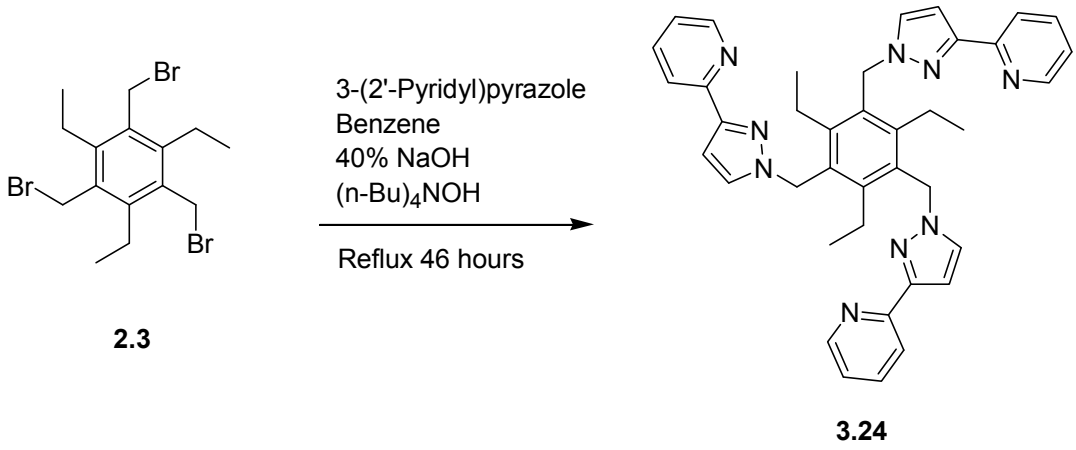

2.3 **3.24**

Scheme 3.8 *– The synthesis of ligand **3.24**.*

The synthetic route to 1,3,5-tri[3-(2'pyridyl)pyrazol-1-ylmethyl]-2,4,6-trimethoxybenzene (**3.25**) was much more difficult. Initially an analogous phase-transfer-catalysed alkylation of pyrazole was tried. Despite multiple attempts, this usually reliable reaction failed to produce more than trace amounts of **3.25**. The reasons for this are unclear. This reaction also worked poorly on **3.18**, so it appears the methoxy groups may be interfering with the reaction. The synthetic route[116] shown in Scheme 3.9 was more successful, providing **3.25** in 58% yield.

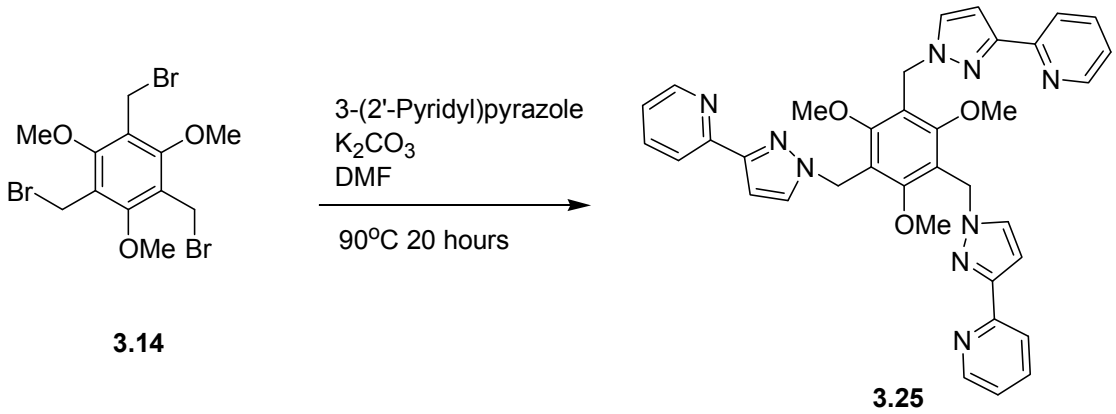

3.14 **3.25**

Scheme 3.9 *– The synthetic route to ligand **3.25**.*

Known compound **3.26**,[59,233] shown in Figure 3.13, is a similar ligand to the series created here, except the ligand arms contain bidentate N,S-donor chelating sites in place of the bidentate N,N-donor chelating sites seen in **3.23**, **3.24** and **3.25**. The crystal structure of the free ligand shows the same two-up-one-down conformation seen in ligand **3.23**.[233]

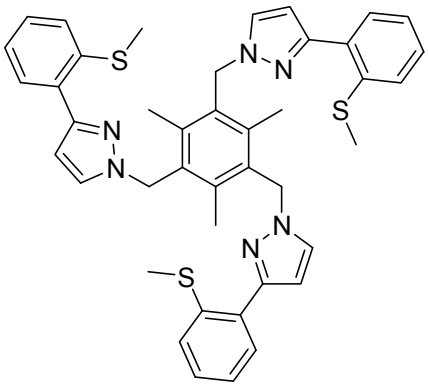

3.26

Figure 3.13 *– A similar ligand to this series,* ***3.26****.*

Ligand **3.26** has been shown to form discrete 1:1 and 3:2 complexes with $AgClO_4$.[233] In both complexes the silver shows the same η^1 interaction with the benzene core of the ligand as **3.20** and related complexes, as the silver atom is held between two arms in the same manner. Reaction with $Cu(CF_3SO_3)$ forms a two-dimensional polymeric sheet,[59] but most importantly, reaction of **3.16** with $Cd(ClO_4)_2$ provided a M_6L_4 cage.[59] Hopefully **3.24** and **3.25** can also act as components to form molecular cages.

Complexes with ligand 3.24

*Crystal structure of the complex with K_2PdCl_4 (**3.27**)*

The orange crystals that spontaneously crystallise from a DMSO solution when potassium tetrachloropalladate is reacted with ligand **3.24** were suitable for X-ray crystallography and the structure solved in trigonal space group R-3. The asymmetric unit contains one third of the ligand, one palladium chloride unit, three water molecules of $^1/_6{}^{th}$ occupancy, and one third of a DMSO solvate molecule.

The structure is shown in Figure 3.14, with hydrogen atoms, solvate water molecules, and the disorder of the DMSO excluded for clarity. The structure consists of three metal atoms and one ligand. Each palladium binds to two ligand nitrogens and two chloride anions in a square planar geometry, slightly distorted due to the restrictions imposed by the nitrogen atoms. Each of the three bidentate arms chelates to one palladium atom.

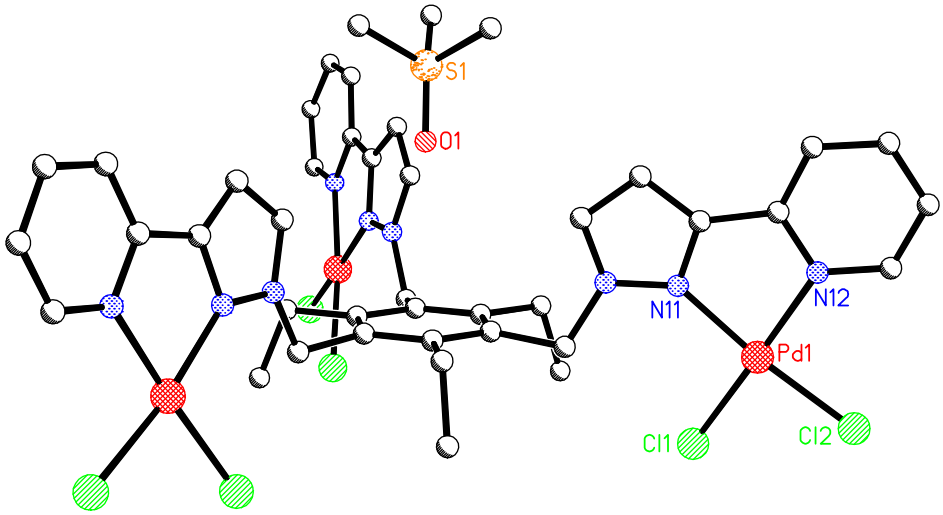

Figure 3.14 *– The discrete trinuclear structure of* ***3.27****. Selected bond lengths (Å) and angles (°): Pd1-N11 2.043(3), Pd1-N12 2.044(4), Pd1-Cl1 2.287(1), Pd1-Cl2 2.270(1), N11-Pd1-N12 79.4(1), N11-Pd1-Cl2 172.7(1), N11-Pd1-Cl1 100.2(1), N12-Pd1-Cl2 93.9(1), N12-Pd1-Cl1 174.8(1), Cl2-Pd1-Cl1 86.74(4).*

The ligand lies in an *ababab* conformation with all three ethyl groups pointing downwards and all three donor arms pointing upwards. The nitrogen donor atoms point downwards, so all the palladium atoms sit level with the plane of the benzene core. A disordered DMSO solvate molecule sits above the complex. The DMSO is the ideal size for the cavity made by the coordinating arms of the ligand, with the oxygen atom pointing towards the central benzene ring. The DMSO is disordered as it does not incorporate the same trigonal symmetry exhibited by the main structure.

In the molecular packing the complexes are aligned. There are multiple short contacts between the chloride anions and hydrogens on the main structure. There are no π-π stacking interactions between molecules.

A sample of **3.27** was transported to the University of Sydney for thermogravimetric analysis measurements, in the hope it might provide information on how strongly the DMSO molecule is interacting with the complex. ThermoGravimetric Analysis (TGA) can be used to investigate the stability of a crystalline framework when solvent molecules are removed from the lattice by measuring the weight change of a sample as

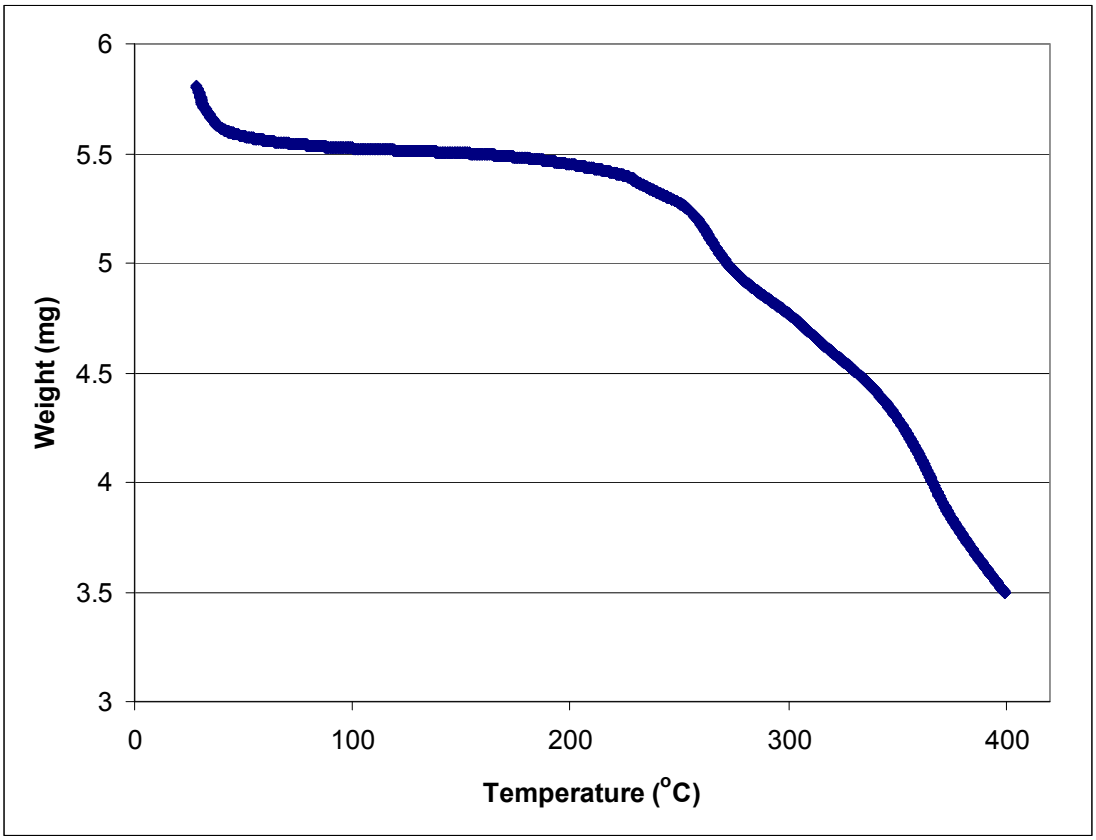

Figure 3.15 *– Thermogravimetric analysis results for complex* ***3.27****. The plot shows the weight change with temperature.*

it is heated. The results are shown in Figure 3.15. The sudden drop in weight at the beginning of measurement is due to rapid solvent removal, probably due to the sample being slightly wet on the surface. The data shows a gradual 5% weight loss to around 200°C, then slow decomposition above this temperature. The DMSO accounts for 6% weight of the structure, so it would make sense that this weight change corresponds to the DMSO being removed from the complex. Possibly 1% of the DMSO had already leaked from the lattice before or at the beginning of the measurements, and increasing temperature allows solvent molecules from deeper within the crystals to escape.

*Crystal structures of the complexes with $CuSO_4$ (**3.28** and **3.29**)*

When ligand **3.24** was reacted with copper sulfate in the methanol layering technique described in the last chapter, large blue crystals were obtained which were stable in solvent for over a year but decompose within seconds upon exposure to air. Eventually a crystal was mounted quickly enough to obtain an X-ray structure from poor quality data, with a final R_1 value of 9.74%. The structure solved in triclinic space group P-1.

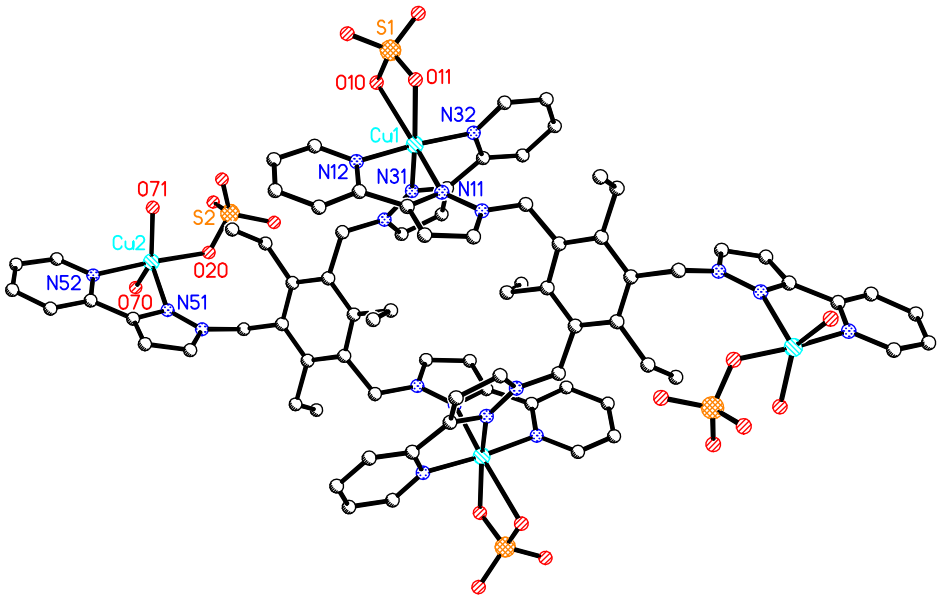

Figure 3.16 *– The discrete M_4L_2 structure* ***3.28****. Selected bond lengths (Å) and angles (°): Cu1-N32 2.006(4), Cu1-N12 2.008(4), Cu1-O11 2.131(6), Cu1-N31 2.113(4), Cu1-N11 2.201(4), Cu1-O10 2.416(8), Cu2-O20 1.955(4), Cu2-N52 1.997(5), Cu2-O70 1.984(5), Cu2-O71 2.035(4), Cu2-N51 2.186(4), N32-Cu1-N12 175.6(2), N32-Cu1-O11 92.7(2), N32-Cu1-N31 79.4(2), N32-Cu1-N11 96.7(2), N32-Cu1-O10 94.5(2), N12-Cu1-O11 89.6(2), N12-Cu1-N31 99.6(1), N12-Cu1-N11 79.1(1), N12-Cu1-O1 89.9(2), O11-Cu1-N31 159.5(2), O11-Cu1-N11 102.2(2), O11-Cu1-O10 62.3(2), N31-Cu1-N11 97.5(2), O20-Cu2-N52 174.6(2), O20-Cu2-O70 92.5(2), O20-Cu2-O71 90.7(2), O20-Cu2-N51 95.7(2), N52-Cu2-O70 90.3(2), N52-Cu2-O71 89.6(2), N52-Cu2-N51 78.9(2), O70-Cu2-O71 146.5(2), O70-Cu2-N51 111.8(2), O71-Cu2-N51 101.1(2).*

The discrete M_4L_2 structure is shown in Figure 3.16, with hydrogen atoms and solvate molecules excluded for clarity. Immediately obvious is the similarity to structure **2.21** and related dimers, which makes the air sensitivity of this complex less surprising. The asymmetric unit contains one ligand **3.24**, two copper atoms and a partially occupied chloroform, a methanol, and a few water solvate molecules. The full structure consists of two ligands and four copper units. The ligands are linked together by two copper atoms, to create a dimeric unit similar to **2.21**. The third arm of both the ligands lies pendant, coordinated to another copper atom. There are two independent metal atoms in the structure. Cu1 chelates to two ligand binding domains and a sulfate anion, binding to four ligand nitrogens and two sulfate oxygens in an octahedral geometry. Cu1 bridges two ligands. The way Cu1 chelates to two sulfate oxygens is different to structure **2.12** and related dimers where the copper atom is five-coordinate. Cu2

chelates to one ligand binding domain, one sulfate oxygen and two water molecules in a five coordinate square pyramidal geometry. In this case, the copper atom has chosen to coordinate extra water molecules rather than chelate to another sulfate oxygen.

A centre of inversion lies in the middle of the structure, and thus, like **2.21**, one ligand reaches over Cu1 and Cu1A, while the other ligand reaches below. The two ligand arms on each ligand that form the dimer lie on the same side of the benzene core, while the third arm lies on the opposite side. The ethyl groups are organised between up and down, with the ethyl group closest the centre of the structure sitting between the "V"-shape formed by the coordinating arms of the opposite ligand. Overall, the ligand lies in an *ababba* conformation.

In the crystal packing the dimers are aligned in channels, with multiple short contacts between the sulfate oxygens and hydrogens on the ligands. There are two sets of π-π stacking interactions between the coordinating arms of ligands on adjacent dimers (3.225Å and 3.428Å).

It is unknown why ligand **3.24** prefers to form this M_4L_2 dimeric structure with only two arms linked, rather than all three arms joining to construct a M_3L_2 molecular cage. To examine the possible variables, such as metal to ligand ratio and presence of a templating guest on the formation of this structure, this reaction was repeated in an H-shaped tube. The ligand was added to one limb of the H-tube with ferrocene, a possible template for the formation of a cage, and copper sulfate was added to the other limb. The solution was left for the components to slowly diffuse together across the bridge of the H-tube. Crystals formed at the region in the tube where the ligand and metal start to mix, and like **3.28** these too were found to be very unstable out of solution. Despite the rapid decomposition, eventually a crystal was mounted quickly enough to retain enough crystallinity for diffraction. Although a solution was obtained, the data are of poor quality and the structure did not refine below 14%. The program *Squeeze*[151] lowers the R_1 value slightly to 10.5% by removing residual electron density. The cell constants from these new crystals were different to **3.28**, although the structure also solved in triclinic space group P-1.

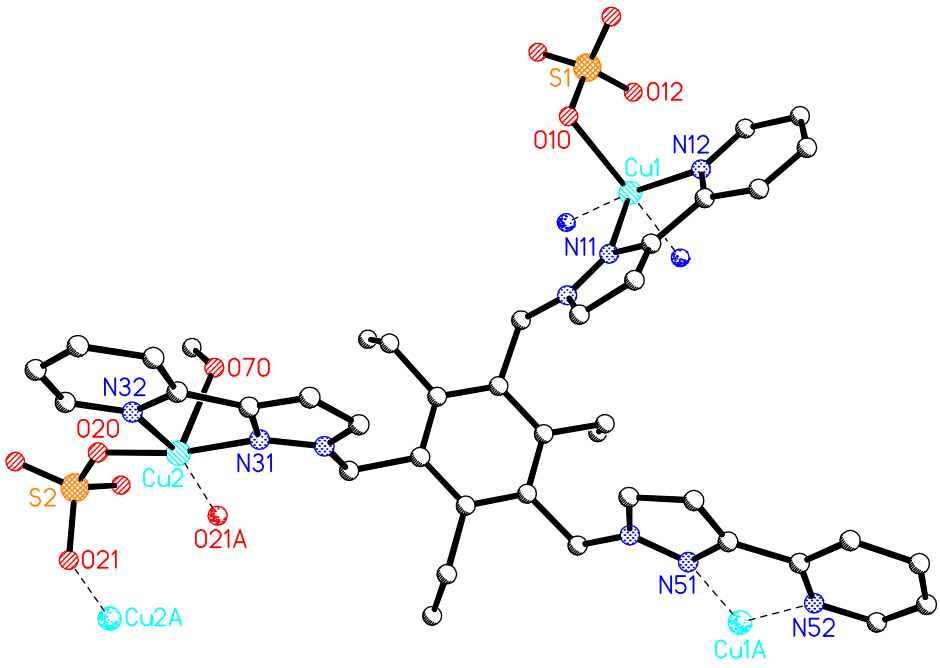

Figure 3.17 *– The asymmetric unit of* ***3.29****, showing the organisation of the ligand. Selected bond lengths (Å) and angles (°): Cu1-N52A 2.019(8), Cu1-N12 2.036(8), Cu1-N51A 2.160(6), Cu1-N11 2.166(7), Cu1-O10 2.30(1), Cu2-O20 1.903(8), Cu2-O21 1.926(8), Cu2-N32 2.024(9), Cu2-N31 2.017(8), Cu2-O70 2.24(1), N52A-Cu1-N12 174.8(3), N52A-Cu1-N51A 80.3(3), N52A-Cu1-N11 97.4(3), N52A-Cu1-O10 93.5(3), N12-Cu1-N51A 95.9(3), N12-Cu1-N11 79.2(3), N12-Cu1-O10 90.7(3), N32-Cu2-N31 81.2(3), O20-Cu2-O21 96.0(3), O20-Cu2-N32 88.9(3), O20-Cu2-N31 169.0(3), O21-Cu2-N31 94.9(3).*

Shown in Figure 3.17 is the asymmetric unit of **3.29**, with hydrogen atoms and solvate molecules excluded for clarity. The asymmetric unit contains one ligand **3.24**, two copper atoms and two sulfate counterions, one coordinated methanol and, due to the poor data, an indeterminable number of methanol and water solvate molecules. Like **3.28**, **3.29** consists of M_4L_2 dimer units, but the structures are quite different. In **3.29**, the ligand lies in an *ababab* organised conformation, with all the binding arms on one side of the benzene core and all the ethyl groups on the other. Cu1 which links together the ligands into dimer units, now binds the sulfate anion monodentate, displaying a five coordinate square pyramidal geometry with a very weak interaction to another sulfate oxygen O12 (2.440Å) causing little distortion of the geometry of the copper centre. Cu2 binds two ligand nitrogens, two sulfate oxygens, and a methanol oxygen in a five coordinate square pyramidal geometry.

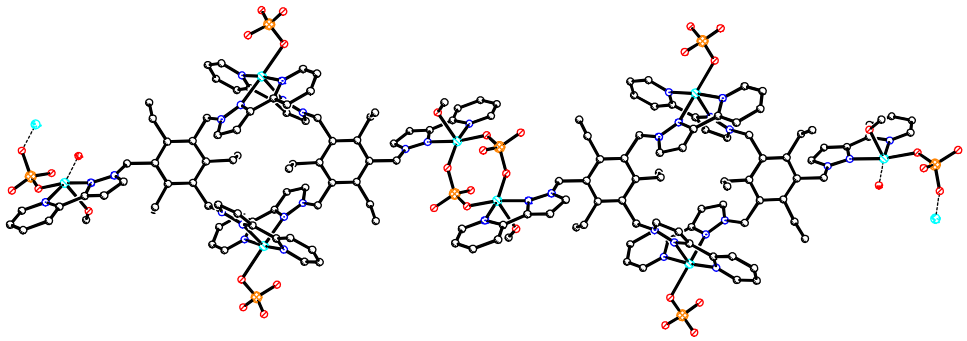

Figure 3.18 *– A section of the M_4L_2 polymeric chain structure of* ***3.29****.*

The M_4L_2 dimers in **3.29** are very similar to those in **3.28**, with the two ligands related by a centre of inversion and sharing two copper atoms to form the dimeric unit. With both the coordinating arms are on the same side of the ligand and an ethyl group lies between the "V"-shape created by the other ligand arms. However Cu1 is now in a five-coordinate geometry, the ligand is now organised with the pendant arm on the same side as the other ligand arms, and Cu2 now coordinates to two sulfate anions and a methanol oxygen. But most significantly, unlike **3.28**, the M_4L_2 dimers in **3.29** are linked together by two bridging sulfate anions to form a one-dimensional polymer, as shown in Figure 3.18. Hydrogen atoms and solvate molecules are excluded for clarity. These two bridging anions create an eight-membered chelate ring between the Cu2 atoms[234] which are also related by a centre of inversion. The sulfate oxygens occupy the equatorial sites on the copper atom along with the ligand nitrogens, and the methanol fills the axial position. The polymer propagates in a linear direction.

Multiple hydrogen bonding interactions between sulfate oxygens and ligand hydrogens link together the one-dimensional strands into a three-dimensional structure. There are also π-π stacking interaction between the coordinating arms (3.268Å) and between the N52 pyridine and the N31 pyrazole rings of adjacent dimers (3.208Å).

Crystal structure of the complex with $Cu(NO_3)_2$ ***(3.30)***

A methanol and toluene solution of ligand **3.24** and copper nitrate produced small green crystals after a few weeks of slow evaporation. Like **3.28** and **3.29**, these crystals were very air sensitive, decomposing seconds after removal from the mother liquor. Despite

the poor diffraction of the crystal a dataset was collected which gave a reasonable R_1 value, considering the circumstances. The structure solved in monoclinic space group $P2_1/c$.

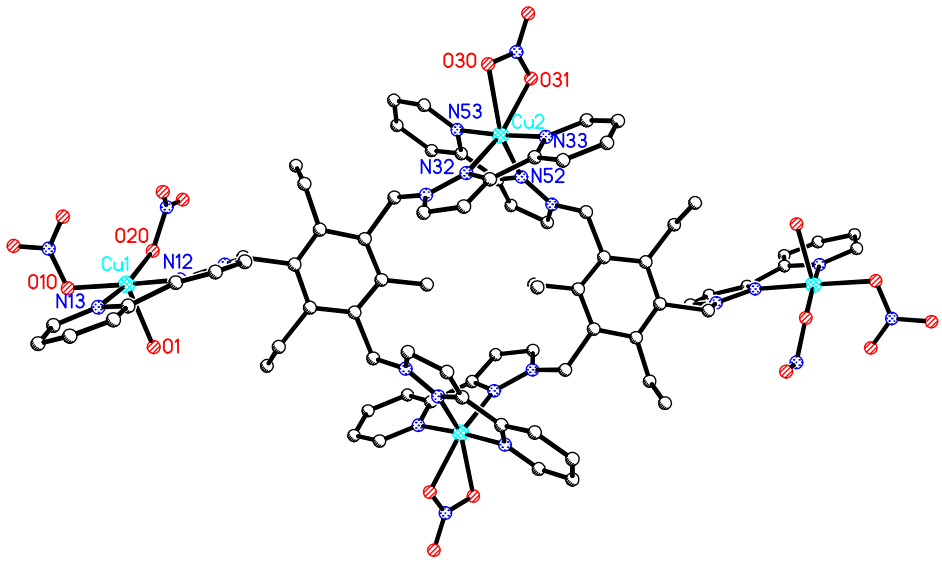

Figure 3.19 *– The discrete M_4L_2 dimer* ***3.30****. Selected bond lengths (Å) and angles (°): Cu1-O10 1.99(1), Cu1-N12 1.99(1), Cu1-N13 2.10(1), Cu1-O20 2.11(1), Cu1-O1-2.23(1), Cu2-N33 1.91(2), Cu2-N53 1.95(2), Cu2-N52 2.06(2), Cu2-N32 2.09(1), Cu2-O31 2.10(2), Cu2-O30 2.40(1), O10-Cu1-N12 168.7(6), O10-Cu1-N13 91.2(7), O10-Cu1-O20 90.9(5), O10-Cu1-O1 96.8(5), N12-Cu1-N13 78.5(9), N12-Cu1-O1 89.5(5), N33-Cu2-N53 176.4(8), N33-Cu2-N52 103.6(8), N33-Cu2-N32 83.0(7), N33-Cu2-O31 84.1(7), N33-Cu2-O30 81.9(5), N53-Cu2-N52 78(1), N52-Cu2-N32 105.8(5), N52-Cu2-O30 155.6(5), N32-Cu2-O31 152.0(5).*

The M_4L_2 dimer **3.30** is shown in Figure 3.19, with hydrogen atoms and solvate molecules excluded for clarity. The asymmetric unit contains one ligand, two copper atoms, three nitrate anions, one coordinated hydroxide anion, and two methanol and one water solvate molecules. The structure is similar to both **3.28** and **3.29**. Two ligands are linked together by two copper atoms into a dimeric structure, with the pendant arm on each ligand binding an extra copper atom. Like **3.29**, the ligand is organised, and like **3.28**, the structure is discrete. Cu2 bridges the two ligands, and also binds a bidentate nitrate anion, coordinating to four ligand nitrogens and two nitrate oxygens in a distorted octahedral geometry. The distortion mainly arises from the restrictions of the nitrate oxygens. Cu1 coordinates to two ligand nitrogens, two monodentate nitrate

anions, and what is presumably a hydroxide with a five coordinate square pyramidal geometry. The ligands are organised into *ababab* conformations, so the central ethyl group sits between the "V" of the adjacent ligand arms and the pendant arm sits on the same face of the benzene core as the bridging arms.

The charge balance is interesting, as there is only one nitrate counterion associated with Cu2. The oxygen attached to the terminal Cu1 atoms must be a hydroxide, giving a localised negative charge over each centre, which would balance the charges over the whole of the dimer, in what is a zwitterionic structure.

In the crystal packing there are hydrogen bonding interactions between the nitrate oxygens, the solvate oxygens and the hydrogens on the ligands. There are π-π stacking interactions between the pendant arms of the ligands of adjacent dimers (3.390Å).

Between these three structures, **3.28**, **3.29**, and **3.30**, it appears that this M_4L_2 moiety is a predominant motif for ligand **3.24**. Unlike a M_3L_2 cage, only two ligand arms are bound together. It may not be possible for **3.24** to act as a component of a M_3L_2 cage, as possibly the orientation of the coordination sites are not suitable for this arrangement, or the benzene cores or ethyl groups may be too close in a M_3L_2 structure to make this structure accessible.

The tendency for ligand **3.24** to decompose in the presence of metal salts, especially those containing copper(II), will be discussed in Chapter Five.

*Other complexes of **3.24***

Complexation of **3.24** was attempted with a large variety of metal salts in many different solvent systems. These metal salts included $AgNO_3$, $AgClO_4$, $AgPF_6$, $AgCF_3SO_3$, CuI, $CuBF_4$, $Cu(NO_3)_2$, $CuSO_4$, $CuCl_2$, $Cu(ClO_4)_2$, $CoCl_2$, $CoBr_2$, $Co(NO_3)_2$, $Co(BF_4)_2$, $NiCl_2$, $Ni(BF_4)_2$, $Ni(ClO_4)_2$, $FeSO_4$, $Fe(SCN)_2$, $Fe(ClO_4)_2$, $ZnBr_2$, $Zn(ClO_4)_2$ and K_2PdCl_4. Four crystal structures of complexes containing **3.24** have been reported in this chapter. More crystal structures were obtained from these reactions which contained ligand decomposition products which will be discussed in Chapter Five. Of the complexes which did not produce crystals, many were not analysed further.

Reaction of **3.24** with $CoCl_2$ produced very air sensitive block-like crystals. These crystals were suitable for X-ray crystallography, but like **3.28**, **3.29** and **3.30**, it was very difficult to get one of these crystals into the cold stream of the diffractometer before too much decomposition had taken place. Eventually a poor quality dataset was obtained. The structure solved in monoclinic space group $P2_1/c$, and showed two ligands linked together into a dimer unit like **3.28**, **3.29** and **3.30**. However in this case, the complex is a M_2L_2 moiety, with the pendant arm uncoordinated and disordered such that it could not be located from the difference map. The cobalt atoms each bind to four ligand nitrogens of two separate ligands, and two chloride anions, in an octahedral geometry. Of the five substituents located, the ligand appears to be in an organised conformation. Once again it has been shown that this dimeric structure appears to be the preferred motif for ligands **3.24** and **2.12**, where an ethyl group of one ligand sits neatly between the arms of the adjacent ligand.

In an attempt to grow better quality crystals, another complex with $CoCl_2$ was prepared, which has a M_2L stoichiometry. Possibly this is the dimeric structure with extra metal atoms coordinated to the pendant ligand arms. Crystals could not be obtained.

The reaction of ligand **3.24** with $Zn(ClO_4)_2$ has been followed by NMR. The complex precipitates out of solution and has been shown by elemental analysis to contain a 1:1 metal to ligand ratio. This could suggest another dimer or a different structure, possibly a polymer. When the ratio of metal to ligand is adjusted this precipitate redissolves and another complex forms, which was not able to be characterised. Reaction with $CoBr_2$ also produced a complex with a 1:1 stoichiometry, whereas complexation with $FeSO_4$ created a complex with a M_3L stoichiometry, which is most likely a discrete structure resembling **3.27**.

Complexes with ligand 3.25

Complexation of ligand **3.25** was attempted with a variety of metal salts, namely CuI, $CuCl_2$, $CuSO_4$, $Cu(NO_3)_2$, $CoBr_2$, $FeSO_4$, $Fe(ClO_4)_2$ and K_2PdCl_4. Unfortunately no crystals suitable for X-ray crystallography could be obtained. Only some of these complexes were analysed further.

Reaction of **3.25** with $FeSO_4$ produced a black solid which was shown to have a M_3L stoichiometry. It is likely this product has a discrete structure similar to **3.27**.

The products of reaction of **3.25** with $CuCl_2$ or $Fe(ClO_4)_2$ were both shown to have a M_4L stoichiometry. One possibility is that the complexes have one metal atom in each binding domain, and then another metal atom interacting with the main structure somehow, possibly with the methoxy groups. Another possibility is that the metal atoms have dimerised into simple square-like units, common for $CuCl_2$ complexes, giving an effective stoichiometry of M_2L, which could conform to a number of different topologies.

Reaction of **3.25** with $CoBr_2$ produced a dark crimson solid that analyses to have a M_5L_2 stoichiometry. This unusual ratio could be consistent with a complex coordination polymer or a large discrete structure.

Synthesis of the 1,3,5-tri(4-pyridylsulfanylmethyl) substituted ligands

Known literature compounds **3.31**[235] and **3.32**[77,236] have been shown to form interesting structures upon complexation with metal salts. As shown in Figure 3.20, both ligands are based on three 4-pyridyl groups linked *via* sulfanylmethyl chains in a 1,3,5-substitution around an aromatic ring. Therefore this seemed a good template for another family of ligands.

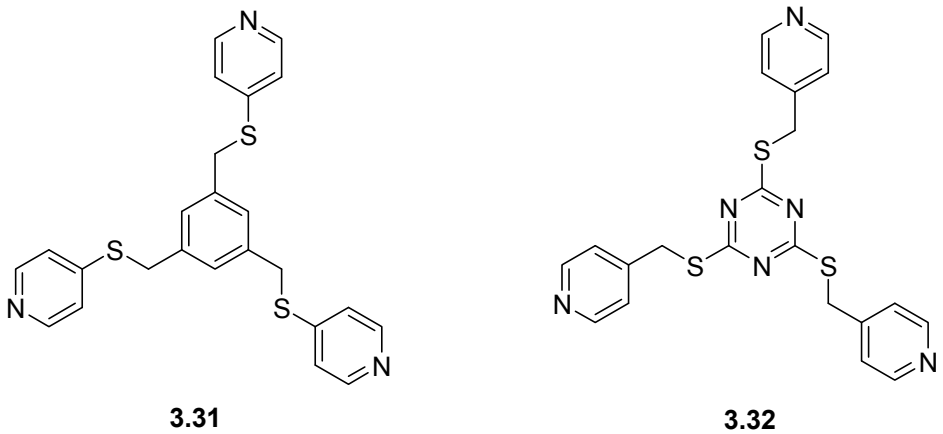

3.31 **3.32**

Figure 3.20 *– Literature compounds which have been shown to form molecular cages upon complexation.*

Ligand **3.31** forms a M_3L_2 cage upon reaction with $AgNO_3$,[235] where the nitrate anions link together the silver atoms. Ligand **3.32** forms a hollow molecular tube of repeating M_3L_2 units upon reaction with $AgClO_4$,[236] and upon complexation with $NiCl_2$ gives a large M_6L_8 cage which encapsulates eight DMF molecules.[77]

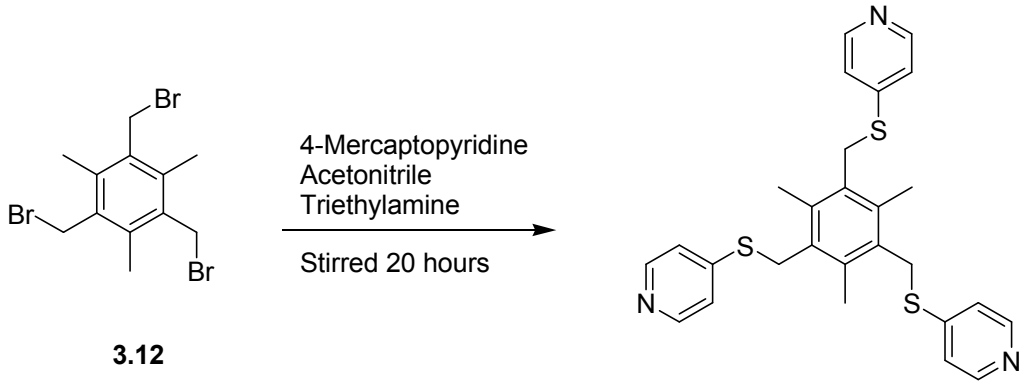

3.12 **3.33**

Scheme 3.10 *– Synthesis of ligand* ***3.33****.*

Known compound 1,3,5-tri(4-pyridylsulfanylmethyl)-2,4,6-trimethylbenzene (**3.33**)[237] was synthesised by the literature procedure,[237] as shown in Scheme 3.10, cooling the reactants to 0^oC on ice and allowing the solution to slowly warm to room temperature over the duration of the experiment, to obtain **3.33** in 45% yield after purification. Although previously made, the coordination chemistry of **3.33** has yet to be investigated as no complexes have been fully characterised. This ligand displays low solubility in common solvents, which is common in 4-pyridyl ligands of this type.[237]

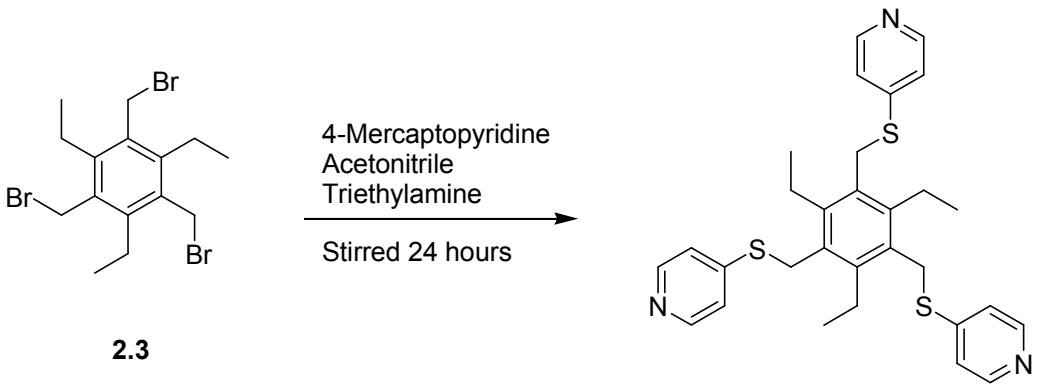

2.3 **3.34**

Scheme 3.11 *– Synthetic route to ligand* ***3.34****.*

New ligand 1,3,5-tri(4-pyridylsulfanylmethyl)-2,4,6-triethylbenzene (**3.34**) was synthesised by an analogous reaction as shown in Scheme 3.11, producing the product in 60% yield. It exhibits low solubility in all common solvents, and differs from **3.33** by the ethyl groups surrounding the core, which will hopefully help induce a preorganised conformation and increase the odds that **3.34** will form cage-like structures like those formed by **3.31** and **3.32**.

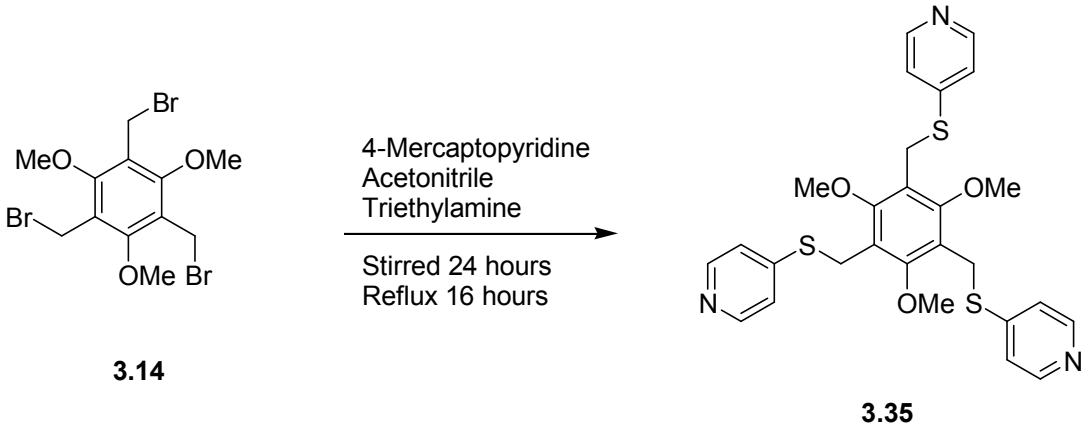

3.14 **3.35**

Scheme 3.12 *– Synthetic route to ligand **3.35**.*

The reaction to produce new ligand 1,3,5-tri(4-pyridylsulfanylmethyl)-2,4,6-trimethoxybenzene (**3.35**) did not run as smoothly. The same procedure used to synthesise **3.33** and **3.34** showed incomplete reaction after 24 hours, so the solution was refluxed overnight to provide **3.35** in 74% yield after purification. Unlike the other two solids, **3.35** is an oil, but also displays low solubility properties. It differs from the other two ligands in this series by the methoxy groups in the 2,4,6-substitution around the ligand core.

*Crystal structure of ligand **3.34***

Slow evaporation of a dichloromethane solution of ligand **3.34** and silver hexafluorophosphate produced a few colourless crystals suitable for X-ray crystallography. The structure solved in orthorhombic space group Ima2.

No silver is present in the structure, as shown in Figure 3.21, with hydrogen atoms, the counterion and solvate water molecules excluded for clarity. The asymmetric unit contains half of ligand **3.34,** half a hexafluorophosphate counterion, and a water

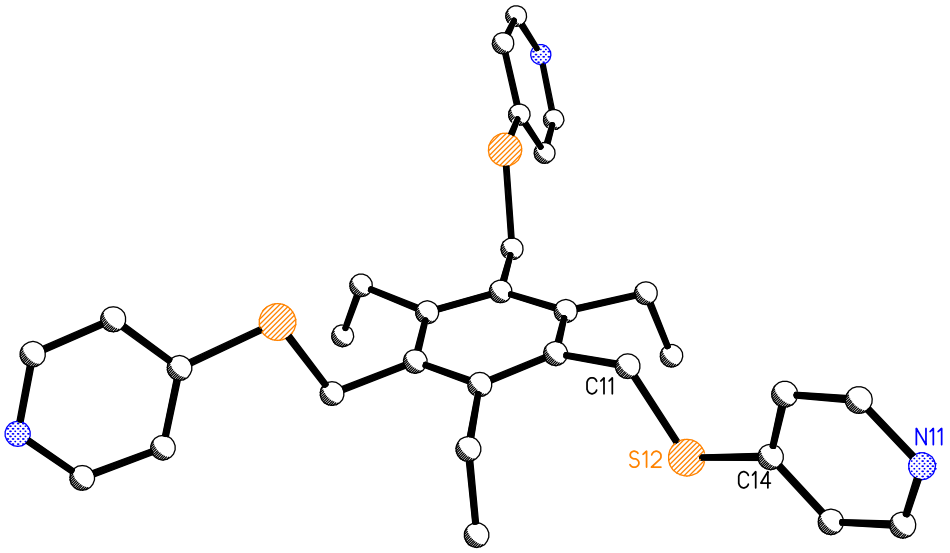

Figure 3.21 *– Ligand* ***3.34****. Selected bond lengths (Å) and angles (°): S12-C14 1.756(5), S12-C11 1.807(5), C11-S12-C14 102.8(2).*

molecule. The extra proton required for charge balance could not be located, so is probably disordered between the water and pyridine sites. All the ethyl groups point down, showing some degree of preorganisation, but two of the sulfur atoms lie above the plane of the benzene ring while the third is below. A mirror plane runs through the middle of the ligand. The pyridine nitrogens point directly out from the ligand. In this orientation it appears that even preorganisation could not alter this ligand to be more than a flat panel capable of acting as a three connector node, but similar ligand **3.31** has shown the sulfanylmethyl linkers to be flexible enough to orient the pyridine nitrogens perpendicular to the benzene core.[235]

Complexes with ligand 3.33

*Crystal structure of the complex with $CoBr_2$ (**3.36**)*

Slow evaporation of a solution containing ligand **3.33** and cobalt bromide provided pink needle-like crystals, which proved to be suitable for X-ray crystallography. The structure solved in orthorhombic space group Pnma.

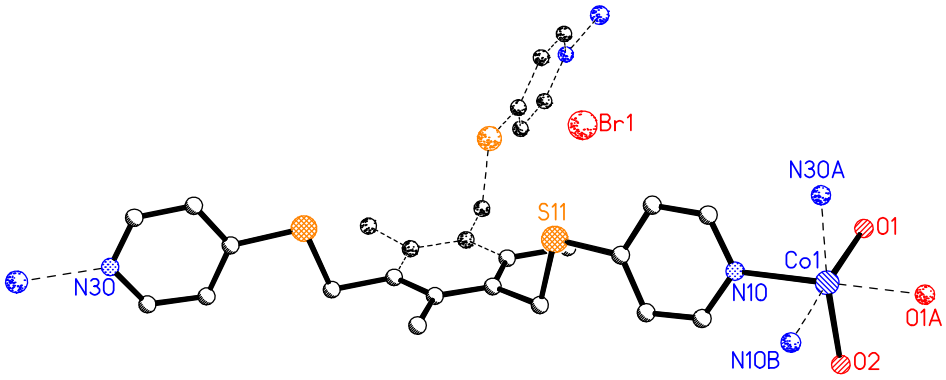

Figure 3.22 *– The asymmetric unit of structure* ***3.36****. Selected bond lengths (Å) and angles (°): Co1-N30A 2.133(7), Co1-O2 2.139(6), Co1-O1 2.146(5), Co1-N10 2.154(6), N30A-Co1-O2 175.1(3), N30A-Co1-O1 87.1(2), N30A-Co1-N10 93.7(2), O2-Co1-O1 89.5(2), O2-Co1-N10 89.6(2), O1-Co1-O1A 89.7(3), O1-Co1-N10 88.7(2), O1-Co1-N10A 178.1(2), N10-Co1-N10A 93.0(3).*

The asymmetric unit is shown in Figure 3.22 with hydrogen atoms, disorder of the bromine atom, and solvate molecules excluded for clarity. The asymmetric unit contains half ligand **3.33**, half a cobalt atom, one and half coordinated water molecules, one non-coordinated bromine atom, and two and a half solvate water molecules disordered over five sites. Each ligand coordinates to three cobalt atoms *via* the pyridine nitrogens. Each cobalt atom binds facially three pyridine nitrogens of separate ligands, and three water molecules with an octahedral geometry. The bromide counterions are not coordinated to the metal centre. Each sits in the lattice disordered over two sites at half occupancy. All three arms on the ligand are bent to the same side of the central benzene core, and a mirror plane runs through the centre of the ligand.

The unit shown in Figure 3.22 is a small section of a polymer. Each polymer strand forms a two-dimensional (6,3) net. Both the central benzene ring of the ligand and the cobalt atoms act as three-connected nodes, as shown in the simplified diagram in Figure 3.23.

Polymer sheets of identical topology are misaligned, with the nodes of each alternating sheet filling the centre of the cavity of the net above and below it. A simplified diagram of two nets is shown in Figure 3.24, with individual polymer chains shown in different colours. While the sheets of polymers interdigitate to fill the large cavities, they do not interpenetrate, as no bonds need to be broken to separate the layers.

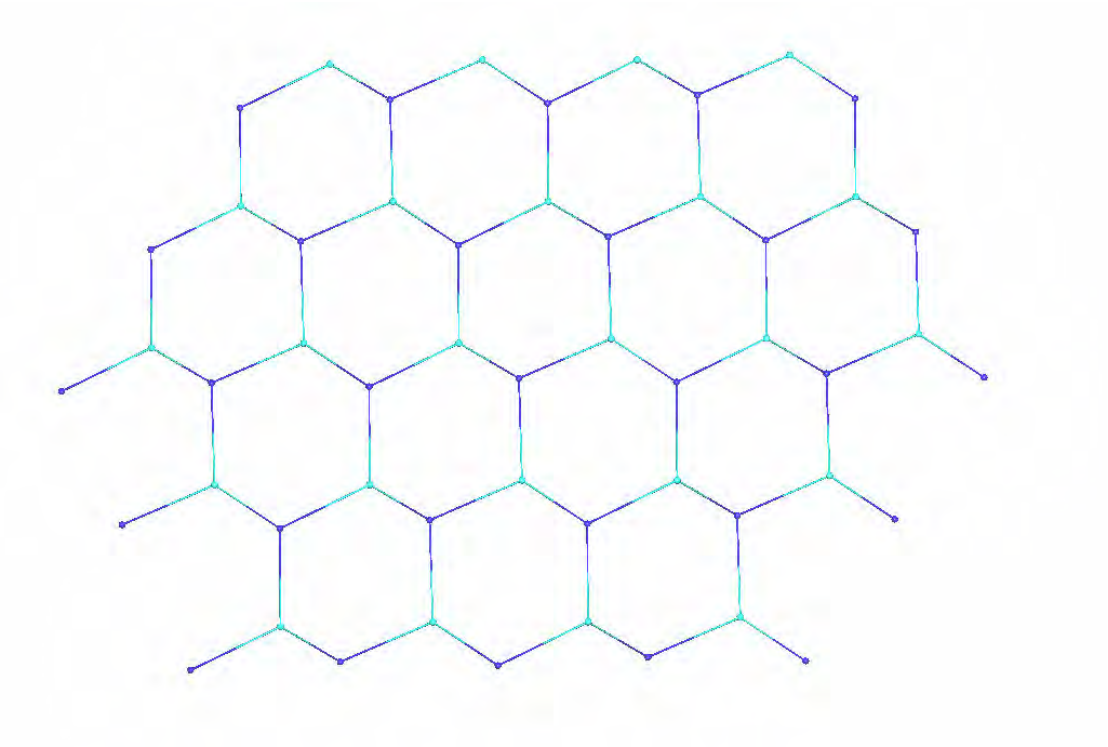

Figure 3.23 *– A simplified view of a section of the polymeric sheet* ***3.36****. The cobalt atoms are shown in dark blue, the ligands pale blue.*

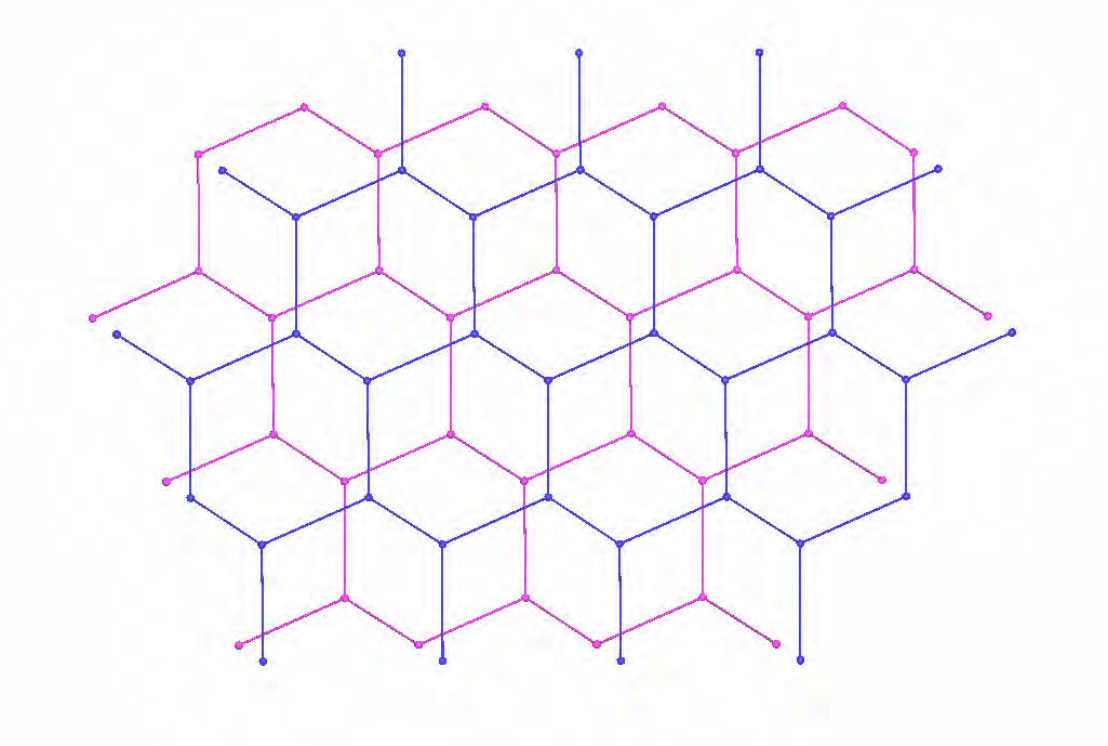

Figure 3.24 *– A simplified diagram of a section of two polymer sheets of* ***3.36****, showing the alignment.*

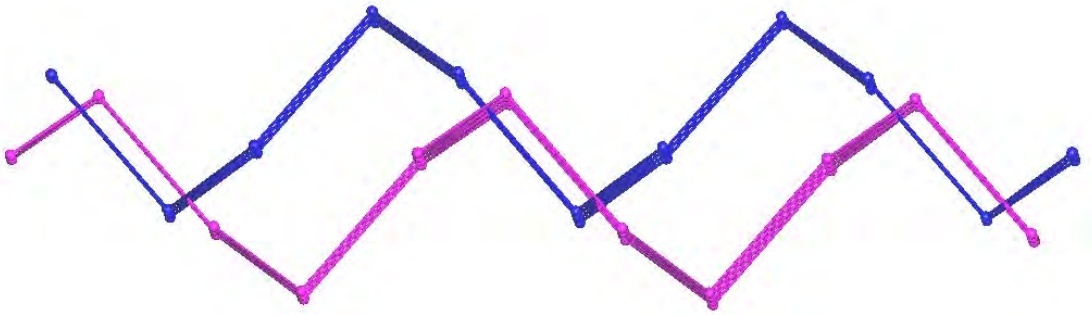

Figure 3.25 *– A simplified diagram of two sheets of polymer* ***3.36****, showing the undulation of the layers.*

When an individual polymer sheet is viewed from the side, a corrugated pattern is seen, as shown in Figure 3.25 by the simplified blue chain. The cobalt atoms are at the crest and base of each wave in this pattern. When two strands are examined from this perspective, it is seen that the lower net is staggered horizontally with respect to the net above, and the average plane of the net is lower, so that it never passes above the higher plane.

An orthogonal view shows the cavities in the (6,3) net of a single sheet, as shown in Figure 3.26 by the blue net. The addition of another sheet shows it is translated down half a unit from the original sheet. The second sheet appears to penetrate into the middle of the original sheet, but this is only due to the undulating nature of the polymer.

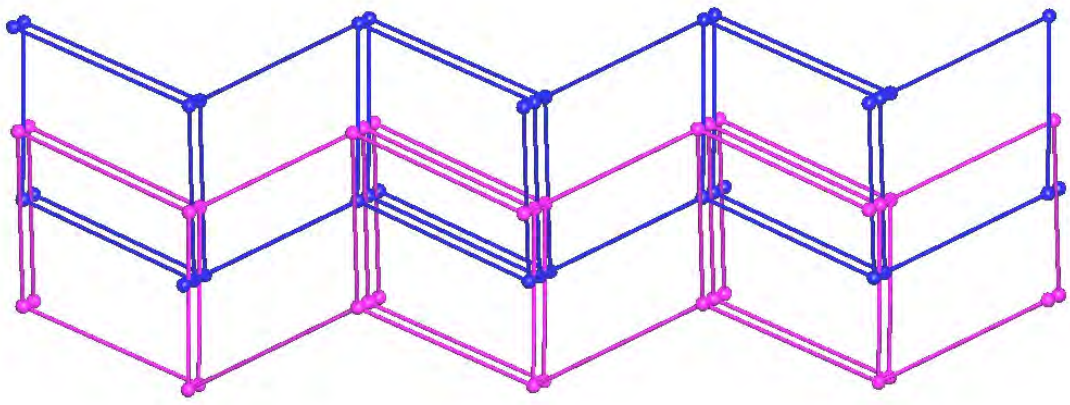

Figure 3.26 *– Another view of two simplified sheets of* ***3.36****, showing the interdigitation between the chains. The different sheets are shown in different colours.*

There are short contacts between the sheets, from the sulfur atoms, bromide counterions and coordinated and solvate water molecules to hydrogens on the ligands. There are no π-π stacking interactions between the chains.

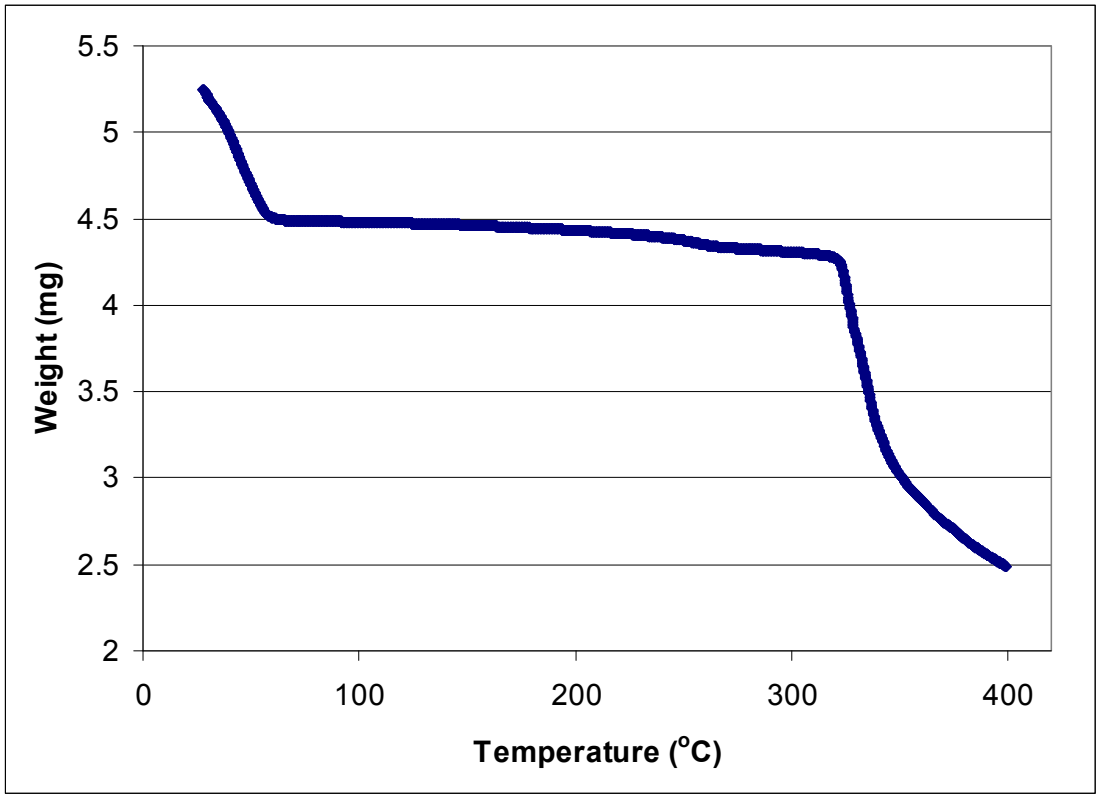

Figure 3.27 *– Thermogravimetric analysis results for two-dimensional polymer* ***3.36****. Weight loss is plotted against temperature.*

Structure **3.36** contains solvent water molecules in the crystal structure. Thermogravimetric analysis (TGA) can be used to investigate the stability of a crystalline framework when solvent molecules are removed from the lattice by measuring the weight change of a sample as it is heated. This instrumentation was used at the University of Sydney. The TGA of structure **3.36** is shown in Figure 3.27. The gradual weight change to around 4.5mg indicates that solvent is being removed from the crystal lattice, while the flattening out of the curve at this weight suggests the framework is stable with the solvent removed. The decline in weight over 300°C is due to the complex decomposing. The weight reduction to 85% of the initial weight seems to correlate to solvent water molecules being removed as well as the coordinated water molecules.

Since the complex seems stable to solvent removal, it was thought it might be possible to remove the solvent and then reabsorb it. This experiment is done by warming the complex enough to remove the solvent, then slowly cooling the sample while blowing water vapour over it. As the sample cools, the solvent vapour can be absorbed, and locked back into the lattice. Unfortunately, structure **3.36** does not resorb water vapour, as shown in Figure 3.28. The pink temperature curve on the graph indicates the heating and cooling process. The blue curve shows the weight change. A very small amount of water is absorbed by the complex, but only 0.5% weight, which correlates to only one water molecule per four unit cells.

It was observed that the sample changes colour from pink to bright blue after solvent removal. It is possible that a structural change is taking place, possibly linked to the removal of the coordinated water molecules on the cobalt atom. A structural change suggests that the solvent channels the water initially resided in may no longer exist, and would explain why the resorption did not occur.

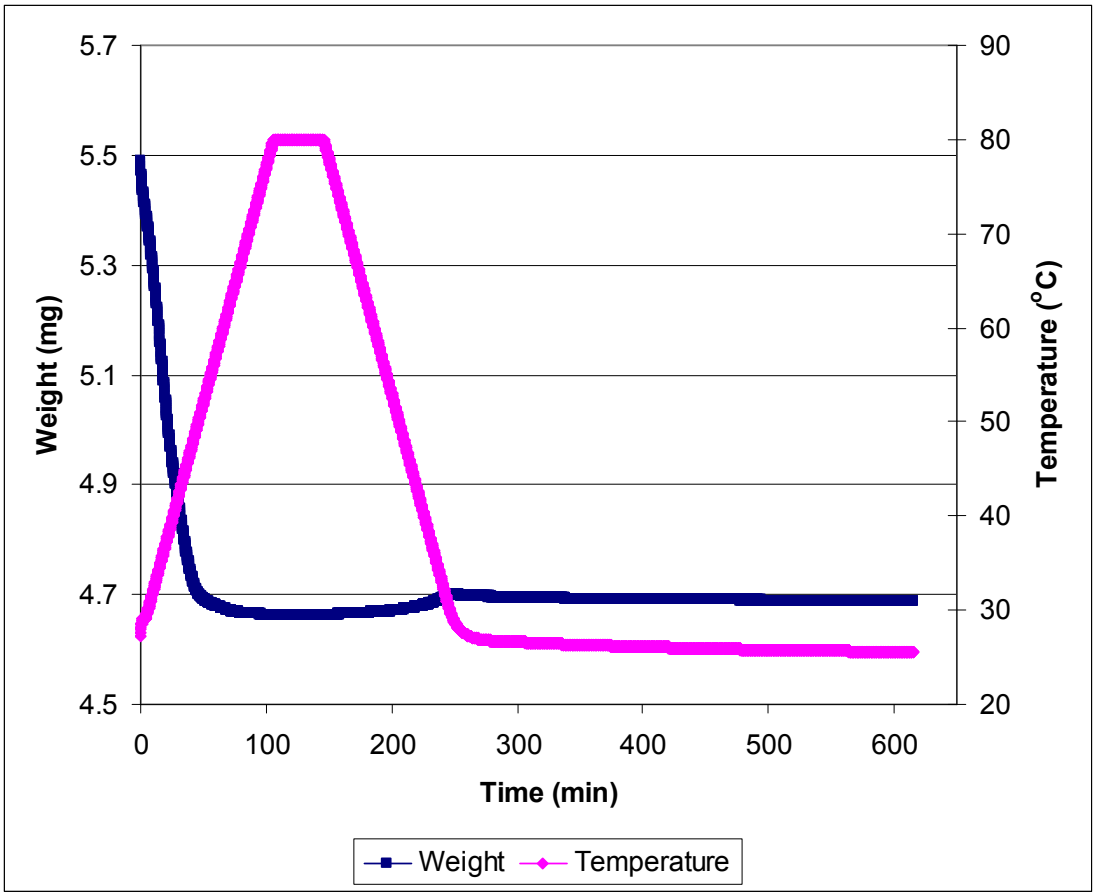

Figure 3.28 *– Thermogravimetric analysis results for resorption attempt on* ***3.36****. The weight change with time is plotted in blue, the temperature change over this time is plotted in pink.*

The colour change upon dehydration of the sample could be significant. Cobalt(II) can change colour from pink to blue if the ligand field around the cobalt atom changes. Obviously if the TGA results are accurate and the coordinated waters have been removed, then the coordination sphere around the cobalt atom has altered. It is possible that the colour change correlates to a change from six-coordinate octahedral cobalt (pink) to tetrahedral four-coordinate cobalt (blue). Possibly a free bromide ion moves to coordinate to the cobalt atom. As this blue sample is no longer crystalline, it is difficult to characterise this new complex.

The resorption of water back into the dehydrated blue complex described above was unsuccessful. The conversion back to pink complex **3.36** was attempted once more, by soaking the dehydrated blue complex in water overnight. By the next morning, some of the blue solid had turned white. The majority of the water was soaked up and this sample (**3.37**) analysed again by TGA as shown in Figure 3.29. The rapid initial weight drop corresponds to surface solvent evaporating as the sample was still wet. It appears

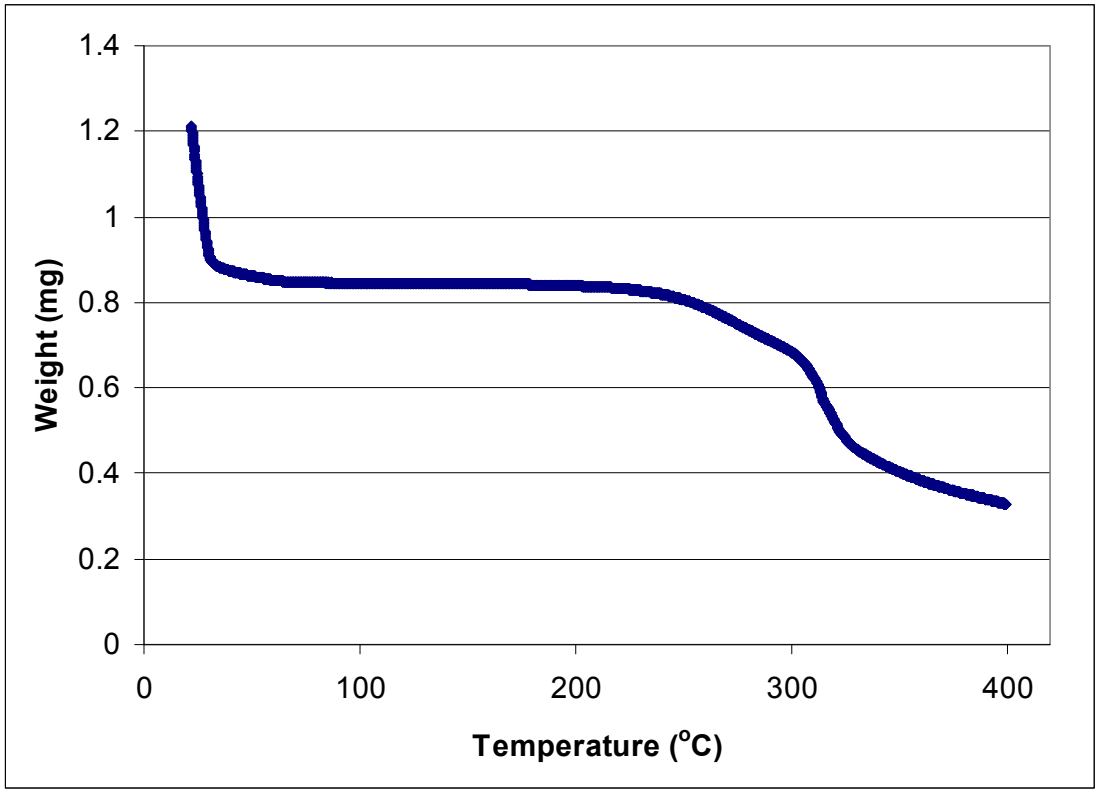

Figure 3.29 *– Thermogravimetric analysis results for dehydrated complex* ***3.37****.*

that no solvent was removed from the lattice. However, complex **3.37** is different to complex **3.36** as the decomposition in **3.37** occurs at a much lower temperature to that observed in **3.36**, and the curves are different shapes.

*Crystal structure of the complex with CuI (**3.38**)*

Crystals of **3.38** were grown by slow evaporation of a methanol and acetonitrile solution of ligand **3.33** and CuI. The structure solved in triclinic space group P-1.

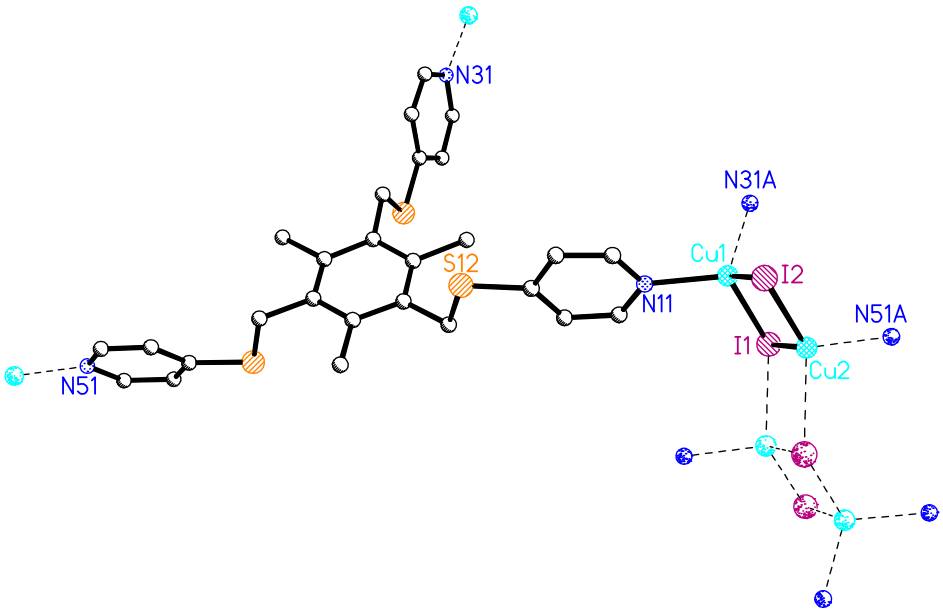

Figure 3.30 *– The asymmetric unit of structure **3.38**. Selected bond lengths (Å) and angles (°): Cu1-N11 2.035(4), Cu1-N13 2.062(5), Cu1-I2 2.6080(7), Cu1-I2 2.6615(7), Cu2-N51A 2.033(4), Cu2-I2 2.6150(6), Cu2-I1 2.6269(6), Cu2-I1A 2.7082(7), N11-Cu1-N31A 111.1(2), N11-Cu1-I2 107.5(1), N11-Cu1-I1 109.6(1), N31A-Cu1-I2 108.1(1), N31A-Cu1-I1 101.8(1), I2-Cu1-I1 118.60(2), N51A-Cu2-I2 109.6(1), N51A-Cu2-I1 106.1(1), N51A-Cu2-I1A 100.0(1), I2-Cu2-I1 119.62(2), I2-Cu2-I1A 108.18(2), I1-Cu2-I1A 111.53(2).*

The asymmetric unit is shown in Figure 3.30 with hydrogen atoms and solvate molecules excluded for clarity. The asymmetric unit contains one ligand, two copper atoms, two iodide counterions and some disordered solvate molecules. The solvate appears to be predominately acetonitrile, but it appears some methanol and water is also present. The complex contains an unusual Cu_4I_4 unit, with two Cu_2I_2 squares stepped parallel. This motif has been reported in the literature, with six examples in the *Cambridge Crystallographic Database*[238-243] (v. 5.26).[130] None of the reported

structures are polymeric compounds. The copper atoms are all tetrahedral, and the iodine atoms two coordinate or three coordinate. The copper to copper distances of 2.663Å and 3.002Å are not thought to represent real bonds.[126,127] Cu1 binds two pyridine nitrogens of separate ligands, and two iodine atoms. Cu2 binds one pyridine nitrogen and three iodide counterions. All inclusive, the Cu_4I_4 unit binds to six ligand nitrogens of six separate ligands. The ligand coordinates to three copper atoms. The sulfur arms on the ligand are organised in a two up and one down conformation.

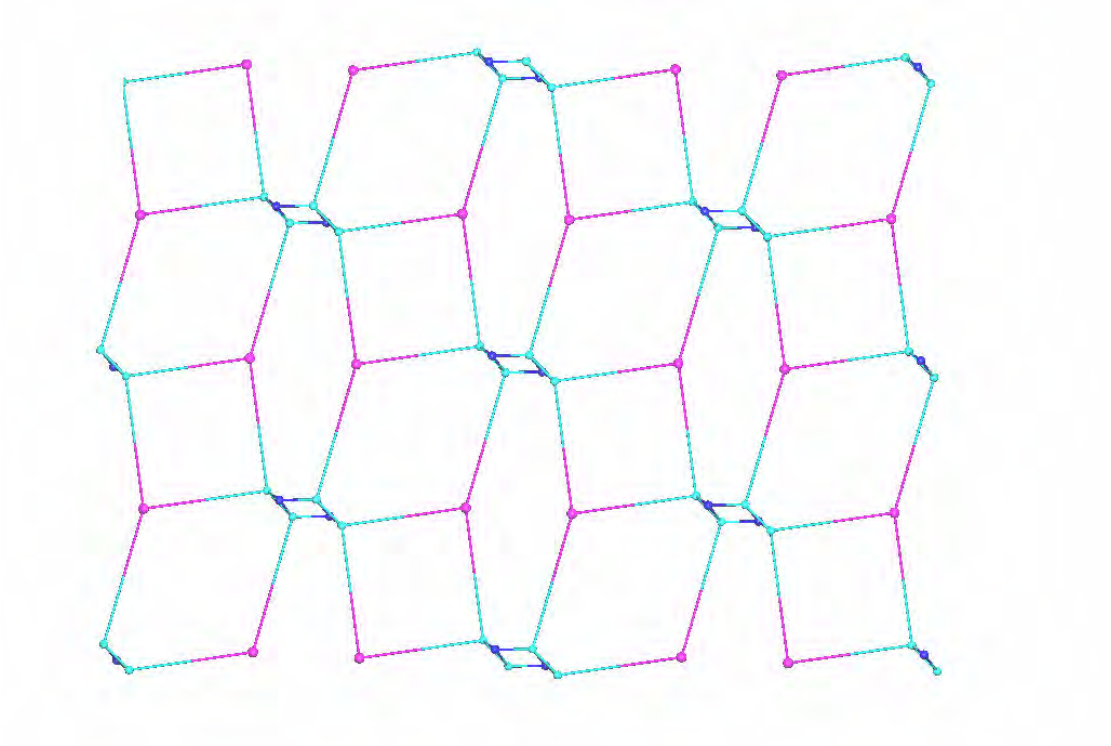

Figure 3.31 *– A simplified diagram of a section of the polymeric sheet of* ***3.38****.*

The complex grows into a two-dimensional polymeric sheet, as shown in the simplified diagram in Figure 3.31. If the Cu_4I_4 units are viewed as two Cu_2I_2 three connector nodes, a (4,3) net is identifiable, as the core of the ligand also acts as a three connector node. These (4,3) nets run in ladders vertically in Figure 3.31. The benzene rings and Cu_2I_2 units act as corners of square-like units. The cavities are partially filled by MeCN solvate molecules. The interaction between Cu_2I_2 squares to form Cu_4I_4 units join what would otherwise be a collection of one-dimensional ladders into a two-dimensional sheet.

The sheets are stacked on top of each other, aligned so the macrocycles in the net align to form channels that run through the crystal. There are iodine-hydrogen, sulfur-hydrogen and sulfur-sulfur interactions between sheets.

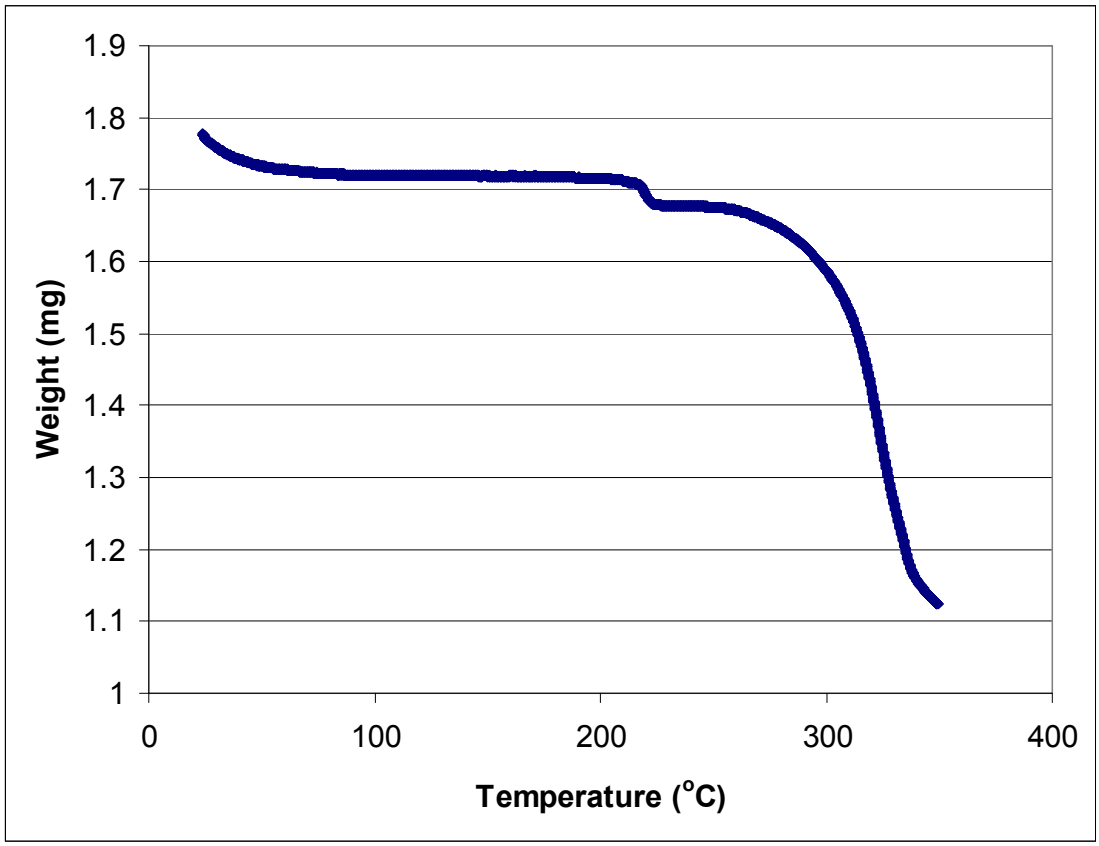

Figure 3.32 *– Thermogravimetric analysis results for* ***3.38****. The weight loss is plotted against temperature.*

As structure **3.38** contains channels of methanol and acetonitrile solvent molecules, it seemed like a good candidate for TGA analysis. The initial plot is shown in Figure 3.32. The slow decrease in weight as the temperature increases indicates that solvent is being removed, and the flattening off of the curve suggests the framework may be stable without the solvent present. Over 200^{o}C the compound decomposes.

Attempts were made to remove the mixture of solvents and replace it with acetonitrile, while monitoring this process with TGA. The results are shown in Figure 3.33. The temperature curve shows when the sample was heated to remove the mixture of methanol and acetonitrile solvent molecules, and then cooled as acetonitrile vapour was blown over the sample. The weight curve shows the loss of solvent during heating, and

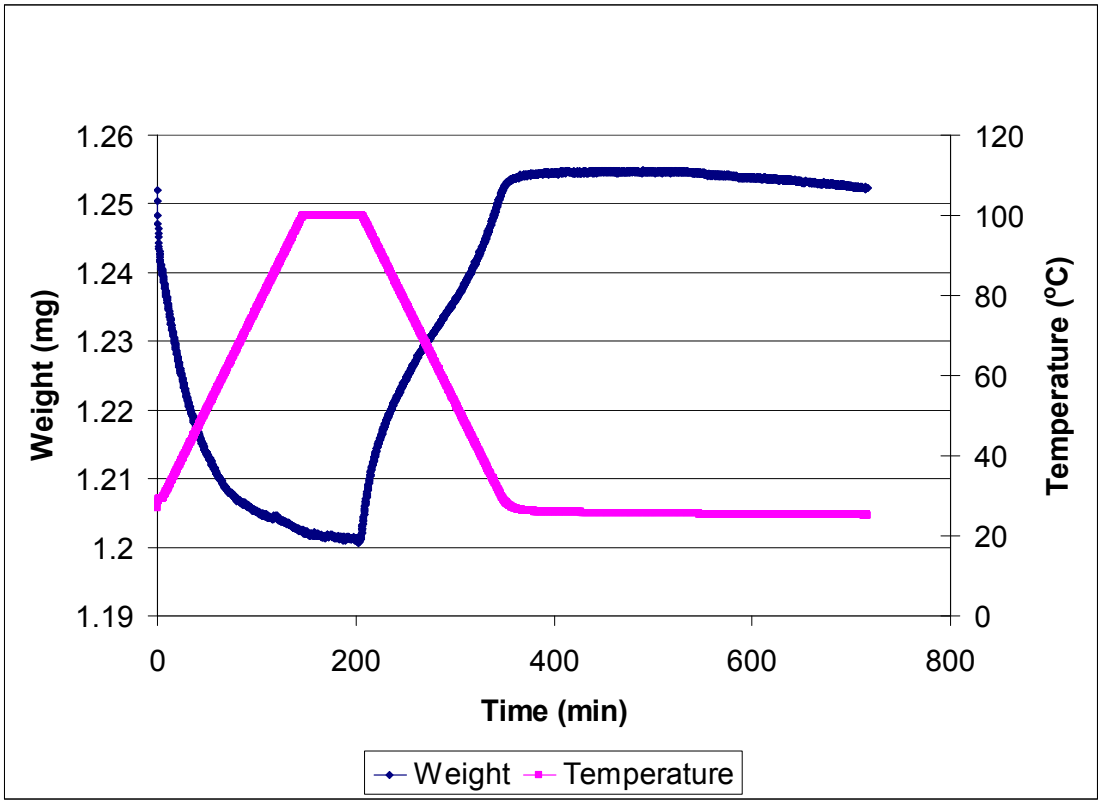

Figure 3.33 *– Resorption attempt on* ***3.38*** *monitored using thermogravimetric analysis. The pink line shows the temperature change with time, while the blue line shows the weight change of the sample over the same time period.*

then the intake of new solvent as the sample was cooled. The sample weighs more after resorption, likely due to acetonitrile molecules weighing more than a mixture of acetonitrile and methanol molecules, and possibly due to a slight dehydration of the starting crystals. So framework **3.38** is stable to solvent removal and resorption, and crystallinity is retained. It seems plausible that the channels in structure **3.38** could host other solvent molecules, unfortunately time was too limited to test this hypothesis.

Other complexes of ***3.33***

Complexation of **3.33** was attempted with a variety of metal salts, namely $AgNO_3$, $AgClO_4$, $AgCF_3SO_3$, CuI, $CuCl_2$, $Cu(NO_3)_2$, $Cu(ClO_4)_2$, $CoBr_2$, $Co(NO_3)_2$, $NiCl_2$, $Pd(en)(NO_3)_2$ and K_2PdCl_4. The two complexes which crystallised as single crystals were fully characterised by X-ray crystallography as discussed, many of those which could not be crystallised were not analysed further.

In support of the TGA analysis which suggests **3.36** loses all water molecules during heating, even the coordinated water molecules, the elemental analysis results of **3.36** are

consistent with the dehydrated product, which presumably formed upon heating to constant weight.

Reaction of **3.33** with $CuCl_2$ or $Cu(ClO_4)_2$ produces complexes with 1:1 metal to ligand stoichiometries. These seem likely to be polymeric structures. The product of reaction with K_2PdCl_4 was shown to have a M_2L stoichiometry, again a polymeric structure seems most likely, considering the ratios of possible simple discrete structures.

When structure **3.38** crystallised, the majority of the complex remained a precipitate. This precipitate was shown to have an M_3L_2 stoichiometry, and is therefore a different complex to **3.38**. As CuI often dimerises into Cu_2I_2 squares, this is likely an effective "M_3L_4"-type stoichiometry, which reveals little about the actual structure.

The very insoluble precipitate obtained from **3.33** and $AgClO_4$ was shown to have a M_3L_2 stoichiometry. This is the right stoichiometry for a cage structure, however the insolubility suggests it may be polymeric.

Reaction with $Pd(en)(NO_3)_2$ also produces a complex of M_3L_2 stoichiometry. The ethylenediamine ancillary ligands do not seem to be present in the final structure.

This same metal to ligand ratio is also seen in the product of reaction of **3.33** with $Cu(NO_3)_2$. Interestingly, the anions seem to be five hydroxides and one nitrate. This unusual scenario repeats through this chapter. It seems possible that this complex may be a cage structure, with one nitrate anion encapsulated and therefore not exchanged for a hydroxide like the rest of the anions.

Complexes with ligand 3.34

*Crystal structure of the complex with CuI (**3.39**)*

This is an example of how subtle changes in ligand design can influence the overall structure. Ligand **3.34** differs from ligand **3.33** by only the substitution of methyl groups for ethyl groups, yet when reacted with copper iodide, the products are almost identical, except one polymer is two-dimensional, and the other three-dimensional.

Solutions of ligand **3.34** in methanol and copper iodide in acetonitrile were combined to give a few orange plate-like crystals after a few days of slow evaporation. These crystals were suitable for X-ray crystallography and the structure solved in monoclinic space group $P2_1/n$.

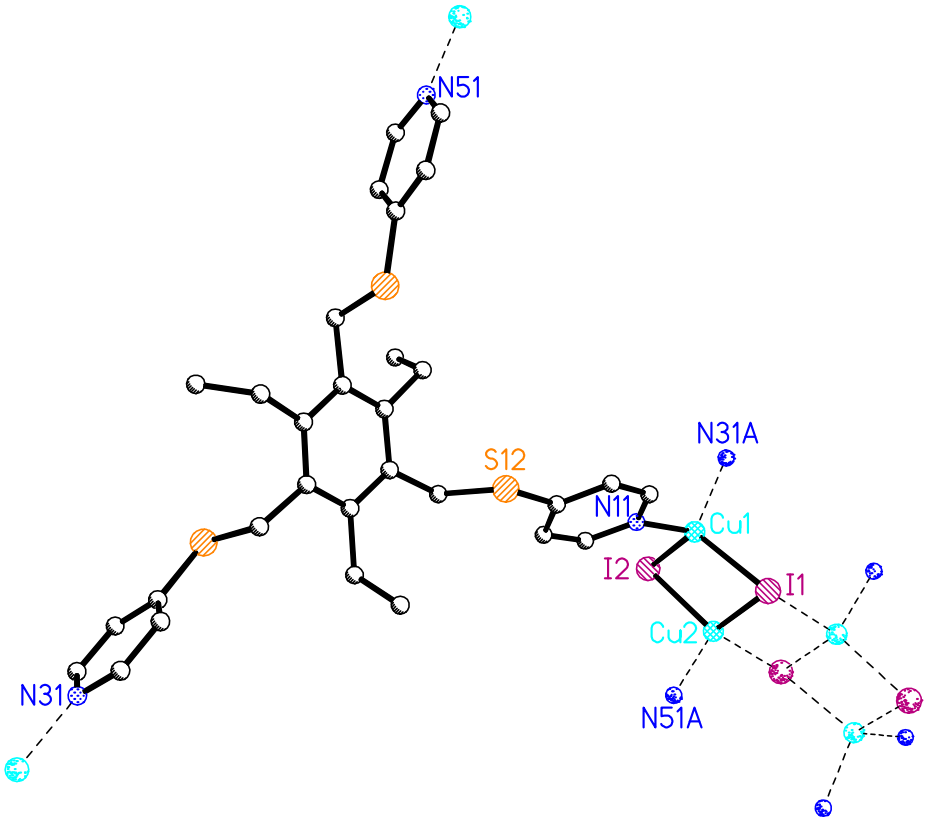

Figure 3.34 *– The asymmetric unit of* ***3.39****. Selected bond lengths (Å) and angles (°): Cu1-N31A 2.037(5), Cu1-N11 2.069(6), Cu1-I2 2.5869(9), Cu1-I1 2.6187(9), Cu2-N51A 2.040(5), Cu2-I2 2.5938(8), Cu2-I1A 2.6278(9), Cu2-I1 2.7077(9), N31A-Cu1-N11 107.9(2), N31A-Cu1-I2 110.0(2), N31A-Cu1-I1 109.4(2), N11-Cu1-I2 108.7(2), N11-Cu1-I1 98.5(2), I2-Cu1-I1 121.20(3), N51A-Cu2-I2 111.3(2), N51A-Cu2-I1A 106.4(2), N51A-Cu2-I1 99.9(2), I2-Cu2-I1A 110.72(3), I2-Cu2-I1 117.60(3), I1-Cu2-I1A 109.91(3).*

The asymmetric unit is shown in Figure 3.34, with hydrogen atoms and solvate molecules excluded for clarity. The asymmetric unit contains one whole ligand, a Cu_2I_2 square unit, and three water molecules. The structure appears very similar to **3.38**. Complex **3.39** displays the same Cu_4I_4 moiety, with two types of copper atoms binding to a total of six ligands. All the copper atoms are tetrahedral, and the iodine atoms

bridge these together to create a stepped structure, like two Cu_2I_2 squares linked. Like **3.38**, the distances between copper atoms in the Cu_2I_2 squares are relatively short (2.649Å Cu1-Cu2) but are not thought to represent a bond.[126,127] The distance between copper atoms in the stepped region is longer (3.064Å Cu2-Cu2A). Like **3.38**, the ligand arms are also arranged in a two up, one down conformation. The ethyl groups are disorganised, giving the ligand an *aabbab* conformation. The steric bulk provided by the ethyl groups has not been enough to preorganise the arms of the ligand in an *ababab* conformation, but seems to have affected the overall structure of this complex.

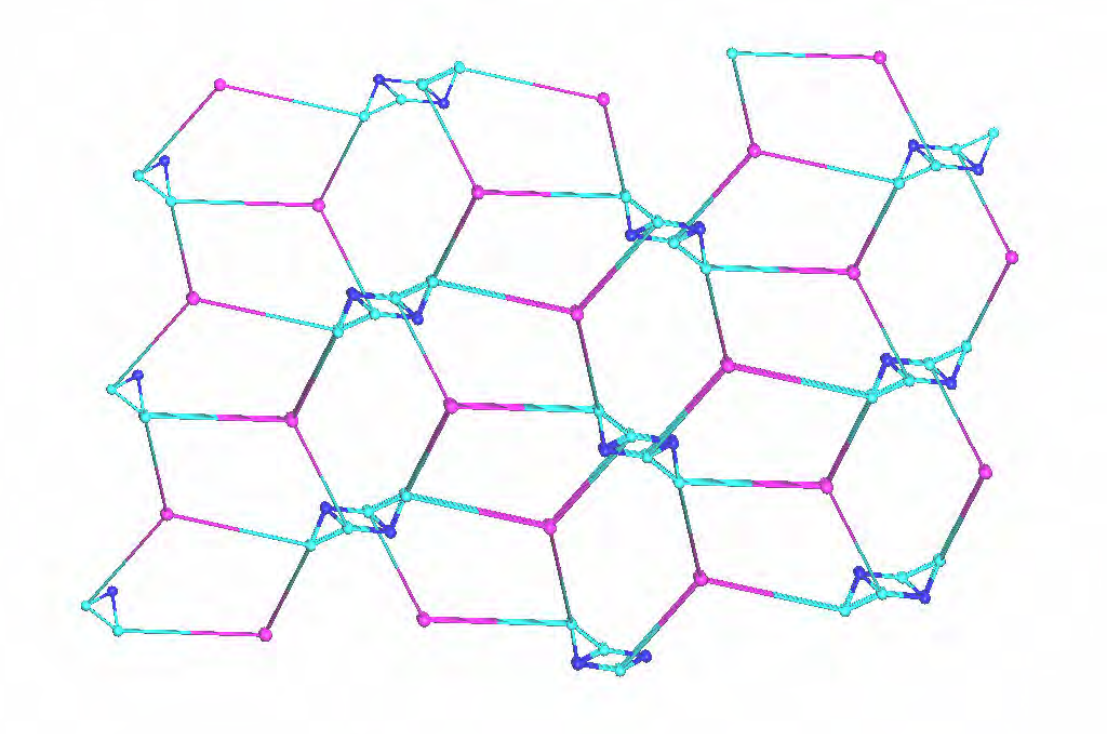

Figure 3.35 *– A view of the simplified structure of* ***3.39****, showing the similarity to* ***3.38****.*

This polymer propagates in three dimensions. The side-on edges of two-dimensional sheets in **3.39** resemble the ladders of **3.38**, as shown running vertically in Figure 3.35. From this view, the two polymers look very similar. These ladders exist if the Cu_4I_4 units are viewed as two three connector Cu_2I_2 units in both these polymers. The ladders are separated by larger elongated macrocycles. If the Cu_2I_2 moieties are viewed as separate units, the polymers in this view are the same, and the ladders can be classified as (4,3) one-dimensional nets.

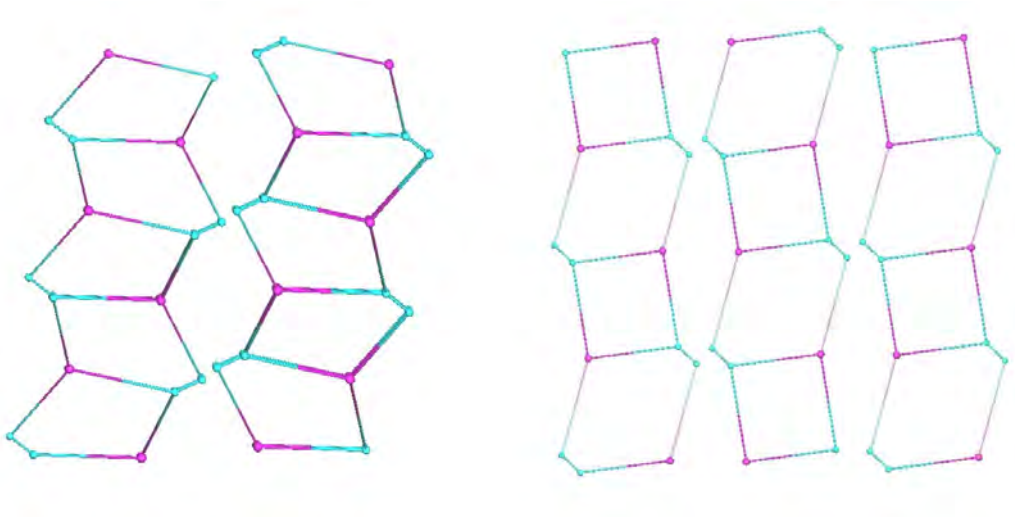

Figure 3.36 *– A comparison of the simplified structures of* ***3.39*** *(left) and* ***3.38*** *(right). The iodine atoms have been removed to emphasise the ladders in the polymers.*

A comparison of the simplified diagrams of polymer **3.39** (left) and **3.38** (right) is shown in Figure 3.36. The iodine atoms have been removed to emphasise the one-dimensional ladders. In these diagrams, the Cu_2I_2 groups are not considered single moieties, but as two copper atoms, bonded together as a simplification of the Cu_2I_2 square. Immediately the difference between the two polymers is obvious. The ladder rungs in **3.39** are symmetrical, as each macrocycle in the diagram includes three copper atoms. The distorted pentagon shapes alternate orientations per rung of the ladder. In **3.38** however, the step sizes between rungs are unsymmetrical, showing that the connectivity is different between the polymers. In **3.38**, the macrocycles alternate between including two copper atoms and four copper atoms. Each rung of the ladder alternates between a square shape and a distorted hexagon shape. It also needs to be noted that the distorted pentagon shapes in **3.39** seen in Figure 3.36 do not actually exist as macrocycles, but as the polymer is two-dimensional these are actually helical channels, as the last bond to complete the macrocycle reaches down to the pentagon below and so on.

Looking at the two-dimensional structure of **3.39**, a (6,3) net can be distinguished if Cu_2I_2 moieties are considered single nodes. Again iodine atoms have been excluded for clarity. This is shown in the simplified diagram in Figure 3.37. Like the last example, the Cu-I interactions which join the Cu_2I_2 squares into Cu_4L_4 units, join together individual polymer strands, so this time the two-dimensional sheets propagate into a

three-dimensional structure. A small section of this three-dimensional structure is shown in the simplified diagram in Figure 3.38. There are no hydrogen bonding or π-π stacking interactions throughout the polymer.

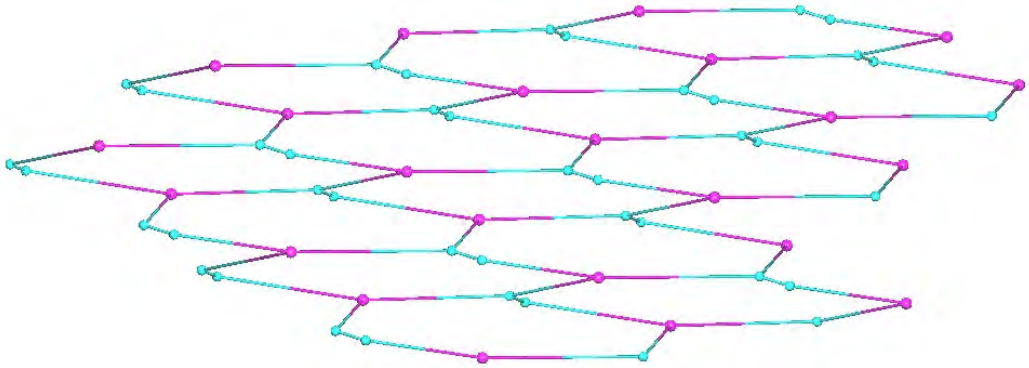

Figure 3.38 *– A simplified view of a section of the two-dimensional sheet in* ***3.39*** *when iodine atoms are excluded, showing the effective (6,3) net if* Cu_2I_2 *units are viewed as a single entity.*

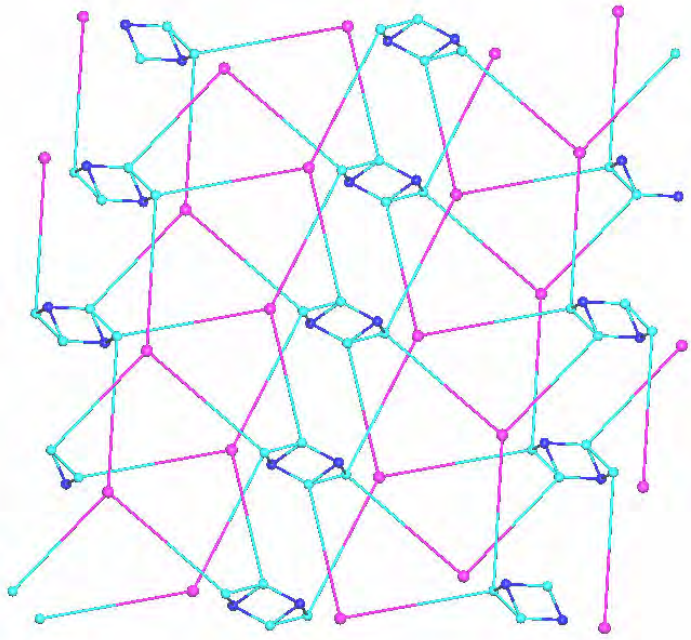

Figure 3.38 *– A simplified view of a section of the three-dimensional polymer* ***3.39****.*

*Crystal structure of the complex with $AgClO_4$ (**3.40**)*

The product of reaction of **3.34** and $AgClO_4$ was dissolved in a mixture of DMF, methanol and dichloromethane. Slow evaporation of this solution produced a few colourless square crystals which proved to be suitable for X-ray crystallography. The structure solved in tetragonal space group $P4_2/n$. Unfortunately the crystals displayed merohedral twinning. The data corresponding to the major twin was able to be mostly isolated, which led to an improvement of the R_1 value to 7.85%.

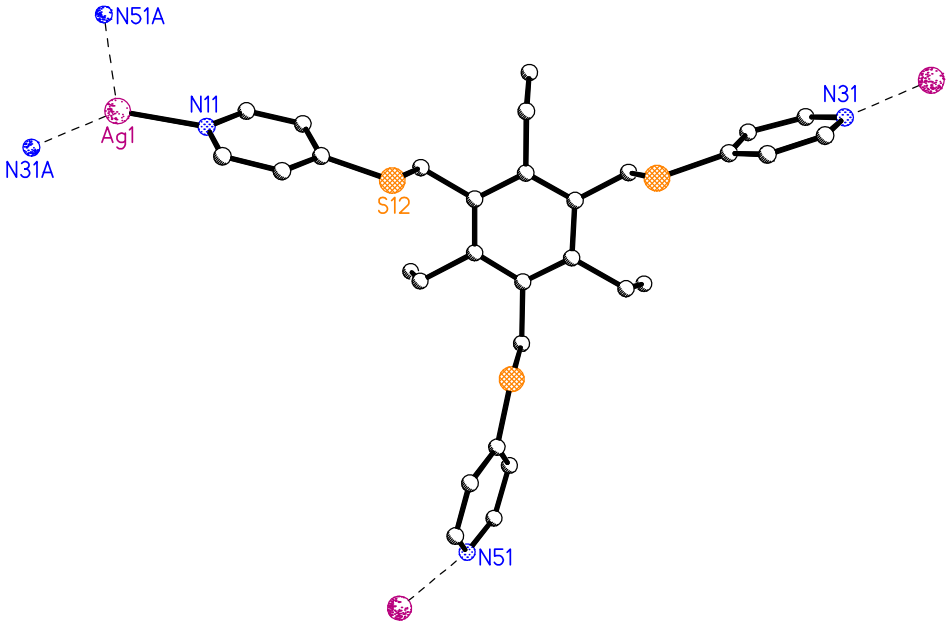

***Figure 3.39** – The asymmetric unit of complex **3.40**. Selected bond lengths (Å) and angles (°): Ag1-N31A 2.194(8), Ag1-N11 2.193(7), Ag1-N51A 2.40(1), N31A-Ag1-N11 145.0(4), N31A-Ag1-N51A 103.7(3), N11-Ag1-N51A 111.1(4).*

The asymmetric unit of **3.40** is shown in Figure 3.39, with hydrogen atoms, solvate molecules and the disorder surrounding the silver atom excluded for clarity. The asymmetric unit contains one ligand, one silver, a perchlorate counterion, a DMF at 75% occupancy, and two water molecules at 33% occupancy. The silver atom is disordered over two sites, 85% of the time residing in the position shown in Figure 3.39. Each ligand bonds to three silver atoms, and each silver atom bonds to three different ligands in a trigonal planar geometry. The bond distance to N51 is relatively long, shown in the diagram at an awkward angle to the plane of the pyridine ring. The

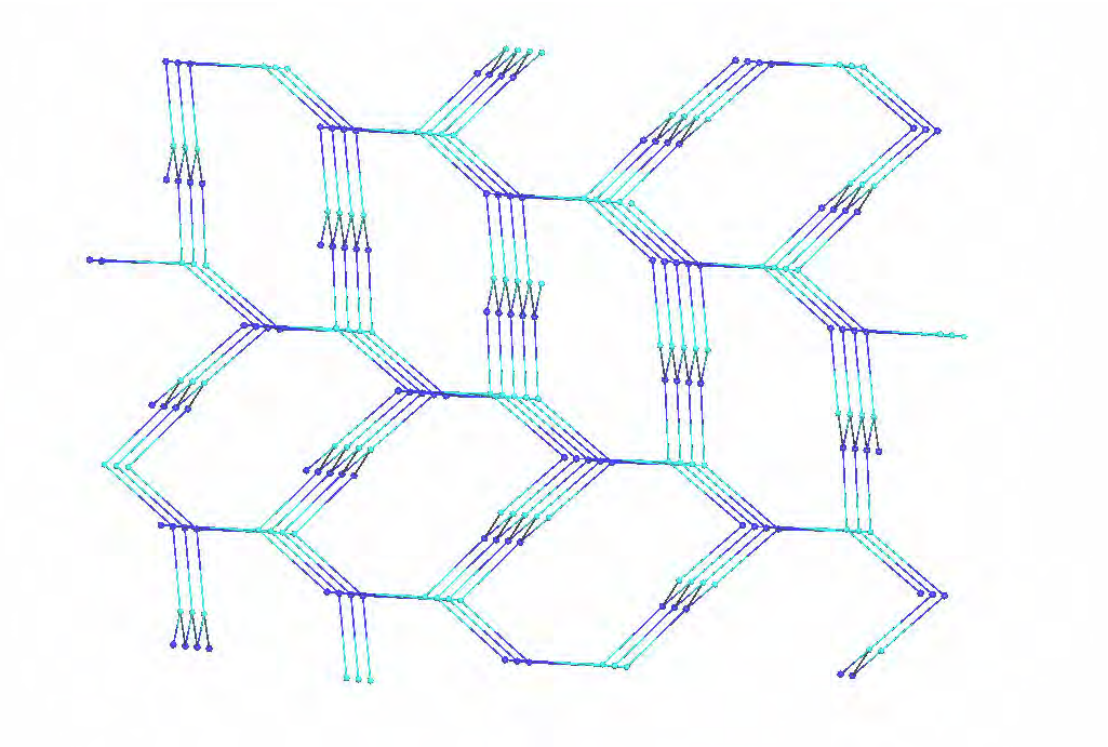

Figure 3.40 *– A simplified diagram of a single (10,3) net of three-dimensional polymer* ***3.40****.*

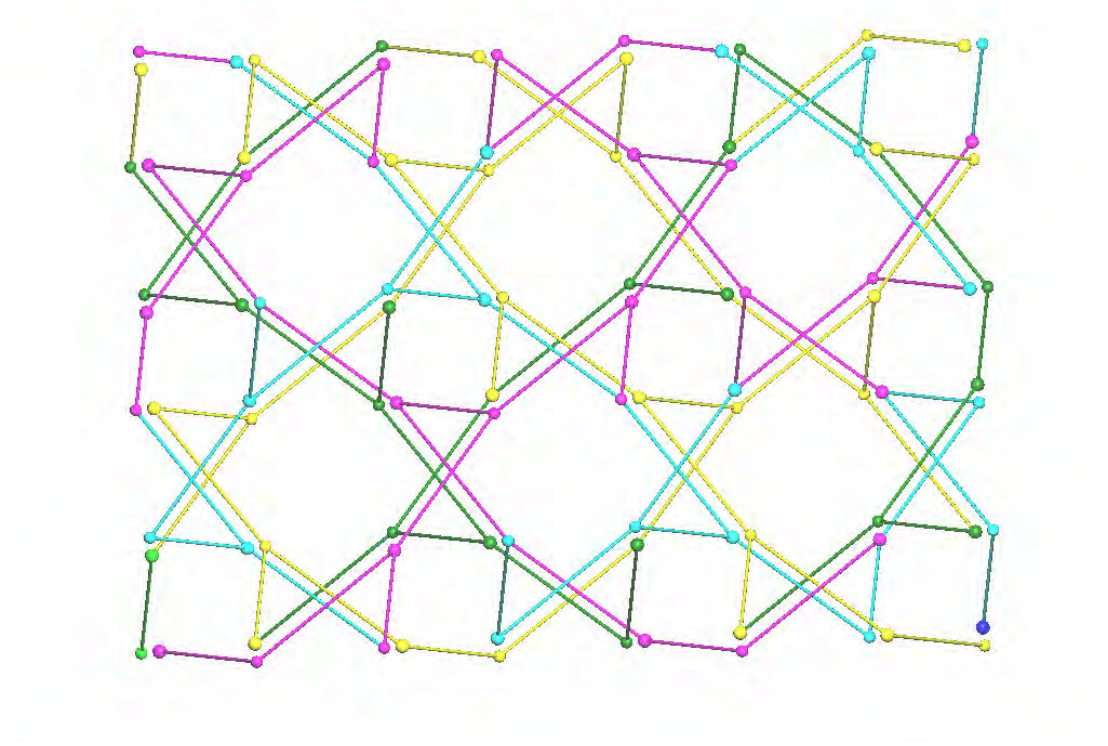

Figure 3.41 *– A simplified view of* ***3.40*** *showing the overall structure of the four interpenetrated polymer strands.*

perchlorate counterion is not coordinated to the metal centre. The ligand is fully organised into an *ababab* conformation around the benzene ring, such that all the ethyl groups point down, and all the sulfurs point up.

The complex grows into a three-dimensional coordination polymer, with both the silver and the central benzene ring of the ligand acting as three connector nodes. The structure fits into the category of (10,3) nets. A simplified diagram of a single net of the structure is shown in Figure 3.40. The oxygens on the perchlorate and DMF molecules create hydrogen bonding networks to the main structure. There are no other interactions such as π-π stacking interactions between ligands in the polymer strands.

Four nets of the polymer interpenetrate, as shown in the simplified diagrams in Figures 3.41, 3.42 and 3.43. Different colours represent different polymer chains. Figure 3.41 shows a view where the polymer strands are aligned and the tetragonal symmetry of the structure can be seen. Square-like units reside in the polymer, with polymer strands crossing between squares. The four nets all follow similar paths, with the cavities in the structure filled with anions and solvate molecules. These channels propagate through the entire crystal, so if this complex could be synthesised in high enough yield TGA analysis or anion exchange reactions to probe the host-guest nature in **3.40** could be interesting. Figure 3.42 shows a different view of the four-fold interpenetration, with the individual (10,3) nets of each chain visible in the diagram. Figure 3.43 shows another view of the four interpenetrated strands, orthogonal to the view in 3.42, where the hexagonal circuits of each net can be distinguished.

*Other complexes with **3.34***

Complexation of ligand **3.34** was attempted with a variety of metal salts, namely $AgNO_3$, $AgClO_4$, $AgPF_6$, $AgCF_3SO_3$, CuI, $CuCl_2$, $Cu(NO_3)_2$, $CoBr_2$, $NiCl_2$, $ZnBr_2$, $Zn(ClO_4)_2$, $Pd(PhCN)_2Cl_2$, $Pd(en)(NO_3)_2$ and K_2PdCl_4. The complexes which crystallised as single crystals have been discussed, many of those that did not crystallise were not analysed further.

Reaction of **3.34** with $NiCl_2$ gave a precipitate that was shown by elemental analysis to have a 1:1 metal to ligand ratio. Given the insolubility, this is likely to be a polymeric complex.

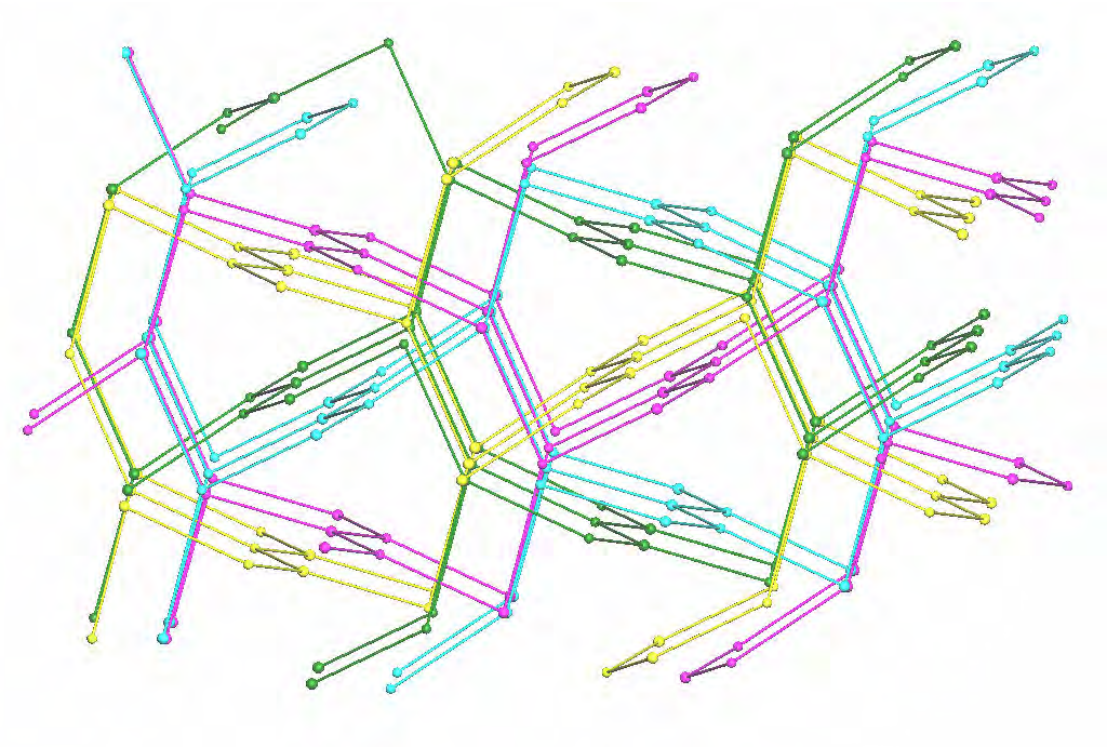

Figure 3.42 *– A simplified view of the four-fold interpenetration in* ***3.40****, showing the (10,3) circuits of each net.*

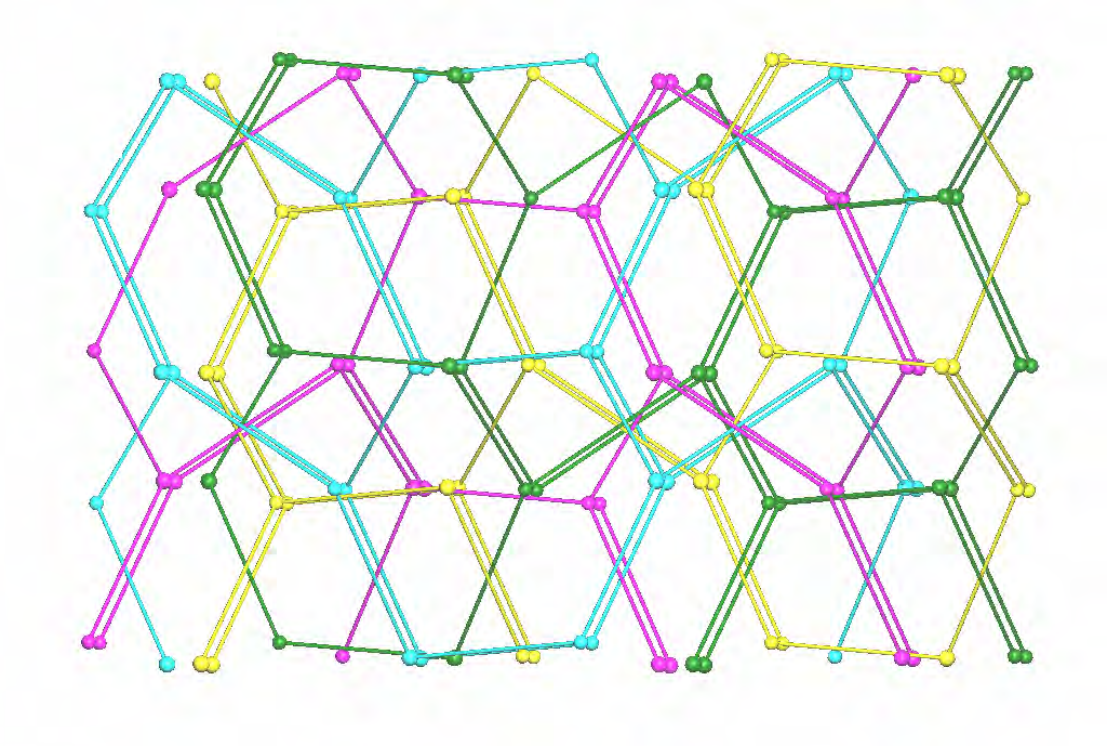

Figure 3.43 *– A simplified view of the four-fold interpenetration in* ***3.40****, showing the hexagonal circuits of each polymer strand.*

The product of reaction of **3.34** with $CuCl_2$ was shown to have a M_4L stoichiometry. This is most likely suggesting that the metal has dimerised into Cu_2X_2 square-like units, quite common for Cu(II), which would give a product with an effective M_2L ratio.

Reaction with $Pd(en)(NO_3)_2$ produced a brown precipitate which was shown to have a M_3L_2 stoichiometry. Again the ethylenediamine groups seem to have been substituted from the final product. The insolubility of this solid prevented characterisation of what may or may not be a cage-like structure. Reaction of **3.34** with $Cu(NO_3)_2$ also produced a complex of M_3L_2 stoichiometry. Once again, the nitrate counterions seem to have been replaced by hydroxide anions. Despite multiple attempts, this complex could not be crystallised.

Complexes with ligand 3.35

Complexation of ligand **3.35** was attempted with a range of metal salts, namely $AgClO_4$, CuI, $CuCl_2$, $Cu(NO_3)_2$, $CoCl_2$ and $CoBr_2$. Unfortunately, despite repeated recrystallisation attempts, none of these complexes could be crystallised. Most of the products were very insoluble precipitates.

The product of reaction of **3.35** with $CoBr_2$ was shown by elemental analysis to have a 1:1 metal to ligand stoichiometry. This is likely to be a coordination polymer. Reaction of **3.35** with either $AgClO_4$ or $CuCl_2$ gives products with M_2L stoichiometries. As the geometries and anion-binding tendencies for the two metal salts are so different, it is unlikely, but still possible, that these complexes have similar structures.

When CuI is reacted with ligand **3.35**, the product has a M_3L ratio. This could suggest a discrete structure, with one copper bound to every pyridine nitrogen, but given the tendency for CuI to dimerise into Cu_2I_2 squares, this is probably an effective M_3L_2 stoichiometry. Reaction of **3.35** with $CoCl_2$ also gives a product with this M_3L_2 stoichiometry. It is possible these complexes are molecular cages, but this stoichiometry could also be provided by coordination polymers.

Synthesis of the 1,3,5-tri(8-quinolyloxymethyl) ligands

Literature compounds 1,3,5-tri(8-quinolyloxymethyl)-2,4,6-trimethylbenzene (**3.41**)[244-246] and 1,3,5-tri(8-quinolyloxymethyl)-2,4,6-triethylbenzene (**3.42**)[244] have been studied for sensor applications, but their coordination chemistry has not yet been investigated. These were designed to grasp the analyte of interest between the three quinolyl arms, holding it in place with hydrogen bonding interactions with the nitrogens. However the flexibility of the oxymethyl chain should allow the arms on these ligands to twist so these molecules could act as interesting synthons in metallosupramolecular chemistry.

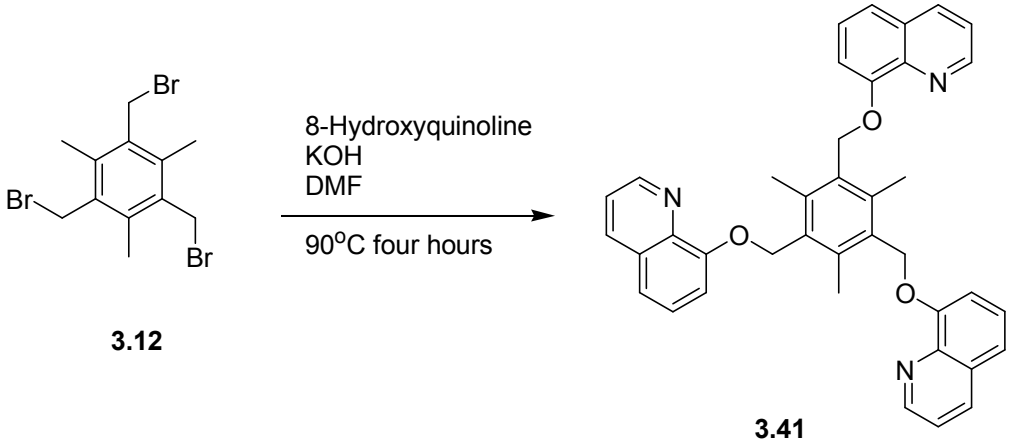

Scheme 3.13 *– Synthesis of ligand* ***3.41****.*

Ligand **3.41** was synthesised by a different literature procedure[171,172] from that reported to produce **3.41**.[244,247] This procedure is shown in Scheme 3.13 and produced **3.41** in 74% yield after four hours of reaction. Ligand **3.42** was synthesised from an analogous

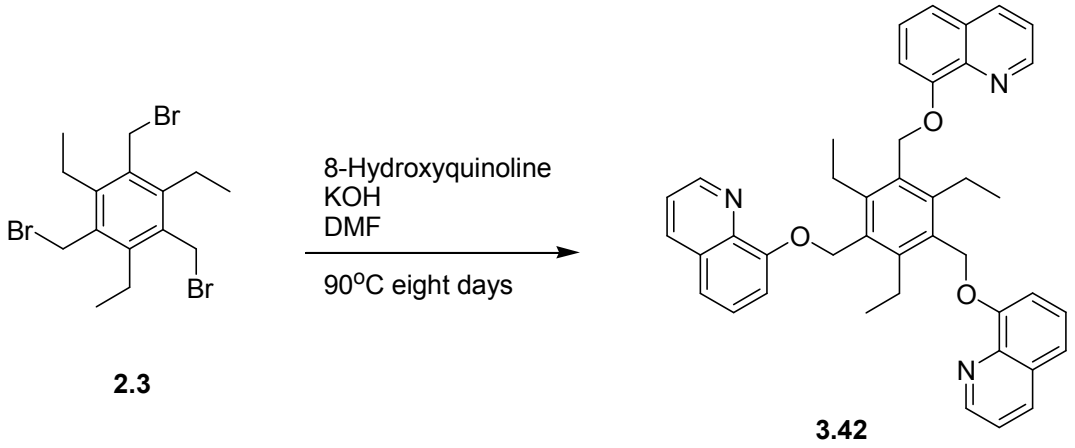

Scheme 3.14 *– The synthetic route to ligand* ***3.42****.*

reaction, as shown in Scheme 3.14, again different to the route reported in the literature.[247] This reaction did not proceed as readily, presumably due to the steric hindrance caused by the ethyl groups, however the product was obtained after eight days of reaction. Extraction from the last traces of DMF proved troublesome, and pure **3.42** was only obtained in 18% yield. This could undoubtedly be improved, but enough product was obtained for this research so optimisation was not pursued. The ligand was obtained as a pale brown solid, proving literature reports of an oil to be incorrect.

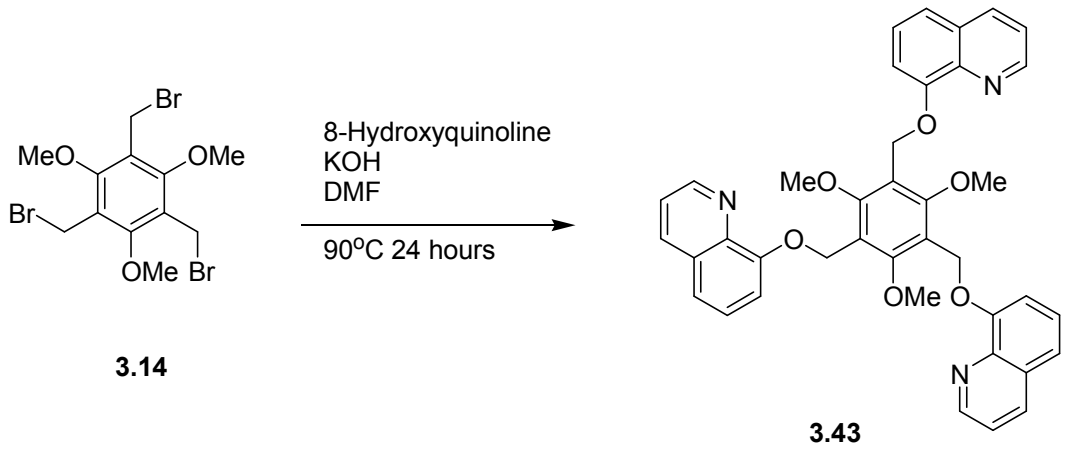

3.14 **3.43**

Scheme 3.15 *– The synthesis of ligand* ***3.43****.*

The analogous reaction to produce 1,3,5-tri(8-quinolyloxymethyl)-2,4,6-trimethoxybenzene (**3.43**) proceeded more readily, providing **3.43** in 70% yield after 24 hours of reaction, as shown in Scheme 3.15. This suggests the methoxy groups may cause less steric hindrance than ethyl groups, leading to a reduced chance these ligands will be preorganised. Like the other trimethoxybenzene-based ligands, **3.43** has lower solubility than the other ligands in the series.

Crystal structure of ligand ***3.42***

Ligand **3.42** crystallises spontaneously from hot acetonitrile. These crystals were suitable for X-ray crystallography, and the structure solved in triclinic space group P-1.

The asymmetric unit is shown in Figure 3.44, with hydrogen atoms excluded for clarity. The ligand is preorganised in an *ababab* conformation, with all three ethyl groups pointing down and the quinoline groups pointing up, with the nitrogens of the quinolines pointing into the centre of the ligand. Three acetonitriles are nestled in the

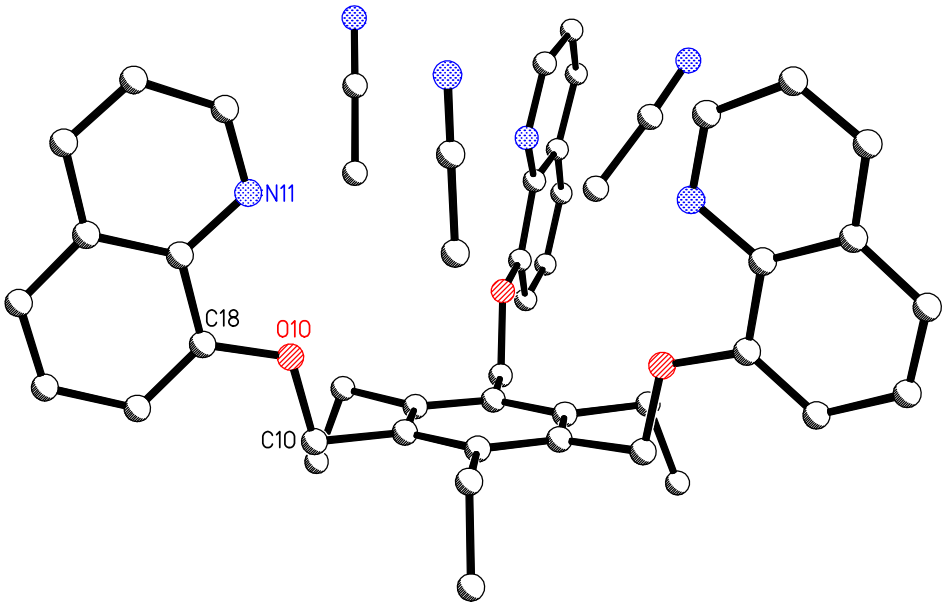

Figure 3.44 *– The structure of ligand* ***3.42****, showing the three interacting acetonitrile solvate molecules. Selected bond lengths (Å) and angles (°): O10-C10 1.443(2), O10-C18 1.361(2), C10-O10-C18 116.9(1).*

cavity made by the quinoline groups over the central benzene ring, resting directly over the ethyl groups. The nitrogens on the acetonitriles point outwards, so the alkyl end is closest to the ligand. There are no obvious hydrogen bonding interactions between the ligand and solvent molecules, although the hydrogens on the solvates point towards the oxygens of the ligand. Two acetonitriles lie close to vertical, while the third is more inclined, destroying the symmetry of the compound. Space filling models in Figure 3.45 show the acetonitriles are packed in tightly and completely fill the inner cavity. This ligand could possibly be used as a sensor to determine the presence of acetonitrile.

In the crystal packing molecules lie directly over one another, and are wedged in tightly beside each other, alternating up and down, with face-end stacking interactions between neighbouring quinolines.

To investigate the strength of the interaction between the acetonitrile guest molecules and the ligand, this compound was studied by thermogravimetric analysis. The results are shown in Figure 3.46. The compound appears stable until around 70°C. This is quite

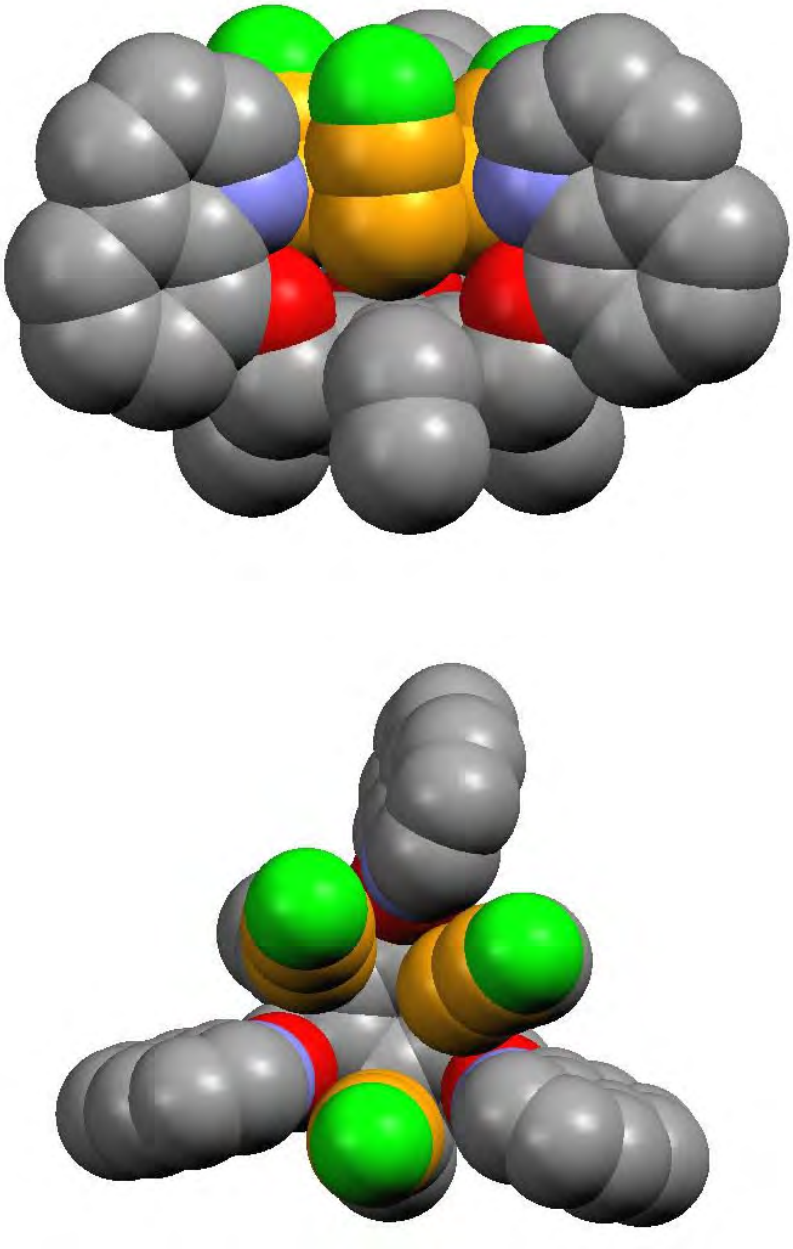

Figure 3.45 *– Space filling diagrams of* ***3.42****, with the acetonitrile molecules shown in yellow and green.*

remarkable as the temperature is approaching the boiling point of acetonitrile. Often solvate molecules will gradually leak out of a crystalline lattice at much lower temperatures than the boiling point of the solvate, so this suggests that the acetonitriles in the structure are held firmly in place by the ligand. Over the next 70^{o}C the weight drops in two steps, the first step appears to correspond to two acetonitriles evaporating, and the second slower step to the final acetonitrile being lost. So once two of the solvate

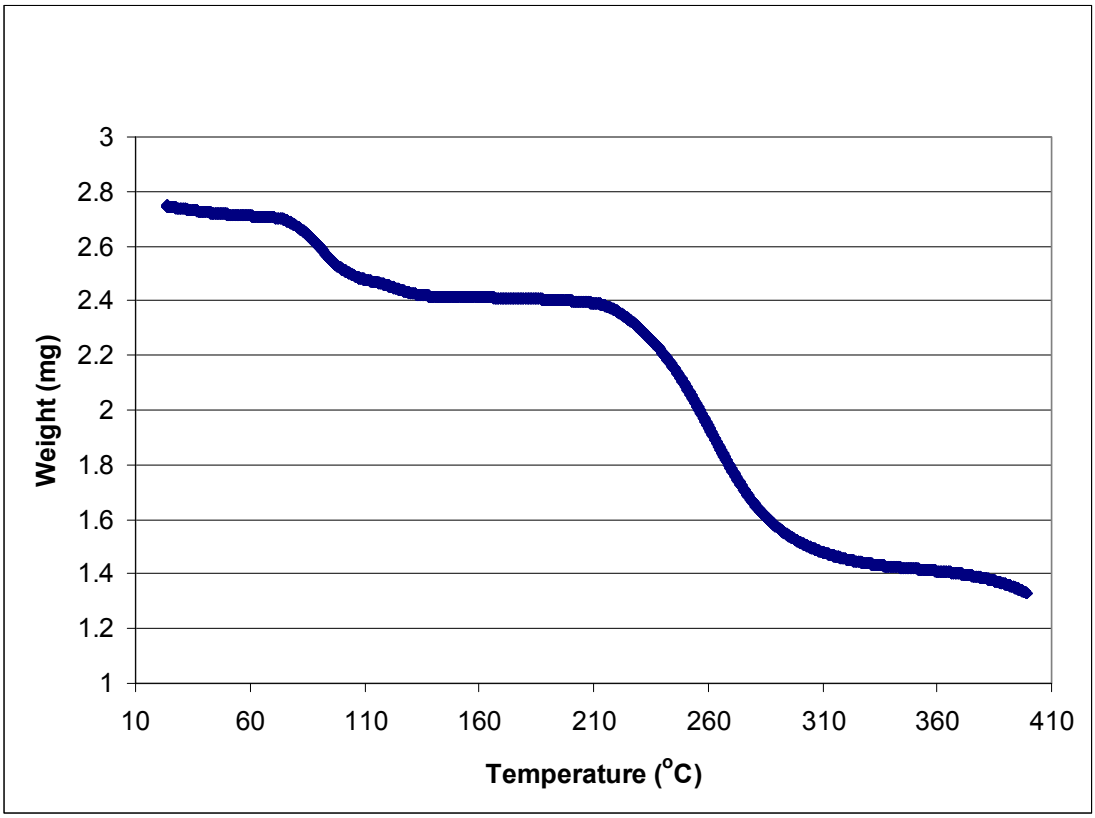

Figure 3.46 *– Thermogravimetric analysis results for ligand* ***3.42*** *crystallised with acetonitrile. The weight change is plotted against temperature.*

molecules have been removed from the lattice, it appears that the ligand interacts more strongly with the final acetonitrile, making it more difficult to remove. Once all the solvate molecules have been removed, the ligand appears stable until decomposition processes start to take place over 200°C. Unfortunately crystallinity is lost after the removal of the acetonitrile molecules, so a crystal structure of the naked ligand could not be obtained.

Complexes with ligand 3.41

Complexation with ligand **3.41** was attempted with a variety of metal salts, namely $AgNO_3$, $AgPF_6$, $AgClO_4$, CuI, $CuCl_2$, $Cu(NO_3)_2$, $CoCl_2$, $ZnBr_2$, $Zn(ClO_4)_2$, $Zn(OAc)_2$, $PdCl_2$, $Pd(en)(NO_3)_2$ and $Cd(OAc)_2$. Unfortunately, despite using a range of different methods and repeated crystallisation attempts, no crystals of complexes of **3.41** could be obtained which were suitable for X-ray crystallography. Only a few of the complexes were analysed further.

Reaction of **3.41** with $PdCl_2$, both in solution and the solid state, has been shown to occur by mass spectrometry and ^1H NMR. The products appear to be different, but this may be due to different metal to ligand ratios used between the experiments, rather than due to the different reaction techniques. Neither of the products could be crystallised, preventing full characterisation. Reaction of ligand **3.41** with $Pd(en)(NO_3)_2$ followed by conversion to the hexafluorophosphate salt, produced a complex with a 1:1 metal to ligand ratio. The ^1H NMR spectrum shows reaction has taken place and that the product is symmetrical.

When ligand **3.41** was reacted with $AgPF_6$, the product was shown to have an M_7L_4 stoichiometry. This ratio seems unusual, but could be possible if the complex is very unsymmetrical.

Amongst other techniques attempted, occasionally a potential templating molecule was added to the reaction solution to see if this would influence the products formed. However as the products were unable to be crystallised, the effectiveness of this technique was unable to be determined. In one such case, **3.41** was reacted with $Zn(OAc)_2$ in the presence of trimesic acid, and the resulting precipitate was shown to have a 4:2:1 metal to ligand to template ratio.

Another reaction of ligand **3.41** with $Pd(en)(NO_3)_2$ produced a product that was shown to have a M_3L_2 stoichiometry, and again the ethylenediamine ligands have been substituted from the metal centre. The anions now appear to be six hydroxides and one nitrate, with one H_3O^+ for charge balance. Although this scenario seems odd, this is a reoccurring theme for ligands in this chapter, with the possibility that a cage has formed encapsulating a nitrate anion, preventing exchange with the other anions.

Complexes with ligand 3.42

*Crystal structure of the complex with CuI (**3.44**)*

Reaction of ligand **3.42** with CuI in an acetonitrile and methanol solvent mixture readily produces crystals of **3.44**; however these crystals are always highly twinned. Photos of the flower-like clusters of extremely thin plate-like crystals are shown in Figure 3.47.

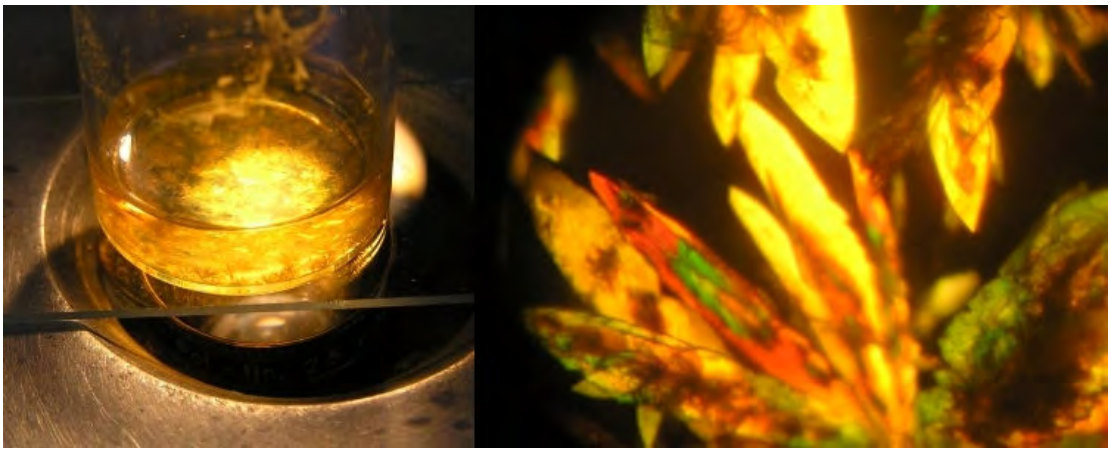

Figure 3.47 *– Photos of the highly twinned plate-like crystals of* ***3.44****.*

Despite repeating the experiment under varying conditions and collecting data on multiple crystals, only a very poor quality X-ray crystallographic structure could be obtained. The solution was coaxed out of a highly twinned crystal, solving in orthorhombic space group $Pb2_1a$.

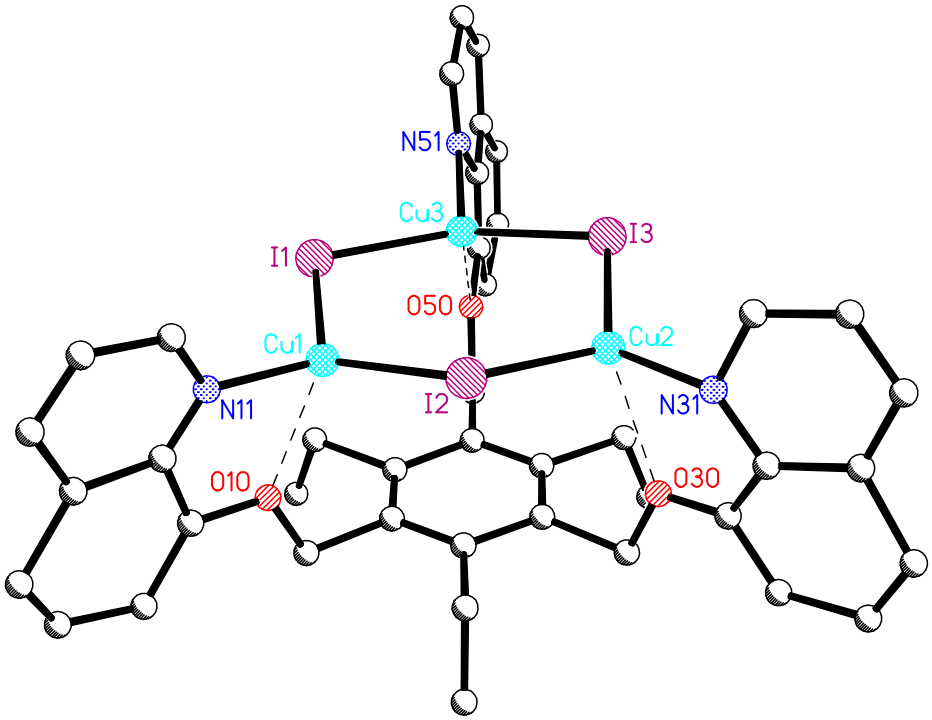

Figure 3.48 *– The discrete structure of* ***3.44****, showing the* Cu_3I_3 *hexagon nestled between the arms of the ligand. Selected bond lengths (Å) and angles (°): Cu1-N11 2.00(3), Cu1-I2 2.555(6), Cu1-I1 2.545(6), Cu2-N31 2.04(2),*

Cu2-I3 2.539(6), Cu2-I2 2.560(6), Cu3-N51 2.15(2), Cu3-I3 2.542(7), Cu3-I1 2.547(6), N11-Cu1-I2 113(1), N11-Cu1-I1 118(1), I2-Cu1-I1 122.8(2), N31-Cu2-I3 122.8(5), N31-Cu2-I2 109.1(5), I3-Cu2-I2 121.5(2), N51-Cu3-I3 109.8(4), N51-Cu3-I1 111.5(5), I3-Cu3-I1 133.0(2), Cu3-I1-Cu1 107.8(2), Cu1-I2-Cu2 115.6(2), Cu3-I3-Cu2 107.3(2).

The asymmetric unit is shown in Figure 3.48, with hydrogen atoms excluded for clarity. The discrete structure consists of copper and iodine atoms forming a hexagon nestled within the arms of the ligand. The ligand is organised in an *ababab* conformation, with the quinoline nitrogens facing inwards to bind a copper atom each. The copper atoms only make three bonds, to two iodines and a ligand nitrogen, with a weak interaction to the oxygen in the ligand (2.40-2.49Å) to give a highly distorted tetrahedral geometry (angles range between 73^{o} and 133^{o}). Three copper atoms and three iodine atoms are linked together in a cyclic structure resembling a hexagon. This Cu_3I_3 hexagon is not planar, as each of the iodines rises a little above of the plane to give a chair conformation, which is probably a compromise between the geometry of a hexagon and the bonding constraints of the copper atoms. The distance across the hexagon is 5.16Å (Cu1-I3), with the copper to copper distances ranging from 4.1-4.3Å.

There are very few reports of isolated Cu_3I_3 hexagons in the literature.[248-251] The motif itself is not unknown, with a few crystal structures of copper iodide clusters forming hexagonal nets,[230,252,253] or of a hexagon capped by another copper or iodide atom to skew the shape.[254,255] In every case in the literature supported by an X-ray structure in the *Cambridge Crystallographic Database* (v 5.26),[130] a Cu_3I_3 hexagon only exists connected to other copper and iodide atoms as part of a larger structure. A few reports of the Cu_3I_3 unit characterised without X-ray crystallography exist,[248-251] but the papers are difficult to obtain, so the relevance to this case was not established.

The closest examples from the *Cambridge Crystallographic Database* to the Cu_3I_3 hexagon identified in **3.44** are shown in Figure 3.49. Upon reaction with Cu(I) halide salts, ligand **3.45** forms a two-dimensional sheet, with a Cu_6X_6 hexagonal prism cluster linking together ligands.[256] Interestingly, ligand **3.45** is similar to the ligands described in this chapter, based on a 1,3,5-triethylbenzene core, with three 2'-pyridyl heterocyclic donor groups linked *via* two-carbon chains to the core. Instead of the ligand holding onto one hexagonal unit, the prisms, consisting of two Cu_3X_3 units joined, link together

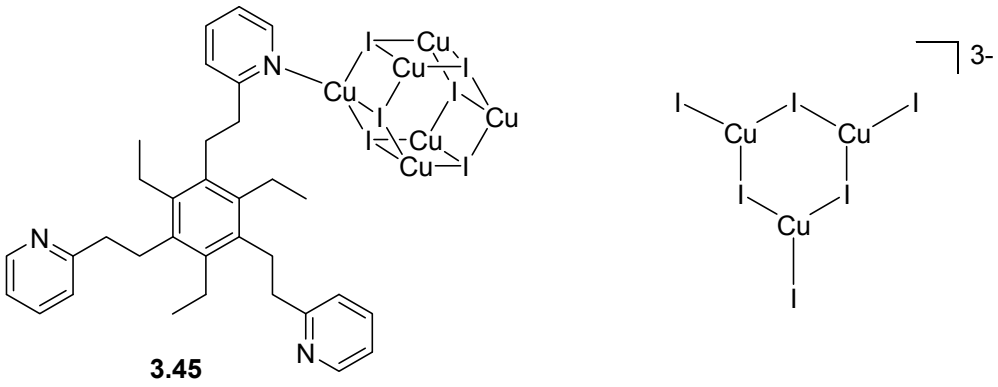

Figure 3.49 *– The closest examples of discrete Cu_3I_3 hexagons in the* Cambridge Crystallographic Database.

six ligands.[256] This is significant as the cavity between the three arms is a similar size as in **3.42**, and instead of one ligand choosing to encompass half of a Cu_6X_6 prism, the arms have rotated so each nitrogen binds to a copper on separate prisms, forming a polymer.[256] A notable difference between the ligands is the presence of an oxygen atom in **3.42**, allowing the copper atom to form a weak interaction and obtain a distorted

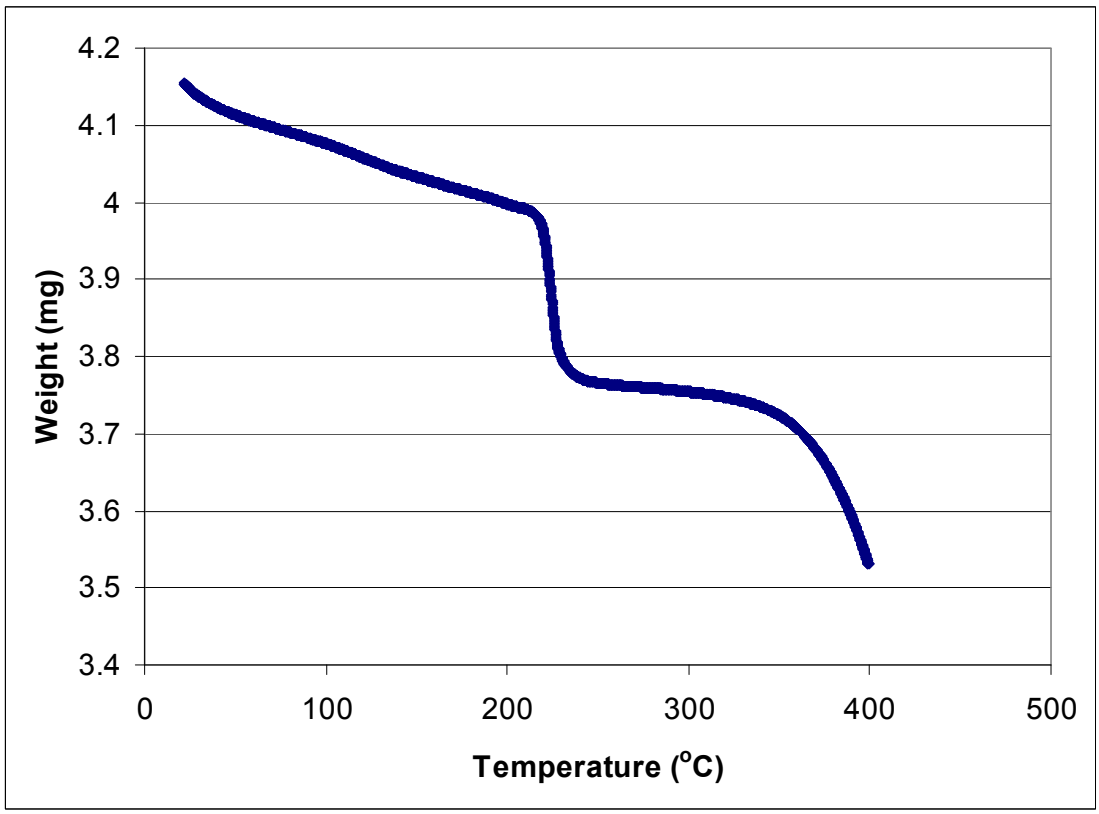

Figure 3.50 *– Thermogravimetric analysis results for **3.44**. The weight loss is plotted against temperature.*

tetrahedral geometry, which is likely to be the driving force for the formation of complex **3.44**. The next closest example to an isolated Cu_3I_3 hexagon is the discrete anion shown in Figure 3.49.[257] Although the hexagon exists it is not isolated, with three extra iodines saturating the copper atoms.

A small sample of **3.44** was removed from the mother liquor and transported to Sydney for thermogravimetric analysis. Unexpectedly, the crystals had changed colour from yellow to jet black upon arrival. What triggered this dramatic colour change is unknown. This black sample was analysed by TGA to give the very unusual results shown in Figure 3.50. A steady weight loss is seen to 220^{o}C before a sharp sudden drop in weight, then the curve stabilises before final decomposition around 350^{o}C. The weight loss before decomposition is about 10% of the total weight. It is unknown how to interpret these results, especially considering the lack of crystallographic information about other solvents present in the lattice, and what processes made the crystals turn black.

*Other complexes with **3.42***

Complexation of **3.42** was attempted with a variety of metal salts, namely $AgNO_3$, $AgClO_4$, $AgPF_6$, CuI, $Cu(ClO_4)_2$, $NiCl_2$, $ZnBr_2$, $Zn(ClO_4)_2$, $PdCl_2$ and $Pd(en)(NO_3)_2$. Despite repeated recrystallisation attempts, the only complex that could be crystallised was **3.44**. Most of the other complexes were not analysed further.

The reaction of **3.42** with $Pd(en)(NO_3)_2$ produced a yellowish powder which was analysed to have a M_3L_2 stoichiometry. Like analogous complexes, once again the ethylenediamine groups have been removed, and the anions replaced by hydroxides. Only a single nitrate anion remains, possibly encapsulated by a cage-like structure. Despite multiple crystallisation attempts, no adequate crystals of this complex could be obtained.

Complexes with ligand 3.43

In the hope of creating complexes, ligand **3.43** was reacted with a few different metal salts, namely $AgClO_4$, CuI, $CoCl_2$ and $CoBr_2$. The solubility of **3.43** is much lower than

3.42, which made complexation more difficult. A suitable solvent combination to attempt to synthesise the equivalent complex to **3.44** was difficult to obtain, and no products could be crystallised. Ligand **3.43** also precipitates if any acetonitrile is present, so the ligand structure similar to **3.42** could not be obtained. Only two of the complexation products were analysed further.

Reaction of **3.43** with $CoBr_2$ gives a green precipitate with a M_2L stoichiometry. This ratio is ambiguous and may suggest either a coordination polymer or a discrete structure. Reaction of **3.43** with $AgClO_4$ gives a product with a M_3L_2 stoichiometry. It is possible that this complex is a cage structure, but it could not be crystallised to confirm this.

Summary

This chapter details the synthesis of eleven tripodal ligands based on hexasubstituted benzene cores, of which seven were previously unknown. The coordination chemistry of these ligands was studied. Eleven crystal structures of complexes were obtained, and three crystal structures of ligands.

Ligand **3.5** is known to form a M_6L_4 cage with $PdCl_2$ which encapsulates a DMSO molecule. It was shown that this cage can be synthesised from different starting materials, and the cage is capable of crystallising in a different space group, with all the ligands fully organised and a chloroform molecule encapsulated. A one-dimensional polymer was also obtained from ligand **3.5** with silver displaying an η^1 interaction with the benzene core of the ligand, typical of complexes of this nature.

Ligand **3.24** forms a discrete trinuclear complex with $PdCl_2$, which interacts with a DMSO molecule. Reaction with copper(II) salts led to the formation of M_4L_2 dimers, similar to those obtained with **2.12**, with crystal structures of both discrete and polymeric examples, and examples of varying ligand conformations.

Ligand **3.33** forms a two-dimensional interdigitated polymer upon reaction with $CoBr_2$. The two-dimensional sheets obtained from reaction with CuI, containing an unusual Cu_4I_4 unit, were shown by TGA to be stable to solvate removal and resorption. A very

similar structure was obtained by reaction of ligand **3.38** with CuI, but the connectivity of the complexes is different, resulting in a three-dimensional polymer. Another three-dimensional polymer was obtained from ligand **3.38** and $AgClO_4$, displaying four-fold interpenetration.

Ligand **3.42** crystallises readily from acetonitrile, interacting with three solvate molecules to form a host-guest complex shown by TGA to be relatively stable. Reaction of **3.42** with CuI creates a complex which contains a Cu_3I_3 hexagon nestled between the arms of the ligand.

Three ligand cores were utilised in this research, based on mesitylene, 1,3,5-triethylbenzene and 1,3,5-trimethoxybenzene. It was hoped the steric bulk of the substituents in the later two cores would be sufficient enough to promote a preorganised *ababab* conformation around the ring. Unfortunately none of the complexes containing ligands based on the 1,3,5-trimethoxybenzene core crystallised. Of the thirteen crystal structures obtained of triethylbenzene-based ligands, 62% of the ligands lie in an organised conformation, consistent with the 64% identified from the *Cambridge Crystallographic Database* (v. 5.26).

Unfortunately, apart from **3.21** and its isomer **3.22**, no crystal structures of molecular cages were obtained from these ligands, although a large number of complexes were shown by elemental analysis to display the M_3L_2 stoichiometry common in molecular cages, but these could not be fully characterised by X-ray crystallography.

Chapter Four

The remaining C_3 symmetric ligands

Chapter Four

The remaining C_3 symmetric ligands

Introduction

As mentioned in previous chapters, a useful concept in ligand design is to tether multiple arms terminating in donor atoms (or heterocycles containing donor atoms) to a suitable core. Expansion of the ligand in this way allows more control over the positioning of the donor atoms, and may allow incorporation of additional features into the metallosupramolecular synthon like flexibility, hydrogen bonding donors or acceptors, or aromatic rings for π-π stacking interactions, all of which may influence the product formed upon reaction with metal salts. So far in this thesis all the ligands discussed are based around a single benzene ring. However many more options exist for core groups that can be built into C_3 symmetric ligands, as will be seen in this chapter.

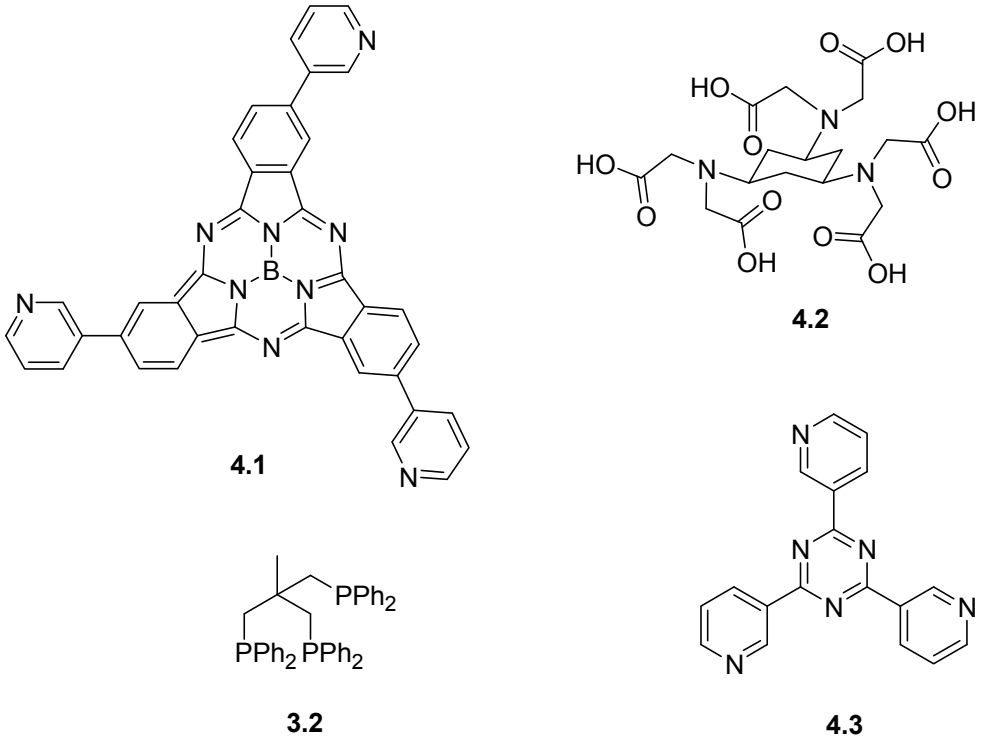

Figure 4.1 *– Examples of ligands not based on benzene cores which are capable of forming molecular cages.*

Figure 4.1 shows some examples of ligands which are not based on benzene cores and are still capable of forming molecular cages.[56,99,258,259] Ligand **4.1**[258] is based on a

subphthalocyanine. The ancillary substituent on the boron atom is not shown. The subphthalocyanine has a curve shaped structure, bringing all the donor atoms onto the same side of the ligand core, making it ideal for the formation of molecular capsules.[258] Ligand **4.2**[259] is based on a cyclohexane core, eliminating the rigidity imposed by aromatic rings. When **4.2** is reacted with iron(III) salts, both the carboxylic acid groups and the amine donors bond to the metal atoms to create a M_6L_2 cluster which resembles a M_3L_2 cage.[259] The ligand arms in **3.2**[56] are tethered to a single carbon atom, the geometry of the central atom directing the ligand arms into a tripodal arrangement. Ligand **4.3**[99] uses a triazine as the aromatic core, a substitute that provides similar benefits to a benzene core and the resulting ligand may be easier to synthesise than the corresponding benzene-based ligand. A subtle difference between a triazine and benzene core is the absence of hydrogen atoms on the central ring, which removes steric hindrance with hydrogens on adjoining aromatic rings in ligands like **4.3**, and encourages the aromatic rings to lie coplanar with the possibility of hydrogen bonding to the triazine nitrogens.[260]

This chapter focuses on C_3 symmetric ligands synthesised during this research that are based on different or more elaborate ligand cores than just a single benzene ring. The first family of ligands to be discussed are based on 4,4',4"-trisubstitution of 1,3,5-triphenylbenzene. Next are related ligands based on the similar core, 1,3,5-triphenyltriazine. Also discussed are a family of ligands based on a single carbon atom core, the tri(4-substituted-phenyl)methanol ligands. And finally the synthetic route towards tri(4-trisubsituted-phenyl)amine ligands will be discussed.

The 4,4',4"-trisubstituted-1,3,5-triphenylbenzene ligands

An array of benzene rings at the centre of a ligand can be desirable to extend the size of the ligand so it can act as a component of a molecular cage with a substantially sized central cavity. A molecular cage is of most use if by encapsulating the desired guest molecule(s) it can separate it from a mixture or initiate a chemical reaction upon the guest. One way to increase the size of the central cavity is to increase the size of the ligand by adding extra linkers into the core or the arms. Ligands based on 1,3,5-triphenylbenzene also incorporate a degree of rigidity caused by the aromatic rings.

Arrays of aromatic rings also have a tendency to π-π stack, an interaction that may encourage the formation of complexes and the crystallisation of these complexes.

1,3,5-Triphenylbenzene has often been used to construct organic cage molecules like cyclophanes.[261-266] The array of aromatic rings helps create a rigid non-collapsible cavity.[263] Ligands based on 1,3,5-triphenylbenzene have been shown to act as components for the formation of coordination cages upon reaction with appropriate metal salts.[8,66,267] Examples of two of these ligands are shown in Figure 4.2.

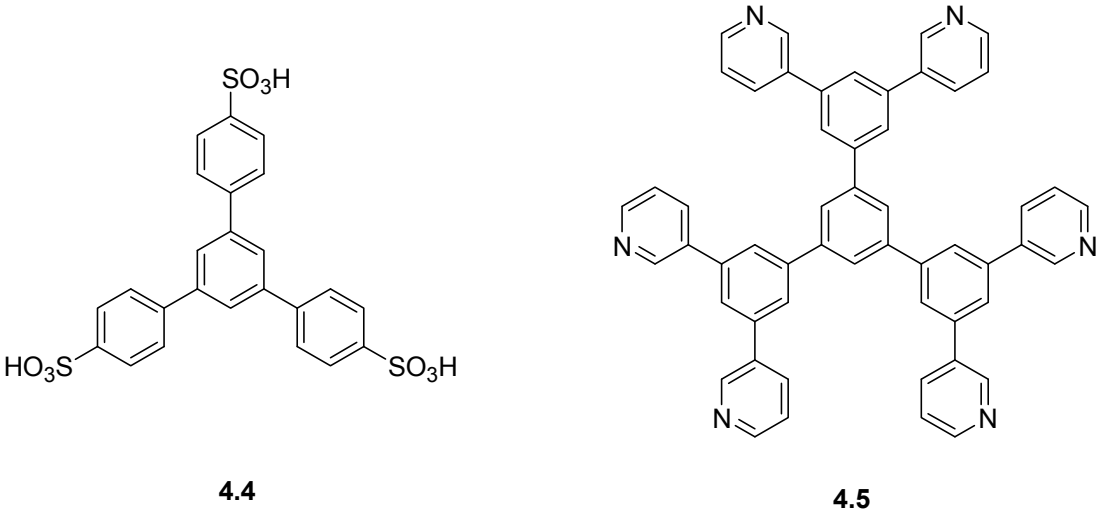

4.4 **4.5**

Figure 4.2 *– Ligands based on 1,3,5-triphenylbenzene which have been shown to act as components of molecular cages.*

Upon reaction with Cu(II) salts, ligand **4.4** has been shown to form a M_3L_2 cage which hosts a pyridine guest molecule.[66] Interestingly, two polymer products are also crystallised from the same solution as the cage, and the ratio of each product is dependent on the anion used.[267] Ligand **4.5** has been shown to form a M_6L_2 cage upon reaction with $Pd(en)(NO_3)_2$,[8] where the planar ligand panel distorts to be as concave as possible to allow the cage to encapsulate a 1,3,5-triphenylbenzene guest. With a smaller guest molecule, a $M_{12}L_4$ elongated cage-like structure is formed.[8] In all of these cases, the aromatic guest π-π stacks strongly with the triphenylbenzene component of the cage.[8,66,267]

Synthesis of ligand precursors

1,3,5-Triphenylbenzene is an attractive core for ligands designed for the construction of molecular cages for the reasons highlighted above. Due to the nature of this research, it was desired to increase the flexibility of the ligand so the heterocyclic group was joined to the central core by a methylene group. This also helps provide a facile synthetic route to these ligands.

Originally $SOCl_2$ was used to cyclotrimerise 4-methylacetophenone (**4.6**) into 4,4',4"-trimethyl-1,3,5-triphenylbenzene (**4.7**),[268] but the method gave poor yields and it was difficult to separate the desired product. Another method was attempted where triflic acid was used as a catalyst with a Dean-Stark trap to remove water,[269] and the reaction proceeded more effectively with a 54% yield after recrystallisation. Bromination of the product was achieved with N-bromosuccinimide[269] over 10 hours to give 4,4',4"-tri(bromomethyl)-1,3,5-triphenylbenzene (**4.8**) in 74% yield. These reactions are shown in Scheme 4.1.

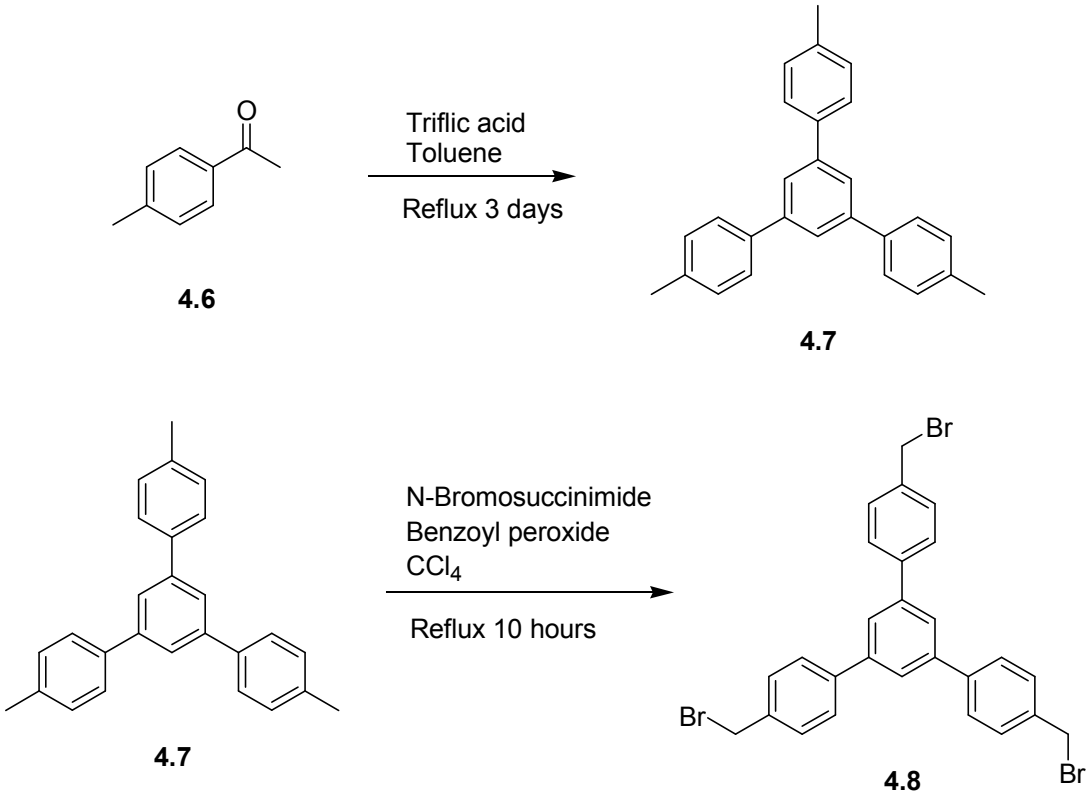

Scheme 4.1 *– The synthetic route to precursor* ***4.8****.*

4,4',4"-Tri(pyrazol-1-ylmethyl)-1,3,5-triphenylbenzene (4.9)

A phase-transfer-catalysed alkylation of pyrazole, shown in Scheme 4.2, provided incorporation of the pyrazoles to **4.8** over four days to give 4,4',4"-tri(pyrazol-1-ylmethyl)-1,3,5-triphenylbenzene (**4.9**) in 94% yield.

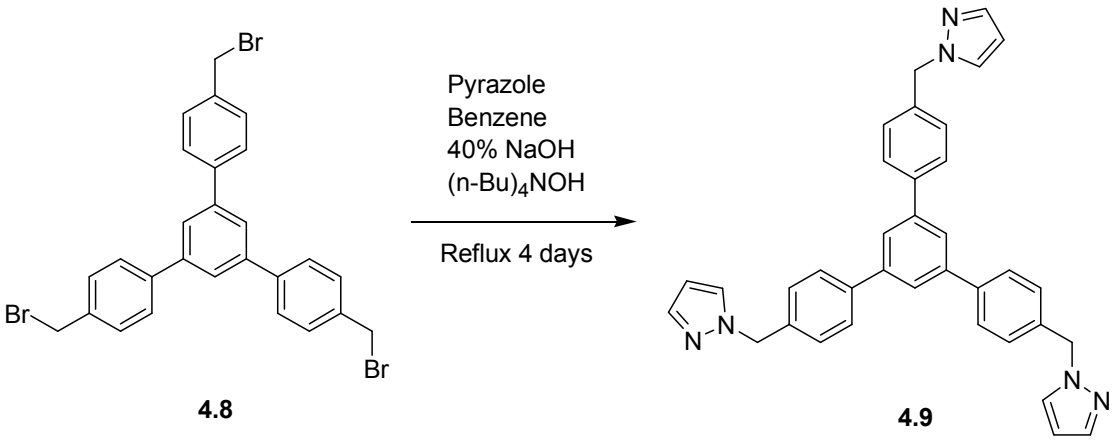

4.8 **4.9**

Scheme 4.2 *– The synthetic route to ligand* ***4.9****.*

Ligand **4.9** has a rigid and mostly planar core, leaving the donor arms well separated from each other, with a degree of conformational flexibility due to the attaching methylene groups. If cage structures could be obtained from this ligand, they would have a greater cavity size than corresponding structures of the benzene based ligands discussed previously.

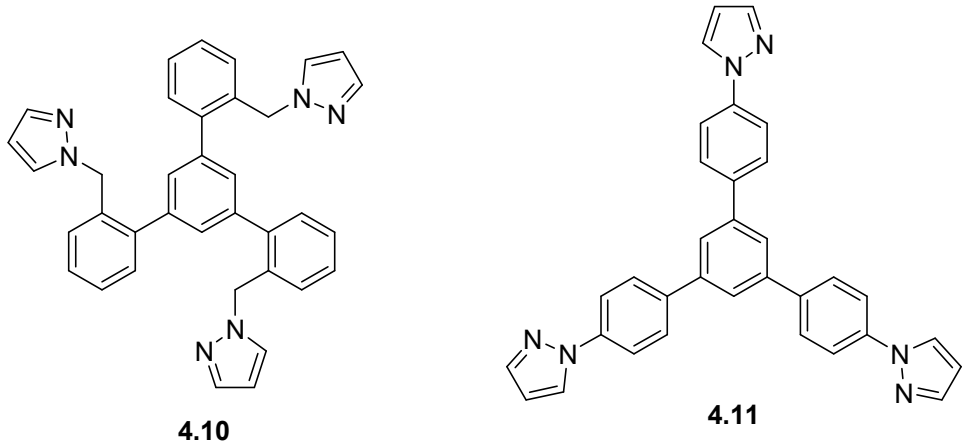

4.10 **4.11**

Figure 4.3 *– Ligands structurally similar to* ***4.9****.*

Two ligands in the literature share structural similarities with **4.9**, and are shown in Figure 4.3. Ligand **4.10**[270] is an isomer of **4.9**, with the pyrazol-1-ylmethyl arms

connected in the ortho- instead of para-positions. This changes the relative position of the nitrogen donors dramatically compared with **4.9**. When reacted with Cu(I) or Ag(I) triflate salts, **4.10** forms chiral coelenterand complexes where the metal coordinates to all three pyrazole nitrogens and the benzene core of the ligand.[270] Ligand **4.11**[271] is a more rigid version of **4.9**, lacking the flexible methylene linker. This ligand forms a double stranded one-dimensional polymer upon reaction with $AgNO_3$.[271]

Complexes with ligand 4.9

*Crystal structure of the complex with $AgClO_4$ (**4.12**)*

Crystals were obtained by reaction of silver perchlorate in toluene with ligand **4.9** in dichloromethane and subsequent recrystallisation by evaporation of an acetonitrile solution. These crystals were suitable for X-ray crystallography and solve in the trigonal space group P-3.

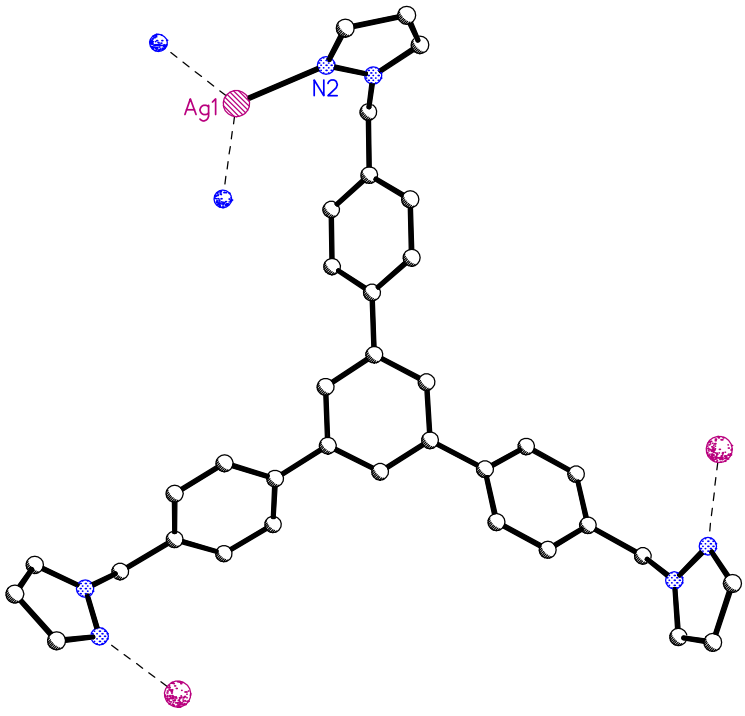

Figure 4.4 *– A section of the two-dimensional polymer **4.12**, showing the connectivity of the ligand and silver atoms. Selected bond lengths (Å) and angles (°): Ag1-N2 2.229(6), N2-Ag1-N2A 119.30(5).*

The asymmetric unit contains one third of a ligand and one third of a silver atom, as well as a third of a disordered perchlorate and a third of a disordered acetonitrile solvate molecule. An expanded section of the structure is shown in Figure 4.4 to display the connectivity. Hydrogen atoms, the disordered perchlorate anion and acetonitrile solvate molecule are excluded for clarity. Each pyrazole is coordinated to a silver atom, and each silver atom is bound to three pyrazoles with a trigonal planar geometry. Each of the aromatic rings surrounding the central benzene is tilted 29.8^{o} from coplanarity, presumably to reduce the steric interactions between hydrogens. Due to the crystallographic 3-fold rotational symmetry, all three rings tilt in the same direction, creating a propeller-like arrangement, and therefore making the ligand chiral in this conformation.

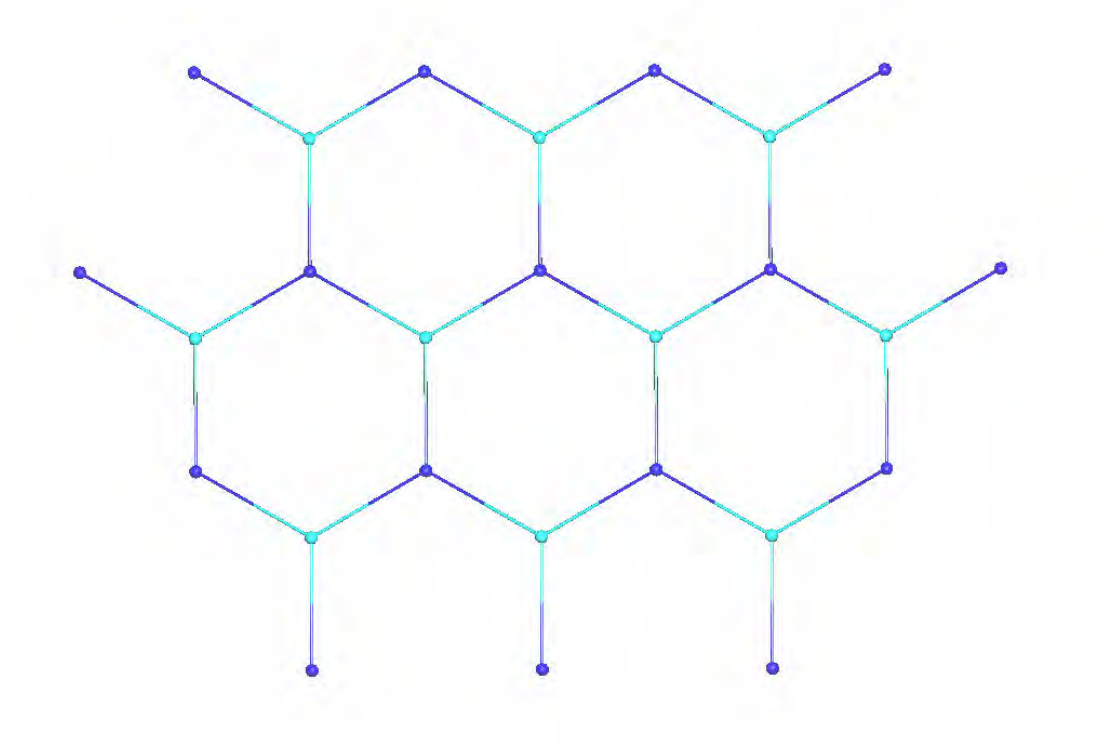

Figure 4.5 *– A simplified diagram of a single (6,3) net of* ***4.12****.*

The unit shown in Figure 4.4 is a small section of a two-dimensional polymer. A larger section of this polymer is shown in the simplified diagram in Figure 4.5. As both the central core of the ligand and the metal atom act as three-connector nodes, the sheet is classified as a (6,3) net. Every ligand in a sheet has the same chirality. Due to the twist of the pyrazole rings, the silver atoms lie out of the plane of the ligand, so the silver

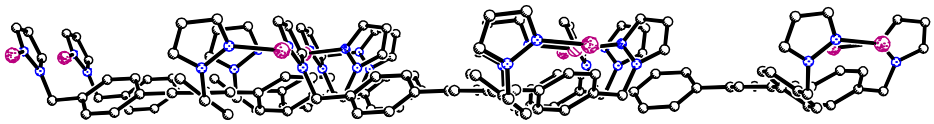

Figure 4.6 *– A side-on view of the unsymmetrical sheet of* ***4.12****, showing how the silver atoms rise above one face of the polymer.*

atoms and coordinated pyrazole rings sit on one side of the polymer sheet, while the ligand cores lie on the other. This is shown in Figure 4.6 for a single sheet. Alternating sheets sit back-to-back, with the silver atoms from one sheet sitting between the silver atoms of another sheet. The sheets are staggered so that the nodes of the ligands in each sheet are aligned, but the silver atoms sit in the middle of the macrocycles in alternating sheets. This is shown in the simplified diagram of two sheets in Figure 4.7. The chirality of the ligands alternates between sheets, so that the crystal itself is achiral, as required by the space group. There are π-π stacking interactions (3.567Å) between the sheets where the central ligand core rings overlap. Each sheet interacts with only one of the adjacent polymers in this way, as the ligands only sit on one face of the sheet. The sheets are also linked by hydrogen bonding to the perchlorate counterions.

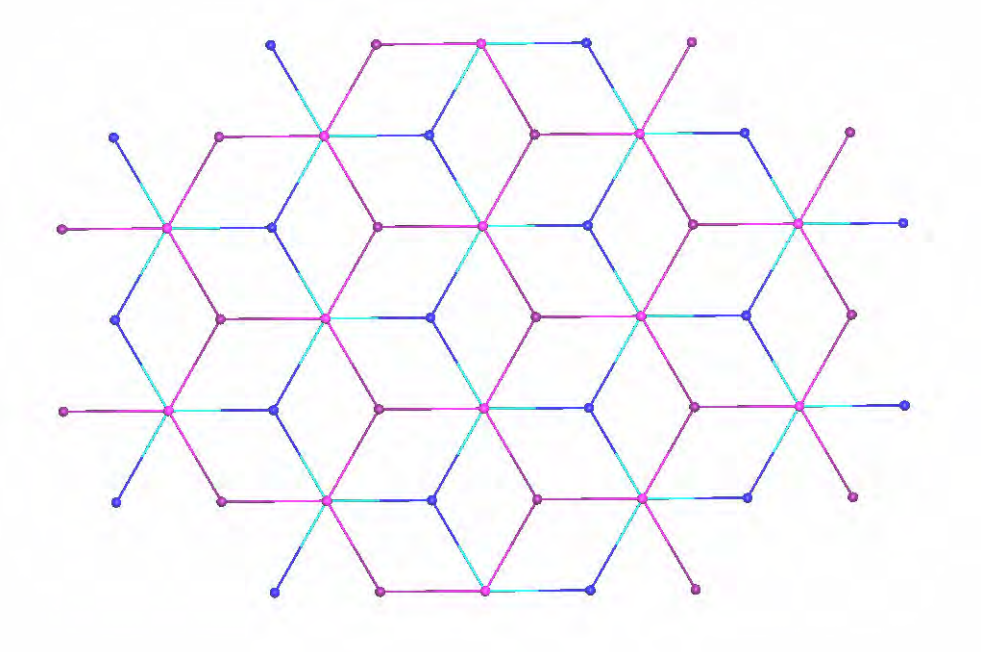

Figure 4.7 *– A simplified diagram of two sheets of* ***4.12****, showing the alignment with respect to each other. The darker points in each strand represent the silver atoms.*

*Other complexes with **4.9***

Attempts were made to complex **4.9** with a variety of metal salts in a variety of different solvents and conditions. The metal salts used included $AgNO_3$, $AgClO_4$, $AgPF_6$, CuI, $CuCl_2$, $Cu(NO_3)_2$, $Cu(ClO_4)_2$, $CoBr_2$, $Zn(OAc)_2$, $Zn(ClO_4)_2$, $PdCl_2$, K_2PdCl_6, $Pd(PhCN)_2Cl_2$, $Pd(CH_3CN)Cl_2$ and $Pd(en)(NO_3)_2$. Unfortunately crystals suitable for X-ray crystallography were only obtained of one of these complexes. Many of the other complexes were not analysed further.

The reaction which produced complex **4.12** was repeated, but including the potential templating molecule, trimesic acid, to ascertain if this could trigger the formation of a cage-like structure. The white precipitate obtained was shown to have a 1:1:1 metal to ligand to template stoichiometry. Unfortunately the crystals grown from slow evaporation of an acetonitrile solution were shown by X-ray crystallography to be polymer **4.12** again, with no trimesic acid present in the crystal lattice.

Reaction of **4.9** with $Pd(en)(NO_3)_2$ was largely unsuccessful due to the low solubility of the ligand in the polar solvents needed to dissolve the metal salt. However the product of reaction with $PdCl_2$ grows into spherical solids using diffusion techniques, which according to elemental analysis possess a M_3L_2 stoichiometry. Given the nature of the components it is possible the product is a molecular cage, although this metal and ligand ratio could also signify a polymer. Unfortunately these solids do not diffract and ^1H NMR and mass spectrometry analyses are ambiguous. This reaction was repeated with the inclusion of the potential templating molecule, trimesic acid. Only thin needle-like crystals could be grown which were not suitable for X-ray crystallography. Elemental analysis showed the yellow product to have a 2:1:3 metal to ligand to template stoichiometry.

The products of reaction of **4.9** with both $AgNO_3$ and $AgPF_6$ were shown to have M_2L stoichiometries by elemental analysis. Finally, triple cyclopalladation[272-274] with $Pd(OAc)_2$ was attempted with this ligand. Initial results looked promising, but the complex could not be converted to the corresponding soluble acetylacetonate salt[274] for characterisation.

4,4',4"-Tri[3-(2'-pyridyl)pyrazol-1-ylmethyl]-1,3,5-triphenylbenzene (4.13)

Like ligand **4.9**, 4,4',4"-tri[3-(2'-pyridyl)pyrazol-1-ylmethyl]-1,3,5-triphenylbenzene (**4.13**) was synthesised by a phase-transfer-catalysed alkylation of pyrazole, as shown in Scheme 4.3. The incorporation of the 3-(2'-pyridyl)pyrazole units to **4.8** over three days gave **4.13** in 85% yield.

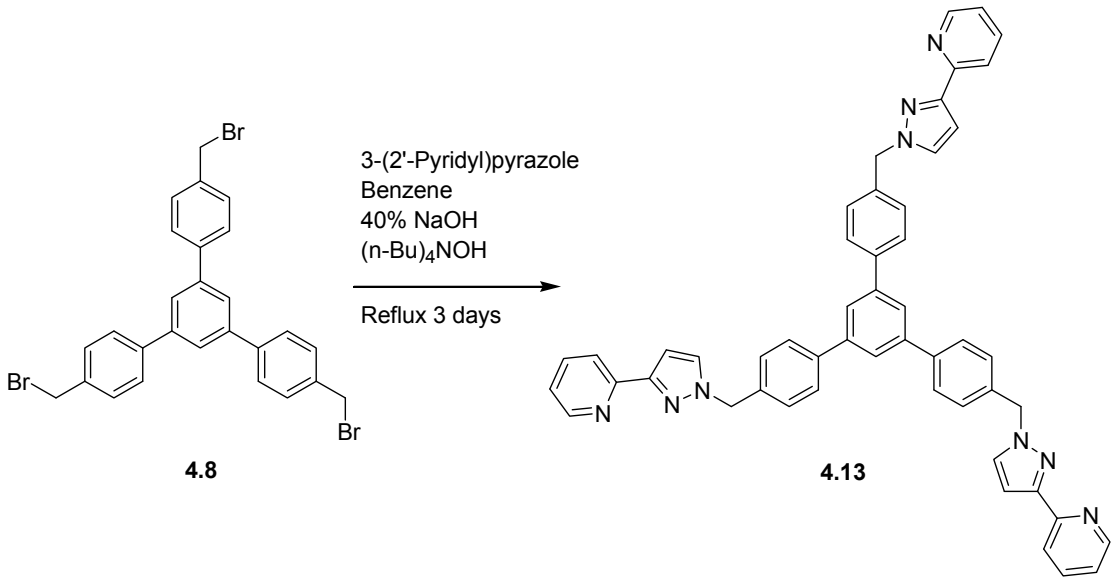

4.8 **4.13**

Scheme 4.3 *– Synthetic route to ligand **4.13**.*

Ligand **4.13** resembles **4.9**, but has an extra pyridine ring attached to each pyrazole to create three bidentate binding domains which will hopefully chelate to metal atoms and form robust structures that crystallise easily. Ligand **4.13** also incorporates the same flexibility seen in **4.9** due to the methylene linkers that join the binding domains to the ligand core. The size and flexibility of this ligand may make complexes containing it less likely to crystallise than complexes containing smaller, more rigid ligands.

Ligand **4.13** displays some structural similarity to the literature compound **4.14**.[275] Ligand **4.14** varies from **4.13** in that the flexibility in the ligand results from an amide connector instead of a methylene connector, and that the flexibility is located around the central core of the ligand rather than closer to the binding domains. Although designed as a ligand, no complexes of **4.14** have been reported.[275]

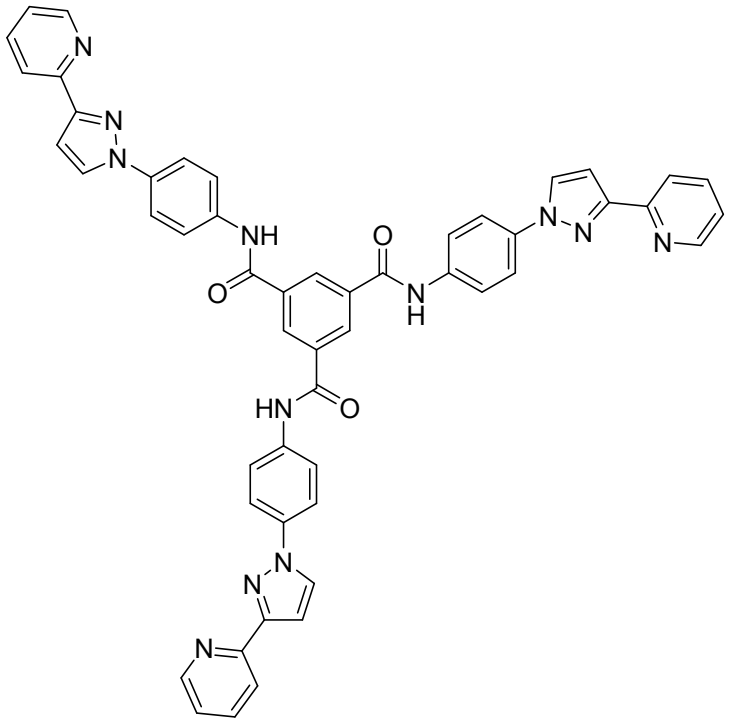

4.14

Figure 4.8 *– A ligand displaying structural similarity to* ***4.9****.*

Complexes with ligand 4.13

*Crystal structure of the complex with $CuSO_4$ (**4.15**)*

Reaction of ligand **4.13** with copper sulfate *via* the methanol layering procedure furnished clusters of green needle-like crystals after a few weeks of slow evaporation. Amongst these clusters were a few very small single crystals which, despite their size and consequent weak diffraction, were suitable for X-ray crystallography. The structure solved in triclinic space group P-1.

The asymmetric unit is shown in Figure 4.9, with hydrogen atoms and solvate molecules excluded for clarity. The asymmetric unit contains two ligands, three copper atoms and sulfate counterions, and fourteen water molecules, two of which are disordered over four sites. Each ligand bridges three copper atoms, one chelated in each binding domain. Each copper binds to two ligands, and coordinates an oxygen of a sulfate counterion with a five coordinate square pyramidal geometry, with short contacts to another sulfate oxygen (2.65-2.69Å). The ligands are highly twisted.

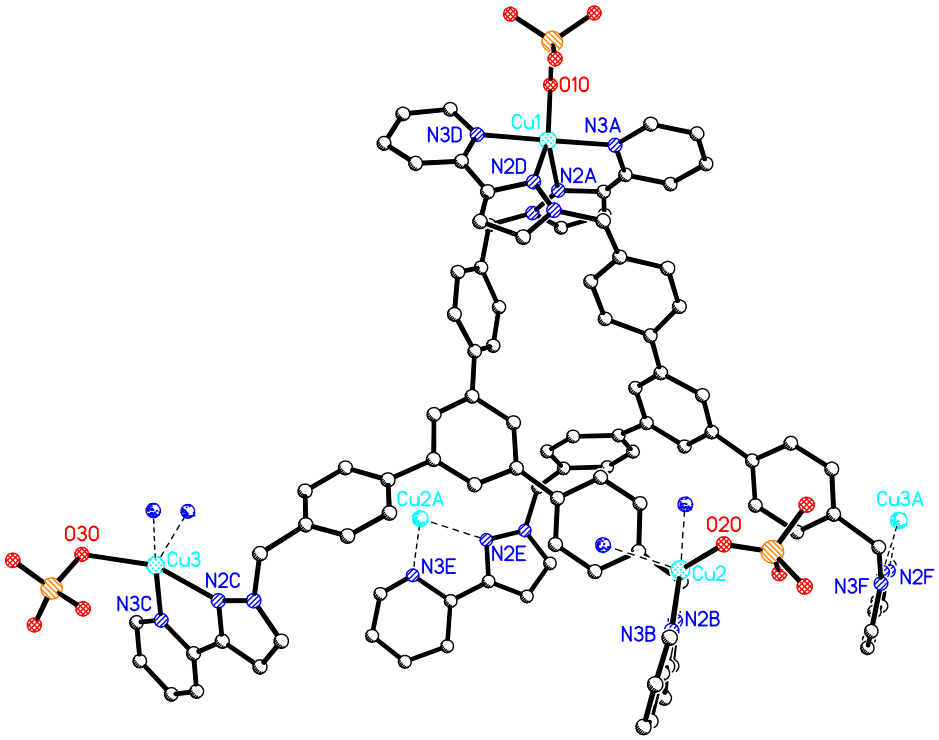

*Figure **4.9** – The asymmetric unit of **4.15**. Selected bond lengths (Å) and angles (°): Cu1-N2D 1.95(1), Cu1-O10 1.97(1), Cu1-N3A 1.952(9), Cu1-N3D 2.06(1), Cu1-N2A 2.235(8), Cu2-N3B 1.89(2), Cu2A-N3E 1.96(2), Cu2-O20 2.12(2), Cu2-N2B 2.14(1), Cu2A-N2E 2.21(1), Cu3A-N3F 1.99(1), Cu3-N3C 2.01(1), Cu3-O30 2.19(1), Cu3-N2C 2.21(2), Cu3A-N2F 2.1(2), N2D-Cu1-O10 159.7(6), N2D-Cu1-N3A 101.4(6), N2D-Cu1-N3D 80.7(8), N2D-Cu1-N2A 101.4(5), O10-Cu1-N3A 90.0(4), O10-Cu1-N3D 88.2(6), O10-Cu1-N2A 97.5(4), N3A-Cu1-N3D 177.7(6), N3A-Cu1-N2A 77.3(2), N3D-Cu1-N2A 101.5(5), N3B-Cu2-N3E 172.3(9), N3B-Cu2-O20 87.1(8), N3B-Cu2-N2B 78.1(8), N3B-Cu2-N2E 93.5(7), N3E-Cu2-O20 88.8(8), N3E-Cu2-N2B 108.7(8), N3E-Cu2A-N2E 81.5(9), O20-Cu2-N2B 146.1(6), O20-Cu2-N2E 107.2(6), N2B-Cu2-N2E 104.0(5), N3F-Cu3-N3C 176.8(8), N3F-Cu3-O30 90.9(5), N3F-Cu3-N2C 96.9(8), N3F-Cu3A-N2F 77(6), N3C-Cu3-O30 92.3(7), N3C-Cu3-N2C 79.9(9), N3C-Cu3-N2F 102(7), O30-Cu3-N2C 158.8(5), O30-Cu3-N2F 99(2), N2C-Cu3-N2F 101(2).*

The structure is a discrete M_6L_4 collapsed cage, as shown in Figure 4.10. The entwining of the ligands makes it difficult to interpret the connectivity of the structure, so symmetry related ligands are shaded similarly in Figure 4.10 to make them easier to distinguish. As the structure is quite complex, an alternative view is shown in Figure 4.11, again with symmetry equivalent ligands shaded similarly. The copper atoms sit at the vertices of the assembly, linked by the ligands which twist through the centre of the

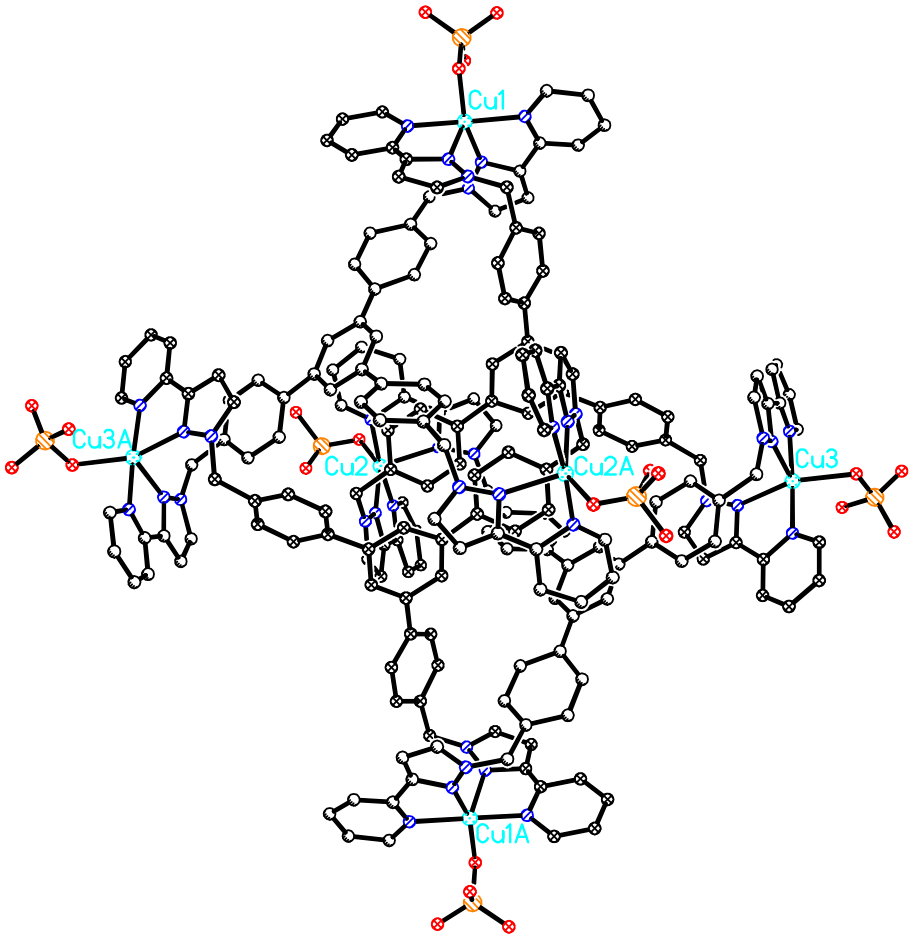

Figure 4.10 *– The M_6L_4 collapsed cages structure* ***4.15****. Ligands related by symmetry are shaded similarly to help simplify the complicated structure.*

structure. Unfortunately, in the conformation the cage has crystallised in, it does not contain a central cavity, as the ligands are aromatically stacked and fill the centre of the structure.

The cage is compressed on one axis, as shown in Figure 4.12, with the distances between opposite copper atoms being Cu1-Cu1A 23.58Å, Cu3-Cu3A 22.48Å and Cu2-Cu2A 12.92Å. Even though the cage is compressed seemingly unevenly, the copper atoms still sit at the vertices of an octahedron that has been shortened in one axis, as shown in Figure 4.13.

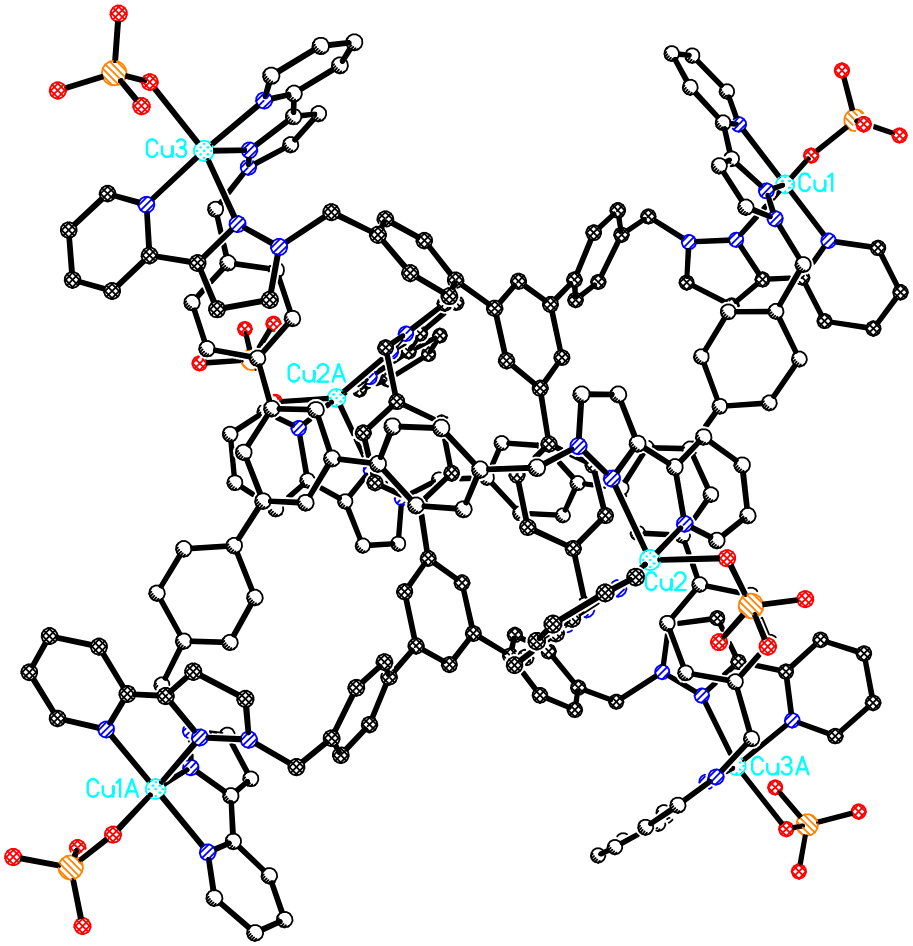

Figure 4.11 *– An alternative view of collapsed M_6L_4 cage* ***4.15****. Symmetry related ligands are shaded similarly.*

The structure is so twisted and entwined that it seems possible that it may be chiral; however it contains a centre of inversion. Even though the overall structure is not chiral, aspects of the structure do display chirality. The copper centres are all chiral, with three of each relative configuration, making the structure heterochiral. The ligand cores display the same helical chirality as seen in complex **4.12**, and the ligand arms also twist in such a way to form helices within the structure.

Each $CuSO_4$ unit hinges together two ligands and sits on a vertex of the structure, the flexibility of the ligand allowing each hinge to twist the structure so as to compress any

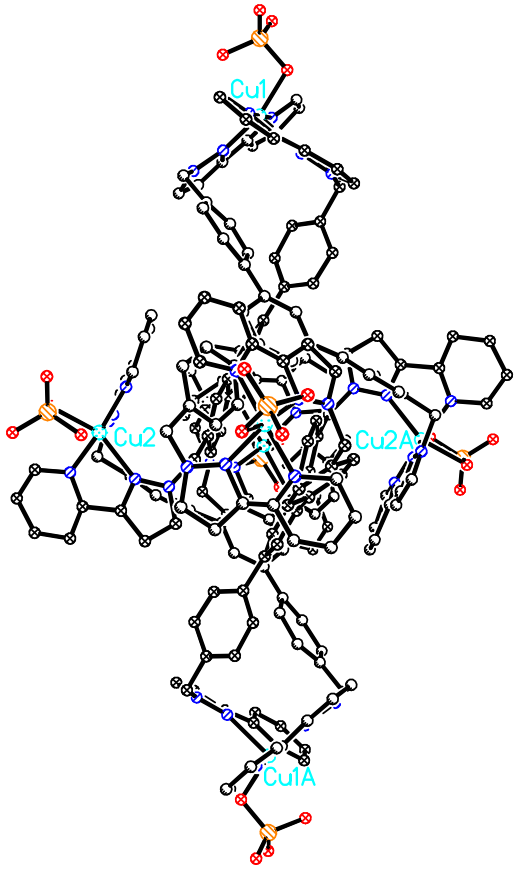

Figure 4.12 *– A side-on view of M_6L_4 assembly* ***4.15*** *showing the compression down one axis, rotated 90° from the view in Figure 4.10.*

potential central cavity. It seems possible that if these $CuSO_4$ hinges were untwisted, the ligands would unwind and each face of the octahedron would expand, providing a molecular cage large enough to encapsulate a substantial guest. The complex crystallised out of a partially aqueous solution which explains why the cage would compress to hide its hydrophobic interior. Therefore, it seems logical that cage expansion and guest encapsulation would be more likely in less polar solvents, but efforts to characterise an encapsulated guest within the cage were unsuccessful. Many potential guest molecules were used in these attempts, mostly aromatic, and many solvent systems were examined. Solubility of the reactants made these experiments difficult, as did the need to crystallise the product for definitive characterisation. In one case, the empty cage **4.15** crystallised from a relatively polar solution containing

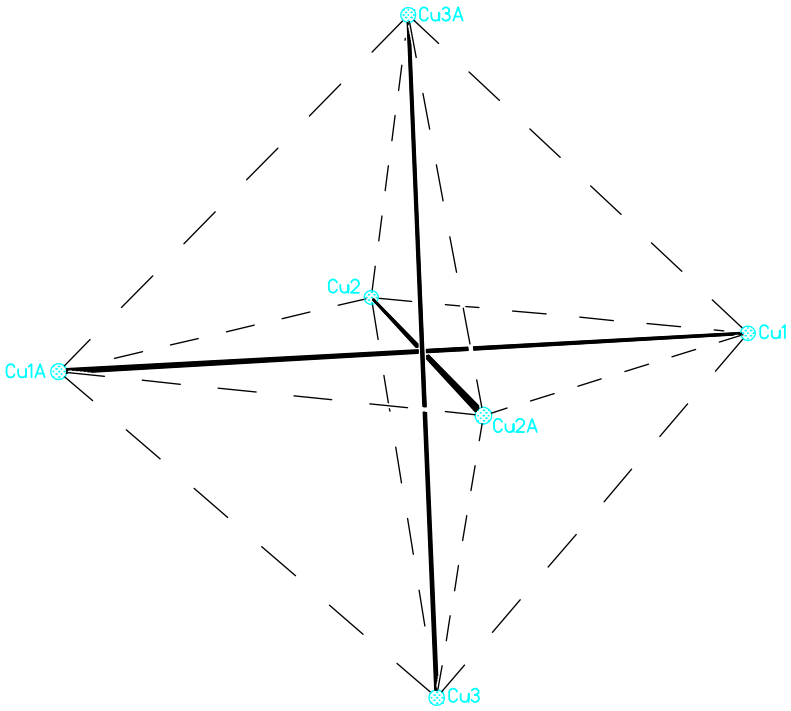

Figure 4.13 *– The compressed octahedron that the copper atoms of* ***4.15*** *form.*

potential guest molecule triphenylamine. Ligand decomposition greatly hindered this investigation, which will be discussed in detail in Chapter Five. The tendency for ligand **4.13** to decompose in the presence of copper(II) salts, including copper(II) sulfate, makes the characterisation of **4.15** all the more impressive.

Traditionally molecular cages are constructed from ligands displaying more rigidity than **4.13**. The advantage of those ligands is now obvious, with the rigidity ensuring that the cavity inside the cage is unyielding under any conditions and always available to seek out a guest molecule. As seen in complex **4.15**, flexibility inherent to the ligand can hinder cage formation by allowing the structure to fold in upon itself and compress the central cavity. However this could offer a new approach to molecular cages. Cages formed by rigid ligands have a central cavity of a defined size, whereas a cage constructed from a flexible ligand like **4.15** may be able to expand or contract to create a cavity of an ideal size to suit a particular guest, thereby acting as a more widely applicable molecular flask if reactions could be undertaken upon the encapsulated guest.

Also interesting in the structure of **4.15** are the solvate water molecules packed in a pocket between the cages. Fourteen water molecules have been located in the crystal lattice in the asymmetric unit, two disordered over four sites, which appears consistent with the elemental analysis results of 29 waters per cage. Eighteen close interactions exist between oxygen atoms in the structure (both between sulfate oxygens and solvate oxygens, and between solvate oxygens) with bond distances between 2.515Å-2.808Å. The average distance is 2.666Å. Solvate water molecules make either one or two short interactions. This is comparable with a recent paper which reports the formation of molecular ice inside a coordination cage,[184] where ten water molecules are located in close proximity, with an average O-O distance of 2.84Å.[184]

The cages are aligned in channels, with π-π stacking interactions between sets of coordinating arms (3.469Å). The water pockets fill the spaces between the bulky structures.

*Other complexes with **4.13***

Complexation of **4.13** was attempted with a variety of metal salts, namely $AgClO_4$, $AgCF_3SO_3$, CuI, $CuBF_4$, $CuCl_2$, $Cu(NO_3)_2$, $CuSO_4$, $CoBr_2$, $Co(BF_4)_2$, $Ni(BF_4)_2$, $FeSO_4$, $Fe(SCN)_2$ and K_2PdCl_4. Only one complex that crystallised was shown to contain ligand **4.13**, as has been discussed. Many of the complexes which did not crystallise were not investigated further.

After the characterisation of complex **4.15**, many attempts were made to synthesise this same assembly with alternative metal salts in the place of $CuSO_4$. Many copper(II) salts were attempted in different solvents, as were octahedral metal atoms. Crystals could not be obtained of any of these complexation attempts.

Although most of the crystals obtained from the solution from which **4.15** crystallised were needle-like clusters, elemental analysis suggests the sample is homogeneous. The metal to ligand ratio of the whole batch is consistent with the crystal structure, as is the unusual ratio of 29 waters per cage. Only 28 waters have been located in the difference map, but it is very likely that another half a water molecule exists in the asymmetric unit, possibly disordered over two or more sites.

The product of reaction of **4.13** with cobalt(II) bromide was shown to have a M_3L_2 stoichiometry, so it is possible that this complex has a similar structure to **4.15**. The product of reaction of **4.13** with copper(I) iodide was shown to have a M_3L stoichiometry; however given the tendency for copper iodide to dimerise into Cu_2I_2 squares this could suggest an effective "M_3L_2"-type stoichiometry. This complex could not have the same connectivity as **4.15**.

The tendency for ligand **4.13** to decompose in the presence of certain metal salts will be discussed in Chapter Five.

4,4',4"-Tri(4-pyridylsulfanylmethyl)-1,3,5-triphenylbenzene (4.16)

As shown in Scheme 4.4, 4,4',4"-tri(4-pyridylsulfanylmethyl)-1,3,5-triphenylbenzene (**4.16**) was synthesised by a base-catalysed substitution reaction over two days to give crude **4.16** in 79% yield. Unfortunately most of the product was lost during column chromatography, so only a small amount of pure product was obtained.

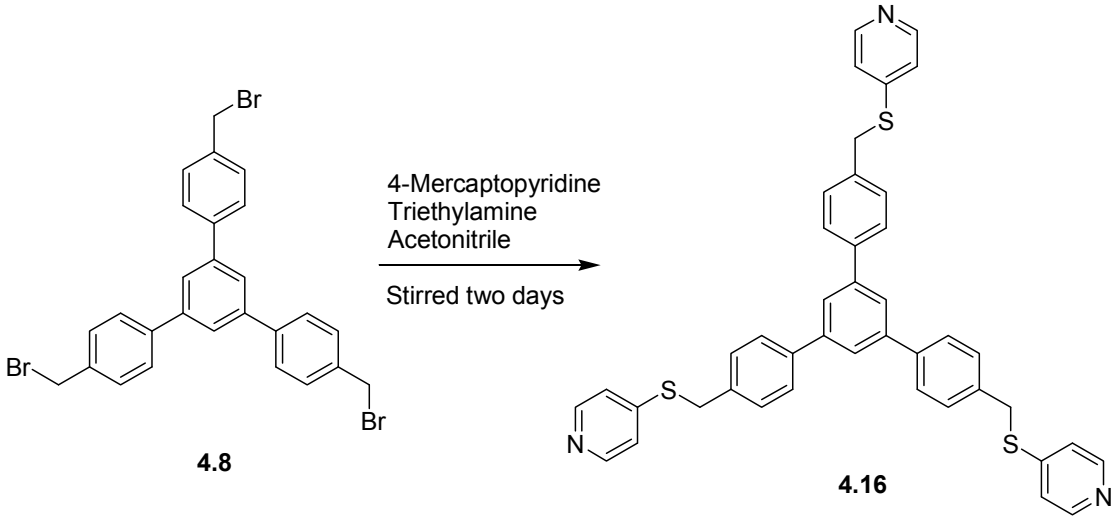

Scheme 4.4 *– The synthetic route to ligand* ***4.16****.*

In addition, $CHBr_2$ impurities in **4.8** affected the reaction, with side-products **4.17** and **4.18** separated from the reaction mixture during column chromatography, as shown in Figure 4.14. Ligand **4.17** is the product resulting from one $CHBr_2$ arm on **4.8**, while the smaller amounts of **4.18** obtained result from the impurity where two $CHBr_2$ arms exist on **4.8**. The coordination chemistry of these ligands was not investigated.

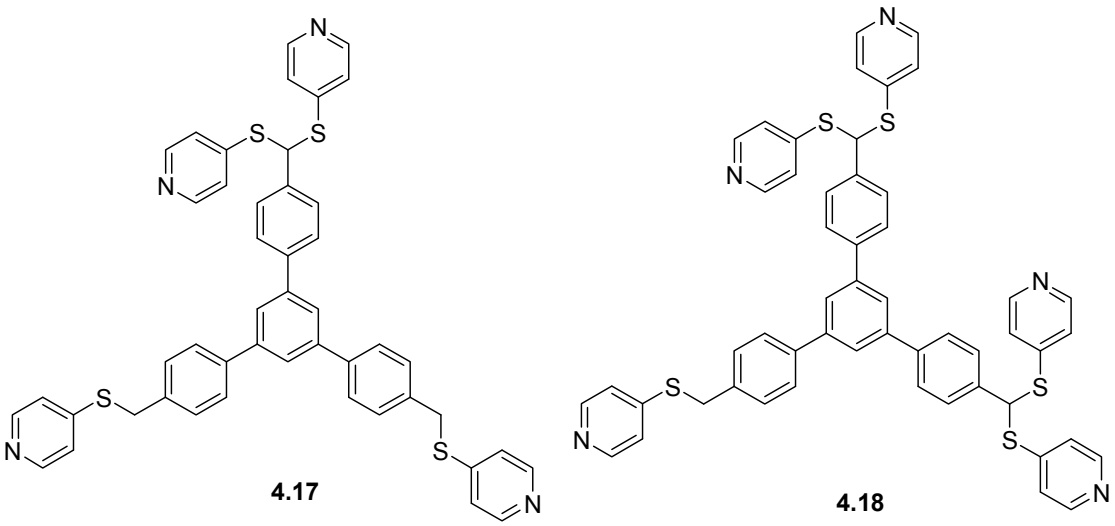

Figure 4.14 *– Side products produced from the reaction to synthesise* ***4.16****, resulting from the tetra- and penta-brominated impurities in* ***4.8****.*

Ligand **4.16** is another large ligand in this series, with flexibility incorporated by the sulfanylmethyl linkers joining the pyridine donor arms to the central core. Unlike **4.9** and **4.13**, the donor atoms in **4.16** point directly out from the ligand core. There are no literature compounds that closely resemble ligand **4.16**.

Complexes with ligand 4.16

The coordination chemistry of **4.16** was not studied in depth as such a small amount of ligand was obtained. It was attempted to complex the ligand with $AgClO_4$, CuI and $Cu(ClO_4)_2$. Unfortunately none of the crystals obtained from these reactions included ligand **4.16**. The precipitate obtained from reaction with CuI was shown by elemental analysis to have a M_2L stoichiometry. As CuI has a tendency to dimerise into Cu_2I_2 squares this could suggest an effective 1:1 stoichiometry. This may indicate a coordination polymer.

4,4',4"-Tri(8-quinolyloxymethyl)-1,3,5-triphenylbenzene (4.22)

An attempt to produce 4,4',4"-tri(8-quinolyloxymethyl)-1,3,5-triphenylbenzene (**4.22**) by the standard procedure used in this thesis was unsuccessful, as shown in Scheme 4.5. It is unknown why the only product of the reaction was the alcohol (**4.19**), and not the desired product **4.22**, as there is no steric hindrance impeding the addition of 8-hydroxyquinoline to the methylene groups.

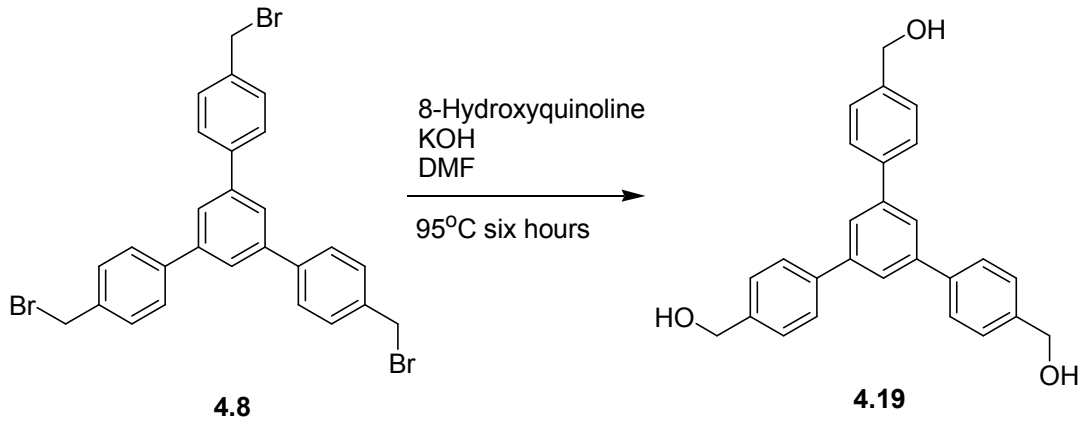

Scheme 4.5 *– The unsuccessful synthetic route to ligand* ***4.22***

Briefly an alternative convergent route to the synthesis of **4.22** and other ligands, including **4.9** was considered. The route is shown in Scheme 4.6. This route seeks to eliminate the $CHBr_2$ impurity from **4.8**, as the equivalent reaction on **4.6** proceeds more cleanly as only one bromine atom is added per molecule, so this would allow a cleaner

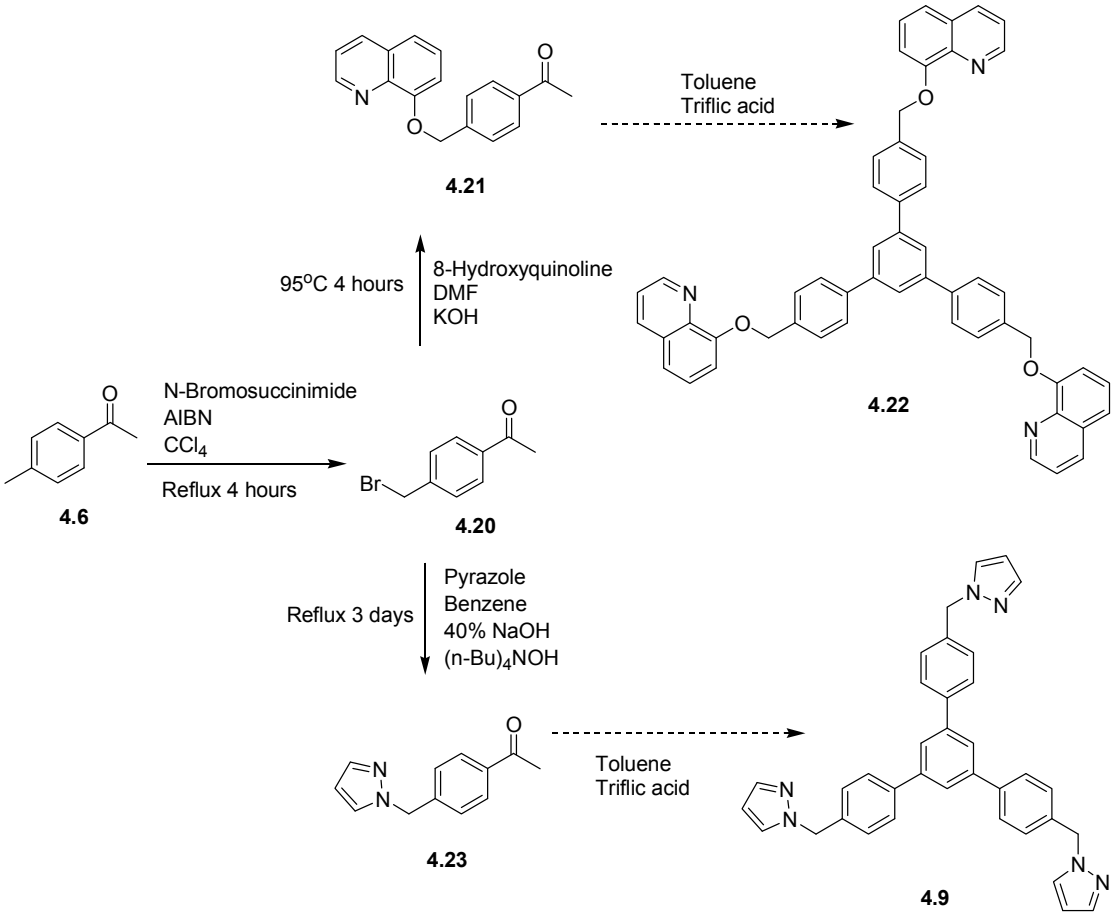

Scheme 4.6 *– An alternative convergent synthetic route to this ligand family which was considered by not pursued to completion.*

route to this family of ligands. The reaction to form **4.20** proceeded best when AIBN was used as an initiator with heating, rather than when dibenzoyl peroxide was used with light. The crude reaction mixture was used directly in the next steps; however this complicated the reactions more than expected. Problems arose due to the need to purify precursor **4.20**, and the difficulty of undertaking the condensation reaction in small quantities without evaporating the whole sample but still heating the solution enough that water can be removed by the Dean-Stark trap. Obviously more adequate glassware needed to be prepared to pursue this reaction scheme. Some of the precursors were prepared but this route to the ligands was abandoned due to time constraints.

The 4,4',4"-Trisubstituted-1,3,5-triphenyltriazine ligands

The cyclotrimerisation of p-toluonitrile (**4.24**) into 4,4',4"-trimethyl-1,3,5-triphenyltriazine (**4.25**) took several attempts. Triflic anhydride did not work as a catalyst,[276] even when the reaction was repeated under an inert atmosphere using dry

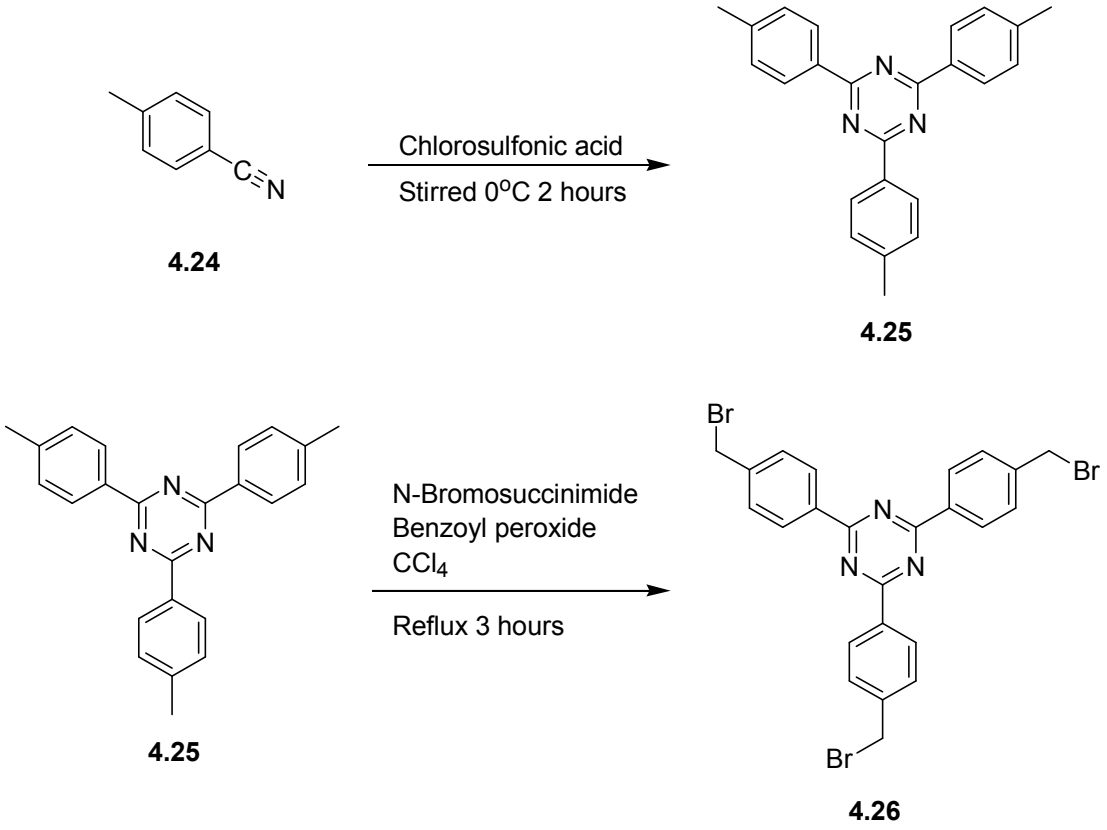

4.24 **4.25** **4.25** **4.26**

***Scheme 4.7** – Synthetic route to precursor **4.26**.*

solvent. However the reaction with chlorosulfonic acid[277,278] proceeded smoothly to give a 97% yield of the triazine product **4.25**, as shown in Scheme 4.7. This was brominated *via* the same procedure used to produce **4.8**, to obtain precursor **4.26** in 96% crude yield. The reaction produced a significant amount of tetrabrominated impurity that was not separated from the product before use in subsequent reactions.

4,4',4"-Tri(pyrazol-1-ylmethyl)-1,3,5-triphenyltriazine (4.27)

A phase-transfer-catalysed alkylation of pyrazole, shown in Scheme 4.8, provided incorporation of the pyrazoles to **4.26** over 68 hours and gave 4,4',4"-tri(pyrazol-1-ylmethyl)-1,3,5-triphenyltriazine (**4.27**) in low yield. Ligand **4.27** closely resembles ligand **4.9**, differing only in the nature of the central aromatic ring.

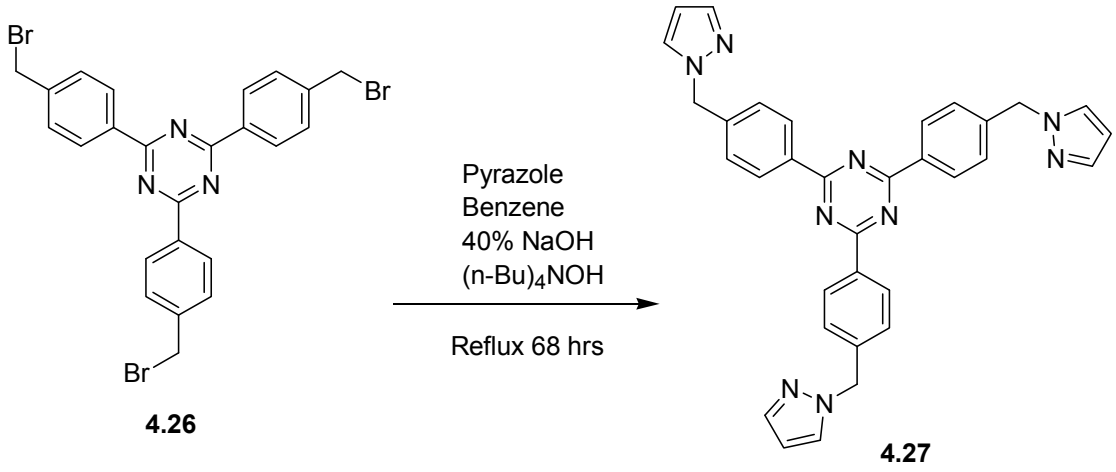

4.26 **4.27**

Scheme 4.8 *– Synthetic route to ligand **4.27**.*

Unintentionally a shortage of pyrazole was used in this reaction. However this was fortunate as it revealed information about the reaction. Two products were produced in this reaction in roughly equimolar amounts, ligand **4.27** and side-product **4.28**, pictured in Figure 4.15. The existence of product **4.28** shows that the mono-brominated arms react preferentially with pyrazole under these conditions. Separation of these two products was not attempted.

Ligand **4.27** is similar to two ligands in the literature, as shown in Figure 4.16. Ligand **4.29**[181] differs from **4.27** by the pyridine heterocycle in place of the pyrazole, with the

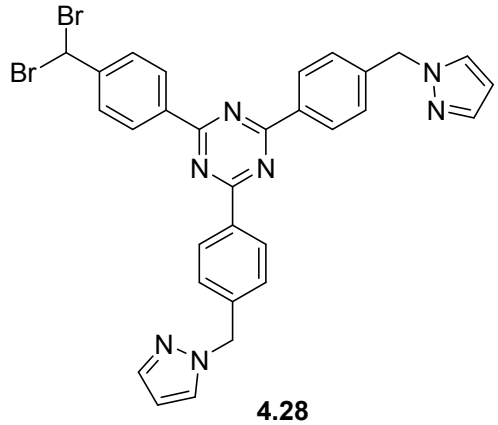

4.28

Figure 4.15 *– Side product produced alongside* ***4.27****.*

donor atom now pointing directly out from the ligand core. The flexibility of the methylene linker in **4.29** allows the ligand to form two interlocked M_3L_2 cages upon reaction with $Pd(en)(NO_3)_2$ and ligand **3.1**.[181] Ligand **4.30**[279-281] only differs from **4.27** by the position of the nitrogen donor atom in the heterocycle. Ligand **4.30** forms two-dimensional polymers upon reaction with $Pd(NO_3)_2$, $Zn(NO_3)_2$ or $NiSO_4$,[280,281] and one-dimensional polymers upon reaction with mercury(II) halide salts.[279]

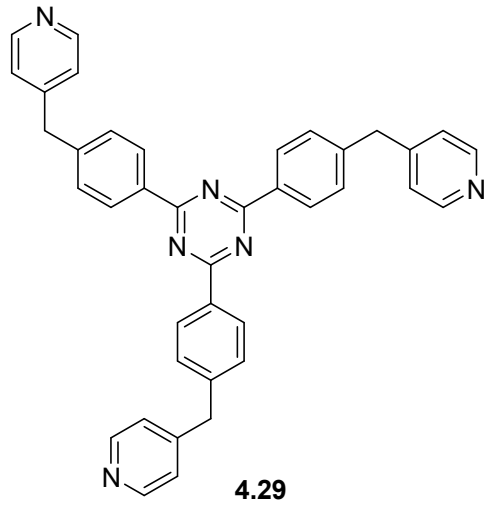

4.29

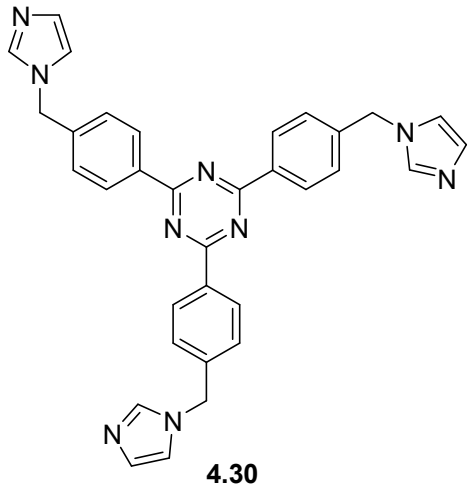

4.30

Figure 4.16 *– Similar ligands to* ***4.27****.*

Crystal structure of ligand ***4.27***

Slow evaporation of a dichloromethane solution of the mixture of **4.27** and **4.28** produced very small yellow crystals which, despite poor diffraction, proved to be suitable for X-ray crystallography. The structure solved in P-1 and was revealed to be ligand **4.27**.

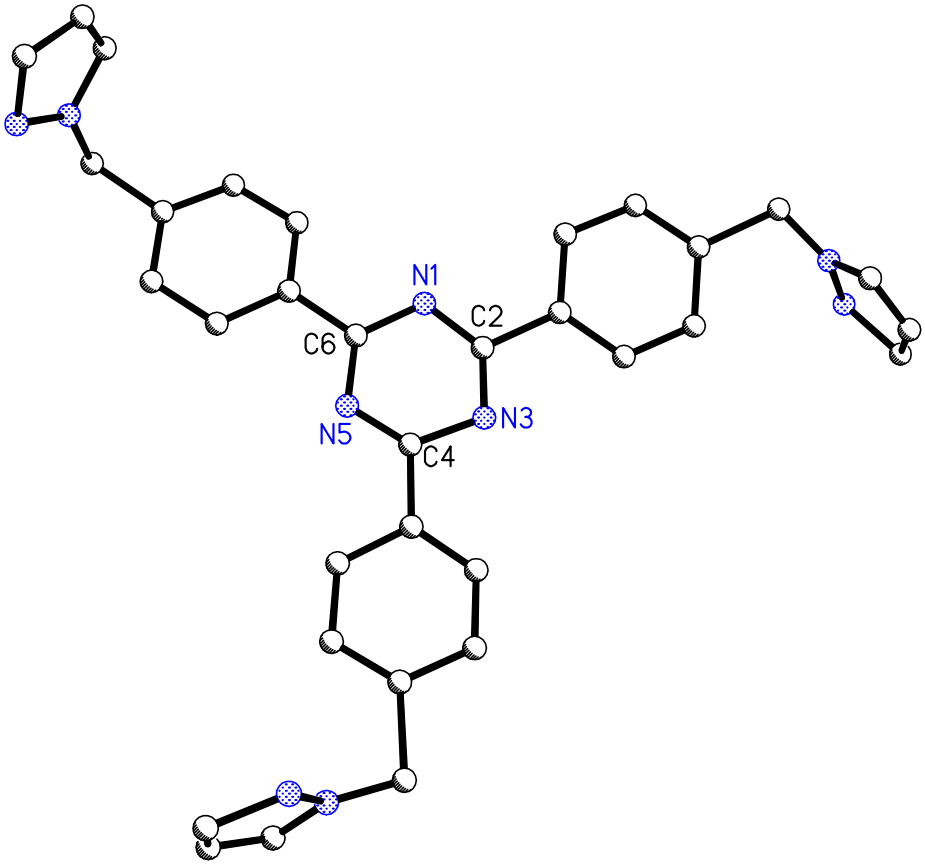

***Figure 4.17** – The structure of ligand **4.27**. Selected bond lengths (Å) and angles (°): N1-C2 1.32(1), N1-C6 1.36(1), N3-C2 1.33(1), N3-C4 1.40(1), N5-C4 1.31 (1), N5-C6 1.34(1), C2-N1-C6 114(1), C2-N3-C4 111(1), C4-N5-C6 117(1).*

A whole ligand lies in the asymmetric unit, as shown in Figure 4.17 with hydrogen atoms omitted for clarity. The array of aromatic rings in the core of the structure lie coplanar, with no steric interactions between aromatic hydrogens as in ligands based on **4.7**. Two pyrazole rings lie sideways in the plane of the ligand, while the third lies perpendicular to the ligand core, destroying the potential C_3 symmetry of the ligand. Of the two pyrazole rings lying sideways in similar orientations, one nitrogen points toward one face of the ligand while the other points towards the other face, presumably to minimise the dipole of the ligand. This also disrupts any potential internal symmetry of the ligand.

The ligands are π-π stacked in layers (3.416Å) through the triazine cores, with edge-face π stacking between pyrazole rings and phenyl rings (3.412Å), and hydrogen bonding interactions between pyrazoles (3.375Å C-N).

It was decided not to investigate the coordination chemistry of **4.27** as it is so similar to ligand **4.9**. It is also possible that metal salts may induce ring-opening reactions on the triazine which is not a possibility in **4.9**.

4,4',4"-Tri[3-(2'-pyridyl)pyrazol-1-ylmethyl]-1,3,5-triphenyltriazine (4.31)

Like ligand **4.13**, 4,4',4"-tri[3-(2'-pyridyl)pyrazol-1-ylmethyl]-1,3,5-triphenyltriazine (**4.29**) was synthesised by a phase-transfer-catalysed alkylation, as shown in Scheme 4.9. The addition of the 3-(2'-pyridyl)pyrazole units to **4.26** over three days gave **4.31** in 80% yield.

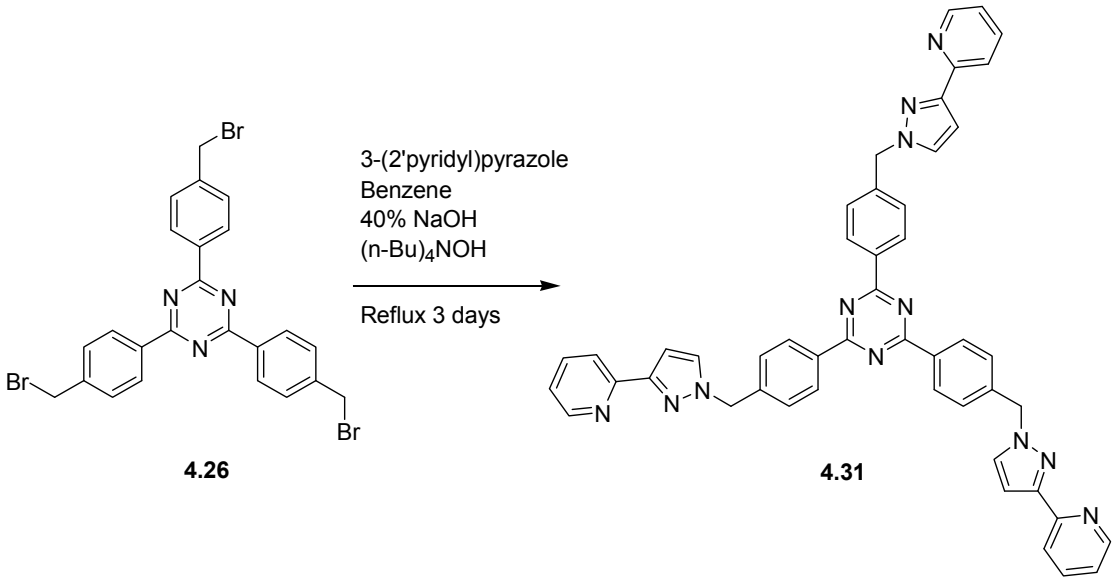

Scheme 4.9 *– The synthesis route to ligand **4.31**.*

Ligand **4.31**, the triazine analogue of **4.13**, was prepared to investigate if it could form an analogous complex to **4.15**. Unfortunately the solubility of **4.31** is different to that of **4.13**, and the same procedure that produced **4.15** only yielded an instant precipitate. As **4.13** was shown to decompose in the presence of $CuSO_4$ in different solvent systems (discussed in Chapter Five), alternative solvent mixtures were not attempted.

The tri(4-substituted-phenyl)methanol ligands

All of the ligands discussed so far from this research have been based on aromatic cores. Aromatic cores are useful for providing a junction that evenly spaces three ligand arms from the central core. Another way to achieve this is to use a single atom of appropriate geometry as the ligand core to provide a suitable junction to tether ligand arms to. The tetrahedral geometry of carbon can allow this, because if only three arms are substituted to the central carbon atom a tripodal ligand can be created. The fourth substituent on the carbon can be a hydrogen, methyl, hydroxyl or other group. Ligands based on carbon atom cores have been shown to act as components of coordination cages, such as those shown in Figure 4.18.[56,282]

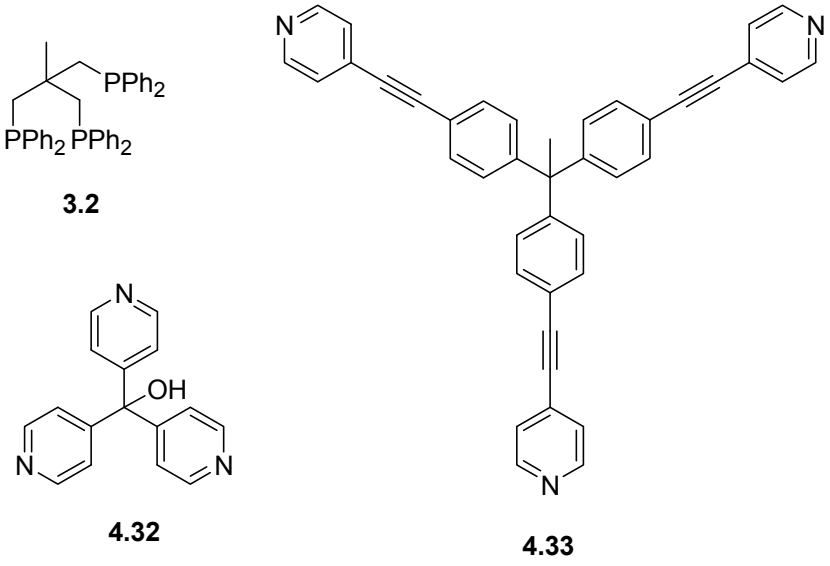

Figure 4.18 *– Examples of ligands based on single carbon atom cores capable of forming molecular cages upon reaction with appropriate metal salts.*

Precursor **4.36** was prepared by known methods,[265] as shown in Scheme 4.10. p-Bromotoluene was turned into a Grignard reagent with magnesium. Ethyl p-toluate (**4.34**) was added to the Grignard in benzene and stirred at room temperature overnight before the reaction was quenched with ice and H_2SO_4 to give a 91% yield of **4.35**. This was subsequently brominated to give precursor **4.36** in 99% yield. This product also contains a small amount of $CHBr_2$ arms as the bromination reaction is not totally selective.

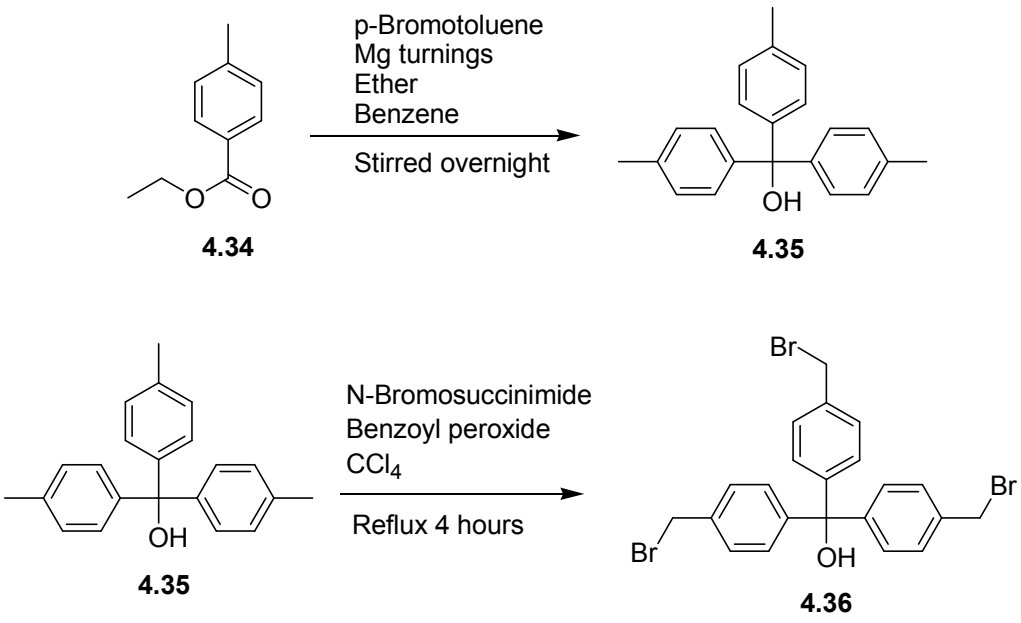

Scheme 4.10 *– Synthetic route to precursor* ***4.36****.*

Precursor **4.36** consists of a carbon atom core with a hydroxyl group substituent to terminate the ancillary position. Three phenyl groups are tethered to the remaining substitution sites around the carbon, extending towards the same face of the core to create a tripodal structure. A methylene linker adds flexibility to the terminating groups, bromine atoms in **4.36**. These bromine atoms can be substituted for donor groups to create a family of ligands that will act as exciting synthons in metallosupramolecular chemistry.

Tri(4-pyrazol-1-ylmethylphenyl)methanol (4.37)

A phase-transfer-catalysed alkylation of pyrazole reaction, shown in Scheme 4.11, provided addition of the pyrazoles to **4.36** over three days to give tri(pyrazol-1-ylmethylphenyl)methanol (**4.37**) in 94% yield. The product was produced cleanly without need for further purification.

As ligand **4.37** has three pyrazole groups extending towards the same side of the ligand core, it seems an ideal candidate to act as a component of a coordination cage. Few ligands in the literature resemble this family of ligands as the triphenylmethanol cores have not yet been utilised by many researchers in this area. No literature compounds are similar enough to **4.37** to mention here.

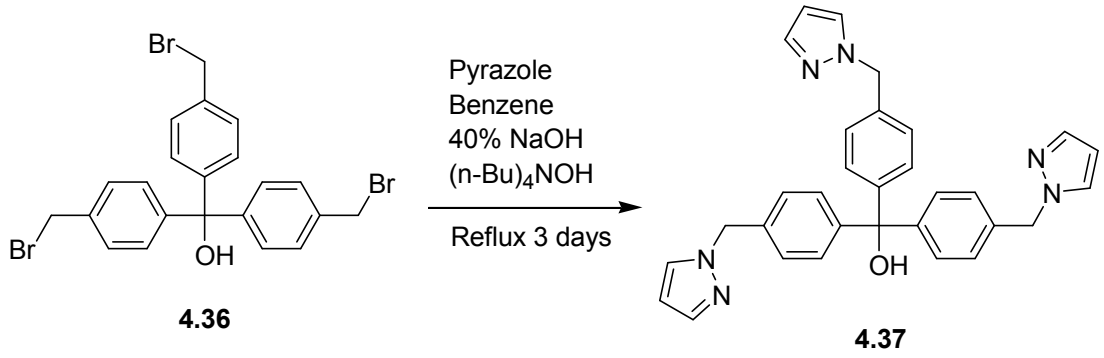

4.36 **4.37**

Scheme 4.11 *– Synthetic route to ligand* ***4.37****.*

Complexes with ligand 4.37

Regrettably, no complexes involving ligand **4.37** could be fully characterised. Complexation was attempted with a variety of metal salts, namely $AgNO_3$, $AgClO_4$, $AgCF_3SO_3$, CuI, $CuBF_4$, $CuCl_2$, $Cu(NO_3)_2$, $CuSO_4$, $Cu(ClO_4)_2$, $CoBr_2$, $ZnBr_2$, $PdCl_2$, K_2PdCl_4, $Pd(PhCN)_2Cl_2$ and $Pd(en)Cl_2$. Unfortunately no suitable single crystals of complexes containing ligand **4.37** could be grown. Many of the complexes synthesised were not analysed further.

Reaction of **4.37** with cobalt(II) bromide gave a complex which was shown by elemental analysis to have a 1:1 metal to ligand stoichiometry. This is ambiguous and could suggest a coordination polymer or possibly a discrete structure such as a M_2L_2 dimer.

Reaction of ligand **4.37** with $Pd(PhCN)_2Cl_2$ produced a product shown to have a M_3L_2 stoichiometry. Given the geometry of the components, it is possible this product is a molecular cage. However despite repeated attempts, the product could not be crystallised to confirm this.

Tri[4-(3-[2'-pyridyl]pyrazol-1-ylmethyl)phenyl]methanol (4.38)

The addition of the 3-(2'-pyridyl)pyrazole units to **4.36** by a phase-transfer-catalysed alkylation reaction over three days gave tri[4-(3-[2'-pyridyl]pyrazol-1-

ylmethyl)phenyl]methanol (**4.38)** in 80% yield, as shown in Scheme 4.12. This product was produced cleanly without need for further purification.

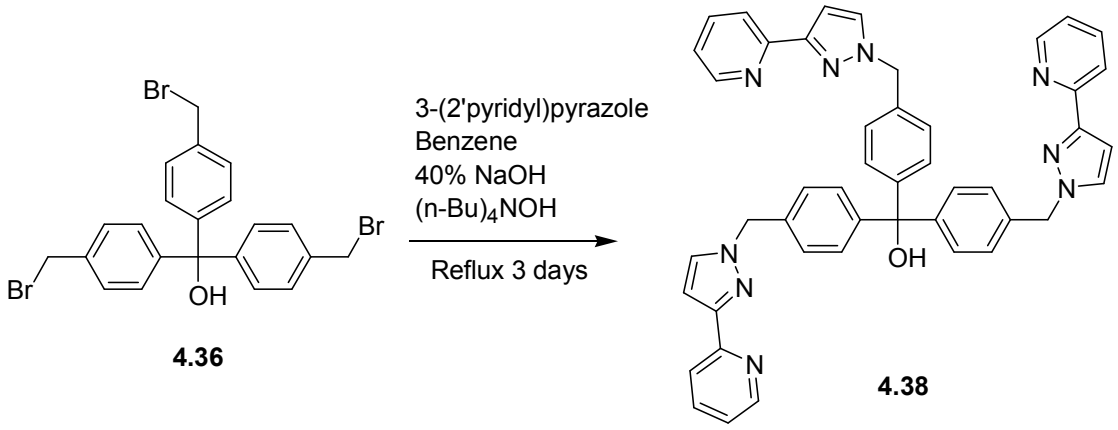

Scheme 4.12 *– The synthetic route to* ***4.38****.*

Ligand **4.38** resembles **4.37**, but with a pyridine ring attached to create a bidentate binding domain on each arm, which will hopefully snare metal ions more effectively than the pyrazole rings in **4.37**. Two ligands in the literature distantly resemble **4.38**, and are shown in Figure 4.19. Ligand **4.39**[283] is much smaller, with the binding arms attached directly to the central carbon. Ligand **4.39** forms a 1:1 complex with $Cu(PF_6)_2$,[283] where two binding arms bond to the metal atom while the third lies pendant.

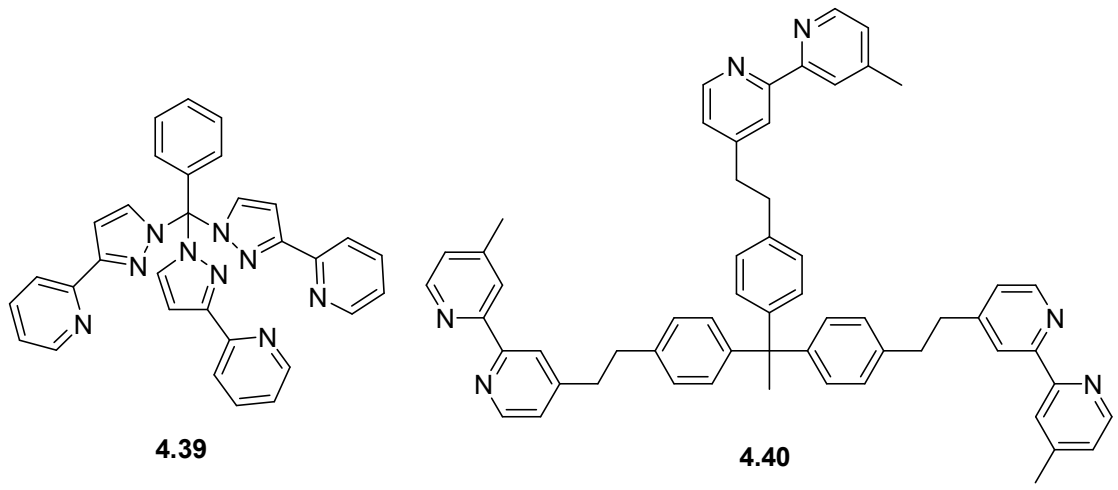

Figure 4.19 *– Similar ligands to* ***4.38****.*

Ligand **4.40**[284] is based on a similar core to **4.38**, with bipyridine bidentate binding domains linked to the ligand core by longer flexible linkers. Ligand **4.40** has been shown to form a 1:1 complex with Ru(II), where all three arms wrap around a single

metal atom to form a hemicage.[284] Ligand **4.38** is designed such that the binding arms should be separated enough to tend to bind to separate metal atoms to create metallosupramolecular structures rather than bind a single metal atom.

Complexes with ligand 4.38

Complexation of ligand **4.38** was attempted with a variety of metal salts, namely $AgClO_4$, $AgCF_3SO_3$, CuI, $CuBF_4$, $CuCl_2$, $Cu(NO_3)_2$, $CuSO_4$, $Cu(ClO_4)_2$, $CoCl_2$, $CoBr_2$, $Co(BF_4)_2$, $Ni(ClO_4)_2$, $FeSO_4$, $Fe(SCN)_2$, $Fe(ClO_4)_2$, $ZnBr_2$, K_2PdCl_4 and $Pd(PhCN)_2Cl_2$. Regrettably, despite many recrystallisation attempts, crystals suitable for X-ray crystallography could not be obtained of any complexes of **4.38**. Most of the complexes were not analysed further.

Reaction of **4.38** with $Co(BF_4)_2$ gave a pink precipitate which has a 1:1 metal to ligand stoichiometry. This ratio is ambiguous and could suggest either a polymer or a discrete complex. Reaction of ligand **4.38** with either $FeSO_4$ or $CuCl_2$ gives solids which were shown to have M_2L stoichiometry. Again this ratio could suggest either a polymeric or discrete structure.

When ligand **4.38** was mixed with $CoBr_2$, a pink precipitate was produced which was shown to have a M_3L_2 stoichiometry. Given the nature of the components, it is possible this ratio may suggest a coordination cage. Unfortunately suitable crystals could not be grown for definitive characterisation of this complex.

Tri[4-(4-pyridylsulfanylmethyl)phenyl]methanol (4.41)

As shown in Scheme 4.20, tri[4-(4-pyridylsulfanylmethyl)phenyl]methanol (**4.41**) was synthesised by a base-catalysed substitution reaction over 22 hours to give **4.41** in 81% yield. Like ligand **4.16**, a small amount of side product of reaction with a $CHBr_2$ impurity in **4.36** is observed (**4.42**). These products were not separated. Ligand **4.41** displays very low solubility in common solvents, being only slightly soluble in DMSO.

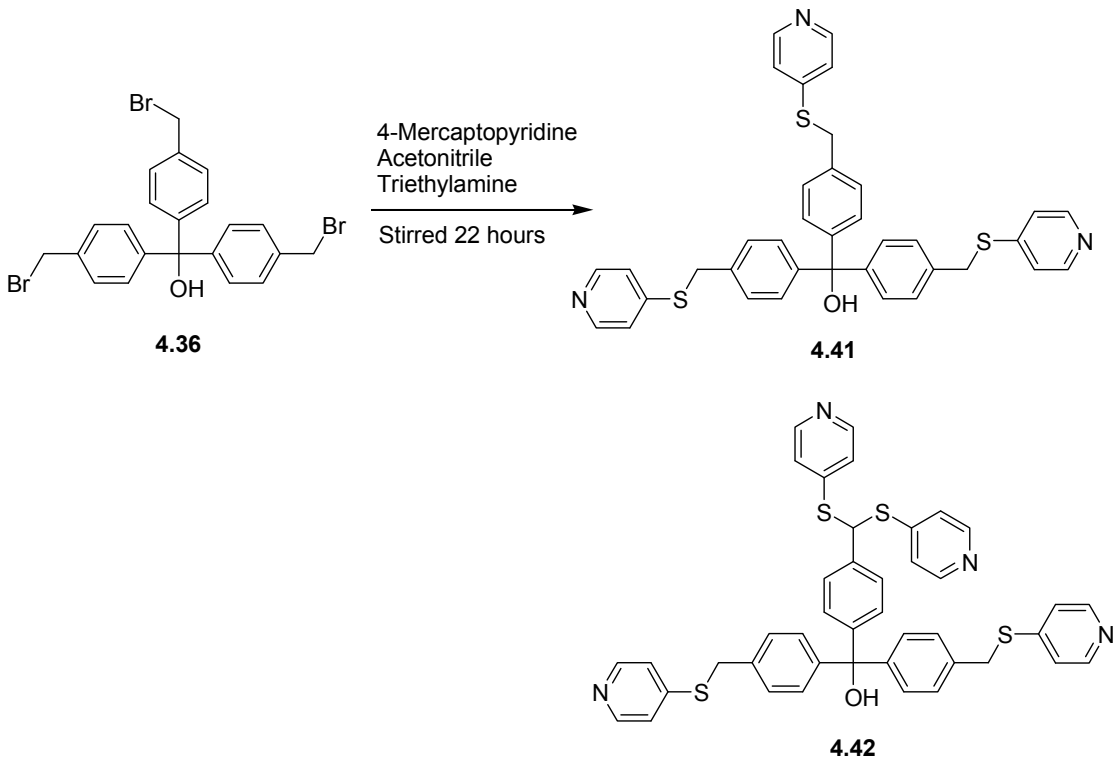

Figure 4.20 *– Synthesis of ligand* ***4.41*** *and side-product* ***4.42****.*

Complexation of **4.41** was attempted with a few different metal salts in various solvent combinations, but the insolubility of the ligand severely hindered complex formation. No products were analysed as complexation did not appear to occur.

Tri[4-(8-quinolyloxymethyl)phenyl]methanol (4.43)

The procedure used to synthesise tri[4-(8-quinolyloxymethyl)phenyl]methanol (**4.43**) is shown in Scheme 4.13, and produced **4.43** in 75% yield after six hours of reaction.

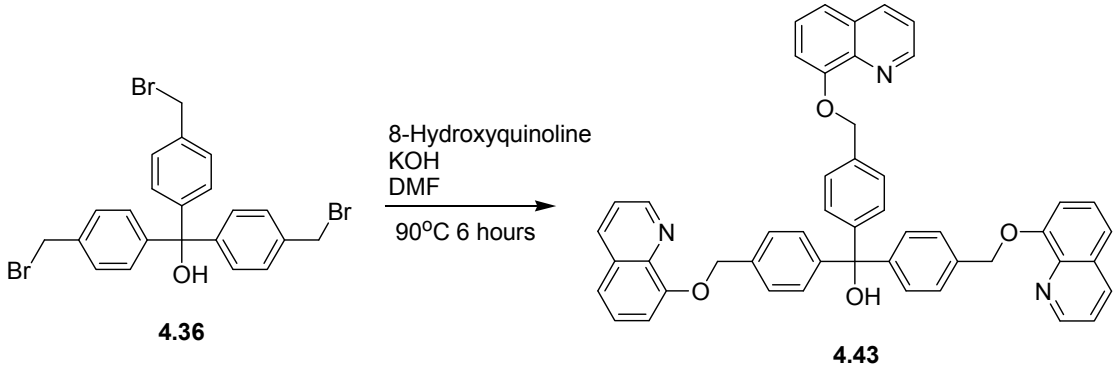

Scheme 4.13 *– The synthesis of* ***4.43****.*

Complexes with ligand 4.43

Complexation of **4.43** was attempted with a variety of metal salts, namely $AgClO_4$, $AgCF_3SO_3$, CuI, $CuBF_4$, $CoCl_2$ and $CoBr_2$. No crystals suitable for X-ray crystallography could be grown which contained ligand **4.43**. Most of these complexes were not analysed further.

Reaction of ligand **4.43** with copper(I) iodide produced a pale brown powder which was shown to have a M_2L stoichiometry. As the metal salt has a tendency to dimerise into Cu_2I_2 squares, this is likely to be an effective 1:1 stoichiometry. This is ambiguous and could suggest a discrete or polymeric structure.

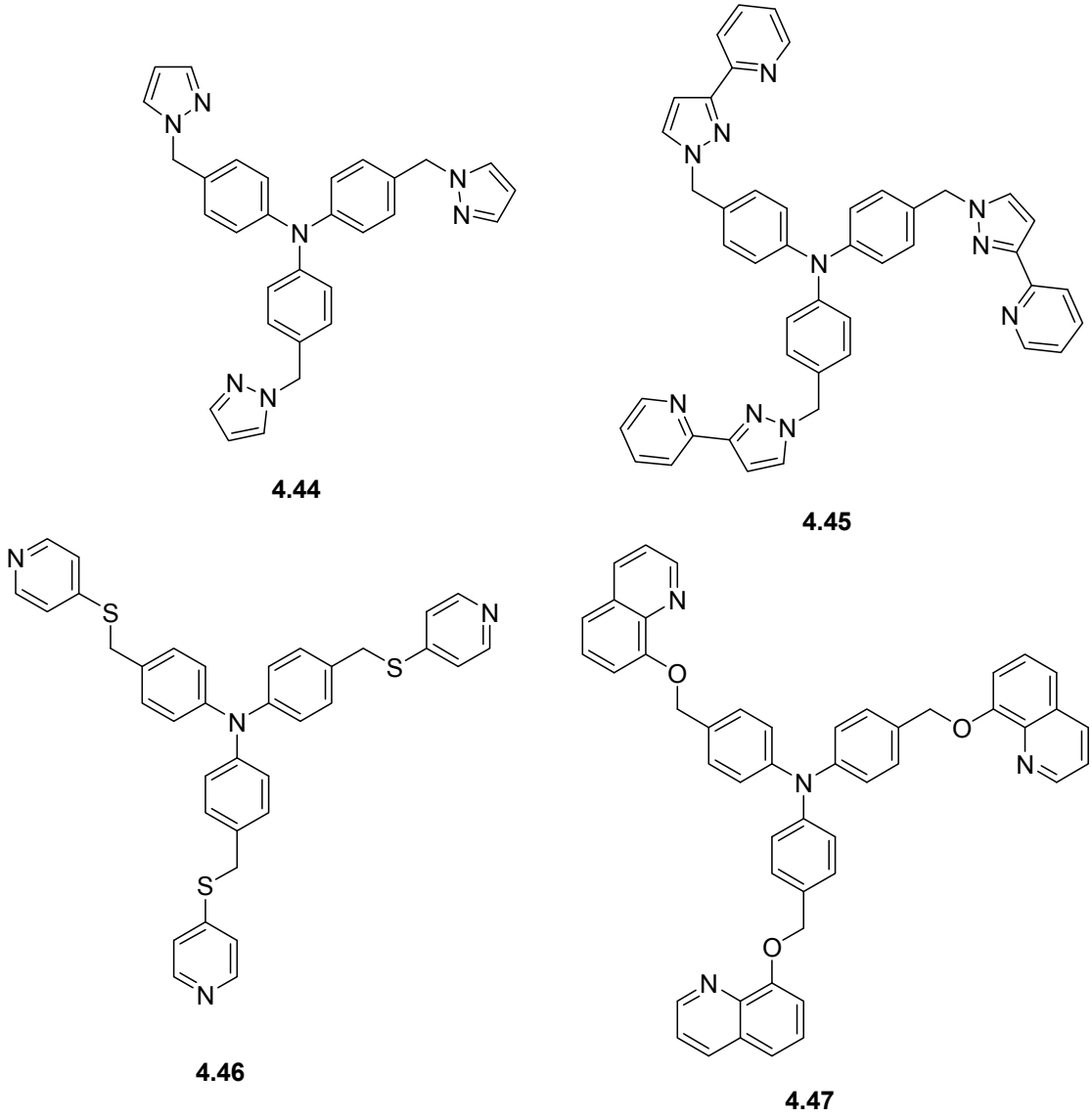

Figure 4.21 *– Proposed ligands based on a triphenylamine core.*

Attempted syntheses of the tri(4-substituted-phenyl)amine ligands

Another attractive atom to use as a ligand core is nitrogen. Not only would an amine core for a three-armed ligand act as a three connector node and planar constituent under normal conditions, but may be able to be protonated to alter the orientation of the ligand arms and create a tripodal ligand. Therefore a family of ligands were designed based on an amine core, as shown in Figure 4.21.

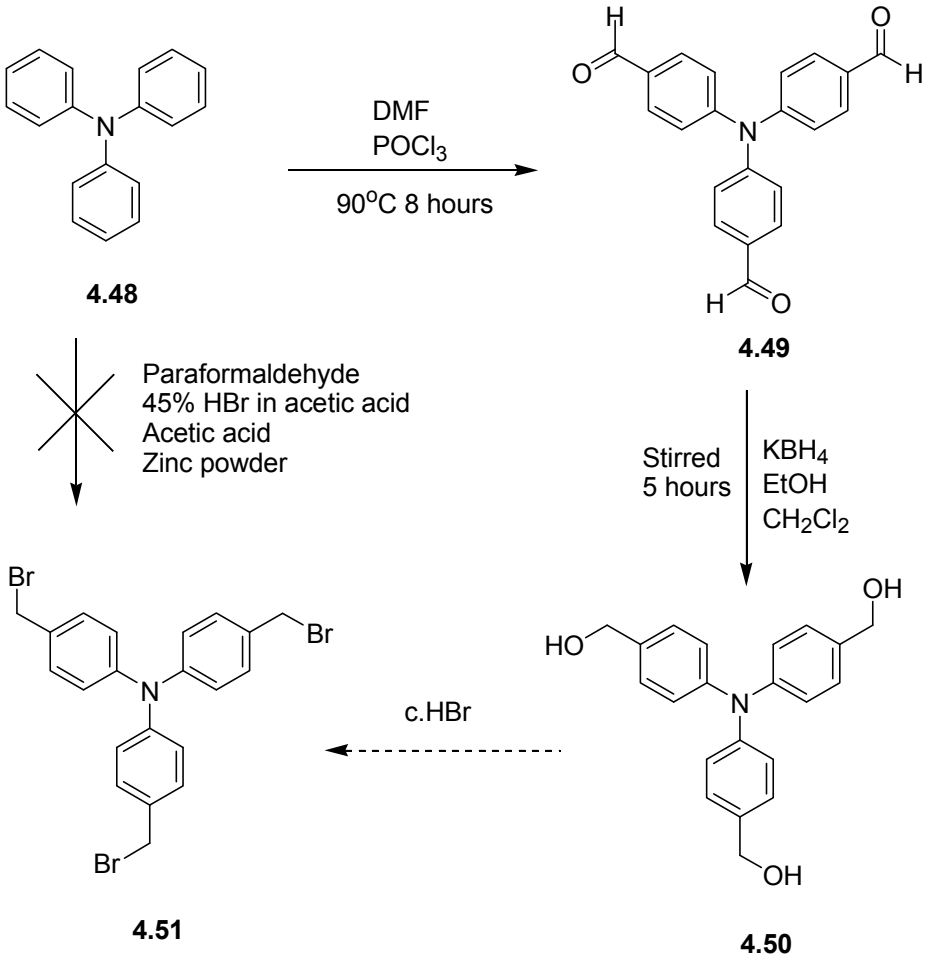

Scheme 4.14 *– Proposed synthetic route to precursor* ***4.51****.*

To create a family of ligands based on triphenylamine (**4.44**, **4.45**, **4.46** and **4.47**), first tri(4-bromomethylphenyl)amine (**4.51**)[285] must be synthesised. Initially a direct route straight from triphenylamine (**4.48**) was investigated, and when this proved unsuccessful the literature route was followed,[285] as shown in Scheme 4.14. The reaction to synthesise **4.49**[285,286] proceeds in two steps, firstly to create the dialdehyde, and then this is converted to the trialdehyde (**4.49**) by repeating the same procedure.[286] This reaction is sensitive and took several attempts to achieve. The subsequent

reduction to the alcohol (**4.50**)[285] proceeded smoothly. However the final step to **4.51** was not as successful as anticipated. O. Mongin and co-workers report an 85% yield of **4.51** after five hours of refluxing in concentrated HBr.[285] However **4.50** was very insoluble in aqueous solution so only trace amounts of very impure **4.51** was obtained from this method. The reaction was repeated, dissolving **4.50** in acetic acid first, and using 33% HBr in acetic acid as the bromination agent. Unfortunately a large amount of insoluble green solid was obtained. Elemental analysis suggests this is the protonated salt of **4.51**, but it is too insoluble for further analysis or subsequent reaction.

Summary

This chapter looked at C_3 symmetric ligands synthesised during this research which are based on a large variety of ligand cores. Despite the fascinating ligands prepared, unfortunately only a few crystal structures of complexes of these ligands could be obtained, so the coordination chemistry of these new ligands is still largely unknown.

Ligands **4.9**, **4.13** and **4.16** are based on a 1,3,5-triphenylbenzene core. Ligand **4.9** was shown to form a two-dimensional coordination polymer upon reaction with $AgClO_4$. The synthesis of ligand **4.16** was hindered by $CHBr_2$ impurities in precursor **4.8**, and briefly an alternative route to these ligands was investigated to try to eliminate this.

Ligand **4.13** was shown to assemble into a large M_6L_4 complex upon reaction with $CuSO_4$. This compound is a collapsed coordination cage. Structure **4.15** was the pinnacle of this research, showing that flexible ligands may not be the most desirable components of a coordination cage as they may allow compression of the central cavity of the cage. Experiments to crystallise **4.15** encapsulating a guest molecule were unsuccessful, so it is unknown if **4.15** could untwist and uptake guest molecules into a central cavity in solution.

Ligands **4.27** and **4.31** were prepared from 1,3,5-triphenyltriazine cores. The crystal structure of ligand **4.27** shows that, unlike **4.9** and **4.13**, the central aromatic rings lie coplanar.

Ligands **4.37**, **4.38**, **4.41** and **4.43** were prepared from triphenylmethanol cores. Unfortunately, no complexes could be characterised of any of these new ligands.

A new family of ligands were designed based on triphenylamine cores, but unfortunately the last step in the synthesis of precursor **4.51** produced an insoluble compound that could not be used in further reactions.

Chapter Five

Complexes of 3-(2’-pyridyl)pyrazole: from decomposition and direct synthesis

Chapter Five

Complexes of 3-(2'-pyridyl)pyrazole: from decomposition and direct synthesis

Introduction

3-(2'-Pyridyl)pyrazole (**5.1**) was first synthesised by Tisler and co-workers in 1980.[287] The attachment of a pyridine ring to a pyrazole ring in this manner creates a ligand with multiple nitrogen donors capable of coordinating to metal atoms. Both the protonated (**5.1**) and deprotonated (**5.2**) forms of 3-(2'-pyridyl)pyrazole are shown in Figure 5.1.

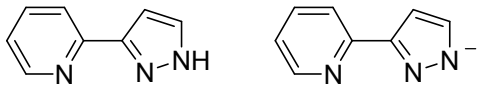

5.1 **5.2**

Figure 5.1 *– 3-(2'-Pyridyl)pyrazole in both its protonated (**5.1**) and deprotonated (**5.2**) states. Only one tautomer and resonance structure are shown.*

This relatively simple ligand has been shown to display three coordination modes,[288,289] as shown in Figure 5.2. Until 1996 only coordination mode a) had been characterised,[288,290] where **5.1** is acting as a bidentate chelating ligand. Since then many complexes involving the deprotonated ligand **5.2** acting as a terdentate bridging ligand as in mode b) have been identified,[289-296] and even one case where **5.2** bridges two different metals,[297] as shown in mode c) in Figure 5.2. A search of *Scifinder Scholar* reveals that 109 complexes have been reported involving **5.1** and/or **5.2**.

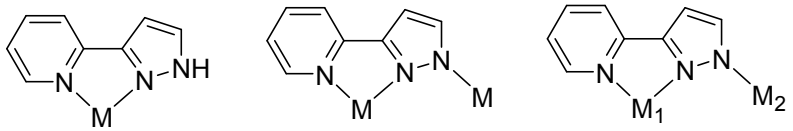

a) b) c)

Figure 5.2 *– The coordination modes of **5.1** and **5.2**.*

Substructure **5.2** is often incorporated into ligands *via* the deprotonated pyrazole nitrogen to add a bidentate binding domain. A huge variety of ligands incorporating **5.2**

have been designed, and some fascinating metallosupramolecular structures constructed from these ligands, such as molecular cages.[69,83,139,140,142,147,148] Shown in Figure 5.3 are the ligands synthesised during this research that incorporate units of **5.2.** Recently complexes involving a simple **5.2**-containing ligand have been shown to possess high cytotoxic activities against cancer cells.[298]

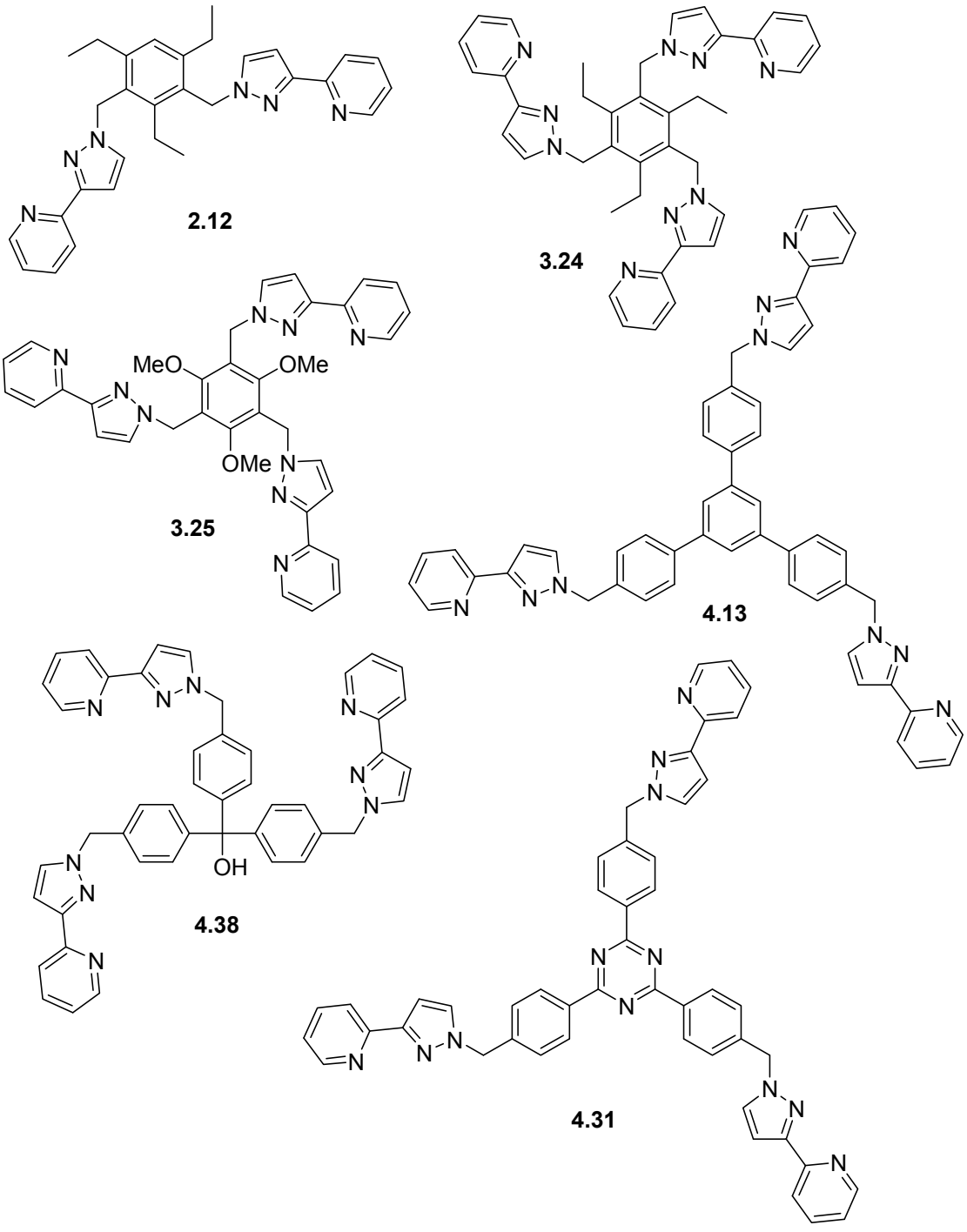

Figure 5.3 *– Ligands synthesised in this research incorporating* ***5.2*** *units.*

Ligand decomposition

Early in this research it was discovered that the numerous crystals resulting from reaction of ligand **3.24** with copper(II) nitrate did not contain **3.24**, but a dimeric complex containing **5.2**. The crystal structure of this complex (**5.3**), shown in Figure 5.4, has already been reported,[288] as this complex can also be synthesised directly by reaction of **5.1** with copper(II) nitrate in ethanol.[288] Two **5.2** ligands bridge two copper atoms, which are coordinatively saturated by nitrate counterions and water molecules. The presence of **5.3** in this reaction was surprising, as although **5.1** was used in the synthesis of ligand **3.24**, no impurity of **5.1** is seen in the ^{1}H NMR spectrum, mass spectrum, or elemental analysis of **3.24**. Therefore, it seems the most likely source of **5.2** from this reaction is from the decomposition of ligand **3.24**, through the breakage of a C-N bond, likely promoted by the metal salt.

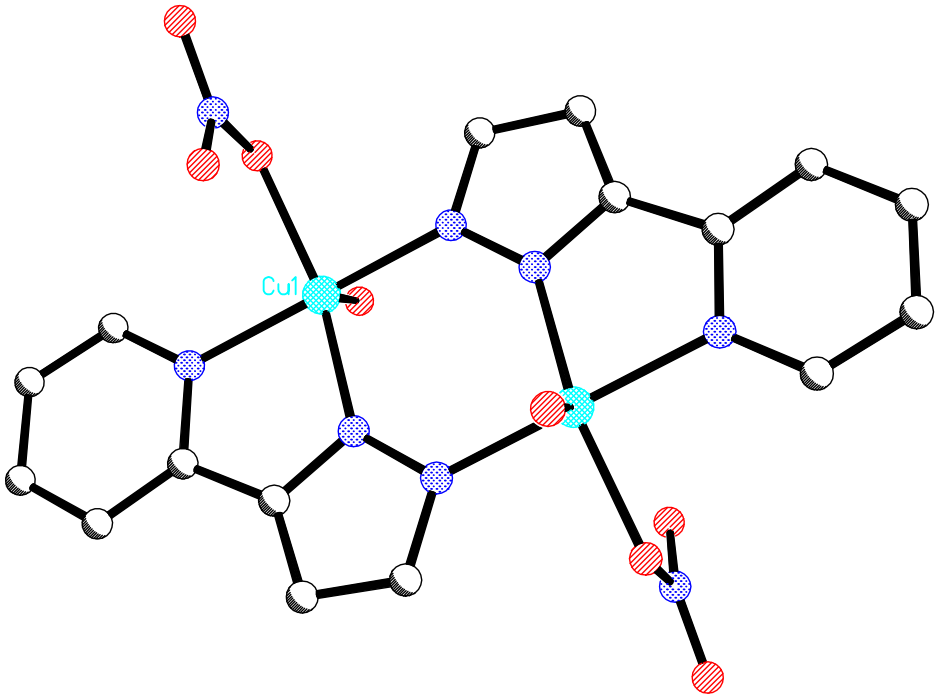

Figure 5.4 *– The decomposition product* ***5.3*** *resulting from reaction of ligand* ***3.24*** *with* $Cu(NO_3)_2$*. Hydrogen atoms are excluded for clarity.*

It soon became apparent that this was not an isolated case. Four examples have been identified in the literature where complexes based on **5.1** and/or **5.2** have originated from the decomposition of ligands incorporating **5.2**.

The first case was reported in 1997 where the reaction of sodium tris[{3-(2'-pyridyl)pyrazol-1-yl}hydroborate] with $FeSO_4$ in methanol caused N-B bond cleavage of the ligand to form an unusual tetranuclear Fe(III) complex $[Fe_4(\mathbf{5.2})_6(\mathbf{5.1})_2(\mu\text{-}O)_2]$.[290] It was noted that this complex could not be synthesised directly from **5.1**, and could only be obtained though decomposition of an intermediate iron(II) complex containing the original ligand.[290]

The next case was reported in 1998 from the decomposition of the same hydroborate ligand in the presence of $PdCl_2$ or $Pd(OAc)_2$ in methanol gave complexes $Pd(\mathbf{5.1})Cl_2$ and $Pd(\mathbf{5.2})_2$ respectively.[291] In the later complex, the deprotonated nitrogen does not coordinate to a metal centre, but forms an intramolecular hydrogen bond.[291]

In 2000 another case of ligand decomposition in the presence of $Pd(OAc)_2$ was reported, with the reaction of bis[3-(2'-pyridyl)pyrazol-1-ylmethyl]biphenyl in methanol.[295] The resulting complex consists of a $[Pd(\mathbf{5.2})]_2$ unit similar to **5.3**, with the free coordination sites on the metal atom occupied by monodentate coordination to the original ligand.[295] While **5.2** makes three coordinative bonds to the metal atoms, the bidentate binding sites on the original ligand is no longer chelated. The authors speculate that the decomposition process and subsequent self assembly is driven by the high thermodynamic preference of Pd(II) for a square planar geometry, which could not be obtained solely with the original ligand.[295] NMR and mass spectrometric data showed that the crystallised complex was only one of many decomposition products.[295]

A more recent paper reported the crystal structure of a copper(I) complex of 1-benzyl-[3-(2'-pyridyl)pyrazole].[296] The crystals were removed from an acetonitrile solution and dissolved in DMF, from which dark blue crystals were obtained from vapour diffusion of $MeCO_2Et$ into this solution.[296] The new complex is a decomposition product of the original complex consisting of a polymer of $[Cu(II)(\mathbf{5.2})]_2$ units, similar to **5.3**, bridged by acetate anions.[296] The authors claim that this debenzylation reaction is the first nonenzymic hydrolysis of an unactivated ester $MeCO_2Et$ by an isolated Cu(II)-

coordinated hydroxide ion. The authors also offer a possible mechanism for the decomposition process.[296]

Ligand	Metal salt	Primary solvent	Complex
3.24	$Cu(NO_3)_2$	Methanol	$[Cu(NO_3)(H_2O)(\mathbf{5.2})]_2$ (**5.3**)
3.24	$Cu(ClO_4)_2$	Acetonitrile	$[Cu(ClO_4)(MeCN)(\mathbf{5.2})]_2$ (**5.9**)
3.24	K_2PdCl_4	DMSO	$[(PdCl)(\mathbf{5.2})]_2$ (**5.8**)
4.13	$CuSO_4$	DMSO	$[Cu(DMSO)(\mathbf{5.2})]_2SO_4$ polymer (**5.14**)
4.13	$CuSO_4$	DMF	$[Cu(\mathbf{5.2})]_2SO_4$ polymer (**5.15**)
4.13	$CuCl_2$	DMSO	$[(CuCl)(\mathbf{5.2})]_2$ polymer (**5.12**)

Table 5.1 *– A summary of the conditions which produced decomposition complexes with ligands containing* ***5.2*** *in this research.*

A summary table of the decomposition products obtained in this research is shown in Table 5.1. Included in the table is the **5.2**-containing ligand which decomposed to yield **5.2**, the metal salt presumably responsible for this decomposition, and the primary solvent used during the reaction, as often mixtures of solvents were used.

As can be seen from the table, mainly copper(II) salts triggered ligand decomposition. The decomposition product **5.3** from reaction of $Cu(NO_3)_2$ and ligand **3.24** was crystallised on three different occasions, from different solvent mixtures, but methanol was the primary solvent each time. On one occasion, a few crystals of the M_4L_2 complex **3.30** (containing **3.24**) were removed from solution and characterised, and a week later darker crystals grew in the same solution that were shown to be decomposition product **5.3**. This could suggest that decomposition of the intermediate complex takes some time to occur.

Ligand **3.24** also decomposed in the presence of K_2PdCl_4 and $AgClO_4$. This is surprising as trinuclear complex **3.27** is formed from K_2PdCl_4 and also crystallises from DMSO. Ward and coworkers[295] suggest that the decomposition of their ligands occurs in the presence of Pd(II) to fulfill the geometrical requirements for the metal atom;[295] however in this case the crystal structure of **3.27** shows that the original ligand can provide an adequate binding geometry for the metal atom.

Similarly, ligand **4.13** has been shown to form a stable structure with $CuSO_4$ (**4.15**) when reacted in methanol, however any attempts to replicate this reaction in alternative

solvents such as DMF or DMSO result in ligand decomposition. Unfortunately this severely hindered efforts to locate an adequate solvent system that would allow solubilisation of all components and subsequent attempts to encapsulate a guest molecule inside complex **4.15**.

Out of all the ligands listed in Figure 5.3, it is unknown why decomposition complexes were only characterised from **3.24** and **4.13**. In all cases, the formation of crystals of the decomposition complexes appeared in solution after long periods of time, usually months. Using DMSO as a solvent appeared to increase the chances that a decomposition complex would be obtained. It is plausible that the decomposition process occurs via a substitution reaction. The coordination of the metal salt would make **5.2** a better leaving group, and encourage a nucleophile such as water to attack the methylene carbon. Therefore it seems likely that the other product of this decomposition would be the alcohol, however this was not confirmed.

Complexes with ligand 5.1 and 5.2

A range of complexes were obtained with **5.2** unintentionally through decomposition of larger ligands. From these complexes it was noticed that the dimeric unit $[M(\mathbf{5.2})]_2$ was a component of many different structures, and could be an interesting synthon in metallosupramolecular chemistry. Therefore the coordination chemistry of **5.1** with a variety of metal salts was studied deliberately, to learn more about this rather interesting ligand. In this section, all complexes involving **5.1** and/or **5.2** will be discussed, regardless of how the complexes were synthesised. The protonated form (**5.1**) was used in all reactions where these complexes were synthesised deliberately, and no base was added to remove the proton to form **5.2**.

*Crystal structure of **5.1** with $CoBr_2$ (**5.4**)*

When solutions of ligand **5.1** and $CoBr_2$ in acetone were combined, a solid precipitates, redissolves, and then large purple crystals grow. These crystals were suitable for X-ray crystallography. The structure solves in triclinic space group P-1.

The asymmetric unit is shown in Figure 5.5, with hydrogen atoms, the disorder of the bromine atoms, and solvate acetone and water molecules excluded for clarity. Two **5.1**

ligands each chelate to the cobalt atom, which is coordinatively saturated by two bromide counterions. The ligands are coordinated in such a way to allow the protons on the pyrazole nitrogens to point towards the bromine atoms.

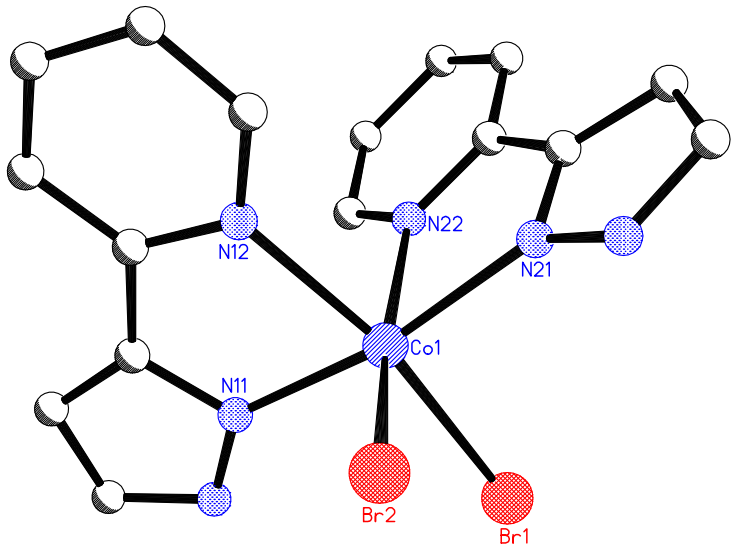

Figure 5.5 *– The asymmetric unit of* ***5.4****. Selected bond lengths (Å) and angles (°): Co1-N11 2.075(7), Co1-N21 2.081(7), Co1-N12 2.179(7), Co1-N22 2.202(7), Co1-Br1 2.599(1), Co1-Br2 2.599(2), N11-Co1-N21 168.9(3), N11-Co1-N12 76.1(3), N11-Co1-N22 94.6(3), N11-Co1-Br1 89.8(2), N11-Co1-Br2 98.3(2), N21-Co1-N12 97.0(3), N21-Co1-N22 75.9(3), N21-Co1-Br1 96.2(2), N21-Co1-Br2 90.35(2), N12-Co1-N22 84.22(3), N12-Co1-Br1 165.4(2), N12-Co1-Br2 90.3(2), N22-Co1-Br1 93.0(2), N22-Co1-Br2 164.4(2), Br1-Co1-Br2 95.86(5).*

The complex packs in the crystal with π-π stacking interactions between the ligands (3.349Å) and short contacts between the bromine atoms and ligand hydrogens.

Crystal structure of ***5.1*** *with* $La(NO_3)_3$ *(****5.5****)*

Slow evaporation of a methanol solution of $La(NO_3)_3$ and **5.1** gave large colourless blocks suitable for X-ray crystallography. The structure solved in monoclinic space group $P2_1/n$.

The discrete structure is shown in Figure 5.6, with hydrogens and a solvate methanol molecule excluded for clarity. Two **5.1** ligands are chelated to the metal atom, along with three chelated nitrate anions and a methanol oxygen, making the lanthanum

eleven-coordinate. The nitrates are bound on one side of the metal atom, while the **5.1** ligands are bound to the other side.

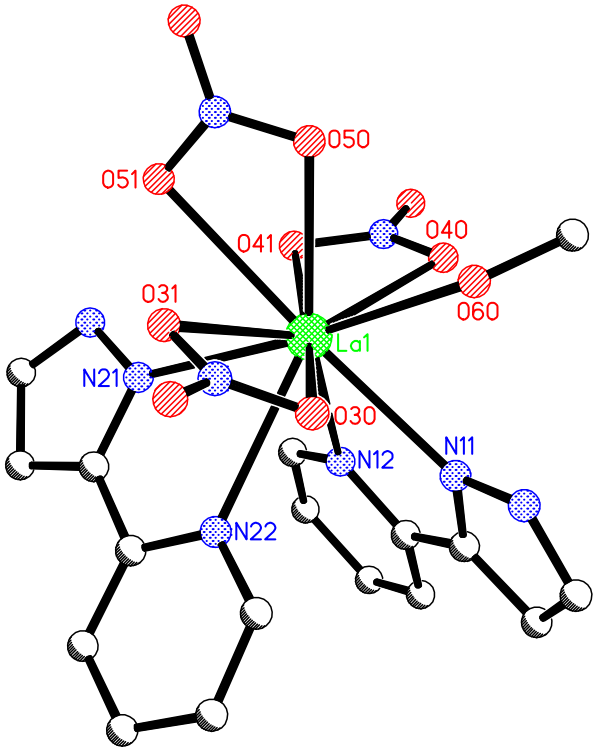

Figure 5.6 *– The asymmetric unit of* ***5.5****. Selected bond lengths (Å) and angles (°): La1-O50 2.580(2), La1-O41 2.596(2), La1-O40 2.608(2), La1-O60 2.614(2), La1-N11 2.615(2), La1-N21 2.655(3), La1-O31 2.660(2), La1-O30 2.710(2), La1-N22 2.796(3), La1-O51 2.820(2), La1-N12 2.822(2), O50-La1-O41 78.48(7), O50-La1-N21 109.70(7), O50-La1-O30 92.30(7), O41-La1-O60 115.49(7), O41-La1-N21 68.24(7), O40-La1-N11 114.60(7), O40-La1-N12 71.70(7), O60-La1-N22 120.46(7), N21-La1-N12 69.48(7), N21-La1-O51 62.89(7), N11-La1-N12 59.67(7), N11-La1-N21 119.99(8), O41-La1-N1 114.92(7), O50-La1-N11 130.09(7), O40-La1-N21 114.60(7).*

The complexes are aligned in channels, with short contacts between nitrate oxygens and hydrogens on **5.1**. There are no π-π stacking interactions between **5.1** rings in adjacent complexes.

Crystal structure of ***5.1*** *with* $ZnBr_2$ *(****5.6****)*

Vapour diffusion of ether into a methanolic solution of ligand **5.1** and zinc bromide grew two large colourless crystals suitable for X-ray crystallography. In retrospect, the

crystal mounted onto the fibre was too large and may have moved during the data collection. This resulted in a poor absorption correction and poor refinement, and subsequently large peaks are present in the difference map that can not be explained. The R_1 value was 16.7%, consistent with the value expected from such poor data. However the complex is identified unambiguously. The structure solved in monoclinic space group $P2_1/n$.

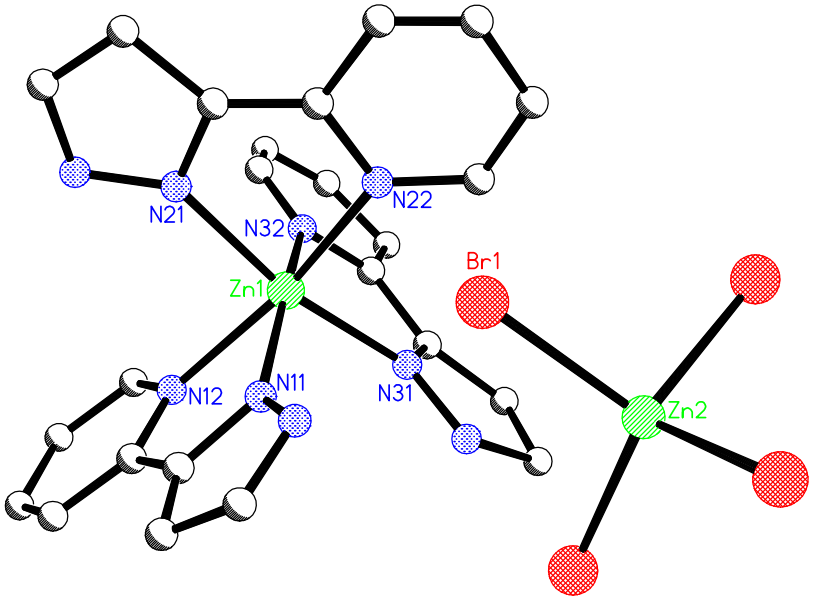

Figure 5.7 *– Trishomoleptic complex* ***5.6*** *with counterion. Selected bond lengths (Å) and angles (°): Zn1-N11 2.09(1), Zn1-N21 2.10(2), Zn1-N31 2.12(2), Zn1-N32 2.16(2), Zn1-N22 2.19(1), Zn1-N12 2.22(1), N11-Zn1-N21 93.9(6), N11-Zn1-N31 95.2(6), N11-Zn1-N32 163.5(5), N11-Zn1-N22 94.8(5), N11-Zn1-N12 75.9(5), N21-Zn1-N31 168.4(6), N21-Zn1-N32 96.1(7), N21-Zn1-N22 77.1(7), N21-Zn1-N12 91.7(6), N31-Zn1-N32 76.8(7), N31-Zn1-N22 95.0(6), N31-Zn1-N12 97.4(5), N32-Zn1-N22 100.2(5), N32-Zn1-N12 90.7(5), N22-Zn1-N12 165.0(5).*

The asymmetric unit is shown in Figure 5.7, with hydrogen atoms and solvate methanol molecule excluded for clarity. Three **5.1** ligands saturate one zinc atom to create a cation, while the other zinc coordinates four bromine atoms to create a $ZnBr_4^{2-}$ anion to balance the charge. The three **5.1** ligands are meridonally bound to the metal atom, and the crystal is a racemic mixture of delta and lambda isomers.

The cations are aligned in stacks, separated by stacks of anions. There are short contacts between the bromine atoms and hydrogen atoms on the ligands. There are no π-π stacking interactions between adjacent complexes.

As the solution evaporated to dryness, more crystals were obtained that were suitable for X-ray crystallography. One of these was analysed in the hope it would provide a better dataset of structure **5.6**. Surprisingly, the cell constants were different and the new structure solved in monoclinic space group C2/c. Unfortunately, despite the better data collection, this new complex is disordered in such a way that is inconsistent with the space group it solves in. A two-fold rotation axis runs through each complex, and correspondingly through the **5.1** ligands, so that ligand **5.1** is generated as two connected pyrazole rings, instead of a pyrazole and pyridine ring. Therefore, no pictures of this complex will be shown. This problem has been encountered in complexes of this type before, however references are difficult to find as the structures are rarely published.

The complex is similar to **5.6**, but contains two half cations in the asymmetric unit, plus one uncoordinated bromide counterion. This suggests that some of the coordinated **5.1** ligands have been deprotonated.

*Crystal structure of **5.1** with $CuCl_2$ (**5.7**)*

A solution of ligand **5.1** in methanol was added to a methanol solution of copper(II) chloride and combined with a solution of cobalt(II) chloride. Slow evaporation of this solution produced large green block-like crystals which were suitable for X-ray crystallography. The geometry of the metal atom in the crystal structure shows unambiguously that copper is the only metal atom present in these crystals. The structure solved in triclinic space group P-1.

The discrete structure is shown in Figure 5.8, with hydrogen atoms excluded for clarity, and consists of two **5.1** ligands, two copper atoms and four chloride counterions. Half the complex is present in the asymmetric unit. The copper atom coordinates to one chelating **5.1** ligand, and three chlorine atoms in a square pyramidal geometry. The two copper atoms are bridged by two chlorine atoms to form a square-like unit. Each bridging chlorine is bonded more strongly to one metal atom than the other, with

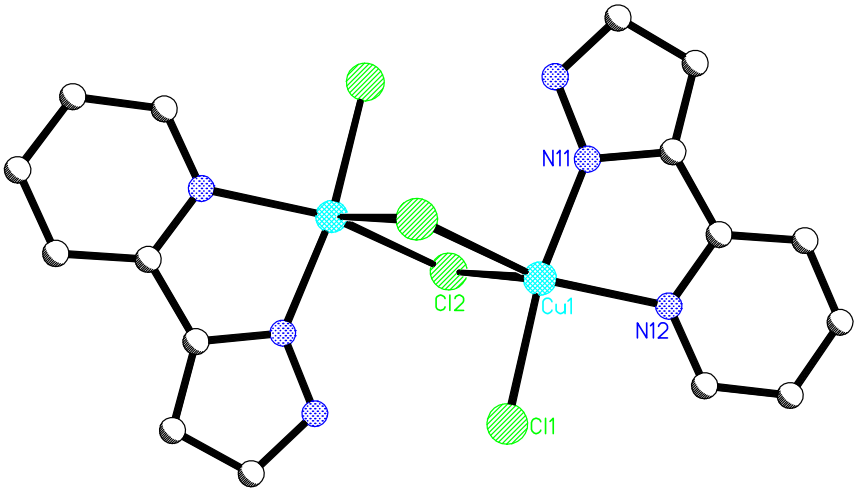

Figure 5.8 *– The discrete structure of complex* ***5.7****. Selected bond lengths (Å) and angles (°): Cu1-N11 1.975(3), Cu1-N12 2.067(2), Cu1-Cl1 2.2421(7), Cu1-Cl2A 2.3316(7), Cu1-Cl2 2.6433(7), N11-Cu1-N12 78.5(1), N11-Cu1-Cl1 170.98(8), N11-Cu1-Cl2A 91.56(8), N11-Cu1-Cl2 91.78(7), N12-Cu1-Cl1 93.36(7), N12-Cu1-Cl2A 158.10(7), N12-Cu1-Cl2 109.12(7), Cl1-Cu1-Cl2A 94.79(3), Cl1-Cu1-Cl2 94.57(3), Cl2-Cu1-Cl2A 90.45 (2).*

distances of 2.332Å and 2.643Å to the copper atoms. The longer distance still represents a bonding interaction to the copper atom as it makes a definite contribution to the geometry of the metal atom. The terminal chlorine atoms do not bridge, but do display short contacts to pyrazole hydrogens. The complexes are π-π stacked in layers (3.418Å)

Crystal structure of ***5.1*** *with* $CdCl_2$ *(****5.8****)*

Thin needle-like crystals were obtained by cooling a hot methanolic solution of ligand **5.1** and cadmium chloride. A week later these crystals had recrystallised into clusters of colourless block-like crystals which were suitable for X-ray crystallography. The structure solved in triclinic space group P-1.

A section of the one-dimensional polymer is shown in Figure **5.9**, with hydrogen atoms and the disorder of the ligands excluded for clarity. The asymmetric unit contains two cadmium atoms, four chloride counterions, and two **5.1** ligands. The structure is very similar to discrete complex **5.7**, except in this case the same motif extends into a

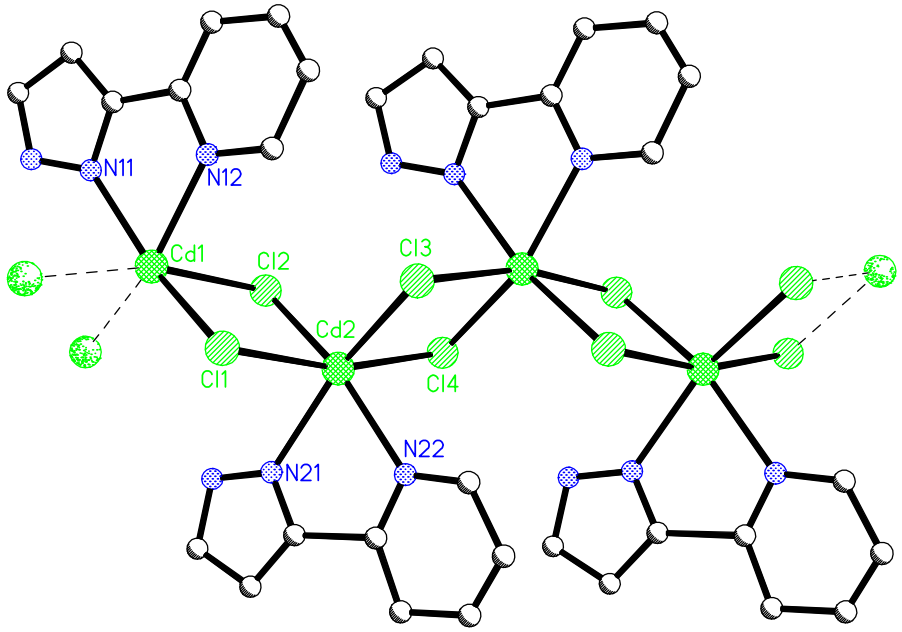

Figure 5.9 *– A section of the polymeric chain of* ***5.8****. Selected bond lengths (Å) and angles (°): Cd1-N12 2.33(2), Cd1-N11 2.35(2), Cd1-Cl1 2.6134(7), Cd1-Cl2 2.6682(8), Cd1-Cl3A 2.6691(7), Cd1-Cl4A 2.6147(6), Cd2-N21 2.40(2), Cd2-N22 2.36(1), Cd2-Cl3 2.6126(6), Cd2-Cl2 2.6131(7), Cd2-Cl4 2.6676(7), Cd2-Cl1 2.6688(7), N12-Cd1-N11 69.7(5), N12-Cd1-Cl1 95.3(4), N12-Cd1-Cl4A 154.6(5), N12-Cd1-Cl2 86.9(4), N12-Cd1-Cl3A 105.5(4), N11-Cd1-Cl1 89.7(4), N11-Cd1-Cl4 157.7(5), N11-Cd1-Cl2 82.4(4), N11-Cd1-Cl3 109.2(4).*

polymeric structure. Interestingly, the ligands can sit facing either of the two possible directions (rotated 180° from each other), so each coordination site is occupied by a pyrazole half of the time, and by a pyridine the other half. This disorder is not shown in Figure **5.9**. Each cadmium atom binds one chelating ligand and four chlorine atoms with an octahedral geometry and each chlorine symmetrically bridges two metal atoms. The cadmium and chlorine atoms make up the backbone of the polymer, forming square-like units which rotate each translation to form a zigzag undulation. The **5.1** ligands serve only to saturate the metal atoms, and do not contribute to the dimensionality of the complex, with no π-π stacking interactions between adjacent chains.

Crystal structure of ***5.2*** *with* K_2PdCl_4 *(****5.9****)*

DMSO solutions of ligand **3.24**, potassium tetrachloropalladate and silver hexafluorophosphate were combined, and the resulting AgCl precipitate was filtered

off. Vapour diffusion of chloroform into the filtrate produced small yellow block-like crystals after five to six months. These crystals were suitable for X-ray crystallography and were shown to be ligand decomposition complex **5.9**. The structure solved in monoclinic space group C2/c.

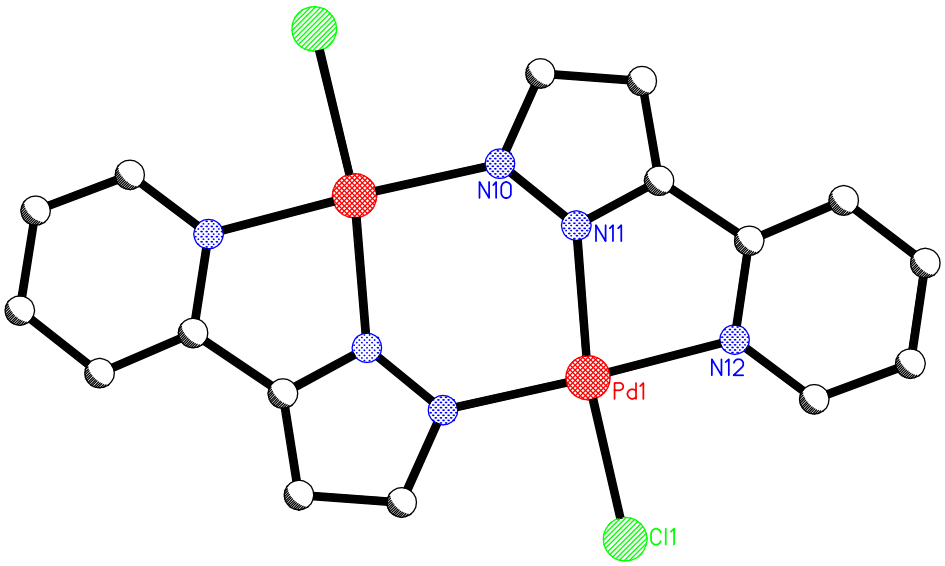

Figure 5.10 *– Dimeric structure* ***5.9****. Selected bond lengths (Å) and angles (°): Pd1-N10A 2.016(9), Pd1-N12 2.050(9), Pd1-N11 2.071(8), Pd1-Cl1 2.299(3), N10A-Pd1-N12 176.8(4), N10A-Pd1-N11 98.0(3), N10A-Pd1-Cl1 90.8(3), N12-Pd1-N11 79.8(3), N12-Pd1-Cl1 91.5(3), N11-Pd1-Cl1 170.6(2).*

Complex **5.9** consists of a discrete dimeric unit containing two **5.2** ligands, two palladium atoms, and two chloride counterions, as shown in Figure 5.10, with hydrogen atoms excluded for clarity. The asymmetric unit contains half of the complex. At first it seemed surprising that chloride anions were still present in the solution, before it was realised that insufficient silver hexafluorophosphate was used, as it was the potassium tetrachloropalladate salt that was used. One chloride per palladium would have still been present in solution, consistent with the complex obtained. Ligand **5.2** acts as a terdentate ligand, chelating to one palladium atom and bridging to the other. Each palladium atom bonds to three ligand nitrogens and one chloride anion. The complex is flat, fulfilling the square planar geometry desired by the metal atom. Like complex **5.3**, this dimeric unit is likely to be very stable, as so many coordinative bonds are formed.

Two five-membered chelate rings are formed, and a six-membered ring containing two metal atoms.

The complexes are packed in a herringbone arrangement, with π-π stacking interactions between pyrazole rings of adjacent complexes (3.319Å).

*Crystal structure of **5.2** with $Cu(ClO_4)_2$ (**5.10**)*

The product of reaction of ligand **3.24** with copper(II) perchlorate was recrystallised by vapour diffusion of ether into an acetonitrile solution. Two types of crystalline material was obtained, dark green opaque crystals and light green rectangular blocks. The later were suitable for X-ray crystallography and were shown to be ligand decomposition complex **5.10**. The structure solved in monoclinic space group $P2_1/c$.

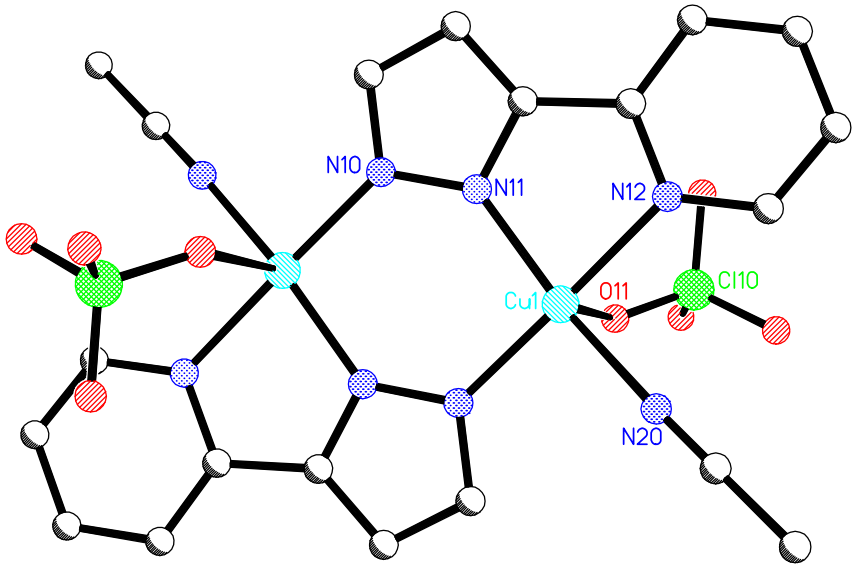

***Figure 5.11** – The dimeric structure of **5.10**. Selected bond lengths (Å) and angles (°): Cu1-N11 1.964(2), Cu1-N10A 1.967(2), Cu1-N20 2.015(3), Cu1-N12 2.054(2), Cu1-O11 2.368(2), N11-Cu1-N10A 97.23(9), N11-Cu1-N20 162.8(1), N11-Cu1-N12 81.54(9), N11-Cu1-O11 99.9(1), N10A-Cu1-N20 91.1(1), N10A-Cu1-N12 178.70(9), N10A-Cu1-O11 93.39(9), N20-Cu1-N12 89.94(9), N20-Cu1-O11 94.6(1), N12-Cu1-O11 87.25(8).*

The structure contains the same dimeric motif seen in complexes **5.3** and **5.9**, as shown in Figure 5.11, with hydrogen atoms excluded for clarity. Two **5.2** ligands bridge two copper atoms, acting as terdentate donors. The copper atoms are saturated with a

perchlorate counterion and an acetonitrile molecule, bonding to four nitrogens equatorially and an oxygen apically with a square pyramidal geometry. Like **5.3** and **5.9**, this structure is also discrete.

The complexes are aligned in a herringbone arrangement through the crystal, with short interactions between perchlorate oxygens and hydrogen atoms on the ligands. There are also π-π stacking interactions between **5.2** rings (3.333Å).

*Crystal structure with **5.2** and $Ni(OAc)_2$ (**5.11**)*

Slow evaporation of a solution containing ligand **5.1** and nickel acetate over three months produced a few blue crystals that were suitable for X-ray crystallography. The structure solved in orthorhombic space group $Pna2_1$.

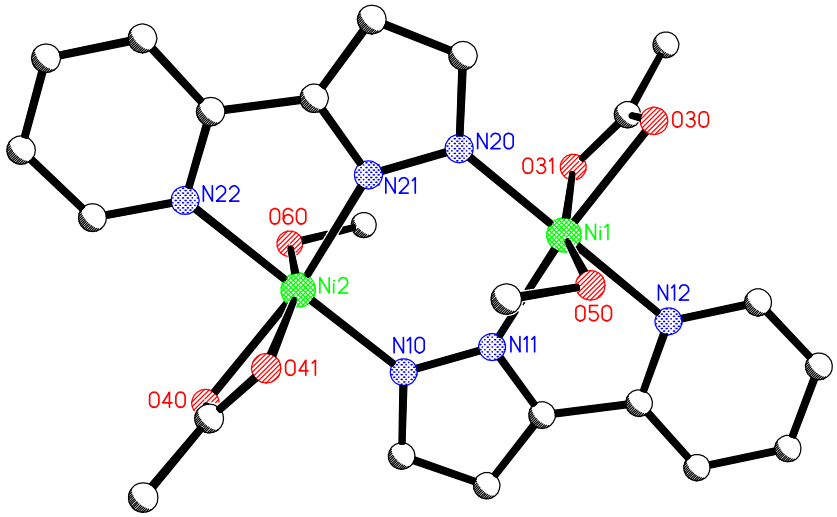

***Figure 5.12** – The dimeric structure of complex **5.11**. Selected bond lengths (Å) and angles (°): Ni1-N11 2.016(2), Ni1-N20 2.023(2), Ni1-N12 2.097(2), Ni1-O50 2.105(2), Ni1-O30 2.110(2), Ni1-O31 2.159(2), Ni2-N21 2.018(2), Ni2-N10 2.026(2), Ni2-O60 2.088(2), Ni2-N22 2.105(3), Ni2-O40 2.121(2), Ni2-O41 2.159(2), N11-Ni1-N20 100.30(9), N11-Ni1-N12 79.60(9), N11-Ni1-O50 91.51(8), N11-Ni1-O30 162.78(8), N11-Ni1-O31 103.97(8), N11-Ni1-O31 103.97(8), N20-Ni1-N12 179.9(1), N20-Ni1-O50 92.67(9), N20-Ni1-O30 89.80(8), N20-Ni1-O31 90.71(9), N12-Ni1-O50 87.27(9), N12-Ni1-O30 90.32(8), N12-Ni1-O31 89.37(9), O50-Ni1-O30 102.00(7), O50-Ni1-O31 163.29(7), O30-Ni1-O31 61.64(7).*

The discrete dimeric structure of **5.11** is shown in Figure 5.12. Hydrogen atoms and the positional disorder surrounding the nickel atoms are excluded for clarity. The whole

molecule lies in the asymmetric unit. Even though there appears to be a centre of inversion in the molecule, this is not recognised crystallographically. The structure consists of two **5.2** ligands, two metal atoms and acetate counterions, and two coordinated methanol molecules. The same dimeric motif where **5.2** is acting as a terdentate ligand and bridging two metal centres to form a planar unit is seen once again. Each nickel atom has a slightly distorted octahedral geometry and binds two **5.2** ligands (one of which chelates), a chelating acetate counterion, and the oxygen of a methanol.

The complexes are packed in a herringbone arrangement, with face-edge π stacking interactions between the ligands in adjacent complexes (3.362Å).

*Crystal structure of **5.2** with $CuCl_2$ (**5.12**)*

A green precipitate was produced from reaction of ligand **4.13** with copper(II) chloride in acetone in the presence of potential guest molecule **4.35**. DMSO was added to the solution to dissolve the precipitate. Slow evaporation of this solution produced clusters of dark green needles suitable for X-ray crystallography. The unit cell had an unusually short axis of 3.774Å. The complex was shown to be ligand decomposition product **5.12**. The complex solved in monoclinic space group $P2_1/c$.

A section of the one-dimensional polymer **5.12** is shown in Figure 5.13, with hydrogen atoms excluded for clarity. The asymmetric unit contains one **5.2** ligand, one copper atom and one chlorine atom. The complex consists of planar dimeric motifs linked into a chain by bridging chlorine atoms. As seen previously, two **5.2** ligands bridge two copper atoms to form a planar dimeric unit. The copper atoms coordinate to three ligand nitrogens and two chlorine atoms with a square pyramidal geometry. Each chlorine atom bridges two copper atoms, but like complex **5.7**, the atoms bond more strongly to one metal atom than the other, with distances of 2.322Å and 2.670Å. The later distance is long for a Cu(II)-Cl bond, but contributes to the coordination sphere of the copper atom as the equatorial copper atom is distorted from the plane away from what would be a square planar geometry. Two chlorine atoms bridge each dimer unit, so that the polymer resembles a ladder, with the dimeric units representing the rungs. The dimeric units are π-π stacked (3.413Å).

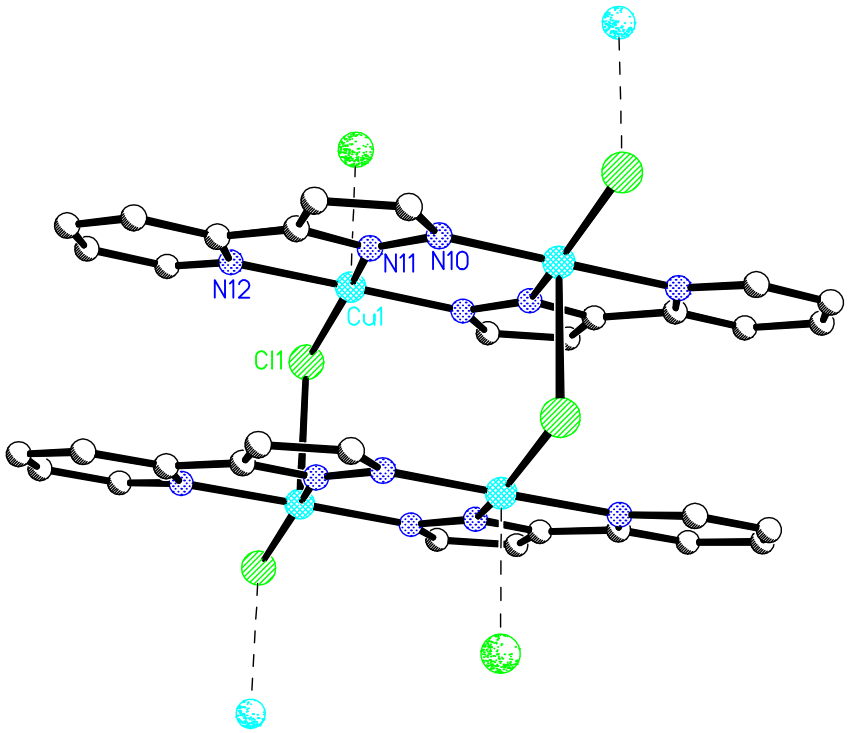

Figure 5.13 *– A section of the one-dimensional polymeric chain* ***5.12****. Selected bond lengths (Å) and angles (°): Cu1-N10A 1.961(2), Cu1-N11 1.994(2), Cu1-N12 2.054(2), Cu1-Cl1 2.3216(6), Cu1-Cl1A 2.6701(7), N10A-Cu1-N11 96.66(7), N10A-Cu1-N12 177.06(7), N10A-Cu1-Cl1 92.32(5), N10A-Cu1-Cl1A 92.54(5), N11-Cu1-N12 80.68(7), N11-Cu1-Cl1 159.25(5), N11-Cu1-Cl1A 100.24(5), N12-Cu1-Cl1 89.81(5), N12-Cu1-Cl1A 89.17(5), Cl1-Cu1-Cl1A 98.00(2).*

Crystal structures of ***5.2*** *with* $CuSO_4$ *(****5.13****,* ***5.14*** *and* ***5.15****)*

In an attempt to incorporate two different bridging ligands into a complex, ligand **5.1** and 4,4'-bipyridine were each dissolved in methanol and combined, and added to a methanolic solution of copper(II) sulfate to give a blue precipitate. Over a period of ten days this precipitate crystallised into large blue diamond-shaped crystals which were suitable for X-ray crystallography. The structure solved in triclinic space group P-1.

The discrete dimeric structure is shown in Figure 5.14, with hydrogen atoms and solvate water molecules excluded for clarity. The asymmetric unit contains half of this material. Although present in the crystal lattice, the 4,4'-bipyridine has not coordinated to the metal atom, instead it is doubly protonated and acts as a cation to balance the charge of

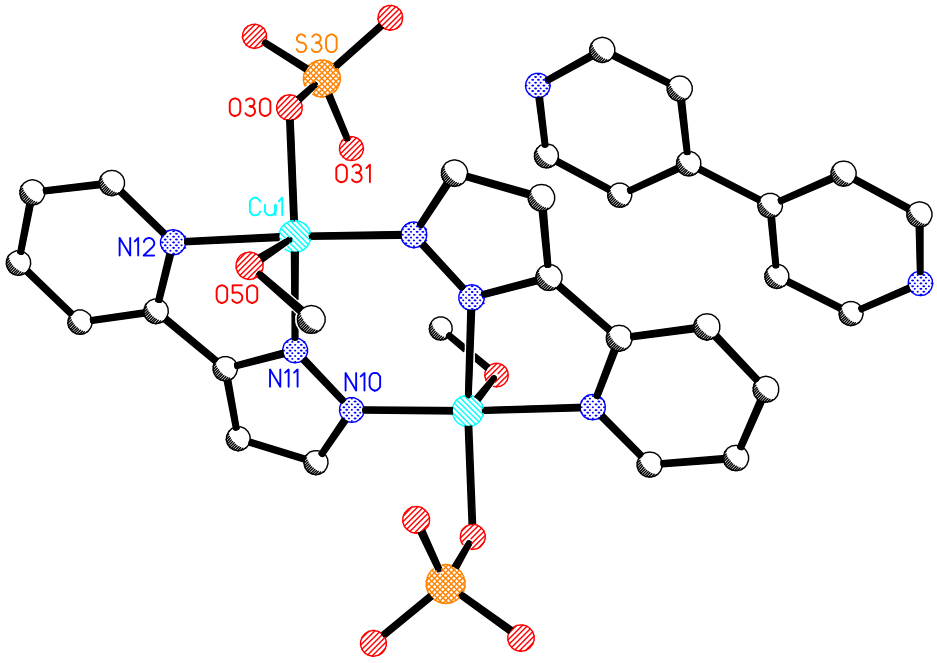

Figure 5.14 *– The discrete structure of complex* ***5.13****, shown with bipyridine cation. Selected bond lengths (Å) and angles (°): Cu1-N10A 1.947(2), Cu1-N11 1.980(2), Cu1-O30 2.015(2), Cu1-N12 2.019(3), Cu1-O50 2.388(2), N10A-Cu1-N11 98.1(1), N10A-Cu1-O30 91.69(9), N10A-Cu1-N12 177.08(9), N10A-Cu1-O50 86.88(8), N11-Cu1-O30 156.11(9), N11-Cu1-N12 80.9(1), N11-Cu1-O50 101.38(8), O30-Cu1-N12 90.27(9), O30-Cu1-O50 100.87(7), N12-Cu1-O50 90.63(8).*

the complex and acts as a space filler for crystallisation. The complex consists of two **5.2** ligands bridging two copper atoms. The copper atoms are bonded to three ligand nitrogens, a sulfate oxygen and a methanol oxygen in a square pyramidal geometry, with an additional weak interaction to O31 of the sulfate (2.776Å).

Between the copper(II) atoms, the two **5.2** ligands and the two coordinated sulfate anions, the complex carries an overall double negative charge, which is counterbalanced by the doubly protonated 4,4'-bipyridine ligand.

There are short contacts between the sulfate oxygens and hydrogen atoms on the ligands. The 4,4'-bipyridine cation is π-π stacked with the adjacent complexes (3.242Å), and this π-π stacking propagates through the crystal as all the aromatic rings are aligned.

Ligand **4.13** and potential guest molecule **4.35** were dissolved in acetone and added to a hot methanol solution of copper(II) sulfate to give a green precipitate. The solution was divided into two portions. DMSO was added to one portion to dissolve the precipitate. Slow evaporation of this solution produced blue plate-like crystals which were suitable for X-ray crystallography. The structure was shown to be ligand decomposition complex **5.14**. The structure solved in monoclinic space group C2/c.

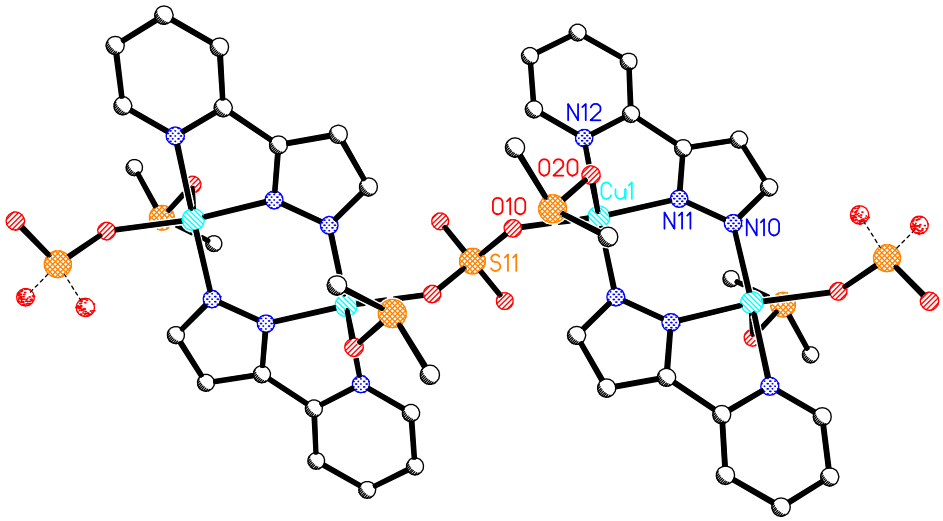

Figure 5.15 *– A section of the one-dimensional polymeric chain **5.14**. Selected bond lengths (Å) and angles (°): Cu1-N10A 1.964(2), Cu1-O10 1.977(1), Cu1-N11 1.992(2), Cu1-N12 2.030(2), Cu1-O20 2.245(1), N10A-Cu1-O10 92.99(6), 97.04(6), N10A-Cu1-N12 176.40(6), N10A-Cu1-O20 93.93(6), O10-Cu1-N11 164.03(6), O10-Cu1-N12 88.51(6), O10-Cu1-O20 85.82(5), N11-Cu1-N12 80.81(6), N11-Cu1-O20 105.78(6), N12-Cu1-O20 89.44(6).*

A section of the polymeric chain structure of complex **5.14** is shown in Figure 5.15 with hydrogen atoms excluded for clarity. The asymmetric unit contains one **5.2** ligand, a copper atom, a coordinated DMSO molecule and half a sulfate anion. The same dimeric motif is seen, where two **5.2** ligands bridge two copper atoms to create a flat panel. Along with three ligand nitrogens, the copper atoms also coordinate to a sulfate oxygen and a DMSO oxygen with a square pyramidal geometry. The sulfate anions bridge the dimeric units, so that only one anion is associated per complex, avoiding the excess charge problem seen in complex **5.13**.

An alternative view of the structure is shown in Figure 5.16, and a slightly longer section of chain, to show the undulation of units along the chain. Every second dimeric panel is tilted from the plane of the dimeric unit on either side, imposed by the angles of the sulfate bridge. The sulfates alternate above and below the plane of the dimers along the chain, to help the chain propagate as linearly as possible. The DMSO ligands are coordinated to the apical site on the copper atom, and do not contribute to the dimensionality of the structure. The DMSO molecules of each dimer sit on opposite sides of the central plane.

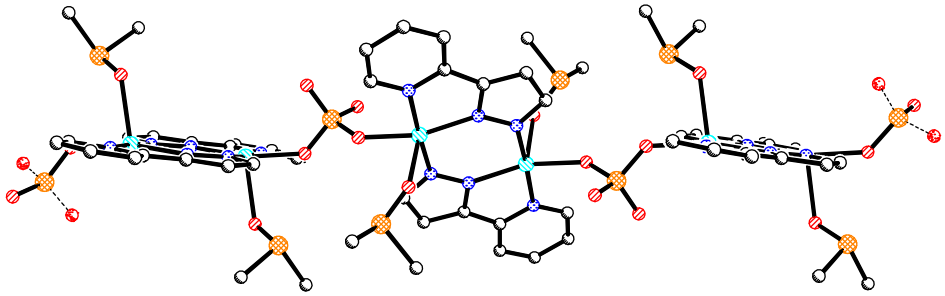

Figure 5.16 *– An alternative view of a section of* ***5.14*** *chain, showing the undulation of each second unit.*

The chains are linked together by short contacts between the non-coordinated sulfate oxygens and the hydrogens on the DMSO ligands on adjacent chains. There are no π-π stacking interactions between or within chains.

Yet another complex containing ligand **5.2** and copper(II) sulfate was obtained from the same reaction mixture. The acetone solution containing the precipitate from ligand **4.13** was split into two portions, the first was redissolved using DMSO and crystallised complex **5.14** upon slow evaporation as discussed. The second portion was redissolved using DMF, and small dark blue blocks grew in solution after a year of slow evaporation. These crystals were suitable for X-ray crystallography, and were shown to be another ligand decomposition complex, **5.15**. The structure solved in orthorhombic space group Pbcn.

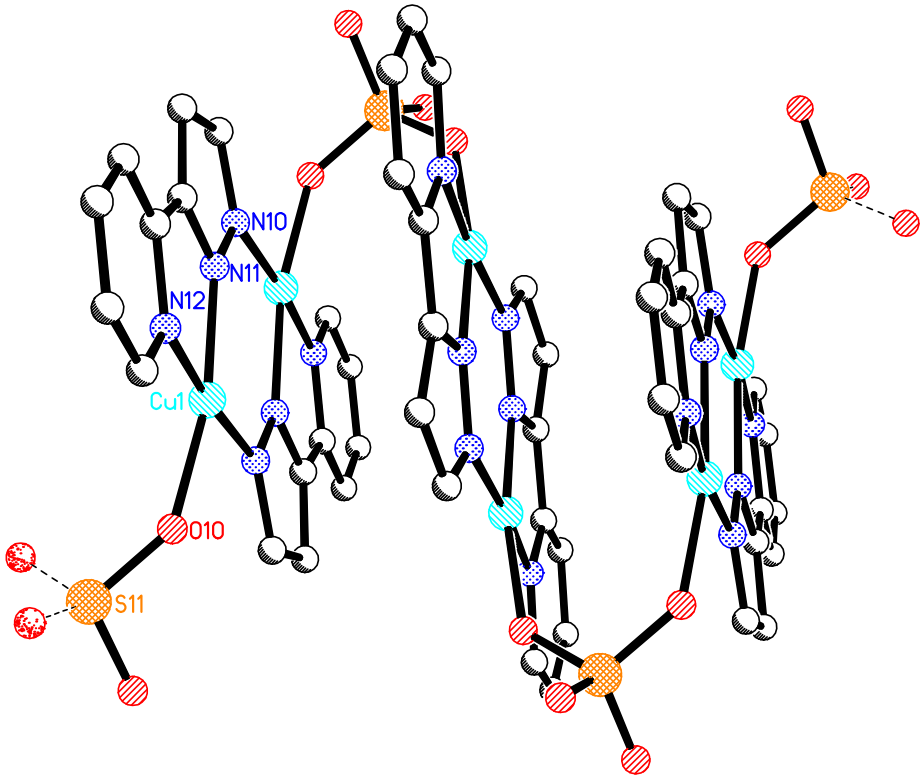

Figure 5.17 *– A section of the one-dimensional polymeric chain* ***5.15****. Selected bond lengths (Å) and angles (°): Cu1-O10 1.956(7), Cu1-N11 1.96(1), Cu1-N10A 1.963(9), Cu1-N12 2.00(1), O10-Cu1-N11 168.1(4), O10-Cu1-N10A 90.6(4), O10-Cu1-N12 91.32(4), N11-Cu1-N10A 98.2(4), N11-Cu1-N12 80.6(5), N10A-Cu1-N12 175.2(4).*

A section of the polymeric chain of **5.15** is shown in Figure 5.17, with hydrogen atoms excluded for clarity. The asymmetric unit contains one **5.2** ligand, one copper atom and half a sulfate anion. Like **5.14**, dimeric panels of two **5.2** ligands and two copper atoms are bridged together by sulfate anions. However the structures are very different. In **5.15** the copper atoms coordinate to three ligand nitrogens and one sulfate oxygen with a square planar geometry. No apical ligands are coordinated in this structure. In **5.14**, the dimeric panels are linked edge on to each other; however in **5.15** the dimers are linked face to face, with strong π-π stacking interactions between dimers (3.220Å). As only one sulfate is associated with each dimer, the charges balance unlike **5.13**. The sulfate anions alternate sides of the dimer, causing a zigzag undulation along the chain. The copper atoms in adjacent dimers are 3.10Å apart.

The chains barely interact with each other, with only a few short contacts between sulfate oxygens and ligand hydrogens.

*Crystal structure with **5.1** and **5.2** with CuI (**5.16**)*

When an acetone solution of **5.1** was added to a solution of copper(I) iodide, a green colour change was observed, suggesting the oxidation of the metal salt. Slow evaporation over a few days gave dark green block-like crystals which were suitable for X-ray crystallography. The structure solved in monoclinic space group $P2_1/n$.

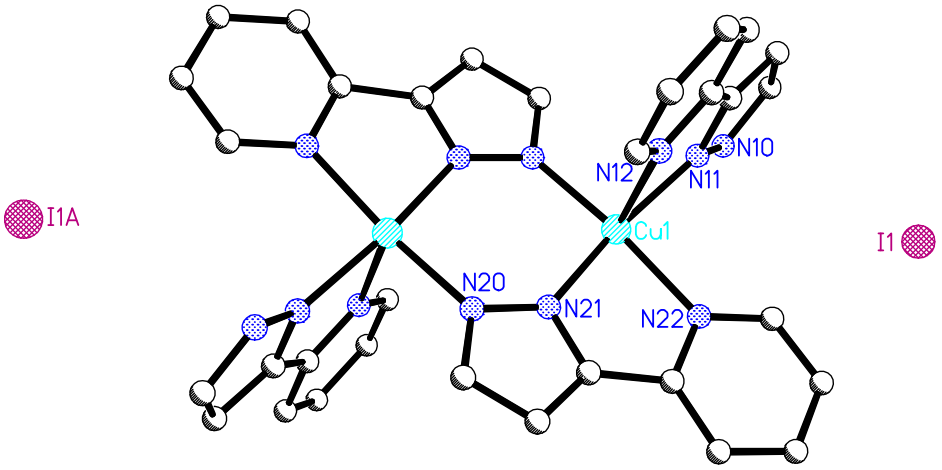

***Figure 5.18** – The discrete structure of **5.16**. Selected bond lengths (Å) and angles (°): Cu1-N20A 1.979(2), Cu1-N21 1.980(2), Cu1-N11 2.028(2), Cu1-N22 2.056(2), Cu1-N12 2.369(2), N20A-Cu1-N21 97.23(7), N20A-Cu1-N11 91.27(7), N20A-Cu1-N22 171.69(7), N20A-Cu1-N12 94.66(7), N21-Cu1-N11 168.22(7), N21-Cu1-N22 80.88(7), N21-Cu1-N12 96.95(7), N11-Cu1-N22 91.83(7), N11-Cu1-N12 74.16(7), N22-Cu1-N12 93.60(7).*

The discrete structure is shown in Figure 5.18, with hydrogen atoms excluded for clarity. Surprisingly, the structure contains both protonated and deprotonated ligands **5.1** and **5.2**. This has been observed in previous complexes.[288,290] The asymmetric unit contains one iodine atom, one copper atom, and one **5.1** and one **5.2** ligand. The same dimeric planar motif seen multiple times in this chapter forms the core of the structure, with two **5.2** ligands bridging two copper(II) atoms. The copper atoms coordinate to five ligand nitrogens with a square pyramidal geometry. Two iodide atoms sit uncoordinated in the crystal lattice, presumably displaced by the **5.1** ligands.

The complexes are stacked in channels, with short contacts between the iodine atoms and ligand hydrogens. There are π-π stacking interactions between **5.1** pyridine rings of adjacent complexes (3.395Å).

From the work already discussed in this chapter, it was established that complexes of **5.1** readily form and crystallise relativity easily. Therefore, it was decided to take this work a step further and investigate whether two different metal atoms could be incorporated into the same complex through a simple "one-pot" self-assembly process. The ultimate goal was to incorporate two different metal atoms into the dimeric motif so often characterised from **5.2**.

*Crystal structure of **5.2** with CuI and $Ni(NO_3)_2$ (**5.17**)*

Methanolic solutions of **5.1** and nickel nitrate were combined to give a purple solution. The addition of an acetonitrile solution of copper(I) iodide triggered a colour change to yellow. Slow evaporation of this solution over a week afforded two different types of crystals, both suitable for X-ray crystallography. The blue prisms were shown to be $[Cu(NO_3)(\mathbf{5.2})(H_2O)]_2$ dimer **5.3**. The other crystals, deep red blocks, solved in triclinic space group P-1.

The discrete M_4L_6 box-like structure of **5.17** is shown in Figure 5.19, complete with $Cu_2I_4^{2-}$ anion, with hydrogen atoms and the rotational disorder of the anion excluded for clarity. Half of this material is present in the asymmetric unit. Two dimeric $[Ni(\mathbf{5.2})]_2$ units are bridged by two other **5.2** ligands, to create a grid-like structure. One nickel atom in each dimer is four coordinate square planar, making four bonds to three different ligands, sitting in the chelating domain of one ligand, and bonding to the pyrazoles of two other ligands. The other nickel atom in each dimer is octahedral, making four bonds to two chelating ligands, a fifth bond to a pyrazole of another ligand, and completed by the nitrogen of an acetonitrile molecule. The dimeric units are locked in position by the bridging axial ligands, and are an ideal distance from each other for π-π stacking interactions (3.385Å).

This M_4L_6 grid structure has been identified before.[288,292,293,299] However every other structure is a slight variation on the Cu(II) analogue of **5.17**. In every structure the copper atoms are always five-coordinate, so it has been presumed that the formation of these grid-like structures is triggered by the stereoelectronic preference of Cu(II) atoms

for a five-coordinate geometry,[292,293] and therefore implying that these structures would not form with other metal atoms.[293] Complex **5.17** proves that this is not the case.

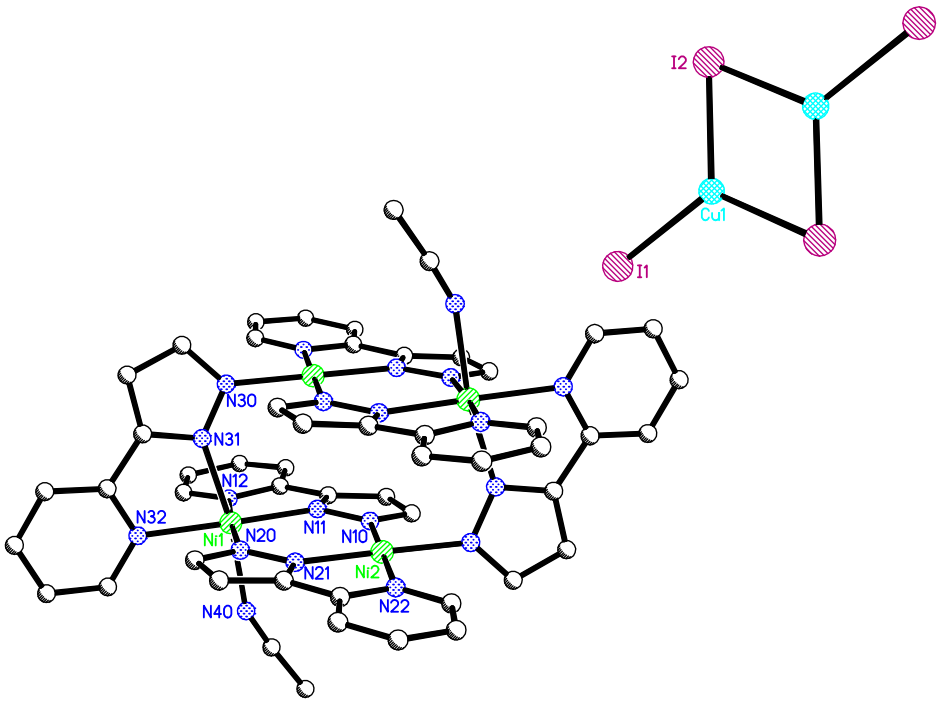

Figure 5.19 *– The M_4L_6 box-like structure of complex* ***5.17****. Selected bond lengths (Å) and angles (°): Cu1-I1 2.4980(7), Cu1-I2A 2.5821(7), Cu1-I2 2.6087(7), Ni1-N11 2.022(3), Ni1-N20 2.034(3), Ni1-N31 2.075(3), Ni1-N12 2.104(3), Ni1-N32 2.117(3), Ni1-N40 2.163(4), Ni2-N10 1.967(3), Ni2-N30A 1.969(3), Ni2-N21 1.969(3), Ni2-N22 2.054(3), I1-Cu1-I2A 121.93(3), I1-Cu1-I2 118.19(3), N11-Ni1-N20 95.9(1), N11-Ni1-N31 101.9(1), N11-Ni1-N12 79.9(1), N11-Ni1-N32 173.2(1), N11-Ni1-N40 86.2(1), N20-Ni1-N31 93.0(1), N20-Ni1-N12 175.5(1), N20-Ni1-N32 90.8(1), N20-Ni1-N40 90.5(1), N31-Ni1-N12 89.6(1), N31-Ni1-N32 78.6(1), N31-Ni1-N40 170.7(1), N12-Ni1-N32 93.37(1), N12-Ni1-N40 87.5(1), N32-Ni1-N40 92.8(1), N10-Ni2-N30A 90.1(1), N10-Ni2-N21 99.0(1), N10-Ni2-N22 179.6(1), N30-Ni2-N21 170.4(1), N30A-Ni2-N22 90.0(1), N21-Ni2-N22 80.9(1).*

The $Cu_2I_4^{2-}$ anion has formed from the CuI added to the solution to balance the charge of the main complex. Each copper atom coordinates to three iodines in a trigonal planar geometry, and two iodines bridge the two copper atoms. The anion is rotationally disordered, 20% of the time lying 90° from where it is pictured, so the copper atoms lie close to where the bridging iodine atoms are pictured in Figure 5.19. This rather unusual anion has been identified before.[300-304]

The complexes are aligned in stacks, with short contacts between iodine atoms and ligand hydrogens, and weak interactions from I2 in the disordered position it occupies 20% of the time to the vacant axial site on Ni2 atoms of adjacent complexes (3.119Å).

*Crystal structure of **5.2** with CuI and $CoBr_2$ (**5.18**)*

Methanolic solutions of ligand **5.1** and cobalt(II) bromide were combined to give an orange solution. The addition of an acetonitrile solution of copper(I) iodide triggered a colour change through dark green to brown. Slow evaporation of this solution provided red (dichroic to green) plate-like crystals that were suitable for X-ray crystallography. The structure solved in monoclinic space group $P2_1/c$.

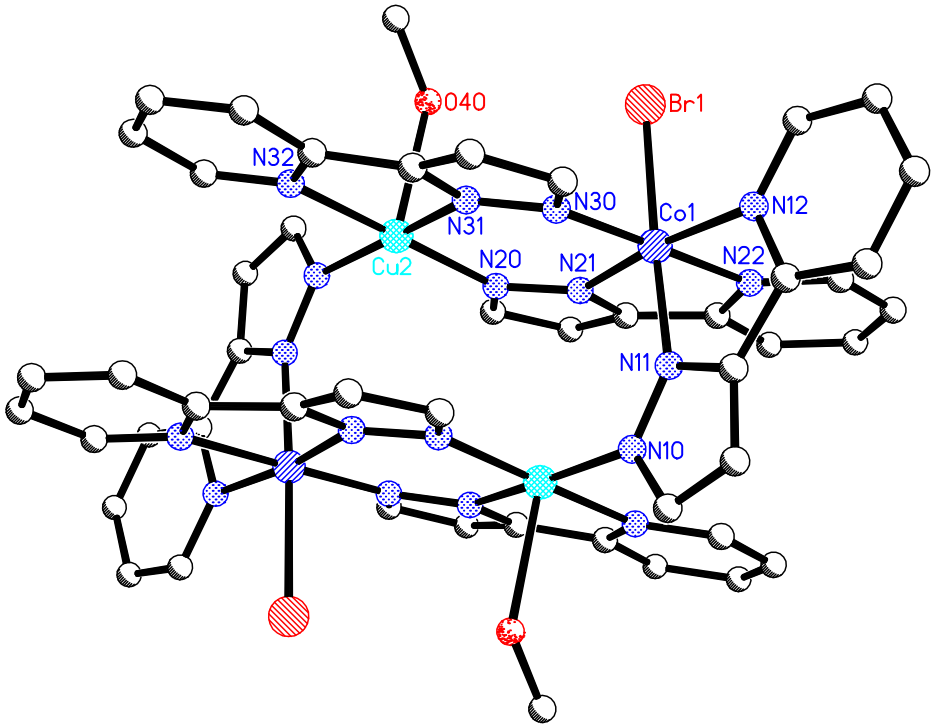

***Figure 5.20** – The M_4L_6 box-like structure of **5.18**. I_3^- counterions are not shown. Selected bond lengths (Å) and angles (°): Co1-N21 1.924(5), Co1-N30 1.935(5), Co1-N11 1.952(6), Co1-N12 1.992(5), Co1-N22 1.997(5), Co1-Br1 2.418(1), Cu2-N31 1.960(5), Cu2-N20 1.971(5), Cu2-N10A 1.979(5), Cu2-N32 2.036(5), Cu2-O40 2.384(4), N21-Co1-N30 97.1(2), N21-Co1-N11 95.6(2), N21-Co1-N12 172.1(2), N21-Co1-N22 82.3(2), N21-Co1-Br1 86.3(2), N30-Co1-N11 90.76(2), N30-Co1-N12 90.4(2), N30-Co1-N22 179.4(2), N30-Co1-Br1 90.5(2), N11-Co1-N12 81.9(2), N11-Co1-N22 89.2(2), N11-Co1-Br1 177.6(2), N12-Co1-N22 90.2(2), N12-Co1-Br1 96.0(2), N22-Co1-Br1 89.7(2),*

N31-Cu2-N20 95.9(2), N31-Cu2-N10A 170.6(2), N31-Cu2-N32 81.2(2), N31-Cu2-O40 92.0(2), N20-Cu2-N10 91.2(2), N20-Cu2-N32 176.4(2), N20-Cu2-O40 87.9(2), N10A-Cu2-N32 91.6(2), N10A-Cu2-O40 94.6(2), N32-Cu2-O40 94.2(2).

The discrete M_4L_6 mixed metal box-like structure (similar to **5.17**) of complex **5.18** is shown in Figure 5.20, with hydrogen atoms, the disorder of the bromine atoms, and the I_3^- anion (and the disorder surrounding the anion) excluded for clarity. The asymmetric unit contains one cobalt atom and one copper atom, three **5.2** ligands, a coordinated bromide anion and a coordinated methanol molecule, and a disordered I_3^- anion. The structure contains two dimeric units containing two different metal atoms each, a cobalt atom and a copper atom. This is only the second example of **5.2** coordinating to two different metal atoms,[297] as shown in mode c) in Figure 5.2, and is the only example of two different metal atoms being incorporated into the dimeric motif favoured by **5.2**. These mixed-metal dimeric units are then linked together by two other **5.2** ligands, each also bonding to two different metal centres. The cobalt atoms each bond to three ligands, two of which chelate, and to a bromine atom to complete an octahedral geometry. The copper atoms also bind to three ligands, but only one of these chelates. The apical position in the square-pyramidal geometry of the copper atom is occupied by a methanol oxygen. During the course of the reaction, Cu(I) has been oxidised to Cu(II), and Co(II) oxidised to Co(III). The deprotonation of six ligands, plus the bromine atoms and two I_3^- anions counterbalance the charge of the metal atoms. Like complex **5.17**, the dimeric units are held closely enough for intramolecular π-π stacking (3.354Å).

The complexes stack in channels, with short contacts between iodine and bromine atoms with hydrogen atoms on the ligands.

*Other complexes of **5.1** and **5.2***

As described, many complexes of **5.2** were obtained unintentionally through the decomposition of ligands **4.13** and **3.24** in the presence of various metal salts. Attempts to deliberately complex **5.1** were undertaken with a variety of metal salts, often in different metal to ligand ratios, and sometimes with potential secondary ligands such as 4,4'-bipyridine or with a mixture of metal salts. The metal salts used include $AgNO_3$, $AgPF_6$, $AgClO_4$, $AgBF_4$, $AgCF_3SO_3$, CuI, $CuCl_2$, $CuSO_4$, $Cu(OAc)_2$, $CoCl_2$, $CoBr_2$, $NiCl_2$, $Ni(NO_3)_2$, $Ni(OAc)_2$, $CdCl_2$, $ZnBr_2$ and $La(NO_3)_3$. Thankfully, single crystals suitable for X-ray crystallography were obtained for a large number of these complexes,

allowing for full characterisation of the products. Almost all of those which did not crystallise were not analysed further.

When **5.1** was reacted with $Ni(OAc)_2$, a few blue crystals were obtained which were shown by X-ray crystallography to be complex **5.11**. The pale pink precipitate that was also formed during the reaction was shown to be a different product, containing a ML_2 stoichiometry. It is likely this product contains two protonated **5.1** ligands attached to each centre, probably discrete but could be polymeric if the acetate anions bridge the metal centres.

When **5.1** is reacted with $Cu(OAc)_2$ in hot methanol, blue square crystals grow within a few days. However these redissolved before they could be analysed, and recrystallised as extremely thin blue needles, not suitable for X-ray crystallography. It seems likely that the first product formed contains a simple product like one **5.1** ligand coordinated to the metal salt, which then recrystallises as the ligand becomes deprotonated and a complex containing the more stable dimeric unit forms. This product was shown to have a 1:1 metal to ligand stoichiometry, so is likely to be a dimeric product, although many structures could form with this metal to ligand ratio.

Complexes with 8-hydroxyquinoline

During the course of this research, a couple of interesting metallosupramolecular structures containing 8-hydroxyquinoline were stumbled upon which are mentioned here.

*Complex of 8-hydroxyquinoline with $CoCl_2$ (**5.19**)*

The reaction of ligand **3.43** with three equivalents of cobalt(II) chloride in an acetone and chloroform solution produced a green precipitate and some very large pink crystals which were shown to be the metal salt. One very small dark red crystal was discovered in the mixture and analysed by X-ray crystallography. The structure was shown not to contain ligand **3.43**, but 8-hydroxyquinoline, probably resulting from a small impurity in the ligand sample. The structure solved in triclinic space group P-1.

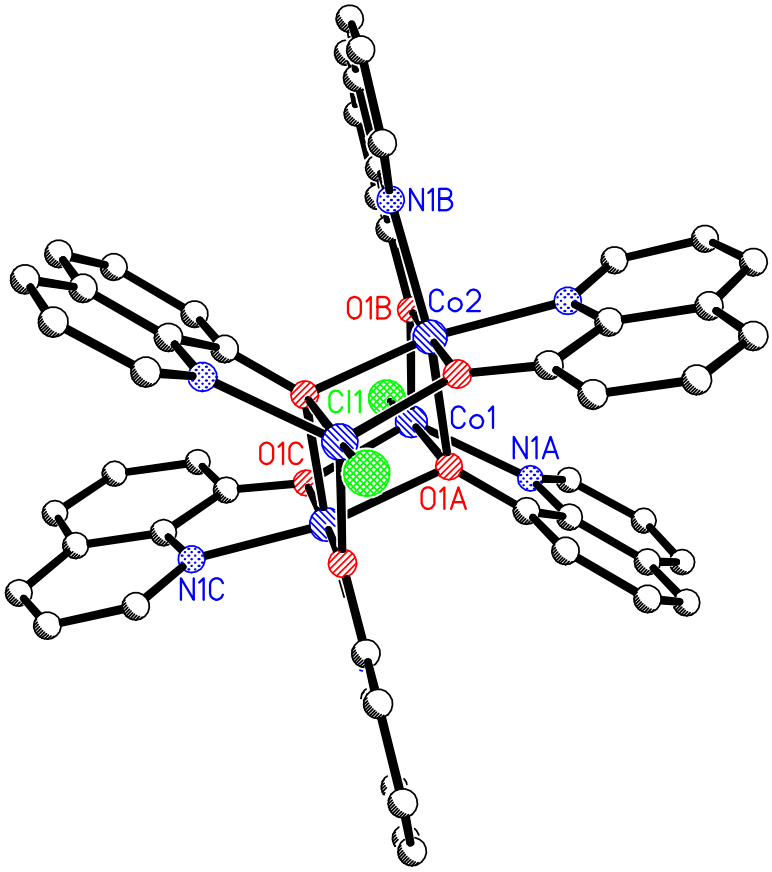

Figure 5.21 *– The $M_4L_6Cl_2$ cluster **5.19**. Selected bond lengths (Å) and angles (°): Co1-O1B 2.002(4), Co1-O1C 2.012(4), Co1-N1A 2.104(5), Co1-O1A 2.271(4), Co1-Cl1 2.299(2), Co2-O1C 2.041(4), Co2-O1B 2.044(4), Co2-O1A 2.084(4), Co2-N1C 2.095(5), Co2-N1B 2.099(5), Co2-O1A 2.134(4), O1B-Co1-O1C 103.6(2), O1B-Co1-N1A 115.2(2), O1B-Co1-O1A 78.0(2), O1B-Co1-Cl1 109.9(1), O1C-Co1-N1A 124.3(2), O1C-Co1-O1A 75.8(2), O1C-Co1-Cl1 105.0(1), N1A-Co1-O1A 75.1(2), N1A-Co1-Cl1 97.7(1), O1A-Co1-Cl1 171.2(1), O1C-Co2-O1B 176.2(2), O1C-Co2-O1A 79.6(2), O1C-Co2-N1C 79.7(2), O1C-Co2-N1B 103.6(2), O1C-Co2-O1A 96.3(2), O1B-Co2-O1A 101.7(2), O1B-Co2-N1C 98.8(2), O1B-Co2-N1B 79.9(2), O1B-Co2-O1A 80.4(2), O1A-Co2-N1C 158.9(2), O1A-Co2-N1B 97.3(2), O1A-Co2-O1A 81.3(2), N1C-Co2-N1B 91.1(2), N1C-Co2-O1A 97.4(2).*

The discrete M_4L_6 structure is shown in Figure 5.21, with chloroform solvate molecules and hydrogen atoms excluded for clarity. Half of the complex lies in the asymmetric unit. The structure consists of six deprotonated ligands linked together by four cobalt atoms in a rectangular cluster. Two of the cobalt atoms (Co2) are six coordinate octahedral, bonding to four ligand oxygens and two ligand nitrogens, of four different

ligands, two of which are chelating. Interestingly, the other two cobalt atoms (Co1) are five coordinate trigonal bipyramidal, binding to three ligand oxygens and one ligand nitrogen of three separate ligands. Only one of these ligands is chelating. There appears to be enough space around Co1 to allow another ligand to approach and bind to reach the preferred octahedral geometry, so the unusual geometry of Co1 must be required by the ligands to form this cluster. Each ligand oxygen bridges two cobalt atoms, forming a double half-cube-like centre to the cluster. The quinoline rings are arrayed on the outside of the cluster, like petals on a flower. The quinoline rings alternate positions at the top and bottom of the rectangular core, the nitrogen atoms of four of these pointing into the centre of the cluster. The nitrogens on the remaining two ligands coordinate to the final metal atom, Co1. The cluster is terminated by chlorine atoms at each end.

This structure is very similar to two others reported in the literature.[305,306] A $Zn(OAc)_2$ analogue exists,[305] as well as a $CoCl_2$ analogue[306] which differs from **5.19** only by the ligand, as a methyl derivative (8-hydroxyquinaldine) of 8-hydroxyquinoline was used. Both structures also display the 5-coordinate metal atom in the terminating position.

*Crystal structure of 8-hydroxyquinoline with $CoBr_2$ (**5.20**)*

In an attempt to directly synthesise an analogue of the above complex in higher yield, cobalt(II) bromide was dissolved in acetone and mixed into a solution of 8-hydroxyquinoline in chloroform, and the resulting solution heated. Many large yellow crystals were obtained which were shown to be the bromide salt of 8-hydroxyquinoline. Only a few small deep red crystals were obtained, one of which was suitable for X-ray crystallography. The structure had a very similar cell to **5.19**, and also solved in triclinic space group P-1.

The M_6L_4 cluster **5.20** is shown in Figure 5.22, with solvate molecules and hydrogen atoms excluded for clarity. The complex is isostructural with **5.19**, with the chlorine atoms replaced by bromines. Again, the asymmetric unit contains half of the complex, along with a solvate molecule. This solvate position is occupied by a chloroform molecule 37% of the time, and an acetone the rest of the time. The structure contains six ligands, each coordinated to the metal atoms *via* the nitrogen and the deprotonated oxygen, the latter bridging two metal atoms. The complex contains four metal atoms

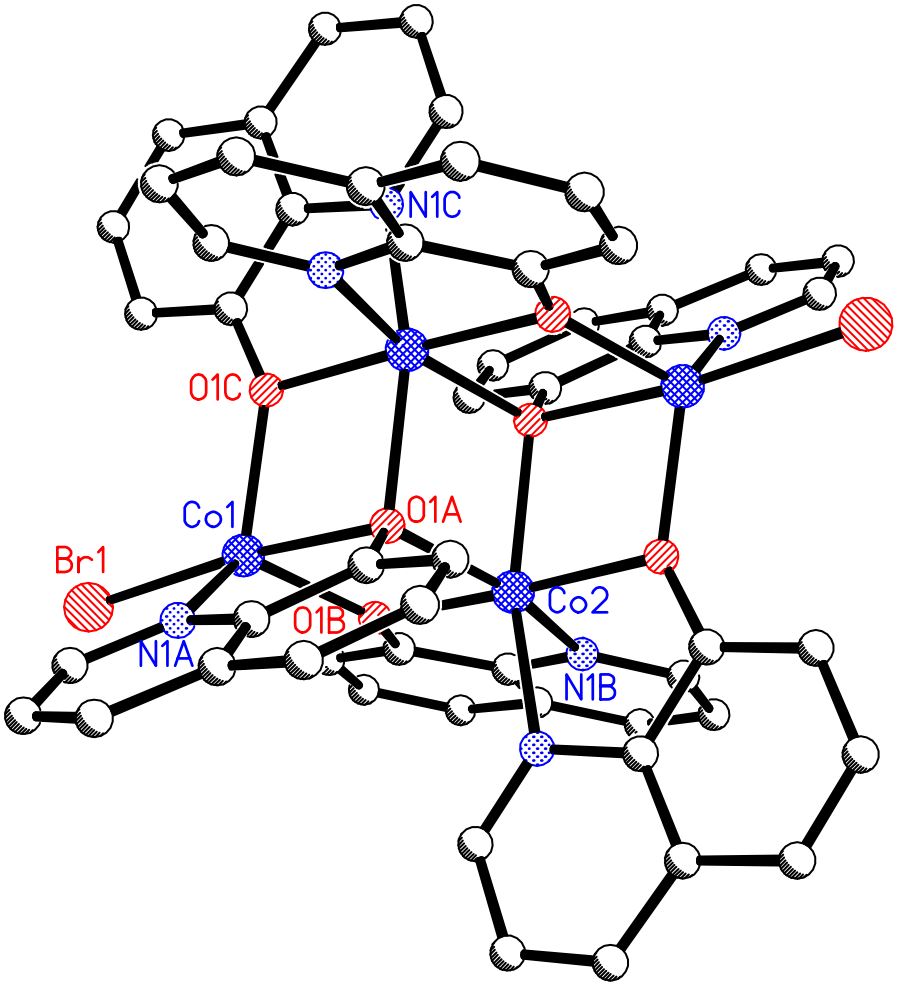

Figure 5.22 *– The $M_4L_6Br_2$ cluster* ***5.20****. Selected bond lengths (Å) and angles (°): Co1-O1C 2.008(2), Co1-O1B 2.020(2), Co1-N1A 2.093(3), Co1-O1A 2.243(2), Co1-Br1 2.4488(6), Co2-O1C 2.040(2), Co2-O1B 2.064(2), Co2-N1C 2.076(3), Co2-O1A 2.080(2), Co2-N1B 2.086(3), Co2-O1A 2.120(2), O1C-Co1-O1B 103.58(9), O1C-Co1-N1A 117.2(1), O1C-Co1-O1A 78.12(8), O1C-Co1-Br1 108.83(6), O1B-Co1-N1A 123.70(9), O1B-Co1-O1A 77.05(8), O1B-Co1-Br1 104.55(6), N1A-Co1-O1A 75.5(1), N1A-Co1-Br1 97.38(8), O1A-Co1-Br1 171.96(6), O1C-Co2-O1B 175.8(1), O1C-Co2-O1A 102.00(8), O1B-Co2-O1A 79.90(8), N1C-Co2-N1B 90.5(1), N1C-Co2-O1A 159.67(9).*

of two types. Co2 is near the middle of the cluster, bonding to four oxygens and two nitrogens in an octahedral geometry. Co1 sits at the edge of the cluster, bonding to three ligand oxygens and one nitrogen, and to the bromine atom in a five-coordinate trigonal bipyramidal geometry. The centre of the cluster is made up of a double half-cube-like unit of cobalt and oxygen atoms, and the quinoline rings radiate out from this core.

Summary

This chapter discussed complexes containing 3-(2'-pyridyl)pyrazole, in either its protonated (**5.1**) or deprotonated (**5.2**) forms. Many of the compounds discussed were synthesised unintentionally, through a ligand decomposition process of unknown origin. There have been four documented cases of related decomposition processes in the literature. Ligands **3.24** and **4.13** were most prone to decomposition in the presence of metal salts, with six different complexes characterised containing **5.2**. This decomposition process appears to be dependent upon the solvents used in the reaction, with different solvent combinations allowing crystallisation of complexes containing ligands **3.24** and **4.13**, or crystallisation of the decomposition complexes.

The decomposition complexes showed that **5.2** could form a dimeric unit that makes a interesting synthon for metallosupramolecular chemistry. Therefore a series of complexes containing **5.1** and **5.2** were prepared deliberately, from direct synthesis from ligand **5.1** and the metal salt.

Discrete and polymeric complexes were synthesised containing ligand **5.1**. Ligand **5.2** prefers to form a dimeric structure with metal salts, where it acts as a terdentate bridging ligand. Discrete and polymeric complexes were obtained containing the **5.2** dimeric unit. It was shown that three different complexes could be obtained from reaction of **5.2** with $CuSO_4$, one discrete and two polymeric. A discrete complex was formed from CuI that contains both **5.2** and **5.1** ligands.

Two grid-like M_4L_6 boxes were crystallised. The first, **5.17**, is constructed from octahedral and square planar nickel(II) atoms, and the charge of the complex is counterbalanced by a $Cu_2I_4^{2-}$ anion. The second, **5.18**, contains both octahedral cobalt atoms and square pyramidal copper atoms, the first case of **5.2** bridging two different metal atoms in the dimeric motif.

3-(2'-Pyridyl)pyrazole is a small and rather simple ligand, but has proved to be a versatile ligand and an interesting synthon in the formation of metallosupramolecular structures.

Chapter Six

Conclusions and future prospects

Conclusions and future prospects

This thesis has covered the synthesis and coordination chemistry of twenty-five nitrogen-containing heterocyclic ligands, nineteen of which were previously unreported. These ligands were designed as potential components for the construction of molecular cages. The majority of molecular cages identified in the literature are based on rigid ligands.[8,50,62,66,79,81,82,99,178,258,282,307] This research has instead focused on incorporating some flexibility into a series of ligands in the form of flexible linkers tethering the heterocyclic donor groups to rigid ligand cores. Rigid ligands act as predictable synthons in metallosupramolecular chemistry, as the fixed conformation of the donor atoms removes a degree of freedom from the self-assembling system, making the complex formed more dependent on the metal salt used and other factors in the system, therefore allowing the chemist more control over directing what product is formed. Consequently, flexible ligands add more variables to the self-assembling system, as more conformations are available. The scientist loses a degree of control over the system, as many more products have the potential to form. The final observed product results due to thermodynamic and kinetic factors, which are not usually predictable, but often justifiable after the characterisation of the product. However, flexible ligands make interesting synthons due to their unpredictability, and can form complexes not accessible from rigid ligands, and it is even possible that the inherent flexibility may add functional properties to the resulting complex.

In this research, it was attempted to restrain the flexibility of some of the ligands by using the concept of preorganisation to encourage the ligand to prefer a single conformation. It was predicted that the high symmetry and thermodynamic stability of coordination cages would help favour the formation of these structures.

A family of two-armed ligands were synthesised based on 1,3-substitution around a 2,4,6-triethylbenzene core, in the hope that the steric bulk around the ligand core would encourage an *ababa* preorganisation around the ring, thereby orientating the donor groups on the same face of the ligand core. There have been multiple examples of similar ligands based on 1,3-substitution around a benzene ring acting as components

for molecular cages,[107,108,147,148] so it was envisaged that these ligands could potentially self-assemble into M_4L_6 tetrahedral cages upon reaction with appropriate metal salts.

However ligand **2.4** seemed to prefer to form coordination polymers, with the exception of cyclic trimer **2.11**, a fascinating discrete structure of which the host-guest chemistry should be further investigated.

Ligand **2.12** proved to be an extremely valuable ligand to this research, forming complexes which crystallised easily. The characterisation of so many [2+2] macrocycles containing **2.12** displays the unpredictability of these systems, as it was not predicted that the ethyl groups designed to preorganise the ligands would have such a strong influence on the product formed, obviously stabilising the complex formed by interacting strongly with the "V"-shape made by the arms of the adjacent ligand. It has been suggested that this ethyl group may be affected enough by the surrounding environment to become susceptible to reaction;[308] hopefully this can be investigated in the future.

The stability of the dimeric unit ultimately led to the formation of the family of M_4L_6 squares, which consist of two dimeric units linked together by two extra ligands. The squares are isomers of the desired tetrahedral cages. The squares are fascinating structures, and act like molecular cages by encapsulating an anion, which is usually perchlorate, but a tetrafluoroborate analogue was also characterised. Anion exchange reactions to probe the degree of encapsulation and investigate which anion is the preferred guest would be interesting, and could be monitored *via* NMR if the Co(III) square could be synthesised. A different anion system may promote spin-crossover properties in **2.33**.[158] Also of interest would be more attention towards the seemingly fragile equilibrium that can allow crystallisation of either the square or the dimer from very similar reaction conditions.

Ligand **2.35** formed very insoluble complexes, of which only one could be crystallised, a one-dimensional coordination polymer. More unfortunately, ligand **2.44** could not be synthesised by the procedure attempted here, and it is hoped other workers will manage to prepare this interesting ligand by another procedure in the future.

The design of these ligands with increased steric bulk around the ring now seems unnecessary, as the ethyl groups did not seem to promote preorganisation. However the ethyl group in the 2-position appears to promote dimerisation in complexes with ligand **2.12**, and therefore the formation of the squares.

A series of three-armed ligands were synthesised based on 1,3,5-substitution around 2,4,6-trialkyl- or trimethoxy-benzene cores. This work began with ligand **3.5** which had been previously shown to form M_6L_4 cage **3.21** upon reaction with $PdCl_2$.[55] Apart from showing that this cage can be synthesised by different procedures, and can crystallise in a different space group with a different guest molecule, no other molecular cages were prepared from **3.5**. However the protonated ligand and a coordination polymer displaying an η^1 silver-benzene interaction were crystallised. A chiral ligand (**3.17**) similar to **3.5** was prepared, which hopefully can be purified in the future so the coordination chemistry can be studied.

Ligand **3.24** differs from **3.5** only by the addition of a pyridine ring to create a bidentate binding domain. It forms M_4L_2 dimeric complexes with Cu(II) salts, rather than the desired M_3L_2 cages. It is unknown why only two arms of the two ligands bridge, but possibly the geometry of the components are not suitable for the formation of a M_3L_2 cage.

Similar ligands **3.33** and **3.34** appear to favour the formation of coordination polymers over discrete structures, although related ligands have been shown to form molecular cages. Ligand **3.33** forms two-dimensional polymers with $CoBr_2$ and CuI, the former shown to undergo changes upon dehydration that are not yet characterised, while the latter contains solvent-filled channels shown to be stable to guest removal and resorption. It is hoped that more study of the resorption properties of **3.38** will be undertaken in the future. Ligand **3.34** forms a similar but three-dimensional net with CuI, and another three-dimensional framework with $AgClO_4$ which displays four-fold interpenetration. If this framework, **3.40**, could be synthesised in sufficient yield, resorption studies should be undertaken.

The only complex crystallised with ligand **3.42** was shown to contain a Cu_3I_3 hexagon nestled inside the arms of the ligand. Despite repeated attempts, no complexes were

fully characterised from ligand **3.41**, but other workers may have more luck growing crystals of complexes from **3.41** and **3.42**.

Similarly, no complexes were fully characterised from the family of ligands based on 1,3,5-trimethoxybenzene. The solubility of these ligands differs from the trialkyl ligands so the same solvent systems are not successful. However these problems may be overcome in the future.

The ligands incorporating ethyl groups were shown to encourage preorganisation only some of the time, consistent with a study of the conformations of similar ligands in the literature.

Chapter Four discusses three-armed ligands based on different cores from those previously discussed. Three large ligands based on 1,3,5-triphenylbenzene ligands were synthesised, including **4.9** which forms a two-dimensional coordination polymer with $AgClO_4$. Reaction of ligand **4.13** with $CuSO_4$ produced complex **4.15**, the pinnacle of this research. This M_6L_4 assembly appears to be a collapsed octahedral coordination cage, twisted in upon itself due to the flexibility of the ligand. It is possible that the complex may open in solution to allow encapsulation of a guest molecule, an exciting prospect considering the size of the cavity within the cage may be adjustable and therefore adaptive to suit the guest. During the course of this research, the characterisation of a guest inside **4.15** was not achieved, but this hopefully will be re-examined in the future.

Two ligands were synthesised from the similar 1,3,5-triphenyltriazine core, but the coordination chemistry of neither was studied. A new family of ligands was synthesised, based on triphenylmethanol cores. Surprisingly, despite repeated attempts, no complexes involving these ligands could be crystallised. This is disappointing as these ligands are likely to be exciting synthons in metallosupramolecular chemistry. Ideally crystals of complexes of these ligands will be obtained in the future.

Unfortunately, ligands **3.24** and **4.13** were shown to decompose in the presence of certain metal salts, a phenomenon that has been noted previously in the literature.[290,291,295,296] Six decomposition complexes were obtained this way, and then the coordination chemistry of **5.1** was studied deliberately to give a range of discrete

and polymeric complexes. Of note is the formation of a M_4L_6 box-like grid that incorporates both copper and cobalt atoms, which is only the second case of **5.2** bridging two different metal centres.

In conclusion, this research could have been improved dramatically if a larger percentage of the complexes synthesised could have been crystallised for full characterisation by X-ray crystallography. Undoubtedly the ligands synthesised are capable of forming a greater range of complexes than just those that were able to be characterised in this time period, so there is likely to be more to be learnt about the coordination chemistry of these ligands.

Likewise, few of the complexes that were fully characterised were studied further. It is possible that some of these complexes possess properties that may be revealed by NMR spectroscopy, thermogravimetric analysis, or magnetic studies.

Unfortunately, the goal of forming a range of molecular cages of controlled size and shape was not met. A few cage-like complexes were identified, such as the M_4L_6 squares and the collapsed M_6L_4 cage. However it is suspected that many more cage-like complexes were made but were not crystallised, as a high proportion of elemental analysis results showed precipitates to have the desired M_3L_2 stoichiometry. Some of these precipitates also showed promising high symmetry ^{1}H NMR spectra and in one case, even a characteristic up-field shift of an encapsulated solvent molecule; however these complexes could not be crystallised for full characterisation.

The difficulty of forming and characterising molecular cages in this research and the collapsed structure of **4.15** suggests that flexible ligands may not be the most desirable components for the formation of molecular cages. A cage constructed from rigid ligands has a cavity of defined size which is unyielding under any conditions and always open to host a guest molecule. However a cage incorporating flexible ligands, such as **4.15**, may be able to expand and contract to create a cavity of an ideal size for a particular guest, which would allow it to act as a more widely applicable molecular flask if reactions could be undertaken upon the encapsulated guest. Therefore it is hoped that molecular cage **4.15** and the other ligands presented in this research which are possibly capable of forming similar structures will be further examined in the future.

Chapter Seven

Experimental

General experimental

Melting points were recorded on an Electrothermal melting point apparatus and are uncorrected. Melting points were not attempted of complexes containing perchlorate salts, in case of explosion. The Campbell microanalytical laboratory at the University of Otago performed elemental analyses. Electrospray (ES) mass spectra were recorded using a Micromass LCT-TOF mass spectrometer.

NMR spectra were recorded on Varian 300 MHz and Varian 500 MHz spectrometers at 23^{o}C, using a 3mm probe. ^{1}H NMR spectra recorded in $CDCl_3$ were referenced relative to the internal standard Me_4Si. ^{1}H NMR recorded in other solvents were referenced to the solvent peak: acetonitrile, 2.0ppm; methanol, 3.3ppm; DMSO, 2.6ppm; acetone, 2.17ppm. When required, 2D COSY and other correlation experiments were performed using standard pulse sequences. Unless otherwise stated, the values given for chemical shifts are to the centre of the mulitplet. Multiplets have been described in terms of their two- and three-bond coupling only, with splitting due to longer coupling being ignored. The ^{1}H NMR assignments for the compounds are denoted with primes to differentiate between rings of the ligand.

Thermogravimetric analyses were performed at the University of Sydney in conjuction with the research group of Cameron Kepert, using a TA instruments H-Res TGA 2950 Analyser under a nitrogen gas atmosphere under the supervison of Greg Halder. Other gases were added to the nitrogen gas stream by bubbling the nitrogen gas through a liquid sample of the desired secondary gas. The data were analysed using the TA instruments Universal Analysis 2000 program.

Spin crossover measurements were undertaken at Monash University (Clayton Campus) by the research group of Keith Murray, using a Quantum Design MPMS SQUID magnetometer.

Unless otherwise stated reagents were obtained from commercial sources and used as received. Solvents were dried by literature procedures and freshly distilled as required. The following compounds were prepared by literature procedures: copper(I) iodide,[309] copper(I) tetrafluoroborate,[310] copper(II) perchlorate,[311] nickel(II) perchlorate,[312] potassium tetrachloropalladate,[313] bis(benzonitrile)palladium(II) dichloride,[314]

bis(ethylenediamine)palladium(II) dichloride,[315,316] and (4S,7R)-7,8,8-trimethyl-4,5,6,7-tetrahydro-4,7-methano-2H-indazole.[317]

Preparation of ligands & ligand precursors

General procedure for phase-transfer-catalysed (PTC) alkylations of pyrazoles

A mixture of the poly(bromomethyl) precursor, the pyrazole (1 equiv. per bromine), benzene (approx. 2mL per mmol of bromomethyl compound), 40% aqueous sodium hydroxide (approx. 0.3mL per mmol of bromomethyl compound) and 40% aqueous tetrabutylammonium hydroxide (1 drop per 10mmol of bromomethyl compound) was refluxed for two to four days. The organic layer was then separated, dried (Na_2SO_4), and concentrated to give the product.

General procedure for the synthesis of 4-pyridylsulfanylmethyl ligands

A mixture of the poly(bromomethyl) precursor and 4-mercaptopyridine (1 equiv. per bromine) was stirred in acetonitrile (approx 20mL per mmol of bromomethyl compound) at 0^{o}C on ice. Triethylamine (approx 0.2mL per mmol of bromomethyl compound) was added and the solution stirred overnight and allowed to slowly warm up to room temperature as the ice melted. Depending on solubility, the product may precipitate out and be filtered off, otherwise the product can be separated from the reaction mixture with ethyl acetate or by washing a chloroform solution with dilute sodium hydroxide.

General procedure for the synthesis of the 8-quinolyloxymethyl ligands

The poly(bromomethyl) precursor and 8-hydroxyquinoline (1 equiv. per bromine) were added to a 90^{o}C solution of DMF (approx 1mL per mmol of bromomethyl compound) containing dissolved potassium hydroxide (approx 0.2g per 10mmol of bromomethyl compound). Reaction can take anywhere from a few hours to a few weeks, depending on the steric bulk surrounding the bromomethyl group. The product is separated from the solution mixture using chloroform and water, with the organic layer being washed with water multiple times to remove any remaining DMF. The organic layer is then dried and the solvent removed *in vacuo* to isolate the desired product.

3-(Dimethylamino)-1-(2-pyridyl)prop-2-en-1-one, ***5.0***

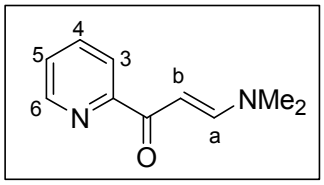

A mixture of 2-acetylpyridine (22mL, 218mmol) and DMF-dimethylacetal (40mL, 301mmol) was refluxed for 42 hours. Upon cooling the solution completely solidified as dark green crystals, which were recrystallised from petroleum ether and chloroform to give the product as light green crystals (26.5g, 69%). ^{1}H N.M.R. (300MHz, $CDCl_3$): δ 3.00 (3H, s, CH_3), 3.18 (3H, s, CH_3), 6.45 (1H, d, Hb), 7.36 (1H, dd, H5), 7.80 (1H, t, H4), 7.92 (1H, d, Ha), 8.15 (1H, d, H3), 8.63 (1H, d, H6).

3-(2'-pyridyl)pyrazole, ***5.1***

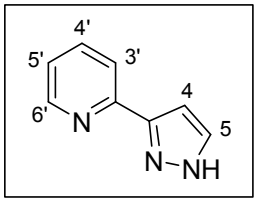

A mixture of **5.0** (26.5g, 151mmol) and hydrazine hydrate (41mL) in ethanol (29mL) was heated at 60^{o}C for 45 minutes. The reaction mixture was cooled and water added (150mL). The product crystallised in the fridge overnight and was filtered to obtain **5.1** as a light brown solid (18.5g, 82%), m.p. 122-127^{o}C (lit.[159,318] 119-120^{o}C). ^{1}H N.M.R. (300MHz, $CDCl_3$): δ 6.82 (1H, d, H4), 7.25 (1H, dd, H5'), 7.67 (1H, d, H5), 7.76 (2H, m, H3',4'), 8.68 (1H, d, H6').

Preparation of the 1,3-disubstituted-2,4,6-triethylbenzene ligands

1,3-Di(bromomethyl)-2,4,6-triethylbenzene, ***2.2***

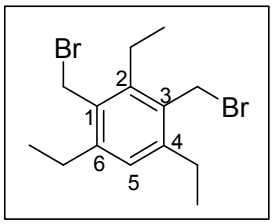

A mixture of 1,3,5-triethylbenzene (4.18g, 25.8mmol), paraformaldehyde (2.50g, 82.5mmol), and hydrobromic acid (33% in H_2O, 8mL) was refluxed in acetic acid (28mL) for six days. During this time an extra 2mL of hydrobromic acid was added to the reaction mixture. Upon cooling a light coloured precipitate formed which was filtered off, to give **2.2** as a pale brown solid (8.97g, 84%), m.p. 81-86^{o}C (lit. not provided[109,110,113-115,117]). ^{1}H N.M.R. (300MHz, $CDCl_3$): δ 1.29 (6H, t, 4,6-CH_3), 1.32 (3H, t, 2-CH_3), 2.76 (4H, q, 4,6-CH_2), 2.93 (2H, q, 2-CH_2), 4.60 (4H, s, 1,3-CH_2), 6.98 (1H, s, H5).

1,3-Di(pyrazol-1-ylmethyl)-2,4,6-triethylbenzene, ***2.4***

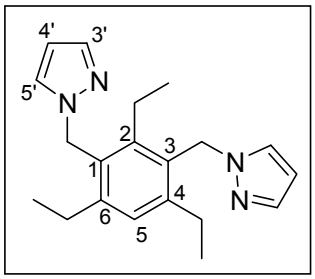

A mixture of **2.2** (1.04g, 3.0mmol), pyrazole (0.41g, 6.0mmol), and 40% aqueous tetrabutylammonium hydroxide (3 drops) was refluxed in benzene (60mL) and 40% aqueous sodium hydroxide (10mL) for 60 hours. The organic layer was separated, dried with Na_2SO_4, and concentrated to give **2.4** as a yellow oil (0.95g, 98%), (Found: C, 74.74; H, 8.29; N, 15.92. $C_{20}H_{26}N_4.{}^1/_2H_2O$ requires C, 74.54; H, 8.15; N, 15.80). ^{1}H N.M.R. (500MHz, $CDCl_3$): δ 0.93 (3H, t, 2-CH_3), 1.15 (6H, t, 4,6-CH_3), 2.66 (6H, m, 2,4,6-CH_2), 5.41 (4H, s, 1,3-CH_2), 6.17 (2H, t, H4'), 6.97 (2H, d, H5'), 7.10 (1H, s, H5), 7.54 (2H, d, H3'). Found M^+ 323.2235, $C_{20}H_{27}N_4$ requires M^+ 323.2236.

1,3-Di[3-(2'-pyridyl)pyrazol-1-ylmethyl]-2,4,6-triethylbenzene, ***2.12***

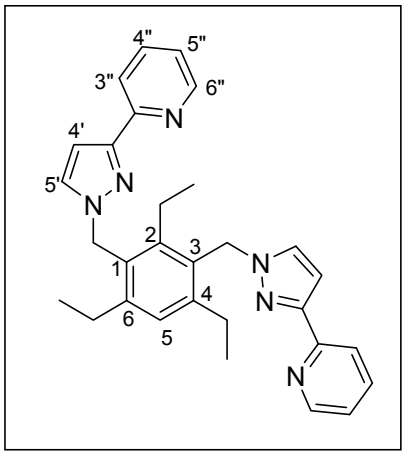

A mixture of **2.2** (1.00g, 2.9mmol), **5.1** (0.87g, 5.8mmol), and 40% aqueous tetrabutylammonium hydroxide (3 drops) was refluxed in benzene (60mL) and 40% aqueous sodium hydroxide (10mL) for 66 hours. The organic layer was separated, dried with Na_2SO_4, and concentrated to give **2.12** as a thick yellow oil (1.34g, 98%), (Found: C, 74.84; H, 6.89; N, 16.66. $C_{30}H_{32}N_6.{}^1/_3C_6H_6.{}^2/_3H_2O$ requires C, 74.68; H, 6.92; N, 16.23). ^{1}H N.M.R. (500MHz, $CDCl_3$): δ 1.03 (3H, t, 2-CH_3), 1.19 (6H, t, 4,6-CH_3), 2.69 (4H, q, 4,6-CH_2), 2.74 (2H, q, 2-CH_2), 5.50 (4H, s, 1,3-CH_2), 6.79 (2H, d, H4'), 6.90 (2H, d, H5'), 7.14 (1H, s, H5), 7.19 (2H, dd, H5"), 7.71 (2H, t, H4"), 7.92 (2H, d, H3"), 8.63 (2H, d, H6"). TOF-MS: Found M^+ 477.2765, $C_{30}H_{33}N_6$ requires M^+ 477.2767.

1,3-Di(4-pyridylsulfanylmethyl)-2,4,6-triethylbenzene, ***2.35***

A mixture of **2.2** (1.00g, 2.9mmol), 4-mercaptopyridine (0.64g, 5.8mmol), and triethylamine (0.60mL) was stirred in acetonitrile (60mL) at 0^{o}C on ice, slowly warming to room temperature over 18 hours. A small amount of precipitate was filtered off. The remaining reaction mixture was concentrated by removing the solvent *in*

vacuo, then stirred overnight in ethyl acetate. The solution was filtered, the precipitate discarded, and the filtrate reduced *in vacuo* to give **2.35** as an orange solid (0.61g, 52%), m.p. 125-131°C. (Found: C, 66.42; H, 6.82; N, 6.74. $C_{24}H_{28}N_2S_2.{}^4/_3H_2O$ requires C, 66.63; H, 7.14; N, 6.47). ^{1}H N.M.R. (500MHz, $CDCl_3$): δ 1.29 (6H, t, 4,6-CH_3), 1.31 (3H, t, 2-CH_3), 2.75 (4H, q, 4,6-CH_2), 2.86 (2H, q, 2-CH_2), 4.23 (4H, s, 1,3-CH_2), 7.02 (1H, s, H5), 7.18 (4H, d, H3',5'), 8.45 (4H, d, H2',6'). Slow evaporation of a chloroform and methanol solution containing ligand **2.35** gave crystals suitable for X-ray crystallography.

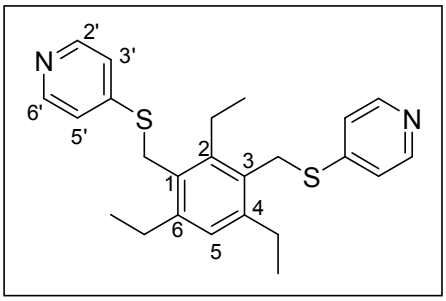

1,3-Di(8-quinolyloxymethyl)-2,4,6-triethylbenzene, ***2.44***

A mixture of **2.2** (1.01g, 2.9mmol), 8-hydroxyquinoline (0.87g, 6.0mmol), and potassium hydroxide (0.63g, 11.2mmol) was stirred in DMF (50mL) at 90°C for four weeks. The products were extracted with dichloromethane (50mL) and water (50mL), the organic layer was washed with water (2x150mL), dried with Na_2SO_4, and concentrated *in vacuo* to give a 1:2 mixture of the desired product and the corresponding alcohol. Column chromatography on silica gel eluting with chloroform failed to isolate **2.44** in sufficient purity.

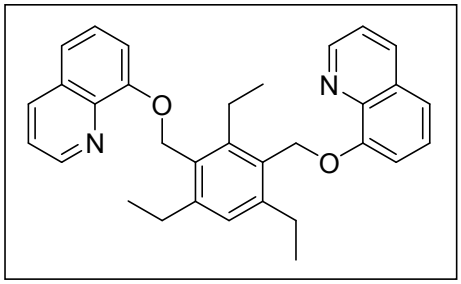

Preparation of the 1,3,5-trisubstituted-2,4,6-trimethylbenzene ligands

1,3,5-Tri(bromomethyl)-2,4,6-trimethylbenzene, ***3.12***

A mixture of mesitylene (7.0mL, 50.3mmol), paraformaldehyde (5.07g, 169mmol), and hydrobromic acid (45% solution in acetic acid, 35mL) was refluxed in acetic acid (29mL) for 18 hours. The orange solution was poured into 100mL of water, and the resulting white precipitate was filtered off to give **3.12** in adequate purity (17.3g, 87%), m.p. 180-181°C (lit.[201] 186°C). ^{1}H N.M.R. (300MHz, $CDCl_3$): δ 2.46 (9H, s, CH_3), 4.58 (6H, s, CH_2).

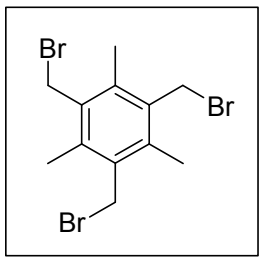

1,3,5-Tri[((4S,7R)-7,8,8-trimethyl-4,5,6,7-tetrahydro-4,7-methano-2H-indazol-2-yl)methyl]-2,4,6-trimethylbenzene, ***3.17***

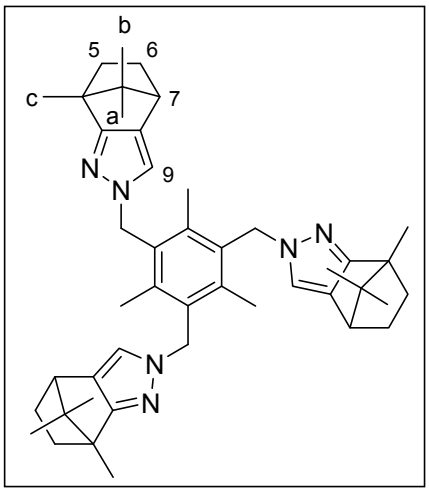

A mixture of **3.12** (0.21g, 0.5mmol), (4S,7R)-7,8,8-trimethyl-4,5,6,7-tetrahydro-4,7-methano-2H-indazole (0.29g, 1.7mmol), and 40% aqueous tetrabutylammonium hydroxide (3 drops) was refluxed in benzene (10mL) and 40% aqueous sodium hydroxide (2mL) for 46 hours. The organic layer was separated and the solvent removed *in vacuo* to give approximately a 2:1 mixture of **3.17** and its structural isomers as a white powder (0.29g, 79%), m.p. 95-99°C (Found: C, 77.01; H, 9.05; N, 11.92. $C_{45}H_{60}N_6.H_2O$ requires C, 76.88; H, 8.89; N, 11.95). ^{1}H N.M.R. (300MHz, $CDCl_3$): δ 0.63 (9H, s, a-CH_3), 0.92 (9H, s, b-CH_3), 1.02 (3H, m, endo-H5), 1.30 (9H, s, c-CH_3), 1.32 (3H, m, endo-H6), 1.81 (3H, m, exo-H5), 2.03 (3H, m, exo-H6), 2.28 (9H, s, CH_3), 2.64 (3H, d, H7), 5.36 (6H, s, CH_2), 6.43 (3H, s, H9).

1,3,5-Tri(4-pyridylsulfanylmethyl)-2,4,6-trimethylbenzene, ***3.33***

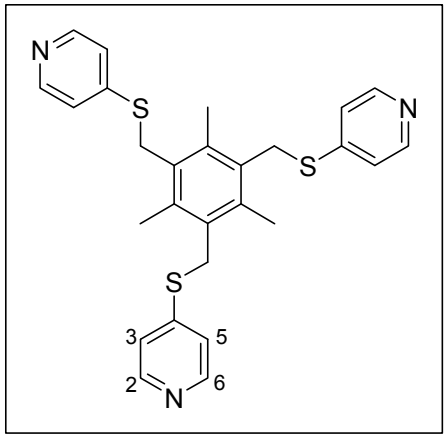

A mixture of **3.12** (2.01g, 5.0mmol), 4-mercaptopyridine (1.83g, 16.5mmol), and triethylamine (3mL) was stirred in acetonitrile (40mL) at 0°C on ice, slowly warming to room temperature over 20 hours. The yellow precipitate was filtered off. This crude product was dissolved in hot ethyl acetate, the insoluble impurities filtered off, and the remaining solvent removed *in vacuo* to give **3.33** as a pale orange powder (1.11g, 45%), m.p. 203-207°C (lit.[237] 229-231°C) (Found: C, 63.21; H, 5.67; N, 8.18. $C_{27}H_{27}N_3S_3.{}^4/_3H_2O$ requires C, 63.12; H, 5.82; N, 8.18). ^{1}H N.M.R. (300MHz, $CDCl_3$): δ 2.50 (9H, s, CH_3), 4.27 (6H, s, CH_2), 7.20 (6H, d, H3,5), 8.45 (6H, d, H2,6).

1,3,5-Tri(8-quinolyloxymethyl)-2,4,6-trimethylbenzene, ***3.41***

A solution of **3.12** (1.00g, 2.5mmol) in DMF (21mL) was added slowly to a hot solution of 8-hydroxyquinoline (1.11g, 7.7mmol) and potassium hydroxide (0.46g,

8.2mmol) in DMF (22mL) and the resulting solution heated at 90°C for four hours. After cooling the KBr was filtered off and the product extracted from the filtrate with dichloromethane and water. The organic layer was washed multiple times with water to remove any remaining DMF. The DCM was removed *in vacuo* to give **3.41** as a crimson powder (1.09g, 74%), m.p.187-193°C (lit.[244,247] 200-202°C) ^{1}H N.M.R. (300MHz, $CDCl_3$): δ 2.51 (9H, s, CH_3), 5.33 (6H, s, CH_2), 7.16-7.49 (12H, m, H3,6,7,8), 8.14 (3H, t, H4), 8.91 (3H, d, H2). TOF-MS: Found M^+ 592.2438, $C_{39}H_{34}N_3O_3$ requires M^+ 592.2600.

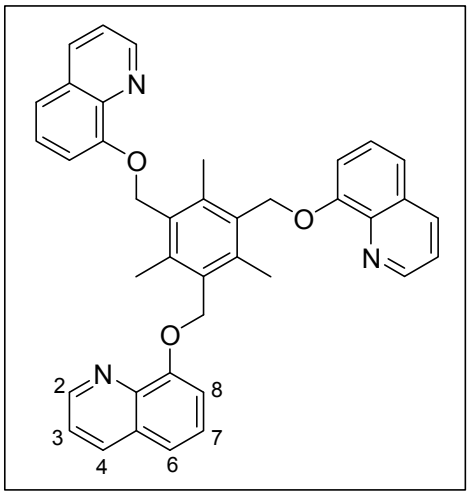

Preparation of the 1,3,5-trisubstituted-2,4,6-triethylbenzene ligands

1,3,5-Tri(bromomethyl)-2,4,6-triethylbenzene, ***2.3***

Zinc powder (1.31g, 20.0mmol) and hydrobromic acid (45% solution in acetic acid, 10mL) were stirred together in acetic acid (26mL) for 20 minutes to get a cloudy yellow solution. 1,3,5-triethylbenzene (2.9mL, 15.4mmol), paraformaldehyde (5.00g, 167mmol), and hydrobromic acid (45% solution in acetic acid, 30mL) were added and the resulting red solution was refluxed for 64 hours. The precipitate which formed upon cooling was filtered off, and the filtrate returned to the reaction flask and refluxed for another 22 hours before more product was obtained by cooling. Again the filtrate was returned to the reaction flask and refluxed for another two days, before the last batch of precipitate was filtered off after cooling. The batches were combined to give **2.3** as a light brown solid in adequate purity (5.28g, 74%), m.p.160-162°C (lit. [109,113-117] 173-174°C). ^{1}H N.M.R. (300MHz, $CDCl_3$): δ 1.34 (9H, t, CH_3), 2.94 (6H, q, 2,4,6-CH_2), 4.58 (6H, s, 1,3,5-CH_2).

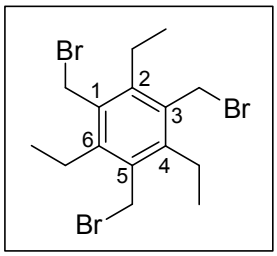

1,3,5-Tri(pyrazol-1-ylmethyl)-2,4,6-triethylbenzene, ***3.5***

A mixture of **2.3** (0.250g, 0.6mmol), pyrazole (0.159g, 2.3mmol), and 40% aqueous tetrabutylammonium hydroxide (2 drops) was refluxed in benzene (10mL) and 40% aqueous sodium hydroxide (2mL) for 40 hours. The organic layer was separated, dried

with Na_2SO_4, and the solvent removed *in vacuo* to give **3.5** as a light brown powder (0.197g, 78%), m.p. 113-116°C (lit.[55] 125-126°C) (Found: C, 71.32; H, 7.83; N, 18.50. $C_{24}H_{30}N_6.{}^3/_4H_2O.{}^1/_2C_6H_6$ requires C, 71.26; H, 7.64; N, 18.47). ^{1}H N.M.R. (300MHz, $CDCl_3$): δ 0.96 (9H, t, CH_3), 2.71 (6H, q, 2,4,6-CH_2), 5.45 (6H, s, 1,3,5-CH_2), 6.20 (3H, t, H4'), 6.98 (3H, d, H5'), 7.55 (3H, d, H3'). TOF-MS: Found M^+ 404.2649, $C_{24}H_{32}N_6$ requires M^+ 404.2688. Crystals grown from slow evaporation of an acetone solution also containing silver hexafluorophosphate were shown by X-ray crystallography to be the hexafluorophosphate salt of this mono-protonated ligand.

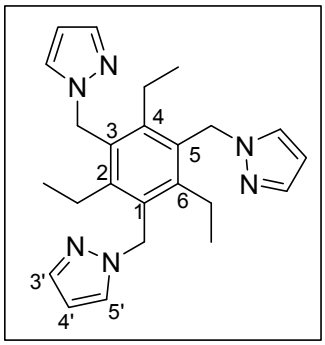

1,3,5-Tri[3-(2'-pyridyl)pyrazol-1-ylmethyl]-2,4,6- triethylbenzene, ***3.24***

A mixture of **2.3** (1.39g, 3.2mmol), **5.1** (1.58g, 10.6mmol), and 40% aqueous tetrabutylammonium hydroxide (6 drops) was refluxed in benzene (50mL) and 40% aqueous sodium hydroxide (10mL) for 46 hours. The organic layer was separated, dried with Na_2SO_4, and the solvent removed *in vacuo* to give **3.24** as a pale yellow powder (1.99g, 96%), m.p. 63-70°C (Found: C, 73.85; H, 6.48; N, 19.17. $C_{39}H_{39}N_9.{}^1/_4H_2O.{}^1/_4C_6H_6$ requires C, 73.95; H, 6.28; N, 19.16). ^{1}H N.M.R. (300MHz, $CDCl_3$): δ 1.07 (9H, t, CH_3), 2.78 (6H, q, 2,4,6-CH_2), 5.55 (6H, s, 1,3,5-CH_2), 6.81 (3H, d, H4'), 7.02 (3H, d, H5'), 7.20 (3H, dd, H5"), 7.72 (3H, t, H4"), 7.91 (3H, d, H3"), 8.64 (3H, d, H6"). TOF-MS: Found M^+ 634.3411, $C_{39}H_{40}N_9$ requires M^+ 634.3407.

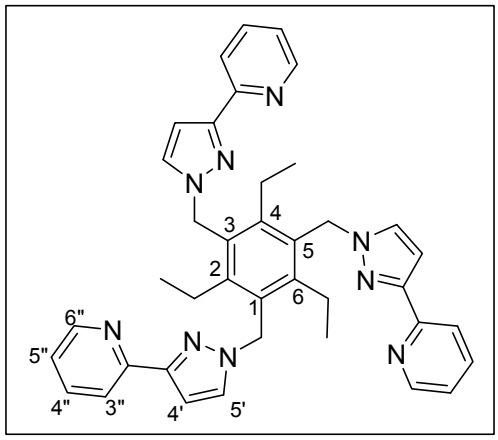

1,3,5-Tri(4-pyridylsulfanylmethyl)-2,4,6-triethylbenzene, ***3.34***

A mixture of **2.3** (1.00g, 2.3mmol), 4-mercaptopyridine (0.84g, 7.6mmol), and triethylamine (0.65mL) was stirred in acetonitrile (30mL) at 0°C on ice, before slowly warming to room temperature over 24 hours. The white precipitate was filtered off to give **3.34** in adequate purity as a white powder (0.73g, 60%), m.p. 148-151°C. (Found: C, 57.07; H, 5.81; N, 6.60. $C_{30}H_{33}N_3S_3.H_2O.HBr$ requires C, 57.13; H, 5.75; N, 6.66).

^{1}H N.M.R. (300MHz, $CDCl_3$): δ 1.33 (9H, t, CH_3), 2.87 (6H, q, 2,4,6-CH_2), 4.23 (6H, s, 1,3,5-CH_2), 7.20 (6H, d, H3',5'), 8.46 (6H, d, H2',6'). TOF-MS: Found M^+ 532.1925, $C_{30}H_{34}N_3S_3$ requires M^+ 532.1915. Crystals grown from the slow evaporation of a dichloromethane solution of ligand **3.34** and silver hexafluorophosphate were shown by X-ray crystallography to be the hexafluorophosphate salt of ligand **3.34**.

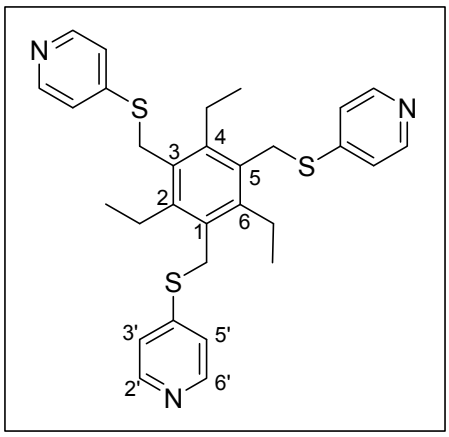

1,3,5-Tri(8-quinolyloxymethyl)-2,4,6-triethylbenzene, ***3.42***

A solution of **2.3** (1.00g, 2.3mmol) in DMF (24mL) was added slowly to a hot solution of 8-hydroxyquinoline (1.01g, 7.0mmol) and potassium hydroxide (0.42g, 7.5mmol) in DMF (23mL) and the resulting solution heated at 90°C for eight days. After cooling the product was extracted from the red solution with dicholoromethane and water. The organic layer was washed multiple times with water to remove any remaining DMF. The dichloromethane was removed *in vacuo* to give the crude product as a thick red oil. The product was purified by washing a chloroform solution with dilute sodium hydroxide to precipitate **3.42** as a light brown solid (0.26g, 18%), m.p.119-125°C (lit.[247] oil). Crystals grown from hot acetonitrile were suitable for X-ray crystallography. ^{1}H N.M.R. (300MHz, $CDCl_3$): δ 1.29 (9H, t, CH_3), 2.97 (6H, q, 2,4,6-CH_2), 5.36 (6H, s, 1,3,5-CH_2), 7.30-7.54 (12H, m, H3',6',7',8'), 8.12 (3H, d, H4'), 8.92 (3H, d, H2'). TOF-MS: Found M^+ 634.3069, $C_{42}H_{40}N_3O_3$ requires M^+ 634.3070.

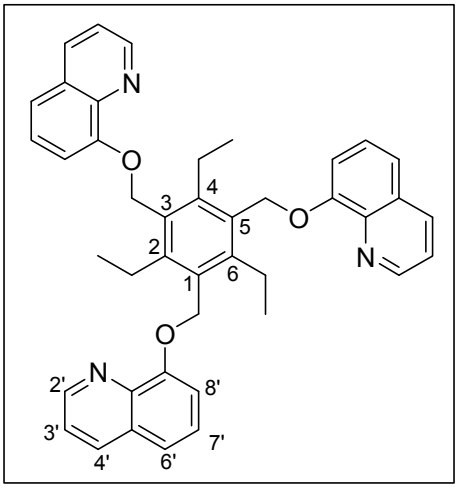

Preparation of the 1,3,5-trisubstituted-2,4,6-trimethoxybenzene ligands

1,3,5-Tri(bromomethyl)-2,4,6-trimethoxybenzene, ***3.14***

A mixture of 1,3,5-trimethoxybenzene (7.55g, 45mmol), paraformaldehyde (4.07g, 137mmol), and hydrobromic acid (45% solution in acetic acid, 25mL) was refluxed in

acetic acid (100mL) for 23 hours. Initially a pink precipitate formed which clogged up the reaction, but this dissolved upon heating. The deep red solution was cooled for 45 minutes, then poured into 200mL of ice water. The resulting red precipitate was filtered off, then dissolved in chloroform and washed with water to remove residual acetic acid. The chloroform was removed *in vacuo*, to give **3.14** in adequate purity as a red solid (12.40g, 61%), m.p. 102-105°C (lit.[220] 126°C). ^{1}H N.M.R. (500MHz, $CDCl_3$): δ 4.15 (9H, s, CH_3), 4.60 (6H, s, CH_2).

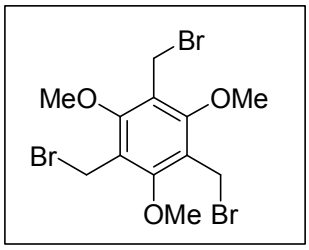

1,3,5-Tri(pyrazol-1-ylmethyl)-2,4,6-trimethoxybenzene, ***3.18***

Method A: A mixture of **3.14** (1.89g, 4.2mmol), pyrazole (0.86g, 12.9mmol), and 40% aqueous tetrabutylammonium hydroxide (5 drops) was refluxed in benzene (75mL) and 40% aqueous sodium hydroxide (10mL) for three days. The red precipitate in the organic layer was filtered off, while the filtrate was dried with Na_2SO_4, and the solvent removed *in vacuo* to give **3.18** as an orange oil which could not be recrystallised (1.25g, 73%), (Found: C, 60.97; H, 6.02; N, 17.49. $C_{21}H_{24}N_6O_3.{}^1/_2C_6H_6.{}^3/_2H_2O$ requires C, 60.75; H, 6.37; N, 17.71). ^{1}H N.M.R. (500MHz, $CDCl_3$): δ 3.68 (9H, s, CH_3), 5.38 (6H, s, CH_2), 6.32 (3H, t, H4), 7.47 (3H, d, H5), 7.78 (3H, d, H3).

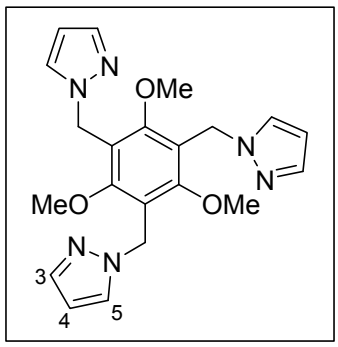

Method B: A mixture of **3.14** (0.81g, 1.8mmol), pyrazole (0.40g, 5.8mmol), and potassium carbonate (1.61g) was heated in DMF (15mL) at 90°C for 20 hours, then cooled. The crude product was extracted from the red solution with dichloromethane (30mL) and water (50mL), then the organic layer was washed with water (3x50mL), and the solvent removed *in vacuo* to give a red oil that was less pure than the product obtained in method A (0.16g, 23%).

1,3,5-Tri[3-(2'-pyridyl)pyrazol-1-ylmethyl]-2,4,6- trimethoxybenzene, ***3.25***

A mixture of **3.14** (0.77g, 1.7mmol), **5.1** (0.61g, 4.1mmol), and potassium carbonate (1.55g) was heated in DMF (16mL) at 90°C for 20 hours, then cooled. The crude product was extracted from the red solution with dichloromethane (30mL) and water (50mL), then the organic layer was washed with water (3x50mL), and the solvent

removed *in vacuo* to give a red oil. Recrystallisation from dichloromethane and ethyl acetate removed some impurity and provided a dark red solid after solvent removal (0.52g, 58%), m.p.89-96°C. ^{1}H N.M.R. (500MHz, $CDCl_3$): δ 3.75 (9H, t, CH_3), 5.45 (6H, q, CH_2), 6.88 (3H, d, H4), 7.17 (3H, dd, H5'), 7.50 (3H, d, H5), 7.67 (3H, t, H4'), 7.89 (3H, d, H3'), 8.59 (3H, d, H6'). TOF-MS: Found M^+ 640.2775, $C_{36}H_{34}N_9O_3$ requires M^+ 640.2785.

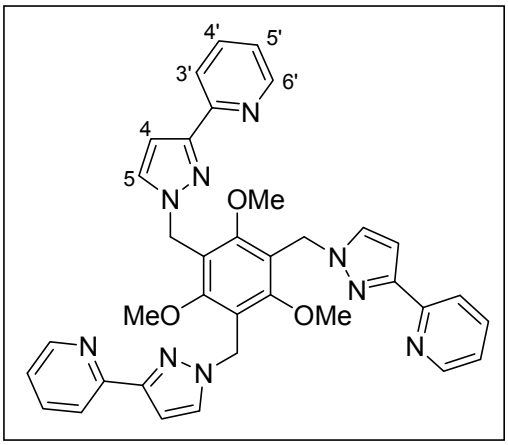

1,3,5-Tri(4-pyridylsulfanylmethyl)-2,4,6-trimethoxybenzene, ***3.35***

A mixture of **3.14** (1.98g, 4.4mmol), 4-mercaptopyridine (1.47g, 13.2mmol), and triethylamine (1.0mL) was stirred in acetonitrile (85mL) at 0°C on ice, before slowly warming to room temperature over 24 hours. The reaction was incomplete at this point so the solution was refluxed for 16 hours to give an orange solution. This was cooled, the precipitate filtered off, and the solvent removed from the filtrate to give the crude product as a bright orange solid. This was purified by stirring in ethyl acetate, filtering and removing the solvent in the filtrate *in vacuo*. Then a chloroform solution was washed with dilute sodium hydroxide to give **3.35** as an orange oil (1.74g, 74%), (Found: C, 56.77; H, 5.05; N, 6.53. $C_{27}H_{27}N_3O_3S_3.{}^2/_3C_4H_8O_2.{}^1/_3CHCl_3$ requires C, 56.63; H, 5.18; N, 6.60). ^{1}H N.M.R. (500MHz, $CDCl_3$): δ 3.97 (9H, s, CH_3), 4.28 (6H, s, CH_2), 7.22 (6H, d, H3,5), 8.44 (6H, d, H2,6).

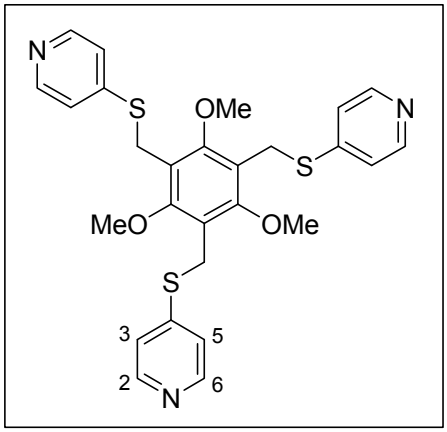

1,3,5-Tri(8-quinolyloxymethyl)-2,4,6-trimethoxybenzene, ***3.43***

A solution of **3.14** (1.04g, 2.3mmol) in DMF (24mL) was added slowly to a hot solution of 8-hydroxyquinoline (1.05g, 7.2mmol) and potassium hydroxide (0.40g, 7.1mmol) in DMF (30mL) and the resulting solution heated at 90°C for 24 hours. After cooling the product was extracted from the red solution with chloroform (50mL) and water (150mL). The organic layer was washed with water (4x150mL) to remove any

remaining DMF. The chloroform was removed *in vacuo* to give **3.43** as an oily dark red solid (1.02g, 70%), m.p. 62-65°C. (Found: C, 69.51; H, 5.34; N, 6.14. $C_{39}H_{33}N_3O_6.2H_2O$ requires C, 69.34; H, 5.54; N, 6.22). ^{1}H N.M.R. (500MHz, $CDCl_3$): δ 4.02 (9H, s, CH_3), 5.37 (6H, s, CH_2), 7.18 (3H, d, H6), 7.33-7.51 (9H, m, H3,7,8), 8.16 (3H, d, H4), 8.85 (3H, d, H2).

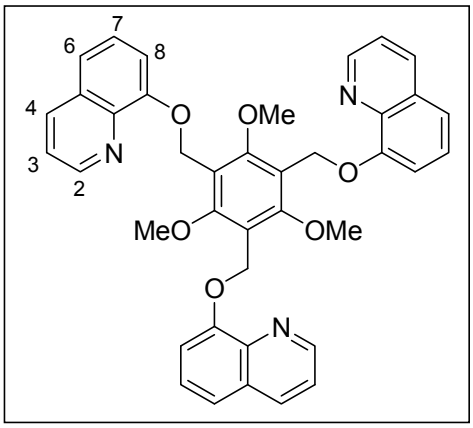

Preparation of the 4,4',4"-trisubstituted-1,3,5-triphenylbenzene ligands

4,4',4''-Trimethyl-1,3,5-triphenylbenzene, ***4.7***

4-Methylacetophenone (13.4mL, 100mmol) was refluxed with triflic acid (0.05mL, 5.65mmol) and toluene (70mL) for three days, using a Dean-Stark trap to remove any water produced during the course of the reaction. After cooling the crystalline product was filtered off, and the remaining filtrate reduced in volume so more product could be precipitated. The crude product was recrystallised from 2:1 dichloromethane:methanol to give **4.7** as yellow crystals (4.67g, 54%), m.p. 169-170°C (lit.[268,269] 178-180°C) ^{1}H N.M.R. (300MHz, $CDCl_3$): δ 2.42 (9H, s, CH_3), 7.28 (6H, d, H3',5'), 7.60 (6H, d, H2',6'), 7.73 (3H, s, H2,4,6).

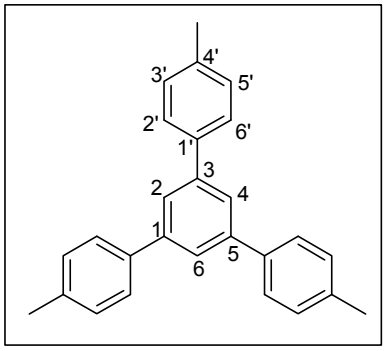

4,4',4''-Tri(bromomethyl)-1,3,5-triphenylbenzene, ***4.8***

A mixture of **4.7** (4.67g, 13.0mmol), *N*-bromosuccinimide (8.40g, 40.2mmol), benzoyl peroxide (66mg) and tetrachloromethane (70mL) was refluxed for five hours, under a 100 watt light bulb. The yellow precipitate was filtered off and discarded, while the product crystallised out of the filtrate upon slow evaporation, to give **4.8** as a pale yellow solid (5.63g, 74%), m.p. 164-166°C

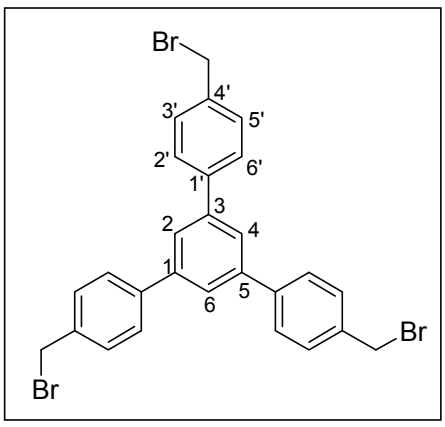

(lit.[262,269] 194-196°C). ^{1}H N.M.R. (300MHz, $CDCl_3$): δ 4.57 (6H, s, CH_2), 7.51 (6H, d, H3',5'), 7.67 (6H, d, H2',6'), 7.77 (3H, s, H2,4,6).

4,4',4''-Tri(pyrazol-1-ylmethyl)-1,3,5-triphenylbenzene, ***4.9***

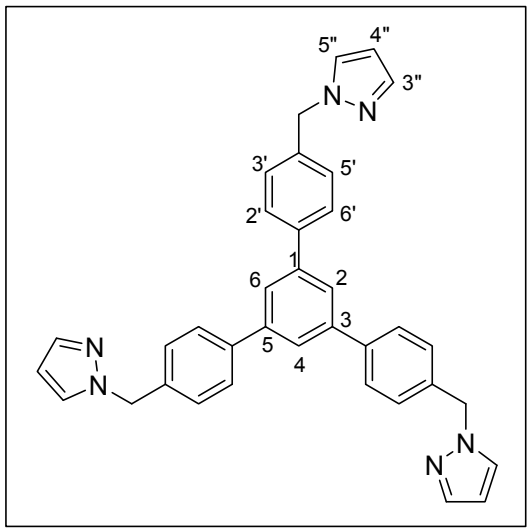

A mixture of **4.8** (5.63g, 9.6mmol), pyrazole (2.16g, 32.0mmol), and 40% aqueous tetrabutylammonium hydroxide (10 drops) was refluxed in benzene (105mL) and 40% aqueous sodium hydroxide (22mL) for four days. The organic layer was separated, dried with Na_2SO_4, and the solvent removed *in vacuo* to give **4.9** as a light yellow powder (4.97g, 94%), m.p. 55-65°C (Found: C, 71.60; H, 5.33; N, 12.70. $C_{36}H_{30}N_6.CH_2Cl_2.^1/_2C_6H_6$ requires C, 71.64; H, 5.26; N, 12.53). ^{1}H N.M.R. (300MHz, $CDCl_3$): δ 5.28 (6H, s, CH_2), 6.21 (3H, t, H4"), 7.21 (6H, d, H3',5'), 7.34 (3H, d, H3"), 7.50 (6H, d, H2',6'), 7.54 (3H, d, H3"), 7.60 (3H, s, H2,4,6).

4,4',4''-Tri[3-(2'-pyridyl)pyrazol-1-ylmethyl]-1,3,5-triphenylbenzene, ***4.13***

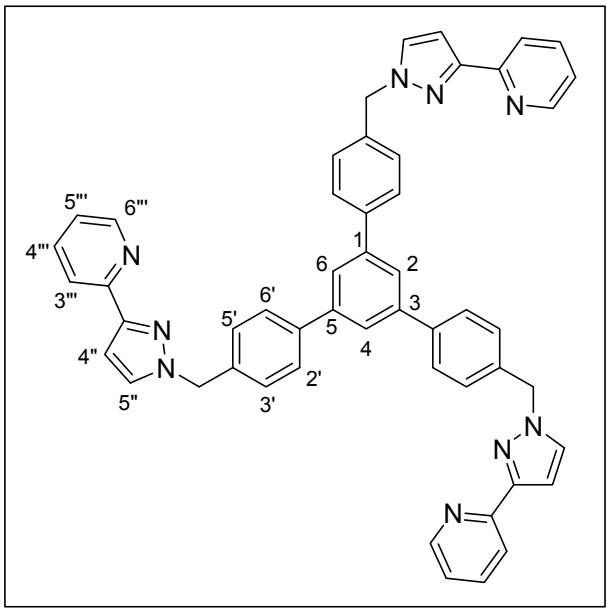

A mixture of **4.8** (1.72g, 2.9mmol), **5.1** (1.47g, 9.8mmol), and 40% aqueous tetrabutylammonium hydroxide (6 drops) was refluxed in benzene (50mL) and 40% aqueous sodium hydroxide (10mL) for three days. The organic layer was separated, dried with Na_2SO_4, and the solvent removed *in vacuo* to give **4.13** as a fluffy light yellow solid (1.96g, 85%), m.p. 115-120°C (Found: C, 74.16; H, 5.19; N, 15.58. $C_{51}H_{39}N_9.^5/_2H_2O$ requires C, 74.43; H, 5.39; N, 15.32). ^{1}H N.M.R. (300MHz, $CDCl_3$): δ 5.45 (6H, s, CH_2), 7.02 (3H, d, H4"), 7.24 (6H, d, H3',5'), 7.36 (3H, dd, H5"'), 7.47

(3H, d, H5”), 7.65 (6H, d, H2’,6’), 7.71 (3H, s, H2,4,6), 7.74 (3H, t, H4”’), 8.00 (3H, d, H3”’), 8.65 (3H, d, H6”’).

4,4’,4’’-Tri(4-pyridylsulfanylmethyl)-1,3,5-triphenylbenzene, ***4.16***

A mixture of **4.8** (1.02g, 1.7mmol), 4-mercaptopyridine (0.63g, 5.7mmol), and triethylamine (1.0mL) was stirred in acetonitrile (30mL) at 0^{o}C on ice, before slowly warming to room temperature over two days. The solvent was removed *in vacuo*, and the product separated out by dissolving in ethyl acetate and filtering off the insoluble impurities. The solvent from the filtrate was removed *in vacuo* to give crude **4.16** as a red oil (1.15g, 79%) Attempts were made to purify this oil further on an alumina column eluting with chloroform, but most of the product was lost. Some more highly substitiuted side products were separated and identified by ^{1}H NMR and mass spectroscopy. Pure **4.16** is also a red oil (0.12g, 10%), (Found: C, 71.36; H, 5.15; N, 5.98. $C_{42}H_{33}N_3S_3.{}^{1}/_{4}CHCl_3.{}^{1}/_{2}CH_3OH$ requires C, 71.14; H, 4.92; N, 5.82). ^{1}H N.M.R. (300MHz, $CDCl_3$): δ 4.28 (6H, s, CH_2), 7.15 (6H, d, H3’,5’), 7.50 (6H, H3”,5”), 7.65 (6H, d, H2’,6’), 7.74 (3H, s, H2,4,6), 8.40 (6H, d, H2”,6”).

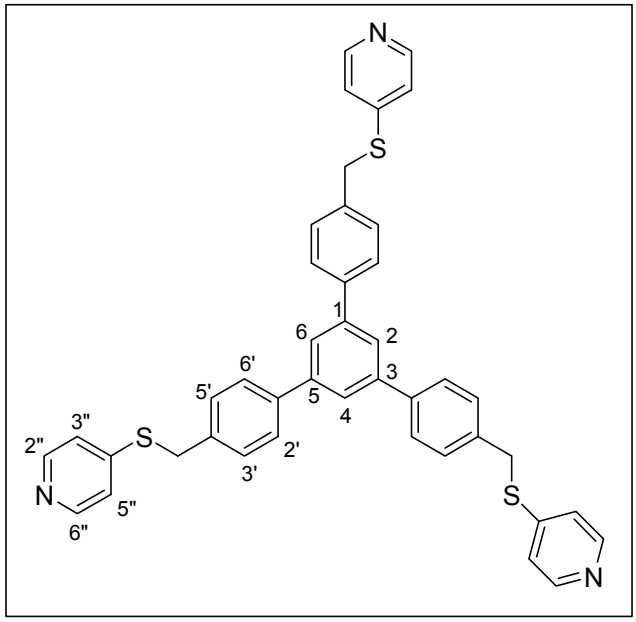

Also isolated from the column were the four- and five-armed side products **4.17** and **4.18** as red oils. **4.17**: ^{1}H N.M.R. (300MHz, $CDCl_3$): δ 4.28 (4H, s, CH_2), 5.89 (1H, s, CH), 7.17 (6H, dd, H3’,5’), 7.51 (4H, H3”,5”), 7.65 (6H, d,

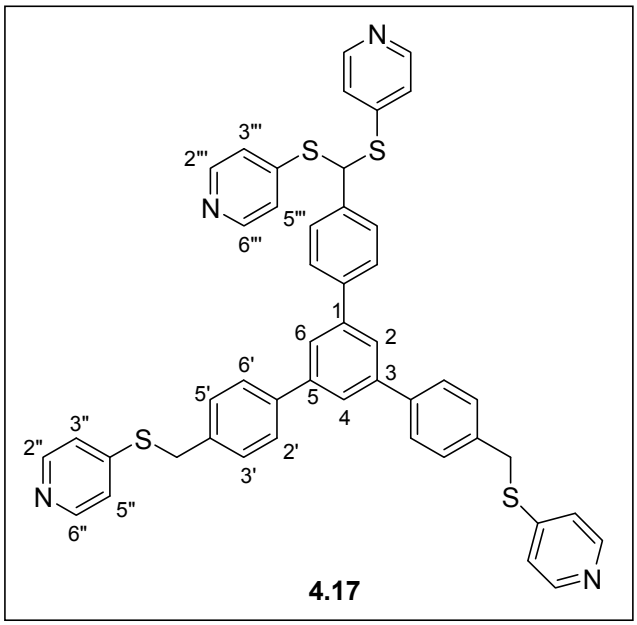

4.17

H2',6'), 7.69 (3H, s, H2,4,6), 7.74 (4H, d, H3''',5'''), 8.40 (4H, d, H2'',6''), 8.45 (4H, d, H2''',6'''). TOF-MS: Found M^+ 785.2697, $C_{47}H_{36}N_4S_4$ requires M^+ 785.1901.

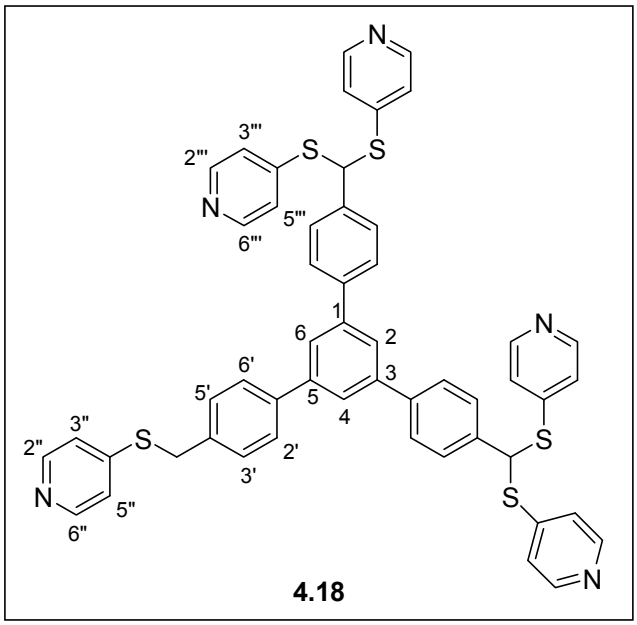

4.18: ^{1}H N.M.R. (300MHz, $CDCl_3$): δ 4.29 (2H, s, CH_2), 5.89 (2H, s, CH), 7.19 (6H, d, H3',5'), 7.51 (2H, H3'',5''), 7.66 (6H, d, H2',6'), 7.70 (3H, s, H2,4,6), 7.75 (8H, d, H3'',5''), 8.40 (2H, d, H2'',6''), 8.45 (8H, d, H2''',6'''). TOF-MS: Found M^+ 894.1902, $C_{52}H_{39}N_5S_5$ requires M^+ 894.1887.

Attempted synthesis of 4,4',4''-Tri(8-quinolyloxymethyl)-1,3,5-triphenylbenzene, ***4.22***

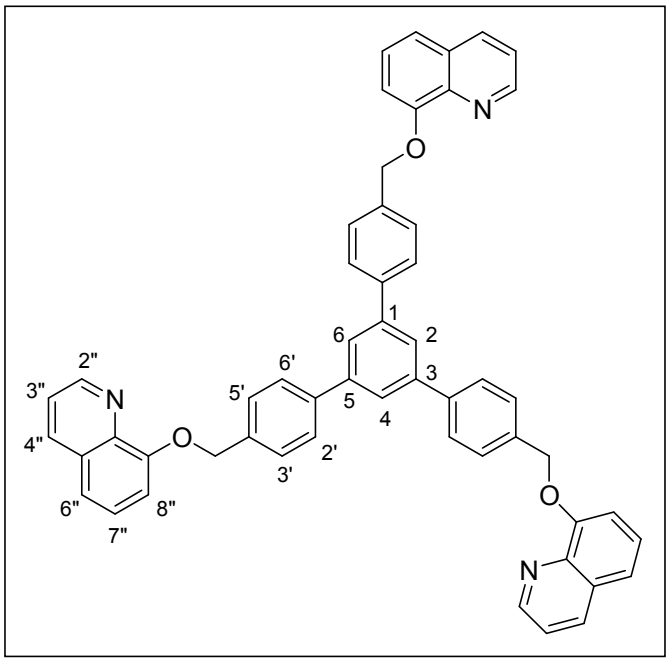

8-Hydroxyquinoline (0.38g, 2.6mmol) and potassium hydroxide (0.159g, 2.8mmol) were dissolved in DMF (16mL) with heating to give an orange solution. A solution of **4.8** (0.500g, 0.86mmol) in DMF (10mL) was added and the reaction mixture heated at 95°C for six hours. The cloudy orange solution was cooled overnight before extraction with dichloromethane (75mL), and water (150mL) basified with a little sodium hydroxide. The organic layer was separated off, washed with water (3x150mL), dried with Na_2SO_4, filtered, and the solvent removed *in vacuo* to give an orange oil still wet with DMF. Over time 8-hydroxyquinoline crystallised out of this oil, leaving the alcohol **4.19** to be separated out.

Preparation of the 4,4',4"-trisubstituted-1,3,5-triphenyltriazine ligands

4,4',4''-Trimethyl-1,3,5-triphenyltriazine, ***4.25***

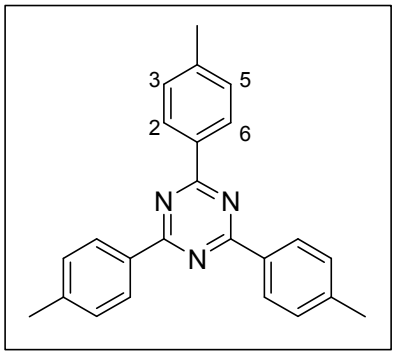

Chlorosulfonic acid (16mL) was cooled to 0°C on ice before p-toluonitrile (7.00g, 60mmol) was added slowly. The resulting green solution was stirred at 0°C for two hours, then transferred to the fridge overnight. The next morning the reaction was quenched by pouring into 100mL ice water (caution – violent reaction) and the precipitate filtered off to give **4.25** as a cream coloured solid (6.79g, 97%), m.p. 265-275°C (lit.[278,319] 278-280°C). ^{1}H N.M.R. (300MHz, $CDCl_3$): δ 2.48 (9H, s, CH_3), 7.37 (6H, d, H3,5), 8.66 (6H, d, H2,6).

4,4',4''-Tri(bromomethyl)-1,3,5-triphenyltriazine, ***4.26***

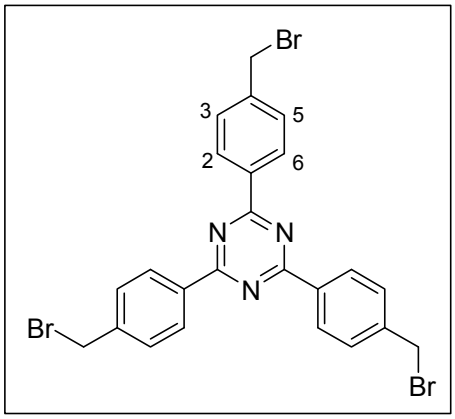

A mixture of **4.25** (0.99g, 2.8mmol), *N*-bromosuccinimide (1.77g, 10.0mmol), benzoyl peroxide (7.4mg) and tetrachloromethane (15mL) was refluxed for three hours, under a 100 watt light bulb for the first 15 minutes. The precipitate was filtered off to give **4.26** and a tetrabrominated side product as a fluffy white solid (1.60g, 96%), m.p. 178-180°C (Found: C, 47.67; H, 3.10; N, 6.76. $C_{24}H_{18}N_3Br_3.H_2O$ requires C, 47.56; H, 3.33; N, 6.93). ^{1}H N.M.R. (300MHz, $CDCl_3$): δ 4.60 (6H, s, CH_2), 7.60 (6H, d, H3,5), 8.72 (6H, d, H2,6).

4,4',4''-Tri(pyrazol-1-ylmethyl)-1,3,5-triphenyltriazine, ***4.27***

A mixture of **4.26** (1.60g, 2.7mmol), pyrazole (0.20g, 3.0mmol), and 40% aqueous tetrabutylammonium hydroxide (4 drops) was refluxed in benzene (32mL) and 40% aqueous sodium hydroxide (6mL) for 42 hours. The organic layer was separated, dried with Na_2SO_4, and the solvent removed *in vacuo* to give an approximately 1:1 mixture of **4.27** and side product **4.28** as a yellow powder (0.57g, 38%), m.p. 75-85°C. Separation of these two products was not attempted. ^{1}H N.M.R. (300MHz, $CDCl_3$): δ 5.45 (6H, s, CH_2), 6.38 (3H, t, H4'), 7.37 (3H, d, H5'), 7.46 (3H, d, H3'), 7.62 (6H, d, H3,5), 8.68 (6H, d, H2,6). TOF-MS: Found M^+ 550.2047, $C_{33}H_{28}N_9$ requires M^+ 550.2468. Also

found M^+ 640.0307, side product $C_{30}H_{23}N_7Br_2$ requires 640.0460. Slow evaporation of a dichloromethane solution of this mixture grew small yellow crystals of **4.27** suitable for X-ray crystallography.

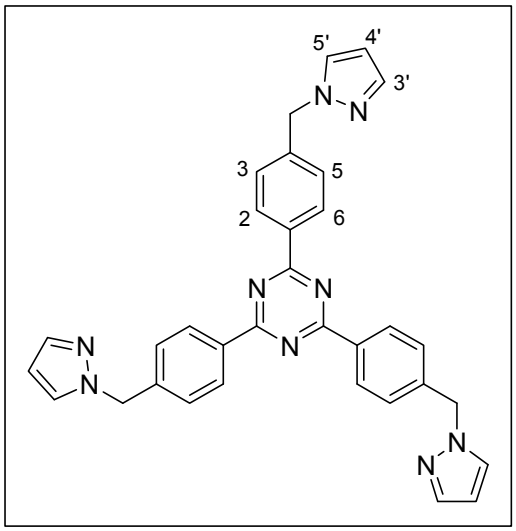

4,4',4''-Tri[3-(2'-pyridyl)pyrazol-1-ylmethyl]-1,3,5-triphenylazine, ***4.31***

A mixture of **4.26** (0.34g, 0.58mmol), **5.1** (0.27g, 1.8mmol), and 40% aqueous tetrabutylammonium hydroxide (3 drops) was refluxed in benzene (33mL) and 40% aqueous sodium hydroxide (4mL) for three days. The organic layer was separated, dried with Na_2SO_4, and the solvent removed *in vacuo* to give **4.31** as a yellow oil (0.36g, 80%). Mulitple recrystallisations from methanol and dichloromethane, followed by recrystallisation from an ethanol, pentane, chloroform mixture gave **4.31** as a fluffy yellow solid (0.18g, 39%), m.p. 101-104°C. (Found: C, 67.66; H, 5.01; N, 18.12. $C_{48}H_{36}N_{12}.2CH_3CH_2OH.^1/_2CHCl_3$ requires C, 67.61; H, 5.24; N, 18.02). ^{1}H N.M.R. (500MHz, $CDCl_3$): δ 5.47 (6H, s, CH_2), 6.98 (3H, d, H4'), 7.21 (3H, dd, H5"), 7.38 (6H, d, H3,5), 7.48 (3H, d, H5'), 7.73 (3H, t, H4"), 7.98 (3H, d, H3"), 8.61 (6H, d, H2,6), 8.66 (3H, d, H6"). Found M^+ 781.3259, $C_{48}H_{37}N_{12}$ requires M^+ 781.3264.

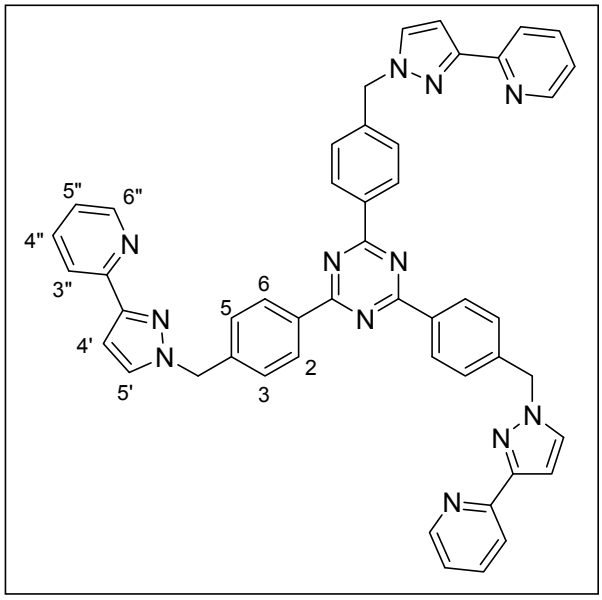

Preparation of the tri(4-substituted-phenyl)methanol ligands

Tri(4-methylphenyl)methanol, ***4.35***

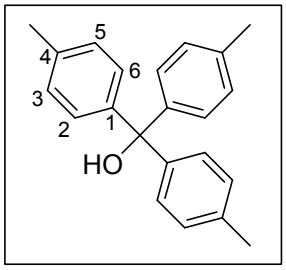

Magnesium turnings (6.62g, 270mmol) were stirred overnight to a fine powder. Dry ether (100mL) was added to the reaction flask and 4-bromotoluene (47.3g, 280mmol) was added dropwise over two hours to form a cloudy solution. A few drops of dibromoethane were added with the first of the 4-bromotoluene to initialise the formation of the Grignard reagent. The resulting green solution was stirred for 30 minutes, then heated for an hour to ensure the first step of the reaction was complete. A mixture of ethyl p-toluate (20.5mL, 128mmol) and benzene (15mL) was added dropwise over 30 minutes. The reaction was stirred overnight to ensure reaction was complete, before the reaction was quenched by pouring into a beaker containing concentrated sulfuric acid (20mL) and ice (600g). The yellow benzene layer was decanted off, then the aqueous layer was washed twice with benzene in a separating funnel. The combined benzene extracts were washed with saturated $NaHCO_3$ solution (100mL), dried with Na_2SO_4, filtered, and the solvent was removed to give **4.35** as a yellow oily solid (35.4g, 91%), m.p. 64-69^{o}C (lit.[265] 92-94^{o}C). ^{1}H N.M.R. (300MHz, $CDCl_3$): δ 2.32 (9H, s, CH_3), 7.09 (6H, d, H3,5), 7.15 (6H, d, H2,6).

Tri(4-bromomethylphenyl)methanol, ***4.36***

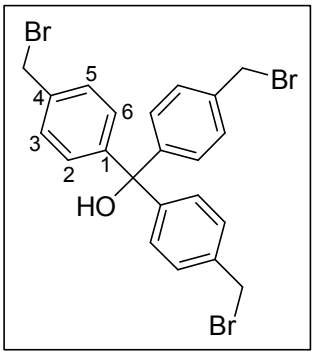

A mixture of **4.35** (20.28g, 67mmol), *N*-bromosuccinimide (36.33g, 204mmol), AIBN (53.2mg), and tetrachloromethane (150mL) was refluxed for 12 hours. Over the next few days benzoyl peroxide (600mg) and additional *N*-bromosuccinimide (5.50g) were added to the reaction solution as neccessary while a 100 watt light shone on the solution until reaction was complete. The solution was cooled and the succinimide filtered off. The solvent in the filtrate was removed *in vacuo*, to give **4.36** as a thick brown oil (36.0g, 99%), (Found: C, 46.59; H, 3.91. $C_{22}H_{19}OBr_3.3H_2O$ requires C, 46.67; H, 3.92). ^{1}H N.M.R. (300MHz, $CDCl_3$): δ 4.46 (6H, s, CH_2), 7.31 (6H, d, H2,6), 7.38 (6H, d, H3,5).

Tri(4-pyrazo-1-ylmethylphenyl)methanol, ***4.37***

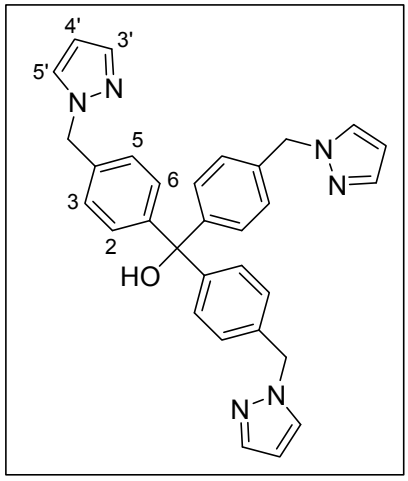

A mixture of **4.36** (2.74g, 5.1mmol), pyrazole (1.05g, 15.4mmol), and 40% aqueous tetrabutylammonium hydroxide (5 drops) was refluxed in benzene (50mL) and 40% aqueous sodium hydroxide (10mL) for three days. The organic layer was separated, dried with Na_2SO_4, and the solvent removed *in vacuo* to give **4.37** as a thick yellow oil (1.78g, 70%), (Found: C, 71.88; H, 5.61; N, 14.62. $C_{31}H_{28}N_6O.^1/_2H_2O.^1/_2NaOH.^1/_2C_6H_6$ requires C, 71.81; H, 5.76; N, 14.78). ^{1}H N.M.R. (300MHz, $CDCl_3$): δ 5.29 (6H, s, CH_2), 6.27 (3H, t, H4'), 7.08 (6H, d, H3,5), 7.24 (3H, d, H5'), 7.36 (6H, d, H2,6), 7.54 (3H, d, H3'). TOF-MS: Found M^+ 501.2413, $C_{31}H_{29}N_6O$ requires M^+ 501.2403.

Tri[4-(3-[2'-pyridyl]pyrazol-1-ylmethyl)phenyl]methanol, ***4.38***

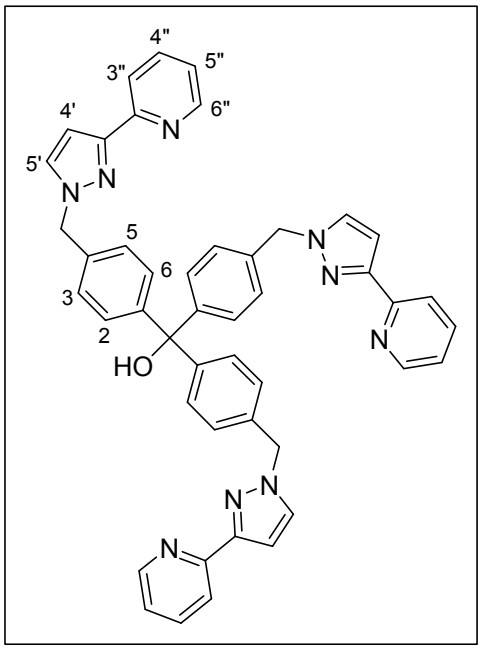

A mixture of **4.36** (2.88g, 5.3mmol), **5.1** (2.41g, 16.1mmol), and 40% aqueous tetrabutylammonium hydroxide (5 drops) was refluxed in benzene (50mL) and 40% aqueous sodium hydroxide (10mL) for three days. The organic layer was separated, dried with Na_2SO_4, and the solvent removed *in vacuo* to give **4.38** as a fluffy yellow solid (2.35g, 60%), m.p. 72-77^{o}C (Found: C, 72.71; H, 5.17; N, 16.98. $C_{46}H_{37}N_9O.^3/_4H_2O$ requires C, 73.09; H, 5.29; N, 16.68). ^{1}H N.M.R. (300MHz, $CDCl_3$): δ 5.37 (6H, s, CH_2), 6.89 (3H, d, H4'), 7.18 (6H, d, H3,5), 7.21 (3H, dd, H5"), 7.37 (6H, d, H2,6), 7.65 (3H, d, H5'), 7.73 (3H, t, H4"), 7.92 (3H, d, H3"), 8.62 (3H, d, H6").

Tri[4-(4-pyridylsulfanylmethyl)phenyl]methanol, ***4.41***

A mixture of **4.36** (2.62g, 4.9mmol), 4-mercaptopyridine (1.63g, 14.7mmol), and triethylamine (1.0mL) was stirred in acetonitrile (55mL) at 0^{o}C on ice, before slowly warming to room temperature over 22 hours. The precipitate was filtered off to give

4.41 as an insoluble yellow powder (2.48g, 81%), m.p. 134-136°C (Found: C, 54.03; H, 4.47; N, 4.68. $C_{37}H_{31}N_3OS_3.2HBr.2H_2O$ requires C, 53.69; H, 4.51; N, 5.08). ^{1}H N.M.R. (500MHz, DMSO): δ 4.61 (6H, s, CH_2), 7.26 (6H, d, H3,5), 7.50 (6H, d, H2,6), 7.84 (6H, d, H3',5'), 8.66 (6H, d, H2',6'). TOF-MS: Found M^+ 630.1716, $C_{37}H_{32}N_3OS_3$ requires M^+ 630.1708. Also found M^+ 739.1724, four-armed side product **4.42** $C_{42}H_{35}N_4OS_4$ requires M^+ 739.1694.

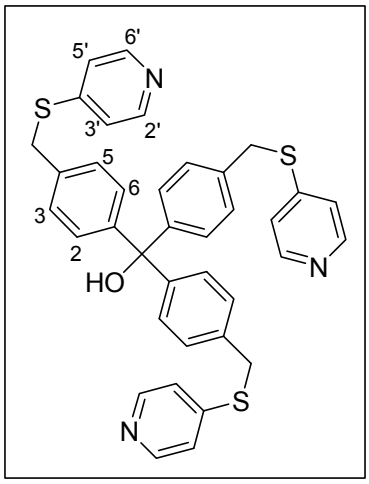

*Tri[4-(8-quinolyloxymethy)phenyl]methanol, **4.43***

A solution of **4.36** (3.02g, 5.6mmol) in DMF (15mL) was added slowly to a hot solution of 8-hydroxyquinoline (2.45g, 16.8mmol) and potassium hydroxide (1.17g, 20.9mmol) in DMF (75mL) and the resulting solution heated at 90°C for six hours. After cooling the product was extracted from the red solution with chloroform (50mL) and water (100mL) basified with a little sodium hydroxide. The organic layer was washed with water (4x150mL) to remove any remaining DMF, then dried with Na_2SO_4, and filtered. The chloroform was removed *in vacuo* to give **4.43** as a deep red solid. (3.07g, 75%), m.p. 77-82°C, (Found: C, 75.47; H, 5.33; N, 5.97. $C_{49}H_{33}N_3O_4.{}^1/_2C_3H_7NO.2H_2O$ requires C, 75.40; H, 5.58; N, 6.09). ^{1}H N.M.R. (300MHz, $CDCl_3$): δ 5.40 (6H, s, CH_2), 7.16-7.58 (24H, m, H2,3,5,6,3',6',7',8'), 8.14 (3H, d, H4'), 8.78 (3H, d, H2').

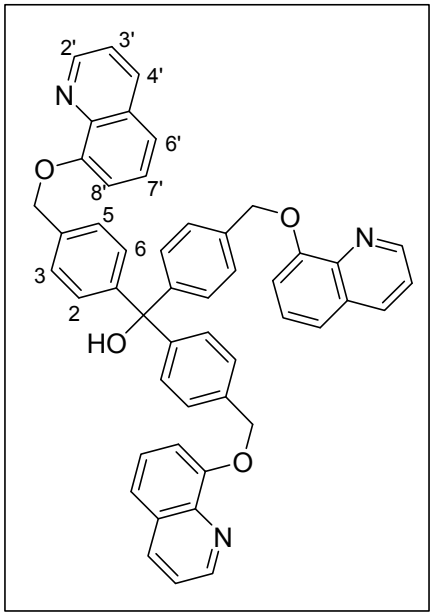

Attempted syntheses of the tri(4-substituted-phenyl)amine ligands

*Tri(4-formylphenyl)amine **4.49***

Step 1: Distilled $POCl_3$ (203mL, 2180mmol) was added slowly over a two hour period *via* a dropping funnel to a 0°C solution of dried DMF (156mL, 2010mmol) under an

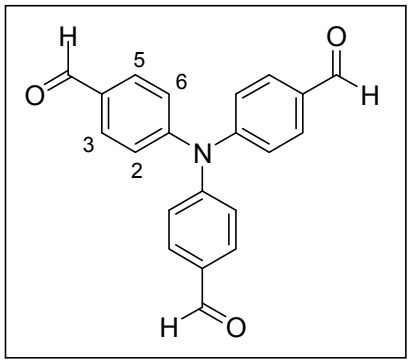

argon atmosphere. Whilst stirring for an hour the solution solidified, and was warmed gently to melt over another hour. Solid triphenylamine (21.18g, 86.3mmol) was added and the resulting brown solution heated at 90°C for four hours. The reaction solution was cooled before pouring into ice water (4L) and neutralising with 40% sodium hydroxide to produce a light coloured solid which was extracted by splitting the aqueous solution into three portions and washing each with dichloromethane (1L total). The organic phase was then washed with water (2x1L in portions), dried with Na_2SO_4 overnight, then filtered through a 2-3cm silica plug to get an orange solution that was reduced *in vacuo* to a light brown solid.

Step 2: Distilled $POCl_3$ (167mL, 1790mmol) was added slowly over an hour *via* a dropping funnel to a 0°C solution of dried DMF (125mL, 1610mmol) under an argon atmosphere. Whilst stirring for an hour the solution solidified, and this was warmed gently to melt over another hour. The light brown solid obtained in the first step was added and the resulting black viscous solution heated at 90°C for four hours. The reaction solution was cooled before pouring into ice water (4L) and neutralising with 40% sodium hydroxide to give a brown solution. The product was extracted by splitting the aqueous solution into three portions and washing each with dichloromethane (1.3L total). The organic phase was then washed with water (3x1L in portions), dried with Na_2SO_4, then the solid removed *in vacuo* to give a black solid (13.72g crude). This black solid was purified by column chromatography on silica gel eluting with dichloromethane to give the product as a yellow solid (4.61g, 16%), m.p. 224-228°C (lit.[286] 233-235°C) ^{1}H N.M.R. (500MHz, $CDCl_3$): δ 7.25 (6H, d, H2,6), 7.84 (6H, d, H3,5), 9.95 (3H, s, CHO).

Tri(4-hydroxymethylphenyl)amine ***4.50***

Sodium borohydride (8.00g, 211mmol) was stirred in distilled ethanol for twenty minutes, before a solution of **4.49** (4.61g, 14mmol) in dichloromethane (120mL) was added to produce a cloudy yellow solution. The solution was stirred at room temperature for five hours, then poured into ice water (400mL). Conc. hydrochloric acid was added dropwise until effervescence stopped, then $NaHCO_3$ solution was added to

raise the pH. The yellow solid was filtered off and dried *in vacuo*. (4.40g, 95%), m.p. 153-155°C (lit not provided[285]) (Found: C, 73.81; H, 6.14; N, 4.02. $C_{21}H_{21}NO_3.{}^1/_3H_2O$ requires C, 73.88; H, 6.40; N, 4.10). ^{1}H N.M.R. (500MHz, DMSO): δ 4.51 (6H, d, CH_2), 5.44 (3H, t, OH), 6.99 (6H, d, H2,6), 7.30 (6H,d, H3,5).

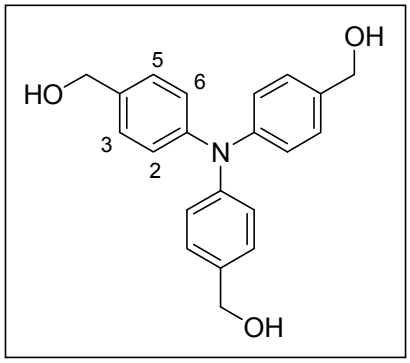

Attempted synthesis of tri(4-bromomethylphenyl)amine ***4.51***

Method A: Product **4.50** (0.56g, 1.7mmol) was refluxed in 63% HBr in H_2O (20mL), however the starting material did not dissolve at all. The addition of acetic acid (50mL) dissolved a little of the material but most was still insoluble. After seven hours of refluxing the solution was cooled and poured into ice (200g), to give a small amount of purple precipitate and a large amount of insoluble black solid. The purple precipitate was filtered off and shown to contain impure product (35.6mg).

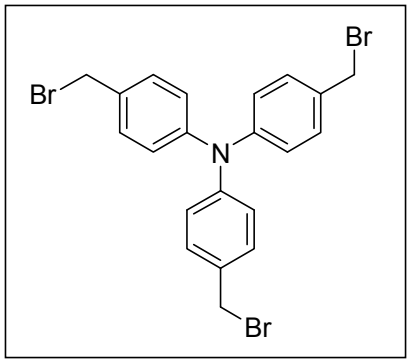

Method B: Product **4.50** (4.30g, 13mmol) was dissolved in acetic acid (100mL) with heating to give a dark green solution. 33% HBr in acetic acid (100mL) was added and the very dark solution refluxed for three hours, before cooling and pouring into 1.5kg of ice to get a purple precipitate and a large amount of dark green solid. These were filtered off and dried. The purple precipitate (1.05g) does not contain the desired product. The dark green solid (5.67g) is insoluble in common solvents, however elemental analysis suggests it may be the desired product, possibly protonated. The insolubility permits further characterisation or reaction to form the proposed ligands. (Found: C, 47.23; H, 3.87; N, 2.74. $C_{21}H_{20}NBr_3.{}^1/_2H_2O$ requires C, 47.22; H, 3.77; N, 2.62).

Preparation of complexes

Preparation of complexes with the 1,3-disubstituted-2,4,6-triethylbenzene ligands

Complexes of 2.4

*With $CoBr_2$, viz **2.7***

Methanolic solutions of ligand **2.4** (24.0mg, 0.075mmol) and cobalt(II) bromide (11.0mg, 0.050mmol) were combined and a light blue precipitate slowly formed. This precipitate was crystallised from acetonitrile and acetone to provide dark blue plates of one-dimensional polymer **2.7** suitable for X-ray crystallography. Yield 12.3mg (43%). M.p. 296-299°C. (Found: C, 45.30; H, 4.97; N, 10.51. $C_{20}H_{26}N_4CoBr_2.{}^1/_3CH_3CN.{}^1/_3(CH_3)_2CO$ requires C, 45.32; H, 5.09; N, 10.57).

*With $ZnBr_2$, viz **2.8***

A methanol solution of zinc bromide (8.8mg, 0.039mmol) was layered upon a solution of ligand **2.4** (17.9mg, 0.056mmol) in chloroform. Colourless crystals appeared over five days, and were analysed by X-ray crystallography to give 1:1 complex one-dimensional polymer **2.8**. Surprisingly, the bulk crystals gave a 2:3 metal to ligand stoichiometry, different to the X-ray analysis and product **2.8a** which has the same melting point. Yield 12.3mg (40%). M.p. 284-288°C. (Found: C, 45.02; H, 4.89; N, 10.33. M_2L_3 complex $C_{60}H_{78}N_{12}Zn_2Br_4.2CHCl_3$ requires C, 44.95; H, 4.87; N, 10.15).

*With $ZnBr_2$, viz **2.8a***

Methanolic solutions of ligand **2.4** (26.3mg, 0.073mmol) and zinc bromide (10.9mg, 0.048mmol) were combined to give a colourless solution which produced clusters of white crystalline material over a few days which were filtered off. Yield 18.1mg (59%). M.p. 285-289°C. (Found: C, 45.73; H, 5.13; N, 10.43. M_5L_6 complex $C_{120}H_{156}N_{24}Zn_5Br_{10}.5H_2O$ requires C, 45.74; H, 5.31; N, 10.67).

*With CuI, viz **2.9***

Ligand **2.4** (19.3mg, 0.060mmol) in methanol was added to a solution of copper(I) iodide (7.5mg, 0.039mmol) in acetonitrile and immediately a large amount of white precipitate formed. Overnight the precipitate redissolved and crystallised as clusters of

highly twinned colourless crystals. X-ray crystallography eventually provided a structure of two-dimensional polymer **2.9**. Yield 13.7mg (66%). M.p. 226-232°C. (Found: C, 47.36; H, 5.29; N, 11.05. 1:1 complex $C_{20}H_{26}N_4CuI.{}^1/_4CH_3CN$ requires C, 47.06; H, 5.15; N, 11.38).

*With CuI, viz **2.10***

Copper(I) iodide (16.2mg, 0.085mmol) was dissolved in acetonitrile and layered upon a chloroform solution of ligand **2.4** (13.9mg, 0.043mmol) to give a small amount of white precipitate at the boundary between the solvents. Over a few days stacks of colourless plates crystallised which were revealed by X-ray crystallography to be three-dimensional polymer **2.10**. Yield 12.0mg (52%). M.p. 230-232°C. (Found: C, 45.37; H, 5.47; N, 10.59. 1:1 complex $C_{20}H_{26}N_4CuI.H_2O$ requires C, 45.25; H, 5.32; N, 10.55).

*With CuI, viz **2.10a***

Copper(I) iodide (18.8mg, 0.099mmol) was dissolved in acetonitrile and added to an acetone solution of ligand **2.4** (15.8mg, 0.049mmol) and immediately a large amount of white fluffy precipitate formed. Overnight the precipitate redissolved and crystallised as clusters of poor quality crystals. These were filtered off to give a pale green solid. Yield 14.6mg (57%). M.p. 228-230°C. (Found: C, 46.03; H, 5.07; N, 10.38. 1:1 ratio complex $C_{20}H_{26}N_4CuI.{}^1/_2H_2O$ requires C, 46.03; H, 5.21; N, 10.74).

*With $Pd(PhCN)_2Cl_2$, viz **2.11***

Ligand **2.4** (20.5mg, 0.064mmol) and bis(benzonitrile)dichloropalladium(II) (16.2mg, 0.043mmol) were each dissolved in acetone and combined to give a yellow precipitate, which slowly redissolved. Slow evaporation over ten days afforded large orange clusters of blocks and smaller yellow squares. Both analysed by X-ray crystallography to be $(PdCl_2)_3L_3$ triangle **2.11**. Yield 11.5mg (52%). M.p. 292-294°C. (Found: C, 48.88; H, 5.61; N, 10.85. M_3L_3 complex $C_{60}H_{78}N_{12}Pd_3Cl_6.(CH_3)_2CO$ requires C, 48.59; H, 5.44; N, 10.79).

With $AgClO_4$

Solutions of ligand **2.4** (20.1mg, 0.062mmol) and silver perchlorate (9.1mg, 0.044mmol) in acetone were combined to give a colourless solution. Slow evaporation of this solution and other solvent combinations failed to produce anything other than an

oily residue. Eventually a small amount of pale pink powder was precipitated from a methanol solution for analysis. Yield 8.3mg (36%). (Found: C, 45.26; H, 4.98; N, 10.57. 1:1 complex $C_{20}H_{26}N_4O_4ClAg$ requires C, 45.34; H, 4.95; N, 10.58).

With $CoCl_2$

Solutions of ligand **2.4** (17.5mg, 0.054mmol) and cobalt(II) chloride (8.3mg, 0.035mmol) in acetone were combined to give a blue solution. By the next morning the solution was filled with dark blue crystalline clusters. Yield 14.9mg (72%). (Found: C, 54.85; H, 6.44; N, 11.25. M_5L_6 complex $C_{120}H_{156}N_{24}Cl_{10}Co_5.5(CH_3)_2CO.4H_2O$ requires C, 55.03; H, 6.64; N, 11.41).

Complexes with 2.12

*With CuI, viz **2.20***

A solution of copper(I) iodide (18.2mg, 0.096mmol) in acetonitrile was added to ligand **2.12** (22.5mg, 0.047mmol) in acetone to give a bright yellow precipitate. After evaporation, this precipitate was partially redissolved in a mixture of acetone, methanol, acetonitrile and chloroform. Slow evaporation of this solution induced a few air sensitive green needle-like crystals to grow on the sides of the vial. These crystals of dimer **2.20** proved to be suitable for X-ray crystallography. Insufficient crystals were obtained for further analysis, and the precipitate did not appear to be homogenous so was not characterised.

*With $CuSO_4$, viz **2.21***

Methanol (12ml) was very carefully layered upon an aqueous solution (4ml) of copper(II) sulfate (7.1mg, 0.028mmol) to create a gradient. Ligand **2.12** (20.1mg, 0.042mmol) was dissolved in a minimal amount of chloroform, and very carefully and slowly added dropwise to the layered solution, so the chloroform floated to the surface of the vial. The nearly colourless solution turned green where the ligand solution touched. A few blue block-like crystals appeared in solution after a few weeks of slow evaporation, followed by a pale green turquoise precipitate. Yield 13.6mg (72%). M.p. 236-239^oC. (Found: C, 54.35; H, 5.53; N, 12.78. 1:1 dimer $C_{60}H_{64}N_{12}O_8S_2Cu_2.3H_2O$ requires C, 54.33; H, 5.32; N, 12.67). These extremely air sensitive blue crystals were shown by X-ray crystallography to be dimer **2.21**.

*With $FeSO_4$, viz **2.22***

Methanolic solutions of ligand **2.12** (24.1mg, 0.051mmol) and iron(II) sulfate (9.5mg, 0.034mmol) were combined to give a yellow solution. Slowly some yellow precipitate formed, which did not redissolve. A few days of slow evaporation saw a few large orange chunky crystals grow on the sides of the vial. Fragments of these proved to be suitable for X-ray crystallography to reveal dimer **2.22**. The bulk precipitate was filtered and shown by elemental analysis to be a different complex to the crystals. Yield 4.7mg (32%). M.p. >320°C. (Found: C, 41.33; H, 4.72; N, 10.28. 2:1 complex $C_{30}H_{32}N_6O_8S_2Fe_2.5H_2O$ requires C, 41.39; H, 4.86; N, 9.65).

*With $CoCl_2$, viz **2.23***

Acetone solutions of ligand **2.12** (23.6mg, 0.050mmol) and cobalt(II) chloride (7.9mg, 0.036mmol) were combined to give a pink solution containing a precipitate. Large pink crystals grew in solution over a week of slow evaporation. Fragments from these stacks of plates proved suitable for X-ray crystallography and led to the dimer structure of complex **2.23**. Yield 11.6mg (51%). M.p. 228-233°C. (Found: C, 57.50; H, 5.47; N, 13.31. 1:1 dimer $C_{60}H_{64}N_6Cl_2Co.2H_2O$ requires C, 57.70; H, 5.49; N, 13.46).

*With $CuCl_2$, viz **2.24***

Methanolic solutions of ligand **2.12** (25.3mg, 0.053mmol) and copper(II) chloride (6.1mg, 0.036mmol) were combined to give a dark green solution. Slow evaporation over two weeks provided green block-like crystals of dimer **2.24** suitable for X-ray crystallography. Yield 9.8mg (43%). M.p. 174-179°C. (Found: C, 56.52; H, 5.58; N, 13.38. 1:1 complex $C_{60}H_{64}N_{12}Cu_2Cl_2.3H_2O$ requires C, 56.47; H, 5.53; N, 13.17). Found M^+ 1050.4376, $C_{60}H_{64}N_{12}ClCu$ requires M^+ 1050.4361.

*With $CuCl_2$, viz **2.24a***

Methanolic solutions of ligand **2.12** (18.8mg, 0.040mmol) and copper(II) chloride (4.5mg, 0.026mmol) were combined to give a dark green solution. Slow evaporation in the fridge provided small grass green block-like crystals which were filtered. Yield 7.0mg (40%). M.p. 173-176°C. (Found: C, 54.55; H, 5.28; N, 12.60. 1:1 complex $C_{60}H_{64}N_{12}Cu_2Cl_2.5H_2O$ requires C, 54.92; H, 5.68; N, 12.81).

*With $Cu(NO_3)_2$, viz **2.25***

Solutions of ligand **2.12** (23.3mg, 0.049mmol) and copper(II) nitrate (8.0mg, 0.033mmol) in methanol were combined to give a dark green solution. Slow evaporation over a few days provided green rectangular block-like crystals for X-ray crystallography of dimer **2.25**. Yield 4.1mg (18%). M.p. 249-251°C. (Found: C, 51.94; H, 4.94; N, 16.01. $C_{60}H_{64}N_{16}O_{12}Cu_2.3H_2O$ requires C, 52.13; H, 5.10; N, 16.21).

*With $ZnBr_2$, viz **2.26***

Zinc bromide (8.7mg, 0.039mmol) in methanol was added to a solution of ligand **2.12** (27.1mg, 0.057mmol) in methanol. Slow evaporation over a few weeks resulted in the growth of colourless block-like crystals of dimer **2.26** on the sides of the vial. These crystals proved suitable for X-ray crystallography. Yield 11.2mg (40%). M.p. 120-135°C. (Found: C, 50.31; H, 4.66; N, 11.73. 1:1 complex $C_{30}H_{32}N_6ZnBr_2.H_2O$ requires C, 50.06; H, 4.76; N, 11.68).

*With $AgClO_4$, viz **2.27***

Ligand **2.12** (23.0mg, 0.048mmol) and silver perchlorate (6.7mg, 0.032mmol) were dissolved in acetone and combined. Evaporation of this solution gave an oil, which was redissolved using methanol, acetonitrile and acetone. Slow evaporation over a few months gave large stacks of colourless plate-like crystals of one-dimensional polymer **2.27** suitable for X-ray crystallography. Yield 13.1mg (52%). (Found: C, 53.75; H, 5.02; N, 12.65. 1:1 complex $C_{30}H_{32}N_6O_4ClAg.(CH_3)_2CO.CH_3CN$ requires C, 53.68; H, 5.28; N, 12.52).

*With $Ni(ClO_4)_2$, viz **2.28***

Solutions of ligand **2.12** (26.3mg, 0.055mmol) and nickel(II) perchlorate (9.5mg, 0.035mmol) in acetone were combined to give a pale yellow solution. Two days later the resultant colourless solution had yielded a mass of very pale purple block-like crystals of Ni_4L_6 square **2.28** suitable for X-ray crystallography. Yield 15.2mg (42%). (Found: C, 54.28; H, 5.12; N, 12.81. $C_{180}H_{192}N_{36}O_{32}Cl_8Ni_4.5H_2O$ requires C, 54.32; H, 5.12; N, 12.67).

*With $Cu(ClO_4)_2$, viz **2.29***

Ligand **2.12** (22.3mg, 0.047mmol) and copper(II) perchlorate (11.8mg, 0.032mmol) were dissolved in acetone and combined to give a bright green solution. Within ten minutes the vial was filling with green needle-like crystals of Cu_4L_6 square **2.29** suitable for X-ray crystallography. Yield 15.5mg (50%). (Found: C, 54.44; H, 5.00; N, 12.64. $C_{180}H_{192}N_{36}O_{32}Cl_8Cu_4.4H_2O$ requires C, 54.30; H, 5.06; N, 12.66).

*With $Co(NO_3)_2$ and $AgClO_4$, viz **2.30***

Solutions of cobalt(II) nitrate (10.8mg, 0.037mmol) and ligand **2.12** (25.2mg, 0.0.53mmol) in acetone were combined to give a light pink precipitate. The addition of an acetone solution of silver perchlorate (10.8mg, 0.052mmol) to this mixture redissolved the precipitate to give a clear pink solution. Slow evaporation over a few days gave orange block-like crystals suitable for X-ray crystallography which revealed the structure of dimer **2.30**. Yield 15.6mg (57%). (Found: C, 49.05; H, 5.03; N, 13.18. Dimer $C_{30}H_{36}N_9O_7ClCo$ requires C, 49.15; H, 4.95; N, 13.38).

*With $Zn(ClO_4)_2$, viz **2.31***

Solutions of ligand **2.12** (26.7mg, 0.056mmol) and zinc perchlorate (13.8mg, 0.037mmol) in acetone were combined to give a colourless solution. Within an hour colourless blocks had started crystallising out of solution. These crystals of Zn_4L_6 square **2.31** were suitable for X-ray crystallography. Yield 15.7mg (41%). (Found: C, 53.19; H, 5.06; N, 12.35. $C_{180}H_{192}N_{36}O_{32}Cl_8Zn_4.8H_2O$ requires C, 53.24; H, 5.16; N, 12.42).

*With $ZnBr_2$ and $AgClO_4$, viz **2.31a***

Solutions of zinc bromide (8.7mg, 0.039mmol) and ligand **2.12** (26.3mg, 0.0.53mmol) in acetone were combined to give a colourless solution. The addition of an acetone solution of silver perchlorate (10.5mg, 0.051mmol) to this mixture gave an instant precipitate of AgBr. This precipitate was filtered off through cotton wool in a pipette to give a slightly cloudy solution which yielded small colourless blocks over a few days. A cell check of these crystals using X-ray crystallography proved this complex was Zn_4L_6 square **2.31**. Yield 10.3mg (27%). (Found: C, 51.63; H, 5.03; N, 12.16. $C_{180}H_{192}N_{36}O_{32}Cl_8Zn_4.14H_2O$ requires C, 51.86; H, 5.32; N, 12.09).

*With $Zn(BF_4)_2$, viz **2.32***

Zinc tetrafluoroborate (10.4mg, 0.044mmol) was dissolved in acetone and added to a solution of ligand **2.12** (26.9mg, 0.057mmol) in acetone. The next morning the vial was filled with colourless blocks of Zn_4L_6 square **2.32** which were suitable for X-ray crystallography. Yield 8.4mg (21%). M.p. 315-319°C. (Found: C, 53.42; H, 5.38; N, 11.82. $C_{180}H_{192}N_{36}F_{32}B_8Zn_4.6CH_3OH.10H_2O$ requires C, 53.34; H, 5.68; N, 12.04).

*With $Fe(ClO_4)_2$, viz **2.33***

Solutions of ligand **2.12** (25.5mg, 0.054mmol) and iron(II) perchlorate (13.1mg, 0.036mmol) in acetone were combined to give a yellow solution. Two days later the vial was filled with yellow block-like crystals of Fe_4L_6 square **2.33** suitable for X-ray crystallography. Yield 11.1mg (30%). (Found: C, 52.66; H, 4.98; N, 12.08. $C_{180}H_{192}N_{36}O_{32}Cl_8Fe_4.12H_2O$ requires C, 52.80; H, 5.32; N, 12.31).

*With $Fe(ClO_4)_2$, viz **2.34***

Solutions of ligand **2.12** (41.0mg, 0.086mmol) and iron(II) perchlorate (21.2mg, 0.058mmol) were dissolved in less than one millilitre of acetone each and were combined to give a yellow solution. Almost a week later yellow octahedral crystals of dimer **2.34** formed which proved suitable for X-ray crystallography. A few days later different crystals formed, but these air sensitive blocks of stacked plates were not suitable for X-ray crystallography. This 1:1 mixture of crystals was filtered, then the intergrown tiny crystals were separated as accurately as possible by hand under a microscope so small samples of each could be submitted independently for elemental analysis. Analysis revealed both crystal types have the same metal to ligand ratio as dimer **2.34**, varying only in solvent incorporation. Total yield 31.0mg (66%). Octahedral crystals: (Found: C, 49.60; H, 5.06; N, 10.98. $C_{60}H_{64}N_{12}O_{16}Cl_4Fe_2.^4/_3(CH_3)_2CO.^2/_3H_2O$ requires C, 49.52; H, 4.76; N, 10.83). Block crystals: (Found: C, 46.94; H, 4.80; N, 10.48. $C_{60}H_{64}N_{12}O_{16}Cl_4Fe_2.(CH_3)_2CO.5H_2O$ requires C, 46.97; H, 5.01; N, 10.43).

With $Co(PF_6)_2$

Methanolic solutions of cobalt bromide (8.0mg, 0.037mmol) and ammonium hexafluorophosphate (28.2mg, 0.173mmol) were combined, then added to a methanol solution of ligand **2.12** (25.6mg, 0.54mmol) to give a peach coloured precipitate, which

was filtered off after multiple recrystallisation attempts failed. Yield 2.7mg (8%). (Found: C, 41.91; H, 3.82; N, 9.62. 1:1 complex $C_{60}H_{64}N_{12}F_{24}P_4Co_2.5H_2O$ requires C, 41.39; H, 4.28; N, 9.65).

With $CdCl_2$ and $AgClO_4$

Cadmium chloride (9.3mg, 0.041mmol) was dissolved in a hot solution of 2:3 acetone:methanol, and added to an acetone solution of silver perchlorate (22.1mg, 0.107mmol) to get an immediate white precipitate which was filtered off through cotton wool in a pipette. The resulting colourless solution was added to a solution of ligand **2.12** (27.1mg, 0.0.57mmol) in acetone to give a colourless solution. Multiple crystallisation attempts were unsuccessful, so the white solid was extracted for analysis, which surprisingly suggests that chloride is still present even though all should have been precipitated by the silver. Yield 16.4mg (56%). (Found: C, 52.70; H, 5.18; N, 11.87. $C_{30}H_{32}N_6Cl_2Cd.^1/_2(CH_3)_2CO.^3/_2H_2O$ requires C, 52.84; H, 5.35; N, 11.74).

With $La(NO_3)_3$

Solutions of ligand **2.12** (21.0mg, 0.044mmol) and lanthanum nitrate (12.7mg, 0.029mmol) in methanol were combined to give a colourless solution. Multiple crystallisation attempts were unsuccessful, so a small amount of product was precipitated from solution as a white powder for analysis. Yield 4.9mg (24%). (Found: C, 36.83; H, 3.79; N, 13.46. M_3L_2 complex $C_{60}H_{64}N_{21}O_{27}La_3.5CH_3OH.2H_2O$ requires C, 36.75; H, 4.18; N, 13.86).

Complexes with 2.35

*With $Cu(NO_3)_2$, viz **2.43***

A solution of copper(II) nitrate (8.4mg, 0.035mmol) in methanol was layered upon a solution of ligand **2.35** (21.0mg, 0.052mmol) in chloroform. Within seconds a few small blue crystals had formed and then a blue solid precipitated. Three hours later this precipitate had redissolved and clusters of dark blue crystalline material had formed. This product was dissolved in DMSO. Initially chloroform was diffused in, then the solution was left to slowly evaporate. A few months later the vial was filled with small purple needles which proved to be suitable for X-ray crystallography to give one-dimensional necklace-like polymer **2.43**. Yield 6.0mg (19%). M.p. 208-214^{o}C. (Found:

C, 51.96; H, 5.95; N, 6.49. ML_2 complex $C_{48}H_{56}N_6O_6S_4Cu.3(CH_3)_2SO.^1/_2H_2O$ requires C, 51.96; H, 6.06; N, 6.73).

With $Pd(PhCN)_2Cl_2$

Ligand **2.35** (24.5mg, 0.060mmol) and bis(benzonitrile)dichloropalladium(II) (15.4mg, 0.040mmol) were dissolved in acetone and combined to give a yellow precipitate, which was filtered off and dried to give a terracotta coloured powder. Yield 15.9mg (64%). M.p. 255-260°C. (Found: C, 46.88; H, 4.90; N, 4.48. 1:1 complex $C_{24}H_{28}N_2S_2PdCl_2.^3/_2H_2O$ requires C, 47.03; H, 5.10; N, 4.57).

With $CoCl_2$

Acetone solutions of ligand **2.35** (21.9mg, 0.054mmol) and cobalt(II) chloride (8.4mg, 0.035mmol) were combined to give a fine blue precipitate, which was filtered off and dried a few weeks later. Yield 6.5mg (33%). M.p. 264-268°C. (Found: C, 52.31; H, 5.27; N, 5.38. 1:1 complex $C_{24}H_{28}N_2S_2CoCl_2.^2/_3H_2O$ requires C, 52.37; H, 5.37; N, 5.09).

With $CuCl_2$

A solution of copper(II) chloride (6.5mg, 0.038mmol) in methanol was layered upon a solution of ligand **2.35** (22.6mg, 0.055mmol) in chloroform, to give a colour change to dark green at the boundary between the solutions. Over time a green precipitate formed which was filtered off weeks later. Yield 11.0mg (50%). M.p. 213-216°C. (Found: C, 49.64; H, 5.47; N, 4.71. 1:1 complex $C_{24}H_{28}N_2S_2CuCl_2.2H_2O$ requires C, 49.78; H, 5.57; N, 4.84).

With $FeSO_4$

Iron(II) sulfate (10.2mg, 0.037mmol) was dissolved in methanol and layered upon a chloroform solution of ligand **2.35** (22.8mg, 0.056mmol). Slowly an orange precipitate formed which was filtered off a few weeks later. Yield 10.1mg (71%). M.p. >320°C. (Found: C, 38.53; H, 4.66; N, 3.64. M_2L complex $C_{24}H_{28}N_2O_8S_4Fe_2.CH_3OH.2H_2O$ requires C, 38.47; H, 4.65; N, 3.59).

With $CuSO_4$

Copper(II) sulfate (11.2mg, 0.045mmol) was dissolved in methanol and layered upon a chloroform solution of ligand **2.35** (27.1mg, 0.066mmol) to give a light coloured precipitate at the boundary between the solutions. This was filtered off weeks later to give a sky blue powder. Yield 13.4mg (37%). M.p. 166-174°C. (Found: C, 52.55; H, 5.77; N, 5.00. M_2L_3 complex $C_{72}H_{84}N_6O_8S_8Cu_2.6H_2O$ requires C, 52.31; H, 5.85; N, 5.08).

With CuI

A solution of copper(I) iodide (7.6mg, 0.040mmol) in acetonitrile was layered upon a solution of ligand **2.35** (23.9mg, 0.059mmol) dissolved in a 2:1 mixture of methanol and chloroform. Immediately a pale brown precipitate was obtained, which was eventually filtered off. Yield 10.8mg (54%). M.p. 183-187°C. (Found: C, 43.11; H, 4.22; N, 4.28. M_4L_3 complex $C_{72}H_{84}N_6S_6Cu_4I_4.H_2O$ requires C, 43.12; H, 4.32; N, 4.19).

Preparation of complexes with the 1,3,5-trisubstituted-2,4,6-trimethylbenzene ligands

Complexes with 3.33

*With $CoBr_2$, viz **3.36***

A solution of cobalt(II) bromide (15.5mg, 0.071mmol) in methanol was layered on top of a solution of ligand **3.33** (22.6mg, 0.046mmol) in chloroform to give a blue solution and a small amount of light blue precipitate. Upon slow evaporation the solution turned pink and pink needle-like crystals grew amongst the white precipitate. These crystals proved suitable for X-ray crystallography and provided the structure of the two-dimensional polymer **3.36**. Yield 25.7mg (78%). M.p. 233-237°C. (Found: C, 45.72; H, 3.92; N, 5.76. Dehydration product $C_{27}H_{27}N_3S_3CoBr_2$ requires C, 45.77; H, 3.84; N, 5.93).

*With CuI, viz **3.38***

A solution of ligand **3.33** (28.6mg, 0.058mmol) in methanol was added to a solution of copper(I) iodide (16.9mg, 0.089mmol) in acetonitrile to give a light coloured precipitate. Upon slow evaporation of this solution clusters of crystalline material grew on the sides of the vial. Fragments of these clusters proved to be suitable for X-ray crystallography and revealed the two-dimensional polymer **3.38**. Yield 9.6mg (17%). M.p. 210-220°C. (Found: C, 38.17; H, 3.56; N, 5.84. $C_{27}H_{27}N_3S_3Cu_2I_2.CH_3CN.CH_3OH$ requires C, 38.18; H, 3.63; N, 5.94). The light brown precipitate was filtered off and shown to be a different complex to the crystals. Yield 30.5mg (62%). M.p. 207-216°C. (Found: C, 38.79; H, 3.63; N, 5.00. M_3L_2 complex requires $C_{54}H_{54}N_6S_6Cu_3I_3.6H_2O$ C, 39.10; H, 4.01; N, 5.07).

With $CuCl_2$

This complex was synthesised by a delicate layering process. Methanol (12ml) was layered very carefully on top of a solution of copper(II) chloride (29.1mg, 0.171mmol) in water to create a gradient. Very carefully and slowly chloroform (2ml) was added dropwise, allowing this solvent to float back to the surface of the solution. Then water (1ml) was very carefully added dropwise to re-enforce the aqueous gradient that holds the chloroform at the top of the solvent layers, preventing mixing too quickly. Equally carefully a solution of ligand **3.33** (26.7mg, 0.055mmol) in methanol (3ml) was added dropwise to float on top on the upper chloroform layer. A precipitate started forming immediately. A few weeks later after the solution had fully mixed the insoluble green precipitate was filtered off. Yield 16.1mg (43%). M.p. 190-195°C. (Found: C, 48.07; H, 4.49; N, 5.82. 1:1 complex $C_{27}H_{27}N_3S_3Cl_2Cu.3H_2O$ requires C, 47.81; H, 4.90; N, 6.20).

With $Cu(ClO_4)_2$

A solution of copper(II) perchlorate (33.7mg, 0.091mmol) in methanol (10ml) was layered on top of a solution of ligand **3.33** (28.6mg, 0.059mmol) in dichloromethane and a small amount of precipitate appeared at the solvent boundary. A few weeks later this precipitate was filtered off. Yield 34.4mg (72%). (Found: C, 42.92; H, 4.30; N, 5.20. 1:1 complex $C_{27}H_{27}N_3O_8S_3Cl_2Cu.2CH_3OH$ requires C, 42.67; H, 4.32; N, 5.15).

With K_2PdCl_4

A solution of ligand **3.33** (20.2mg, 0.041mmol) in methanol (15ml) was layered on top of a solution of potassium tetrachloropalladate (20.3mg, 0.062mmol) in DMSO. A pale yellow precipitate formed between the layers and was filtered off a few weeks later when the solution had fully mixed. Yield 46.1mg (91%). (Found: C, 34.14; H, 4.45; N, 3.21. M_2L complex $C_{27}H_{27}N_3S_3Cl_4Pd_2.4(CH_3)_2SO.4H_2O$ requires C, 34.21; H, 4.84; N, 3.42).

With $AgClO_4$

Silver perchlorate (14.9mg, 0.072mmol) was dissolved in acetone and layered on top of a solution of ligand **3.33** (23.0mg, 0.047mmol) in dichloromethane. Immediately a light coloured precipitate formed at the boundary between the solutions. A few weeks later this very insoluble brown precipitate was filtered off. Yield 24.2mg (59%). (Found: C, 39.93; H, 3.59; N, 5.12. $Ag_3L_2(ClO_4)_3$ complex $C_{54}H_{54}N_6O_{12}S_6Cl_3Ag_3.CH_2Cl_2.C_3H_6O$ requires C, 39.93; H, 3.58; N, 4.82).

With $Pd(en)(NO_3)_2$

Dinitrato(ethylenediamine)palladium(II) was generated *in situ* by stirring and heating (80°C) a solution of dichloro(ethylenediamine)palladium(II) (30.1mg, 0.130mmol) in 5ml of water, with nitric acid (two drops) to dissolve. An aqueous solution of silver nitrate (45.5mg, 0.268mmol) in water (2ml) was added dropwise to precipitate AgCl. This solution was stirred at 80°C for two hours, before filtering the precipitate off through cotton wool in a pipette. The yellow filtrate was stirred at 80°C while ligand **3.33** (41.8mg, 0.086mmol) was added as a solid, and the heating continued for 24 hrs. The solution was filtered to give a colourless filtrate and a bright red precipitate, which was insoluble in all common solvents and therefore unable to be crystallised. Yield 56.4mg (76%). M.p. 252-274°C (Found: C, 37.35; H, 3.84; N, 9.53. $Pd_3L_2(NO_3)_6$ complex $C_{54}H_{54}N_6S_6Pd_3.6NO_3.4H_2O$ requires C, 37.21; H, 3.59; N, 9.64).

With $Cu(NO_3)_2$

A solution of copper(II) nitrate (18.4mg, 0.080mmol) in methanol (3ml) was layered on top of a solution of ligand **3.33** (24.5mg, 0.050mmol) in dichloromethane and a pale blue precipitate appeared at the solvent boundary. DMSO was added in an attempt to dissolve the precipitate, but it was mostly insoluble. After an extended period of time

the teal green precipitate was filtered off. Yield 7.6mg (21%). (Found: C, 45.82; H, 4.39; N, 6.64. M_3L_2 complex $C_{54}H_{54}N_6S_6Cu_3.5OH.NO_3.DCM.H_2O$ requires C, 45.94; H, 4.56; N, 6.82).

Complexes with 3.41

With $PdCl_2$

Palladium chloride (8.6mg, 0.049mmol) was dissolved in dilute hot hydrochloric acid, and added dropwise to a solution of ligand **3.41** (19.4mg, 0.033mmol) in hot methanol. The solution was stirred and heated for an hour before the yellow precipitate was filtered off. Yield 7.7mg (32%). M.p. >250°C (dec). (Found: C, 46.79; H, 3.79; N, 4.38. M_2L complex $C_{39}H_{33}N_3O_3Cl_4Pd_2.3H_2O$ requires C, 46.82; H, 3.93; N, 4.20). TOF-MS: Found M^+ 732.1239, $C_{39}H_{33}N_3O_3ClPd$ requires M^+ 732.1245. ^{1}H N.M.R. (300MHz, DMSO): δ 2.40, 5.33, 7.46, 7.76, 7.85, 8.79, 8.97, 9.11.

With $PdCl_2$

Solid palladium chloride (17.0mg, 0.096mmol) and solid ligand **3.41** (21.1mg, 0.036mmol) were ground together using a glass mortar and pestle for 15 minutes. The resulting sample was then analysed without purification. M.p. >170°C (dec). (Found: C, 40.92; H, 3.26; N, 3.69. M_3L complex $C_{39}H_{33}N_3O_3Cl_6Pd_3.H_2O$ requires C, 41.03; H, 3.09; N, 3.68). TOF-MS: Found M^+ 1101.8943, $C_{39}H_{35}N_3O_4Cl_5Pd_3$ requires M^+ 1101.8174. ^{1}H N.M.R. (300MHz, DMSO): δ 2.60, 5.25, 5.37, 7.03, 7.27, 7.77, 7.86, 8.71, 8.79, 8.96, 9.43.

With $Pd(en)(PF_6)_2$

Dinitrato(ethylenediamine)palladium(II) was generated *in situ* by stirring and heating (90°C) a solution of dichloro(ethylenediamine)palladium(II) (29.7mg, 0.125mmol) in water (4ml), with nitric acid (two drops) to dissolve. An aqueous solution of silver nitrate (42.5mg, 0.250mmol) in water (2ml) was added dropwise to precipitate AgCl. This solution was stirred at 90°C for two and a half hours, before filtering the precipitate. Methanol was added to the yellow filtrate to double the volume, and the solution was cooled to room temperature. It was attempted to dissolve ligand **3.41** (49.9mg, 0.084mmol) in MeOH (5ml), however the undissolved ligand dissolved when the $Pd(en)(NO_3)_2$ solution was added dropwise. The reaction was stirred at room

temperature for two hours before an excess of ammonium hexafluorophosphate was added. Immediately the vial filled with a yellow precipitate. The solution was stirred for a further 30 minutes before the precipitate was filtered off. Yield 25.7mg (28%). M.p. >320°C (Found: C, 46.41; H, 4.28; N, 6.36. Pd(en)L$(PF_6)_2$ complex $C_{41}H_{39}N_5O_3F_{12}P_2Pd.CH_3OH.{}^1/_2H_2O$ requires C, 46.40; H, 4.08; N, 6.44). ^{1}H N.M.R. (300MHz, DMSO): δ 2.60, 5.36, 7.93, 8.91, 9.02.

With $AgPF_6$

A dichloromethane solution of silver hexafluorophosphate (14.4mg, 0.057mmol) was added dropwise to a solution of ligand **3.41** (18.2mg, 0.031mmol) in dichloromethane to give an immediate precipitate. This light brown powder was filtered off a few days later. Yield 4.1mg (13%). M.p. >320°C. (Found: C, 44.02; H, 3.60; N, 4.08. M_7L_4 complex $C_{156}H_{132}N_{12}O_{12}F_{42}P_7Ag_7.CH_2Cl_2.2H_2O$ requires C, 44.29; H, 3.27; N, 3.95).

With $Zn(OAc)_2$

Ligand **3.41** (10.1mg, 0.017mmol) was dissolved in dichloromethane. Possible templating molecules benzene (2 drops) and trimesic acid (3.2mg, 0.015mmol) in methanol, were layered on top of the ligand solution, then on top of that was layered a solution of zinc acetate (5.7mg, 0.026mmol) in methanol. A light coloured precipitate started forming immediately. Three days later this peach coloured precipitate was filtered off. M.p. >320°C (Found: C, 54.61; H, 4.00; N, 3.82. M_2L complex $C_{47}H_{45}N_3O_{11}Zn.{}^1/_2(COOH)_3C_6H_3.CH_2Cl_2$ requires C, 54.90; H, 4.39; N, 3.66).

With $Pd(en)(NO_3)_2$

Dinitrato(ethylenediamine)palladium(II) was generated in situ by stirring and heating (90°C) a solution of dichloro(ethylenediamine)palladium(II) (23.1mg, 0.097mmol) in water (4ml), with nitric acid (two drops) to dissolve. An aqueous solution of silver nitrate (36.6mg, 0.215mmol) in water (2ml) was added dropwise to precipitate AgCl. This solution was stirred at 90°C for ninety minutes, before filtering the precipitate. The yellow filtrate was stirred at 90°C while ligand **3.41** (41.8mg, 0.064mmol) was added as a solid, and the heating continued for 24 hrs. The solution was filtered to give a green filtrate and brown precipitate, which could not be crystallised. Yield 35.1mg (65%). M.p. >320°C (Found: C, 55.19; H, 4.09; N, 5.73. $[Pd_3(OH)_6L_2(NO_3)]^-$ complex

$C_{78}H_{66}N_6O_6Pd_3.NO_3.6OH.H_3O$ requires C, 55.57; H, 4.48; N, 5.82). ^{1}H N.M.R. (300MHz, DMSO): δ 2.27, 2.34, 4.37, 4.64, 7.03, 7.22, 7.56, 7.76, 8.55, 8.68.

Preparation of complexes with the 1,3,5-trisubstituted-2,4,6-triethylbenzene ligands

Complexes with 3.5

*With $AgPF_6$, viz **3.5***

Solutions of silver hexafluorophosphate (13.1mg, 0.052mmol) and ligand **3.5** (13.2mg, 0.033mmol) in dichloromethane were combined to give a pink solution which did not yield crystals upon slow evaporation. Extra silver hexafluorophosphate (32.1mg, 0.127mmol) in acetone (5ml) was added to the residue. Repeated attempts at slow evaporation from an acetone solution eventually provided a few colourless crystals of protonated ligand **3.5**, suitable for X-ray crystallography. The quantity of crystals obtained was insufficient for weighing or further analysis.

*With $AgClO_4$, viz **3.20***

Ligand **3.5** (20.2mg, 0.053mmol) in dichloromethane (2ml) was added to a solution of silver perchlorate (15.9mg, 0.077mmol) in acetonitrile. As initial attempts to grow crystals were unsuccessful, extra silver perchlorate (21.8mg, 0.105mmol) in acetone (2ml) was added. Again slow evaporation did not furnish suitable crystals, so the residue was redissolved in acetonitrile, which provided a few suitable crystals of one-dimensional polymer **3.20** for X-ray crystallography upon slow evaporation. The quantity of crystals obtained was insufficient for weighing or further analysis.

*With K_2PdCl_4, viz **3.21***

Solutions of ligand **3.5** (5.1mg, 0.013mmol) and potassium tetrachloropalladate (6.5mg, 0.020mmol) were dissolved in D_6-DMSO and combined into an NMR tube. ^{1}H NMR did not show any signs of complex formation. Vapour diffusion of chloroform into this solution eventually led to orange block-like crystals over a period of ten months. These crystals were suitable for X-ray crystallography, and led to the structure of M_6L_4 cage **3.21**. ^{1}H N.M.R. (300MHz, DMSO): δ 0.88, 2.86, 5.47, 6.32, 7.52, 7.56.

*With K_2PdCl_6, viz **3.22***

Solutions of ligand **3.5** (7.8mg, 0.019mmol) and potassium hexachloropalladate (9.5mg, 0.024mmol) were dissolved in D_6-DMSO and combined into an NMR tube. ^{1}H NMR did not show any signs of complex formation. Vapour diffusion of dichloromethane into this solution eventually led to orange block-like crystals over a month. These crystals were suitable for X-ray crystallography, and led to the structure of M_6L_4 cage **3.22**. ^{1}H N.M.R. (300MHz, DMSO): δ 0.87, 2.86, 5.47, 6.33, 7.54, 7.57.

*With $Pd(en)(NO_3)_2$, viz **3.22***

Dinitrato(ethylenediamine)palladium(II) was generated *in situ* by stirring and heating a solution of dichloro(ethylenediamine)palladium(II) (44.8mg, 0.188mmol) in water (6ml), with nitric acid (one drop) to dissolve. An aqueous solution of silver nitrate (64.3mg, 0.378mmol) in water (4ml) was added dropwise to precipitate AgCl. This solution was stirred at 80^{o}C for ninety minutes, before filtering the precipitate. The yellow filtrate was cooled to room temperature, and added dropwise to a stirred solution of ligand **3.5** (49.3mg, 0.123mmol) in 5ml of methanol, and the solution stirred for an hour. Refrigeration over several days provided a white precipitate, which was filtered. Yield 63.8mg (57%). M.p. 210-220^{o}C (Found: C, 39.13; H, 5.48; N, 18.21. $Pd_6(en)_6L_4(NO_3)_{12}$ complex $C_{108}H_{165}N_{48}O_{45}Pd_6.9CH_3OH$ requires C, 38.72; H, 5.33; N, 18.52). TOF-MS: Found M^+ 613.9807, $C_{24}H_{30}N_6Pd_2$ requires M^+ 614.0601. ^{1}H N.M.R. (300MHz, DMSO): δ 0.88, 1.86(DMSO encapsulated), 2.72, 2.86, 3.72, 5.48, 5.52, 5.77, 6.33, 7.47, 7.54. Zinc chloride (13.5mg, 0.099mmol) was dissolved in water (1ml) and HCl (1 drop). This solution of $ZnCl_4^{2-}$ counterion was layered on top of a solution of the white product (5.2mg, 0.001mmol) in DMSO (1ml) and left to mix. After an extended period of time a yellow precipitate was filtered off (2.6mg). This precipitate was dissolved in DMSO and large orange crystals were obtained by vapour diffusion of dichloromethane and ethyl acetate into this solution over a long period of time. These crystals were suitable for X-ray crystallography and revealed $(PdCl_2)_6L_4$ cage **3.22**.

With $Pd(en)(PF_6)_2$

Dinitrato(ethylenediamine)palladium(II) was generated in situ by stirring and heating a solution of dichloro(ethylenediamine)palladium(II) (27.9mg, 0.117mmol) in water (4ml), with nitric acid (one drop) to dissolve. An aqueous solution of silver nitrate

(41.5mg, 0.244mmol) in water (3ml) was added dropwise to precipitate AgCl. This solution was stirred and heated for two hours, before filtering the precipitate. The yellow filtrate was cooled to room temperature, before adding dropwise a solution of ligand **3.5** (66.6mg, 0.166mmol) in methanol (5ml), and the solution stirred for an hour, before an excess of ammonium hexafluorophosphate was added to give a white precipitate. The solution was stirred at room temperature for a further 18 hours before the white precipitate was filtered. Yield 73.4mg (55%). M.p. 225^{o}C (Found: C, 39.40; H, 4.83; N, 13.21. $Pd_5(en)_5L_6(PF_6)_{10}$ complex $C_{156}H_{215}N_{46}F_{60}P_{10}Pd_5.6CH_3OH$ requires C, 39.38; H, 4.83; N, 13.20). ^{1}H N.M.R. (300MHz, DMSO): δ 0.98, 2.97, 3.80, 5.58, 6.43, 7.63, 7.67. ^{1}H N.M.R. (300MHz, MeCN): δ 0.83, 0.95, 1.05, 2.82, 4.52, 5.49, 5.84, 6.29, 6.54, 6.64, 7.12, 7.50, 7.72, 7.94, 8.25.

Complexes with 3.24

*With K_2PdCl_4, viz **3.27***

Solutions of ligand **3.24** (24.6mg, 0.038mmol) and potassium tetrachloropalladate (18.8mg, 0.058mmol) were dissolved in D_6-DMSO and combined into an NMR tube, and complex formation was observed by ^{1}H NMR. Over the weekend the NMR tube filled with orange crystals, suitable for X-ray crystallography, and led to the structure of Pd_3L complex **3.27**. Yield 25.3mg (85%). M.p. >320^{o}C. (Found: C, 33.44; H, 3.44; N, 8.28. $C_{39}H_{39}N_9Cl_6Pd_3.2(CH_3)_2SO.KCl$ requires C, 33.41; H, 3.33; N, 8.16). ^{1}H N.M.R. (300MHz, DMSO): δ 1.02, 2.36 (interacting DMSO), 2.76, 5.55, 5.81, 6.11, 6.98, 7.38, 7.43, 7.59, 7.73, 8.02, 8.17, 8.31, 8.66, 9.05.

*With $CuSO_4$, viz **3.28***

Methanol (10ml) was carefully layered upon an aqueous solution (5ml) of copper(II) sulfate (15.8mg, 0.063mmol) to create a gradient. Ligand **3.24** (27.1mg, 0.042mmol) was dissolved in chloroform (3ml), and added dropwise to the layered solution. Initially the organic solvent floated back up to the surface, but due to a combination of incorrect solvent ratio and poor layering, soon some of the chloroform solution sank to the bottom of the vial, disrupting the delicate slow mixing process. However the green solution still yielded air sensitive blue block-like crystals within a few days, which were shown by X-ray crystallography to be Cu_4L_2 dimer **3.28**. Yield 8.1mg (25%). M.p.

300°C (dec). (Found: C, 46.68; H, 4.41; N, 12.38. M_4L_2 complex $C_{39}H_{39}N_9O_8S_2Cu_2.6H_2O$ requires C, 46.51; H, 4.50; N, 12.52).

*With $CuSO_4$, viz **3.29***

Ligand **3.24** (24.3mg, 0.037mmol) and the potential templating molecule ferrocene (6.9mg, 0.037mmol) were dissolved in the minimum amount of chloroform and transferred to the same limb of a H-shaped crystallisation tube. Copper sulfate (14.0mg, 0.056mmol) was dissolved in the minimum amount of water and transferred to the other limb of the H-tube. Methanol was carefully layered on top of both of these solutions until the H-tube was filled with solvent. A few extremely air sensitive blue plate-like crystals grew in the bridging region of the H-tube and were shown by X-ray crystallography to be a polymer of Cu_4L_2 dimers **3.29**. Yield 1.7mg (3%). (Found: C, 36.26; H, 4.26; N, 9.38. $C_{40}H_{43}N_9O_9S_2Cu_2.2CHCl_3.9H_2O$ requires C, 36.40; H, 4.58; N, 9.10).

*With $Cu(NO_3)_2$, viz **3.30***

A solution of copper(II) nitrate (14.8mg, 0.061mmol) in methanol was layered on top of a solution of ligand **3.24** (25.3mg, 0.039mmol) in 1:4 toluene:methanol (10ml) to give a green solution. A few weeks of slow evaporation yielded a few air sensitive small green crystals which were suitable for X-ray crystallography and revealed Cu_4L_2 dimer **3.30**. A week after these crystals were removed from solution and analysed, a few dark blue crystals appeared in solution. These were also suitable for X-ray crystallography and were shown to be ligand decomposition complex **5.3**. Upon almost full evaporation, green clusters of crystalline material grew. These clusters were filtered and analysed and appear to be the same Cu_4L_2 product as the original crystals. Yield 5.9mg (20%). M.p. 233-236°C. (Found: C, 49.39; H, 4.91; N, 16.27. $C_{39}H_{41}N_{11}O_8Cu_2.{}^5/_2H_2O$ requires C, 49.47; H, 4.79; N, 16.27).

With $CoCl_2$

A methanolic solution of cobalt(II) chloride (11.0mg, 0.046mmol) was layered over a solution of ligand **3.24** (20.2mg, 0.031mmol) in dichloromethane. As slow evaporation did not yield crystals, vapour diffusion of ether into this solution was successfully attempted to give a few extremely air sensitive pink block-like crystals which X-ray

crystallography could only reveal a poor quality structure of a Co_2L_2 dimer. The quantity of crystals obtained was insufficient for weighing or further analysis.

With $CoCl_2$

Acetone solutions of cobalt(II) chloride (11.1mg, 0.047mmol) and ligand **3.24** (20.4mg, 0.031mmol) were combined to give a pink precipitate. Although this precipitate was soluble in methanol, no crystals could be obtained by slow evaporation or vapour diffusions, so the dark purple solid was extracted. Yield 11.9mg (55%). M.p. 281-287°C. (Found: C, 51.28; H, 4.82; N, 13.48. M_2L complex $C_{39}H_{39}N_9Cl_4Co_2.{}^1/_2CH_3OH.H_2O$ requires C, 51.15; H, 4.67; N, 13.59).

With $Zn(ClO_4)_2$

Zinc perchlorate (18.8mg, 0.050mmol) and ligand **3.24** (36.2mg, 0.056mmol) were dissolved in D_4-methanol and combined into an NMR tube. Immediately a white precipitate formed, however complex formation was still observed by ^{1}H NMR. A few days later this white precipitate was filtered off. Yield 23.8mg (43%). (Found: C, 49.05; H, 4.81; N, 13.00. 1:1 complex $C_{39}H_{39}N_9O_8Cl_2Zn.CH_3OH.3H_2O$ requires C, 48.82; H, 5.02; N, 12.81). ^{1}H N.M.R. (300MHz, CD_3OD): δ -0.34, 0.87, 2.19, 2.51, 3.14, 3.83, 5.31, 7.16, 7.47, 7.74, 8.06, 8.87.

With $CoBr_2$

A methanolic solution of cobalt(II) bromide (15.5mg, 0.071mmol) was layered over a solution of ligand **3.24** (30.5mg, 0.047mmol) in chloroform. Mutiple crystallisation attempts from various solvents were unsuccessful, so eventually the crimson powder was filtered off. Yield 16.4mg (36%). M.p. 278-285°C. (Found: C, 49.09; H, 4.86; N, 13.08. 1:1 complex $C_{39}H_{39}N_9Br_2Co.3H_2O.{}^1/_2CHCl_3$ requires C, 49.10; H, 4.75; N, 13.05).

With $FeSO_4$

Methanolic solutions of iron(II) sulfate (13.4mg, 0.048mmol) and ligand **3.24** (21.0mg, 0.032mmol) were combined to give a bright yellow solution which slowly precipitated. After recrystallisations were unsuccessful this orange precipitate was filtered off. Yield 11.7mg (57%). M.p. >320°C. (Found: C, 36.76; H, 4.68; N, 10.10. M_3L complex $C_{39}H_{39}N_9O_{12}S_3Fe_3.10H_2O$ requires C, 36.89; H, 4.68; N, 9.93).

*With $Cu(NO_3)_2$, viz **5.3***

This complex was synthesised by a layering process. Methanol (8ml) was layered very carefully on top of a solution of copper(II) nitrate (31.9mg, 0.132mmol) in water (3ml) to create a gradient. Very carefully and slowly chloroform (2ml) was added dropwise, allowing this solvent to float back to the surface of the solution. Then water (1ml) was added very carefully dropwise to re-enforce the aqueous gradient that holds the chloroform at the top of the solvent layers, preventing mixing too quickly. Equally carefully a solution of ligand **3.24** (28.8mg, 0.044mmol) in methanol (3ml) was added dropwise to float on top of the upper chloroform layer. The upper layer of solution turned green. Slow mixing over time and slow evaporation failed to produce crystals, so vapour diffusion of ether into this mixture of solvents was used to produce clusters of dark blue plates which were revealed by X-ray crystallography to be ligand decomposition complex **5.3**. Yield 1.2mg (3%).

*With K_2PdCl_4 and $AgPF_6$, viz **5.9***

Ligand **3.24** (42.8mg, 0.066mmol) and potassium tetrachloropalladate (32.3mg, 0.099mmol) were dissolved in DMSO and combined, then a DMSO solution of silver hexafluorophosphate (75.0mg, 0.297mmol) was added to precipitate AgCl. The solution was stirred at 60^{o}C for an hour, before the precipitate was filtered off. Vapour diffusion of chloroform into the filtrate produced small yellow block-like crystals after a period of five to six months. X-ray crystallography showed these crystals to be ligand decomposition product **5.9**. The quantity of crystals obtained was insufficient for weighing or further analysis.

*With $Cu(ClO_4)_2$, viz **5.10***

A solution of copper(II) perchlorate (27.8mg, 0.075mmol) in methanol was layered onto a solution of ligand **3.24** (30.2mg, 0.046mmol) in dichloromethane to give a green precipitate at the boundary between solvents. Six weeks later attempts were made to crystallise this precipitate from other solvents. Vapour diffusion of ether into an acetonitrile solution of this precipitate led to a few opaque poor quality dark green crystals, and a few light green rectangular blocks which proved to be suitable for X-ray crystallography, and led to the structure of ligand decomposition complex **5.10**. The quantity of crystals obtained was insufficient for weighing or further analysis.

Complexes with 3.34

*With $AgPF_6$, viz **3.34***

Silver hexafluorophosphate (11.2mg, 0.044mmol) and ligand **3.34** (13.3mg, 0.025mmol) were each dissolved in dichloromethane and the solutions combined. Slow evaporation produced a few colourless crystals which X-ray crystallography showed to contain only protonated ligand and anion, rather than a silver complex. The quantity of crystals obtained was insufficient for weighing or further analysis.

*With CuI, viz **3.39***

Copper(I) iodide (11.7mg, 0.061mmol) was dissolved in acetonitrile (8ml) and added to a solution of ligand **3.34** (21.2mg, 0.040mmol) in methanol (8ml) to give a white precipitate and yellow solution. A few days later orange plate-like crystals had grown on the sides of the vial. These were suitable for X-ray crystallography, and shown to be three-dimensional polymer **3.39**. Yield 7.7mg (26%). M.p. 171-176^{o}C. (Found: C, 37.36; H, 3.82; N, 4.26. $C_{30}H_{33}N_3S_3Cu_2I_2.3H_2O$ requires C, 37.27; H, 4.07; N, 4.35).

*With $AgClO_4$, viz **3.40***

A solution of silver perchlorate (7.6mg, 0.037mmol) in acetone (2ml) was added to a solution of ligand **3.34** (11.1mg, 0.021mmol) in methanol (4ml) to produce an immediate white precipitate. Evaporation of the solvent did not produce crystals, so the white solid was dissolved in a mixture of DMF, methanol and dichloromethane solvents. Slow evaporation of this solution produced a few colourless square crystals, which X-ray crystallography showed to be four-fold three-dimensional interpenetrating polymer **3.40**. The quantity of crystals obtained was insufficient for weighing or further analysis.

With $NiCl_2$

A solution of nickel(II) chloride (8.7mg, 0.037mmol) in DMF (4ml) was added to a solution of ligand **3.34** (25.9mg, 0.049mmol) in hot acetonitrile (5ml) to give an immediate precipitate. The solution was stirred and heated for 4.5 hours, before the green precipitate was filtered off. Vapour diffusion of various solvents in the yellow filtrate only produced crystals of the metal salt. Yield 8.6mg (25%). M.p. 308-309^{o}C. (Found: C, 51.02; H, 5.29; N, 5.78. 1:1 complex $C_{30}H_{33}N_3S_3Cl_2Ni.{}^{5}/_{2}H_2O$ requires C, 51.01; H, 5.42; N, 5.95).

With $CuCl_2$

Methanol (15ml) was carefully layered upon an aqueous solution (4ml) of copper(II) chloride (18.7mg, 0.110mmol) to create a gradient. Then an ethanol solution (7ml) of ligand **3.34** (19.5mg, 0.037mmol) was carefully layered on top of the methanol layer, to give a green precipitate at the solvent boundary. Slow evaporation to dryness produced an orange solid. Yield 15.2mg (49%). M.p. 123-126^{o}C. (Found: C, 31.50; H, 3.96; N, 3.69. M_4L complex requires $C_{30}H_{33}N_3S_3Cl_8Cu_4.4H_2O$ requires C, 31.56; H, 3.62; N, 3.68).

With $Pd(en)(NO_3)_2$

Dinitrato(ethylenediamine)palladium(II) was generated *in situ* by stirring and heating a solution of dichloro(ethylenediamine)palladium(II) (32.4mg, 0.136mmol) in water (5ml), with nitric acid (two drops) to dissolve. An aqueous solution of silver nitrate (48.6mg, 0.286mmol) in water (2ml) was added dropwise to precipitate AgCl. This solution was stirred at 85^{o}C for ninety minutes, before filtering the precipitate. Solid ligand **3.34** (48.2mg, 0.091mmol) was added to the warm yellow filtrate, and the solution stirred and heated at 65^{o}C for 24 hours to get a pinkish brown mixture, which was filtered to provide an insoluble brown powder. Yield 61.2mg (70%). M.p. 265-275^{o}C (Found: C, 37.21; H, 4.04; N, 8.37. $Pd_3L_2(NO_3)_6$ complex $C_{60}H_{66}N_{12}O_{18}Pd_3.9H_2O$ requires C, 37.59; H, 4.42; N, 8.77).

With $Cu(NO_3)_2$

A solution of copper(II) nitrate (15.0mg, 0.063mmol) in methanol was layered upon a solution of ligand **3.34** (21.3mg, 0.040mmol) in dichloromethane to give an immediate blue precipitate at the boundary between the solvents. This precipitate was mostly insoluble even in DMSO, and was eventually filtered to give a bright blue powder. Yield 3.7mg (12%). M.p. 231-234^{o}C. (Found: C, 49.33; H, 5.22; N, 5.38. M_3L_2 complex $C_{60}H_{66}N_6S_6Cu_3.6OH.CH_2Cl_2.(CH_3)_2SO.H_2O$ requires C, 49.22; H, 5.38; N, 5.47).

Complexes with 3.42

*With CuI, viz **3.44***

Ligand **3.42** (24.9mg, 0.039mmol) was dissolved in methanol and added to a solution of copper(I) iodide (22.6mg, 0.119mmol) in acetonitrile to give a yellow solution. Within

an hour, flowers of plate-like crystal clusters had formed. Although highly twinned, these crystals were suitable for X-ray crystallography, and shown to be discrete Cu_3I_3L complex **3.44**. Unexpectedly, the crystals turn black after filtering, and the elemental analysis results are different to the stoichiometry seen in the crystal structure. Yield 24.0mg (64%). M.p. >320°C (Found: C, 29.37; H, 2.68; N, 2.39. $C_{42}H_{39}N_3O_3Cu_6I_6.4CH_3OH$ requires C, 29.01; H, 2.91; N, 2.21%).

With $Pd(en)_2(NO_3)_2$

Dinitrato(ethylenediamine)palladium(II) was generated *in situ* by stirring and heating a solution of dichloro(ethylenediamine)palladium(II) (22.8mg, 0.096mmol) in water (4ml), with nitric acid (two drops) to dissolve. An aqueous solution of silver nitrate (34.1mg, 0.200mmol) in water (2ml) was added dropwise to precipitate AgCl. This solution was stirred at 85°C for ninety minutes, before filtering the precipitate through cotton wool in a pipette. Solid ligand **3.42** (36.2mg, 0.057mmol) was added to the warm yellow filtrate, and the solution stirred and heated at 85°C for 24 hours to get a brown solution, which was filtered to give a yellow-brown powder. Yield 26.5mg (52%). M.p. 235-245°C (Found: C, 56.48; H, 4.72; N, 5.27. $Pd_3L_2.NO_3.6OH$ complex $C_{84}H_{84}N_7O_{15}Pd_3.H_2O.H_3O^+$requires C, 56.43; H, 5.02; N, 5.48). TOF-MS: Found M^+ 1654.6456, $C_{84}H_{82}N_8O_{15}Pd_2$ requires M^+ 1654.3969. ^{1}H N.M.R. (300MHz, DMSO): δ 1.18, 2.78, 2.96, 4.32, 4.63, 7.02, 7.20, 7.54, 7.74, 8.55, 8.65.

Preparation of complexes with the 1,3,5-trisubstituted-2,4,6-trimethoxybenzene ligands

Complexes with 3.18

With CuI

Ligand **3.18** (23.0mg, 0.056mmol) was dissolved in methanol and added to a solution of copper(I) iodide (32.5mg, 0.171mmol) in acetonitrile to give an instant brown precipitate, which was filtered off a few days later. Yield 30.6mg (56%). M.p. 175-186°C. (Found: C, 23.68; H, 2.56; N, 6.82. M_4L complex $C_{21}H_{24}N_6O_3Cu_4I_4.3CH_3OH.{}^1/_2CH_3CN$ requires C, 23.33; H, 2.94; N, 7.07%).

With $CuCl_2$

Methanolic solutions of **3.18** (19.7mg, 0.048mmol) and copper(II) chloride (12.6mg, 0.074mmol) were combined to give a pale green solution, which slowly formed a yellow precipitate. Multiple crystallisation attempts from various solvents were unsuccessful. Yield 9.1mg (16%). M.p. 146-151°C. (Found: C, 40.15; H, 4.27; N, 10.44. M_2L complex $C_{21}H_{24}N_6O_3Cl_4Cu_2.{}^3/_2(CH_3)_2CO.{}^1/_2CH_3OH$ requires C, 40.01; H, 4.52; N, 10.77%.)

With $Pd(PhCN)_2Cl_2$

A solution of bis(benzonitrile)dichloropalladium(II) (35.1mg, 0.092mmol) in acetone was added to an acetone solution of ligand **3.18** (24.9mg, 0.061mmol) to give a yellow precipitate which was filtered the next morning. Yield 39.1mg (92%). M.p. >320°C. (Found: C, 36.80; H, 3.83; N, 10.36. M_2L complex $C_{21}H_{24}N_6O_3Cl_4Pd_2.C_6H_5CN.3H_2O$ requires C, 36.54; H, 3.83; N, 10.65). ^{1}H N.M.R. (500MHz, DMSO): δ 2.83, 4.45, 4.51, 4.95, 5.03, 5.39, 5.45, 5.64, 6.61, 6.81, 6.83, 6.91.

Complexes with 3.25

With $FeSO_4$

A solution of iron(II) sulfate (15.1mg, 0.054mmol) in methanol was layered upon a solution of ligand **3.25** (20.5mg, 0.036mmol) in chloroform to give a small amount of precipitate at the solvent boundary. Crystallisation attempts from various solvents were unsuccessful, so the black solid was filtered off. Yield 24.1mg (92%). M.p. >320°C. (Found: C, 40.85; H, 4.10; N, 8.46. M_3L complex $C_{36}H_{33}N_9O_{15}S_3Fe_3.4(CH_3)_2CO.CHCl_3$ requires C, 40.67; H, 4.04; N, 8.71%).

With $CuCl_2$

A methanolic solution of copper(II) chloride (9.7mg, 0.057mmol) was layered upon a chloroform solution of ligand **3.25** (21.5mg, 0.038mmol) to give a colour change to dark brown near the solvent boundary. Evaporation to dryness gave a brown solid, which was filtered after crystallisation attempts from various solvents were unsuccessful. Yield 3.6mg (16%). (Found: C, 39.01; H, 3.49; N, 7.91. M_4L complex $C_{36}H_{33}N_9O_3Cl_8Cu_4.4(CH_3)_2CO.{}^3/_2CH_2Cl_2$ requires C, 38.68; H, 3.93; N, 8.20%).

With $Fe(ClO_4)_2$

A solution of iron(II) perchlorate (22.2mg, 0.061mmol) in acetone was layered upon a solution of ligand **3.25** (22.9mg, 0.040mmol) in chloroform to give a precipitate at the solvent boundary. Crystallisation attempts from various solvents were unsuccessful, so the dark brown solid was filtered. Yield 11.7mg (28%). (Found: C, 41.78; H, 4.13; N, 8.91. M_2L complex $C_{36}H_{33}N_9O_{19}Cl_4Fe_2.4(CH_3)_2CO$ requires C, 41.47; H, 4.30; N, 8.54%).

With $CoBr_2$

A solution of cobalt(II) bromide (9.8mg, 0.045mmol) in acetone was layered upon a solution of ligand **3.25** (19.8mg, 0.030mmol) in 1:2 acetone:chloroform to give a precipitate at the solvent boundary. Crystallisation attempts from various solvents were unsuccessful, so the dark crimson solid was extracted. Yield 7.0mg (31%). M.p. >320°C. (Found: C, 41.73; H, 4.14; N, 8.52. M_5L_2 complex $C_{72}H_{66}N_{18}O_6Br_{10}Co_5.10(CH_3)_2CO$ requires C, 41.47; H, 4.30; N, 8.54%).

Complexes with 3.35

With $CoBr_2$

A solution of cobalt(II) bromide (13.7mg, 0.063mmol) in acetone was layered upon a solution of ligand **3.35** (21.9 mg, 0.041mmol) in 1:2 acetone:chloroform to give a blue precipitate at the boundary between the solvents. Crystallisation from methanol and acetonitrile was unsuccessful, so the precipitate was filtered off to give a dark green powder. Yield 14.3mg (39%). M.p. 208-214°C. (Found: C, 42.58; H, 3.87; N, 4.65. 1:1 complex $C_{27}H_{27}N_3O_3S_3Br_2Co.{}^1/_2CHCl_3.{}^3/_2(CH_3)_2CO$ requires C, 26.60; H, 2.55; N, 3.32%).

With $AgClO_4$

An acetone solution of silver(I) perchlorate (21.7mg, 0.105mmol) was layered upon a chloroform solution of ligand **3.35** (27.0 mg, 0.050mmol) to slowly give a white precipitate, which was washed out with methanol and filtered off after slow evaporation to dryness. Yield 31.0mg (56%). (Found: C, 33.16; H, 3.02; N, 3.77. M_2L complex $C_{27}H_{27}N_3O_{11}S_3Cl_2Ag_2.{}^1/_2CHCl_3.{}^3/_2CH_3OH$ requires C, 32.86; H, 3.19; N, 3.96%).

With $CuCl_2$

A solution of copper(II) chloride (11.9mg, 0.070mmol) in methanol (3ml) was layered upon a solution of ligand **3.35** (27.4mg, 0.046mmol) in dichloromethane, to give a precipitate at the boundary between the solutions. Weeks later this precipitate was filtered off to give the product as a mustard yellow powder. Yield 16.3mg (56%). M.p. 177-182^{o}C. (Found: C, 40.43; H, 3.74; N, 4.78. M_2L complex $C_{27}H_{27}N_3O_3S_3Cl_4Cu_2.CH_3OH$ requires C, 40.10; H, 3.73; N, 5.01%).

With CuI

A solution of copper(I) iodide (21.7mg, 0.114mmol) in acetonitrile was layered upon a solution of ligand **3.35** (20.2 mg, 0.038mmol) in 4:1 methanol:chloroform to give an orange precipitate, which was washed and filtered off after slow evaporation to dryness. Yield 29.1mg (61%). M.p. 184-189^{o}C. (Found: C, 26.54; H, 2.45; N, 3.03. M_3L complex $C_{27}H_{27}N_3O_3S_3Cu_3I_3.CHCl_3.H_2O$ requires C, 26.60; H, 2.55; N, 3.32%).

With $CoCl_2$

A solution of cobalt(II) chloride (14.4mg, 0.066mmol) in methanol was layered upon a chloroform solution of ligand **3.35** (21.5mg, 0.040mmol) to give an immediate blue precipitate. The solution was evaporated to dryness, before the solid washed out and filtered off to give a teal green powder. Yield 13.2mg (41%). M.p. >320^{o}C. (Found: C, 43.68; H, 4.21; N, 4.87. M_3L_2 complex $C_{54}H_{54}N_6O_6S_6Cl_6Co_3.5CH_3OH$ requires C, 43.60; H, 4.59; N, 5.17%).

Complexes with 3.43

With $CoBr_2$

Ligand **3.43** (24.0 mg, 0.038mmol) barely dissolved upon heating in a 1:10 solution of acetone:chloroform, but was used anyway as enough dissolved for equilibrium processes to take place. An acetone solution of cobalt(II) bromide (13.3mg, 0.061mmol) was layered upon the ligand solution to give a precipitate at the boundary between the solvent solutions. A few weeks later the solution appeared to have mixed and all reacted, so the brown precipitate was filtered off. Yield 13.8mg (36%). M.p. >320^{o}C. (Found: C, 46.03; H, 4.08; N, 3.50. M_2L complex $C_{39}H_{33}N_3O_6Br_4Co_2.3(CH_3)_2CO$ requires C, 46.07; H, 4.11; N, 3.36%).

With $AgClO_4$

An acetone solution of silver(I) perchlorate (14.5mg, 0.070mmol) was layered upon a chloroform solution of ligand **3.43** (21.7 mg, 0.034mmol) to give an immediate precipitate. This deep crimson powder was washed out with methanol and filtered off after slow evaporation to dryness. Yield 19.6mg (48%). (Found: C, 40.72; H, 3.17; N, 3.41. M_3L_2 complex $C_{78}H_{66}N_6O_{24}Cl_3Ag_3.4CHCl_3.2H_2O$ requires C, 40.78; H, 3.09; N, 3.48%).

Preparation of complexes with the 4,4',4"-trisubstituted 1,3,5-triphenylphenyl ligands

Complexes with 4.9

*With $AgClO_4$, viz **4.12***

Ligand **4.9** (13.2mg, 0.024mmol) was dissolved in dichloromethane and added to a solution of silver perchlorate (7.9mg, 0.038mmol) in toluene to give a white precipitate which was filtered off. Yield 8.6mg (45%) (Found: C, 66.68; H, 4.91; N, 10.80. M_2L_3 complex $C_{108}H_{90}N_{18}O_8Cl_2Ag_2.3C_7H_8$ requires C, 66.47; H, 4.93; N, 10.82). Slow evaporation of an acetonitrile solution of this solid gave a few colourless crystals suitable for X-ray crystallography which showed it to be two-dimensional polymer **4.12**.

*With $AgClO_4$, viz **4.12a***

A solution of silver perchlorate (42.1mg, 0.203mmol) in toluene was layered upon a dichloromethane solution containing ligand **4.9** (73.4mg, 0.134mmol) and the potential templating molecule trimesic acid (14.2mg, 0.068mmol). The solution was left overnight to slowly mix together, then stirred for seven hours the next day, allowed to sit for three days, stirred for an extra half hour before the white precipitate was filtered off. Yield 66.6mg (44%). (Found: C, 49.75; H, 3.54; N, 7.51. 1:1:1 complex $C_{36}H_{30}N_6O_4ClAg.C_6H_3(COOH)_3.2CH_2Cl_2$ requires C, 49.78; H, 3.56; N, 7.41). Slow evaporation of an acetonitrile solution gave a few colourless crystals suitable for X-ray crystallography to reveal again the two-dimensional polymer **4.12**.

With $PdCl_2$

A solution of palladium(II) chloride (31.5mg, 0.178mmol) dissolved in hot hydrochloric acid (2M, 3ml) was added dropwise to a solution of ligand **4.9** (62.1mg, 0.114mmol) in methanol (3ml) to give a light coloured precipitate which was stirred for 15 minutes and filtered the next morning to give a cream powder. Yield 72.1mg (72%). M.p. >320°C. Vapour diffusion of methanol into a DMSO solution of this powder gave yellow spheres which did not diffract. (Found: C, 48.80; H, 3.84; N, 8.75. Pd_3L_2 complex $C_{72}H_{60}N_{12}Cl_6Pd_3.3(CH_3)_2SO.CH_2Cl_2$ requires C, 48.79; H, 4.15; N, 8.64). ^{1}H N.M.R. (300MHz, DMSO): δ 5.50, 6.39, 7.44, 7.55, 7.93, 7.98.

With $PdCl_2$

A solution of palladium(II) chloride (18.8mg, 0.106mmol) dissolved in hot dilute hydrochloric acid (5ml) was added dropwise to a solution of ligand **4.9** (34.9mg, 0.064mmol) and possible templating molecule trimesic acid (27.4mg, 0.130mmol) in hot acetonitrile (30ml) to give a light coloured precipitate which was stirred for 23 hours then filtered to give a yellow powder. Yield 25.2mg (36%). M.p. >320°C. (Found: C, 50.70; H, 3.59; N, 9.11. M_2L complex $C_{36}H_{30}N_6Cl_4Pd_2.3C_6H_3(COOH)_3.4CH_3CN$ requires C, 50.48; H, 3.66; N, 8.87). ^{1}H N.M.R. (300MHz, DMSO): δ 5.49, 6.04, 6.14, 6.39, 6.62, 7.36, 7.44, 7.51, 7.58, 7.67, 7.92, 7.98, 8.14, 8.23.

With $AgNO_3$

A solution of silver nitrate (10.6mg, 0.062mmol) in water was added to a solution of ligand **4.9** (19.9mg, 0.036mmol) in acetone. The next day a pale brown precipitate was filtered off. Yield 26.0mg (81%). M.p. 70°C. (Found: C, 50.59; H, 3.61; N, 10.68. Ag_2L complex $C_{36}H_{30}N_8O_6Ag_2.2(CH_3)_2CO$ requires C, 50.32; H, 4.22; N, 11.18).

With $AgPF_6$

Ligand **4.9** (39.2mg, 0.072mmol) and silver hexafluorophosphate (32.2mg, 0.127mmol) were each dissolved in dichloromethane and combined to give an immediate precipitate. Two days later this pale purple precipitate was filtered off. Yield 47.7mg (58%). M.p. 135-150°C. (Found: C, 38.49; H, 3.03; N, 6.97. Ag_2L complex $C_{36}H_{30}N_6F_{12}P_2Ag_2.CHCl_3.H_2O$ requires C, 38.47; H, 2.97; N, 7.27).

Complexes with 4.13

*With $CuSO_4$, viz **4.15***

Methanol (12ml) was very carefully layered upon an aqueous solution (4ml) of copper(II) sulfate (14.2mg, 0.057mmol) to create a solvent gradient. Ligand **4.13** (29.5mg, 0.038mmol) was dissolved in the minimum amount of chloroform, and very carefully and slowly added dropwise to the layered solution, whereupon the chloroform floated to the surface of the vial. The nearly colourless solution turned green where the solutions met. After a few weeks of slow evaporation, clusters of needle-like green crystals appeared, along with a few very small green single crystals. These single crystals proved to be suitable for X-ray crystallography and revealed Cu_6L_4 cage-like complex **4.15**. Months later the solution was filtered, and the mixture of crystals sent for elemental analysis, the results of which suggest all the material may be homogeneous. Yield 14.2mg (33%). M.p. 307-311^oC. (Found: C, 53.02; H, 4.34; N, 11.26. M_6L_4 complex $C_{204}H_{156}N_{32}O_{24}S_6Cu_6.29H_2O$ requires C, 53.36; H, 4.70; N, 10.98).

*With $CuSO_4$, viz **4.15a***

Methanol (18ml) was very carefully layered upon an aqueous solution (4ml) of copper(II) sulfate (16.8mg, 0.067mmol) to create a solvent gradient. Ligand **4.13** (35.0mg, 0.045mmol) and the possible guest molecule triphenylamine (4.7mg, 0.019mmol) were dissolved in the minimum amount of chloroform, and very carefully and slowly added dropwise to the layered solution, whereupon the chloroform floated to the surface of the vial. The nearly colourless solution turned green where the solutions met. A little extra chloroform (1ml) was added to increase the solubility of the organic molecules as the solution was slightly cloudy. After a month of slow evaporation, clusters of needle-like green crystals appeared in solution, along with a few very small green single crystals. These single crystals proved to be suitable for X-ray crystallography and revealed empty Cu_6L_4 cage-like complex **4.15**.

With $CoBr_2$

A solution of cobalt(II) bromide (10.6mg, 0.048mmol) in methanol was layered upon a chloroform solution of ligand **4.13** (24.8mg, 0.032mmol) to give a pink solution. Vapour diffusion and slow evaporation of various solvents only produced a precipitate, which was eventually filtered off. Yield 21.7mg (57%). M.p. 228-232^oC. (Found: C,

54.86; H, 4.34; N, 11.87. M_3L_2 complex $C_{102}H_{78}N_{18}Br_6Co_3.2CH_3CN.3CH_3OH$ requires C, 54.77; H, 4.05; N, 11.72).

With CuI

An acetonitrile solution of copper(I) iodide (11.4mg, 0.060mmol) was layered upon a 10:1 toluene:methanol solution of ligand **4.13** (30.2mg, 0.039mmol) to give a yellow solution which slowly precipitated. The solution was slowly evaporated to dryness, and the pale brown powder washed out with acetone and filtered off. Yield 18.7mg (61%). M.p. 206-210°C. (Found: C, 47.06; H, 3.52; N, 10.83. M_3L complex $C_{51}H_{39}N_9Cu_3I_3.{}^1/_3C_7H_8.3CH_3CN.{}^3/_2H_2O$ requires C, 47.02; H, 3.59; N, 10.88).

*With $CuCl_2$, viz **5.12***

Ligand **4.13** (29.5mg, 0.038mmol) and possible guest molecule **4.35** (6.5mg, 0.022mmol) were each dissolved in acetone, combined, then added to a solution of copper(II) chloride (9.9mg, 0.058mmol) in acetone to give a green precipitate. DMSO was added to dissolve the precipitate. Vapour diffusion of more acetone into this solution failed to produce crystals, however clusters of dark green needle-like crystals grew upon slow evaporation of this solution. These crystals were suitable for X-ray crystallography and were shown to be ligand decomposition complex **5.12**. Yield 0.1mg (0.6%). The quantity of crystals obtained was insufficient for further analysis.

*With $CuSO_4$, viz **5.14** and **5.15***

Copper(II) sulfate (12.6mg, 0.050mmol) was dissolved in hot methanol (2ml). Ligand **4.13** (26.3mg, 0.034mmol) and the possible guest molecule **4.35** (5.4mg, 0.018mmol) were each dissolved in acetone (1ml), and added to the copper solution to give a turquoise green precipitate. The solution was heated and stirred for an hour, before it was divided into portions. DMSO was added to one portion to dissolve the precipitate. Vapour diffusion of more acetone into this solution failed to produce crystals, however blue plate-like crystals grew upon slow evaporation of this solution. These crystals were suitable for X-ray crystallography and were shown to be ligand decomposition complex **5.14**. Yield 0.3mg (2%). DMF was added to the other portion to dissolve the precipitate. Vapour diffusion of ether into this solution failed to produce crystals, however small dark blue blocks grew after a year of slow evaporation. These crystals were suitable for X-ray crystallography and shown to be a different ligand decomposition complex

polymer, **5.15**. Yield 0.1mg (0.7%). The quantity of each batch of crystals obtained was insufficient for further analysis.

Complex with 4.16

With CuI

An acetonitrile solution of copper(I) iodide (5.9mg, 0.031mmol) was layered upon a solution of ligand **4.16** (14.0mg, 0.021mmol) in dichloromethane to give a small amount of precipitate slowly forming at the boundary between the solvents. Crystallisation attempts of this brown solid from various solvents were unsuccessful. Yield 13.1mg (71%). M.p. 183-191^{o}C. (Found: C, 43.18; H, 3.42; N, 3.68. M_2L complex $C_{42}H_{33}N_3S_3Cu_2I_2.CH_2Cl_2.3H_2O$ requires C, 43.19; H, 3.46; N, 3.51).

Preparation of complexes with the 4,4',4"-trisubstituted triphenylhydroxymethane ligands

Complexes with 4.37

With $CoBr_2$

A solution of cobalt(II) bromide (16.0mg, 0.073mmol) in acetone (10ml) was layered upon a solution of ligand **4.37** (24.0mg, 0.048mmol) in chloroform (10ml). A small amount of precipitate appeared at the boundary between the solutions. A few weeks later a turquoise blue precipitate was filtered off. Yield 11.7mg (27%). M.p. >320^{o}C (Found: C, 47.06; H, 3.64; N, 8.95. 1:1 complex $C_{31}H_{28}N_6OCoBr_2.CHCl_3.(CH_3)_2CO$ requires C, 46.88; H, 3.93; N, 9.37).

With $Pd(PhCN)_2Cl_2$

A solution of bis(benzonitrile)dichloropalladium(II) (23.1mg, 0.061mmol) in acetone (10ml) was layered upon a solution of ligand **4.37** (20.1mg, 0.040mmol) in chloroform (10ml). Immediately a precipitate formed at the boundary between the solutions. A few weeks later this pale yellow precipitate was filtered off. Yield 14.4mg (41%). M.p. >320^{o}C (Found: C, 48.37; H, 3.78; N, 9.38. M_3L_2 complex $C_{62}H_{56}N_{12}O_2Cl_6Pd_2.{}^{1}/_{2}CHCl_3.{}^{5}/_{2}(CH_3)_2CO$ requires C, 48.37; H, 4.15; N, 9.67).

Complexes with 4.38

With $Co(BF_4)_2$

A solution of cobalt(II) tetrafluoroborate (14.8mg, 0.064mmol) was added to a solution of ligand **4.38** (31.1mg, 0.043mmol) in acetone to give an orange solution and pink precipitate. Multiple crystallisation attempts of this precipitate from various solvents were unsuccessful, so the pink solid was filtered off. Yield 30.4mg (69%). M.p. >320°C. (Found: C, 55.77; H, 4.01; N, 13.56. 1:1 complex $C_{46}H_{37}N_9OB_2F_8Co.CH_3CN.^3/_2H_2O$ requires C, 55.84; H, 4.20; N, 13.57).

With $FeSO_4$

A methanolic solution of iron(II) sulfate (18.0mg, 0.065mmol) was layered upon a chloroform solution of ligand **4.38** (30.7mg, 0.042mmol) to give an orange solution and slowly forming precipitate. Crystallisation of this yellow precipitate from various solvents was unsuccessful. Yield 23.0mg (62%). M.p. 281-286°C. (Found: C, 48.10; H, 4.21; N, 11.56. M_2L complex $C_{46}H_{37}N_9O_9S_2Fe_2.^1/_2CH_3CN.^{13}/_2H_2O$ requires C, 48.11; H, 4.42; N, 11.34).

With $CuCl_2$

Ligand **4.38** (40.3mg, 0.055mmol) and copper(II) chloride (14.6mg, 0.086mmol) were each dissolved in acetone (10ml) with a little acetonitrile, and combined to give a pale green precipitate which was filtered off. Yield 11.3mg (26%). M.p. 186-189°C (Found: C, 54.76; H, 4.03; N, 13.10. M_2L complex $C_{46}H_{37}N_9Cl_4Cu_2.^1/_2CH_3CN.^1/_2H_2O$ requires C, 54.79; H, 3.86; N, 12.92).

With $CoBr_2$

Ligand **4.38** (23.8mg, 0.033mmol) and cobalt(II) bromide (10.8mg, 0.049mmol) were each dissolved in hot acetone and combined to give a pink precipitate which was filtered off. Yield 21.4mg (58%). M.p. 218-220°C (dec). (Found: C, 52.38; H, 4.22; N, 12.31. Co_3L_2 complex $C_{92}H_{74}N_{18}O_2Co_3Br_6$ requires C, 52.12; H, 3.52; N, 11.89).

Complexes with 4.43

With CuI

An acetonitrile solution of copper(I) iodide (11.5mg, 0.060mmol) was layered upon a chloroform solution of ligand **4.43** (29.6mg, 0.041mmol) to give a small amount of

light precipitate at the boundary between solutions. The solution was slowly evaporated to dryness, and the pale brown powder washed out with acetone and filtered off. Yield 20.8mg (59%). M.p. >320°C. (Found: C, 52.93; H, 3.84; N, 4.02. M_2L complex $C_{49}H_{37}N_3O_4Cu_2I_2.{}^1/_2CH_3CN.{}^1/_2(CH_3)_2CO.{}^1/_2H_2O$ requires C, 52.81; H, 3.66; N, 4.19).

Complexes of 5.1

*With $CoBr_2$, viz **5.4***

Acetone solutions of ligand **5.1** (19.3mg, 0.129mmol) and cobalt(II) bromide (28.1mg, 0.128mmol) were combined to give a light coloured precipitate. By the next morning this precipitate had redissolved and the solution contained large pink crystals of **5.4** suitable for X-ray crystallography. Yield 6.1mg (17%). M.p. 294-299°C. (Found: C, 35.57; H, 2.85; N, 15.54. $C_{16}H_{12}N_6CoBr_2.2H_2O$ requires C, 35.39; H, 2.97; N, 15.47).

*With $La(NO_3)_3$, viz **5.5***

Solutions of ligand **5.1** (20.9mg, 0.139mmol) and lanthanum nitrate (60.2mg, 0.139mmol) in methanol were combined to give a colourless solution. Slow evaporation over a week gave colourless block-like crystals of **5.5** suitable for X-ray crystallography. Yield 35.0mg (77%). M.p. 197-202°C. (Found: C, 31.13; H, 2.79; N, 19.10. $C_{17}H_{18}N_9O_{10}La.{}^1/_2H_2O$ requires C, 31.11; H, 2.92; N, 19.21).

*With $ZnBr_2$, viz **5.6***

Both ligand **5.1** (20.2mg, 0.135mmol) and zinc bromide (30.2mg, 0.134mmol) were dissolved in methanol and combined to give a colourless solution. Vapour diffusion of ether into this solution in the fridge gave two large colourless crystals of **5.6** suitable for X-ray crystallography. More crystals were obtained upon evaporation to dryness, one of which was shown to be a different complex to **5.6**. The bulk of material appears to be a mixture of different products. Yield 29.3mg (64%). M.p. >320°C. (Found: C, 27.95; H, 2.03; N, 12.12. $C_{48}H_{42}N_{18}Zn_5Br_{10}.3H_2O$ requires C, 28.11; H, 2.36; N, 12.29).

*With $CuCl_2$ and $CoCl_2$, viz **5.7***

Copper(II) chloride (15.3mg, 0.090mmol) in methanol was added to a solution of ligand **5.1** (26.5mg, 0.177mmol) in methanol to give a cloudy teal green solution. The addition

of a methanol solution of cobalt(II) chloride (21.2mg, 0.089mmol) had little effect on the appearance of the solution. Slow evaporation over two weeks and the addition of a little acetonitrile gave large green block-like crystals amongst a fine crystalline green precipitate. One of the large block-like crystals was analysed by X-ray crystallography and shown to be dimer **5.7**. Yield 13.7mg (53%). M.p. 304-306^{o}C. (Found: C, 35.44; H, 2.59; N, 15.54. $C_8H_7N_3Cl_2Cu.^1/_4CH_3CN$ requires C, 35.22; H, 2.69; N, 15.70). Found M^+ 388.0217, $C_{16}H_{14}N_6ClCu$ requires M^+ 388.0264.

*With $CdCl_2$, viz **5.8***

Hot methanolic solutions of ligand **5.1** (19.1mg, 0.127mmol) and cadmium chloride (29.2mg, 0.128mmol) were combined, and produced thin needle-like crystals upon cooling. A week later these thin crystals had recrystallised into clusters of block-like colourless crystals. These new crystals were suitable for X-ray crystallography and were analysed to reveal one-dimensional polymer structure **5.8**. Yield 35.8mg (83%). M.p. 319-324^{o}C. (Found: C, 28.17; H, 2.15; N, 12.24. $C_8H_7N_3Cl_2Cd$ requires C, 28.47; H, 2.39; N, 12.45).

*With $Ni(OAc)_2$, viz **5.11***

Ligand **5.1** (25.6mg, 0.147mmol) and nickel acetate (42.6mg, 0.171mmol) were both dissolved in hot methanol. When the ligand solution was added to the metal solution, it triggered a colour change from pale green to purple. A pale pink coloured precipitate formed upon cooling, which was filtered off a few months later, and was shown by elemental analysis to be a different product to the few crystals obtained. Yield 4.3mg (12%). M.p. >320^{o}C. (Found: C, 50.72; H, 3.69; N, 20.32. ML_2 complex $C_{18}H_{15}N_6O_2Ni.H_2O$ requires C, 50.98; H, 4.04; N, 19.82). A few blue crystals of dimer **5.11** suitable for X-ray crystallography grew on the sides of the vial over a three month period.

*With $CuSO_4$, viz **5.13***

Methanolic solutions of ligand **5.1** (21.9mg, 0.146mmol) and 4,4'-bipyridine (22.7mg, 0.145mmol) were combined, then added to a methanol solution of copper(II) sulfate (36.6mg, 0.147mmol) to give a light blue precipitate. Over a period of ten days the precipitate crystallised to give large blue diamond-shaped crystals of dimer **5.13** suitable for X-ray crystallography. Yield 37.7mg (58%). M.p. >320^{o}C. (Found: C,

37.76; H, 3.95; N, 12.51. $C_{28}H_{30}N_8O_{10}S_2Cu_2.{}^7/_2H_2O$ requires C, 37.67; H, 4.18; N, 12.55).

*With CuI, viz **5.16***

Ligand **5.1** (22.0mg, 0.147mmol) dissolved in acetone was added to a solution of copper(I) iodide (14.1mg, 0.074mmol) in acetonitrile. The colourless solutions turned green upon combination. Slow evaporation over a few days gave dark green block-like crystals of Cu_2L_4 complex **5.16** suitable for X-ray crystallography. Yield 18.8mg (54%). M.p. 292-295°C. (Found: C, 40.20; H, 2.80; N, 17.60. $C_{16}H_{12}N_6CuI$ requires C, 40.14; H, 2.53; N, 17.55).

*With CuI and $Ni(NO_3)_2$, viz **5.17***

A methanolic solution of nickel nitrate (14.8mg, 0.081mmol) was added to a solution of ligand **5.1** (24.0mg, 0.160mmol) in methanol to give a purple solution. The addition of an acetonitrile solution of copper(I) iodide (15.3mg, 0.080mmol) caused another colour change to yellow. Slow evaporation over a week afforded two different types of crystals, both suitable for X-ray crystallography. Total yield 26.9mg. The different crystal types were separated by hand under a microscope. The blue prisms proved to be copper complex **5.3**. Yield 6.0mg (26%). M.p. 303°C (Caution: explosive). (Found: C, 33.69; H, 2.81; N, 19.59. $C_{16}H_{16}N_8O_8Cu_2$ requires C, 33.40; H, 2.80; N, 19.47). The deep red blocks revealed Ni_4L_6 box structure **5.17**. Yield 17.7mg (46%). M.p. >320°C. (Found: C, 33.05; H, 2.36; N, 14.78. $C_{26}H_{21}N_{10}CuNi_2I_2.4H_2O$ requires C, 33.07; H, 2.67; N, 14.83).

*With CuI and $CoBr_2$, viz **5.18***

Methanolic solutions of cobalt(II) bromide (17.5mg, 0.080mmol) and ligand **5.1** (26.5mg, 0.177mmol) were combined to give an orange solution. The addition of an acetonitrile solution of copper(I) iodide (15.3mg, 0.080mmol) caused the solution colour to change slowly through dark green to brown. Slow evaporation gave red (dichroic to green) plate-like crystals of mixed metal M_4L_6 box complex **5.18** suitable for X-ray crystallography. Yield 9.4mg (34%). M.p. 318-321°C. Found M^+ 850.9697, $C_{33}H_{27}N_{12}OCu_2Co_2$ requires M^+ 850.9687.

With $Cu(OAc)_2$

Copper(II) acetate (30.1mg, 0.151mmol) was dissolved in hot methanol, cooled to room temperature, and added to a solution of ligand **5.1** (22.3mg, 0.149mmol) in methanol. After a few days in the fridge, blue square blocks formed which were suitable for X-ray crystallography; however before they could be analysed the entire mass of crystals redissolved and then crystallised as blue needles not suitable for X-ray crystallography. Yield 35.7mg (90%). M.p. 293-296^{o}C. (Found: C, 45.24; H, 3.41; N, 15.82. 1:1 complex $C_{10}H_9N_3O_2Cu$ requires C, 45.03; H, 3.40; N, 15.75).

Appendices

Crystallography

Tables A1-A14 list the crystal data and X-ray experimental details for the fifty-six crystal structures discussed in this thesis. Throughout the text, selected bond lengths and angles are discussed and listed under the appropriate figures, while the remaining distances and angles, as well as atomic coordinates, anisotropic displacement factors and hydrogen atom coordinates are available on request from the Department of Chemistry, University of Canterbury.

The data for the crystal structures reported in this thesis were collected on two different X-ray diffractometers. Both detectors used graphite monochromatised Mo Kα (λ=0.71073Å) radiation.

The first diffractometer used was a Siemens CCD area detector mounted on a P4 four-circle diffractometer. Data collection and cell determination was performed with SMART and data reduction with SAINT.

The second diffractometer used was a Bruker-Nonius APEX II system. Data collection, cell determination and data reduction were all performed with the APEX software package.

All structures had intensities corrected for Lorentz and polarization effects and for absorption using SADABS. All structures were solved by direct methods using SHELXS and refined on F^2 using all data by full-matrix least squares procedures using SHELXL-97. All non-hydrogen atoms were refined with anisotropic displacement parameters, except one example which is alluded to in the text. Hydrogen atoms were included in calculated positions with isotropic displacement parameters 1.2 or 1.5 times the isotropic equivalent of their carrier carbon atoms. It is possible that some of the refinements reported may change slightly upon preparation for publication.

R_1 values in brackets quote the values prior to the application of *Squeeze*.[151]

Table A1. Crystal data and structure refinement for 27, 2.8, 2.9 and 2.10.

Compound		**2.7**	**2.8**	**2.9**	**2.10**
Empirical formula		$C_{22}H_{28}N_5CoBr_2$	$C_{85}H_{109}N_{16}Cl_{15}Zn_4Br_8$	$C_{20}H_{26}N_4CuI$	$C_{178}H_{210}N_{36}Cl_{30}Cu_{16}I_{16}$
Formula weight		581.24	2787.39	512.89	6964.53
Temperature (K)		93(2)	93(2)	93(2)	93(2)
Crystal system		Triclinic	Monoclinic	Monoclinic	Orthorhombic
Space group		P-1	$P2_1/n$	$P2_1/n$	$P2_12_12_1$
Unit cell dimensions:	a (Å)	9.1795(2)	17.2370(3)	7.5512(1)	15.8068(6)
	b (Å)	10.8369(2)	16.3013(4)	19.1785(3)	18.0782(7)
	c (Å)	13.0784(2)	19.4473(4)	14.0020(2)	21.6641(8)
	α (°)	92.433(1)	90	90	90
	β (°)	97.773(1)	93.695(1)	96.220(1)	90
	γ (°)	104.254(1)	90	90	90
Volume ($Å^3$)		1245.47(4)	5453.0(2)	2002.4(11)	6190.7(4)
Z		2	2	4	1
Density (calculated) (Mg/m^3)		1.550	1.698	1.701	1.868
Absorption coefficient (mm^{-1})		3.915	4.217	2.644	3.712
F(000)		584	2772	1024	3352
Crystal size (mm^3)		0.35 x 0.24 x 0.08	0.42 x 0.16 x 0.03	0.30 x 0.20 x 0.08	0.35 x 0.25 x 0.15
Theta range for data collection (°)		2.60 to 27.49	2.37 to 27.52	2.59 to 30.52	1.47 to 25.05
Reflections collected		17188	84304	7799	78781
Independent reflections [R(int)]		5553 [0.0376]	12456 [0.0564]	7626 [0.0347]	10962 [0.0887]
Completeness to theta (°/%)		27.49/97.2	27.52/99.3	30.52/97.7	25.05/99.9
Data / restraints / parameters		5553 / 0 / 273	12456 / 0 / 586	7626 / 0 / 237	10962 / 6 / 641
Goodness-of-fit on F^2		1.082	0.970	1.221	1.116
Final R_1 [I>2sigma(I)]		0.0290	0.0322	0.0564	0.0573
wR_2 (all data)		0.0802	0.0839	0.1579	0.1566
Largest diff. peak and hole ($e.Å^{-3}$)		1.043 and -0.534	1.382 and -1.669	3.208 and -2.049	2.084 and -1.132
Detector		APEX II	APEX II	APEX II	APEX II
Flack parameter (if applicable)				0.02(4)	

Table A2. Crystal data and structure refinement for 2.11, 2.20, 2.21 and 2.22.

Compound	**2.11**	**2.20**	**2.21**	**2.22**
Empirical formula	$C_{63}H_{84}N_{12}OCl_6Pd_3$	$C_{35}H_{33}N_{6O}Cl_6Cu_2I_2$	$C_{62.33}H_{64}N_{12}O_{21.75}S_2ClCu_2$	$C_{72}H_{70}N_{12}O_{20}S_2Fe_2$
Formula weight	1557.32	1147.27	1555.55	1599.24
Temperature (K)	93(2)	108(2)	93(2)	93(2)
Crystal system	Monoclinic	Triclinic	Triclinic	Triclinic
Space group	$P2_1/n$	P-1	P-1	P-1
Unit cell dimensions: a (Å)	15.5405(4)	9.6422(9)	12.6991(15)	12.089(3)
b (Å)	15.9842(5)	11.9765(14)	17.238(2)	12.846(3)
c (Å)	27.5654(7)	19.002(2)	17.672(2)	14.020(4)
α (°)	90	77.002(7)	85.283(8)	105.501(7)
β (°)	90.465(1)	86.384(7)	82.101(8)	105.499(7)
γ (°)	90	75.038(7)	73.085(7)	94.451(10)
Volume ($Å^3$)	6847.1(3)	2065.7(4)	3662.4(7)	1995.7(9)
Z	4	2	2	1
Density (calculated) (Mg/m^3)	1.511	1.845	1.411	1.331
Absorption coefficient (mm^{-1})	1.063	2.949	0.753	0.491
F(000)	3176	1118	1605	830
Crystal size (mm^3)	0.45 x 0.24 x 0.12	0.26 x 0.07 x 0.01	0.44 x 0.36 x 0.22	0.36 x 0.26 x 0.08
Theta range for data collection (°)	1.48 to 25.05	1.10 to 25.54	1.16 to 25.05	2.23 to 25.05
Reflections collected	84560	26844	41457	17394
Independent reflections [R(int)]	12127 [0.0689]	7304 [0.2827]	12379 [0.1757]	7013 [0.0811]
Completeness to theta (°/%)	25.05/100.0	25.54/94.5	25.05/92.5	25.05/99.1
Data / restraints / parameters	12127 / 0 / 804	7304 / 0 / 244	12379 / 0 / 937	7013 / 0 / 515
Goodness-of-fit on F^2	1.072	0.870	1.076	0.965
Final R_1 [I>2sigma(I)]	0.0457	0.0836	0.1667	0.0726
wR_2 (all data)	0.1323	0.3017	0.4987	0.1971
Largest diff. peak and hole ($e.Å^{-3}$)	1.341 and -0.966	1.946 and -1.230	4.943 and -1.756	0.977 and -0.568
Detector	APEX II	APEX II	APEX II	APEX II

Table A3. Crystal data and structure refinement for 2.23, 2.24, 2.25 and 2.26.

Compound	**2.23**	**2.24**	**2.25**	**2.26**
Empirical formula	$C_{69}H_{82}N_{12}O_3Cl_4Co_2$	$C_{29}H_{31}N_6O_3Cl_2Cu$	$C_{67}H_{64}N_{16}O_{19}Cu_2$	$C_{65}H_{70}N_{12}O_7Br_4Zn_2$
Formula weight	1387.13	1446.43	1524.44	1581.71
Temperature (K)	93(2)	93(2)	93(2)	93(2)
Crystal system	Monoclinic	Monoclinic	Monoclinic	Monoclinic
Space group	C2/c	$P2_1/n$	$P2_1/c$	$P2_1/c$
Unit cell dimensions: a (Å)	14.0823(4)	12.0972(5)	12.0787(4)	12.023(2)
b (Å)	20.6136(5)	20.2048(8)	20.0822(8)	18.262(5)
c (Å)	24.1671(6)	14.4515(6)	15.0498(5)	16.616(3)
α (°)	90	90	90	90
β (°)	102.957(1)	94.273(2)	95.918(2)	96.271(10)
γ (°)	90	90	90	90
Volume ($Å^3$)	6836.8(3)	3522.4(2)	3631.1(2)	3626.6(14)
Z	4	2	2	2
Density (calculated) (Mg/m^3)	1.348	1.364	1.394	1.449
Absorption coefficient (mm^{-1})	0.697	0.816	0.667	2.921
F(000)	2904	1520	1576	1600
Crystal size (mm^3)	0.31 x 0.20 x 0.17	0.28 x 0.22 x 0.08	0.55 x 0.20 x 0.08	0.40 x 0.26 x 0.14
Theta range for data collection (°)	2.63 to 25.05	2.35 to 25.05	1.98 to 25.05	1.66 to 26.43
Reflections collected	26115	29252	37992	35215
Independent reflections [R(int)]	6043 [0.0613]	6194 [0.0845]	6415 [0.0562]	7407 [0.0793]
Completeness to theta (°/%)	25.05 / 99.9	25.05 / 99.0	25.05 / 99.9	26.43 / 99.3
Data / restraints / parameters	60.43 / 12 / 407	6194 / 0 / 430	6415 / 0 / 564	7407 / 0 / 415
Goodness-of-fit on F^2	0.953	1.004	1.054	1.085
Final R_1 [I>2sigma(I)]	0.0348	0.0547	0.0473	0.0960
wR_2 (all data)	0.0841	0.1673	0.1431	0.3231
Largest diff. peak and hole ($e.Å^{-3}$)	0.376 and -0.346	1.234 and -0.533	0.636 and -0.845	3.879 and -1.568
Detector	APEX II	APEX II	APEX II	APEX II

Table A4. Crystal data and structure refinement for 2.27, 2.28, 2.29 and 2.30.

Compound	**2.27**	**2.28**	**2.29**	**2.30**
Empirical formula	$C_{61}H_{64}N_{12}O_{10.3}Cl_2Ag_2$	$C_{191.1}H_{156}N_{36}O_{35}Cl_8Ni_4$	$C_{185}H_{136}N_{36}O_{29}Cl_7Cu_4$	$C_{60}H_{72}N_{14.4}O_{17.6}Cl_{1.6}Co_2$
Formula weight	1416.90	4035.0	3829.65	1451.10
Temperature (K)	113(2)	93(2)	93(2)	93(2)
Crystal system	Monoclinic	Orthorhombic	Orthorhombic	Triclinic
Space group	C2/c	Pmmn	Pmmn	P-1
Unit cell dimensions: a (Å)	26.701(4)	22.6490(17)	22.997(7)	11.1126(4)
b (Å)	24.008(3)	38.029(3)	38.992(10)	12.1848(5)
c (Å)	11.5973(15)	12.0735(9)	12.221(3)	13.0225(5)
α (°)	90	90	90	112.782(2)
β (°)	115.364	90	90	97.694(2)
γ (°)	90	90	90	93.964(2)
Volume ($Å^3$)	6717.7(15)	10399.3(13)	10958(5)	1596.92(11)
Z	4	2	2	1
Density (calculated) (Mg/m^3)	1.401	1.289	1.161	1.509
Absorption coefficient (mm^{-1})	0.726	0.535	0.535	0.670
F(000)	2899	4165	3930	755
Crystal size (mm^3)	0.35 x 0.24 x 0.09	0.24 x 0.15 x 0.07	0.80 x 0.11 x 0.08	0.26 x 0.09 x 0.05
Theta range for data collection (°)	2.39 to 25.05	1.05 to 25.05	1.03 to 25.04	2.43 to 27.97
Reflections collected	34317	94443	69564	23433
Independent reflections [R(int)]	5922 [0.0784]	9626 [0.2193]	9945 [0.2783]	7249 [0.0706]
Completeness to theta (°/%)	25.05 / 99.6	25.05 / 99.9	25.04 / 98.2	27.97 / 94.4
Data / restraints / parameters	5922 / 1 / 498	9626 / 0 / 647	9945 / 0 / 624	7249 / 6 / 451
Goodness-of-fit on F^2	0.942	0.938	1.507	0.849
Final R_1 [I>2sigma(I)]	0.0526	0.1065	0.2095	0.0386
wR_2 (all data)	0.1617	0.3570	0.5668	0.0706
Largest diff. peak and hole ($e.Å^{-3}$)	0.547 and -0.579	1.787 and -1.492	2.113 and -2.526	0.472 and -0.434
Detector	APEX II	APEX II	APEX II	APEX II

Table A5. Crystal data and structure refinement for 2.31, 2.32, 2.33 and 2.34.

Compound	**2.31**	**2.32**	**2.33**	**2.34**
Empirical formula	$C_{180}H_{192}N_{36}O_{33}Cl_8Zn_4$	$C_{180}H_{156}B_9N_{36}F_{34}Zn_4$	$C_{180}H_{152}N_{36}O_{28}Cl_7Fe_4$	$C_{76}H_{62}N_{12}O_{26}Cl_4Fe_2$
Formula weight	3932.86	3828.26	3738.93	1812.88
Temperature (K)	93(2)	93(2)	93(2)	113(2)
Crystal system	Orthorhombic	Orthorhombic	Orthorhombic	Orthorhombic
Space group	Pmmn	Pmmn	Pmmn	Cmca
Unit cell dimensions: a (Å)	22.648(4)	22.671(5)	22.603(4)	21.7465(12)
b (Å)	38.200(7)	37.924(7)	38.069(7)	17.7100(8)
c (Å)	12.0384(17)	12.0662(15)	12.0023(13)	20.9686(11)
α (°)	90	90	90	90
β (°)	90	90	90	90
γ (°)	90	90	90	90
Volume ($Å^3$)	10415(3)	10374(3)	10328(3)	8075.6(7)
Z	2	2	2	4
Density (calculated) (Mg/m^3)	1.254	1.226	1.202	1.491
Absorption coefficient (mm^{-1})	0.630	0.542	0.435	0.579
F(000)	4088	3918	3862	3720
Crystal size (mm^3)	0.70 x 0.16 x 0.11	0.55 x 0.27 x 14	0.56 x 0.16 x 13	0.31 x 0.22 x 0.14
Theta range for data collection (°)	1.05 to 25.05	1.05 to 25.11	1.05 to 25.05	2.50 to 27.60
Reflections collected	58092	103006	128961	92914
Independent reflections [R(int)]	9169 [0.0960]	9587 [0.3492]	9546 [0.1123]	4796 [0.0925]
Completeness to theta (°/%)	25.05 / 95.1	25.11 / 99.1	25.05 / 99.9	27.60 / 99.5
Data / restraints / parameters	9169 / 6 / 625	9587 / 0 / 630	9546 / 0 / 620	4796 / 0 / 311
Goodness-of-fit on F^2	0.865	2.234	0.931	0.948
Final R_1 [I>2sigma(I)]	0.0711 (0.0939)	0.2187	0.0925 (0.1310)	0.0727
wR_2 (all data)	0.1902	0.4567	0.2945	0.2390
Largest diff. peak and hole ($e.Å^{-3}$)	0.638 and -1.113	2.004 and -1.303	1.677 and -0.997	0.720 and -0.849
Detector	APEX II	APEX II	APEX II	APEX II

Table A6. Crystal data and structure refinement for 2.35, 2.43, 3.19 and 3.20.

Compound	**2.35**	**2.43**	**3.19**	**3.20**
Empirical formula	$C_{26}H_{36}N_2O_2S_2$	$C_{48}H_{56}N_4S_4Cu$	$C_{24}H_{33}N_6O_{1.4}F_6P$	$C_{28}H_{36}N_8O_4ClAg$
Formula weight	472.69	880.80	572.93	691.97
Temperature (K)	93(2)	123(2)	90(2)	113(2)
Crystal system	Orthorhombic	Hexagonal	Monoclinic	Monoclinic
Space group	Pnma	P6/m	$P2_1/c$	$P2_1/c$
Unit cell dimensions: a (Å)	8.398(2)	20.0090(15)	9.2680(13)	8.526(2)
b (Å)	31.672(8)	20.0090(15)	16.045(2)	23.950(6)
c (Å)	9.1814(19)	16.0959(19)	18.692(3)	15.320(3)
α (°)	90	90	90	90
β (°)	90	90	101.350(3)	104.681(4)
γ (°)	90	120	90	90
Volume ($Å^3$)	2442.1(11)	5580.8(9)	2725.4(7)	3026.2(12)
Z	4	3	4	4
Density (calculated) (Mg/m^3)	1.286	0.786	1.396	1.519
Absorption coefficient (mm^{-1})	0.244	0.429	0.173	0.802
F(000)	1016	1395	1197	1424
Crystal size (mm^3)	1.20 x 0.20 x 0.02	0.23 x 0.06 x 0.03	0.46 x 0.25 x 0.05	0.13 x 0.12 x 0.10
Theta range for data collection (°)	2.31 to 25.05	1.18 to 25.11	2.22 to 25.00	2.19 to 26.39
Reflections collected	15014	51130	19224	26704
Independent reflections [R(int)]	2188 [0.1295]	3452 [0.3228]	4754 [0.0880]	6190 [0.1885]
Completeness to theta (°/%)	25.05 / 99.8	25.11 / 99.6	25.00 / 99.3	26.39 / 99.8
Data / restraints / parameters	2188 / 6 / 155	3452 / 6 / 138	4754 / 0 / 378	6190 / 12 / 400
Goodness-of-fit on F^2	1.079	0.705	0.801	0.819
Final R_1 [I>2sigma(I)]	0.0673	0.0671 (0.1076)	0.0425	0.0590
wR_2 (all data)	0.1372	0.1620	0.0928	0.1719
Largest diff. peak and hole ($e.Å^{-3}$)	0.406 and -0.391	0.310 and -0.476	0.233 and -0.330	0.494 and -0.496
Detector	APEX II	APEX II	SMART CCD	SMART CCD

Table A7. Crystal data and structure refinement for 3.22, 3.27, 3.28 and 3.29.

Compound		**3.22**	**3.27**	**3.28**	**3.29**
Empirical formula		$C_{96}N_{24}S_{14}Cl_{12}Pd_6$	$C_{41}H_{45.03}N_9O_{2.53}SCl_6Pd_3$	$C_{81.31}H_{79.31}N_{18}O_{30}S_4Cl_{3.92}Cu_4$	$C_{40}H_{42}N_9O_9S_2Cu_2$
Formula weight		3002.10	1268.82	2309.98	984.07
Temperature (K)		93(2)	93(2)	93(2)	93(2)
Crystal system		Orthorhombic	Trigonal	Triclinic	Triclinic
Space group		Pbcn	R-3	P-1	P-1
Unit cell dimensions:	a (Å)	27.270(3)	18.6691(4)	13.2616(8)	11.3145(7)
	b (Å)	19.9066(18)	18.6691(4)	13.9056(9)	12.5583(9)
	c (Å)	24.857(2)	25.6922(12)	16.2800(11)	19.3745(13)
	α (°)	90	90	79.051(4)	85.872(4)
	β (°)	90	90	84.390(4)	87.296(4)
	γ (°)	90	120	63.431(4)	85.093(4)
Volume ($Å^3$)		13494(2)	7754.9(4)	2636.0(3)	2733.4(3)
Z		4	6	1	2
Density (calculated) (Mg/m^3)		1.478	1.629	1.455	1.196
Absorption coefficient (mm^{-1})		1.284	1.426	1.055	0.906
F(000)		5792	3780	1179	1014
Crystal size (mm^3)		0.65 x 0.26 x 0.11	0.30 x 0.27 x 0.25	0.50 x 0.28 x 0.20	1.10 x 0.54 x 0.18
Theta range for data collection (°)		1.99 to 26.46	2.18 to 27.49	1.66 to 34.27	1.05 to 25.05
Reflections collected		114446	32698	58374	37856
Independent reflections [R(int)]		13699 [0.0904]	3953 [0.0337]	18938 [0.0487]	9676 [0.1056]
Completeness to theta (°/%)		26.46 / 98.4	27.49 / 99.8	34.27 / 86.3	25.05 / 99.9
Data / restraints / parameters		13699 / 0 / 321	3953 / 0 / 220	18938 / 0 / 650	9676 / 0 / 559
Goodness-of-fit on F^2		3.712	1.122	1.661	0.885
Final R_1 [I>2sigma(I)]		0.1837	0.0419	0.0977	0.1055 (0.1444)
wR_2 (all data)		0.5180	0.1300	0.3035	0.3152
Largest diff. peak and hole ($e.Å^{-3}$)		4.873 and -3.081	0.980 and -0.561	4.440 and -2.245	1.237 and -1.163
Detector		SMART CCD	APEX II	APEX II	APEX II

Table A8. Crystal data and structure refinement for 3.30, 3.34, 3.36 and 3.38

Compound		**3.30**	**3.34**	**3.36**	**3.38**
Empirical formula		$C_{41}H_{39}N_{12}O_{13}Cu_2$	$C_{30}H_{35}N_3OF_6PS_3$	$C_{27}H_{27}N_3O_8S_3CoBr_2$	$C_{28}H_{27}N_3O_4S_3Cu_2I_2$
Formula weight		1034.94	694.79	836.45	946.59
Temperature (K)		93(2)	93(2)	93(2)	93(2)
Crystal system		Monoclinic	Orthorhombic	Orthorhombic	Triclinic
Space group		$P2_1/c$	Ima2	Pnma	P-1
Unit cell dimensions:	a (Å)	17.651(4)	18.848(5)	9.4406(9)	9.3178(13)
	b (Å)	14.741(4)	19.302(5)	15.389(2)	14.3744(14)
	c (Å)	17.891(3)	8.6825(19)	23.704(3)	16.9921(18)
	α (°)	90	90	90	67.077(4)
	β (°)	99.516(8)	90	90	88.616(6)
	γ (°)	90	90	90	79.727(5)
Volume ($Å^3$)		4591.1(18)	3158.8(13)	3443.6(7)	2060.0(4)
Z		4	4	4	2
Density (calculated) (Mg/m^3)		1.497	1.463	1.613	1.526
Absorption coefficient (mm^{-1})		1.003	0.351	3.049	2.713
F(000)		2124	1448	1676	920
Crystal size (mm^3)		0.20 x 0.10 x 0.01	0.31 x 0.11 x 0.10	0.55 x 0.09 x 0.01	0.21 x 0.20 x 0.08
Theta range for data collection (°)		1.81 to 27.74	2.11 to 25.05	1.58 to 25.04	2.22 to 25.05
Reflections collected		43844	9249	40179	32726
Independent reflections [R(int)]		10340 [0.6482]	2806 [0.0490]	3174 [0.1922]	7119 [0.0311]
Completeness to theta (°/%)		27.74 / 95.7	25.05 / 99.6	25.04 / 99.7	25.05 / 97.7
Data / restraints / parameters		10340 / 0 / 613	2806 / 1 / 224	3174 / 0 / 249	7119 / 0 / 369
Goodness-of-fit on F^2		0.671	0.886	0.883	1.042
Final R_1 [I>2sigma(I)]		0.0737	0.0384	0.0531	0.0393
wR_2 (all data)		0.2455	0.0758	0.1520	0.1173
Largest diff. peak and hole ($e.Å^{-3}$)		0.340 and -0.403	0.318 and -0.289	0.557 and -0.521	2.093 and -0.806
Detector		APEX II	SMART CCD	APEX II	APEX II

Table A9. Crystal data and structure refinement for 3.39, 3.40, 3.42 and 3.44.

Compound		**3.39**	**3.40**	**3.42**	**3.44**
Empirical formula		$C_{30}H_{35}N_3OS_3Cu_2I_2$	$C_{32.25}H_{38.25}N_{3.75}O_{5.43}S_3ClAg$	$C_{48}H_{48}N_6O_3$	$C_{50}N_4O_3Cu_9I_9$
Formula weight		926.72	804.59	756.92	2418.59
Temperature (K)		93(2)	93(2)	90(2)	93(2)
Crystal system		Monoclinic	Tetragonal	Triclinic	Orthorhombic
Space group		$P2_1/n$	$P4_2/n$	P-1	$Pb2_1a$
Unit cell dimensions:	a (Å)	9.3364(5)	19.0103(6)	9.9767(13)	14.135(2)
	b (Å)	32.2292(17)	19.0103(6)	12.3796(18)	19.981(3)
	c (Å)	13.2120(6)	22.7281(10)	18.451(3)	34.336(6)
	α (°)	90	90	100.845(3)	90
	β (°)	100.962(2)	90	91.064(2)	90
	γ (°)	90	90	110.502(2)	90
Volume ($Å^3$)		3903.0(3)	8213.7(5)	2087.5(5)	9697(3)
Z		4	8	2	4
Density (calculated) (Mg/m^3)		1.638	1.301	1.204	1.656
Absorption coefficient (mm^{-1})		2.863	0.748	0.076	4.823
F(000)		1888	3306	804	4360
Crystal size (mm^3)		0.35 x 0.21 x 0.03	0.28 x 0.25 x 0.22	0.56 x 0.18 x 0.12	0.40 x 0.19 x 0.01
Theta range for data collection (°)		1.26 to 27.50	0.90 to 25.05	1.91 to 26.38	0.59 to 25.05
Reflections collected		31695	53910	18462	172484
Independent reflections [R(int)]		8943 [0.0325]	7276 [0.0728]	8345 [0.0301]	17077 [0.3818]
Completeness to theta (°/%)		27.50 / 99.9	25.05 / 99.9	26.38 / 97.6	25.05 / 100.0
Data / restraints / parameters		8943 / 0 / 389	7276 / 42 / 444	8345 / 0 / 517	17077 / 1 / 315
Goodness-of-fit on F^2		1.178	0.952	0.864	1.702
Final R_1 [I>2sigma(I)]		0.0537	0.0785	0.0429	0.2015
wR_2 (all data)		0.1457	0.2336	0.0981	0.4394
Largest diff. peak and hole ($e.Å^{-3}$)		1.664 and -1.176	1.340 and -0.575	0.521 and -0.481	8.396 and -7.831
Detector		APEX II	APEX II	SMART CCD	APEX II
Flack parameter (if applicable)				0.0(8)	

Table A10. Crystal data and structure refinement for 4.12, 4.15, 4.25 and 5.4.

Compound		**4.12**	**4.15**	**4.25**	**5.4**
Empirical formula		$C_{74.02}H_{63.06}N_{13.02}O_{7.98}Cl_2Ag_2$	$C_{204}H_{156}N_{36}O_{52}S_6Cu_6$	$C_{33}H_{27}N_9$	$C_{18.65}H_{19.29}N_6O_{1.88}CoBr_{2.08}$
Formula weight		1549.27	4517.25	549.64	582.92
Temperature (K)		88(2)	93(2)	93(2)	93(2)
Crystal system		Trigonal	Triclinic	Triclinic	Triclinic
Space group		P-3	P-1	P-1	P-1
Unit cell dimensions:	a (Å)	13.5935(14)	17.329(5)	8.626(7)	11.1901(6)
	b (Å)	13.5935(14)	18.311(5)	11.291(10)	11.2812(7)
	c (Å)	10.450(2)	18.329(5)	14.449(12)	11.7033(7)
	α (°)	90	84.926(8)	83.25(3)	62.148(3)
	β (°)	90	78.428(6)	79.79(3)	63.095(3)
	γ (°)	120	63.839(4)	88.62(2)	70.425(3)
Volume ($Å^3$)		1672.3(4)	5114(2)	1375(2)	1.683
Z		1	1	2	2
Density (calculated) (Mg/m^3)		1.538	1.467	1.327	1.683
Absorption coefficient (mm^{-1})		0.734	0.765	0.083	4.389
F(000)		790	2318	576	576
Crystal size (mm^3)		0.16 x 0.13 x 0.12	0.25 x 0.07 x 0.03	0.19 x 0.11 x 0.02	0.70 x 0.40 x 0.30
Theta range for data collection (°)		2.61 to 25.05	1.37 to 27.64	2.40 to 25.05	2.07 to 25.05
Reflections collected		13347	62813	17711	13243
Independent reflections [R(int)]		1992 [0.1124]	22965 [0.5308]	4866 [0.4842]	3946 [0.0363]
Completeness to theta (°/%)		25.05 / 99.8	27.64 / 96.3	25.05 / 99.9	25.05 / 96.9
Data / restraints / parameters		1992 / 0 / 171	22965 / 0 / 1356	4866 / 0 / 352	3946 / 0 / 280
Goodness-of-fit on F^2		0.860	0.616	0.644	1.222
Final R_1 [I>2sigma(I)]		0.0589	0.0679	0.0693	0.0669
wR_2 (all data)		0.1557	0.1718	0.01763	0.1525
Largest diff. peak and hole ($e.Å^{-3}$)		0.674 and -0.732	0.305 and -0.289	0.196 and -0.215	1.183 to -1.245
Detector		SMART CCD	APEX II	APEX II	APEX II

Table A11. Crystal data and structure refinement for 5.5, 5.6, 5.7 and 5.8.

Compound		**5.5**	**5.6**	**5.7**	**5.8**
Empirical formula		$C_{18}H_{22}N_9O_{11}La$	$C_{25}H_{18}N_9OZn_3Br_4$	$C_{16}H_{14}N_6Cl_4Cu_2$	$C_{32}H_{27}N_{12}Cl_8Cd_4$
Formula weight		679.36	976.25	559.21	1312.90
Temperature (K)		93(2)	93(2)	93(2)	93(2)
Crystal system		Monoclinic	Monoclinic	Triclinic	Triclinic
Space group		$P2_1/n$	$P2_1/n$	P-1	P-1
Unit cell dimensions:	a (Å)	8.3195(6)	12.6730(10)	7.6480(3)	6.8180(2)
	b (Å)	29.341(2)	12.8119(11)	8.1529(3)	8.8696(3)
	c (Å)	10.6876(6)	20.6790(16)	8.7868(3)	17.7325(6)
	α (°)	90	90	68.561(2)	103.333(2)
	β (°)	103.963(2)	90.680(6)	71.627(2)	94.660(2)
	γ (°)	90	90	78.451(3)	94.689(2)
Volume ($Å^3$)		2531.8(3)	3357.3(5)	481.74(3)	1034.39(6)
Z		4	4	1	1
Density (calculated) (Mg/m^3)		1.782	1.931	1.928	2.108
Absorption coefficient (mm^{-1})		1.762	6.921	2.778	2.587
F(000)		1352	1876	278	631
Crystal size (mm^3)		0.50 x 0.38 x 0.17	0.74 x 0.72 x 0.54	0.70 x 0.55 x 0.16	1.17 x 0.19 x 0.18
Theta range for data collection (°)		2.08 to 35.35	1.87 to 31.18	2.58 to 25.04	1.19 to 35.62
Reflections collected		40681	39305	3884	26369
Independent reflections [R(int)]		9509 [0.0552]	10352 [0.2174]	1584 [0.0160]	8433 [0.0226]
Completeness to theta (°/%)		35.35 / 82.9	31.18 / 95.1	25.04 / 92.5	35.62 / 88.4
Data / restraints / parameters		9509 / 0 / 372	10352 / 0 / 379	1584 / 0 / 127	8433 / 0 / 451
Goodness-of-fit on F^2		1.263	1.622	1.032	1.131
Final R_1 [I>2sigma(I)]		0.0490	0.1671	0.0374	0.0201
wR_2 (all data)		0.0862	0.4959	0.1041	0.0536
Largest diff. peak and hole ($e.Å^{-3}$)		1.297 and -3.963	4.662 and -5.143	1.207 and -1.085	0.809 and -0.810
Detector		APEX II	APEX II	APEX II	APEX II

Table A12. Crystal data and structure refinement for 5.9, 5.10, 5.11 and 5.12.

Compound		**5.9**	**5.10**	**5.11**	**5.12**
Empirical formula		$C_{16}H_{12}N_6Cl_2Pd_2$	$C_{20}H_{18}N_8O_8Cl_2Cu_2$	$C_{22}H_{26}N_6O_6Ni_2$	$C_8H_6N_3ClCu$
Formula weight		572.06	696.42	587.87	243.16
Temperature (K)		93(2)	93(2)	93(2)	93(2)
Crystal system		Monoclinic	Monoclinic	Orthorhombic	Monoclinic
Space group		C2/c	$P2_1/c$	$Pna2_1$	$P2_1/c$
Unit cell dimensions:	a (Å)	23.052(3)	7.7945(7)	15.9653(7)	3.7741(6)
	b (Å)	5.0571(7)	9.9911(9)	8.5578(3)	15.390(2)
	c (Å)	15.034(2)	16.6231(16)	17.8313(7)	13.995(3)
	α (°)	90	90	90	90
	β (°)	105.892(4)	100.720(5)	90	94.184(9)
	γ (°)	90	90	90	90
Volume ($Å^3$)		1685.6(4)	1271.9(2)	2436.25(17)	810.7(2)
Z		4	2	4	4
Density (calculated) (Mg/m^3)		2.254	1.819	1.603	1.992
Absorption coefficient (mm^{-1})		2.464	1.946	1.596	2.967
F(000)		1104	700	1216	484
Crystal size (mm^3)		0.22 x 0.14 x 0.10	0.25 x 0.12 x 0.08	0.65 x 0.28 x 0.18	0.82 x 0.07 x 0.03
Theta range for data collection (°)		2.82 to 25.05	22.39 to 30.61	2.64 to 25.05	2.65 to 35.44
Reflections collected		6713	15366	28915	17706
Independent reflections [R(int)]		1468 [0.0630]	3618 [0.0408]	4308 [0.0316]	3377 [0.0407]
Completeness to theta (°/%)		25.05 / 99.0	30.61 / 92.3	25.05 / 99.9	35.44 / 91.8
Data / restraints / parameters		1468 / 0 / 118	3618 / 0 / 193	4308 / 1 / 338	3377 / 0 / 118
Goodness-of-fit on F^2		1.180	1.042	0.950	1.187
Final R_1 [I>2sigma(I)]		0.0568	0.0359	0.0261	0.0388
wR_2 (all data)		0.1610	0.0956	0.0793	0.0810
Largest diff. peak and hole ($e.Å^{-3}$)		2.498 and -1.389	0.705 and -0.814	0.495 and -0.397	0.910 and -0.841
Detector		APEX II	APEX II	APEX II	APEX II
Flack parameter (if applicable)				0.397(11)	

Table A13. Crystal data and structure refinement for 5.13, 5.14, 5.15 and 5.16.

Compound	**5.13**	**5.14**	**5.15**	**5.16**
Empirical formula	$C_{28}H_{34}N_8O_{12}S_2Cu_2$	$C_{20}H_{24}N_6O_6S_3Cu_2$	$C_{16}H_{12}N_6O_4SCu_2$	$C_{32}H_{26}N_{12}Cu_2I_2$
Formula weight	865.87	667.76	511.49	959.55
Temperature (K)	93(2)	93(2)	108(2)	93(2)
Crystal system	Triclinic	Monoclinic	Orthorhombic	Monoclinic
Space group	P-1	C2/c	Pbcn	$P2_1/n$
Unit cell dimensions: a (Å)	9.2256(8)	24.4406(9)	13.052(2)	11.5644(6)
b (Å)	9.8974(7)	8.2065(3)	16.854(3)	9.6523(5)
c (Å)	10.2828(9)	17.3304(11)	7.1935(10)	16.4318(9)
α (°)	74.545(2)	90	90	90
β (°)	68.932(2)	131.3140(10)	90	109.077(2)
γ (°)	70.650(2)	90	90	90
Volume ($Å^3$)	815.00(12)	2610.8(2)	1582.4(4)	1733.44(16)
Z	1	4	4	2
Density (calculated) (Mg/m^3)	1.764	1.699	2.147	1.838
Absorption coefficient (mm^{-1})	1.511	1.917	2.864	3.051
F(000)	444	1360	1024	932
Crystal size (mm^3)	0.50 x 0.26 x 0.10	0.63 x 0.31 x 0.03	0.21 x 0.13 x 0.08	0.70 x 0.18 x 0.05
Theta range for data collection (°)	2.74 to 25.05	2.36 to 28.29	3.12 to 25.11	2.48 to 25.05
Reflections collected	8156	11404	13728	17359
Independent reflections [R(int)]	2879 [0.0384]	3231 [0.0322]	1412 [0.3321]	3060 [0.0317]
Completeness to theta (°/%)	25.05 / 99.9	28.29 / 99.8	25.11 / 99.5	25.05 / 100.0
Data / restraints / parameters	2879 / 0 / 235	3231 / 0 / 159	1412 / 90 / 132	3060 / 0 / 217
Goodness-of-fit on F^2	1.029	1.064	0.810	1.084
Final R_1 [I>2sigma(I)]	0.0326	0.0270	0.0565	0.0178
wR_2 (all data)	0.0865	0.0758	0.1600	0.0462
Largest diff. peak and hole ($e.Å^{-3}$)	0.592 and -0.574	1.455 and -1.053	0.879 and -0.644	0.512 and -0.844
Detector	APEX II	APEX II	APEX II	APEX II

Table A14. Crystal data and structure refinement for 5.17, 5.18 and 5.20.

Compound		**5.17**	**5.18**	**5.20**
Empirical formula		$C_{26}H_{21}N_{10}CuNi_2I_2$	$C_{50}H_{44}N_{18}O_2Co_2Cu_2Br_2I_6$	$C_{58.50}H_{44.26}N_6O_{7.25}Cl_{2.24}Co_4Br_2$
Formula weight		908.58	2095.45	1422.41
Temperature (K)		93(2)	93(2)	108(2)
Crystal system		Triclinic	Monoclinic	Triclinic
Space group		P-1	$P2_1/c$	P-1
Unit cell dimensions:	a (Å)	9.4397(3)	14.151(4)	11.7688(5)
	b (Å)	13.0456(4)	14.262(3)	12.3717(5)
	c (Å)	13.3103(4)	15.199(3)	12.4909(9)
	α (°)	62.036(2)	90	97.214(3)
	β (°)	88.476(2)	95.612(9)	111.823(4)
	γ (°)	89.868(2)	90	116.941(2)
Volume ($Å^3$)		1447.13(8)	3052.9(12)	1406.93(13)
Z		2	2	1
Density (calculated) (Mg/m^3)		2.085	2.279	1.679
Absorption coefficient (mm^{-1})		4.189	5.620	2.745
F(000)		876	1972	711
Crystal size (mm^3)		0.20 x 0.20 x 0.05	0.50 x 0.35 x 0.01	0.92 x 0.19 x 0.16
Theta range for data collection (°)		1.80 to 30.51	2.51 to 25.05	2.49 to 27.77
Reflections collected		26713	22713	20128
Independent reflections [R(int)]		8609 [0.0504]	5354 [0.0684]	6485 [0.0693]
Completeness to theta (°/%)		30.51 / 97.4	25.05 / 99.3	27.77 / 97.5
Data / restraints / parameters		8609 / 0 / 398	5354 / 7 / 399	6485 / 0 / 389
Goodness-of-fit on F^2		1.050	0.972	0.827
Final R_1 [I>2sigma(I)]		0.0398	0.0387	0.0381
wR_2 (all data)		0.1108	0.0975	0.0660
Largest diff. peak and hole ($e.Å^{-3}$)		2.489 and -1.827	1.376 and -0.835	0.462 and -0.486
Detector		APEX II	APEX II	APEX II

References

References

(1) Lehn, J.-M. *Supramolecular Chemistry*; VCH: Weinheim, 1995.
(2) Lehn, J.-M. *Proc. Nat. Acad. Sci.* **2002**, *99*, 4763-4768.
(3) Steed, J. W.; Atwood, J. L. *Supramolecular Chemistry*; John Wiley & Sons Ltd: New York, 2000.
(4) Sumby, C. J., PhD Thesis, University of Canterbury, Christchurch, 2003.
(5) Fitchett, C. M., PhD Thesis, University of Canterbury, Christchurch, 2002.
(6) Biotechnology Australia, http://www.biotechnologyonline.gov.au/biotec/dnalook.cfm.
(7) Cram, D. J.; Tanner, M. E.; Thomas, R. *Angew. Chem. Int. Ed. Engl.* **1991**, *30*, 1024.
(8) Kumazawa, K.; Yamanoi, Y.; Yoshizawa, M.; Kusukawa, T.; Fujita, M. *Angew. Chem. Int. Ed.* **2004**, *43*, 5936-5940.
(9) Saalfrank, R. W.; Demleitner, B. In *Transition Metals in Supramolecular Chemistry*; Sauvage, J.-P., Ed., 1999.
(10) Sauvage, J.-P.; Dietrich-Buchecker, C.; (Eds.) *Molecular Catenanes, Rotaxanes and Knots*; Wiley-VCH: Weinheim, 1999.
(11) Balzani, V.; Credi, A.; Raymo, F. M.; Stoddart, J. F. *Angew. Chem. Int. Ed.* **2000**, *39*, 3348-3391.
(12) Balzani, V.; Credi, A.; Silvi, S.; Venturi, M. *Chem. Soc. Rev.* **2006**, *35*, 1135-1149.
(13) Credi, A.; Tian, H. *Adv. Funct. Mater.* **2007**, *17*, 679-682.
(14) Addison, A. W.; Rao, T. N.; Reedjik, J.; van Rijn, J.; Verschoor, G. C. *J. Chem. Soc., Dalton Trans.* **1984**, 1349-1355.
(15) Fujita, M.; Sasaki, O.; Mitsuhashi, T.; Fujita, T.; Yazaki, J.; Yamaguchi, K.; Ogura, K. *Chem. Commun.* **1996**, 1535-1536.
(16) Blake, A. J.; Greig, J. A.; Schroder, M. *J. Chem. Soc., Dalton Trans.* **1991**, 529-532.
(17) Roche, S.; Haslam, C.; Adams, H.; Heath, S. L.; Thomas, J. A. *Chem. Commun.* **1998**, 1681-1682.
(18) Steel, P. J. *Molecules* **2004**, *9*, 440-448.
(19) Reedijk, J. In *Comprehensive Coordination Chemistry*; Wilkinson, G., Gillard, R. D., McCleverty, J. A., Eds.; Pergamon Press: Oxford, 1987; Vol. 2.
(20) Fujita, M.; Oka, H.; Ogura, K. *Tetrahedron Lett.* **1995**, *36*, 5247-5250.
(21) Janka, M.; Anderson, G. K.; Rath, N. P. *Inorg. Chim. Acta* **2004**, *357*, 2339-2344.
(22) Reddy, L. S.; Bhogala, B. R.; Nangia, A. *Cryst. Eng. Comm.* **2005**, *7*, 206-209.
(23) Yang, H.-B.; Ghosh, K.; Northrop, B. H.; Stang, P. J. *Org. Lett.* **2007**, *9*, 1561-1564.
(24) Chand, D. K.; Balaji, G.; Manivannan, R.; Athilakshmi, J. *Tetrahedron Lett.* **2006**, *47*, 2867-2869.
(25) Kuehl, C. J.; Yamamoto, T.; Seidel, S. R.; Stang, P. J. *Org. Lett.* **2002**, *4*, 913-915.
(26) Hasegawa, S.; Horike, S.; Matsuda, R.; Furukawa, S.; Mochizuki, K.; Kinoshita, Y.; Kitagawa, S. *J. Am. Chem. Soc.* **2007**, *129*, 2607-2614.
(27) Liu, C.-M.; Gao, S.; Zhang, D.-Q.; Zhu, D.-B. *Cryst. Growth Des.* **2007**, *7*, 1312-1317.

(28) Batten, S. R.; Robson, R. *Angew. Chem. Int. Ed.* **1998**, *37*, 1460-1494.
(29) Robson, R. *J. Chem. Soc., Dalton Trans.* **2000**, 3735-3744.
(30) Dinca, M.; Long, J. R. *J. Am. Chem. Soc.* **2007**, *129*, 11172-11176.
(31) Han, S. S.; Deng, W.-Q.; Goddard, W. A. *Angew. Chem. Int. Ed.* **2007**, *46*, 6289-6292.
(32) Mulfort, K. L.; Hupp, J. T. *J. Am. Chem. Soc.* **2007**, *129*, 9604-9605.
(33) Hupp, J. T.; Poeppelmeier, K. R. *Science* **2005**, *309*, 2008-2009.
(34) Kitagawa, S.; Uemura, K. *Chem. Soc. Rev.* **2005**, *34*, 109-119.
(35) Kitagawa, S.; Kitaura, R.; Noro, S. *Angew. Chem. Int. Ed.* **2004**, *43*, 2334-2375.
(36) Chen, C.-T.; Suslick, K. S. *Coord. Chem. Rev.* **1993**, *128*, 293-322.
(37) Evans, O. R.; Lin, W. *Acc. Chem. Res.* **2002**, *35*, 511-522.
(38) Llabres i Xamena, F. X.; Abad, A.; Corma, A.; Garcia, H. *J. Catal.* **2007**, *250*, 294-298.
(39) Alvaro, M.; Carbonell, E.; Ferrer, B.; Llabres i Xamena, F. X.; Garcia, H. *Chem. Eur. J.* **2007**, *13*, 5106-5112.
(40) Hong, M.-C. *Cryst. Growth Des.* **2007**, *7*, 10-14.
(41) Xu, Z. *Coord. Chem. Rev.* **2006**, 2745-2757.
(42) Mueller, U.; Schubert, M.; Teich, F.; Puetter, H.; Schierle-Arndt, K.; Pastre, J. *J. Mater. Chem.* **2006**, *16*, 626-636.
(43) Fujita, M.; Yazaki, J.; Katsuyuki, O. *J. Am. Chem. Soc.* **1990**, *112*, 5645-5647.
(44) Sharma, C. V.; Griffin, S. T.; Rogers, R. D. *Chem. Commun.* **1998**, 215-216.
(45) Wurthner, F.; You, C.-C.; Saha-Moller, C. R. *Chem. Soc. Rev.* **2004**, *33*, 133-146.
(46) Leininger, S.; Olenyuk, B.; Stang, P. J. *Chem. Rev.* **2000**, *100*, 853-907.
(47) Olenyuk, B.; Fechtenkotter, A.; Stang, P. J. *J. Chem. Soc., Dalton Trans.* **1998**, 1707-1728.
(48) Stang, P. J.; Olenyuk, B. *Acc. Chem. Res.* **1997**, *30*, 502-518.
(49) Maurizot, V.; Yoshizawa, M.; Kawano, M.; Fujita, M. *Dalton Trans.* **2006**, 2750-2756.
(50) Fujita, M.; Ogura, D.; Miyazawa, M.; Oka, H.; Yamaguchi, K.; Ogura, K. *Nature* **1995**, *378*, 469-471.
(51) Seidel, S. R.; Stang, P. J. *Acc. Chem. Res.* **2002**, *35*, 972-983.
(52) Liu, Z.-M.; Liu, Y.; Zheng, S.-R.; Yu, Z.-Q.; Pan, M.; Su, C.-Y. *Inorg. Chem.* **2007**, *46*, 5814-5816.
(53) Jones, C. J. *Chem. Soc. Rev.* **1998**, *27*, 289-299.
(54) Ghosh, S.; Mukherjee, P. S. *J. Org. Chem.* **2006**, *71*, 8412-8416.
(55) Hartshorn, C. M.; Steel, P. J. *Chem. Commun.* **1997**, 541-542.
(56) James, S. L.; Mingos, D. M. P.; White, A. J. P.; Williams, D. J. *Chem. Commun.* **1998**, 2323-2324.
(57) Leininger, S.; Fan, J.; Schmitz, M.; Stang, P. J. *Proc. Nat. Acad. Sci.* **2000**, *97*, 1380-1384.
(58) Schweiger, M.; Yamamoto, T.; Stang, P. J.; Blaeser, D.; Boese, R. *J. Org. Chem.* **2005**, *70*, 4861-4864.
(59) Ronson, T. K.; Adams, H.; Ward, M. D. *Cryst. Eng. Comm.* **2006**, *8*, 497-501.
(60) Su, C.-Y.; Cai, Y.-P.; Chen, C.-L.; Lissner, F.; Kang, B.-S.; Kaim, W. *Angew. Chem. Int. Ed.* **2000**, *41*, 3371-3375.
(61) Pluth, M. D.; Raymond, K. N. *Chem. Soc. Rev.* **2007**, *36*, 161-171.
(62) Tominaga, M.; Suzuki, K.; Kawano, M.; Kusukawa, T.; Ozeki, T.; Sakamoto, S.; Yamaguchi, K.; Fujita, M. *Angew. Chem. Int. Ed.* **2004**, *43*, 5621-5625.

(63) Liu, H.-K.; Sun, W.-Y.; Ma, D.-J.; Yu, K.-B.; Tang, W.-X. *Chem. Commun.* **2000**, 591-592.
(64) Fan, J.; Zhu, H.-F.; Okamura, T.-a.; Sun, W.-Y.; Tang, W.-X.; Ueyama, N. *Chem. Eur. J.* **2003**, *9*, 4724-4731.
(65) Sun, W.-Y.; Xie, J.; Yu, K.-B. *Chem. Lett.* **2001**, *4*, 342-343.
(66) Mahmoudkhani, A. H.; Cote, A. P.; Shimizu, G. K. H. *Chem. Commun.* **2004**, 2678-2679.
(67) Lindner, E.; Hermann, C.; Baum, G.; Fenske, D. *Eur. J. Inorg. Chem.* **1999**, *4*, 679-685.
(68) Fujita, M.; Nagao, S.; Ogura, K. *J. Am. Chem. Soc.* **1995**, *117*, 1649-1650.
(69) Fleming, J. S.; Mann, K. L. V.; Carraz, C.-A.; Psillakis, E.; Jeffery, J. C.; McCleverty, J. A.; Ward, M. D. *Angew. Chem. Int. Ed.* **1998**, *37*, 1279-1281.
(70) Paul, R. L.; Argent, S. P.; Jeffery, J. C.; Harding, L. P.; Lynam, J. M.; Ward, M. D. *Dalton Trans.* **2004**, 3454-3458.
(71) Beissel, T.; Powers, R. E.; Raymond, K. N. *Angew. Chem. Int. Ed. Engl.* **1996**, *35*, 1084-1086.
(72) Caulder, D. L.; Powers, R. E.; Parac, T. N.; Raymond, K. N. *Angew. Chem. Int. Ed.* **1998**, *37*, 1841-1844.
(73) Saalfrank, R. W.; Horner, B.; Stalke, D.; Salbeck, J. *Angew. Chem. Int. Ed. Engl.* **1993**, *32*, 1179-1182.
(74) Saalfrank, R. W.; Burak, R.; Breit, A.; Stalke, D.; Herbst-Irmer, R.; Daub, J.; Porsch, M.; Bill, E.; Muther, M.; Trautwein, A. X. *Angew. Chem. Int. Ed. Engl.* **1994**, *33*, 1621-1623.
(75) He, C.; Wang, L.-Y.; Wang, Z.-M.; Liu, Y.; Liao, C.-S.; Yan, C.-H. *J. Chem. Soc., Dalton Trans.* **2002**, 134-135.
(76) Steel, P. J.; Sumby, C. J. *Chem. Commun.* **2002**, 322-323.
(77) Hong, M.-C.; Zhao, Y.-J.; Su, W.-P.; Cao, R.; Fujita, M.; Zhou, Z.-Y.; Chan, A. S. C. *J. Am. Chem. Soc.* **2000**, *122*, 4819-4820.
(78) Liu, H.-K.; Tong, X. *Chem. Commun.* **2002**, 1316-1317.
(79) Umemoto, K.; Yamaguchi, K.; Fujita, M. *J. Am. Chem. Soc.* **2000**, *122*, 7150-7151.
(80) Abrahams, B. F.; Egan, S. J.; Robson, R. *J. Am. Chem. Soc.* **1999**, *121*, 3535-3536.
(81) Umemoto, K.; Tsukui, H.; Kusukawa, T.; Biradha, K.; Fujita, M. *Angew. Chem. Int. Ed.* **2001**, *40*, 2620-2622.
(82) Takeda, N.; Umemoto, K.; Yamaguchi, K.; Fujita, M. *Nature* **1999**, *398*, 794-796.
(83) Bell, Z. R.; Jeffery, J. C.; McCleverty, J. A.; Ward, M. D. *Angew. Chem. Int. Ed.* **2002**, *41*, 2515-2518.
(84) Caulder, D. L.; Bruckner, C.; Powers, R. E.; Konig, S.; Parac, T. N.; Leary, J. A.; Raymond, K. N. *J. Am. Chem. Soc.* **2001**, *123*, 8923-8938.
(85) Fujita, M.; Umemoto, K.; Yoshizawa, M.; Fujita, N.; Kusukawa, T.; Biradha, K. *Chem. Commun.* **2001**, 509-518.
(86) Gray, I. In *Chemical Science*, 2006; Vol. 7.
(87) Caulder, D. L.; Powers, R. E.; Parac, T. N.; Raymond, K. N. *Angew. Chem. Int. Ed.* **1998**, *37*, 1840-1843.
(88) Fiedler, D.; Leung, D. H.; Bergman, R. G.; Raymond, K. N. *Acc. Chem. Res.* **2005**, *38*, 349-358.
(89) Kusukawa, T.; Fujita, M. *Angew. Chem. Int. Ed.* **1998**, *37*, 3142-3144.

(90) Sun, W.-Y.; Kusukawa, T.; Fujita, M. *J. Am. Chem. Soc.* **2002**, *124*, 11570-11571.
(91) Kusukawa, T.; Fujita, M. *J. Am. Chem. Soc.* **2002**, *124*, 13576-13582.
(92) Tashiro, S.; Tominaga, M.; Kawano, M.; Therrien, B.; Ozeki, T.; Fujita, M. *J. Am. Chem. Soc.* **2005**, *127*, 4546-4547.
(93) Kusukawa, T.; Fujita, M. *J. Am. Chem. Soc.* **1999**, *121*, 1397-1398.
(94) Yoshizawa, M.; Kusukawa, T.; Fujita, M.; Yamaguchi, K. *J. Am. Chem. Soc.* **2000**, *122*, 6311-6312.
(95) Yoshizawa, M.; Kusukawa, T.; Fujita, M.; Sakamoto, S.; Yamaguchi, K. *J. Am. Chem. Soc.* **2001**, *123*, 10454-10459.
(96) Yoshizawa, M.; Kumazawa, K.; Fujita, M. *J. Am. Chem. Soc.* **2005**, *127*, 13456-13457.
(97) Iwasawa, T.; Mann, E.; Rebek, J. *J. Am. Chem. Soc.* **2006**, *128*, 9308-9309.
(98) Kusukawa, T.; Yoshizawa, M.; Fujita, M. *Angew. Chem. Int. Ed.* **2001**, *40*, 1879-1884.
(99) Yoshizawa, M.; Takeyama, Y.; Kusukawa, T.; Fujita, M. *Angew. Chem. Int. Ed.* **2002**, *41*, 1347-1349.
(100) Yoshizawa, M.; Takeyama, Y.; Okano, T.; Fujita, M. *J. Am. Chem. Soc.* **2003**, *125*, 3243.
(101) Yoshizawa, M.; Miyagi, S.; Kawano, M.; Ishiguro, K.; Fujita, M. *J. Am. Chem. Soc.* **2004**, *126*, 9172-9173.
(102) Nishioka, Y.; Yamaguchi, T.; Yoshizawa, M.; Fujita, M. *J. Am. Chem. Soc.* **2007**, *129*, 7000-7001.
(103) Chen, B.; Ma, S.; Zapata, F.; Fronczek, F. R.; Lobkovsky, E. B.; Zhou, H.-C. *Inorg. Chem.* **2007**, *46*, 1233-1236.
(104) Thetiot, F.; Triki, S.; Pala, J. S.; Galan-Mascaros, J.-R.; Martinez-Agudo, J. M.; Dunbar, K. R. *Eur. J. Inorg. Chem.* **2004**, 3783-3791.
(105) Sung, N.-D.; Yun, K.-S.; Kim, T.-Y.; Choi, K.-Y.; Suh, M.; Kim, J.-G.; Suh, I.-H.; Chin, J. *Inorg. Chem. Commun.* **2001**, *4*, 377-380.
(106) Hoskins, B. F.; Robson, R. *J. Am. Chem. Soc.* **1990**, *112*, 1546-1554.
(107) Su, C.-Y.; Cai, Y.-P.; Chen, C.-L.; Smith, M. D.; Kaim, W.; zur Loye, H.-C. *J. Am. Chem. Soc.* **2003**, *125*, 8595-8613.
(108) Liu, H.-K.; Su, C.-Y.; Quin, C.-M.; Liu, J.; Tan, H.-Y.; Kang, B.-S. *J. Chem. Soc., Dalton Trans.* **2001**, 1167-1168.
(109) Riordan, C. G.; Rheingold, A. L.; Lam, K. C.; Voo, J. K. *J. Chem. Soc., Dalton Trans.* **2001**, 1803-1805.
(110) Ohi, H.; Tachi, Y.; Itoh, S. *Inorg. Chem.* **2006**, *45*, 10825-10835.
(111) Fitzgerald, E. A.; Tadros, S. P.; Almeida, R. F.; Sienko, G. A.; Honda, K.; Sarubbi, T. *J. App. Pol. Sci* **1992**, *45*, 363-370.
(112) Tsang, S. K.; Cheh, J.; Isaacs, L.; Joseph-McCarthy, D.; Choi, S.-K.; Pevear, D. C.; Whitesides, G. M.; Hogle, J. M. *Chem. Biol.* **2001**, *8*, 33-45.
(113) Anslyn, E. V.; Monahan, M.-K.; Perreault, D. M.; Schneider, S. E.; Lavigne, J. J.; Best, M. D.; Cabell, L. A. *J. Chem. Soc., Perkin Trans. 2* **2001**, 315-323.
(114) Pohl, S.; Saak, W.; Walsdorff, C. *J. Chem. Research* **1996**, 282-283.
(115) Anslyn, E. V.; Lynch, V. M.; Metzger, A. *Angew. Chem. Int. Ed. Engl.* **1997**, *36*, 862-865.
(116) Hartshorn, C. M., PhD Thesis, University of Canterbury, Christchurch, 1996.
(117) Schatz, J.; Schmaderer, H.; Frank, M.; Fahlbusch, T. *Eur. J. Org. Chem.* **2006**, 1899-1903.

(118) Chin, J.; Oh, J.; Jon, S. Y.; Park, S. H.; Walsdorff, C.; Stranix, B.; Ghoussoub, A.; Lee, S. J.; Chung, H. J.; Park, S.-M.; Kim, K. *J. Am. Chem. Soc.* **2002**, *124*, 5374-5379.
(119) Chin, J.; Walsdorff, C.; Stranix, B.; Oh, J.; Chung, H. J.; Park, S.-M.; Kim, K. *Angew. Chem. Int. Ed.* **1999**, *38*, 2756-2759.
(120) Sasaki, S.-i.; Amano, T.; Monma, G.; Otsuka, T.; Iwasawa, N.; Citterio, D.; Hisamoto, H.; Suzuki, K. *Anal. Chem.* **2002**, *74*, 4845-4848.
(121) Sorrell, T. N.; Jameson, D. L. *J. Am. Chem. Soc.* **1982**, *104*, 2053-2054.
(122) Balamurugan, V.; Mukherjee, R. *Cryst. Eng. Commun.* **2005**, *7*, 337-341.
(123) Balamurugan, V.; Mukherjee, R. *Inorg. Chim. Acta.* **2006**, *359*, 1376-1382.
(124) Gupta, R.; Mukherjee, R. *Polyhedron* **2000**, *19*, 719-724.
(125) Bondi, A. *J. Phys. Chem.* **1964**, *68*, 441-451.
(126) Huang, C.; Gou, S.; Zhu, H.; Huang, W. *Inorg. Chem.* **2007**, *46*, 5537-5543.
(127) Cotton, F. A.; Feng, X.; Matusz, M.; Poli, R. *J. Am. Chem. Soc.* **1988**, *110*, 7077-7083.
(128) Zhang, J.-P.; Wang, Y.-B.; Huang, X.-C.; Lin, Y.-Y.; Chen, X.-M. *Chem. Eur. J.* **2005**, *11*, 552-561.
(129) Carvajal, M. A.; Alvarez, S.; Novoa, J. J. *Chem. Eur. J.* **2004**, *10*, 2117-2132.
(130) Allen, F. H. *Acta Cryst.* **2002**, *B58*, 380-388.
(131) Wikipedia; http://en.wikipedia.org/wiki/Tricorne.
(132) National Park Service Museum Collection, http://www.nps.gov/history/museum/exhibits/revwar/image_gal/morrimg/hattricorn.html.
(133) Tamura, T.; Tamura, N.; Cejka, Z.; Hegerl, R.; Lottspeich, F.; Baumeister, W. *Science* **1996**, *274*, 1385-1389.
(134) Baker, A. T.; Cass, J. K.; Maniska, M.; Craig, D. C. *Inorg. Chim. Acta* **1995**, *230*, 225-229.
(135) Ruttimann, S.; Bernardinelli, G.; Williams, A. F. *Angew. Chem. Int. Ed. Engl.* **1993**, *32*, 392-394.
(136) Carina, R. F.; Williams, A. F. *Inorg. Chem.* **2001**, *40*, 1826-1832.
(137) Wojacczynski, J.; Latos-Grazynski, L.; Olmstead, M. M.; Balch, A. L. *Inorg. Chem.* **1998**, *36*, 4548.
(138) Chaudhuri, P.; Karpenstein, I.; Winter, M.; Butzlaff, C.; Bill, E.; Trautwein, A. X.; Florke, U.; Haupt, H.-J. *J. Chem. Soc., Chem. Commun.* **1992**, 321-322.
(139) Al-Rasbi, N. K.; Sabatini, C.; Barigelletti, F.; Ward, M. D. *Dalton Trans.* **2006**, 4769-4772.
(140) Argent, S. P.; Adams, H.; Riis-Johannessen, T.; Jeffery, J. C.; Harding, L. P.; Mamula, O.; Ward, M. D. *Inorg. Chem.* **2006**, *45*, 3905-3919.
(141) Bell, Z. R.; McCleverty, J. A.; Ward, M. D. *Aust. J. Chem.* **2003**, *56*, 665-670.
(142) Argent, S. P.; Adams, H.; Riis-Johannessen, T.; Jeffery, J. C.; Harding, L. P.; Ward, M. D. *J. Am. Chem. Soc.* **2006**, *128*, 72-73.
(143) Hartshorn, C. M.; Steel, P. J. *Inorg. Chem. Commun.* **2000**, *3*, 476-481.
(144) Argent, S. P.; Adams, H.; Riis-Johannessen, T.; Jeffery, J. C.; Harding, L. P.; Clegg, W.; Harrington, R. W.; Ward, M. D. *Dalton Trans.* **2006**, 4996-5013.
(145) Fleming, J. S.; Mann, K. L. V.; Couchman, S. M.; Jeffery, J. C.; McCleverty, J. A.; Ward, M. D. *J. Chem. Soc., Dalton Trans.* **1998**.
(146) McMorran, D. A.; Steel, P. J. *Inorg. Chem. Commun.* **2003**, *6*, 43-47.
(147) Bell, Z. R.; Harding, L. P.; Ward, M. D. *Chem. Commun.* **2003**, 2432-2433.
(148) Argent, S. P.; Adams, H.; Harding, L. P.; Ward, M. D. *Dalton Trans.* **2006**, 542-544.

(149) Gerloch, M.; Constable, E. C. *Transition Metal Chemistry*; VCH: Weinheim, 1994.
(150) Figgis, B. N.; Hitchman, M. A. *Ligand Field Theory and Its Applications*; Wiley-VCH: New York, 2000.
(151) Speck, R. L. *PLATON, a multipurpose crystallographic tool*; Utrecht University: Utrecht, The Netherlands, 2001.
(152) Yam, V. W.-W.; Yeung, P. K.-Y.; Cheung, K.-K. *Angew. Chem. Int. Ed. Engl.* **1996**, *35*, 739-740.
(153) Eastland, G. W.; Mazid, M. A.; Russell, D. R.; Symons, M. C. R. *J. Chem. Soc., Dalton Trans.* **1980**, 1682-1687.
(154) Amoroso, A. J.; Jeffery, J. C.; Jones, P. L.; McCleverty, J. A.; Psillakis, E.; Ward, M. D. *J. Chem. Soc., Chem. Commun.* **1995**, 1175-1176.
(155) Singh, K.; Long, J. R.; Stavropoulos, P. *J. Am. Chem. Soc.* **1997**, *119*, 2942-2943.
(156) Nelson, S. M.; McFall, S. G.; Drew, M. G. B.; Othman, A. H. B. *J. Chem. Soc., Chem. Commun.* **1977**, 370-371.
(157) Pyykko, P. *Chem. Rev.* **1997**, *97*, 597-636.
(158) Murray, K. S. *Personal Communication* **2007**.
(159) Sugiyarto, K. H.; Goodwin, H. A. *Aust. J. Chem.* **1988**, *41*, 1645-1663.
(160) Harimanow, L. S.; Sugiyarto, K. H.; Craig, D. C.; Scudder, M. L.; Goodwin, H. A. *Aust. J. Chem.* **1999**, *52*, 109-122.
(161) Yue, N. L. S.; Jennings, M. C.; Puddephatt, R. J. *Inorg. Chem.* **2005**, *44*, 1125-1131.
(162) Sun, S.-S.; Lees, A. J.; Zavalij, P. Y. *Inorg. Chem.* **2003**, *42*, 3445-3453.
(163) Qin, Z.; Jennings, M. C.; Puddephatt, R. J. *Inorg. Chem.* **2003**, *42*, 1956-1965.
(164) Qin, Z.; Jennings, M. C.; Puddephatt, R. J. *Chem. Commun.* **2002**, 354-355.
(165) Atherton, Z.; Goodgame, D. M. L.; Menzer, S.; Williams, D. J. *Polyhedron* **1999**, *18*, 273-279.
(166) Zhao, Y.; Hong, M.; Su, W.; Cao, R.; Zhou, Z.; Chan, A. S. C. *Chem. Lett.* **2000**, 28-29.
(167) Zhao, Y.-J.; Hong, M.-C.; Liang, Y.-C.; Su, W.-P.; Cao, R.; Zhou, Z.-Y.; Chan, A. S. C. *Polyhedron* **2001**, *20*, 2619-2625.
(168) Wang, R.-H.; Hong, M.-C.; Su, W.-P.; Liang, Y.-C.; Cao, R.; Zhao, Y.-J.; Weng, J.-B. *Bull. Chem. Soc. Japan* **2002**, *75*, 725-730.
(169) Hartshorn, C. M.; Steel, P. J. *J. Chem. Soc., Dalton Trans.* **1998**, 3935-3940.
(170) Albrecht, M.; Fiege, M.; Osetska, O. *Coord. Chem. Rev.* **2007**, In Press.
(171) Steel, P. J.; Al-Mandhary, M. R. A. *Acta Cryst.* **2004**, *E60*, o346-o347.
(172) Steel, P. J.; Al-Mandhary, M. R. A. *Eur. J. Inorg. Chem.* **2004**, 329-334.
(173) Al-Mandhary, M. R. A.; Steel, P. J. *Inorg. Chem. Commun.* **2002**, *5*, 954-957.
(174) Ibukuro, F.; Kusukawa, T.; Fujita, M. *J. Am. Chem. Soc.* **1998**, *120*, 8561-8562.
(175) Kumazawa, K.; Biradha, K.; Kusukawa, T.; Okano, T.; Fujita, M. *Angew. Chem. Int. Ed.* **2003**, *42*, 3909-3913.
(176) Yoshizawa, M.; Nakagawa, J.; Kumazawa, K.; Nagao, M.; Ozeki, T.; Fujita, M. *Angew. Chem. Int. Ed.* **2005**, *44*, 1810-1813.
(177) Ono, K.; Yoshizawa, M.; Kato, T.; Watanabe, K.; Fujita, M. *Angew. Chem. Int. Ed.* **2007**, *46*, 1803-1806.
(178) Manimaran, B.; Rajendran, T.; Lu, Y.-L.; Lee, G.-H.; Peng, S.-M.; Lu, K.-L. *Eur. J. Inorg. Chem.* **2001**, 633-636.
(179) Mukherjee, P. S.; Das, N.; Stang, P. J. *J. Org. Chem.* **2004**, *69*, 3526-3529.

(180) Moon, D.; Kang, S.; Park, J.; Lee, K.; John, R. P.; Won, H.; Seong, G. H.; Kim, Y. S.; Kim, G. H.; Rhee, H.; Lah, M. S. *J. Am. Chem. Soc.* **2006**, *128*, 3530-3531.
(181) Fujita, M.; Fujita, N.; Ogura, K.; Yamaguchill, K. *Nature* **1999**, *400*, 52-55.
(182) Sakamoto, S.; Fujita, M.; Kim, K.; Yamaguchi, K. *Tetrahedron* **2000**, *56*, 955-964.
(183) Yoshizawa, M.; Tamura, M.; Fujita, M. *J. Am. Chem. Soc.* **2004**, *126*, 6846-6847.
(184) Yoshizawa, M.; Kusukawa, T.; Kawano, M.; Ohhara, T.; Tanaka, I.; Kurihara, K.; Niimura, N.; Fujita, M. *J. Am. Chem. Soc.* **2005**, *127*, 2798-2799.
(185) Tashiro, S.; Fujita, M. *Bull. Chem. Soc. Japan* **2006**, *79*, 833-837.
(186) Kobayashi, Y.; Kawano, M.; Fujita, M. *Chem. Commun.* **2006**, 4377-4379.
(187) Ito, H.; Kusukawa, T.; Fujita, M. *Chem. Lett.* **2000**, 598-599.
(188) Kusukawa, T.; Nakai, T.; Okano, T.; Fujita, M. *Chem. Lett.* **2003**, *32*, 284-285.
(189) Nakabayashi, K.; Kawano, M.; Yoshizawa, M.; Ohkoshi, S.; Fujita, M. *J. Am. Chem. Soc.* **2004**, *126*, 16694-16695.
(190) Hosoi, H.; Yamaguchi, S.; Tahara, T. *Chem. Lett.* **2005**, *34*, 618-619.
(191) Karthikeyan, S.; Ramamurthy, V. *Tetrahedron Lett.* **2005**, *46*, 4495-4498.
(192) Yoshizawa, M.; Fujita, M. *Pure Appl. Chem.* **2005**, *77*, 1107-1112.
(193) Nakabayashi, K.; Kawano, M.; Fujita, M. *Angew. Chem. Int. Ed.* **2005**, *44*, 5322-5325.
(194) Yoshizawa, M.; Sato, N.; Fujita, M. *Chem. Lett.* **2005**, *34*, 1392-1393.
(195) Takaoka, K.; Kawano, M.; Ozeki, T.; Fujita, M. *Chem. Commun.* **2006**, 1625-1627.
(196) Yoshizawa, M.; Tamura, M.; Fujita, M. *Science* **2006**, *312*, 251-254.
(197) Kawano, M.; Kobayashi, Y.; Ozeki, T.; Fujita, M. *J. Am. Chem. Soc.* **2006**, *128*, 6558-6559.
(198) Cronin, L. *Angew. Chem. Int. Ed.* **2006**, *45*, 3576-3578.
(199) Karthikeyan, S.; Ramamurthy, V. *J. Org. Chem.* **2007**, *72*, 452-458.
(200) Su, C.-Y.; Cai, Y.-P.; Chen, C.-L.; Lissner, F.; Kang, B.-S.; Kaim, W. *Angew. Chem. Int. Ed.* **2002**, *41*, 2002.
(201) van der Made, A. W.; van der Made, R. H. *J. Org. Chem.* **1993**, *58*, 1262-1263.
(202) Constable, E. C.; Harverson, P. *Chem. Commun.* **1996**, 33-34.
(203) Liu, H.-K.; Sun, W.-Y.; Tang, W.-X.; Yamamoto, T.; Ueyama, N. *Inorg. Chem.* **1999**, *38*, 6313-6316.
(204) Sun, W.-Y.; Xie, J.; Huang, C.-K.; Okamura, T.-a.; Ueyama, N. *Chem. Commun.* **2000**, 1429-1430.
(205) Grawe, T.; Schrader, T.; Zadmard, R.; Kraft, A. *J. Org. Chem.* **2002**, *67*, 3755-3763.
(206) Yun, S.; Ihm, H.; Kim, H. G.; Lee, C.-W.; Indrajit, B.; Oh, K. S.; Gong, Y. J.; Lee, J. W.; Yoon, J.; Lee, H. C.; Kim, K. S. *J. Org. Chem.* **2003**, *68*, 2467-2470.
(207) Reger, D. L.; Semeniuc, R. F.; Smith, M. D. *Inorg. Chem.* **2003**, *42*, 8137-8139.
(208) Mazik, M.; Cavga, H.; Jones, P. G. *J. Am. Chem. Soc.* **2005**, *127*, 9045-9052.
(209) Kim, J.; Kim, Y. K.; Park, N.; Hahn, J. H.; Ahn, K. H. *J. Org. Chem.* **2005**, *70*, 7087-7092.
(210) Oyler, K. D.; Coughlin, F. J.; Bernhard, S. *J. Am. Chem. Soc.* **2007**, *129*, 210-217.
(211) Aversa, M. C.; Barattucci, A.; Bonaccorsi, P.; Faggi, C.; Papalia, T. *J. Org. Chem.* **2007**, *72*, 4486-4496.

(212) Murray, P.; Willans, C.; Bredenkamp, M. W.; Gertenbach, J. A. *Acta Cryst.* **2007**, *E63*, o224-o225.
(213) Walsdorff, C.; Park, S.; Kim, J.; Heo, J.; Park, K.-M.; Oh, J.; Kim, K. *J. Chem. Soc., Dalton Trans.* **1999**, 923-929.
(214) Kamper, A.; Apostolakis, J.; Rarey, M.; Marian, C. M.; Lengauer, T. *J. Chem. Inf. Model* **2006**, *46*, 903-911.
(215) Fahlbusch, T.; Frank, M.; Schatz, J.; Schmaderer, H. *Eur. J. Org. Chem.* **2006**, 1899-1903.
(216) Hennrich, G.; Anslyn, E. V. *Chem. Eur. J.* **2002**, *8*, 2218-2224.
(217) Lampkins, A. J.; Abdul-Rahim, O.; Li, H.; Castellano, R. K. *Org. Lett.* **2005**, *7*, 4471-4474.
(218) Morgans, G. L.; Otterlo, W. A. L. v.; Michael, J. P.; Fernandes, M. A. *Acta Cryst.* **2006**, *E62*, o168-o170.
(219) Li, H.; Homan, E. A.; Lampkins, A. J.; Ghiviriga, I.; Castellano, R. K. *Org. Lett.* **2005**, *7*, 443-446.
(220) Cho, B. R.; Chajara, K.; Oh, H. J.; Son, K. H.; Jeon, S.-J. *Org. Lett.* **2002**, *4*, 1703-1706.
(221) Chang, W.-K.; Sheu, S.-C.; Lee, G.-H.; Wang, Y.; Ho, T.-I.; Lin, Y.-C. *J. Chem. Soc., Dalton Trans.* **1993**, 687-694.
(222) Hartshorn, C. M.; Steel, P. J. *Aust. J. Chem.* **1995**, *48*, 1587-1599.
(223) Hartshorn, C. M.; Steel, P. J. *Angew. Chem. Int. Ed. Engl.* **1996**, *35*, 2655-2657.
(224) Oh, K. S.; Lee, C.-W.; Choi, H. S.; Lee, S. J.; Kim, K. S. *Org. Lett.* **2000**, *2*, 2679-2681.
(225) Watson, A. A., PhD Thesis, University of Canterbury, Christchurch, 1987.
(226) Shelly, K.; Finster, D. C.; Lee, Y. J.; Scheidt, W. R.; Reed, C. A. *J. Am. Chem. Soc.* **1985**, *107*, 5955-5959.
(227) Munakata, M.; Wu, L. P.; Ning, G. L. *Coord. Chem. Rev.* **2000**, *198*, 171-203.
(228) Munakata, M.; Ning, G. L.; Suenaga, Y.; Kuroda-Sowa, T.; Maekawa, M.; Ohta, T. *Angew. Chem. Int. Ed.* **2000**, *39*, 4555-4557.
(229) Munakata, M.; Wu, L. P.; Kuroda-Sowa, T.; Maekawa, M.; Suenaga, Y.; Ohta, T.; Konaka, H. *Inorg. Chem.* **2003**, *42*, 2553-2558.
(230) Li, G.; Shi, Z.; Liu, X.; Dai, Z.; Feng, S. *Inorg. Chem.* **2004**, *43*, 6884-6886.
(231) Graham, P. M.; Pike, R. D.; Sabat, M.; Bailey, R. D.; Pennington, W. T. *Inorg. Chem.* **2000**, *39*, 5121-5132.
(232) Zou, R.-Q.; Liu, C.-S.; Huang, Z.; Hu, T.-L.; Bu, X.-H. *Cryst. Growth Des.* **2006**, *6*, 99-108.
(233) Ronson, T. K.; Adams, H.; Ward, M. D. *Eur. J. Inorg. Chem.* **2005**, 4533-4549.
(234) Telfer, S. G.; Sato, T.; Harada, T.; Kuroda, R.; Lefebvre, J.; Leznoff, D. B. *Inorg. Chem.* **2004**, *43*, 6168-6176.
(235) Bray, D. J.; Liao, L.-L.; Antonioli, B.; Gloe, K.; Lindoy, L. F.; McMurtrie, J. C.; Wei, G.; Zhang, X.-Y. *Dalton Trans.* **2005**, 2082-2083.
(236) Hong, M.-C.; Zhao, Y.-J.; Su, W.-P.; Cao, R.; Fujita, M.; Zhou, Z.-Y.; Chan, A. S. C. *Angew. Chem. Int. Ed.* **2000**, *39*, 2468-2469.
(237) McMorran, D. A.; Steel, P. J. *Tetrahedron* **2003**, *59*, 3701-3707.
(238) Healy, P. C.; Pakawatchai, C.; Raston, C. L.; Skelton, B. W.; White, A. H. *J. Chem. Soc., Dalton Trans.* **1983**, 1905.
(239) Su, C.-Y.; Kang, B.-S.; Sun, J. *Chem. Lett.* **1997**, 821.
(240) Xie, Y.-B.; Ma, Z.-C.; Wang, D. *J. Mol. Struct.* **2006**, *784*, 93.
(241) Song, R.-F.; Xie, Y.-B.; Li, J.-R.; Bu, X.-H. *Cryst. Eng. Comm.* **2005**, *7*, 249.
(242) Ma, Z.-C.; Xian, H.-S. *Cryst. Eng. Comm.* **2006**, *36*.

(243) Diez, J.; Panera, M. *Inorg. Chem.* **2006**, *45*, 10043.
(244) Kumar, S.; Kaur, S.; Singh, G. *Supramolecular Chem.* **2003**, *15*, 65-67.
(245) Singh, P.; Kumar, S. *Tetrahedron Lett.* **2006**, *47*, 109-112.
(246) Mittal, S. K.; Kumar, A. S. K.; Gupta, N.; Kaur, S.; Kumar, S. *Anal. Chim. Act.* **2007**, *585*, 161-170.
(247) Singh, P.; Kumar, S. *Tetrahedron* **2006**, *62*, 6379-6387.
(248) Liu, Y.; Wu, G.; Liao, M. *Geodeng Xuexiao Hauxue Xuebao* **1986**, *7*, 815-820.
(249) Krabbes, G.; Oppermann, H. *Z. Anorg. Allg. Chem.* **1977**, *435*, 33-44.
(250) Potts, A. W.; Lyus, M. L. *J. Electron. Spec. Rel. Phenom.* **1978**, *13*, 305-315.
(251) Butaev, B. S.; Gershikov, A. G.; Spiridonov, V. P. *Vestn. Mosk. Uni., Ser. 2:Khim.* **1978**, *19*, 734.
(252) Cariati, E.; Ugo, R.; Cariati, F.; Roberto, D.; Masciocchi, N.; Galli, S.; Sironi, A. *Adv. Mater.* **2001**, *13*, 1665.
(253) Buravov, L. I.; Zvarikina, A. V.; Kartsovnik, M. V.; Kuschch, N. D.; Laukhin, V. N.; Lobkovskaya, R. M.; Merzhanov, V. A.; Fedutin, D. N.; Shibaeva, R. P.; Yagubskii, E. B. *J. Exp. Theor. Phys.* **1987**, *92*, 594.
(254) Heller, M.; Sheldrich, W. S. *Z. Anorg. Allg. Chem.* **2004**, *630*, 1191.
(255) Bowmaker, G. A.; Camus, A.; Hart, R. D.; Kildea, J. D.; Skelton, B. W.; White, A. H. *J. Chem. Soc., Dalton Trans.* **1990**, 3753.
(256) Ohi, H.; Tachi, Y.; Kunimoto, T.; Itoh, S. *Dalton Trans.* **2005**, 3146-3147.
(257) Solntsev, P. V.; Sieler, J.; Krautscheid, H.; Domasevitch, K. V. *Dalton Trans.* **2004**, 1153-1158.
(258) Claessens, C. G.; Torres, T. *J. Am. Chem. Soc.* **2002**, *124*, 14522-14523.
(259) Cooper, G. J. T.; Abbas, H.; Kogerler, P.; Long, D.-L.; Cronin, L. *Inorg. Chem.* **2004**, *43*, 7266-7268.
(260) Polson, M. I. J.; Taylor, N. J.; Hanan, G. S. *Chem. Commun.* **2002**, 1356-1357.
(261) Blanchard, P.; Svenstrup, N.; Rault-Berthelot, J.; Amedee, R.; Becher, J. *Eur. J. Org. Chem.* **1998**, 1743-1757.
(262) Vogtle, F.; Hohner, G.; Weber, E. *J. Chem. Soc. Chem. Comm.* **1973**, 366-367.
(263) Rajakumar, P.; Srisailas, M. *Tetrahedron Lett.* **2002**, *43*, 1909-1913.
(264) Schmohel, E.; Ott, F.; Breitchbach, J.; Nieger, M.; Vogtle, F. *Chem. Ber.* **1993**, *126*, 2477-2482.
(265) Hohner, G.; Vogtle, F. *Chem. Ber.* **1977**, *110*, 3052-3077.
(266) Vogtle, F.; Hohner, G. *Angew. Chem.* **1975**, *87*, 522-523.
(267) Mahmoudkhani, A. H.; Shimizu, G. K. H. *Inorg. Chem.* **2007**, *46*, 1593-1602.
(268) Hu, Z. G.; Liu, J.; Li, G. A.; Dong, Z. B. *J. Chem. Research* **2003**, 778-779.
(269) Kim, Y. H.; Beckerbauer, R. *Macromolecules* **1994**, *27*, 1968-1971.
(270) Stilbury, R. T.; Zhang, C.; Emge, T. J.; Schugar, H. J.; Potenza, J. A.; Knapp, S. *Inorg. Chem.* **2006**, *45*, 9713-9720.
(271) Shu, M.; Tu, C.; Xu, W.; Jin, H.; Sun, J. *Cryst. Growth Des.* **2006**, *6*, 1890-1896.
(272) Caygill, G. B.; Steel, P. J. *J. Organomet. Chem.* **1987**, *327*, 115-123.
(273) de Gueest, D. J., PhD Thesis, University of Canterbury, Christchurch, 1998.
(274) O'Keefe, B. J., PhD Thesis, University of Canterbury, Christchurch, 1999.
(275) Roessler, K.; Kluge, T.; Schubert, A.; Sun, Y.; Herdtweck, E.; Thiel, W. R. *Z. Naturforsch., B* **2004**, *59*, 1253-1263.
(276) Herrera, A.; Martinez-Alvarez, R.; Ramiro, P.; Chioua, M.; Chioua, R. *Synthesis* **2004**, 503-505.
(277) Thalladi, V. R.; Muthuraman, M.; Nangia, A.; Desiraju, G. R. *Acta Cryst.* **1999**, *C55*, 698-700.

(278) Cook, A. H.; Jones, D. G. *J. Chem. Soc.* **1941**, 278-282.
(279) Wang, X.-F.; Lv, Y.; Okamura, T.-a.; Kawaguchi, H.; Wu, G.; Sun, W.-Y.; Ueyama, N. *Cryst. Growth Des.* **2007**, *7*, 1125-1133.
(280) Wan, S.-Y.; Li, Y.-Z.; Okamura, T.-a.; Fan, J.; Sun, W.-Y.; Ueyama, N. *Eur. J. Inorg. Chem.* **2003**, 3783-3789.
(281) Wan, S.-Y.; Fan, J.; Okamura, T.-a.; Zhu, H.-F.; Ouyang, X.-M.; Sun, W.-Y.; Ueyama, N. *Chem. Commun.* **2002**, 2520-2521.
(282) Kuehl, C. J.; Kryschenko, Y. K.; Radhakrishnan, U.; Seidel, S. R.; Huang, S. D.; Stang, P. J. *Proc. Nat. Acad. Sci.* **2002**, *99*, 1932-1936.
(283) Humphrey, E. R.; Mann, K. L. V.; Reeves, Z. R.; Behrendt, A.; Jeffery, J. C.; Maher, J. P.; McCleverty, J. A.; Ward, M. D. *New J. Chem.* **1999**, *23*, 417-423.
(284) Beeston, R. F.; Aldridge, W. S.; Treadway, J. A.; Fitzgerald, M. C.; DeGraff, B. A.; Stitzel, S. E. *Inorg. Chem.* **1998**, *37*, 4368-4379.
(285) Mongin, O.; Porres, L.; Katan, C.; Pons, T.; Mertz, J.; Blanchard-Desce, M. *Tetrahedron Lett.* **2003**, *44*, 8121-8125.
(286) Mallegol, T.; Gmouth, S.; Meziane, M. A. A.; Blanchard-Desce, M.; Mongin, O. *Synthesis* **2005**, 1771-1774.
(287) Tisler, M.; Stanovnik, B.; Versek, B. *Vestn. Slov. Kem. Drus.* **1980**, *27*, 65.
(288) Hu, T.-L.; Li, J.-R.; Liu, C.-S.; Shi, X.-S.; Zhou, J.-N.; Bu, X.-H.; Ribas, J. *Inorg. Chem.* **2006**, *45*, 162-173.
(289) Hu, T.-L.; Wang, J.-J.; Li, J.-R.; Bu, X.-H. *J. Mol. Struct.* **2006**, *796*, 18-22.
(290) Jones, P. L.; Jeffery, J. C.; McCleverty, J. A.; Ward, M. D. *Polyhedron* **1997**, *16*, 1567-1571.
(291) Ward, M. D.; Mann, K. L. V.; Jeffery, J. C.; McCleverty, J. A. *Acta Cryst.* **1998**, *C54*, 601-603.
(292) Mann, K. L. V.; Psillakis, E.; Jeffery, J. C.; Rees, L. H.; Harden, N. M.; McCleverty, J. A.; Ward, M. D.; Gatteschi, D.; Totti, F.; Mabbs, F. E.; McInnes, E. J. L.; Riedi, P. C.; Smith, G. M. *J. Chem. Soc., Dalton Trans.* **1999**, 339-348.
(293) Jeffery, J. C.; Jones, P. G.; Mann, K. L. V.; Psillakis, E.; McCleverty, J. A.; Ward, M. D.; White, C. M. *Chem. Commun.* **1997**, 175-176.
(294) Liu, C.-S.; Shi, X.-S.; Li, J.-R.; Wan, J.-J.; Bu, X.-H. *Cryst. Growth Des.* **2006**, *6*, 656-663.
(295) Paul, R. L.; Couchman, S. M.; Jeffery, J. C.; McCleverty, J. A.; Reeves, Z. R.; Ward, M. D. *J. Chem. Soc., Dalton Trans.* **2000**, 845-851.
(296) Mukherjee, J.; Mukherjee, R. *Dalton Trans.* **2006**, 1611-1621.
(297) Lam, M. H. W.; Cheung, S. T. C.; Fung, K.-M.; Wong, W.-T. *Inorg. Chem.* **1997**, *36*, 4618-4619.
(298) Liu, C.-S.; Zhang, H.; Chen, R.; Shi, X.-S.; Bu, X.-H.; Yang, M. *Chem. Pharm. Bull.* **2007**, *55*, 996-1001.
(299) Singh, K.; Long, J. R.; Stravropoulos, P. *Inorg. Chem.* **1998**, *37*, 1073-1079.
(300) Canty, A. J.; Engelhardt, L. M.; Healy, P. C.; Kildea, J. D.; Minchin, N. J.; White, A. H. *Aust. J. Chem.* **1987**, *40*, 1881.
(301) Basu, A.; Bhaduri, S.; Sapre, N. Y.; Jones, P. G. *J. Chem. Soc., Chem. Commun.* **1987**, 1724.
(302) Allen, D. W.; Mifflin, J. P. L.; Coles, S. *Chem. Commun.* **1998**, 2115.
(303) Su, C.-Y.; Cai, Y.-P.; Chen, C.-L.; Lissner, F.; Kang, B.-S.; Kaim, W. *Angew. Chem. Int. Ed.* **2002**, *41*, 3371.
(304) Su, C.-Y.; Cai, Y.-P.; Chen, C.-L.; Smith, M. D.; Kaim, W.; Zur Loye, H.-C. *J. Am. Chem. Soc.* **2003**, *125*, 8595.
(305) Xu, Y.; Ran, C.; Wang, H.; Song, M. *J. Zhejiang Univ. Sci. Ed.* **2005**, *37*, 86.

(306) Telfer, S. G.; Kuroda, R.; Lefebvre, J.; Leznoff, D. B. *Inorg. Chem.* **2006**, *45*, 4592.
(307) Yamanoi, Y.; Sakamoto, S.; Kusukawa, T.; Fujita, M.; Sakamoto, Y.; Yamaguchi, K. *J. Am. Chem. Soc.* **2001**, *123*, 980-981.
(308) Constable, E. C. *Personal Communication* **2007**.
(309) Kodak, N. V. *Preparation of cuprous iodide*; Neth. Appl., 1967.
(310) Hathaway, B. J.; Holah, D. G.; Postlethwaite, J. D. *J. Chem. Soc.* **1961**, 3215-3218.
(311) Pfeiffer, P.; Glasser, H. *J. Prakt. Chem* **1938**, *151*, 134.
(312) Goodgame, D. M. L.; Venanzi, L. M. *J. Chem. Soc.* **1963**, 616.
(313) Narath, A.; Tiilikka, A. *Journal of Photographic Science* **1961**, *9*, 303-311.
(314) Heck, R. F. *Palladium Reagents in Organic Synthesis*; Academic Press: London, 1985.
(315) Hohmann, H.; Eldik, R. V. *Inorg. Chim. Acta* **1990**, *174*, 87.
(316) Fujita, M.; Aoyagi, M.; Ogura, K. *Inorg. Chim. Acta* **1996**, *246*, 53-57.
(317) Lecloux, D. D.; Tokar, C. J.; Osawa, M.; Houser, R. P.; Keyes, M. C.; Tolman, W. B. *Organometallics* **1994**, *13*, 2855.
(318) Ward, M. D.; McCleverty, J. A.; Jones, P. L.; Jeffery, J. C.; Thompson, A. M. C.; Amoroso, A. J. *J. Chem. Soc., Chem. Commun.* **1994**, 2751-2752.
(319) Yanagida, S.; Yokoe, M.; Katagiri, I.; Ohoka, M.; Komori, S. *Bull. Chem. Soc. Jpn* **1973**, *46*, 306-310.